Molecular and functional characterization of the long non-coding RNA SSR42 in *Staphylococcus aureus*

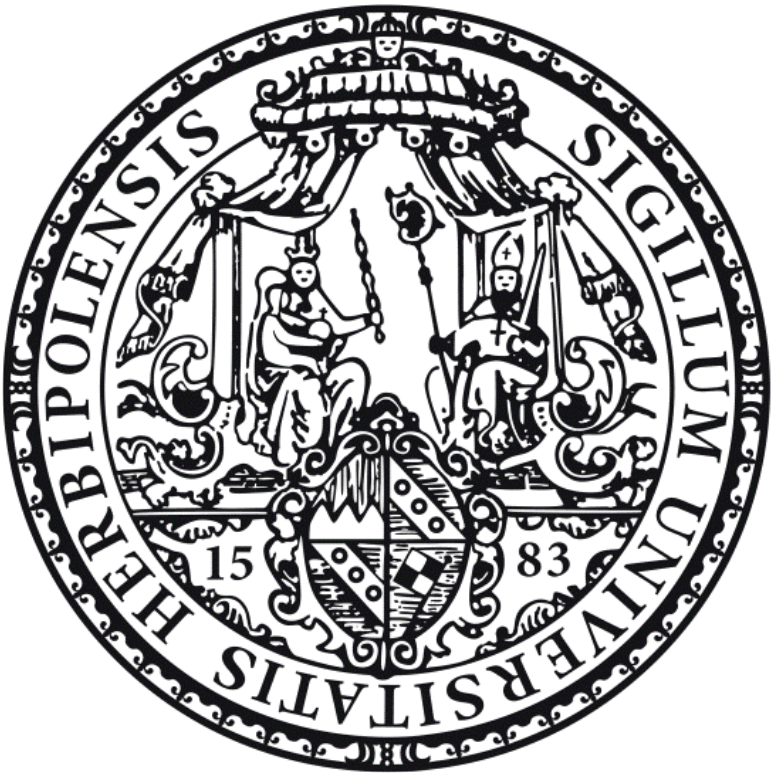

DISSERTATION

zur Erlangung des naturwissenschaftlichen Doktorgrades

doctor rerum naturalium

(Dr. rer. nat.)

im Fach Biologie

eingereicht an der Fakultät für Biologie

der Julius-Maximilians-Universität Würzburg

vorgelegt von

M.Sc. Biol.

Jessica Horn

geboren am 01.11.1989 in Würzburg

Würzburg, 2018

Eingereicht am:

Mitglieder der Promotionskommission:

Vorsitzender:

Erstgutachter: Prof. Dr. Thomas Rudel

Zweitgutachter: Prof. Dr. Cynthia Sharma

Tag des Promotionskolloquiums:

Doktorurkunde ausgehändigt am:

TABLE OF CONTENT

1 SUMMARY

1.1 Abstract

Staphylococcus aureus asymptomatically colonizes the skin and anterior nares of 20-30% of the healthy human population. As an opportunistic human pathogen it elicits a variety of infections ranging from skin and soft tissue infections to highly severe manifestations such as pneumonia, endocarditis and osteomyelitis. Due to the emergence of multi resistant strains, treatment of staphylococcal infections becomes more and more challenging and the WHO therefore classified *S. aureus* as a "superbug". The variety of diseases triggered by *S. aureus* is the result of a versatile expression of a large set of virulence factors. The most prominent virulence factor is the cytotoxic and haemolytic pore-forming α-toxin whose expression is mediated by a complex regulatory network involving two-component systems such as the agr quorum-sensing system, accessory transcriptional regulators and alternative sigma-factors. However, the intricate regulatory network is not yet understood in its entirety. Recently, a transposon mutation screen identified the AraC-family transcriptional regulator 'Repressor of surface proteins' (Rsp) to regulate haemolysis, cytotoxicity and the expression of various virulence associated factors. Deletion of *rsp* was accompanied by a complete loss of transcription of a 1232 nt long non-coding RNA, SSR42.

This doctoral thesis focuses on the molecular and functional characterization of SSR42. By analysing the transcriptome and proteome of mutants in either SSR42 or both SSR42 and *rsp*, as well as by complementation of SSR42 in trans, the ncRNA was identified as the main effector of Rsp-mediated virulence. Mutants in SSR42 exhibited strong effects on transcriptional and translational level when compared to wild-type bacteria. These changes resulted in phenotypic alterations such as strongly reduced haemolytic activity and cytotoxicity towards epithelial cells as well as reduced virulence in a murine infection model. Deletion of SSR42 further promoted the formation of small colony variants (SCV) during long term infection of endothelial cells and demonstrated the importance of this molecule for intracellular bacteria. The impact of this ncRNA on staphylococcal haemolysis was revealed to be executed by modulation of *sae* mRNA stability and by applying mutational studies functional domains within SSR42 were identified.

Moreover, various stressors modulated the transcription of SSR42 and antibiotic challenge resulted in SSR42-dependently increased haemolysis and cytotoxicity. Transcription of SSR42 itself was found under control of various important global regulators including AgrA, SaeS, CodY and σB, thereby illustrating a central position in *S. aureus* virulence gene regulation.

The present study thus demonstrates SSR42 as a global virulence regulatory RNA which is important for haemolysis, disease progression and adaption of *S. aureus* to intracellular conditions via formation of SCVs.

1.2 Zusammenfassung

Staphylococcus aureus kolonisiert asymptomatisch als Kommensal die Haut und Nasenschleimhäute von circa 20-30% der gesunden Weltbevölkerung. Als opportunistisches Humanpathogen löst *S. aureus* dagegen eine Reihe von Krankheiten aus, die von leichten Hautinfektionen und Abszessen bis hin zu schwerwiegenden und lebensbedrohlichen Krankheitsformen wie Pneumonie, Endokarditis und Osteomyelitis reichen können. Die Behandlung von Staphylokokken-Infektionen stellt aufgrund der Entstehung multi-resistenter Stämme vermehrt eine Herausforderung dar, weshalb *S. aureus* von der WHO als „superbug" klassifiziert wurde. Die Vielzahl an möglichen Krankheitsformen sind das Ergebnis der anpassungsfähigen und koordinierten Expression einer Vielzahl von Virulenzfaktoren. Der dabei wohl bedeutendste und am besten charakterisierte Virulenzfaktor ist das porenbildende α-toxin, dessen zytotoxische und hämolytische Aktivität für eine Reihe diverser Krankheiten verantwortlich ist. Die Expression dieses Toxins wird durch ein komplexes, bis jetzt noch nicht komplett verstandenes, regulatorisches Netzwerk gesteuert, das sowohl Zwei-Komponentensysteme wie das agr Quorum-sensing System, diverse akzessorische transkriptionelle Regulatoren sowie alternative Sigmafaktoren beinhaltet. Kürzlich wurde in einem Transposon-Mutanten-Screen der AraC-Familie transkriptionelle Regulator „Repressor of surface proteins" (Rsp) identifiziert, der die Expression diverser Virulenz-assoziierter Faktoren beeinflusste. Eine Deletion von *rsp* ging, neben reduzierter Hämolyse und Zytotoxizität, auch mit dem kompletten Verlust der Transkription einer 1232 nt langen nicht-kodierenden RNA, SSR42, einher.

Diese Doktorarbeit befasst sich mit der molekularen und funktionellen Charakterisierung dieser nicht-kodierenden RNA. Mittels Transkriptom- und Proteomanalysen wurden eine SSR42 Deletionsmutante sowie eine Doppelmutante in SSR42 und *rsp* charakterisiert und SSR42 als Hauptfaktor der Rsp-vermittelten Virulenzregulation identifiziert. Neben weitreichenden Veränderungen auf trans-kriptioneller und translationaler Ebene wiesen Mutanten in SSR42 eine stark reduzierte hämolytische und zytotoxische Aktivität sowie verringerte Virulenz in einem murinen Infektionsmodell auf. Eine Deletion von SSR42 begünstigte weiterhin die Bildung von sog. „small colony variants" während Langzeit-Infektionen von Endothelzellen und demonstrierte die Bedeutung dieser nicht-codierenden RNA für intrazelluläre Staphylokokken. Die regulatorische Wirkung von SSR42 auf die hämolytische Aktivität von *S. aureus* wurde in dieser Arbeit aufgeklärt. Dabei konnte ein stabilisierender Einfluss der nicht-kodierenden RNA auf *sae* mRNA nachgewiesen werden. Weiterhin wurde SSR42 durch Mutagenese-Studien auf molekularer Ebene charakterisiert, wobei funktionelle und stabilisierende Domänen identifiziert wurden.

Ebenso wurden in dieser Arbeit diverse Stressoren und Antibiotika erfasst, die eine modulatorische Wirkung auf die Transkription von SSR42 ausüben. Neben einer Erhöhung der Transkription von SSR42

resultierte eine Behandlung von *S. aureus* mit sub-inhibitorischen Konzentrationen von Antibiotika in einer drastischen, SSR42-abhängigen, Steigerung der hämolytischen und zytotoxischen Aktivität. Mithilfe von Promotoraktivitätsstudien wurde der Einfluss diverser Regulatoren wie AgrA, SaeS, CodY und σB auf die transkriptionellen Regulation von SSR42 identifiziert und SSR42 somit eine zentrale Rolle in der Regulation von Virulenzgenen verliehen.

SSR42 wurde demnach als ein neuartiger globaler Regulator identifiziert, der eine wichtige Rolle für Hämolyse, den Krankheitsverlauf sowie bei der Anpassung an intrazelluläre Bedingungen, über die Bildung von „small colony variants“, spielt.

2 INTRODUCTION

2.1 *Staphylococcus aureus*

2.1.1 General Information

Staphylococcus aureus, subsp. *aureus* is a gram-positive, catalase positive, nitrate reducing, facultative anerobic, coccoid bacterium which was first identified by Sir Alexander Ogston while examinating purulence from abscesses of a human patient after surgery in 1880 (Aberdeen, United Kingdom; Ogston, 1882). The name *Staphylococcus aureus* was later established by the German researcher Friedrich Julius Rosenbach (1884). The name derives from the Greek words 'staphyle' and 'kokkos' translating to bunch of grapes and the Latin word 'aureus' meaning golden thereby describing the appearance of this 0.8 – 1.2 µm yellow pigmented, coccoid bacterium that appears in microscopic images in grape-like clusters (Fig. 2.1). Friedrich Julius Rosenbach initially classified *S. aureus* in an own genus, 'Staphylococcus' (Rosenbach, 1884). While taxonomic classification was later reversed twice (Flügge, 1886; Götz et al., 2006), Staphylococci were finally placed into the family of Staphylococcaceae (2010) containing 44 different species. *S. aureus* further belongs to the phylum of Firmicutes and the class of Bacilli. *S. aureus* contains a circular genome encompassing ~2.8 Mbp with a GC-content of 33 mol% (Kuroda et al., 2001). The genome can be subdivided into a 'core genome' and a variable part, the 'accessory genome'. The core genome constitutes genes encoding essential cellular functions such as metabolism, replication and growth which are conserved in all strains. In contrast approximately 22% of the genes of *S. aureus* compose the 'accessory genome' including pathogenicity islands (SaPIs), genomic islands, transposons, integrated plasmids and prophages that often encode virulence factors and resistance genes (Lindsay et al., 2006; reviewed in Feng et al., 2008).

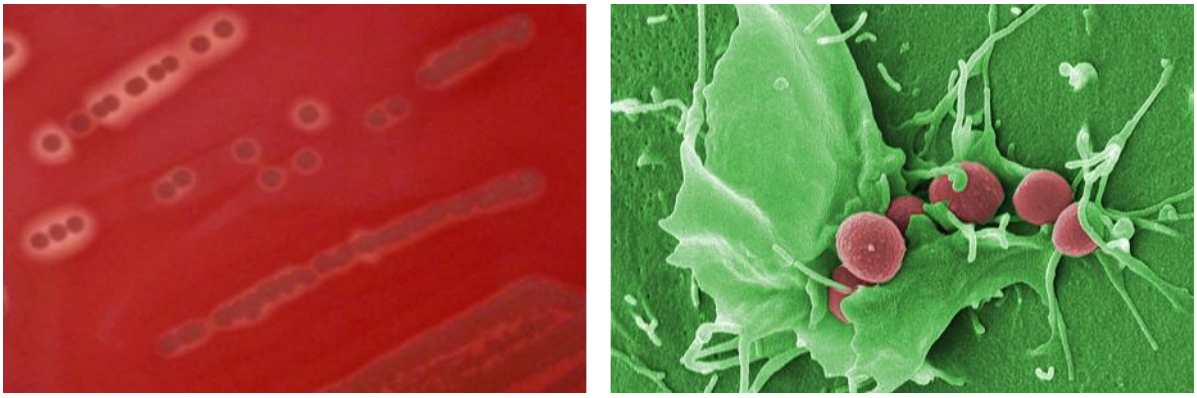

Figure 2.1: Macroscopic and microscopic images of *Staphylococcus aureus*. *S. aureus* colonies on agar supplemented with sheep blood (left) and electron-microscopic presentation of *S. aureus* invading into an epithelial cell (right, source: www.helmholtz-hzi.de).

2.1.2 Host colonization

As a facultative pathogen *S. aureus* represents a frequent cause of community- and hospital-acquired infections while colonizing asymptomatically about 25-30% of the healthy population as a human commensal (Kluytmans et al., 1997). Despite humans *S. aureus* further colonizes animals including dogs, horses, cattle and pigs (Khanna et al., 2008; Morgan, 2008; Hasman et al., 2010) thereby depicting a potential risk factor for zoonosis (Hanselman et al., 2006, Voss et al., 2005; Witte et al., 2007; Wulf et al., 2008; reviewed in Springer et al., 2009). With healthy humans being a natural asymptomatic reservoir for *S. aureus* colonization takes place at mucosal surfaces, primarily the anterior nares, but also skin, gastro-intestinal tract, throat, rectum and vagina (Cook et al., 2007; Senn et al., 2012; reviewed in Wertheim et al., 2005; Fig. 2.2). Approximately 20% of the human population is permanently colonized asymptomatically, while 60% are intermittent carriers characterized by only short-term colonization, whereas 20% are never or seldom colonized by *S. aureus* (Eriksen et al., 1995; reviewed in Kluytmans et al., 1997; Williams, 1963). Nasal carriage of *S. aureus* seldom results in overt infections which can partially be explained by the down-regulation of virulence factor expression which was observed during the colonization phase (Burian et al., 2010). The attachment of *S. aureus* to host surfaces is an important step in colonization and is dependent on bacterial adhesins and surface structures (Weidenmaier et al., 2012; Speziale et al., 2009). Pre-existing diseases like rheumatoid arthritis as well as other host factors such as gender, age, diet, smoking and drug addiction have been associated with influencing nasal carriage (Sollid et al., 2014; Choi et al., 2006; Laudien et al., 2010; Olsen et al., 2012; Tuazon et al., 1975; Berman et al., 1987; Miller et al., 2003). However, the genetic determinants influencing colonization remain elusive.

Nasal carriage of *S. aureus* constitutes a major risk factor for ensuing infections. This was demonstrated in a bacteraemia study which identified the colonizing strains as the source of infection in 80% of the cases (von Eiff et al., 2001).

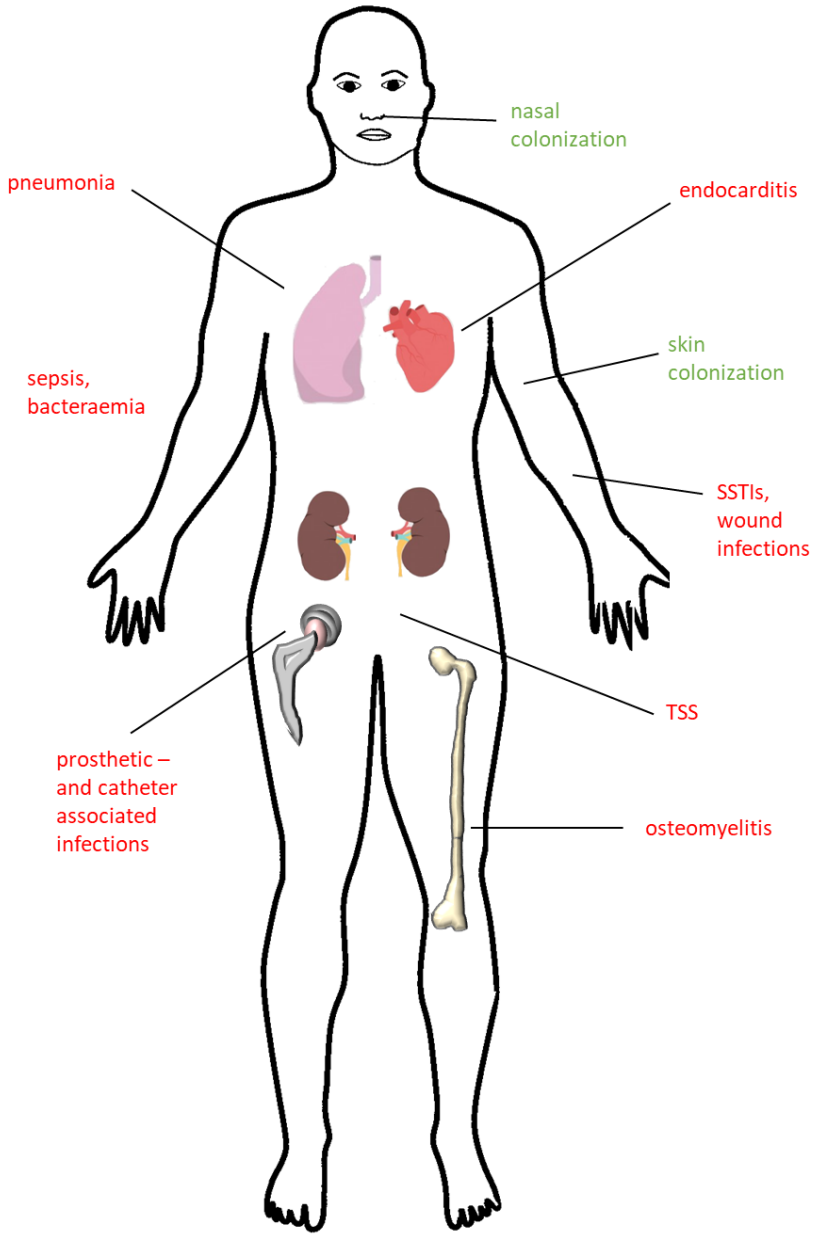

Figure 2.2: *S. aureus* infection manifestations. *S. aureus* is both a human commensal and colonizes skin and nares (green) as well as an opportunistic pathogen that is responsible for a variety of infections (red). (Figure modified after https://upload.wikimedia.org/wikipedia/commons/2/29/Human_body_schemes.png and https://www.freepik.com/free-vector/ human-organs_595348.htm#term=kidney&page=1&position=2)

2.1.3 Methicillin-resistant *Staphylococcus aureus* (MRSA)

A major problem regarding staphylococcal infection represents the emergence of antibiotic resistances in *S. aureus* impeding treatment and rendering many infections untreatable. Already shortly after introduction of the first antibiotic in use, the β-lactam antibiotic Penicillin, resistances arose in *S. aureus* impairing the treatment of infections. Thus, in 1959 the β-lactam derivate methicillin (also known as oxacillin) was introduced into clinical settings. However, methicillin-resistant *S. aureus*

strains were already reported in the early 1960s (Jevons, 1961; Sutherland and Rolinson, 1964). Resistance against β-lactam antibiotics such as methicillin and penicillin is conferred in *S. aureus* by acquisition of a mobile genetic element, the methicillin cassette chromosome (SCC) mec. SCCmec harbours the resistance gene *mec*A encoding a low affinity Penicillin-binding protein, PBP21 (Ubukata et al., 1990), which was most likely acquired by horizontal gene transfer from coagulase-negative staphylococcal species (Tsubakishita et al., 2010). *S. aureus* strains harbouring the SCCmec cassette are referred to as methicillin-resistant *S. aureus* (MRSA) and are mainly accountable for treatment impairment of staphylococcal infections (Mera et al., 2011). Despite MRSA strains, the emergence of strains with resistance against vancomycin (VRSA) further contributes to this problem (Appelbaum, 2007). In the US, the prevalence of MRSA accounting to staphylococcal infections increased to over 50% over the last decade thereby playing a major role for both nosocomial as well as community-acquired infections (Mera et al., 2011). Although in 2011 the prevalence of invasive MRSA infections with an estimated number of 80,461 dropped by 30,800 compared to the prevalence of MRSA infections in 2005 (Dantes et al., 2013), MRSA are still considered the predominant pathogenic bacteria in the US regarding skin and soft tissue infections (Talan et al., 2011). Among these approximately 48,000 were found to be hospital-acquired (HA)-MRSA whereas 16,000 infections were community-acquired (CA-) infections. In addition to the dropping number of total MRSA infections the prevalence of hospital-acquired infections decreased in the last decade (Dantes et al., 2013). However, the prevalence of community-acquired (CA-) MRSA infections increased especially regarding invasive infections in children, which have risen from 1.1 in 2005 to 1.7 incidents in 2010 per 100,000 infections (Iwamoto et al., 2013).

Using pulse-field electrophoresis (PFGE) methicillin-resistant *S. aureus* strains from the US were classified according to their electrophoresis pattern and designated from “USA100” to “USA800”. In the US, the most common community-acquired *S. aureus* infections result from USA300 strains belonging to sequence type (ST) 8 (McDougal et al., 2003). USA300 strains are characterized by acquisition of the SCCmec type IV cassette conferring methicillin-resistance, presence of the arginine catabolic mobile element (ACME) and Panton-Valentine leukocidin encoding operon *pvl*. Apart from the importance of USA300 in the US, USA300 strains were reported to be responsible for approximately 40% of all *S. aureus* infections in Europe thereby representing the most prevalent *S. aureus* sequence type in Europe (Rolo et al., 2012).

2.1.4 *S. aureus* infections and diseases

Upon breaking of natural barriers, such as the skin or mucosal surfaces, the commensal bacterium *S. aureus* becomes an opportunistic pathogen eliciting a multitude of infections such as skin and soft-

tissue infections (SSTIs), surgical-site infections (SSIs), septic arthritis, osteomyelitis, urinary tract infections, toxic-shock syndrome (TSS), endocarditis, bacteraemia (SAB) and sepsis (Engemann et al., 2003; Bunikowski et al., 2000; Corey, 2009; Hartman et al., 1984; Stryjewski and Chambers, 2008; reviewed in Tong et al., 2015).

Being the leading cause of SSTIs the importance of S*. aureus* has increased over the last decade climaxing in a worldwide epidemic of community-acquired (CA-) MRSA infections (DeLeo et al., 2010; David and Daum, 2010). Staphylococcal skin and soft-tissue infections encompass impetigo, necrotising skin lesions, cutaneous abscesses and purulent cellulitis. In some cases, complex manifestations of SSTIs can result in life-threatening conditions such as systemic inflammation and subsequent bacteraemia (Burton et al., 2009).

In addition to its importance in SSTIs *S. aureus* represents a major cause of blood stream infections in humans with an incidence ranging from 10-30 per 100,000 persons in industrialized countries (Laupland et al., 2013). Staphylococcal bacteraemia (SAB) often results from SSTIs, catheter-related infections, or infections of orthopaedic implants (Engemann et al., 2003) and is associated with a high morbidity and mortality. The occurrence of complications such as infective endocarditis and metastatic infections can even worsen the outcome of SAB (Fowler et al., 2005; Troidle et al., 2007). SAB thereby represents one of the leading causes of *S. aureus*-related morbidities.

S. aureus further constitutes the leading cause of osteomyelitis (Sheehy et al., 2010; Inoue et al., 2013), an invasive bone infection resulting in inflammation and necrosis of the bone and can be identified in 30-60% of clinical osteomyelitis manifestations (reviewed in Tong et al., 2015). Although healthy bone tissue is highly resistant against bacterial infections, *S. aureus* established several mechanisms to overcome this natural resistance: The expression of surface proteins aids in the adherence to the bone matrix (Darouiche et al., 1997), the formation of biofilms on catheters and orthopaedic implants confers protection against antimicrobial agents (Fischer et al., 1996) and the bacterial invasion of osteoblasts (Shi and Zhang, 2012) is important to evade the host immune system.

Another manifestation of *S. aureus* infection represents the toxic shock syndrome, which is characterized by symptoms including fever, strong decrease of blood pressure and organ failure (McCormick et al., 2001). TSS was first associated with tampon usage in menstruating women in the 1980s (Herzer, 2001; Issa and Thompson, 2001) and results from the expression of a superantigen, the toxic-shock syndrome toxin 1 (TSST-1), which elicits a strong inflammatory response in the human host (Crass and Bergdoll, 1986; Musser et al., 1990; Fraser et al., 2000). Apart from tampon-associated TSS, non-menstrual cases of TSS are common and often associated with proceeding SSTIs (DeVries et al.,

2011; Descloux et al., 2008). Nowadays the incidence of menstrual and non-menstrual associated TSS is comparable with 0.32 incidents per 100,000 total population (DeVries et al., 2011).

S. aureus frequently induces infections of the lower respiratory tract and acute pneumonia with a high morbidity and mortality. In this connection MRSA represents one of the most common causes for healthcare-associated, hospital-acquired as well as ventilator-associated pneumonia (Shorr et al., 2006; Shorr et al., 2010; Kollef et al., 2005; Rubinstein et al., 2008).

2.2 Virulence factors of *S. aureus*

The human host possesses several lines of defence against invading pathogens ranging from coagulation of blood, the production of antimicrobial peptides, the complement system to phagocytic cells efficiently killing intruding bacteria. In order to overcome the host defence and to successfully establish an infection in the host, *S. aureus* expresses a plethora of virulence factors (Fig. 2.3). These virulence factors can be generally classified into two groups: surface-associated factors including adhesins and secreted proteins including toxins and immuno-modulatory proteins.

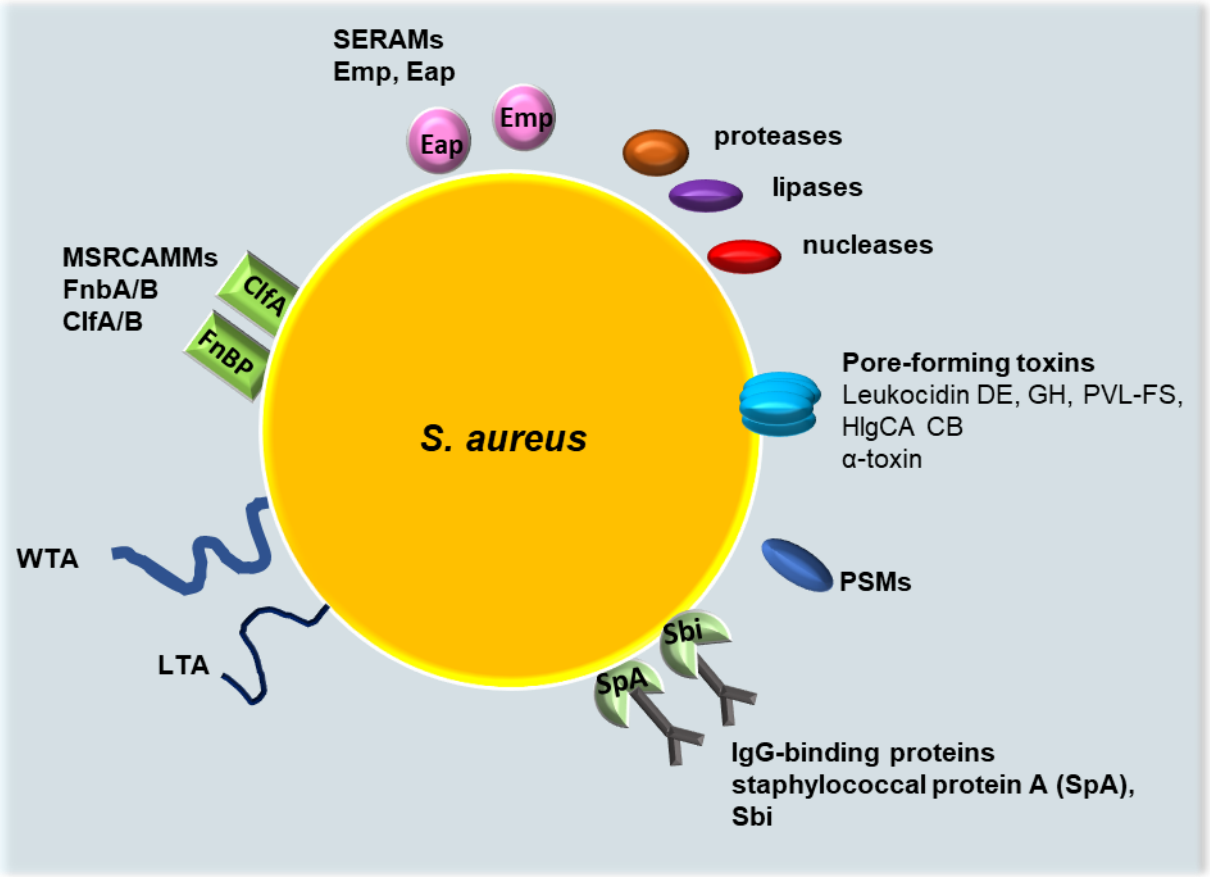

Figure 2.3: Graphical overview of virulence factors. Depicted are selected cell-surface associated and secreted staphylococcal virulence factors. Figure adapted from Choi et al., 2014 and Lowy, 1998.

2.2.1 Surface-associated virulence factors

As representative for gram-positive bacteria the cell wall of *S. aureus* consists of a peptidoglycan multi-layer. In *S. aureus* the peptidoglycan strands are further characteristically cross-linked by a pentaglycine bridge (Ghuysen and Strominger, 1963). The cell surface of *S. aureus* is highly decorated with proteins and glycopolymers mediating the attachment to host cells and non-organic surfaces and the evasion of the host immune system (Mempel et al., 1998; Foster and McDevitt, 1994; Foster et al., 2014). Those surface-associated virulence factors of *S. aureus* are either covalently linked to the cell wall or interact with it via hydrophobic or ionic bonds (reviewed in Heilmann, 2011).

2.2.1.1 Teichoic acids

S. aureus produces two types of teichoic acids which are either covalently linked to the peptidoglycan layer (wall teichoic acids, WTA) or to the lipid bilayer of the cytoplasm membrane (lipoteichoic acid, LTA) (Xia et al., 2010). Staphylococcal teichoic acids consist of repetitive polyol-phosphate subunits that are linked by phosphodiester bonds. While the expression of LTA has been linked to various phenotypes in *S. aureus* such as bacterial growth and cell division (Gründling and Schneewind, 2007), biofilm formation and penetration of the blood-brain barrier in the host (Fedtke et al., 2007; Sheen et al., 2010), the expression of WTA instead is associated with adherence to nasal epithelial cells and nasal colonization (Weidenmaier et al., 2012). Further roles for WTA and LTA in *S. aureus* constitute the protection against cell damage caused by various stressors (Peschel et al., 1999; Peschel et al., 2000; Hoover and Gray, 1977; reviewed in Xia et al., 2010) and the mediation of receptor interactions (Greenberg et al., 1996; Dunne et al., 1994; reviewed in Xia et al., 2010).

2.2.1.2 Microbial surface components recognizing adhesive matrix molecules (MSCRAMMs)

S. aureus expresses a variety of cell-wall anchored proteins that aid in interaction with extracellular matrix components of the host and thus are crucial for colonization (Foster and Hook, 1998). These proteins belong to the family of microbial surface components recognizing adhesive matrix molecules (MSCRAMMs) and are exported via a sortase-mediated mechanism and attached to the cell wall via an LPXTG-motif (reviewed in Marraffini et al., 2006). Examples for MSCRAMMS in *S. aureus* are protein A (SpA), Fibronectin-binding proteins, (FnBPs) and Clumping factors (Clf) (Foster and Hook, 1998). Despite mediating the binding to host matrix components such as fibronectin, fibrinogen and collagen, MSCRAMMs play a crucial role for evading the host immune system and the establishment of infections especially endovascular, bone and orthopaedic or prosthetic device-associated infections (Darouiche et al., 1997; Hudson et al., 1999).

The MSCRAMM Staphylococcal protein A (SpA) mediates the attachment to the host protein von Willebrand factor (Hartleib et al., 2000) and binds to the Fc domain of human immunoglobulin G (IgG)

and the Fab domains of immunoglobulin M (IgM), thereby inhibiting opsonisation by host immunoglobulins and the subsequent phagocytosis by immune cells (Forsgren and Nordstrom, 1974; Cedergren et al., 1993). SpA has been associated with various infection manifestations especially skin lesions (Patel et al., 1987) and inflammation of airway epithelia cells (Gomez et al., 2004). Moreover, protein A was reported to activate host RhoA-GTPases, thus influencing cellular trafficking and facilitating invasion of *S. aureus* via a zipper-like mechanism (Soong et al., 2011).

S. aureus expresses two Clumping factors (ClfA, ClfB) implicated in attachment to fibrinogen, plasma clots and non-organic material (Deivanayagam et al., 2002; McDevitt et al., 1995; Ganesh et al., 2011; reviewed in Foster et al., 2014). While ClfA further mediates the binding to human platelets and was associated with endocarditis in a rat infection model (Siboo et al., 2001; George et al., 2006; Shinji et al., 2011; Que et al., 2005; Veloso et al., 2013), ClfB was shown to mediate the attachment to human type 1 cytokeratin 10 and cell clumping in the presence of soluble fibrinogen (Walsh et al., 2004; O´Brien et al., 2002). Since both Clumping factors were demonstrated to recognize different parts of fibrinogen it was hypothesized that they could act in synergy to promote a firm attachment to thrombi under the harsh conditions faced in the bloodstream of the eukaryotic host (Entenza et al., 2000; Kerrigan et al., 2008; reviewed in Foster et al., 2014).

S. aureus expresses two distinct fibronectin-binding proteins (FnbA, FnbB), which are crucial for the invasion of non-phagocytic host cells. The fibronectin-binding proteins bind to the N-terminal domain of fibronectin, an abundant extracellular matrix protein of host cells (Keane et al., 2007; Burke et al., 2011), thereby bridging host integrin molecules, which allows the subsequent invasion via a zipper-like mechanism (Peacock et al., 1999; Sinha et al., 2000; see section 2.3.1). Apart from mediating invasion FnbPs have been associated with platelet aggregation (Heilmann et al., 2004), eliciting pro-inflammatory responses in the host (Palmqvist et al., 2005), virulence in an experimental endocarditis model (Que et al., 2005) and biofilm formation (O´Neill et al., 2008). Biofilms constitute sessile microbial communities, which are attached to a surface and embedded in a matrix consisting of microbial cells, water, proteins, DNA, polysaccharides and nutrients. The formation of a bacterial biofilm is executed in three different stages including the initial attachment, the maturation of the biofilm and the eventual dispersal (Archer et al., 2011; Costerton et al., 1995). The expression of various surface-adhesive proteins such as the above-mentioned fibronectin binding proteins plays a crucial role for the initial stage of biofilm formation by mediating the adherence to non-organic surfaces (O´Neill et al., 2008; Zapotoczna et al., 2015). The adherence to and formation of biofilms on non-organic surfaces such as medical devices and orthopaedic implants, depicts a major problem in hospital settings promoting various disease manifestations (Archer et al., 2011; Costerton et al., 1999; Stewart and Costerton, 2001; Reffuveille et al., 2017). Bacteria residing in biofilms are largely protected from the impact of antimicrobial substances and components of the host immune system (Ferran et

al., 2016; Scherr et al., 2014). Staphylococcal biofilms thus not only promote infections but further impair the treatment of such infection manifestations.

2.2.1.3 Secretable expanded repertoire adhesive molecules (SERAMs)

Besides MSCRAMMs, which are covalently linked to the cell wall *S. aureus* further expresses surface-associated virulence factors that are linked to the cell envelope via hydrophobic or ionic bonds and can subsequently dissociate from the cell wall. These factors are referred to as secretable expanded repertoire adhesive molecules (SERAMs) and include proteins such as the von Willebrand-factor binding protein (vWbp), the extracellular fibrinogen binding protein (Efb), the staphylocoagulase (Coa), the extracellular adherence protein (Eap) and the extracellular matrix binding protein (Emp). Apart from attachment to surfaces SERAMs have been reported to play a role in the interference with the host immune system and other host defence mechanisms (Chavakis et al., 2005; Chavakis et al., 2002). Both vWbp and staphylocoagulase activate human prothrombin resulting in blood coagulation and formation of fibrin cables (Friedrich et al., 2003; Thomer et al., 2013; Kroh et al., 2009; Hendrix et al., 1983) thereby promoting the establishment of infections such as sepsis, endocarditis and abscess formation which has been demonstrated in various experimental infection models (Cheng et al., 2010; McAdow et al., 2011; Panizzi et al., 2011).

The extracellular fibrinogen binding protein (Efb) instead triggers the accumulation of fibrinogen on the bacterial cell surface resulting in a capsule-like protective barrier against phagocytosis by host immune cells (Ko et al., 2013). Efb was further demonstrated to prevent aggregation of platelets thereby contributing to staphylococcal virulence by inhibiting the wound healing process and prolonging the bleeding time in an experimental murine wound infection model (Shannon and Flock, 2004; Shannon et al., 2005).

The extracellular adherence protein Eap exhibits a diverse role for staphylococcal virulence facilitating bacterial aggregation (Palma et al., 1999), invasion into host cells (Hussain et al., 2002, Haggar et al., 2003), wound healing and angiogenesis (Athanasopoulos et al., 2006) as well as leukocyte recruitment (Chavakis et al., 2002, Lee et al., 2002, Xie et al., 2006). Expression of Eap was further shown to enhance disease severity in a bacteraemia model (Edwards et al., 2012). The complex function of Eap is thought to be executed via formation of protein-protein interactions with various ligands such as host plasma and extracellular matrix molecules (Hussain et al., 2001; Palma et al., 1999, Boden and Flock, 1992, McGavin et al., 1993), interaction with host surface adhesion molecule ICAM-1 (Chavakis et al., 2002) and by rebinding of Eap to the staphylococcal cell surface-located neutral phosphatase (Flock and Flock, 2001).

The SERAM protein Emp binds to various host extracellular matrix molecules such as fibrinogen, fibronectin, vitronectin and collagen (Geraci et al., 2017) thereby executing a versatile role regarding

staphylococcal virulence. Emp was demonstrated to interfere with abscess formation and persistence in host tissue by promoting staphylococcal accumulation (Cheng et al., 2009). Expression of Emp was further shown to promote biofilm formation under low-iron conditions (Johnson et al., 2008) and was found enhanced in *S. aureus* osteomyelitis isolates (Kalinka et al., 2014).

2.2.2 Secreted virulence factors

S. aureus secretes a wide array of small peptides, exotoxins and immuno-modulatory proteins to establish infections, inducing cytotoxicity, evading the host immune system and to survive inside the host.

2.2.2.1 Pore-forming toxins

Pore-forming toxins constitute a class of specific lipid-binding proteins, which disrupt the cellular integrity via formation of membranous pores. *S. aureus* expresses and secretes a variety of such pore-forming toxins targeting several different host cell types.

The water-soluble, β-barrel structured staphylococcal α-toxin is one of the best-studied pore-forming toxins. α-toxin targets various cell types including epithelial and endothelial cells, fibroblasts and immune cells such as lymphocytes, macrophages and monocytes and exhibits cytolytic as well as dermonecrotic properties (Bhakdi et al., 1989; Bhakdi and Tranum-Jensen, 1991; Walev et al., 1994). α-toxin, also known as α-haemolysin, further features haemolytic properties characterized by the release of haeme from ruptured erythrocytes (Cassidy and Harshman, 1976; Cooper et al., 1964; Freer et al., 1973; Bhakdi and Tranum-Jensen, 1991). This α-toxin-mediated erythrocyte lysis is represented by characteristic clearance zones around the staphylococcal colonies on sheep or rabbit blood agar. α-toxin is secreted as 33 kDa hydrophilic single chain monomers (Bhakdi and Tranum-Jensen, 1991). At low dosages of α-toxin a receptor-mediated contact with the host membrane triggers oligomerization of α-toxin monomers leading to formation of homo-heptameric pre-pores (Walker et al., 1992; Valeva et al., 1995; Valeva et al., 2001). The high affinity receptor involved in this process was identified to be A Disintegrin And Metalloprotease 10 (ADAM10), which is expressed on various eukaryotic cell types (Wilke and Bubeck Wardenburg, 2010). A subsequent conformational change of the pre-pore and the insertion of the β-barrel domain into the host cell lipid bilayer results in a heptameric, water-filled trans-membrane pore (Fig. 2.4). With a diameter of approximately 1-2 nm α-toxin trans-membrane pores allow the flow of water, ions such as K^+, ATP and molecules up to a weight of 4 kDa (Menestrina, 1986; Bhakdi and Tranum-Jensen 1991, Song et al., 1996). Low dosages of α-toxin were shown to activate caspases thereby inducing apoptosis (Bantel et al., 2001). Interaction with ADAM10 was further reported to facilitate cleavage of adherence junction protein E-cadherin resulting in a

subsequent disruption of epithelial barrier function promoting pathogenesis in a lung infection model (Inoshima et al., 2011). In contrast, when α-toxin is present in high concentrations (>6 µg/ml) it adsorbs non-specifically to the host cell membrane. This triggers the formation of larger pores resulting in a massive influx of extra-cellular Ca^{2+} promoting necrotic cell death (Essmann et al., 2003, Suttorp and Habben, 1988). Apart from α-toxin, *S. aureus* expresses another toxin with haemolytic properties, the neutral sphingomyelinase (SMase), β-toxin. β-toxin is further known as the "hot-cold" haemolysin since apart from binding to erythrocytes at 37°C, lysis is only triggered after exposure to a cold shock (Smyth et al., 1975). Due to insertion of a prophage (ϕSa3mw) into the *hlb* gene β-toxin is not expressed by a variety of *S. aureus* strains (Coleman et al., 1991).

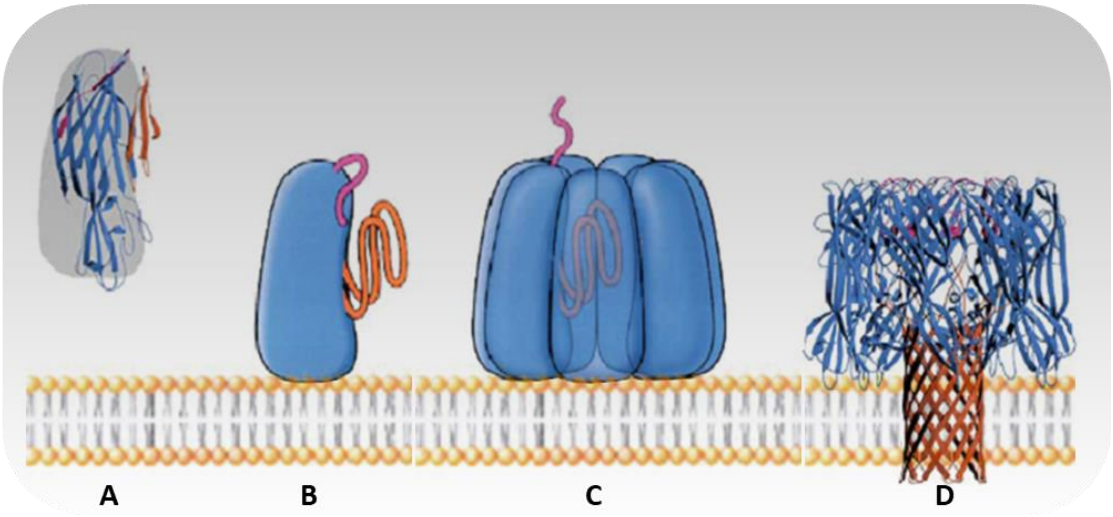

Figure 2.4: Graphical illustration of the oligomerization of α-toxin monomers and formation of β-barrel pores. α-toxin is secreted as 33 kDa hydrophilic single chain monomers (**A**) which upon receptor-mediated contact with the host membrane (**B**) oligomerize resulting in formation of a homo-heptameric pre-pore (**C**). Formation of the pre-pore is followed by a subsequent conformational change and insertion of the β-barrel domain into the host cell lipid bilayer resulting in a heptameric, water-filled trans-membrane pore (**D**). Figure modified after Montoya and Gouaux, 2003.

Leukocidins are a family of bi-component toxins consisting of the two different subunits S (slow eluting) and F (fast eluting) that together induce formation of cation selective pores in the plasma membrane of host immune cells (Finck-Barbancon et al., 1991). Cation flux through the leukocidin-induced pores results in osmotic imbalance subsequently leading to cell death (Menestrina et al., 2003). Seven leukocidins have been identified so far in *S. aureus*: HlgAB, HlgCB, LukAB/HG (Ventura et al., 2010), LukED (Gravet et al., 1998), Panton-Valentine leukocidine (LukSF-PV/PVL; Panton and Valentine, 1932), LukMF (Barrio et al., 2006) and LuKPQ (Koop et al., 2017), among which the latter two are exclusively found in zoonotic *S. aureus* strains (Koop et al., 2017). HlgAB, HlgCB and LukAB/HG are encoded in the core genome of *S. aureus* and thus conserved among all *S. aureus* strains. LukED is encoded on the

common pathogenicity island (vSaβ) (Baba et al., 2002), whereas Panton-Valentine leukocidine, LukMF and LukPQ are encoded on prophages (Zou et al., 2000; Koop et al., 2017). Leukocidins target host cells of both innate and adaptive immunity such as leukocytes, natural killer cells, T-lymphocytes and dendritic cells (DuMont et al., 2011; Alonzo et al., 2012; Alonzo et al., 2013; Alonzo and Torres, 2014) and were found to be crucial for the survival of *S. aureus* by mediating killing of host immune cells and promoting immune evasion. Leukocidins were further shown to be vital during the establishment and for the dissemination of staphylococcal infections (Yoong and Torres 2013, Alonzo and Torres 2014). HlgAB and HlgCB are further able to lyse erythrocytes and are thus often referred to as γ-haemolysin (Prévost et al., 1995). Expression of PVL is characteristic for highly cytotoxic and clinically relevant isolates and is associated with abscess formation and severe forms of necrotizing pneumonia (Gillet et al., 2002).

Leukocidins only exhibit their cytolytic properties after self-assembly of the water-soluble components on host cell surfaces and subsequent pore-formation (Vandenesch et al., 2012). For this, each polypeptide subunit first binds as a monomer to the cell surface. This step is followed by oligomerization of each four molecules of S and F polypeptides resulting in an alternating arrangement of F and S subunits into a hetero-octamer β-barrel pore (Olson et al., 1999; Menestrina et al., 2001). Formation of the β-barrel pore provokes ion fluxes through the cell membrane and extrusion of cellular contents resulting in osmotic imbalance and subsequent host cell death (Menestrina et al., 2001; Alonzo and Torres, 2014).

Phenol soluble modulins (PSMs) constitute a family of small alpha-helical, amphipathic membrane active peptides ranging from 20-44 amino acids in length and are found in several staphylococcal species (Peschel and Otto, 2013). PSMs were first identified in the phenol-soluble fraction of *S. epidermidis* culture supernatants after hot phenol extraction (Mehlin et al., 1999). PSMs exhibit both cytolytic and biosurfactant properties (Wang et al., 2007) and were reported to activate neutrophils (Kretschmer et al., 2010) and induce allergic skin reactions (Nakamura et al., 2013). Further, a crucial role for PSMs in bacterial escape from phagolysosomes of host cells into the host cytoplasm was demonstrated (Grosz et al., 2014). Their ability to interfere with host cell membranes independent of a specific receptor accounts to their large activity spectrum. PSMs target a large subset of host cell ranging from osteoblasts to a variety of human immune cells such as erythrocytes, monocytes and neutrophils (Wang et al., 2007, Cheung et al., 2012, Cassat et al., 2013). PSMs play a crucial role for many different manifestations of *S. aureus* infections such as SSTIs (Wang et al., 2007) by promoting abscess formation in murine infection models, atopic dermatitis (Nakamura et al., 2013) and osteomyelitis (Cassat et al., 2013). At least 8 PSMs are expressed in *S. aureus* which differ in their size. PSMα and PSMβ are encoded on the core genome from three different genetic locations and

contribute to the success of community-acquired staphylococcal isolates (Wang et al., 2007). δ-toxin is encoded within the regulatory RNA RNAIII (Janzon et al., 1989). The only PSM not encoded on the core genome is PSM-mec, which is encoded on the staphylococcal chromosome cassette SCCmec and is thus only present in a subset of *S. aureus* isolates (Queck et al., 2009). With only 20-25 amino acids in length α-type PSMs (PSMα 1-4), δ-toxin and PMS-mec are about half the size of β-type PSMs (PSMβ 1-2), which consists of approximately 44 amino acids (Cheung et al., 2014). PSMs are exported into the culture supernatant via a four-component system transporter (phenol-soluble modulin transporter, Pmt) whose functionality is crucial for self-protection against the highly cytolytic PSMs, which otherwise would accumulate in the bacterial cytosol resulting in damage of the cell membrane, abnormal cell division culminating in severe growth defects. Besides conferring self-resistance against PSMs expression of Pmt was further shown to grant resistance against non-self PSMs (Chatterjee et al., 2013).

2.2.2.2 Immune evasion proteins

In order to evade the host immune system *S. aureus* established different strategies enabling the establishment of infection and disease progression. Disinfection by host immune cells is prevented by expression of various immune evasion proteins such as the chemotaxis-inhibitory protein (CHIPS), staphopain A (ScpA), which inhibit neutrophil communication and chemotaxis. A further defence mechanism is represented by lysis of immune cells by the action of various toxins as described in chapter 2.2.3.1, and inhibition of opsonisation by proteins such as SpA as described in chapter 2.2.1.2.

CHIPS is a secreted protein binding to host formyl peptide receptors (FPRs) thereby inhibiting the recruitment of phagocytes such as neutrophils and monocytes by blocking the interaction of those receptors with their natural ligands (de Haas et al., 2004; Postma et al., 2004). The gene encoding CHIPS (*chs*), together with staphylococcal complement inhibitor (SCIN), staphylokinase (SAK) and enterotoxin A or P (SEA, SEP) is encoded on the β-haemolysin converting-bacteriophage (van Wamel et al., 2006). With SAK inhibiting neutrophil defensins (Jin et al., 2004) and the superantigens SEA and SEP inhibiting phagocyte function (Xu et al., 2014, Lei et al., 2001, Hopkins et al., 2005) this mobile genetic element constitutes a so-called immune evasion cluster (IEC).

ScpA was likewise shown to inhibit neutrophil chemotaxis. In contrast to CHIPS the chemotaxis inhibitory function of ScpA is mediated via cleavage of the N-terminal region of chemokine receptor CVCR2 thereby blocking signal transduction by chemokines such as IL-8 and GROα (Laarman et al., 2012).

2.2.3 Iron acquisition

Iron is an important cofactor for diverse biochemical reactions and therefore essential for growth of bacteria. As a part of defence against invading pathogens, vertebrate hosts sequester iron within proteins, such as transferrin and lactoferrin, thereby limiting free iron. Pathogenic bacteria therefore established several iron acquisition mechanisms (Weinberg, 1978) to overcome the iron limitation.

One mechanism of iron acquisition established by bacteria is the expression of siderophores, small secreted molecules characterized by a high affinity towards iron (Saha et al., 2013). *S. aureus* expresses two of such iron-chelators (staphylofferin A and B), which both were demonstrated to be crucial for survival of *S. aureus* in serum (Beasley et al., 2009). The import of iron bound to staphyloferrin A is mediated via the lipoprotein HtsA and the permease HtsBC (Beasley et al., 2009) whereas transport of staphyloferrin B across the cytoplasma membrane is executed via lipoprotein SirA and permease SirBC (Dale et al., 2004, reviewed in Hammer and Skaar, 2011).

Besides chelated by proteins such as lactoferrin and transferrin the primary source of iron within the vertebrate host constitutes haeme. Using isotope labelling haeme-iron was identified as the preferential iron source of *S. aureus* during the course of infection (Skaar et al., 2004a). The most abundant haemoprotein represents haemoglobin which can be, upon lysis of erythrocytes, liberated and used as an iron source (Pishchany et al., 2013). For this, *S. aureus* expresses a variety of so-called haemolysins, erythrocyte lysing proteins (see chapter 2.2.2.1). Enabling the transport of haeme *S. aureus* expresses the iron-regulated surface determinant system (Isd), which is encoded by five different operons (*isd*A, *isd*B, *isd*CDEF*srt*B*isd*G, *isd*H and *isd*I) (Hammer and Skaar, 2011). The haeme transport apparatus constitutes of the proteins IsdA, IsdB and IsdH, that are anchored via a Sortase A-dependent mechanism to the cell-wall of *S. aureus*, IsdC which is embedded into the cell wall by SrtB and IsdDEF constituting a membrane-localized ABC-transporter (Mazmanian et al., 2003). IsdA, IsdB, IsdH and IsdC have been shown to bind haeme via an N-terminal NEAr iron transporter (NEAT) motif (Grigg et al., 2007) thereby triggering the passage of haeme across the cell wall to the haeme-receptor lipoprotein IsdE. The transport across the cytoplasm membrane is mediated by IsdF and energised by the ATP-hydrolysing activity of IsdD (Grigg et al., 2007; Liu et al., 2008; Muryoi et al., 2008). Upon reaching the cytoplasm, haeme is degraded by IsdG and IsdI resulting in release of iron and production of staphylobilin (Reniere et al., 2010; Skaar et al., 2004b). Besides acquisition of iron Isd proteins were associated with resistance to innate host defence represented by neutrophil derived-H_2O_2 (Palazzolo-Ballance et al., 2008). IsdA was further shown to be crucial for resistance against bactericidal human skin fatty acids and peptides thereby enabling survival on and colonizing of human skin (Clarke et al., 2007).

2.3 Intracellular virulence and persistence of *S. aureus*

2.3.1 Adhesion

Although previously considered an exclusive extracellular pathogen *S. aureus* was recently shown to be able to invade a variety of non-professional phagocytes ranging from epithelial and endothelial cells, fibroblasts to osteoblasts (Strobel et al., 2016; Jevon et al., 1999; Lammers et al., 1999; Dziewanowska et al., 1999; Peacock et al., 1999; Kintarak et al., 2004; Fraunholz and Sinha, 2012). As a prerequisite for invasion, the adhesion of *S. aureus* to matrix molecules of host cells is mediated by the combined action of the expressed surface adhesive molecules (MSCRAMM; SERAM; see section 2.2.1). Adhesion of *S. aureus* to host cells is mainly mediated via the fibronectin binding proteins (FnbPs) (Edwards et al., 2010). Binding of the C-terminal fibronectin-binding motifs of FnbA or FnbB to the N-terminal F1 domain of the host molecule fibronectin triggers a zipper-like invasion mechanism (Foster et al., 2014). Fibronectin in turn binds the host receptor α5β1 integrin (Huveneers et al., 2008) thereby bridging bacterial FnbPs and host integrin (Sinha et al., 1999). One FnbP molecule can simultaneously bind 6-9 fibronectin molecules (Bingham et al., 2008) which subsequently results in clustering of host receptor α5β1 integrin molecules at the adherence site (Josse et al., 2017; Schwarz-Linek et al., 2004; Schwarz-Linek et al., 2003). This in turn triggers Src kinase-mediated rearrangement of host cytoskeleton resulting in invasion of *S. aureus* (Agerer et al., 2003).

2.3.2 Intracellular fate of *S. aureus*

The fate of *S. aureus* inside the infected host cells is dependent on the staphylococcal strain or isolate and the expressed genes and virulence determinants as well as on the host cell type and their susceptibilities towards staphylococcal virulence factors (Strobel et al., 2016). Upon invasion *S. aureus* thrives in an endosomal vesicle (Fig. 2.5), which will undergo a subsequent maturation process involving various fusion events resulting in the formation of a lysosome (Desjardins et al., 1994; Fairn and Grinstein, 2012). The lysosomal formation includes acidification of the endosomal vesicle and the accumulation of reactive oxygen and nitrogen species as well as hydrolases which eventually leads to degradation of the endosomal content (Fairn and Grinstein, 2012). In order to avoid degradation, a variety of bacteria established different mechanism to escape the endosomal vesicle (Gaillard et al., 1987; Clemens et al., 2004; Sansonetti et al., 1986). In *S. aureus* this process is referred to as phagosomal escape and was first described in 1998 for bovine mastitis isolates which escaped from endosomes of MAC-T cells. The escape from the endosomal compartment was followed by induction of host cell death (Bayles et al., 1998). However, phagsomal escape was reported to occur at rather late time points during infection (~2.5 h) and to proceed replication and subsequent host cell death (Grosz et al., 2014).

Initially phagosomal escape was attributed to the pore-forming action of α-toxin since *agr* expression was found to be increased in bacteria residing in phagosomes (Grosz et al., 2014) and mutants in *agr* were not capable of escaping the phagosome (Blättner et al., 2016; Münzenmayer et al., 2016; Shompole et al., 2003). However, in epithelial cells α-toxin was not required for phagosomal escape (Giese et al., 2009), whereas overexpression of both β-toxin and the phenol soluble modulin δ-toxin indicated a synergistic role in triggering phagosomal escape (Giese et al., 2011). In contrast another agr-regulated factor, the cytolytic phenol soluble modulin PSMα has been identified as a vital factor contributing to phagsosomal escape (Grosz et al., 2014). Further, only recently, a crucial role for a non-ribosomal peptide synthetase (NRPS) in eliciting phagosomal escape has been identified (Blättner et al., 2016). Upon escape from the phagosome, a prerequisite for proliferation, *S. aureus* triggers host cell death either via apoptotic or necrotic pathways (Grosz et al., 2014; Bayles et al., 1998; reviewed in Horn et al., 2018a; Fraunholz and Sinha, 2012), which involves the coordinated action of various cytotoxins (see chapter 2.3.2).

The most frequent form of cell death observed in *S. aureus* infected cells represents the caspase-mediated programmed cell death, apoptosis (Menzies and Kourteva, 2000; Bayles et al., 1998; Haslinger-Löffler et al., 2005; Haslinger et al., 2003; Genestier et al., 2005). Induction of apoptosis during *S. aureus* infection was associated with the regulatory action of agr and the alternative sigma-factor σB (Haslinger-Löffler et al., 2005; Wesson et al., 1998). As an agr-regulated factor, the pore-forming α-toxin was identified to activate caspases thereby triggering the apoptotic pathway (Haslinger et al., 2003; Bantel et al., 2001; Essmann et al., 2003). In contrast, however, high dosages of α-toxin triggered necrosis, which was accompanied by release of cytokines in the same studies (Haslinger et al., 2003; Bantel et al., 2001; Essmann et al., 2003).

Despite escaping the phagolysosome, *S. aureus* has been reported to reside inside phagocytes or endothelial cells for extended periods (Hamill et al., 1986; Kubica et al., 2008; Tuchscherr et al., 2011). Prolonged intracellular residence has been associated with chronic staphylococcal infections (Plouin-Gaudon et al., 2006; Proctor et al., 1995). This so-called persistency is most often accompanied by a small colony phenotype (SCV), which displays a metabolically steady phenotype characterized by a much slower growth rate and a higher resistance towards different antibiotic compounds (Proctor et al., 1994; Proctor et al., 1995; Proctor et al., 2006; Sendi and Proctor, 2009). SCVs further bypass the activation of the host immune system (Tuchscherr et al., 2010; Tuchscherr et al., 2011). SCVs are characterized by changes in the transcriptome and proteome (Garzoni et al., 2007; Kriegeskorte et al., 2011), are most often non-haemolytic and non-pigmented and display a thick cell wall (Bulger and Bulger, 1967; Proctor et al., 1994). In many cases SCV possess reversible auxothrophies regarding oxidative phosphorylation and heme biosysnthesis as well as alterations in electron transport due to

mutations in menadione and hemin biosynthesis genes (Proctor et al., 1994; Proctor et al., 2006). Further mutants in *agr* and *sar*A are often found in persistent *S. aureus*-induced infections. Such mutants are characterized by an enhanced expression of σB indicating the involvement of this alternative sigma-factor in SCV formation and adaption to host environments (Tuchscherr et al., 2015). The harsh intracellular conditions are thought to select for SCV phenotypes (Vesga et al., 1996), since small colony variants display higher resistance against ROS (Painter et al., 2015) and can thus withstand host defence mechanisms (Kahl et al., 1998; Proctor et al., 1995). Recently it was demonstrated that during infection a high amount of the initial inoculum can switch to the stress-resistant SCV phenotype (Tuchscherr et al., 2011). Hence, SCV formation represents a potential intracellular reservoir for reoccurring infections (Kipp et al., 2003; Proctor et al., 1995; Proctor et al., 2006; Schröder et al., 2006).

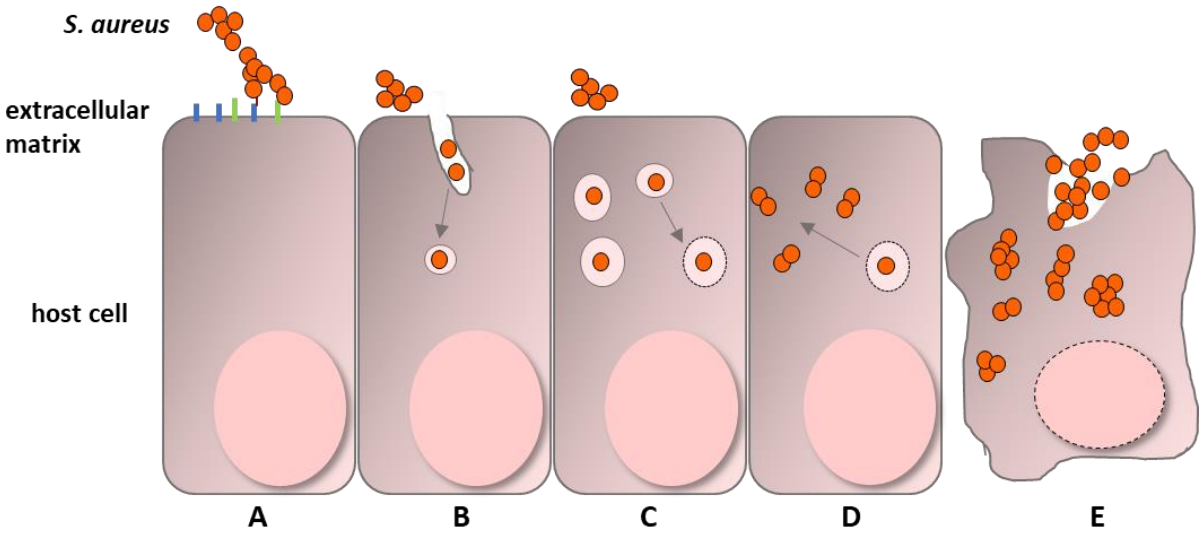

Figure 2.5: Schematic representation of the intracellular fate of *S. aureus* in host cells. *S. aureus* binds to components of the host extracellular matrix (**A**), which triggers internalization via a zipper-like mechanism (**B**). *S. aureus* resides in phagosomes inside the host cells from which it can escape via a mechanism called phagosomal escape (**C**). Once escaped from the phagosome *S. aureus* replicates inside the cytoplasm (**D**) and subsequently induces the death of the host cell (**E**). Adapted from Horn et al., 2018a.

2.4 Regulation of virulence

The ability to cause a plethora of different infection manifestations is dependent on both the virulence factors and the coordination of their expression during infection. The expression of staphylococcal virulence factors is governed by a vast array of regulators, including two-component systems, alternative sigma-factors, accessory DNA-binding proteins as well as non-coding RNAs.

2.4.1 Two-component systems

2.4.1.1 The agr quorum-sensing system

A major virulence regulatory element in *S. aureus* is the well-studied agr quorum-sensing system, which constitutes an extended two-component system with sensor histidine kinase AgrC and the DNA-binding response regulator AgrA (reviewed in Junecko et al., 2012; Novick, 2003, Ji et al., 1995). Kinase AgrC senses the extracellular concentration of an octapeptide, AIP (auto-inducing peptide), which is encoded by *agr*D as a precursor peptide. This precursor peptide is secreted and modified by a further component of the agr quorum-sensing system, AgrB (Zhang and Ji, 2004; Thoendel and Horswill, 2009). Upon perceiving high extracellular concentrations of AIP, which can either result from high bacterial density or a limitation of available space, as found in a phagosome, AgrC auto-phosphorylates (Ji et al., 1995; Lina et al., 1998). Thus, the agr system constitutes both a quorum-sensing and a diffusion-sensing system (Shompole et al., 2003) illustrating its important role for both extracellular and intracellular Staphylococci. Autophosphorylation of AgrC subsequently triggers the transfer of a phosphate group to the response regulator AgrA (Fig. 2.6). The *agr* locus encompasses two divergent transcriptional units whose transcription is driven from two divergent promoters, P2 and P3. Phosphorylation of AgrA facilitates the binding to these two *agr* promotor regions thereby enhancing transcription of both transcriptional units (Novick, 2003, Koenig et al., 2004). Binding to the P2 promotor region, which drives transcription of RNAII, encoding the components of the *agr* quorum-sensing system (*agr*BDCA), provokes a positive feedback loop (Novick et al., 1995). Instead, binding of AgrA-P to P3 enhances transcription of RNAIII, a 514 nt long non-coding regulatory RNA, which constitutes the major effector of the agr quorum-sensing system (Novick et al., 1993; Queck et al., 2008). RNAIII comprises a short open reading frame (ORF) encoding the PSM δ-toxin (Janzon et al., 1989; Janzon and Arvidson, 1990, see section 2.2.3.1).

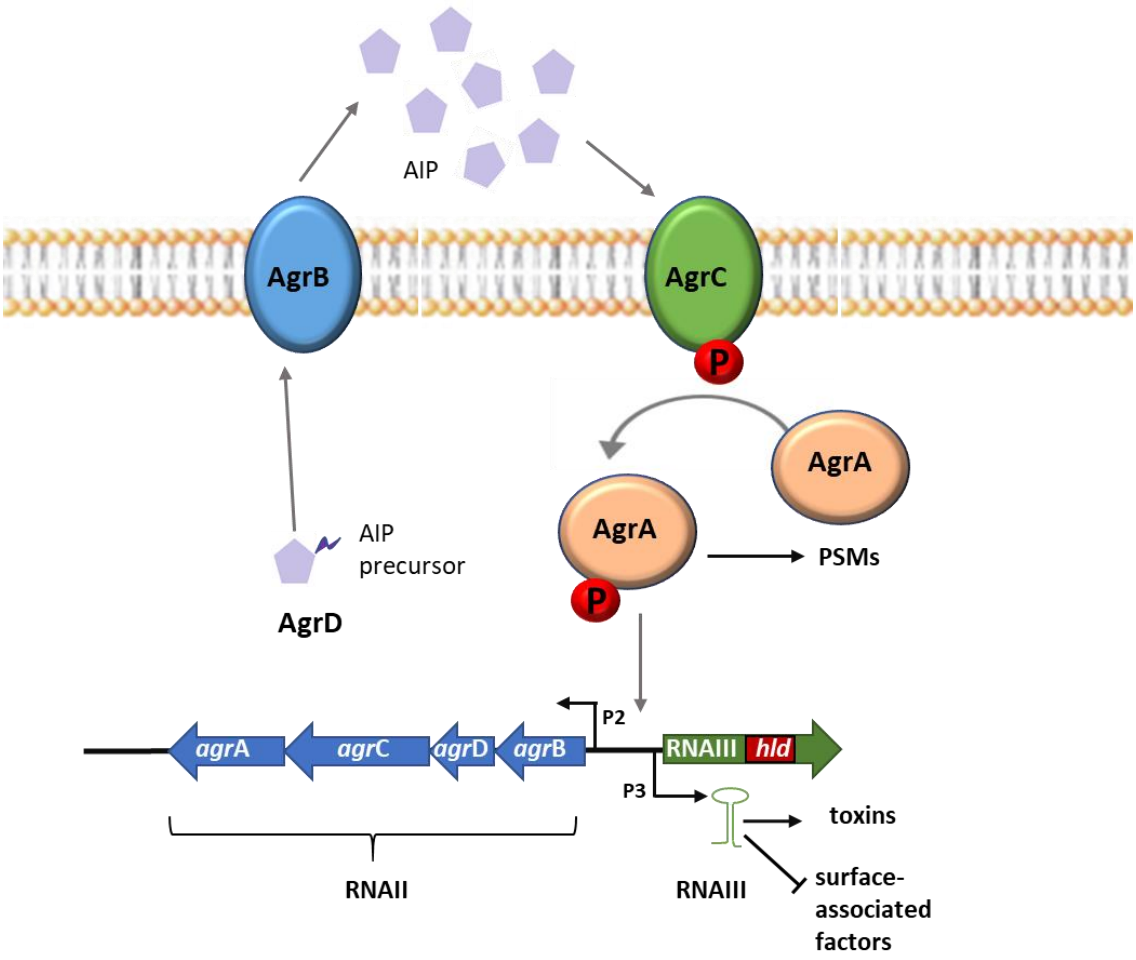

Figure 2.6: Schematic representation of the *S. aureus* accessory gene regulator. Expression of the *agr* operon is driven by two divergent promotors, P2 and P3, which control the expression of the two transcripts RNAII and RNAIII. AgrD constitutes the AIP precursor peptide which is secreted and modified by the transmembrane protein AgrB. Upon sensing high AIP concentrations kinase AgrC gets autophosphorylated and subsequently transfers a phosphate group to response regulator AgrA. Phosphorylated AgrA binds to the promotor of the *agr* operon thereby initiating a feedback loop and activating the expression of various toxins such as the phenol soluble modulins. Further target genes are regulated by RNAIII. Figure adapted from Painter et al., 2014.

The agr quorum-sensing system was reported to both directly as well as indirectly regulate 174 genes among which 90 genes were found to be regulated in a RNAIII-independent manner (Queck et al., 2008). Independently of RNAIII, the agr system positively regulates transcription of PSMα1-4 and PSMβ1-2 via direct binding of AgrA-P to the respective promotor region (Queck et al., 2008). The agr regulon further includes a variety of virulence factors associated with immune evasion (e.g. *sp*A, *sbi*), cytotoxicity (e.g. *hla*, *hlb*) and metabolism (e.g. *ure*ABCEF). While the expression of exoproteins and extracellular proteases is induced by the agr system, the expression of Repressor of toxins (Rot) and immune evasion factors such as SpA and Sbi instead is repressed (Queck et al., 2008, Geisinger et al., 2006; Boisset et al., 2007). Mutations in *agr* are associated with strongly impaired virulence in various infection models including pneumonia, endocarditis, osteomyelitis and SSTIs as well as with enhanced biofilm formation (Cheung et al., 1994; Gillaspy et al., 1995; Bubeck Wardenburg et al., 2007; Schwan

et al., 2003; Boles and Horswill, 2008; Beenken et al., 2010) emphasizing the importance of a functional agr quorum-sensing system for establishing various disease manifestations in *S. aureus*.

2.4.1.2 The SaeRS two-component system

Besides agr, a major regulatory system of *S. aureus* is the SaeRS two-component system. Deletion of *sae*RS results in reduced virulence phenotypes similar to those observed in *agr* mutants regarding necrotizing pneumonia and skin infections (Montgomery et al., 2010). Further a role for the SaeRS two-component system in invasion of lung epithelial cells was reported (Liang et al., 2006). Despite the resemblance of virulence phenotypes of both *agr* and *sae*RS mutants the SaeRS system was demonstrated to be epistatic as well as downstream of the agr quorum-sensing system (Montgomery et al., 2010; Novick and Jiang, 2003). The SaeRS two-component system consists of the sensor kinase SaeS and the DNA-binding regulator SaeR and is transcribed from a four gene operon *sae*PQRS from two divergent promotors, P1 and P3 (Steinhuber et al., 2003, Jeong et al., 2011). The *sae* operon further encompasses the auxiliary genes *sae*P and *sae*Q, which encode a lipoprotein and a membrane protein, respectively (Novick and Jiang, 2003), which were demonstrated to be vital for activation of the phosphatase activity of histidine kinase SaeS by forming a ternary complex (Jeong et al., 2012). Promotor *sae* P1 drives transcription of the unstable transcript T1, which comprises the whole four gene operon. T1 is subsequently processed by endoribonuclease RNase Y resulting in the *sae*QRS encoding stable transcript T2 (Geiger et al., 2008; Adhikari and Novick, 2008, Marincola et al., 2012). Transcription initiated at the weaker but constitutively active promotor P3 results in transcript T3 encoding only *sae*RS, which provides basal expression levels of SaeRS sufficient for receiving and responding to correspondent signals (Geiger et al., 2008; Jeong et al., 2011). A fourth transcript (T4) encoding only lipoprotein SaeP is driven by P1 and results either from premature termination or from RNase Y-dependent processing of transcript T1 (Fig. 2.7; Steinhuber et al., 2003; Adhikari and Novick, 2008).

The bifunctional histidine kinase SaeS consists of a kinase, a transmembrane domain and an α-helical region, which is typical for bacterial sensors, the so called HAMP domain. The transmembrane domain comprises two transmembrane helices connected by a nine aa long linker peptide (Liu et al., 2015; Adhikari and Novick, 2008). With 9 aa in length the linker peptide is considered too small to function as a ligand binding domain which is why SaeS is classified as an intermembrane sensing histidine kinase (Mascher, 2014). As a bifunctional histidine kinase, SaeS possesses both a kinase and phosphatase activity (Jeong et al., 2012). The kinase function of SaeS displays a low basal activity which is sufficient for activation of a subset of target genes. Those so-called class II genes contain high affinity binding sites for SaeR-P and include the haemolysins *hla* and *hlb*. Instead, a further subset of target genes, the class I genes, which include *coa*, *eap*, *emp*, *fnb*A, *fib* and *sae*P is characterized by low affinity binding

sites for SaeR-P and hence require activation of the SaeRS two-component system to ensure high levels of SaeR-P for transcriptional activation (Mainiero et al., 2010; Liu et al., 2015).

The SaeRS system was shown to be activated by presence of human neutrophil peptides, calprotectin, H_2O_2, an acidic pH and sub-inhibitory concentrations of β-lactam antibiotics, while 1 M NaCl and presence of silkworm apolipophorin protein inhibited the two-component system (Cho et al., 2015; Geiger et al., 2008; Kuroda et al., 2007; Weinrick et al., 2004). However, the sensing mechanism of those stimuli is not yet understood.

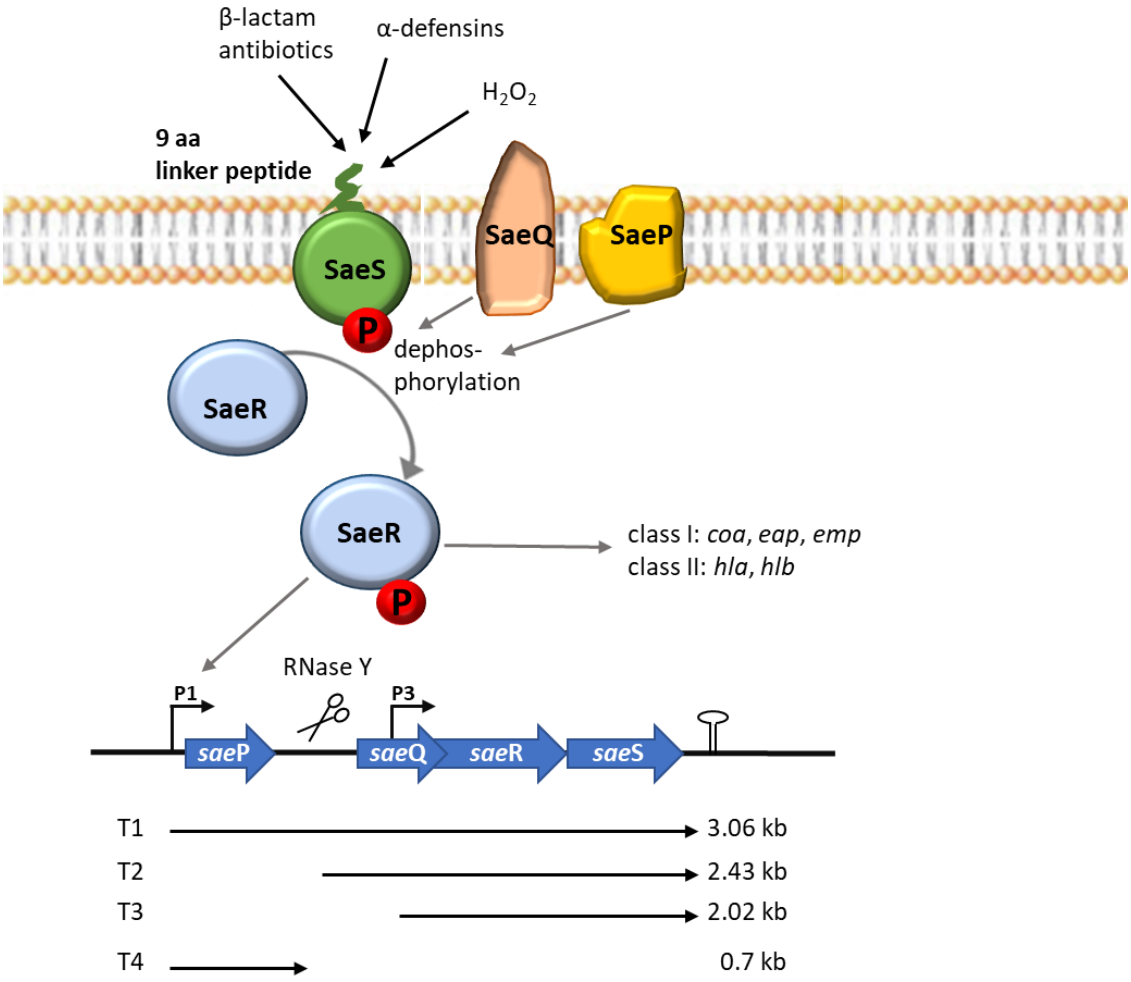

Figure 2.7: Graphical representation of the *S. aureus sae* operon and regulation mechanism by two-component system SaeRS. The *sae* operon constitutes besides *sae*S and *sae*R the two auxiliary genes *sae*P and *sae*Q. Expression of the *sae* operon is driven by two divergent promotors, P1 and P3, which control the expression of four different transcripts. Expression of transcript T1 which encodes the whole *sae* operon is driven by P1 while transcription initiated at P3 results in transcript T3. Transcript T2 instead results from processing of T1 by RNase Y. The smallest of the four transcripts T4 results either from a processing event or premature termination. Different stimuli such as β-lactam antibiotics activate the SaeRS system. Upon sensing differnt stimuli histidine kinase SaeS gets autophosphorylated and subsequently transfers a phosphate group to response regulator SaeR. Phosphorylation activiates the response regulator SaeR which regulates the expression of a variety of target genes that are subdivided into two classes (I and II) according to their affinities towards SaeR-P. The auxiliary proteins SaeQ and SaeP are vital for the phosphatase activity of kinase SaeS. Adapted from Haag and Bagnoli, 2017.

2.4.1.3 Further two-component systems regulating virulence

Further important two-component systems regulating staphylococcal virulence are the ArlRS, VraRS and SrrAB two-component system.

Disruption of the two-component system ArlRS results in an increase in production of secreted virulence factors such as α-toxin, lipases, coagulase, serine proteases and SpA thus resulting in an opposite phenotype compared to mutants in *agr*. ArlRS induces the expression of the transcriptional regulator SarA, which is thought to be responsible for the observed effects on exoprotein production in an *arl*RS mutant (Fournier et al., 2001). Besides SarA, ArlRS was shown to activate the expression of another important regulator, the MarR-type transcriptional regulator, MgrA (Crosby et al., 2016). Regulation of MgrA is thought to account to the clumping defect observed in an *arl*RS mutant (Walker et al., 2013). The two-component system ArlRS was further shown to positively regulate the expression of the agr quorum-sensing system. Regulation was mostly observed in stationary growth phase of *S. aureus* (Liang et al., 2005). Disruption of ArlRS was linked to various virulence phenotypes ranging from endothelial cell damage, endocarditis, haematogenous pyelonephritis and systemic infection (Seidl et al., 2018; Liang et al., 2005; Benton et al., 2004). ArlRS was further identified as one of the key regulators in biofilm formation on implanted catheters thereby contributing to catheter-related infections (Burgui et al., 2018). The importance of ArlRS in infection is further illustrated by its role in reducing the demand for manganese, which is thought to confer resistance against neutrophil-derived calprotectin-induced manganese starvation (Radin et al., 2016). While the signals to which ArlRS is responding remain rather ambiguous, a role for ArlRS in pyruvate-induced expression reprofiling was recently identified (Harper et al., 2018).

The two-component system SrrAB is induced during hypoxia (Kinkel et al., 2013) and was associated with virulence in a murine endocarditis (Pragman et al., 2004) and pyelonephritis model (Throup et al., 2001). SrrAB induces the transcription of both virulence factors and metabolism associated genes involved in cytochrome assembly (*quox*ABCD, *cyd*AB, *hem*ABCX), anaerobic metabolism (*pfl*AB, *adh*E, *nrd*DG), iron-sulfur cluster repair (*scd*A) and NO detoxification (*hmp*) (Kinkel et al., 2013). The regulation of the virulence associated target genes such as *tsst*-1 and *sp*A is executed partly via inhibition of RNAIII expression (Yarwood et al., 2001).

Another two-component system of *S. aureus*, VraRS, was reported to respond to various cell-wall targeting antibiotics such as oxacillin, vancomycin, teicoplanin and d-cycloserine (Gardete et al., 2006; Steidl et al., 2008; Kuroda et al., 2003; Yin et al., 2006) and to play a crucial role in resistance against glycopeptide antibiotics (Galbusera et al., 2011). VraRS regulates the expression of genes associated with cell wall peptidoglycan biosynthesis (*pbp*2, *sgt*B, *mur*Z, *fmt*A, *tca*A/*tca*B) and proteolytic quality control (*sps*A, *ctp*A) but also virulence genes such as *coa*, *sae*RS, *sbi*, *hlg*A, *hlg*B and *hlg*C (Kuroda et al., 2003).

2.4.2 SarA-family of transcriptional regulators

Regulation of virulence in *S. aureus* is further executed by a family of staphylococcal transcriptional regulators (Sar) including the prototypic member SarA, a 124 aa long DNA binding protein (Liu et al., 2006). The SarA-family is a protein family of DNA-binding proteins which exploit Helix-turn-Helix motifs to facilitate DNA-binding and thereby regulate the transcription of virulence associated genes (Cheung et al., 2008). The members of the SarA-family can be subdivided into three classes regarding sequence alignment and secondary structure: single-domain proteins such as SarA, SarR, SarT, SarV, SarX and Rot, double-domain proteins including SarS, SarU and SarY and homologues to the *E.coli* MarR-protein family MgrA and SarZ.

Different possible mechanisms of gene regulation by SarA homologues are proposed. Some Sar-proteins, for instance SarR, are able to bend DNA facilitating the contact of the regulatory protein with DNA. SarA has the ability to form dimers whereof three of such dimers can be covered by promotor DNA. This configuration is not accessible for the transcription machinery thereby inhibiting transcription of target genes (Liu et al., 2006; Cheung et al., 2004). Binding of Sar homodimers to target DNA sequences can be interfered by formation of heterodimers with a different Sar protein (Liu et al., 2001) or by displacement of the Sar protein from the target DNA sequence by another homolog (Manna and Cheung, 2006a). By binding to the promotor region of *agr* SarA induces up-regulation of several exotoxins including α-toxin, β-toxin, and δ-toxin during post-exponential growth phase (Cheung et al., 2004) thereby contributing to several manifestations of *S. aureus* pathogenesis such as septic arthritis and endocarditis (Cheung et al., 1994, Nilsson et al., 1996).

Another member of the single-domain subclass is the SarA antagonist SarR, a 115-residue protein. SarR was shown to bind to the promotor region of *sarA* thereby repressing the transcription of SarA (Manna and Cheung, 2001). Besides its action on transcriptional regulation of SarA, both molecules were shown to compete for the same binding site within the P2 promotor region of *agr* (Manna and Cheung, 2006a). The higher affinity of SarR towards the *agr* P2 region leads to displacement of SarA during transition to late stationary growth phase resulting in a subsequent repression of *agr* expression (Reyes et al., 2011). Similar to SarR, SarX was identified as another repressor of *agr* expression (Manna and Cheung, 2006b).

Instead, SarT and SarV are under negative control of single-domain protein SarA (Manna et al., 2004, Schmidt et al., 2001). While SarV contributes to autolysis (Manna et al., 2004) SarT was reported to negatively influence expression of α-toxin (Schmidt et al., 2001).

While mostly repressing toxins and enhancing the expression of surface proteins a single-domain member of the SarA-family proteins, a 14.3 kDa protein, was entitled repressor of toxins (Rot). Compared to the regulatory action of the agr quorum-sensing system, Rot displays an opposing role regarding the regulation of a plethora of virulence genes including various toxins and surface proteins

(Saïd-Salim et al., 2003; Killikelly et al., 2015). Translation of *rot* mRNA was further shown to be impeded by RNAIII, illustrating the complex regulatory cascades in *S. aureus* (Boisset et al., 2007). The double-domain protein SarS was implicated in regulation of protein A (SpA) expression (Tegmark et al., 2000) while being under negative control of agr and another member of the SarA-familiy, MgrA (Ingavale et al., 2005). Expression of SarS was further shown to be positively regulated by single-domain SarA-family protein SarT (Schmidt et al., 2003).

While the double-domain protein SarU serves as an activator of agr (Cheung et al., 2004) and was demonstrated to be under negative transcriptional control of SarT (Manna and Cheung, 2003), the regulatory role of homologue SarY, however, remains elusive.

The MarR-like proteins MgrA and SarZ display higher sequence identity to the MarR protein from *E. coli* than to SarA of *S. aureus* and were thus grouped into a special class of SarA-family proteins. MgrA represents a major virulence factor positively influencing a total of 175 genes including capsular biosynthesis genes, serine proteases, leukocidins as well as SarA (Luong et al., 2006), *agr* and *hla* (Ingavale et al., 2005) while repressing the expression of 180 genes including urease subunit encoding genes, *sarS* and *spA* (Luong et al., 2006). *mgrA* mRNA itself was shown to be stabilized by the agr effector RNAIII (Gupta et al., 2015). Mutants in *mgrA* are characterized by increased autolysis (Ingavale et al., 2005) which is thought to result from regulation of SarV (Manna et al., 2004; Cheung et al., 2008). MgrA, features a particular cysteine residue which oxidizes in the presence of reactive oxygen species (ROS) hence serving as an oxidation-sensing mechanism. Oxidation triggers dissociation of MgrA from DNA thereby changing the expression pattern resulting in subsequent activation of antibiotic resistance genes (Chen et al., 2006).

The last member of the SarA-family, SarZ is involved in regulation of haemolysis by binding to the promotor region of α-toxin encoding gene *hla*. SarZ was further demonstrated to play a crucial role for virulence in a silkworm infection model (Kaito et al., 2006).

2.4.3 Alternative σ-factors

Regulation of virulence in bacteria is often achieved by the action of dissociable subunits of prokaryotic RNA polymerase, the so-called sigma-factors (Kazmierczak et al., 2005). Besides the house-keeping sigma-factor σA *S. aureus* expresses the alternative sigma-factors σH, σB and the extracytoplasmatic function (ECF) sigma-factor σS. While σH was shown to regulate the natural competence of *S. aureus* (Fagerlund et al., 2014; Morikawa et al., 2012) σB plays a major role in virulence regulation of *S. aureus* regulating the expression of over 100 genes: SarA, catalase (*kat*A), the alkaline shock protein (*asp*23), Na^+/H^+ antiporters as well as capsular genes were identified among the σB regulon (Bischoff et al., 2004, Pané-Farré et al., 2006). σB-dependent regulation of virulence occurs mainly in stationary growth phase of *S. aureus* or when bacteria are challenged with heat, alkaline conditions, $MnCl_2$ or

NaCl (Entenza et al., 2005; Nicholas et al., 1999; Pané-Farré et al., 2006; Ziebandt et al., 2004; Ziebandt et al., 2001). σB activity itself depends on the σB-activating protein RsbU (Giachino et al., 2001; Pané-Farré et al., 2009). In absence of stress the anti-sigma-factor RsbW binds to σB thereby blocking interaction with the RNA polymerase and subsequent gene expression (Miyazaki et al., 1999). Further, RsbW phosphorylates and thus inactivates the anti-sigma antagonist RsbV whose activity is dependent on its phosphorylation state. Only when in its un-phosphorylated state, RsbV competes with σB for RsbW binding, which subsequently results in release of σB. Dephosphorylation of RsbV-P occurs in response to stress by the action of two phosphatases RsbU and RsbP (Pané-Farré et al., 2009; Miyazaki et al., 1999; Senn et al., 2005; Palma and Cheung, 2001).

The third alternative sigma-factor, the ECF sigma-factor σS, protects *S. aureus* against both cytoplasmic and extracytoplasmic stresses thereby contributing to the overall fitness of this pathogen (Miller et al., 2012; Shaw et al., 2008). Growth in serum-rich media and phagocytosis by RAW264.7 murine macrophage-like cells was shown to induce the activity of ECF sigma-factor σS (Miller et al., 2012). However, the regulon of σS remains still elusive.

2.4.4 Repressor of surface proteins (Rsp)

Expression of bacterial genes can further be modulated by DNA-binding regulators of the AraC/XylS family of transcriptional regulators, which were named after AraC from *E. coli* (Wallace et al., 1980; Schleif, 2010) and XylS from *Pseudomonas putida* (Inouye et al., 1986). Members of this family harbour two helix-turn-helix domains facilitating binding to the target DNA. AraC/XylS transcriptional regulators are found in a large variety of bacterial species and are implicated in regulation of various processes of metabolism and virulence (Gallegos et al., 1997).

S. aureus expresses five AraC/XylS transcriptional regulators (Ibarra et al., 2013) among which Rbf and Rsp have been implicated in regulation of biofilm formation (Cue et al., 2009, Lei et al., 2011). Rsp was further shown to play a crucial role for regulation of cytotoxicity (Das et al., 2016, Li et al., 2016).

The AraC-type transcriptional regulator Rsp, a 701 amino acid protein, harbours both the characteristically helix-turn-helix motifs as well as a glycosyl hydrolase domain of yet unknown function. Rsp was initially identified to repress the expression of surface proteins such as FnbA and was thus implicated in repressing biofilm formation (Lei et al., 2011). Due to its repressive action on surface protein expression it was referred to as 'Repressor of surface proteins' (Rsp). Recently a role for Rsp in regulation of a multitude of virulence factors, including *hla*, *sae*RS, *luk*A, *chs*, *scp*A and *hlg*C, was identified (Das et al., 2016; Li et al., 2016). Regulation of those virulence factors was found to be partially executed by induction of *agr* expression via binding to the P2 promotor region (Li et al., 2016). Further, the loss of functional Rsp resulted in a complete absence of transcription of a ncRNA whose

length was determined by TEX-treatment RNA-seq to be 1232 nt (Das et al., 2016; Fig. 2.8). In this study transcription of *rsp* itself was inducible upon stimulation with hydrogen peroxide, which further resulted in an enhancement of expression of a subset of Rsp-regulated virulence genes such as SSR42, *isd*A, *luk*AB and *lukS*-PV (Das et al., 2016). Rsp was further demonstrated to be a crucial regulator especially with regard to intracellular virulence and disease establishment in murine pneumonia and skin infection models (Das et al., 2016, Li et al., 2016). Mutants in *rsp* are characterized by a loss of haemolysis, strong reduction and delay of cytotoxicity due to reduced cytotoxin production and a prolonged intracellular residence within host cells. However, the ability to establish bloodstream infection was unaltered in mutants lacking Rsp (Das et al., 2016).

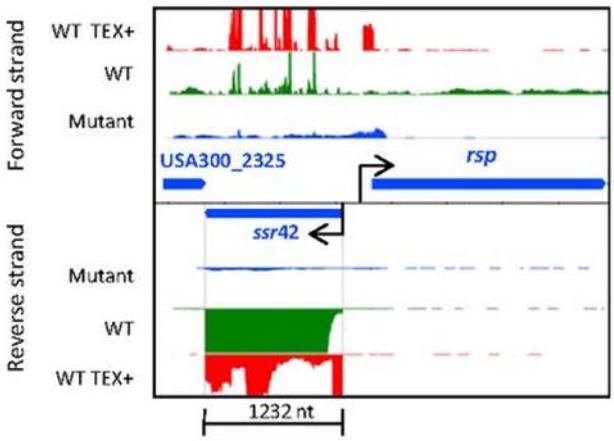

Figure 2.8: Long non-coding RNA SSR42. TEX-treatment RNA-seq shows absence of a 1232 nt long primary transcript encoding ncRNA SSR42 in mutants lacking functional Rsp. Figure modified from Das et al., 2016.

2.4.5 Regulatory link between metabolism and virulence regulation

S. aureus exploits a wide array of host niches for growth and thus requires mechanism to adapt to the different environments. For this reason, metabolism and virulence gene regulation must be linked closely. *S. aureus* possesses several regulatory factors bridging metabolism and virulence regulation such as the global repressor CodY, transcriptional regulator RpiRc and catabolite control protein E (CcpE).

The global repressor CodY regulates the expression of a large variety of virulence genes including *agr*, *sae*S, *sodA*, *hla* and *hlb* and genes involved in nucleotide metabolism (Pohl et al., 2009, Majerczyk et al., 2010). Only when bound to GTP or branched chain amino acids (BCAAs) CodY executes its repressive function (Majerczyk et al., 2010). During nutrient depletion, characterized by a shortage of BCAA and GTP, CodY remains unbound resulting in a subsequent de-repression of the CodY regulon (Majerczyk et al., 2010). Amino acid starvation further induces the synthesis of alarmones ((p)ppGpp) thereby reducing the availability of GTP (Geiger et al., 2014; Manav et al., 2018). The synthesis of

alarmones subsequently triggers transcriptional repression of the protein synthesis machinery resulting in proliferation arrest. Both stringent response and CodY are connected via the GTP-pool and the expression of most Cody-regulated genes was shown to be affected by the production of alarmones (Geiger et al., 2012) thereby bridging metabolism and virulence regulation in *S. aureus*.

Another factor contributing to the connection between virulence regulation and the metabolic state of *S. aureus* is RpiRc, a member of the RpiR family of transcriptional regulators. RpiRc positively regulates the expression of genes from the pentose phosphate pathway (Zhu et al., 2011) while repressing the transcription of RNAIII (Gaupp et al., 2016) and leukocidins (Balasubramanian et al., 2016). RpiRc was implicated in pathogenicity with mutants displaying an attenuated virulence phenotype in a murine pneumonia model (Gaupp et al., 2016). In contrast, loss of RpiRc further resulted in an increase in abscess formation in visceral organs in the same study (Gaupp et al., 2016) and lead to an increase in killing of host neutrophils as well as in pathogenesis of blood stream infections (Balasubramanian et al., 2016). RpiRc was proposed to execute virulence regulation partially indirectly by means of σB and SarA (Gaupp et al., 2016).

The presence of glucose was reported to repress the expression of both virulence factors such as *hla*, *psmα* and regulatory RNA RNAIII as well as metabolic genes corresponding to the TCA cycle via the regulatory action of catabolite control protein CcpE (Hartmann et al., 2014). Mutants in CcpE exhibit enhanced virulence in murine lung, skin and systemic infection models (Ding et al., 2014, Hartmann et al., 2014) and CcpE is hence thought to contribute to virulence of intracellular *S. aureus* by regulating the transition between different host environments via sensing the varying glucose concentrations (reviewed in Horn et al., 2018a).

2.5 Non-coding RNAs

2.5.1 Gene regulation by non-coding RNAs

Besides regulation by two-component systems and other regulatory proteins a major part of the virulome of *S. aureus* is regulated by non-coding RNAs (ncRNA). Regulatory ncRNAs either base-pair to their respective target mRNA forming RNA duplexes thereby modulating the efficiency of translation or stability of the target mRNA (Fig. 2.9). The formation of RNA-RNA duplexes is often facilitated by RNA-binding proteins such as Hfq (reviewed in Guillet et al., 2013). A further regulatory mechanism employed by ncRNAs is via binding to proteins. By mimicking the protein binding sequence of mRNAs ncRNAs can titrate binding affinities of proteins and mRNAs thereby modulating their activities (Chambers and Sauer, 2013; Svensson and Sharma, 2016).

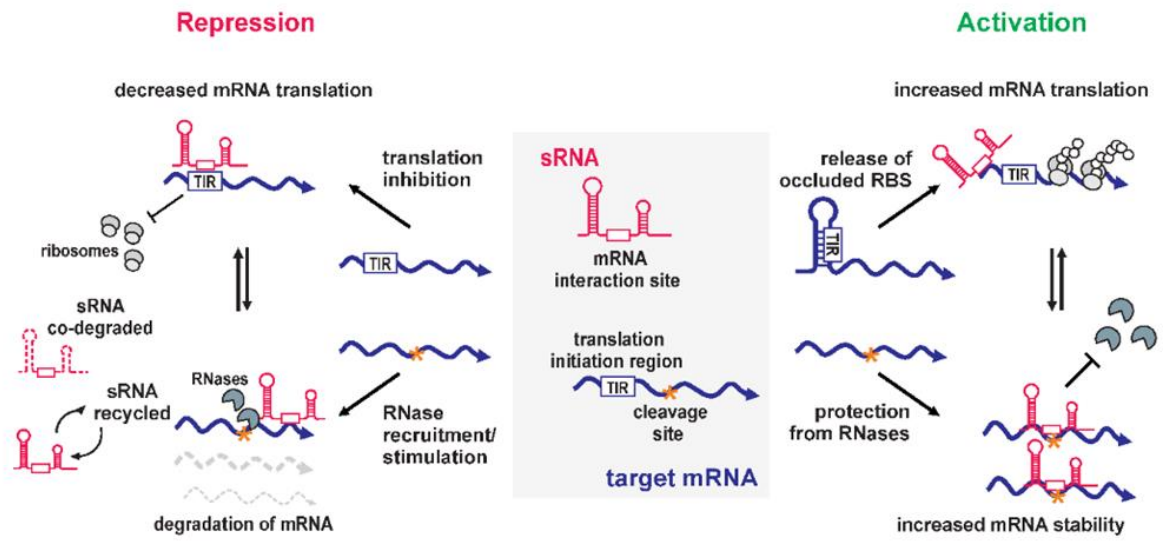

Figure 2.9: Mechanism of posttranscriptional regulation by regulatory RNAs. Expression repression and activation mechanisms employed by ncRNAs (red). Base-pairing of ncRNAs to the target mRNA (blue) can either block the ribosomal access or lead to recruitment of Rnases thereby decreasing mRNA translation. In contrast, base-pairing of ncRNA and mRNAs can result in release of occluded ribosomal binding sites or protect the mRNA from RNases thus increase mRNA stability or translation. Figure modified from Svensson and Sharma, 2016.

Non-coding RNAs can be subdivided into two classes: cis- and trans-encoded ncRNAs (Fig. 2.10). While cis-encoded ncRNAs are transcribed on the opposite DNA strand of their target mRNA and thus execute their regulatory properties via perfect complementary base-pairing, trans-encoded ncRNAs are transcribed from a different genetic locus than the respective target mRNA. Trans-encoded RNAs thus only share partial complementarity to their target mRNA (Thomason and Storz, 2010). While in *E.coli* a so-called seeding sequence of 6-7 nucleotides is sufficient for initiation of a ncRNA-mRNA interaction (Papenfort and Vogel, 2010), this was shown to be not sufficient for ncRNAs of *S. aureus*. For most ncRNAs of S*. aureus* the interaction of ncRNA and mRNA involves a much longer sequence. This is thought to result from the high A-T content of the *S. aureus* genome (Guillet et al., 2013).

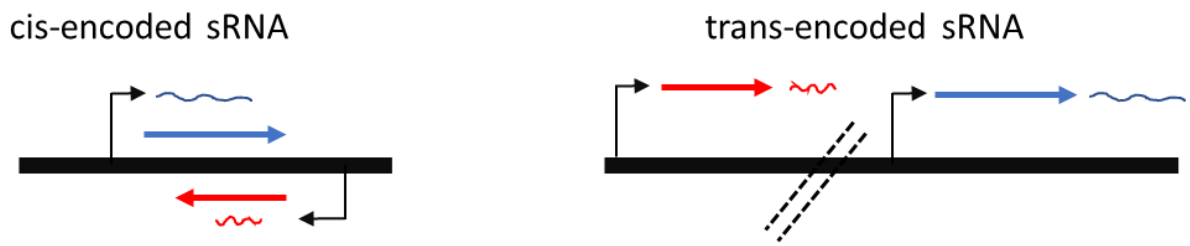

Figure 2.10: Graphical representation of the mode of action of cis- and trans-encoded sRNAs. A) While cis-encoded sRNAs (red) are encoded on the same genetic locus as their target mRNAs (blue) trans-encoded sRNAs are located on different genetic loci than their target mRNA. Adapted from Prasse et al., 2013.

2.5.2 RNA-binding protein Hfq

The imperfect complementarity of trans-encoded ncRNAs to their respective target-mRNA often requires the aid of auxiliary factors such as Hfq. This RNA-binding protein can be found in a large array of bacterial species and serves as an RNA-chaperone stabilizing the interaction of trans-encoded ncRNAs and their respective target mRNAs (Vogel and Luisi, 2011; Valentin-Hansen et al., 2004). Hfq forms a homo-hexameric ring-like structure featuring two single-stranded RNA binding domains located on opposing sites of the molecule (Fig. 2.11). While the distal RNA-binding domain only interacts with poly-A sequences the proximal domain binds ncRNAs via interaction with AU-rich sequences thereby allowing a simultaneous interaction with both ncRNA and their respective target mRNA (Link et al., 2009; Schumacher et al., 2002).

While in *E. coli* Hfq not only facilitates ncRNA-mRNA interactions but was further shown to interfere with RNA turnover by recruiting RNase E (Bandyra et al., 2012; Urban und Vogel, 2007), the exact function for Hfq in *S. aureus* remains elusive and needs further investigation. Deletion of *hfq* was analysed in three different *S. aureus* strains (RN6390, COL and Newman) where it had no impact on more than 2,000 different phenotypes of *S. aureus* (Bohn et al., 2007). However, inactivation of Hfq in strain 8325-4, a natural *rsb*U mutant, altered the expression of 116 genes including the carotenoid pigment staphyloxanthin (Liu et al., 2010). This Hfq-dependent differential regulation of staphyloxanthin expression was observed in strain N315 as well (Castro et al., 2011). While involvement of Hfq in base-pairing of RNAIII to *sp*A or *sa*1000 mRNA was excluded (Huntzinger et al., 2005), RNAIII and Hfq could be co-purified using a Hfq-pulldown approach (Liu et al., 2010). In this study Hfq was further co-purified with *sbi*, *sucD* and *rot* mRNA, which are regulated by the non-coding RNAs SprD, RsaE and RNAIII, respectively (Liu et al., 2010), hence indicating a potential role for Hfq in facilitating ncRNA-mediated regulation of target genes in *S. aureus*. However, the role of Hfq in ncRNA-dependent regulation of target genes remains rather ambiguous and requires further investigation. The discrepancies in the regulatory impact of Hfq in the different studies could result from the expression levels of *hfq,* which vary drastically in different *S. aureus* strains (Liu et al., 2010).

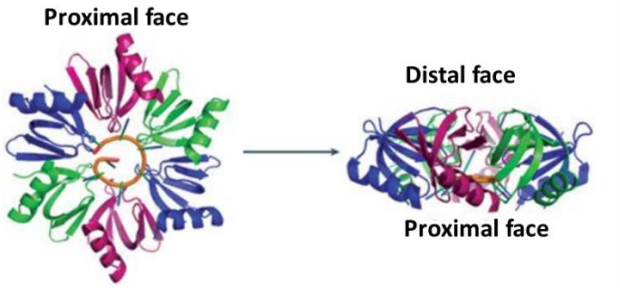

Figure 2.11: Two-dimensional structure of RNA-binding protein Hfq. Hfq forms a homo-hexameric ring-like structure exhibiting two faces for binding of RNAs (represented in orange). The distal domain interacts with poly-A sequences while the proximal part binds ncRNAs via AU-rich sequences. Modified from Vogel and Luisi, 2011.

2.5.3 RNA-turnover

In *E. coli* the turnover of mRNA is mainly executed by endoribonuclease RNase E followed by the activities of PNPase, DEAD-box RNA helicase RhlB and enolase constituting the so-called degradosome (Carpousis, 2007). However, most gram-positive bacteria do not express RNase E but orthologues of RNase E and the other components of the degradosome (Cho, 2017). In *S. aureus* the RNase E function is executed via the orthologous endoribonuclease RNase Y, which was reported to initiate degradation of approximately one hundred mRNA species and some sRNAs (Khemici et al., 2015, Marincola et al., 2012). Cleavage by RNase Y triggers subsequent mRNA decay. The resulting RNA fragments are thought to be further degraded by the 5´-3´exoribonuclease activity of RNase J1 and by PNPase (Durand et al., 2012; Lehnik-Habrink et al., 2012; Cho, 2017). While not required for growth RNase Y was reported to be crucial for virulence in a murine bacteraemia model and implicated in regulation of transcription of virulence genes including *sp*A and *hlg*C. A further important role regarding virulence gene regulation is executed via processing the unstable primary transcript T1 encoding *sae*PQRS to obtain the more stable transcript T2 (Marincola et al., 2012; see section 2.4.1.2). Recently a further protein, the DEAD-box helicase CshA, was identified to interact with components of the RNA degradosome of *S. aureus* (Giraud et al., 2015) thus acting as a functional homologue for RhlB of *E. coli*. Besides affecting bulk mRNA turnover, CshA was reported to affect virulence phenotypes such as biofilm formation and haemolysis via modulating the stability of *agr* mRNA (Oun et al., 2013) and to be required for formation and subsequent stabilization of sRNA teg049 encoded in the 5´UTR of *sar*A mRNA (Kim et al., 2016). Moreover, interaction with CshA confers a protective role against the endoribonuclease activity of toxin MazF. While induction of MazF results in cleavage of a majority of virulence-associated mRNAs, most house-keeping mRNAs, *sarA* mRNA and several sRNAs are protected by presence of the RNA-binding protein CshA and their stability was reported to be significantly reduced in mutants lacking *csh*A (Kim et al., 2016).

2.5.4 Non-coding RNAs in *Staphylococcus aureus*

In *S. aureus* more than 250 genes encoding small RNAs (sRNA), mostly encoded on the core genome, were identified by various experimental approaches (Abu-Qatouseh et al., 2010; Anderson et al., 2006; Beaume et al., 2010; Bohn et al., 2010; Geissmann 2009; Novick et al., 1989; Novick et al., 1993; Pichon and Felden, 2005). However, the function of most sRNAs in *S. aureus* remains elusive. The best characterized ncRNA of *S. aureus* is RNAIII, the main effector of the agr quorum-sensing system (see chapter 2.4.1.1, Boisset et al., 2007, Bronesky et al., 2016, Huntzinger et al., 2005). The regulation of target genes by RNAIII is executed mainly via base-pairing to target mRNAs thereby modulating translation by granting or blocking access to the Shine-Dalgarno sequence (Morfeldt et al., 1995; Geisinger et al., 2006) or facilitating degradation (Chevalier et al., 2010; Fig. 2.12). By these means

RNAIII facilitates the translation of α-toxin. The high complementarity between the 5´end of RNAIII and the 5´untranslated region (UTR) of *hla* mRNA leads to formation of a RNA-duplex which prevents the intramolecular base-pairing of *hla* mRNA that would block translation. Regulation of α-toxin expression by RNAIII is hence executed by enabling ribosomal access to the Shine-Dalgarno sequence via base complementarity to *hla* mRNA (Morfeldt et al., 1995). RNAIII was further shown to block the translation of a major transcription, factor repressor of toxins (rot), by blocking its translation (Geisinger et al., 2006).

The ncRNA psm-mec, which is encoded on the SCCmec mobile genetic element was reported to repress translation of *agr*A mRNA thereby attenuating the virulence potential of *S. aureus* (Kaito et al., 2013). Another ncRNA of *S. aureus* SprD, encoded on a pathogenicity island (Pichon and Felden, 2005) was implicated in regulation of *sbi* translation (Chabelskaya et al., 2014). Recently AgrA-repressed toxin regulating sRNA (ArtR) was identified to regulate α-toxin expression via binding to the 5´ UTR of *sar*T mRNA thereby facilitating its degradation (Xue et al., 2014).

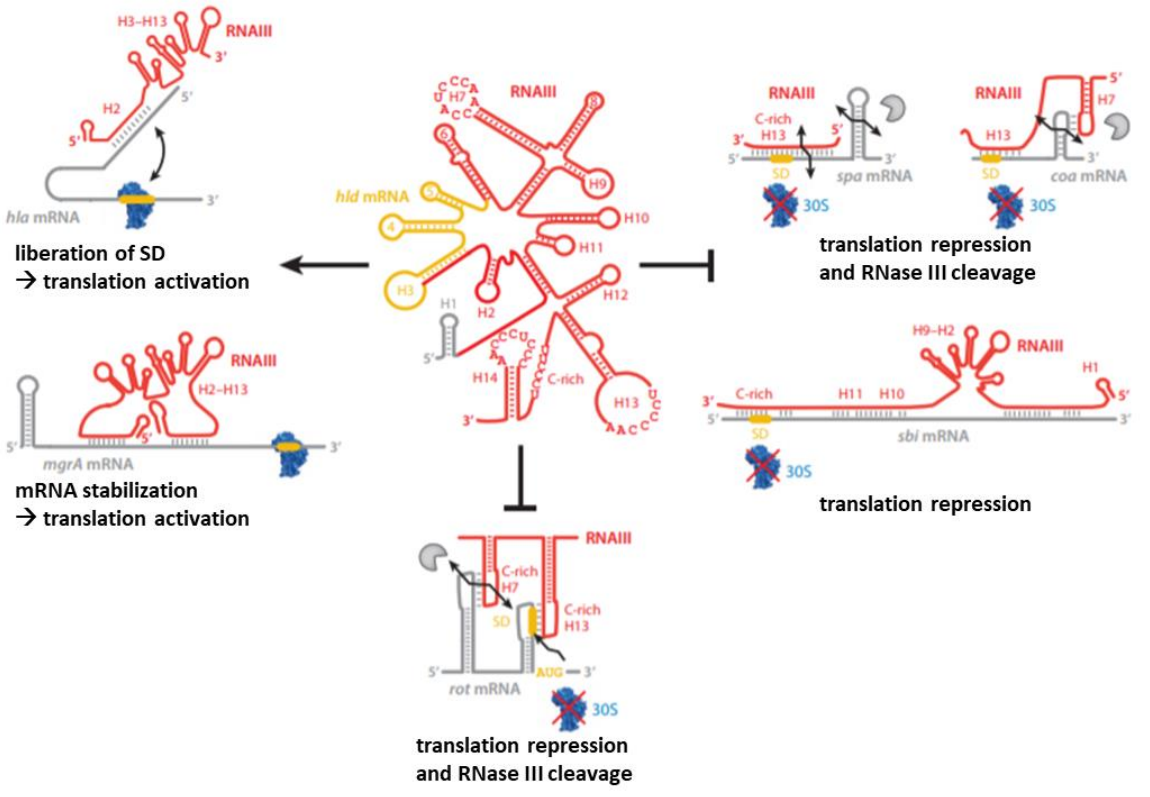

Figure 2.12: Two-dimensional structure of ncRNA RNAIII of *S. aureus* and mechanisms of expression regulation. RNAIII consist 14 stem loop structures that are involved in virulence factor regulation by liberation of ribsosomal binding sites, stabilization, translation activation, translation repression or recruitment of RNase III. Modified from Bronesky et al., 2016.

Several sRNAs of *S. aureu*s such as sRNAs from the Rsa family and RNAIII share a common motif featuring the consensus sequence UCCC, which is involved in the initial pairing to the target mRNA (Geissmann et al., 2009). RNAIII harbours such UCCC motifs in loop H7, H13 and H14 which were demonstrated to be involved in the interaction with the Shine-Dalgarno sequence of target mRNAs such as *sp*A, *coa* and *rot* mRNA (Benito et al., 2000; Chevalier et al., 2010; Geisinger et al., 2006; Guillet et al., 2013). Such UCCC motifs can further be found in other gram-positive bacteria and are hypothesized to be a common feature of translation regulation by ncRNAs (Gaballa et al., 2008; Mandin et al., 2007; Nielsen et al., 2008; Toledo-Arana et al., 2009).

While for most ncRNAs in *S. aureus* the exact function remains elusive a role for ncRNA SSR42 in regulation of haemolysis and expression of 80 mRNA species has been proposed (Morrison et al., 2012a). SSR42 was identified as 891 nt long ncRNA which was stabilized during stationary growth phase in *S. aureus* (Olson et al., 2011; Morrison et al., 2012a). SSR42 has also been detected in other studies although with slightly different length estimates: Teg27: 1176 nt (Beaume et al., 2010), srn_4470: 1174 nt (Sassi et al., 2015), or RsaX28: 1177 nt (Khemici et al., 2015). A genome-wide identification of RNase Y processing sites identified a single cleavage site within the SSR42 molecule (Khemici et al., 2015). SSR42 was grouped into the so-called small stable RNAs, which are thought to adopt crucial functions during otherwise detrimental conditions (Anderson et al., 2006; Anderson et al., 2010; Olson et al., 2011; Roberts et al., 2006). Mutants in SSR42 were shown to display reduced haemolysis, resistance towards human neutrophil killing and virulence in a murine model of SSTIs. Regulation of haemolysis was demonstrated to be executed via modulation of the *hla* promotor activity (Morrsion et al., 2012a). In a recent study SSR42 was identified as a major target of global regulator Rsp (see section 2.4.4). Lack of Rsp resulted in a complete loss of SSR42 transcription, reduced haemolysis and cytotoxicity. SSR42 was thus proposed to be a potential effector of Rsp-mediated virulence. However, in this study, the length of the primary transcript of SSR42 was determined to encompass 1232 nt via TEX-treatment RNA-seq (Das et al., 2016).

2.6 Aim of the study

S. aureus regulates virulence to a large proportion via ncRNAs. Whereas, the mostly non-coding RNA RNAIII is well-studied, little is known about the regulatory role of other ncRNAs. Recently, the ncRNA SSR42 was identified as main target of Repressor of surface proteins, Rsp, however, the regulatory role of SSR42 remained largely elusive.

The aim of this study hence was the functional characterization of SSR42 by phenotypic analysis, thereby investigating the effects resulting from deletion of this ncRNA on staphylococcal haemolysis, cytotoxicity and virulence. In order to gain insight into the regulatory properties of SSR42 the regulon of this ncRNA will be identified by employing high-throughput analyses on RNA and protein level. Apart from phenotypic analysis this study aims to characterize ncRNA SSR42 on a molecular level by employing secondary structure predictions as well as mutational approaches in order to identify functional domains within this molecule. Promotor activity studies will be applied to study the expression of SSR42 during different growth phases and to identify stressors influencing the transcription of this ncRNA. These promotor activity studies will further be applied in different *S. aureus* regulator mutants to resolve the position of SSR42 in the virulence regulatory network of *S. aureus*.

3 MATERIAL AND METHODS

3.1 Material

3.1.1 Bacterial strains

Table 3.1: Bacterial strains used in this study.

Strain	Description	Source
Staphylococcus aureus		
UAMS-1	Osteomyelitis isolate, Little Rock, AR, USA	Gillaspy et al., 1995
UAMS-1 pP_{SSR42}-GFP	UAMS-1 expressing GFP under control of the promotor of SSR42; used for analysis of SSR42 promotor activity	This study
UAMS-1 pP_{rsp}-GFP	UAMS-1 expressing GFP under control of the promotor of *rsp*; used for analysis of *rsp* promotor activity	This study
HG003	NCTC8325, *rsb*U$^+$, *tca*R$^+$	Herbert et al., 2010
HG003 pP_{SSR42}-GFP	HG003 expressing GFP under control of the promotor of SSR42; used for analysis of SSR42 promotor activity	This study
N315	Pharyngeal smear isolate, Japan, 1985, ORSA	Kuroda et al., 2001
N315 pP_{SSR42}-GFP	N315 expressing GFP under control of the promotor of SSR42; used for analysis of SSR42 promotor activity	This study
COL	Archaic MRSA strain from UK	Gill et al., 2005
COL pP_{SSR42}-GFP	COL expressing GFP under control of the promotor of SSR42; used for analysis of SSR42 promotor activity	This study
MW2	Community-acquired isolate causing septicaemia and septic arthritis, North Dakota	Baba et al., 2002
MW2 pP_{SSR42}-GFP	MW2 expressing GFP under control of the promotor of SSR42; used for analysis of SSR42 promotor activity	This study
Cowan I	Non-haemolytic, protein A overproducer	ATCC 12598
Cowan I pP_{SSR42}-GFP	Cowan I expressing GFP under control of the promotor of SSR42; used for analysis of SSR42 promotor activity	This study
Newman	Strong producer of clumping factor	Duthie and Lorenz, 1952

Newman pP_{SSR42}-GFP	Newman expressing GFP under control of the promotor of SSR42; used for analysis of SSR42 promotor activity	This study
RN4220	Derivative of NCTC8325-4 accepting foreign DNA	Kreiswirth et al., 1983
RN4220 pP_{SSR42}-GFP	RN4220 expressing GFP under control of the promotor of SSR42; used for analysis of SSR42 promotor activity	This study
JE2	USA300 LAC MRSA, plasmid-cured; erm^S	Fey et al., 2013
JE2 pP_{SSR42}-BgaB	JE2 expressing BgaB under control of the promotor of SSR42; used for analysis of SSR42 promotor activity in disc diffusion assays	This study
JE2 pAHT-SSR42	JE2 expressing SSR42 under control of an AHT-inducible promotor	This study
JE2 pP_{SSR42}-GFP	JE2 expressing GFP under control of the promotor of SSR42; used for analysis of SSR42 promotor activity	This study
JE2 pP_{rsp}-GFP	JE2 expressing GFP under control of the promotor of *rsp*; used for analysis of *rsp* promotor activity	This study
JE2 pP_{hla}-GFP	JE2 expressing GFP under control of the promotor of *hla*; used for analysis of *hla* promotor activity	This study
NE1614	JE2, SAUSA300_2325::Bursa	Fey et al., 2013
NE954	JE2, SAUSA300_2327::Bursa	Fey et al., 2013
NE1622	JE2, *sae*R::Bursa (SAUSA300_0691)	Fey et al., 2013
NE1622 pAHT-SSR42	NE1622 expressing SSR42 under control of an AHT-inducible promotor	This study
NE1622 pP_{SSR42}-GFP	NE1622 expressing GFP under control of the promotor of SSR42; used for analysis of SSR42 promotor activity	This study
NE1532	JE2, *agr*A::Bursa (SAUSA300_1992)	Fey et al., 2013
NE1532 pP_{SSR42}-GFP	NE1532 expressing GFP under control of the promotor of SSR42; used for analysis of SSR42 promotor activity	This study

NE1532 pP_{rsp}-GFP	NE1532 expressing GFP under control of the promotor of *rsp*; used for analysis of *rsp* promotor activity	This study
NE217	JE2, *pkn*B ::Bursa (SAUSA300_1113)	Fey et al., 2013
NE217 pP_{SSR42}-GFP	NE217 expressing GFP under control of the promotor of SSR42; used for analysis of SSR42 promotor activity	This study
NE1296	JE2, *sae*S::Bursa (SAUSA300_0690)	Fey et al., 2013
NE1296 pP_{SSR42}-GFP	NE1296 expressing GFP under control of the promotor of SSR42; used for analysis of SSR42 promotor activity	This study
NE1296 pP_{rsp}-GFP	NE1296 expressing GFP under control of the promotor of *rsp*; used for analysis of *rsp* promotor activity	This study
NE1304	JE2, *rsp*::Bursa (SAUSA300_2326)	Fey et al., 2013
NE1304 pS2217-3xFLAG	NE1304 expressing triple FLAG-tagged Rsp under control of native promotor	Sudip Das, PhD thesis
NE1304 pP_{SSR42}-GFP	NE1304 expressing GFP under control of the promotor of SSR42; used for analysis of SSR42 promotor activity	This study
NE1109	JE2, *rpo*F::Bursa (SAUSA300_2022)	Fey et al., 2013
NE1109 pP_{SSR42}-GFP	NE1109 expressing GFP under control of the promotor of SSR42; used for analysis of SSR42 promotor activity	This study
NE1109 pP_{rsp}-GFP	NE1109 expressing GFP under control of the promotor of *rsp*; used for analysis of *rsp* promotor activity	This study
NE1607	JE2, *rsb*U::Bursa (SAUSA300_2025)	Fey et al., 2013
NE1607 pP_{SSR42}-GFP	NE1607 expressing GFP under control of the promotor of SSR42; used for analysis of SSR42 promotor activity	This study
NE1607 pP_{rsp}-GFP	NE1607 expressing GFP under control of the promotor of *rsp*; used for analysis of *rsp* promotor activity	This study
NE1560	JE2, *ccp*E::Bursa (SAUSA300_0658)	Fey et al., 2013
NE1560 pP_{SSR42}-GFP	NE1560 expressing GFP under control of the promotor of SSR42; used for analysis of SSR42 promotor activity	This study

NE1560 pP$_{rsp}$-GFP	NE1560 expressing GFP under control of the promotor of *rsp*; used for analysis of *rsp* promotor activity	This study
NE1555	JE2, *cod*Y::Bursa (SAUSA300_1148)	Fey et al., 2013
NE1555 pP$_{SSR42}$-GFP	NE1555 expressing GFP under control of the promotor of SSR42; used for analysis of SSR42 promotor activity	This study
NE1555 pP$_{rsp}$-GFP	NE1555 expressing GFP under control of the promotor of *rsp*; used for analysis of *rsp* promotor activity	This study
NE554	JE2, *vra*R::Bursa (SAUSA300_1865)	Fey et al., 2013
NE554 pP$_{SSR42}$-GFP	NE554 expressing GFP under control of the promotor of SSR42; used for analysis of SSR42promotor activity	This study
NE823	JE2, *vra*S::Bursa (SAUSA300_1866)	Fey et al., 2013
NE823 pP$_{SSR42}$-GFP	NE823 expressing GFP under control of the promotor of SSR42; used for analysis of SSR42 promotor activity	This study
NE229	JE2, *vfr*B::Bursa (SAUSA300_1119)	Fey et al., 2013
NE229 pP$_{SSR42}$-GFP	NE229 expressing GFP under control of the promotor of SSR42; used for analysis of SSR42 promotor activity	This study
NE229 pP$_{rsp}$-GFP	NE229 expressing GFP under control of the promotor of *rsp*; used for analysis of *rsp* promotor activity	This study
NE1684	JE2, *arl*R::Bursa (SAUSA300_1308)	Fey et al., 2013
NE1684 pP$_{SSR42}$-GFP	NE1684 expressing GFP under control of the promotor of SSR42; used for analysis of SSR42 promotor activity	This study
NE1684 pP$_{rsp}$-GFP	NE1684 expressing GFP under control of the promotor of *rsp*; used for analysis of *rsp* promotor activity	This study
NE1183	JE2, *arl*S::Bursa (SAUSA300_1307)	Fey et al., 2013
NE1183 pP$_{SSR42}$-GFP	NE1183 expressing GFP under control of the promotor of SSR42; used for analysis of SSR42 promotor activity	This study
NE1309	JE2, *srr*A::Bursa (SAUSA300_1442)	Fey et al., 2013

NE1309 pP$_{SSR42}$-GFP	NE1309 expressing GFP under control of the promotor of SSR42; used for analysis of SSR42 promotor activity	This study
NE1309 pP$_{rsp}$-GFP	NE1309 expressing GFP under control of the promotor of *rsp*; used for analysis of *rsp* promotor activity	This study
NE588	JE2, *srr*B::Bursa (SAUSA300_1441)	Fey et al., 2013
NE588 pP$_{SSR42}$-GFP	NE588 expressing GFP under control of the promotor of SSR42; used for analysis of SSR42 promotor activity	This study
NE588 pP$_{rsp}$-GFP	NE588 expressing GFP under control of the promotor of *rsp*; used for analysis of *rsp* promotor activity	This study
JE2-217	JE2 Δ*rny*, deletion of gene *rny* encoding RNase Y (SAUSA300_1179)	Marincola et al., 2012
JE2-217 pCG296	JE-217 complemented in trans with *rny* under control of its native promotor	Marincola et al., 2012
JE2-217 pP$_{SSR42}$-GFP	JE-217 expressing GFP under control of the promotor of SSR42; used for analysis of SSR42 promotor activity	This study
JE2 Δ*relp* Δ*relq* Δ*rsh*	JE2, deletion of alarmone production encoding genes *relp, relq* and *rsh*	Geiger et al., 2014
JE2 Δ*relp* Δ*relq* Δ*rsh* pP$_{SSR42}$-GFP	JE2 Δ*relp* Δ*relq* Δ*rsh* expressing GFP under control of the promotor of SSR42; used for analysis of SSR42 promotor activity	This study
JE2 Δ*rpi*Rc	JE2, deletion of gene *rpi*Rc (SAUSA300_2264)	Gaupp et al., 2016
JE2 Δ*rpi*Rc pP$_{SSR42}$-GFP	JE2 Δ*rpi*Rc expressing GFP under control of the promotor of SSR42; used for analysis of SSR42 promotor activity	This study
JE2 Δ*rpi*Rc pP$_{rsp}$-GFP	JE2 Δ*rpi*Rc expressing GFP under control of the promotor of *rsp*; used for analysis of *rsp* promotor activity	This study
JE2 Δ*sigS*	JE2, markerless deletion of gene *sig*S encoding alternative sigma factor σS	This study
JE2 Δ*sigS* pP$_{SSR42}$-GFP	JE2 Δ*sig*S expressing GFP under control of the promotor of SSR42; used for analysis of SSR42 promotor activity	This study

JE2 2500639R	JE2, SSR42::Bursa	Fey et al., 2013
JE2 2500639R pSSR42	JE2 2500639R complemented in trans for SSR42 and upstream ORF RSAU_002216 under control of the native promotors	This study
JE2 2500639R pP_{hla}-GFP	JE2 2500639R expressing GFP under control of the promotor of *hla*; used for analysis of *hla* promotor activity	This study
6850	MSSA, isolated from a patient with a skin abscess, progressed to bacteraemia, osteomyelitis, septic arthritis, and multiple systemic abscesses	Vann and Proctor, 1987
6850 p$_{PagrP3}$-GFP	6850 expressing GFP under control of *agr* P3 the *agr* P3 promotor; used for analysis of SSR42 promotor activity	This study
6850 pP_{SSR42}-BgaB	6850 expressing BgaB under control of the promotor of SSR42; used for analysis of SSR42 promotor activity in disc diffusion assays	This study
6850 pP_{SSR42}-GFP	6850 expressing GFP under control of the promotor of SSR42; used for analysis of SSR42 promotor activity	This study
6850 pP_{rsp}-GFP	6850 expressing GFP under control of the promotor of *rsp*; used for analysis of *rsp* promotor activity	This study
6850 pP_{hla}-GFP	6850 expressing GFP under control of the promotor of *hla*; used for analysis of *hla* promotor activity	This study
6850 pP_{saeP1}-GFP	6850 expressing GFP under control of the promotor of *sae* P1; used for analysis of *sae* P1 promotor activity	This study
6850 pP_{coa}-GFP	6850 expressing GFP under control of the promotor of *coa*; used for analysis of *coa* promotor activity	This study
6850 pP_{ldhD}-GFP	6850 expressing GFP under control of the promotor of *ldh*D; used for analysis of *ldh*D promotor activity	This study

6850 pP$_{psm\alpha}$-GFP	6850 expressing GFP under control of the promotor of *psm*α; used for analysis of *psm*α promotor activity	This study
6850 Δ*rsp*	6850 with targeted deletion of gene locus RSAU_002217 (*rsp*)	Das et al., 2016
6850 Δ*rsp* pS2217-3xFLAG	JE2 expressing triple FLAG-tagged Rsp under control of native promotor	Sudip Das, PhD thesis
6850 Δ*rsp* pP$_{SSR42}$-BgaB	6850 Δ*rsp* expressing BgaB under control of the promotor of SSR42; used for analysis of SSR42 promotor activity in disc diffusion assays	This study
6850 Δ*rsp* pRsp-P$_{SSR42}$-BgaB	6850 Δ*rsp* complemented in trans for ORF RSA_002217 (*rsp*) expressing BgaB under control of the promotor of SSR42; used for analysis of SSR42 promotor activity in disc diffusion assays	Stefanie Feuerbaum, Master thesis
6850 Δ*rsp* pP$_{SSR42}$-GFP	6850 Δ*rsp* expressing GFP under control of the promotor of SSR42; used for analysis of SSR42 promotor activity	This study
6850 Δ*hla*	6850 with targeted deletion of gene locus RSAU_001044 (*hla* gene)	Sudip Das, PhD thesis
6850 ΔSSR42	6850 with targeted deletion of ncRNA SSR42	This study
6850 ΔSSR42 pP$_{hla}$-GFP	6850 ΔSSR42 expressing GFP under control of the promotor of *hla*; used for analysis of *hla* promotor activity	This study
6850 ΔSSR42 pP$_{saeP1}$-GFP	6850 ΔSSR42 expressing GFP under control of the promotor of *sae* P1; used for analysis of *sae* P1 promotor activity	This study
6850 ΔSSR42 pP$_{coa}$-GFP	6850 ΔSSR42 expressing GFP under control of the promotor of *coa*; used for analysis of *coa* promotor activity	This study
6850 ΔSSR42 pP$_{psm\alpha}$-GFP	6850 ΔSSR42 expressing GFP under control of the promotor of *psm*α; used for analysis of *psm*α promotor activity	This study
6850 ΔSSR42 pP$_{ldhD}$-GFP	6850 ΔSSR42 expressing GFP under control of the promotor of *ldh*D; used for analysis of *ldh*D promotor activity	This study

6850 ΔSSR42 pSSR42	6850 ΔSSR42 complemented in trans for SSR42 and upstream ORF RSAU_002216 under control of the native promotors	This study
6850 ΔSSR42 pSSR42-rsp	6850 ΔSSR42 complemented in trans for SSR42, upstream ORF RSAU_002216 and *rsp* under control of the native promotors	This study
6850 ΔSSR42 p2216-2218	6850 ΔSSR42 complemented in trans for SSR42, upstream ORF RSAU_002216, *rsp* and downstream ORF RSAU_002218 under control of the native promotors	This study
6850 ΔSSR42 pAHT-SSR42	6850 ΔSSR42 complemented in trans for SSR42 under control of an AHT-inducible promotor	This study
6850 ΔSSR42 pAHT-SSR42-5ms2	6850 ΔSSR42 complemented in trans for SSR42 under control of an AHT-inducible promotor; SSR42 is tagged at the 5´end with a ms2-aptamer	This study
6850 ΔSSR42 pAHT-MS2-Ter	6850 ΔSSR42 expressing a ms2-aptamer under control of an AHT-inducible promotor	This study
6850 ΔSSR42 pAHT-SSR42-14mer	6850 ΔSSR42 complemented in trans for SSR42 under control of an AHT-inducible promotor; SSR42 is tagged at the 5´end with a 14 nt long aptamer	This study
6850 ΔSSR42 pAHT-14mer-Ter	6850 ΔSSR42 expressing a 14 nt long aptamer under control of an AHT-inducible promotor	This study
6850 ΔSSR42 pSSR42Δ1	6850 ΔSSR42 complemented in trans for SSR42 under control of the native promotor; SSR42 harbours a small deletion encompassing bp 2,352,023-2,352,099	This study
6850 ΔSSR42 pSSR42Δ2	6850 ΔSSR42 complemented in trans for SSR42 under control of the native promotor; SSR42 harbours a small deletion encompassing bp 2,352,157-2,352,221	This study
6850 ΔSSR42 pSSR42Δ3	6850 ΔSSR42 complemented in trans for SSR42 under control of the native promotor; SSR42 harbours a small deletion encompassing bp ,2352,282-2,352,348	This study

6850 ΔSSR42 pSSR42Δ4	6850 ΔSSR42 complemented in trans for SSR42 under control of the native promotor; SSR42 harbours a small deletion encompassing bp 2,352,415-2,352,483	This study
6850 ΔSSR42 pSSR42Δ5	6850 ΔSSR42 complemented in trans for SSR42 under control of the native promotor; SSR42 harbours a small deletion encompassing bp 2,352,535-2,352,607	This study
6850 ΔSSR42 pSSR42Δ6	6850 ΔSSR42 complemented in trans for SSR42 under control of the native promotor; SSR42 harbours a small deletion encompassing bp 2,352,688-2,352,742	This study
6850 ΔSSR42 pSSR42Δ7	6850 ΔSSR42 complemented in trans for SSR42 under control of the native promotor; SSR42 harbours a small deletion encompassing bp 2,352,858-2,352,794	This study
6850 ΔSSR42 pSSR42Δ8	6850 ΔSSR42 complemented in trans for SSR42 under control of the native promotor; SSR42 harbours a small deletion encompassing bp 2,352,917-2,352,978	This study
6850 ΔSSR42 pSSR42-rsp-RNaseY-mutG	6850 ΔSSR42 complemented in trans for SSR42 under control of the native promotor; SSR42 harbours a nucleotide exchange in the RNase Y-cleavage initiating guanosine (bp 2,352,899)	This study
6850 ΔSSR42 pSSR42-rsp-mutORF	6850 ΔSSR42 complemented in trans for SSR42 under control of the native promotor; SSR42 harbours a nucleotide exchange in the putative ORF 3 (bp 2,352,818)	This study
6850 ΔSSR42 pSSR42-rsp-delRNaseY	6850 ΔSSR42 complemented in trans for SSR42 under control of the native promotor; SSR42 harbours a small deletion encompassing the RNase Y cleavage sequence (bp 2,352,844-2,352914)	This study
6850 ΔSSR42 pSSR42 mini-1	6850 ΔSSR42 complemented in trans for a drastically reduced to 780 nt long SSR42 under control of the native promotor	This study

	(deleted nucleotides: bp 2,352,219 - 2,352,658)	
6850 ΔSSR42 pSSR42 mini-2	6850 ΔSSR42 complemented in trans for a drastically reduced to 643 nt long SSR42 under control of the native promotor (deleted nucleotides: bp 2,352,916-2,353,044)	This study
6850 ΔSSR42 pStemLoop2-Term	6850 ΔSSR42 complemented in trans for only a certain, stem loop featuring region of SSR42 under control of the native promotor (bp 2,351,984-2,352,137)	This study
6850 ΔSSR42-*rsp*	6850 with targeted deletion of ncRNA SSR42 and gene locus RSAU_002217 (*rsp*)	This study
6850 ΔSSR42-*rsp* pSSR42	6850 ΔSSR42-*rsp* complemented in trans for SSR42 and upstream ORF RSAU_002216 under control of the native promotors	This study
6850 ΔSSR42-*rsp* pS2217	6850 ΔSSR42-*rsp* complemented in trans for ORF RSAU_002217 (*rsp*) under control of the native promotor	This study
6850 ΔSSR42-*rsp* pSSR42-2217	6850 ΔSSR42-*rsp* complemented in trans for SSR42, upstream ORF RSAU_002216 and *rsp* under control of the native promotors	This study
6850 ΔSSR42-*rsp* p2216-2218	6850 ΔSSR42-*rsp* complemented in trans for SSR42, upstream ORF RSAU_002216, *rsp* and downstream ORF RSAU_002218 under control of the native promotors	This study
6850 ΔSSR42-*rsp* pAHT-SSR42	6850 ΔSSR42-*rsp* complemented in trans for SSR42 under control of an AHT-inducible promotor	This study
6850 ΔSSR42-*rsp* pAHT-rsp	6850 ΔSSR42-*rsp* complemented in trans for RSAU_002217 (*rsp*) under control of an AHT-inducible promotor	This study
6850 ΔSSR42-spec^r	6850 with targeted deletion of ncRNA SSR42. SSR42 locus was exchanged with spectinomycin resistance cassette	This study
HG001 *lex*A-G94E	HG001, *lex*A-G94E	Schröder et al., 2013
HG001 *lex*A-G94E pP_{SSR42}-BgaB	HG001 *lex*A-G94E expressing BgaB under control of the promotor of SSR42; used for	This study

	analysis of SSR42 promotor activity in disc diffusion assays	
Escherichia coli		
DH5α	*fhu*A2 *lac(del)U169 pho*A *glnV44* Φ80' *lac*Z(del)M15 *gyr*A96 *rec*A1 *relA1 end*A1 *thi*-1 *hsd*R17*;* used for cloning	Hanahan, 1983; BRL Life Technology

3.1.2 Plasmids

Table 3.2: Used plasmids in this study.

Name	Description/ purpose	Source
p2085	Derivative of pALC2084 (Bateman et al., 2001), shuttle vector with pC194 and pUC19 backbones, containing *tet*R and $P_{xyl/tet}$ promoter driving GFPuvr expression, Cm^R	Giese et al., 2009
pBASE6	Derivate of pBT2 vector for targeted deletion	Geiger et al., 2012
pJL78	Vector expressing *gfp* in *S. aureus* under control of the constitutive sarAP1 promoter	Liese et al., 2013
pBASE6-SSR42	Derivate of pBASE6, plasmid for targeted, markerless deletion of SSR42	This study
pBASE6-SSR42-rsp	Derivate of pBASE6, plasmid for targeted, markerless deletion of SSR42 and ORF RSAU_002217 (*rsp*)	This study
pBASE6-SSR42-spek	Derivate of pBASE6, plasmid for targeted deletion of SSR42 and insertion of spectinomycin resistance cassette	This study
pSSR42	Complementation of SSR42; expression driven by native promotor	This study
pSSR42-rsp	Complementation of SSR42; expression driven by native promotor	This study
p2216-2218	Complementation of SSR42, upstream and downstream genes	This study
pS2217	Complementation of *rsp;* expression driven by native promotor	Das et al., 2016
pAHT-SSR42	Complementation of SSR42 under control of AHT-inducible promotor	This study
pAHT-rsp	Complementation of *rsp* under control of AHT-inducible promotor	This study

pS2217-3xFLAG	Complementation of *rsp* with triple FLAG-tag; expression driven by native promotor	Sudip Das, PhD thesis
pP_{agrP3}-GFP	GFP transcription under control of *agr* P3 Promotor; used for promotor activity studies	This study
pP_{SSR42}-GFP	GFP transcription under control of SSR42 Promotor; used for promotor activity studies	This study
pP_{rsp}-GFP	GFP transcription under control of *rsp* Promotor; used for promotor activity studies	This study
pP_{saeP1}-GFP	GFP transcription under control of *sae* P1 Promotor; used for promotor activity studies	This study
pP_{coa}-GFP	GFP transcription under control of *coa* Promotor; used for promotor activity studies	This study
pP_{hla}-GFP	GFP transcription under control of *hla* Promotor; used for promotor activity studies	This study
pP_{ldhD}-GFP	GFP transcription under control of *ldh*D Promotor; used for promotor activity studies	This study
p$P_{psm\alpha}$-GFP	GFP transcription under control of *psm*α Promotor; used for promotor activity studies	This study
pP_{SSR42}-BgaB	β-galactosidase (BgaB)transcription under control of SSR42 Promotor	Stefanie Feuerbaum; Master thesis
pRsp-P_{SSR42}-BgaB	β-galactosidase (BgaB)transcription under control of SSR42 Promotor; including ORF *rsp* (RSAU_002217)	Stefanie Feuerbaum; Master thesis
pSSR42Δ1	Complementation of SSR42 with small deletion in 2,352,023-2,352,099 bp; native promotor	This study
pSSR42Δ2	Complementation of SSR42 with small deletion in 2,352,157-2,352,221bp; native promotor	This study
pSSR42Δ3	Complementation of SSR42 with small deletion in 2,352,282-2,352,348 bp; native promotor	This study
pSSR42Δ4	Complementation of SSR42 with small deletion in 2,352,415-2,352,483 bp; native promotor	This study
pSSR42Δ5	Complementation of SSR42 with small deletion in 2,352,535-2,352,607 bp; native promotor	This study
pSSR42Δ6	Complementation of SSR42 with small deletion in 2,352,688-2,352,742 bp; native promotor	This study
pSSR42Δ7	Complementation of SSR42 with small deletion in 2,352,858-2,352,794 bp; native promotor	This study

pSSR42Δ8	Complementation of SSR42 with small deletion in 2,352,917-2,352,978 bp; native promotor	This study
pSSR42 mini-1	Derivate of pSSR42 for creation of minimal, 793 nt long ncRNA SSR42 mini-1; transcription driven by native promotor (deleted nucleotides: bp 2,352,219 -2,352,658)	This study
pSSR42 mini-2	Derivate of pSSR42 for creation of minimal, 643 nt long ncRNA SSR42 mini-1; transcription driven by native promotor (deleted nucleotides: bp 2,352,916-2,353,044)	This study
pGCG296	Complementation of *rny;* transcription driven by native promotor	Marincola et al., 2012
pSSR42-rsp-delRNaseY	Derivate of pSSR42-rsp with 69 nt deletion encompassing RNase Y cleavage site in SSR42 (bp 2,352,844-2,352914); SSR42 transcription driven by native promotor	This study
pSSR42-rsp-mutORF	Derivate of pSSR42-rsp encompassing a nucleotide exchange in the putative ORF 3 (bp 2,352,818); native promotor	This study
pSSR42-rsp-RNaseY_mutG	Derivate of pSSR42-rsp; SSR42 harbours a nucleotide exchange in the RNase Y-cleavage initiating guanosine (bp 2,352,899; G→ U)	This study
pAHT-SSR42-5ms2	AHT-inducible expression of SSR42 with 5´-ms2-tag; used for MS2-pulldown	This study
pAHT-MS2-Ter	AHT-inducible expression of ms2-tag; used for MS2-pulldown as negative control	This study
pMS2-Ter	Constitutive expression of ms2-tag; used for MS2-pulldown as negative control	This study
pAHT-SSR42-14mer	AHT-inducible expression of SSR42 with 5´-14 nt tag; used for oligo capture-pulldown	This study
pAHT-5S-14mer	AHT-inducible expression of 5S rRNA with 5´-14 nt tag; used for oligo capture-pulldown as positive control	This study
pAHT-14mer-Ter	AHT-inducible expression of 14 nt tag; used for oligo capture-pulldown as negative control	This study
pStemLoop2-Ter	Complementation plasmid for only a certain, stem loop featuring region of SSR42 (bp 2,351,984-	This study

	2,352,137); SSR42 transcription driven by native promotor

3.1.3 Cell lines

Table 3.3: Cell lines used in this study.

Cell line	Description	Source
HeLa 2000	Adherent tumour epithelial cell line; derived from human cervix adenocarcinoma	DSMZ; ACC 57
EA.Hy926	Human umbilical vein endothelial cells fused with permanent human cell line A549	Edgell et al., 1983

3.1.4 Oligonucleotides and Northern blot probes

Table 3.4: Oligonucleotides used for cloning.

Name	Sequence	purpose
Af_base6	CCGGAGCTCGGTACCCAACACTCTATTATCATTTTAT	Construction of various deletion and complementation constructs
Ar_SacII	CTAGCCGCGGCCGCACTATCTCTTTCTTTTTGTGTTTA	Construction of ΔSSR42 and ΔSSR42-*rsp*
Br_Base6	GATCTGCGCGCTAGCCCGACGATCTAAATAACCAT	Construction of ΔSSR42
Bf_SacII	TGCGGCCGCGGCTAGCACCAAATAATTTAATTAGAC	Construction of ΔSSR42
Cr_BASE6	GATCTGCGCGCTAGCCCAGCTAACATGTTCAATTGCTGG	Construction of various deletion and complementation constructs
Cf_SacII	TGCGGCCGCGGCTAGTACTAACAGTCCTCTTGTGTTTAG	Construction of ΔSSR42-*rsp*
upstream A	TGCTTATAATTCATATATTTAGCCTCC	Verification of SSR42 and SSR42-*rsp* deletion mutant
downstream B	TCTATAATACTTTGACCTATAATTTTCCCC	Verification of SSR42 deletion mutant
downstream C	TATTACATAAAATTAATTTAAAAAGACACACC	Verification of SSR42-*rsp* deletion mutant
vek_pbase-SSR4_F	TTTATTACTTTAATTTACCGCGGCTAGCACCAAATAATTTAATTAGAC	Construction of SSR42 deletion construct harbouring spectinomycin resistance cassette
vek_pbase-SSR4_R	TACTCTTCTTTTTAAGGGTGCCGCGGCCGCACTATCTCTTTCTTTTTG	Construction of SSR42 deletion construct harbouring spectinomycin resistance cassette

inf-spek F	TAGTGCGGCCGCGGCACCCTTAAAAAAGAAGAGTAATGGAATTAGAAAAAG	Construction of SSR42 deletion construct harbouring spectinomycin resistance cassette
inf-spek r	TTGGTGCTAGCCGCGGTAAATTAAAGTAATAAAGCGTTCTCTAATTTC	Construction of SSR42 deletion construct harbouring spectinomycin resistance cassette
delspek	TAGCCAAATCAGGATCATAGCTTGGTTCCTG	Verification of SSR42 deletion mutant with spectinomycin resistance
compvek-f	GGGCTAGCGCGCAGATCTGTCGACGACTGGCCGTCGTTTTACAAC	Cloning of pSSR42, pSSR42-rsp and p2216-2218
compvek-r	GGTACCGAGCTCCGGAATTCGTCGAGTTATCGATACCGTC	Cloning of pSSR42, pSSR42-rsp and p2216-2218
comp_no_rsp_rev	GATCTGCGCGCTAGCCCGTTGAATATTTTTGAAAAGGTAATAGTG	Cloning of pSSR42
comp_no2218_r	GATCTGCGCGCTAGCCCCTTATGATATAAATAGCCTTTACG	Cloning of pSSR42-rsp
Ssr-vec-f_vec1-f	CTATCTCTTTCTTGAATTCACTGGCCGTCGTTTTACAAC	Cloning of pAHT-SSR42 and pAHT-SSR42-5ms2
ssr-vec-r_vec1-r	GTTTGAAATCTATATTAAACGCGTTATTTTAATTATACTCTATC	Cloning of pAHT-SSR42 and pAHT-SSR42-5ms2
ssr42-r	CGACGGCCAGTGAATTCAAGAAAGAGATAGATTG	Cloning of pAHT-SSR42
ssr42-f	TAACGCGTTTAATATAGATTTCAAACC	Cloning of pAHT-SSR42
2217ORF-PmeI-f	GACGTTTAAACATGACATGCCAACTTAAAATACATC	Cloning of pAHT-rsp
2127ORF_EcoRI_R	AATATAGAATTCCCTCATTAGCTAGGTTTAAAGCAAATATATTTAA	Cloning of pAHT-rsp
2217_ssrProm-SF-r	GATGAATTCATTAATTATGCACCAAATAATTTAATTAGAC	Cloning of pJL78-P_{rsp}-gfp
2217_ssrProm-SF-f	GATCGGTACCAGCATGCTTAGCTAGGTTTAAAGC	Cloning of pJL78-P_{rsp}-gfp
bgab-sf-f	CATCGAATTCTTAGGAGGTGATTATTTATGAATGTGTTATCCTCAATTTG	Cloning of pRsp-P_{SSR42}-BgaB
bgab-sf-r	CTATGGCGCGCCCTAAACCTTCCCCGGCTTCATCATGC	Cloning of pRsp-P_{SSR42}-BgaB
pGFP-Inf-Prom F	GAATTCTTAGGAGGATGATTATTTATGAGTAAAGGAGAAGAAC	Cloning of GFP-promotor reporter plasmids (*hla*, *coa*, *rsp*, *ldh*D, *psm*α)
pGFP vec R	GCATGCAAGCTTTTAAAAAGCAAATATGAGCCAAATAAA	Cloning of GFP-promotor reporter plasmids (*hla*, *coa*, *rsp*, *ldh*D, *psm*α)

P3-Inf-Prom F	TTTAAAAGCTTGCATGCTCACTGTCATTATACGATTAG TACA	Cloning of pP_{agrP3}-GFP
P3-Inf-Prom R	CATCCTCCTAAGAATTCTCTAGTTATATTAAAACATGC TAAAAGCATTTA	Cloning of pP_{agrP3}-GFP
hla-Inf-Prom R	CATCCTCCTAAGAATTCTATTTTTTAAAACGATTTGAG GAAACAATAA	Cloning of pP_{hla}-GFP
hla prom F	CTAGCATGCTCCTGAATTTTTCGAAATTTTATAG	Cloning of pP_{hla}-GFP
Rsp-Inf-Prom F	TTTAAAAGCTTGCATGCTGCACCAAATAATTTAATTAG ACT	Cloning of pP_{rsp}-GFP
rsp-Inf-Prom R	CATCCTCCTAAGAATTCTATACCTATTATAGTTGAATA TTTTTGAAAA	Cloning of pP_{rsp}-GFP
SaeP1 rev	CATCCTCCTAAGAATTCTGTTAAGTTTAAAATGAAGGC AAATAATATG	Cloning of pP_{saeP1}-GFP
SaeP1 fwd	TTTAAAAGCTTGCATGCTAATACCAAAACTATAAAAC ACTTCTG	Cloning of pP_{saeP1}-GFP
coa Prom Inf R2	CCTCCTAAGAATTCAATTTTTTAATTCCTCCAAAATGTA ATTGCCC	Cloning of P_{coa}-GFP
coa Prom Inf F2	TTTAAAAGCTTGCATGCTTTCATTCGTTTATAATCATAT GACAAG	Cloning of P_{coa}-GFP
PpsmA1 F	TTTAAAAGCTTGCATGCCTGCATAACCTCCTTATTTCT AATCTCTCGC	Cloning of $P_{psm\alpha}$-GFP
PpsmA1 R	CATCCTCCTAAGAATTCTAAGATTACCTCCTTTGCTTAT GAGTTAACT TC	Cloning of $P_{psm\alpha}$-GFP
PldhD F2	TTTAAAAGCTTGCATGCGCTCGCTGTATCTAATTGTTT CGCTGCAC	Cloning of P_{ldhD}-GFP
PldhD R2	CATCCTCCTAAGAATTCTATTAAAAACCTCGCTTTTAA AAGATTGAAA AGTAAATG	Cloning of P_{ldhD}-GFP
P3-Inf-Prom R	CATCCTCCTAAGAATTCTCTAGTTATATTAAAACATGC TAAAAAGCATT	Cloning of P_{agrP3}-GFP
P3-Inf-Prom F	TTTAAAAGCTTGCATGCTCACTGTCATTATACGATTTA GTACA	Cloning of P_{agrP3}-GFP
sig-S-Dr-Base6	GATCTGCGCGCTAGCCCGCCTGTTACCTTGCTAATGC	Construction of Δ*sig*S
SSR42 trunc 2 fwd	CCCTTAATTATTACATTGTTTAGTAGAAATTGAGTGTG AAAGT	Construction of pSSR42Δ1
SSR42 trunc 2 rev	TAAACAATGTAATAATTAAGGGTATAAATTG	Construction of pSSR42Δ1
SSR42 trunc 3 fwd	CTAGTAACATAATTAATTCGCTATTCTAGATGAGTTTC TTAG	Construction of pSSR42Δ2
SSR42 trunc 3 rev	GAATTAATTATGTTACTAGCTAAATCATC	Construction of pSSR42Δ2

SSR42 trunc 4 fwd	ATGAAGTTATCTATGATGTTACTATCTTGGTGACGTTTCTAG	Construction of pSSR42Δ3
SSR42 trunc 4 rev	TAACATCATAGATAACTTCATCAAGACAGG	Construction of pSSR42Δ3
SSR42 trunc 5 fwd	TGATGTAAAATCTAAGATGTTGCATTTTCTCATGATGAATC	Construction of pSSR42Δ4
SSR42 trunc 5 rev	AACATCTTAGATTTTACATCAAGAGATGCG	Construction of pSSR42Δ4
SSR42 trunc 6 fwd	TCATTGATGTGTGCTGTTTCCGGCAATAACTAGATGGATT	Construction of pSSR42Δ5
SSR42 trunc 6 rev	GAAACAGCACACATCAATGAATTAACACC	Construction of pSSR42Δ5
SSR42 trunc 7 fwd	TAGATGTTTATACTTATCTTGGTTGTTGATTTGAATAATTTG	Construction of pSSR42Δ6
SSR42 trunc 7 rev	CAAGATAAGTATAAACATCTAGAAAAGTG	Construction of pSSR42Δ6
SSR42 trunc 8 fwd	TTGTAACAGGGCTACTAAGAACCAAACTTAAATAATGGCG	Construction of pSSR42Δ7
SSR42 trunc 8 rev	TTCTTAGTAGCCCTGTTACAAAATATTCG	Construction of pSSR42Δ7
SSR42 trunc 9 fwd	TACATTTAATGTTTTTTGATTGCAAGTTAGTTCAAAATGGC	Construction of pSSR42Δ8
SSR42 trunc 9 rev	AATCAAAAAACATTAAATGTACCCATGAC	Construction of pSSR42Δ8
miniSSR42_1J rev	CTTATCTTGATGTTTTCTAAACAGAACTTTTAAACG	Cloning of minimal SSR42 complementation plasmid pSSR42 mini-1
miniSSR42_1J fwd	GTTCTGTTTAGAAAACATCAAGATAAGTTCATCAAGAACAGTATCTAAC	Cloning of minimal SSR42 complementation plasmid pSSR42 mini-1
miniSSR42_2 rev	TTATGCACCAAATAATTTAATTAGACTC	Cloning of minimal SSR42 complementation plasmid pSSR42 mini-2
miniSSR42_2 fwd	TAAATTATTTGGTGCATAACATTAAATGTACCCATGACTTAA	Cloning of minimal SSR42 complementation plasmid pSSR42 mini-2
dRnaseY-rev	GATTCAAACTTCCATTTTGGTCAATTTGC	Cloning of plasmid pSSR42-rsp-delRNaseY
dRnaseY-fwd	CCAAAATGGAAGTTTGAATCCATCAAACGCTGAAAATTAGTAC	Cloning of plasmid pSSR42-rsp-delRNaseY
RNaseY G mut R	TTTAAGTCATGGGTATATTTAATGTTTTTTG	Cloning of plasmid pSSR42-rsp-RNaseY_mutG

RNaseY G mut F	CAAAAAACATTAAATATACCCATGACTTAAA	Cloning of plasmid pSSR42-rsp-RNaseY_mutG
deltaOrfL-r	CAAGAAGTGATTTCGATCGTACTAATTTTC	Cloning of plasmid pSSR42-rsp-mutORF
deltaOrfL-F	GAAAATTAGTACGATCGAAATCACTTCTTG	Cloning of plasmid pSSR42-rsp-mutORF
Stem loop 2 neu R	CAGGTCGTCCTGCTGGCAGATACCATACACATTTAATTAGTTACAGC	Cloning of plasmid pStemLoop2-Term
Stem loop 2 neu F	GTATAATTAAAATAACGTGACTATATATGAATTAATTATGTTACTAG	Cloning of plasmid pStemLoop2-Term
Vek Term F2	GCCAGCAGGACGACCTGCTGGTTTT	Cloning of plasmid pStemLoop2-Term
Vek Term R	CGTTATTTTAATTATACTCTATCAATGATAGAGTGTC	Cloning of plasmid pStemLoop2-Term
5ms2-fwd	CAGGGTACGTTTTTCAGACACCATCAGGGTCTGCAGTTAATATAGATTTC	Cloning of plasmid pAHT-SSR42-5ms2
5ms2-rev	GTCTGAAAAACGTACCCTGATGGTGTACGCGTATTTTAATTATACTCTATC	Cloning of plasmid pAHT-SSR42-5ms2
PE-term-f	GCCAGCAGGACGACCTGCTGGTTTTTTTTG	Cloning of pAHT-MS2-Ter
PE-term-r	AATTCAAAAAAAACCAGCAGGTCGTCCTGCTGGCTGCA	Cloning of pAHT-MS2-Ter
deltaTetRf	TAATTCCTCCTTTTTGTTGACACTC	Cloning of pMS2-Ter
deltaTetRr	AAGCAGCATAACCTTTTTCCGTGATGG	Cloning of pMS2-Ter
Oligo capture	2´MeOH-AGGCUAGGUCUCCC-Biotin	Oligo-capture pulldown

Table 3.5: Oligonucleotides used for Quantitative real time PCR.

Name	Sequence 5´-3´	target
RT-gyrB-F	CGACTTTGATCTAGCGAAAG	*gyr*B
RT-gyrB-R	ATAGCCTGCTTCAATTAACG	*gyr*B
RT agrB F	GCAGGTCTTAGCTGTAAATATAGG	*agr*B
RT agrB R	CACCATGTGCATGTCTTC	*agr*B
RT-RNAIII-F	ACATAGCACTGAGTCCAAGG	RNAIII
RT-RNAIII-R	TCGACACAGTGAACAAATTC	RNAIII
RT-saeS-F	TTGCAACCATATGAGCAAC	*sae*S
RT-saeS-R	AATATCAATGCGACTACCAAC	*sae*S

RT-SSR42-F	TATCTTGTTGCTGCTAATTCTATTG	SSR42
RT-SSR42-R	CACCTAACATCAAAGAATATTCATC	SSR42
RT-2217-F	TTCACTCGTTTCCAAGATTAC	*rsp*
RT-2217-R	GACTTCGATCTTTCGGATT	*rsp*
RT-hla-F	CAATTTGTTGAAGTCCAATG	*hla*
RT-hla-R	GATCCTAACAAAGCAAGTTCTC	*hla*
RT-CHIPS-F	ATCAGTACACACCATCATTCAG	*chs*
RT-CHIPS-R	ATCAGTACACACCATCATTCAG	*chs*
RT-scpA-F	TTAATGTCGAGGACAAGAGTG	*scp*A
RT-scpA-R	GGTTCACCAAGTGTATACGAG	*scp*A
RT_2216_F	AATGCTTTTGATCATATGTGG	RSAU_2216
RT_2216_R	TCTAATAAAGTTTGGGTGTCGA	RSAU_2216
isdB-RT-F	GGTTTACAATCAGGTCAATTTT	*isd*B
isdB-RT-R	TGAGTTGAACTTACAATTTTAACG	*isd*B
clfA-RT-F	GTGACGGTATCGATAAACCT	*clf*A
clfA-RT-R	TCTGAACCGCTATCTGAATC	*clf*A
ffh-RT-F	GTAGGGAAACAAATTGATATTCC	*ffh*
ffh-RT-R	GTTCATCAATGCTTCATCG	*ffh*
WxG-RT-F	GAGTCCAGAGGAAATCAGAG	*esx*A
WxG-RT-R	GACTAAGTTGTTGGAATTGCTC	*esx*A
RT-PSMalpha-f	GGCCATTCACATGGAATTCGT	*psmα*
RT-PSMalpha-r	GCCATCGTTTTGTCCTCCTG	*psmα*
ureB-RT-F	CTCCAGCTGGAATATCTAAATG	*ure*B
ureB-RT-R	CAGAGGTTGAAATTAATAACCAT	*ure*B
capD-RT-F	CAGCTGAAAAAAGTTGAAGTAG	*his*D
capD-RT-R	CGTTCTGGATAGAAATTACAAAC	*his*D
ldhD-RT-F	CACAACATTGTGATATCTAACGT	*his*D
ldhD-RT-R	TGGTTTAGACATGATTTCTGC	*his*D
coa RT F	AGTGACGAATCAACGTACTG	*coa*
coa RT R	AGCATCAAATCCATCTTTATG	*coa*
eap RT F	CCCAGTAACAATAAATAAATTTGA	*eap*
eap RT R	ACACTTTATACACTGCGCG	*eap*
emp RT F	GTACAAAGAAATTAATAATCGCG	*emp*
emp RT R	CTTTCTTGTAGTGGGTTTGC	*emp*
hisD RT F	AGCATATCAAGAAAGTATTAAGCA	*his*D
hisD RT R	CTTGTGCTAAAGTCGCTGT	*his*D
isaB RT F	ACCAGTAAAGTTTGTGTAGCAG	*isa*B

isaB RT R	CCAGAATAAAATTAGCATTATTACC	*isa*B
ssaA3 RT F	AGGTAACTACCATTACACATGGA	*ssa*A3
ssaA3 RT R	GTAGTTGTTGTAACGGCTGTAG	*ssa*A3
RT-lukG-forward	CATGACCATACGAGACAATTAAC	*luk*G
RT-lukG-reverse	GATTAAACCCTTCAGACACAGT	*luk*G
RT-sigB-F	CTTTGAACGGAAGTTTGAAG	*rpo*F
RT-sigB-R	GGCCCAATTTCTTTAATACG	*rpo*F
codY RT F	GGAAATCTTACGTGAGAAGC	*cod*Y
codY RT R	CAACTTTTGATGCGATTAATAG	*cod*Y
pSL RT F	TCACACTCAATTTCTACATCTAATCATC	SSR42 pStemLoop2
pSL RT R:	ACCATACACATTTAATTAGTTACAGC	SSR42 pStemLoop2

Table 3.6: Northern blot probes used in this study.

Name	Sequence 5´-3´	target
RT-SSR42-F	TATCTTGTTGCTGCTAATTCTATTG	SSR42 = probe 2
RT-SSR42-R	CACCTAACATCAAAGAATATTCATC	
NB-SSR42-up-F	ATAGATTTCAAACCTATGTATTTC	SSR42 5´end = probe 1
NB-SSR42-up-R rev	ATAAAATTTAAGTCATGGGTAC	
RT-saeS-F	TTGCAACCATATGAGCAAC	*saeS*
RT-saeS-R	AATATCAATGCGACTACCAAC	
SSR42 trunc-RT rev	TTTCTAAACAGAACTTTTAAACGC	SSR42 minimal versions =
SSR42 trunc-RT fwd	TATCGCCATTATTTAAGTTTGG	probe 3

Table 3.7: Antibodies

Name	Origin	Dilution	Reference
α-toxin	rabbit polyclonal	1:2000	Sigma
SaeS	rabbit polyclonal	1:1000	Jeong et al., 2011
SaeR	rabbit polyclonal	1:1000	Jeong et al., 2011
FLAG	mouse monoclonal	1:1000	Sigma

3.1.5 Media and buffers

Table 3.8: Cell culture media.

Media and solutions for cell culture	ingredients
RPMI full medium	RPMI 1640 Glutamax™

	10% FCS
	Penicillin-Streptomycin (1000 U/ml)
	Sodium Pyruvate (1 mM)
RPMI infection medium	RPMI 1640 Glutamax™
	10% FCS
	Sodium Pyruvate (1 mM)
LDH assay medium	RPMI 1640 Glutamax™ (without phenol red)
	1% FCS
	Sodium Pyruvate (1 mM)
Cryopreservative medium	90% FCS
	10% DMSO
Dulbecco's Phosphate Buffer Saline (1x)	1x PBS

Table 3.9: Bacterial culture media used in this study.

Bacterial culture media	ingredients
50% Glucose solution	D-(+)-Glucose (500 g/l) in dH_2O
Tryptic Soy Broth (TSB)	27.5 g/l Tryptone Soya Broth without glucose
	5 ml/l 50% glucose solution
Tryptic Soy Agar (TSA)	30 g/l Tryptic Soy Broth
	15 g/l European agar
Columbia Blood Agar	44 g/l Columbia Blood agar base
	5% v/v defibrinated sheep blood
Müller-Hinton Agar	23 g/l Müller-Hinton broth
	15 g/L European agar
Luria-Bertani broth (LB)	10 g/l Tryptone
	10 g/l NaCl
	5 g/l yeast extract
Luria-Bertani agar	10 g/l Tryptone
	10 g/l NaCl
	5 g/l yeast extract
	15 g/l European agar
Luria-Bertani softagar	10 g/l Tryptone
	10 g/l NaCl
	5 g/l yeast extract
	6 g/l European agar
Phage top agar	10 g/l Tryptone
	10 g/l NaCl

	5 g/l yeast extract
	6 g/l European agar
	20 mM $Na_3C_6H_5O_7$

Table 3.10: Buffers for cloning used in this study.

Buffer	Composition
Annealing buffer	100 mM NaCl
	50 mM Tris-HCl pH 7.9
	10 mM $MgCl_2$
	1 mM DTT

Table 3.11: Buffers for agarose gel electrophoresis, SDS-PAGE, staining and Western blot.

Buffer	Composition
1 x TAE buffer	40 mM Tris-HCl (pH 8.5)
	1 mM EDTA
	20 mM acetic acid
2.5 x Laemmli buffer	62.5 mM Tris-HCl pH 8
	10% (w/v) glycine
	2% (w/v) SDS
	5% (w/v) 2-mercaptoethanol
	0.05 % (w/v) bromphenol blue
SDS-PAGE running buffer	25 mM Tris
	0.25 M glycin
	0.1% (w/v) SDS
4% PAA stacking gel	1 ml Acrylamid/bis (37.5/1)
	750 µl 1.5 M Tris pH 6.8
	0.1 % (w/v) SDS
	4.1 ml dH_2O
	60 µl 10 % (w/v) ammonium persulphate (APS) 4 µl tetramethylethylenediamine (TEMED)
12% PAA dissolving gel	4 ml Acrylamid/Bis (37.5/1)
	2.5 ml 1.5 M Tris pH 8.8
	0.1 % (w/v) SDS
	3.3 ml dH_2O

	100 µl 10 % (w/v) ammonium persulphate (APS) 8 µl tetramethylethylenediamine (TEMED)
Colloidal coomassie fixation solution	7% acetic acid 40% methanol
Colloidal coomassie staining solution A	2.375% phosphoric acid, 10% (w/v) ammonium sulphate
Colloidal coomassie staining solution B	5% (w/v) Coomassie G-250
Colloidal coomassie neutralization solution	1.2% (w/v) Tris, adjust with phosphoric acid to pH 6.5
Colloidal coomassie washing solution	25% methanol
Silver staining fixation solution	50% (v/v) ethanol 12% (v/v) acetic acid 0.5 ml/L formaldehyde (37%)
Silver staining washing solution	50% (v/v) ethanol
Silver staining senistizing solution	0.2 g/l $Na_2S_2O_3$ x $5H_2O$
Silver staining solution	2 g/l $AgNO_3$ 0.750 ml/l formaldehyde (37%)
Silver staining developer	60 g/l Na_2CO_3 4 mg/l $Na_2S_2O_3$ x $5H_2O$ 0.5 ml/l formaldehyde (37%)
Silver staining stop solution	1% (v/v) glycine
1 x TBS (tris buffered saline)	20 mM Tris-HCl pH 7.6 137 mM NaCl
1 x TBS-T	20 mM Tris-HCl pH 7.6 137 mM NaCl 0.05% (w/v) Tween-20
Transferbuffer	44 mM Tris 40 mM glycine 1.3 mM SDS 20% (v/v) methanol
Western blot blocking buffer	1x TBS-T 5% non-fatty milk powder
ECL solution 1	2.5 mM luminol 0.4 mM p-coumaric acid
ECL solution 2	100 mM Tris-HCl pH 8.5 0.02% H_2O_2

Table 3.12: Buffers for RNA extraction, gels and Northern blots.

Buffer	Composition
Buffer A	10 % (v/v) glucose 12.5 mM Tris-HCl pH 7.6 10 mM EDTA
10x MOPS running buffer	0.2 M 3-(N-Morpholino)propanesulfonic acid 10 mM EDTA 50 mM sodium acetate 40 mM NaOH
RNA loading dye	750 µl deionized formamide 150 µl 10x MOPS buffer 262 µl 37% formaldehyde 50 µg ethidiumbromide
Blue juice	65% sucrose 10 mM Tris-HCl pH 7.5 10 mM EDTA 0.3% (v/v) bromphenol blue 0.3% (v/v) xylenecyanol
1% agarose RNA gel	0.8 g agarose 68 ml DEPC-treated H_2O 8 ml 10x MOPS 4 ml 37% formaldehyde
5x phosphate buffer	0.5 M Na_2HPO_4 0.5 M NaH_2PO_4
Alkaline transfer buffer	3 M NaCl 2mM N-Lauroylsarcosin 8 mM NaOH
20x SSC	3 M NaCl 0,3 M $Na_3C_6H_5O_7$ pH 7
High SDS hybridization buffer	2.5 M SSC 100 ml 10x blocking solution (Roche Digoxigenin labeling and detection kit)
Buffer 1	100 mM maleic acid 150 mM NaCl adjust to pH 7.5
Washing buffer	Buffer 1 + 0.3% (v/v) Tween-20

Blocking solution (Buffer 2)	Buffer 1 1x blocking solution (Roche Digoxigenin labeling and detection kit)
Buffer 3	100 mM Tris-HCl pH 9.5 100 mM NaCl 50 mM $MgCl_2$
Oligo-capture pulldown lysis buffer	50 mM Tris-HCl pH 8 150 mM KCl 5% glycerol 1 mM DTT 1 mM AEBSF 1 mM $MgCl_2$ 0.05 % Tween-20
Oligo-capture pulldown wash buffer 1	Lysis buffer + 300 mM KCl
Oligo-capture pulldown wash buffer 2	Lysis buffer + 0.1% Triton X-100
MS2 pulldown lysis buffer	20 mM Tris pH8.0 150 mM KCl 1 mM $MgCl_2$ 1 mM DTT
MS2 pulldown lysis buffer	Lysis buffer + 15 mM maltose

Table 3.13: Buffer for working with *S. aureus.*

Buffer	Composition
Electroporation buffer:	0.5 M saccharose 10% (v/v) glycerol
Phage buffer	LB media 0.5 mM $CaCl_2$
Genomic DNA lysis buffer	200 µg/ml lysostaphin 20 mM Tris-HCl pH 8.0 2 mM EDTA 1.2% (v/v) Triton X-100 160 µg/ml RNase A
Protein lysis buffer	20 mM Tris-HCl pH 8.0 150 mM KCl 1 mM $MgCl_2$ 1 mM DTT

3.1.6 Antibiotics and chemicals

Table 3.14: Concentration of antibiotics used in this study.

Antibiotic stock solutions	Composition
Chloramphenicol	10 µg/ml in EtOH for selection of *S. aureus*
Erythromycin	5 µg/ml in EtOH for selection of *S. aureus*
Ampicillin	100 µg/ml in dH_2O for selection of *E. coli*
Spectinomycin	150 µg/ml in dH_2O for selection of *S. aureus*
Anhydrous tetracycline	200 µg/ml in EtOH for induction of inducible plasmids in *S. aureus*

Table 3.15: Chemicals used in this study.

Chemicals	Manufacturer
Acrylmide Rotiphorese Gel 30 (37.5:1)	Carl-Roth
Ammonium persulphate (APS)	Merck
Ampicillin	Carl-Roth
Antimicrobial Susceptibility Discs	Thermo Scientific (Oxoid)
Aqua-Phenol	Carl-Roth
Chloramphenicol	Sigma
Columbia blood agar base	Sigma
Coomassie G-250	Carl-Roth
D-(+)-Glucose	Sigma
Diethylpyrocarbonat (DEPC)	Carl-Roth
Dimethyl sulfoxide (DMSO)	Intas
dNTPS	Genaxxon Bioscience
Dulbecco's Phosphate Buffer Saline (1x)	Sigma
European agar	Oxoid
Erythromycin	Carl-Roth
Fetal calf serum	GIBCO
Intas HD Green	Quanta Biosciences
Lysostaphin	Carl-Roth
MIC strips (Oxacillin, Imipenem)	Thermo Scientific (Oxoid)
Müller-Hinton broth	BD
Penicillin-Streptomycin	GIBCO
Rifampicin	Fluka Analytica
RPMI 1640 Glutamax™	GIBCO
Sodium Pyruvate	PAA

Spectinomycin	AppliChem
Tetramethylethylenediamine (TEMED)	Fluka Analytics
TRI Reagent™ Solution	Thermo Scientific
Tryptone	BD
Tryptone Soya Broth without Dextrose	Sigma (Lot: BCBP7262V)
Tryptic Soy Broth	Sigma (Lot: SLBW1709)
Quanta Biosciences Perfecta SYBR Green FastMix	Quanta Biosciences
Yeast extract	Carl-Roth

All other chemicals were obtained from Carl-Roth, Sigma-Aldrich, Serva, Merck Chemicals or Fluka Analytica if not stated otherwise.

3.1.7 Enzymes

Table 3.16: Enzymes used in this study.

Enzymes	Manufacturer
Restriction enzymes	Thermo Scientific
Phusion High-Fidelity DNA polymerase	Thermo Scientific
Taq Polymerase	Genaxxon Bioscience
T4 DNA ligase	Thermo Scientific
FastAP (Thermosensitive alkaline phosphatase)	Thermo Scientific
TURBO™ DNase	Thermo Scientific
RNase A	Thermo Scientific
T4 DNA ligase	Thermo Scientific
T4 Polynucleotide kinase (PNK)	Thermo Scientific

3.1.8 Size standards

Table 3.17: Size standards used in this study.

Size standard/ loading dye	Manufacturer
GeneRuler 1 kb DNA ladder	Thermo Scientific
GeneRuler 50 bp DNA ladder	Thermo Scientific
Page Ruler Prestained Protein Ladder	Thermo Scientific
RNA Molecular Weight Marker I, DIG-labeled	Sigma Aldrich
loading dye 6x	Thermo Scientific

3.1.9 Kits

Table 3.18: Kits used in this study.

Name	Purpose	Manufacturer
Cytotoxicity Detection Kit (LDH)	Cytotoxicity assay	Roche
In-Fusion HD Cloning Kit	Cloning	Takara
NucleoSpin Gel and PCR Clean up	PCR purification	Machery-Nagel
NucleoSpin Plasmid QuickPure	Plasmid isolation *E. coli*	Machery-Nagel
QIAmp DNA Mini Kit	Genomic DNA isolation	Qiagen
QIAprep Spin Miniprep Kit	Plasmid isolation *S. aureus*	Qiagen
RevertAid First Strand cDNA Synthesis Kit	Reverse transcriptase	Thermo Scientific
TURBO DNA free kit	Digestion of DNA	Thermo Scientific
DIG DNA labeling and detection kit	Labeling of DNA probes and detection of RNA via Northern blot	Sigma-Aldrich

3.1.10 Technical equipment

Table 3.19: Technical equipment used in this study

Equipment	Manufacturer
Autoclave	WEBECO, Sytec VX 150
Chemiluminescence camera system (Intas LabImage Chemostar)	Intas
Electrophoresis power supplies (Peqlab EV202)	Peqlab Biotechnology
FastPrep FP120	MP Biomedicals
Gel imager (BiostepDark hood DH-40/50)	Biostep GmbH
Megafuge 1.0R	Heraeus
MicroPulserTM	Bio-Rad
Microcentrifuge (Hettich MIKRO 200)	Hettich Lab tech
NanoDrop 1000 spectrophotometer	Peqlab Biotechnology
PCR Thermocycler (PEQLAB peqSTAR)	VWR International
PerfectBLue^{TM} Gel system	Peqlab Biotechnology
PerfectBLue^{TM} Semi-Dry Elektroblotter	Peqlab Biotechnology
pH electrode SenTix	WTW series inolab
Photometer Ultraspec 3100 Pro	Amersham Biosciences
Plate reader (TECAN Infinite M200)	TECAN
refrigerated Microcentrifuge (Hitachi himac CT15RE)	Hitachi-Koki

Step One Plus real-time PCR system	Applied Biosystems
Thermo mixer comfort	Eppendorf
UV Crosslinker	Stratalinker
Vortex REAX 2000	Heidolph

3.1.11 Applied Software

Table 3.20: Applied Software and web tools.

Software	Manufacturer/ homepage
ApE A plasmid Editor 8.5.2.0	M. Wayne Davis (biologylabs.utah.eu)
Argus x1 version 7.6.17	Biostep GmbH
Artemis	Sanger Institute
CLC Workbench tool	QIAGEN Bioinformatics
Coral Draw X8	Corel Corporation
CodonCode Aligner 4.0.4	CodonCode Corporation
EndNoteX8.1	Thomson Reuters
ImageJ	W. Rasband, National Institutes of Health; Schneider et al., 2012
IntaRNA	http://rna.informatik.uni-freiburg.de/IntaRNA
LabImage Chemostar	Intas, Science imaging
NCBI blast	http://blast.ncbi.nlm.nih.gov
ND-100 V3.7.1	NanoDrop Technologies, Inc. Wilmington
Office 2010	Microsoft
Pfam	https://pfam.xfam.org
RNAfold	http://rna.tbi.univie.ac.at/cgi-bin/RNAWebSuite/RNAfold.cgi
StepOne Software v.2.3	Life Technologies
TECAN i-Control	TECAN

3.2 Methods

3.2.1 Cultivation of bacteria

3.2.1.1 Bacterial culture conditions

For growth of *Escherichia coli* LB broth or agar supplemented with the required antibiotics was used. All *Staphylococcus aureus* strains were grown on Tryptic soy agar (TSA), or in Tryptic soy broth supplemented with glucose (0.25%, w/vol) and appropriate antibiotics. All strains were cultivated aerobically at 37°C overnight at 180 rpm. Only when bacteria were transformed with plasmid pBASE6, harbouring a temperature sensitive origin of replication, bacteria were grown aerobically overnight at 30°C.

3.2.1.2 Bacterial cryo-stocks for preservation

For generation of bacterial cryo-stocks bacteria were grown in liquid culture and mixed with sterile 50% glycerol to an end concentration of 12.5% (v/v) and stored at -80°C.

3.2.1.3 Bacterial growth curves and determination of minimum inhibitory concentration (MIC)

In order to determine differences in growth bacterial growth was recorded over time in a 48 micro-well plate using a TECAN Infinite M200 plate reader. For this, *S. aureus* strains were grown overnight in TSB in triplicates. Bacterial cultures were diluted to an OD_{600} of 0.1 in 400 µl fresh TSB. Sterile medium was used as a reference. The plate reader was preheated to 37°C before starting the measurement. Optical density at 600 nm was measured every ten minutes for a time course of 23 h. The micro-well plate was shaken between each measurement at an amplitude of 6 mm.

When the MIC of a test substance was investigated, the respective substance was added directly to the bacterial cultures at t=0. Growth rates were determined from the mean of all three biological replicates at every time point.

3.2.1.4 Determination of MIC of antibiotics on agar plates

To determine the MIC of antibiotics *S. aureus* strains were grown aerobically overnight in Müller-Hinton broth at 37°C. Bacterial cultures were normalized to their optical densities and plated on Müller-Hinton agar. Commercially available MIC strips were laid on top. The plates were incubated overnight at 37°C. The minimum inhibitory concentration was determined according to the manufacturer´s instructions.

3.2.2 Genetic manipulation of bacteria

3.2.2.1 Preparation of competent *E. coli*

E. coli DH5α were grown overnight at 37°C in 10 ml LB. 100 ml fresh LB was inoculated with 1 ml of the overnight culture and grown until logarithmic growth phase was reached (OD_{600} 0.4-0.7). Bacteria were harvested at 4000 rpm for 10 min, resuspended in 20 ml 0.1 M $CaCl_2$ and incubated on ice for 30 min. Afterwards bacteria were harvested again and resuspended in 10 ml 0.1 $CaCl_2$ containing 20% glycerol. Bacteria were aliquoted and stored at -80°C.

3.2.2.2 Transformation of *E. coli*

100 µl of chemically competent *E. coli* were thawed on ice and incubated with a plasmid on ice for 30 minutes. Bacteria were heat-shocked for 90 sec at 42°C and chilled afterwards for 2 min on ice. After addition of 1 ml LB bacteria were incubated for 1 h at 37°C and 180 rpm shaking. After incubation bacteria were plated on LB agar supplemented with the respective antibiotics.

3.2.2.3 Preparation of electro-competent *S. aureus*

S. aureus strains were grown overnight at 37°C. Bacterial cultures were diluted to OD_{600}=0.05 in 100 ml fresh TSB. Bacteria were grown aerobically at 37°C and 180 rpm until OD_{600}=0.6-0.8 was reached. Bacteria were incubated on ice for 15 min before harvested at 3000 x g for 10 min at 4°C. Bacterial pellet was washed three times with 30, 25 and 10 ml of sterile ice-cold water. Pellet was afterwards washed twice with 10 and 5 ml of ice cold sterile 10% glycerol and harvested at 3500 x g for 15 min. After the last washing step the pellet was resuspended in 1-2.5 ml ice cold 10% glycerol and divided into 50 µl aliquots which were kept at -80°C.

3.2.2.4 Electroporation of *S. aureus*

Electro-competent *S. aureus* were thawed for 5 min on ice. After incubation for 15 min at room temperature, 120 µl of electroporation buffer and 5 µg of plasmid DNA were added. This mixture was incubated for 20 min at room temperature before bacteria were electroporated in 2 mm electroporation cuvettes. For electroporation of *S. aureus* a Bio-Rad MicroPulser was used at 1.8 kV for a 2.5 milli-second pulse. Immediately after electroporation 1 ml of BHI broth was added and bacteria were incubated for 1.5 h at 37°C at 200 rpm before plating on TSB agar supplemented with the respective antibiotic.

3.2.2.5 Transduction of DNA via phage transduction

To transduce genetic material into *S. aureus* Bacteriophage 11, 80 or 85 were used. This method was either used for transduction of plasmid DNA or for transducing insertional mutations from one strain into another.

Amplifying of phages: *S. aureus* RN4220 was grown overnight in phage buffer. Bacteria were incubated at 53°C for 2 min. Bacteriophages were added to 300 µl of the bacterial culture and incubated for 2 h at room temperature. Using LB-softagar containing 0.5 mM $CaCl_2$ bacteria were plated on TSA. After incubation overnight at 37°C the softagar was scraped off and incubated with 3 ml phage buffer for 3 h. Afterwards the bacteriophages were harvested via centrifugation at 2000 rpm for 10 min.

Preparation of transducing phages: Donor strain RN4220 harbouring the respective plasmid or a strain harbouring an insertional mutation were grown overnight in 5 ml phage buffer. Bacterial cultures were diluted 100-fold in 5 ml phage buffer and grown until OD_{600}=1.0. 1 ml of donor bacteria were diluted with 1 ml of fresh phage buffer and incubated at 30°C with 100 µl of bacteriophage 11, 80 or 85 solution until lysis was visible. Cellular debris was separated from transducing phages by centrifugation at 14000 rpm for 1 min. For transduction of plasmid DNA or insertional mutation the recipient strain was grown in phage buffer overnight. 300 µl of bacterial culture was heat-shocked at 53°C for 2 min before 100 µl of the transducing phage solution was added. Bacteria were incubated with phage solution for 2.5 h at room temperature before they were plated on TSA with the respective antibiotics using 0.6% of LB phage top agar containing sodium citrate. To avoid secondary site mutations, all *S. aureus* insertional transposon mutants obtained from the Nebraska library were transduced via phage 11, 80 or 85 into the genetic background of wild-type *S. aureus* JE2.

3.2.3 Desoxyribonucleic acid techniques

3.2.3.1 Isolation of Plasmid DNA from *E. coli*

For Isolation of plasmid DNA from *E. coli* strains NucleoSpin Plasmid Kit (Machery Nagel) was used according to manufacturer´s protocol. Briefly, *E. coli* was grown in 5 ml LB overnight at 37°C. Bacteria were harvested and plasmid was isolated by passing through spin columns. Elution was performed using 30 µl of prewarmed elution buffer.

3.2.3.2 Isolation of Plasmid DNA from *S. aureus*

For Isolation of plasmid DNA from *S. aureus* strains QIAprep Spin Miniprep Kit (Qiagen) was used according to manufacturer´s protocol. Briefly, *S. aureus* were grown in TSB overnight at 37°C. 2 ml of bacteria were harvested and resuspended in buffer A1. In order to lyse cells 50 µg of lysostaphin was

added and bacteria were incubated at 37°C at 1400 rpm. The plasmid DNA was afterwards isolated according to the manufacturer´s protocol by passing through spin columns. DNA was eluted from columns using 30 µl of prewarmed elution buffer.

3.2.3.3 Isolation of genomic DNA from *S. aureus*

For isolation of genomic DNA of *S. aureus* DNA mini kit (Qiagen) was used with some modifications. *S. aureus* strains were grown overnight in TSB, harvested and resuspended in 180 µl of Lysisbuffer and incubated at 37°C at 1400 rpm. After visible lysis of bacterial cells 200 µl of buffer AL and 20 µl of proteinase K solution were added. Lysed bacteria were incubated at 56°C for 30 min. After incubation 200 µl of absolute EtOH was added and the solution was vigorously vortexed. The mixture was loaded onto spin columns and washed according to manufacturer´s protocol. DNA was eluted from columns using 50 µl of water.

3.2.3.4 Polymerase-Chain-Reaction (PCR)

Polymerase chain reactions were performed in a volume of 50 µl using 50 ng template DNA, 1x polymerase buffer, 0.2 pmol of each forward and reverse primer, 0.2 µM dNTPs and 1U thermostable polymerase. Depending on the application Phusion polymerase (Invitrogen) with 3´-5´exonuclease activity or Taq polymerase (Genaxxon) without proofreading activity was used. After an initial step at 95°C for 5 min reaction continues with 30 cycles of each 30 sec at 95°C, 30 sec at 50-60°C (depending on the primer´s melting temperatures) and 72°C elongation step and a final step for 10 min at 72°C. The duration of the elongation step is dependent on product length (30 sec/ kb for Phusion and 1 min /kb for Taq). PCR products were subsequently analysed on 0.8-2% TAE agarose gels. For visualization of DNA under UV light 0.005% HD Green Plus was added to the agarose gel. PCR products were purified using Nuclespin Gel and PCR Clean-up kit (Machery-Nagel) according to manufacturer's protocol.
For screening of bacterial cultures expressing a transformed plasmid colony PCRs were performed using 10 µl of heat-lysed bacterial suspensions.

3.2.3.5 Quickchange mutagenesis PCR

Quickchange polymerase chain reactions were performed in a volume of 50 µl using 50 ng template plasmid DNA, 1x polymerase buffer, 0.2 pmol of each forward and reverse primer, 0.2 µM dNTPs and 1U thermostable phusion polymerase. The oligonucleotides for quickchange mutagenesis PCR were designed reverse complementary harbouring the base exchange in the middle. After an initial step at 98°C for 30 sec the reaction continues with 18 cycles of each 15 sec at 98°C, 30 sec at 62°C and a 72°C

elongation step and a final step for 10 min at 72°C. Remaining wild-type plasmids were removed by DpnI digestion for 1 h at 37°C, followed by inactivation of DpnI at 80°C for 20 min.

3.2.3.6 Annealing of oligonucleotides

For annealing of oligonucleotides 20 µM of each oligonucleotide was mixed with 1 /10 of annealing buffer and heated for 5 min at 95°C. Annealing occurred by slowly cooling the heated oligonucleotides to room temperature.

3.2.3.7 Phosphorylation of DNA

DNA obtained via PCR amplification was phosphorylated using 1 µl of PNK in 1/10 of ligase buffer for 20 min at 37°C.

3.2.3.8 Cloning of DNA into a vector

Purified PCR fragments and cloning vectors were digested using appropriate restriction enzymes and buffers. Serial digestion was performed in case of incompatible restriction enzyme buffers. The vector was dephosphorylated afterwards using FastAP Thermosensitive Alkaline Phosphatase (Invitrogen) for 15 min at 37°C. Ligation was performed using T4 DNA ligase (Invitrogen) using an insert vector ratio of 3:1 in a total volume of 10 µl at 16°C overnight. The ligation mixture was transformed into chemo-competent *E. coli* DH5α.

3.2.3.9 In-Fusion cloning

Cloning of plasmids was done using the In-Fusion HD Cloning kit (Takara). For this, fragments contained 15-19 bp overlaps to each other or the vector. Cloning was performed according to manufacturer´s recommendation. Resulting plasmids were transformed into chemo-competent *E. coli* DH5α and sequenced via Sanger sequencing (SeqLab, Göttingen).

3.2.3.10 Generation of targeted deletion mutants in *S. aureus*

Targeted deletions in *S. aureus* were obtained by the help of plasmid pBASE6 which derived from fusing a fragment of plasmid pKOR1 with parts of pBT2. Approximately 500 bp fragments flanking the target ORF or gene region were amplified by PCR and cloned via In-Fusion cloning into SmaI opened pBASE6. The plasmid was transformed into *E. coli* DH5α. Recombinant plasmids were confirmed via Sanger sequencing (SeqLab, Göttingen), and subsequently transformed via electroporation into *S. aureus*. Such recombinant *S. aureus* were grown in TSB containing 10 µg/ml chloramphenicol (Cam) at 30°C. Recombinant bacteria were plated on TSA/Cam overnight at 30 °C. For inducing homologous

recombination bacteria were grown in TSB containing 5 µg/ml Cam overnight at 42°C. Bacteria were streaked on TSA. Resulting colonies were grown overnight in TSB without any antibiotic thereby allowing co-integrate resolution. Cultures were diluted 1:10,000 and plated on TSA containing 100 ng/ml anhydrous tetracycline. The cultures were grown overnight at 37°C. Resulting colonies were tested for successful deletion via PCR using genomic DNA and primers flanking the integration site.

Construction of SSR42 and SSR42-*rsp* knockout mutants: Targeted deletion of 1232 nt long SSR42 and SSR42-*rsp* in *S. aureus* 6850 was obtained by the help of plasmid pBASE6. For this, approximately 500 bp fragments flanking the 1232 bp long DNA-sequence of ncRNA SSR42 were amplified by PCR using the primers Af_base6 and Ar_SacII to amplify the upstream sequence and primers Br_Base6 and Bf_SacII to amplify the downstream sequence. SSR42 and the downstream ORF RSAU_002217 encoding *rsp* were deleted from the genome of *S. aureus* 6850 by the help of plasmid pBASE6-SSR42-rsp. This plasmid was constructed by amplification of approximately 500 bp fragments flanking the sequences of ncRNA SSR42 and *rsp* using the primer pairs Af_base6 and Ar_SacII and Cr_BASE6 and Cf_SacII. For construction of a spectinomycin resistant SSR42 knockout mutant the resistance cassette was amplified using oligonucleotides inf-spek F and inf-spek R from the genomic DNA of *S. aureus* strain N315. The vector was amplified from pBASE6-SSR42 using oligonucleotides vek_pbase-SSR4_F and vek_pbase-SSR4_R. The plasmids were transferred in *S. aureus* 6850 which was subsequently screened for knockout mutants. Successful deletion was confirmed via amplifying the flanking genome regions using the primers listed in table 3.4.

3.2.3.11 Construction of plasmids used in this study

Construction of SSR42 complementation plasmids: The oligonucleotides compvek-rev and compvek-fwd were used for amplifying a linearized vector from plasmid p2085. For construction of pSSR42, pSSR42-rsp and p2216-2218 the respective sequences were amplified with the primers listed in table 3.4 and cloned via the In-Fusion system in the prepared vector.

Construction of BgaB reporter constructs: The ORF encoding *rsp* and SSR42 promotor sequence were amplified from genomic DNA of *S. aureus* 6850 using primers 2217_ssrProm-SF-rev and 2217_ssrProm-SF-fwd and cloned via SphI and EcoRI in pJL78 containing a *gfpmut2* sequence. The resulting plasmid was called pJL78-Pr-rsp-gfp. β-galactosidase encoding ORF (*bga*B) was amplified from pMAD using primers bgab-sf-fwd and bgab-sf-rev. *bga*B sequence was cloned via EcoRI and AscI into pJL78-Pr-rsp-gfp. After digestion with EcoRI and KasI the resulting DNA fragment consisting of *rsp*, *bga*B and SSR42 promotor sequence was cloned into p2085. The resulting plasmid was called pRsp-P_{SSR42}-BgaB. Plasmid pRsp-P_{SSR42}-BgaB was digested with PacI and XhoI and religated in order to remove the ORF encoding *rsp* resulting in plasmid pP_{SSR42}-BgaB.

Construction of GFP reporter constructs: For construction of pP_{SSR42}-GFP the SSR42 promotor, *rsp* and *gfpmut2* encoding sequences were obtained from digestion of plasmid pJL78-Pr-rsp-gfp with KasI and SphI and cloned into vector p2085. The plasmid was subsequently digested with PacI and XhoI and religated in order to remove the *rsp* encoding ORF. For construction of pP_{hla}-GFP, pP_{coa}-GFP, $pP_{psm\alpha}$-GFP, pP_{ldhD}-GFP, pP_{saeP1}-GFP and pP_{agrP3}-GFP the respective promotor sequences were amplified using the primers listed in table 3.4. Using oligonucleotides pGFP-Inf-Prom F and pGFP vec R a vector was amplified using plasmid pP_{SSR42}-GFP as a template. The promotor sequences were cloned in the prepared vector using the In-Fusion system.

Construction of a vector for AHT-induced transcription of SSR42 or *rsp*: For inducible complementation plasmids pAHT-SSR42 and pAHT-rsp were constructed. Using oligonucleotides ssr-vec-f_vec1-f and ssr-vec-r_vec1-r the linearized vector containing an AHT-inducible promotor sequence was amplified from plasmid p2085. Sequence of SSR42 was amplified from genomic DNA of *S. aureus* 6850 using oligonucleotides ssr42-r and ssr42-f and cloned via In-Fusion cloning into the prepared vector. The open reading frame of *rsp* was amplified from genomic DNA using oligonucleotides 2217ORF-PmeI-f and 2127ORF_EcoRI_Reverse. The resulting 2134 bp sequence was initially TA-cloned into pCR2.1 TOPO TA (Invitrogen). Digestion with PmeI and EcoRI created a 2216 bp fragment which was cloned into accordingly treated p2085. For induction of gene transcription 200 ng/ml AHT was added to a *S. aureus* liquid culture in TSB. If not stated otherwise transcription was induced in exponential phase cultures of *S. aureus*. (OD_{600}=0.4) for 1.5 at 37°C.

Construction of plasmids harbouring small deletions in SSR42: Small deletion mutants in SSR42 were contructed by amplifying the sequence of SSR42 from plasmid pSSR42 using the oligonucleotides listed in table 3.4 via mutagenesis PCR. Remaining wild-type pSSR42 sequence was digested with DpnI.

Construction of minimal versions of SSR42: Minimal versions of SSR42 were constructed by amplifying SSR42 from pSSR42 using primer miniSSR42_1J rev and miniSSR42_1J fwd for pSSR42_mini-1 and miniSSR42_2 rev and miniSSR42_2 fwd for cloning of pSSR42_mini-2, via mutagenesis PCR respectively. Remaining wild-type pSSR42 sequence was digested with DpnI.

Construction of pStemLoop2: For construction of pStemLoop2, a complementation plasmid harbouring only a certain stemn loop featuring region of SSR42 (bp 2,351,984-2,352,137), the SSR42 sequence, was amplified from genomic DNA of *S. aureus* 6850 using primers Stem loop 2 neu R and Stem loop 2 neu F and cloned using In-Fusion cloning in the prepared vector. The vector was prepared

via amplification of pMS2-Ter using the primer Vek Term R and Vek Term F2 thereby cutting-out the ms2-tag encoding sequence.

Construction of RNase Y cleavage site mutants: The plasmid pSSR42-rsp-delRNaseY harbouring a 69 nt long deletion (bp 2,352,844-2,352914) in the RNase Y cleavage site in SSR42 was constructed by amplifying SSR42 from plasmid pSSR42-rsp using primer dRnaseY-rev and dRnaseY-fwd via mutagenesis PCR. A mutation of the RNase Y-cleavage initiating guanosine in SSR42 was accomplished by amplifying SSR42 from plasmid pSSR42-rsp using the oligonucleotides RNaseY G mut R and RNaseY G mut F via mutagenesis PCR. The resulting plasmid pSSR42-rsp-RNaseY_mutG harbours an adenosine instead of a guanosine at position bp 2,352,899. In both cases the remaining wild-type plasmid sequence was digested using DpnI.

Construction of pSSR42-rsp-mutORF harbouring a mutation in putative ORF 3: The plasmid pSSR42-rsp-mutORF was constructed via mutagenesis PCR from plasmid pSSR42-rsp using the oligonucleotides deltaOrfL-r and deltaOrfL-f. The remaining wild-type plasmid sequence was digested using DpnI. The resulting plasmid pSSR42-rsp-mutORF harbours a guanosince instead of a thymidine at position bp 2,352,818 in the sequence encoding SSR42.

Construction of plasmids for RNA pulldowns: For the MS2-pulldown plasmid pAHT-SSR42-5ms2 and pAHT-SSR42-5ms2 were constructed. pAHT-SSR42-5ms2 was constructed by amplifying SSR42 from genomic DNA of *S. aureus* 6850 using the oligonucleotides 5ms2-rev and 5ms2-fwd. The vector was amplified from plasmid p2085 using the primer vec1-f and vec1-r. The 1295 nt long SSR42 encompassing sequence was cloned using In-Fusion cloning in the prepared vector. As a negative control for MS2-pulldown the plasmid pAHT-MS2-Ter was amplified by annealing the oligonucleotides PE-term-f and PE-term-r encompassing a terminator sequence. The annealed oligonucleotides were cloned into the PstI and EcoRI digested pAHT-SSR42-5ms2 therby cutting-out the SSR42 encoding sequence. A further negative control plasmid, referred to as pMS2-Ter, was constructed. For this, plasmid pAHT-MS2-Ter was amplified using the oligonucleotides deltaTetRf and deltaTetRr thereby removing the tet repressor. The PCR product was phosphorylated and religated.
For the oligo-capture pulldown the plasmids pAHT-SSR42-14mer, pAHT-5S-14mer and pAHT-14mer-Ter were contructed. The vector was prepared from plasmid pAHT-SSR42 via PCR using the oligonucleotides Vek 14 mer F and Vek 14 mer R thereby cutting-out the SSR42 encoding sequence. The inserts were amplified from genomic DNA of *S. aureus* 6850 using the primer 5S-14mer F and 5S-In-Fusion R or SSR42-14mer F and SSR42-Infusion R, respectively. The obtained fragments were used in a further PCR to add a 14 nt long aptamer. For this, a PCR with oligonucleotides 5S-14mer-Infus F

and 5S-Infusion R or SSR42-14mer Infusion F and SSR42-Infusion R was performed respectively. The inserts were cloned via In-Fusion cloning in the prepared vector. As negative control plasmid pAHT-14mer-Ter was constructed by digesting pAHT-me2-Ter with MluI and PstI. The oligonucleotides 14mer anneal F and 14mer MluI PstI R were annealed and ligated into the prepared vector.

3.2.4 Ribonucleic acid techniques

3.2.4.1 RNA isolation

Bacterial RNA was extracted using the TRIzol method (Lasa et al., 2011). Bacteria were harvested at desired optical densities, flash-frozen in liquid nitrogen and stored at -80°C. Pellets were thawed on ice with addition of EDTA to a final concentration of 65 mM and resuspended in Buffer A. Bacteria were lysed using Lysin matrix B tubes (MP Biomedicals) containing 500 µl of acidic phenol, using a FastPrep FP120 at 6 m/s for 45 seconds. Every step was performed in a cooling centrifuge or on ice if not mentioned otherwise. Phases were separated at 10,000 x g for 10 min at 4°C. The upper, aqueous layer was transferred to 1 ml TRI reagent and incubated for 5 min at room temperature. Afterwards 100 µl chloroform was added and sample was shaken vigorously and incubated for 3 min at room temperature. Phases were separated again at 17,900 x g for 10 min. The aqueous phase was mixed with 200 µl chloroform and incubated at room temperature for 5 min. After another phase separation step the aqueous phase was precipitated using isopropanol. After 15 min incubation at room temperature RNA was precipitated for at least 30 min at 17,900 x g. The resulting pellet was washed once with 75% ethanol, air-dried in a fume-hood and dissolved in DEPC-treated water. RNA was stored at -80°C.

After isolation of total RNA residing DNA contamination was digested using TURBO DNase I (Thermo Scientific). For this, 10 µg of total RNA was digested according to manufacturer´s protocol for 30 min at 37°C. The digestion reaction was stopped by addition of a DNase I-inactivation reagent and incubation for 5 min. RNA was separated from the inactivation reagent via centrifugation at 10,000 x g for 2 min. RNA samples were tested via PCR for residual DNA contamination.

3.2.4.2 Generation of cDNA via reverse transcription

cDNA was generated from DNase I-treated RNA using RevertAid Kit (Thermo Scientific) according to manufacturer's protocol. For this, 1 µg of RNA was used. The resulting cDNA was diluted 5-fold and kept at -20°C.

3.2.4.3 Quantitative real time PCR (qRT-PCR)

Real time PCR was performed using Quanta Biosciences Perfecta SYBR Green FastMix (2x, Quanta Biosciences) on a StepOne® Plus Real Time PCR system (Applied Biosystems) in 96 well format. Composition of reaction mixture and cycle settings were chosen according to manufacturer´s recommendation. The SYBR Green master mix was diluted to 1X in dH_2O and mixed with each 0.9 µM of forward and reverse primers. Approximately 10 ng of template cDNA in a total volume of 20 µl per well was used. Reactions were performed in technical triplicates.

Reactions were run for 40 cycles. After an initial step at 95°C for 10 min, each cycle was run for 15 sec at 95°C followed by 60°C for 1 min. Analysis of relative transcription was done according to the $2^{-\Delta\Delta CT}$ method (Livak and Schmittgen, 2001). For normalization of the relative transcript levels the expression of target genes was compared to the expression of housekeeping gene *gyrB* (gyrase subunit B).

3.2.4.4 Northern blotting

For Northern blot 10 µg of DNase I-treated RNA was used. RNA was mixed with 3x volumes of RNA loading buffer before heating at 65°C for 15 min. Afterwards 1/6 volumes of blue juice was added. RNA was loaded onto a 1% formaldehyde agarose gel. RNA was separated in MOPS-buffer at 50 V for approximately 3.5 h. RNA was visualized under UV light, washed three times in DEPC-treated water and transferred to a nylon membrane using alkaline transfer for 2.5 h. The nylon membrane was incubated in 1x phosphate buffer for 5 min and RNA was UV-cross-linked to the membrane according to manufacturer´s recommendation (Stratalinker). The membrane was pre-hybridized at 64°C for 30 min. Digoxigenin-labelled DNA-fragments were used as probes and produced using PCR DIG Labeling kit (Roche Digoxigenin Detection kit) according to manufacturer´s protocol. The DNA probes were heated for 10 min at 95°C and subsequently added to fresh hybridization buffer. The nylon membrane was hybridized overnight at 64°C. The nylon membrane was washed twice with 2x SSC containing 0.1% SDS for 5 min at room temperature and twice with 0.2x SSC containing 0.1% SDS for 15 min at 64°C. To detect the digoxigenin labelled probes the membrane was equilibrated in maleic acid washing buffer and blocked in buffer 2 (all buffers from Roche Digoxigenin Detection kit). Anti-Digoxigenin antibody (Roche Digoxigenin Detection kit) was used in a 1:10,000-fold dilution. The Northern blot was incubated in the antibody for 30 min. The membrane was washed twice with maleic acid washing buffer for 20 min and once with buffer 3 for 3 min. The signal was developed using CSPD readymade solution (Roche) according to manufacturer´s recommendation and recorded using Intas LabImage Chemostar imager.

3.2.4.5 Investigation of transcript stabilities by rifampicin assay

To test the stability of transcripts a rifampicin assay was used. For this, *S. aureus* was grown overnight in TSB or until the respective growth phase was reached. rifampicin was added to a final concentration of 500 µg/ml in DMSO. Bacteria were harvested at time point 0 and at the respective time points, flash-frozen in liquid nitrogen and stored at -80°C until RNA was isolated. RNA was separated and detected using Northern blotting. Signal strength was measured quantitatively using ImageJ.

3.2.4.6 RNA-Sequencing (RNA-seq)

DNase I-treated RNA samples were rRNA depleted and converted into cDNA libraries for Illumina sequencing by Max-Planck Genome Centre Cologne, Cologne, Germany. Paired-end read sequencing was performed on an Illumina HiSeq2000 machine aiming for a total of 5 million reads for sequencing of each cDNA library. RNA-seq was performed in biological triplicates.

Statistical analysis was performed by Maximilian Klepsch (Department of Microbiology, University Würzburg, Germany). In short quality control of reads was performed with FASTQ, followed by trimming using trimmomatic (sliding window: 4, 12). Mapping to the genome of *S. aureus* 6850 was performed using bowtie2 (default parameter: very sensitive local). Data was converted, sorted and compressed in a bamfile using samtools before quantification of reads was performed using feature counts. Differential analysis was performed via Deseq2 and reporting tools.

3.2.4.7 Gradient profiling by sequencing (Grad-seq)

Grad-Seq was performed as described in Smirnov et al., 2016. In short bacteria were lysed; cleared lysates were fractionated into 20 equal fractions using linear 10–40% (wt/vol) glycerol gradients. Fractionating was performed in Beckman SW40Ti tubes at 100,000 × *g* for 17 h at 4 °C. RNA was isolated from the fractions and sequenced on an Illumina HiSeq 2000 platform. Statistical analysis was performed by Konrad Förstner.

3.2.4.8 RNA pulldown approaches

MS2-tagged RNA pulldown

The MS2-tagged RNA pulldown approach was adapted from Yoon et al., 2012. Bacteria at an OD_{600} of 50 were resuspended in 600 ml lysis buffer and lysed in Lysing matrix B tubes in a a fast prep at 6 m/s for 45 s. Cellular debris was pelleted for 10 min at 16, 000 x g at 4°C. The cleared lysate was added to the prepared column. For preparation of the resin (2 ml Bio-spin disposable chromatography columns; BioRad) 70 µl of amylose beads (BioRad) was added and washed three times with 2 ml lysis buffer before 250 pmol of purified MS2-MPB was added to the column. The cleared lysate was added and incubated with the resin for 5 min at 4°C. Afterwards the resin was washed five times with 2 ml lysis

buffer. Bound proteins and RNA was eluted using 300 µl elution buffer. RNA and proteins were separated by Phenol-Chloroform precipitation. RNA was further precipitated with EtOH:NaAcetate (30:1).

Oligo-capture RNA pulldown

The Oligo-capture pulldown approach was adapted from Treiber et al., 2017. Bacterial cells at an OD_{600} of 50 of the respective *S. aureus* strain expressing a target RNA with a 14 nt tag were lysed in 500 µl lysis buffer in lysine matrix B tubes using a fast prep at 6 m/s for 45 s. Cellular debris was pelleted by centrifugation for 30 min at 20,000 x g. 50 µl of streptavidin beads were washed three times with 500 µl lysis buffer. Beads were incubated with 4 µg of biotin-labeled 2´OH methylated RNA oligo (Oligo-capture) in 500 µl lysis buffer for 1 h at 4°C. After incubation the beads were washed twice with 500 µl lysis buffer.

The prepared lysate was added to the oligo-labelled beads and incubated over night at 4°C. Afterwards beads were washed once with wash buffer 1, once with wash buffer 2 and once with lysis buffer. For eluation of bound proteins beads were resuspended in 30 µl of Laemmli buffer and incubated for 5 min at 95°C. Proteins were separated on a 12% PAA gel and stained with colloidal coomassie or silver staining.

3.2.5 Investigation of promotor activities

β-galactosidase assay for testing the effect of antibiotics on the activity of promotors: SSR42 promotor activity upon treatment with chemical substances was analysed using a β-galactosidase reporter construct. Strains harbouring such reporter plasmids were grown overnight at 37°C in TSB supplemented with 10 µg/ml chloramphenicol. 100 µl of bacterial culture was added to 5 ml soft agar containing 40 mg/ml 5-bromo-4-chloro-3-indolyl-β-D-galactopyranoside (X-Gal). Softagar was poured on LB agar containing 40 mg/ml X-Gal. Diffusion discs containing the substance of interest were placed on top of the softagar. Bacteria were incubated overnight at 37°C. Formation of indigo colour indicated induction of promotor activity.

Fluorescence-based promotor activity assay: Promotor activities during planktonic growth were assessed by monitoring GFP fluorescence (excitation: 488±9 nm, emission: 518±20 nm) and optical density (600 nm) over a time course of 23 h. GFP and optical density were measured using a TECAN Infinite M200 plate reader. For this, bacteria were cultured overnight at 37°C. Bacterial cultures were diluted in 400 µl TSB to OD600=0.1 in triplicates and grown for 23 h in a 48 microwell plate. Optical density and GFP fluorescence was measured every ten minutes for a time course of 23 h. The micro-well plate was shaken between each measurement at an amplitude of 6 mm.

Heatmaps were generated via calculating the difference in relative fluorescence units between each tested mutant and respective wild-type for each time point. Using the library pheatmap from R the resulting matrix was visualized.

3.2.6 Investigation of haemolytic capacities in *S. aureus*

Quantitative haemolysis assay: *S. aureus* possesses virulence factors, e.g. α-toxin, which lead to disruption of erythrocytes and release of haemoglobin. This release of haemoglobin can be measured in order to determine the haemolytic potential of *S. aureus*. For such quantitative measurements sheep erythrocytes (Fiebig Nährstofftechnik, Germany) were washed twice with 0.9% NaCl and diluted in 0.9% NaCl to a final concentration of 1% erythrocytes. Bacteria were grown for 16 h in TSB at 37°C, normalized according to their optical densities, harvested and supernatants were collected. Supernatants were sterile filtered (0.45 µm). 5% (v/v) of sterile-filtered supernatant of *S. aureus* was added to 1 ml of a 1% erythrocyte dilution. This mixture was incubated for 1 h at 37°C at 550 rpm. The suspension was centrifuged and supernatants were analysed for liberated haemoglobin by measuring the absorbance at 405± 9 nm using a TECAN Infinite M200 plate reader. As negative control erythrocytes were incubated with sterile TSB. Relative haemolysis was determined as a percentage of *S. aureus* wild-type haemolysis potential.

Haemolysis assay using sheep blood agar: For analysis of haemolysis of *S. aureus* in a non-quantitative way bacteria were grown overnight in TSB at 37°C, diluted 100-fold and spotted on Columbia agar (BD Biosciences) supplemented with 5% of defibrinated sheep blood (Fiebig Nährstofftechnik, Germany).

3.2.7 Protein techniques

3.2.7.1 Isolation of bacterial proteins

Isolation of cytosolic bacterial proteins: For isolation of cytosolic proteins of stationary phase *S. aureus* bacteria were grown overnight in TSB at 37°C and harvested at 4,200 rpm for 20 min at 4°C. Bacterial pellet was washed once with PBS and flash-frozen. For analysis of exponential phase proteins bacteria were inoculated in fresh TSB to OD_{600}=0.05 and grown until exponential phase (OD_{600}=0.6) was reached. Bacteria were harvested, washed and pellet was flash-frozen.

Samples were thawed on ice, resuspended in 300 µl protein lysis buffer and transferred to Lysing matrix B tubes (MP Biomedicals). Bacteria were lysed using a FastPrep FP120 (MP Biomedicals) at 6 m/s for 45 seconds. Cellular debris was removed by centrifugation at 14,000 rpm for 10 min. Supernatant was collected and stored at -20°C.

Isolation of secreted bacterial proteins: For analysing the secreted protein fraction of *S. aureus* bacteria were grown overnight in TSB at 37°C and harvested or inoculated in fresh TSB to OD_{600}=0.05 and grown until exponential phase was reached (OD_{600}=0.6). Bacteria were harvested at the given time

points at 4,200 rpm for 20 min at 4°C. Supernatant was sterile filtered (0.45 µm) and proteins were precipitated with acetone. For the precipitation of proteins from bacterial supernatants the supernatant was mixed with 4x the volume ice-cold acetone in order to precipitate secreted proteins. Precipitation was performed overnight at -20°C followed by centrifugation for 60 min at 6,000 rpm at 4°C. Precipitated proteins were washed once with ice cold acetone, air-dried and resuspended in an appropriate amount of PBS. Proteins were stored at -20°C.

3.2.7.2 Bradford assay

For measuring the protein amount of a sample Bradford assay was performed using Roti Quant according to manufacturer's protocol (Roth). A calibration line was performed using a 1 mg/ml BSA solution.

3.2.7.3 SDS PAGE

For separation of proteins according to their masses via electrophoresis SDS-PAGE was performed. For this, the samples were denatured with Laemmli buffer by heating at 95°C for 5 min. The gel consisted of a 4% PAA stacking and a 7-15% PAA resolving gel. Proteins were separated at 150 V and 25 mA.

3.2.7.4 Staining of proteins

Colloidal coomassie staining: For visualization of proteins separated by SDS-PAGE colloidal coomassie G-250 was used. Gels were fixed for 1 h in fixing solution before staining overnight in colloidal staining solution. Staining solution was prepared freshly by mixing 400 ml of Staining A, 10 ml of Staining B and 100 ml of methanol. Gels were incubated afterwards for 5 min in neutralizing solution, washed for 15 min in washing solution and until destaining was sufficient in dH_2O.

Silver staining: Small amounts of proteins were visualized using silver staining. For this, gels were fixed for 1 h in fixing solution, washed twice for 20 min in washing solution and incubated for 1 min in the sensitizer. The gel was washed three times for 20 sec with dH_2O before silver staining solution was added for 20 min. After staining the gel was washed twice for 20 sec with dH_2O before the developing solution was added. The gel was incubated until the strength of the staining was sufficient and developing was stopped by incubating the gel for 2 min in stop solution. The gel was afterwards washed with dH_2O.

3.2.7.5 Western blotting

The transfer of proteins from SDS-PAGE on a polyvinylidene fluoride (PVDF) membrane was carried out using semi-dry blotting for 1.5 h at 0.9 mA/ cm^2. The membrane was blocked in 5% skim milk in

TBS-T for 2 h. Incubation with the first antibody was done at 4°C overnight. Afterwards the membrane was washed once for 15 min and three times for 5 min in TBS-T before it was incubated with the HRP-linked secondary antibody (diluted 1:3000 in TBS-T) for 1 h at room temperature. The membrane was washed three times afterwards with TBS-T for 30 min. To develop the Western blot ECL-1 and ECL-2 solution were mixed in equivalent amounts and added to the membrane. The signal was detected using an Intas LabImage Chemostar system.
Signal strength was measured quantitatively using ImageJ. As loading control proteins separated via SDS-PAGE were stained using silver staining.

3.2.7.6 Mass spectrometry analysis

Isolated cytosolic and secreted proteins were sent to University of Greifswald, Institute for Microbiology, for Mass spectrometry. Experiment was performed in biological triplicates by Andreas Otto and Dörte Becher.
Statistical analysis was performed by Maximilian Klepsch (Department of Microbiology, University Würzburg, Germany) using MeV 4.9.0 for two-way Anova, followed by Tukey´s HSD test as post-hoc test.

3.2.8 Cell culture techniques

3.2.8.1 Cultivation of cell lines

HeLa 2000 cells were cultivated in cell culture medium supplemented with 10% FCS and 10% sodium-pyruvate in 75 cm^2 cell culture flasks at 37°C and 5% CO_2.
For revitalizing frozen cell pellet was washed in 10 ml of cell culture medium at 1,500 rpm for 10 min. Cells were resuspended in 20 ml fresh medium and transferred into a cell culture flask.
Passaging of cells occurred every second day in order to maintain confluency of approximately 80-90%. For this, cells were washed twice with PBS before 1 ml of trypsin was added. Cells were incubated for 5 min at 37°C and reaction was stopped afterwards by addition of 10 ml cell culture medium.
For cryopreservation cells were grown until reaching confluency, detached using trypsin, washed once with PBS and harvested at 1,500 rpm for 10 min. The cell pellet was resuspended in an appropriate amount of FCS supplemented with 10% DMSO and transferred to cryo tubes. The cryo tubes were kept at -80°C in an isopropanol chamber for short term storage. For long term storage cells were transferred to a liquid nitrogen container.

3.2.8.2 Infection of HeLa cells with *S. aureus*

Cells were seeded in a 12 well microwell plate at density of $1*10^5$/ well in cell culture media and grown for approximately 24 h. 30-60 min before starting the experiment cells were washed twice with PBS and cell culture medium was replaced by 500 µl infection media.

For infection *S. aureus* strains were grown overnight in TSB at 37°C. Bacterial cultures were inoculated in fresh TSB to OD_{600}=0.4 and grown at 37°C for 45 min until reaching logarithmic growth phase. Bacteria were harvested, washed once with infection media and resuspended in infection media. Using a Thoma chamber bacteria were counted. A MOI of 10 was used to infect the cells. For this, bacteria were added to the cells and cells were centrifuged at 1,000 rpm for 10 min to sediment the bacteria. 1 h post infection cells were washed once with PBS and medium was replaced by 500 µl infection media containing 20 µg/ml lysostaphin to digest extracellular bacteria. 1.5 h post infection cells were washed twice with PBS and medium was replaced by 500 µl infection media containing 2 µg/ml lysostaphin.

3.2.8.3 CFU enumeration

CFU enumeration of *S. aureus* from infected cells was performed at the indicated time points. For this, infected cells were washed once with PBS and once with sterile dH_2O. Cells were incubated for approximately 20 min in 500 µl dH_2O at 37°C until lysis of cells was observed. Cells were mechanically cracked and bacteria were diluted and plated on TSA. Bacteria were incubated overnight at 37°C. CFU were counted.

3.2.8.4 Cytotoxicity assay (LDH release assay)

For analysis of *S. aureus*-induced cell death LDH assay was performed according to manufacturer's protocol (Roche). Infection of cells was performed as described earlier (chapter 3.2.8.5). 1.5 h post infection cells were washed twice with PBS and medium was replaced by 500 µl infection media without phenol red supplemented with 1% FCS and 2 µg/ml lysostaphin. 4 h post infection LDH assay was performed according to manufacturer's protocol (Roche) using 100 µl of supernatant. Experiment was performed in technical duplicates. Uninfected cells were used as a control. LDH release was measured at 492 nm ± 9 nm using a TECAN M200 plate reader. Cytoxicity (%) was calculated according to manufacturer´s recommendation.

3.2.8.5 Long-term infection of EA.Hy926 cells

Infection of EA.Hy926 cells with *S. aureus* for CFU and SCV count was performed by Lorena Tuchscherr (Institute University clinics, Jena). Confluent cell monolayers were washed, invasion medium (containing 1% human serum albumin and 25 mM HEPES) was added to the cells, and cells were infected with *S. aureus* using a MOI of 50. Infected cells were incubated for 30 min at room

temperature to allow sedimentation before they were shifted for 3 h to 37°C to allow invasion of the bacteria. Afterwards, cells were washed and lysostaphin was added to a final concentration of 20 µg/ml for 30 min. After the incubation time cells were washed and incubated with fresh culture medium (M199, 10% human serum, penicillin, 100 IU/ml; streptomycin, 10 µg/ml). The infected cells were incubated for 7 days. Lysostaphin treatment and medium exchange was repeated every 24 h. CFU were enumerated and bacteria were plated on TSA.

3.2.9 *In vivo* infection models

Acute and chronic infection model in mice: C57BL/6 female mice (8 weeks old) were purchased from Harlan-Winkelmann (Borchen, Germany), kept under pathogen-free conditions and housed in microisolator cages. For infection with *S. aureus* 6850 mice were inoculated with 1×10^6 CFU of *S. aureus* in 0.2 ml of PBS via a lateral tail vein. Mice were sacrificed by CO_2 asphyxiation at the indicated time point (day 2 for acute; day 7 and day 14 for chronic infection). For CFU counting homogenates of kidneys, liver and tibia were prepared in PBS and plated by 10-fold serial dilutions on blood agar. Infection and CFU assay were performed by Eva Medina (Helmholtz Centre Braunschweig).

3.2.10 Statistics

If not declared otherwise, statistical analysis was performed using two tailed Student´s t-test using Excel 2010: *: $p < 0.05$; ***: $p < 0.001$.

4 RESULTS

4.1 Characterization of SSR42, a long ncRNA of *S. aureus*

ncRNAs have been identified to play a crucial role for virulence regulation in *S. aureus* (Felden et al., 2011). Among these, small stable RNAs (SSR) are often found to enhance pathogen survival in detrimental conditions (Anderson et al., 2006; Anderson et al., 2010; Olson et al., 2011). One of such SSRs SSR42, was implicated in regulating virulence in two *S. aureus* strains, UAMS-1 and USA300. However, the authors of this study determined the length of SSR42 at 891 nt (Morrsion et al., 2012a) while TEX-treatment RNA-seq in a recent study identified a 1232 nt long primary transcript of SSR42 (Das et al., 2016). Thus, potentially a processed form of the transcript was analysed instead of the full-length ncRNA. The prescence of this longer ncRNA was therefore analysed in this chapter.

4.1.1 SSR42 sequence conservation

Investigating a potential conservation of ncRNA SSR42 in other species, the DNA-sequence encoding 1232 nt long ncRNA SSR42 of *S. aureus* 6850 was analysed by NCBI BLASTN (https://blast.ncbi.nlm.nih.gov/Blast.cgi) applying ´discontiguous megablast´ against the ´nucleotide collection´ (see Appendix Table 7.1). The complete sequence encoding SSR42 was only found in *Staphylococcus aureus sp. aureus* and *Staphylococcus argenteus* but not in other members of the Staphylococcaceae family. In *S. agenteus* the SSR42 encoding sequence exhibited 94% identity (E-value=0) towards the sequence of *S. aureus* 6850. 18 gaps and several nucleotide exchanges were present within the sequence in *S. agenteus* (see Appendix table 7.2, Fig. 7.1). The SSR42 sequence of strain 6850 further showed an identity of 77% (E-value=2.3) towards 63 nt of a sequence found in *Ceratosolen solmsi marchali* mRNA encoding the WASH complex subunit 7, an identity of 82% (E-value= 2.3) towards 44 nt of a sequence found in the genome of *Dracunculus medinensis* and 85% identity (E-value= 8.1) towards 38 nt of a sequence found in the genome of *Schistosoma curassoni* (see Appendix table 7.2).

The complete sequence of SSR42 displayed high conservation with 99% identity in all *S. aureus* strains and isolates existing in the NCBI datatbase. Moreover, the more precise analysis revealed that in most strains only single nucleotide exchanges differed from the SSR42 sequence of *S. aureus* 6850. For example, in the USA300 isolate COL the SSR42 sequence exhibited a single nucleotide exchange at nt 334 compared to the sequence of *S. aureus* 6850 (Fig. 4.1). Thus, while only further found in *S. argenteus*, the sequence encoding SSR42 is highly conserved within *Staphylococcus aureus sp. aureus.*

6850	301	ACAATAACCATCAACTAAGAAATTTTAAACAATCCACTAAAAAATAAAGCGTTTAAAAGT	360
COL		ACAATAACCATCAACTAAGAAATTTTAAACAATCTACTAAAAAATAAAGCGTTTAAAAGT	

Figure 4.1: SSR42 is highly conserved among *S. aureus* strains. Sequence comparison of SSR42 from *S. aureus* strain 6850 and strain COL revealed one nucleotide exchange at nucleotide 334 (highlighted in yellow).

4.1.2 The genomic locus of SSR42 in *S. aureus*

The SSR42 encoding gene is located directly upstream on the opposite DNA strand of the gene encoding the AraC-transcriptional regulator Rsp. Transcription start site analysis revealed divergent transcription start sites for both SSR42 and *rsp*. While both genes are transcribed bidirectionally, distinct predicted -10 and -35 boxes for both *rsp* an SSR42 were found indicating the transcription from divergent, independent promotors (Das et al., 2016). Upstream of SSR42 on the other DNA strand the 385 bp encompassing ORF RSAU_002216 is located. The ORF of RSAU_002216 overlaps by 5 nucleotides at the 3' end with the 3' end of the sequence encoding SSR42. Protein family analysis using the web tool Pfam (https://pfam.xfam.org) characterized RSAU_002216 as a protein of unknown function belonging to the DUF1722 family of proteins (E-value= $7*10^{-23}$). The 432 bp encompassing gene downstream of *rsp* on the same DNA strand is the general stress protein 26 RSAU_002218 (Fig. 4.2). Further analysis using Pfam characterized the encoded protein as putative pyridoxamine 5'-phosphate oxidase (E-value= $2.8*10^{-15}$). The whole genomic locus around SSR42 is highly conserved in all *S. aureus* strains (see Appendix table 7.3).

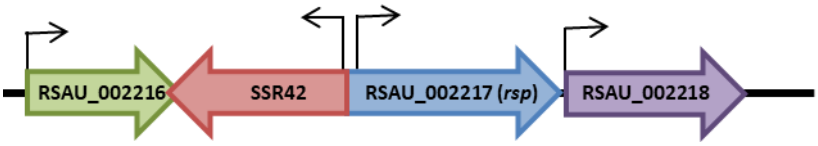

Figure 4.2: Genomic localization of SSR42 in the genome of *S. aureus*. SSR42 is encoded upstream in antiparallel orientation to *rsp.* RSAU_002216 and SSR42 overlap at both 3'ends. Arrows indicate transcription start sides.

4.1.3 Evidence for full-length SSR42 and procession by RNase Y

In a previous study the length of SSR42 was determined by RACE to be 891 nt (Olson et al., 2011). However, in a recently performed TEX-treatment RNA-seq a transcript for SSR42 encompasing 1232 nt has been detected (Das et al., 2016). Analysing the role of this 1232 nt long transcript of SSR42 a deletion mutant was constructed. The 1232 nt long SSR42 encoding sequence was therefore deleted from the genome of *S. aureus* 6850 using a targeted deletion approach (Fig. 4.3A; see section 3.2.3.10).

The mutant, *S. aureus* 6850 ΔSSR42, did not show any growth defects when grown in TSB medium compared to wild-type bacteria from the same strain background (Fig. 4.3B). The existence of a 1232 nt SSR42 transcript was verified using Northern blotting (Fig. 4.4). For this, a probe binding to the very 5´end of 1232 nt SSR42 (Fig. 4.4A,D; see Appendix Fig. 7.9; probe 1; nt 6-167 of SSR42) and a probe binding to the middle part of SSR42 (Fig. 4.4B,D; probe 2; nt 889-991 of SSR42) were used. Total RNA extracts of *S. aureus* 6850 wild-type bacteria, ΔSSR42 mutant and mutant complemented in trans for SSR42 (pSSR42) were used. While employing probe 1 an approximately 1200 nt long transcript was found for wild-type bacteria and complemented mutant verifying the via TEX-treatment RNA-seq determined 5´end of full-length SSR42. This transcript was designated transcript 1 (T1). Using probe 2 a further approximately 1000 nt long transcript (T2) was detected indicating a potential processing of SSR42. Both signals were absent in a ΔSSR42 mutant confirming the successful knockout and the specificity of the used probes. The full-length transcript (T1) was further detected in *S. aureus* USA300 JE2 and strain UAMS-1, although for the latter much higher amounts of RNA had to be used (Fig. 4.4C). Both strains were used in the previous studies characterizing 891 nt long SSR42 (Morrison et al., 2012a). Thus, the existence of a ~1200 nt transcript of SSR42 was not only verified in *S. aureus* strain 6850 but also in various other strains. Northern blotting hence demonstrated that SSR42 exists in at least two distinct transcripts lengths. Especially in *S. aureus* JE2 the longer transcript was found as the predominant form in stationary phase bacteria while the smaller transcript, T2, potentially resulting from a processing event was found at lower amounts.

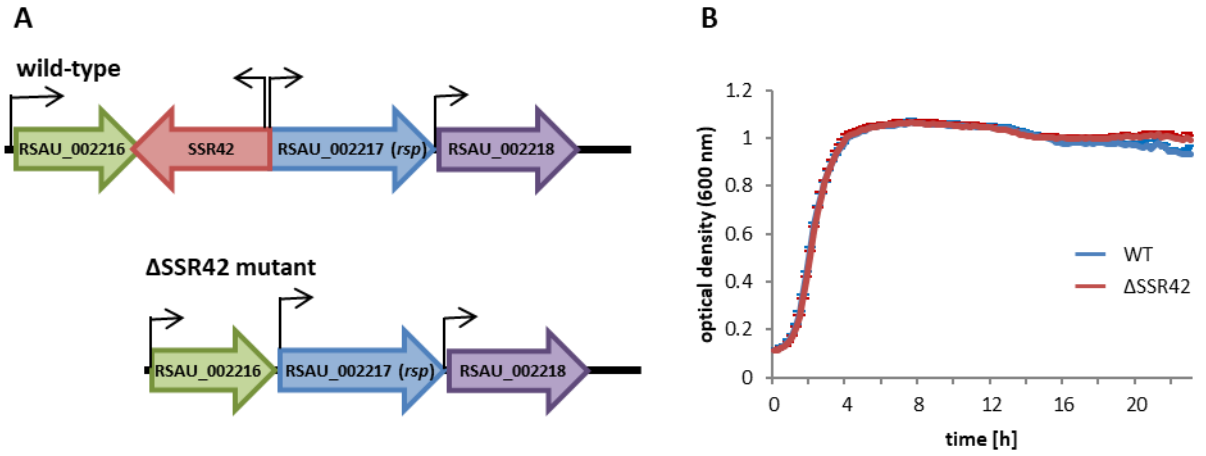

Figure 4.3: Deletion of SSR42 does not influence growth of *S. aureus* 6850. A) Schematic representation of deletion of the 1232 nt long SSR42 encoding sequence. Genomic localization of SSR42 in wild-type *S. aureus* (upper panel) and genomic situation in a ΔSSR42 mutant (lower panel). **B)** Growth curve of *S. aureus* 6850 wild-type bacteria and ΔSSR42 mutant does not reveal any differences between the two groups. Growth curve was monitored over a time course of 23 h.

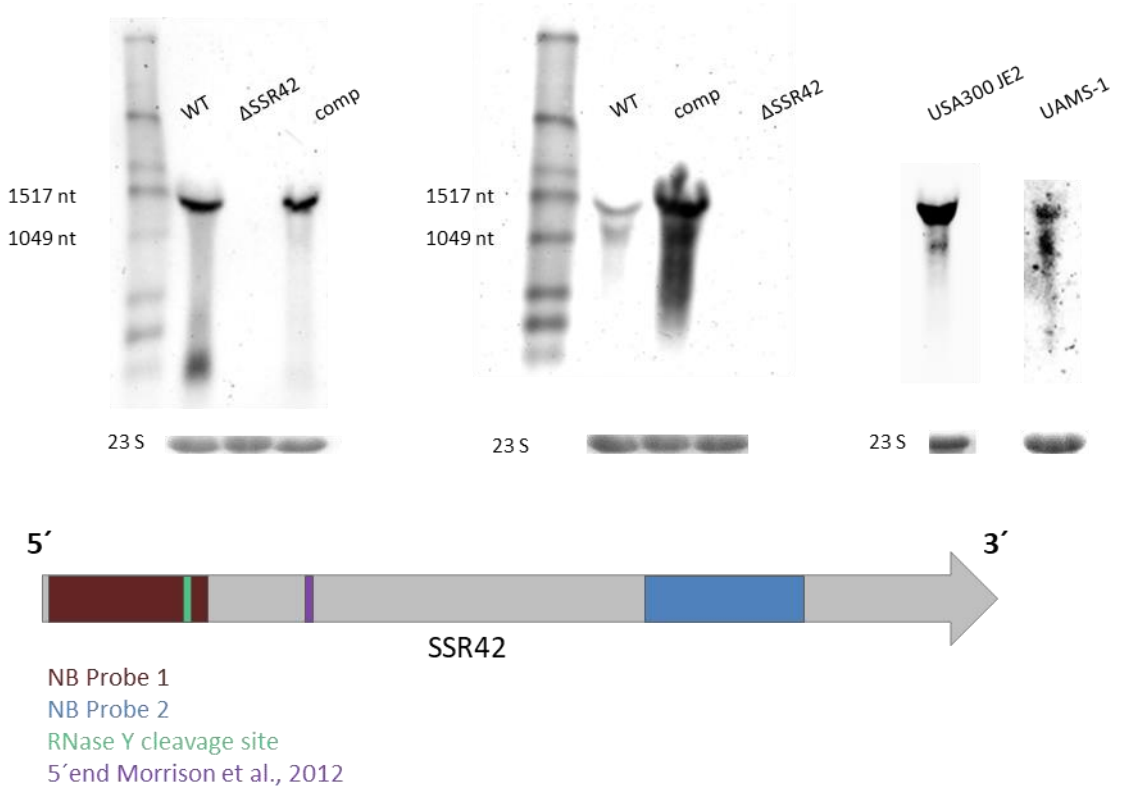

Figure 4.4: SSR42 exists in at least two transcripts in *S. aureus*. Northern blot using RNA (10 µg) extracted from stationary growth phase *S. aureus* 6850 wild-type, ΔSSR42 mutant and complemented mutant. Hybridization with **A)** probe 1 (5'end of SSR42) and **B)** probe 2 (850-989 nt of SSR42) reveals the existence of two SSR42 transcript forms (T1 and T2). **C)** Northern blot using RNA obtained from stationary growth phase *S. aureus* JE2 (10 µg) and UASM-1 (40 µg). For detection of SSR42 probe 2 was used. **D)** Schematic representation of the sequence encoding SSR42. Highlighted are the sequences encompassing binding of probe 1 and 2 as well as the 5'end suggested by Morrison et al., 2012a and the predicted RNase Y cleavage site (Khemici et al., 2015).

In *S. aureus* processing of a hundred of mRNAs and ncRNAs occurs by RNase Y, which is thought to initiate the further decay of RNAs (Khemici et al., 2015). During a global EMOTE screen a potential cleavage site of endoribonuclease RNase Y within the sequence of SSR42 has been predicted (bp 2,352,898 of SSR42; Khemici et al., 2015, Fig. 4.4D). It was therefore hypothesized that cleavage by RNase Y could result in the smaller SSR42 transcript T2. To confirm this hypothesis Northern blotting was performed using RNA from *S. aureus* JE2 wild-type bacteria, a RNase Y knockout mutant (Δ*rny*) and the mutant complemented for *rny* (pCG296) (Fig. 4.5A). Using probe 2 for Northern blotting a complete loss of smaller SSR42 transcripts was detected in the Δ*rny* mutant. The presence of transcript T2 was restored in the Δ*rny* mutant complemented in trans for *rny* (pCG296) verifying the emergence of transcript T2 via processing by RNase Y. Using qRT-PCR SSR42 transcript levels were analysed in the Δ*rny* mutant which revealed a slight but not significant increase (Fig. 4.5B; FC: 3.02, p=0.088) compared to the transcript levels found in wild-type bacteria. Further, transcript levels of SSR42 were found significantly increased in the complemented mutant (FC: 2.89, p=0.002). Therefore, a role of RNase Y

in transcriptional regulation of SSR42 was ruled out. Further analysing this processing event a 70 nt sequence spanning the predicted RNase Y cleavage site within the 5´end of SSR42 was deleted. This mutated SSR42 sequence was re-introduced in the ΔSSR42 mutant via complementation plasmid pSSR42-rsp-delRNaseY. A global EMOTE screen not only identified a cleavage site within SSR42 but further found a guanosine marking the RNase Y-cleavage site in most of the target RNAs (Khemici et al., 2015). In order to prevent cleavage of SSR42 by RNase Y the ΔSSR42 mutant was likewise complemented in trans for SSR42 using plasmid pSSR42-rsp-RNaseY_mutG, thereby replacing the RNase Y-cleavage site preceding guanosine (nt 145) by uracil. The RNA of both complemented mutants was analysed via Northern blotting for the presence of smaller SSR42 transcripts (Fig. 4.5C). Neither deletion of the cleavage site encompassing sequence nor changing the cleavage site preceding nucleotide prevented the processing of SSR42 into smaller transcripts.

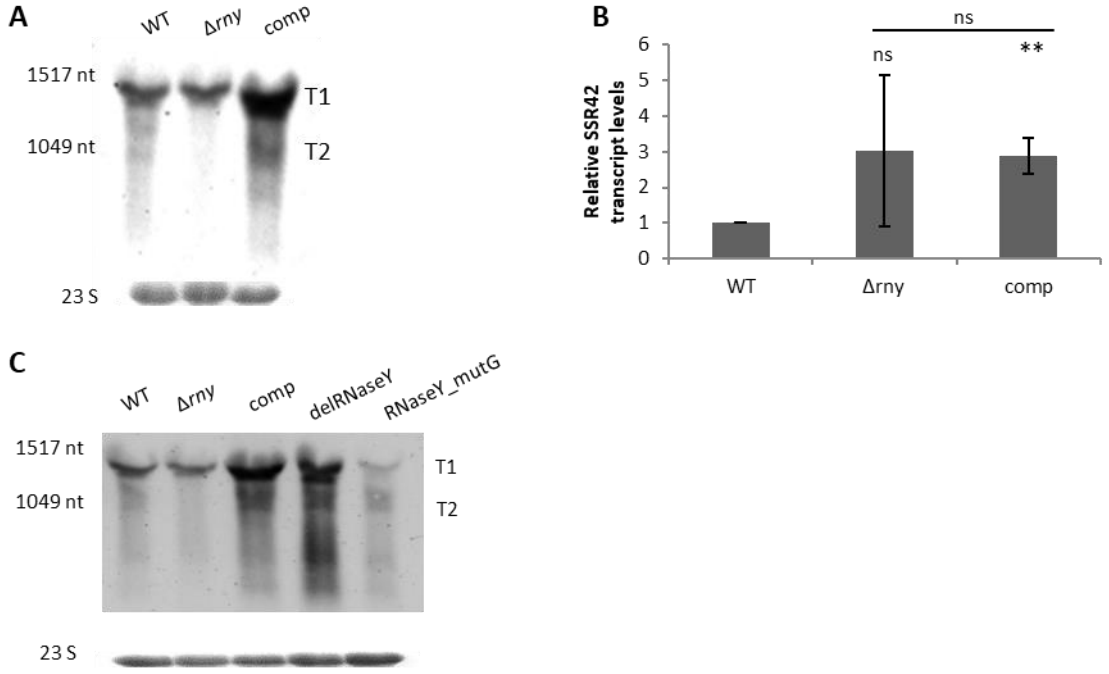

Figure 4.5: RNase Y cleaves SSR42 producing an approximately 1050 nt product. A) Northern blot using RNA obtained from stationary growth phase *S. aureus* JE2 wild-type, Δ*rny* and complemented mutant demonstrated involvement of RNase Y in production of smaller SSR42 transcript T2. The approximately 1050 nt cleavage product was lost in a Δ*rny* mutant. For hybridization probe 2 was used. **B)** qRT-PCR analysis revealed no significant differences in total SSR42 transcript levels in absence of RNase Y. Statistical analysis was performed using Student´s t-test. **C)** Cleavage of SSR42 by RNase Y is independent of the, by a global EMOTE assay, predicted sequence encompassing a guanosine as demonstrated by Northern blot analysis. Northern blot of total RNA extracted from stationary growth phase bacteria of *S. aureus* JE2 wild-type, Δ*rny* and complemented mutant as well as complemented ΔSSR42 mutants harbouring either a ~70 nt deletion encompassing the RNase Y cleavage site (delRNaseY) or a nucleotide exchange in the cleavage initiating guanosine (RNaseY_mutG).

Whether processing of SSR42 by RNase Y has an effect on the stability of SSR42 was investigated using rifampicin to arrest de novo transcription, followed by Northern blot analysis (Fig. 4.6). For this, wild-type *S. aureus* JE2 and isogenic Δ*rny* mutant were challenged with rifampicin. No significant differences in the overall stability of the SSR42 T1 transript could be detected in the Δ*rny* mutant (FC= 0.67, p=0.156). In summary, RNase Y-mediated cleavage did neither influence overall transcription of SSR42 nor stability of the T1 transcript but the emergence of the smaller transcript T2.

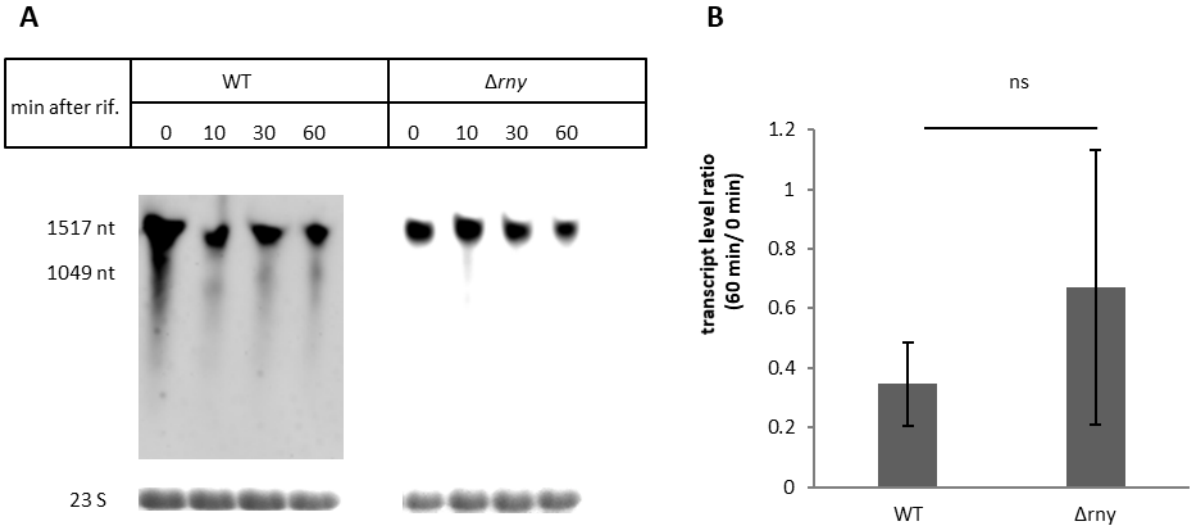

Figure 4.6: *rny* deletion does not affect SSR42 transcript stability. A) Lack of RNase Y (Δ*rny*) does not influence the transcript stability of SSR42 as demonstrated by rifampicin assay followed by Northern blotting. **B)** Quantification of chemiluminescence signals using ImageJ. Statistical analysis was performed using Student´s t-test.

4.1.4 Putative protein-coding sequences in SSR42

The nucleotide sequence of SSR42 from *S. aureus* 6850 was analysed for potential protein-coding sequences within the sequence of SSR42 using the ´find open reading frame´ function of the CLC Workbench tool. Using a minimum codon length of 12 and all known start codons as default settings 12 putative ORFs were identified ranging from 12 to 40 aa in length. All putative ORFs were not preceeded by typical ribosomal binding sites (AGGAGGU) (McLaughlin et al., 1981) and are thus not likely translated into a peptide. The putative peptide sequences were used to perform a BLAST search using the collection of non-redundant protein sequences. For some of the potential protein encoding sequences high similarities to small parts of proteins from various bacterial and other species were found. However, the E-values of the found hits were rather high thus implying a high probability that the hits were merely found by chance (Table 4.1; see Appendix table 7.4). No significant similarity was found for the translated protein sequence of the largest ORF, ORF 3.

ORF 1 was predicted to encompass 39 bp and covered nucleotides 21-59 of SSR42. For the deduced amino acid sequence an identity of 67% to a hypothetical protein of *Chryseobacterium sp*. OV279 was found. The E-value (Expect) was 2.9 (Table 4.1; see Appendix). For ORF 12 the highest of all similarities with a protein from the NCBI database was found. The deduced amino acid sequence of ORF 12 exhibited an identity of 91% to a pentatricopeptide repeat containing protein from *Apostasia shenzhenica*, a member of the family of orchids. However, with an E-value of 40 the alignment of both aa sequences most likely occurred by chance and does not verify the existence of the putative peptide encoded by ORF 12.

Since all ORFs were lacking a preceding typical Shine-Dalgarno sequence and the respective putative protein sequences could not be aligned with any proteins of *S. aureus* it was concluded that the SSR42 encoding gene harbours various potential ORFs, which are not translated into proteins and thus do not contribute to the regulatory function of ncRNA SSR42. A more complex analysis of a potential regulatory role of the largest predicted ORF (ORF 3) was performed in section 4.7.3.

Table 4.1: Analysis of putative ORFs within SSR42 (*S. aureus* strain 6850).

ORF_ID	Position in SSR42 gene	length (bp)	nucleotide sequence	aa sequence	BLAST hit	E-value
ORF 1	21-59	39	atgtatttcaaaaaacaata catagccattttgaactaa	MYFKKQYIAI LN*	Hypothetical protein (*Chryseobacterium sp.)*	2.9
ORF 2	240-314	75	ttggacatacacttttgtcat caaacgctgaaaattagtac gattgaaatcacttcttgtta taaaaattcttag	LDIHFCHQTL KISTIEITSC YKNS	Hypothetical protein (*Flavobacteriaceae bacterium*)	3.6
ORF 3	225-347	123	ttgaaatcacttcttgttata aaaattcttagtagccctgtt acaaaatattcgctacaaat tattcaaatcaacaacaata accatcaactaagaaatttt aaacaatccactaaaaaat aa	LKSLLVIKILSS PVTKYSLQIIQ INNNNHQLR NFKQSTKK*	-	-
ORF 4	262-318	57	ctgttacaaaatattcgctac aaattattcaaatcaacaac aataaccatcaactaa	LLQNIRYKLF KSTTITIN*	Hypothetical protein (*Dictyostelium purpureum*)	5.9
ORF 5	362-406	45	ctgtttagaaaacatcaaga taagtataaacatctagaaa agtga	LFRKHQDKY KHLEK*	AAA family ATPase (*Burkholderia cepacian)*	3.0
ORF 6	457-498	42	ttgaaaaagtgcattagaca gcgaaattcaccatcaagat aa	LKKCIRQRNS PSR*	Conserved hypothetical protein (*Leishmania mexicana*)	9.8
ORF 7	498-542	45	atgaagcaacaagaaacag cacacatcaatgaattaaca ccttag	MKQQETAHI NELTP*	Structural maintenance of chromosomes protein 2	0.74

					(*Schistosoma haematobiu*)	
ORF 8	550-591	42	atgagaaaatgcatggcac aactagatttaccatcaaga taa	MRKCMAQL DLPSR*	DUF4038 domain-containing protein (*Lachnoclostridium sp.*)	2.5
ORF 9	558-620	63	atgcatggcacaactagatt taccatcaagataattcttaa gcagcgaagaattaacatct ag	MHGTTRFTI KIILKQRRINI *	Putative uncharacterized protein (*Bacteroides unifomis*)	4.0
ORF 10	623-694	72	atgcataaacatcttagattt tacatcaagagatgcgataa ctataaacaactagaaacgt caccaagatag	MHKHLRFYIK RCDNYKQLE TSPR*	Glytaminyl-peptide cyclotransferase, putative (*Plasmodium sp. Gorilla clade G3*)	8.7
ORF 11	876-965	90	ttgactatatatgaattaatt atgttactagctaaatcatct attattaactttcacactcaa tttctacatctaatatca	LTIYELIMLLA KSSIINFHTQF LHLIS	Hypothetical protein (*Psychroserpens damuponensi*)	0.24
ORF 12	1075-1119	45	atgtgtatggtatcttctaac atcaagaaacgcattttaat atag	MCMVSSNIK KRILI*	Pentatricopeptide repeat containing protein (*Apostasia shenzenica*)	40

4.1.5 Secondary structure analysis

The secondary structure of ncRNA SSR42 was predicted using the RNAfold WebServer (http://rna.tbi.univie.ac.at/cgi-bin/RNAWebSuite/RNAfold.cgi; Gruber et al., 2008). The 1232 nt long SSR42 nucleotide sequence was analysed by RNAfold using the default settings minimum free energy (MFE) and partition function and avoid isolated base pairs. The WebServer provided two predictions for the secondary structure of SSR42 (Fig. 4.7). The first structure was predicted via calculation of the minimum free energy (MFE) while the second prediction was based on a thermodynamic ensemble prediction and resulted in a centroid secondary structure. The calculated minimum free energy of the SSR42 secondary structure was -192.8 kcal/mol while the free energy of the thermodynamic ensemble was -216.15 kcal/mol. Both predicted secondary structures exhibited several stem loop structures and a base-pairing between the 5´- and 3´-ends. Prediction using the Mfold web server (version 4.7; http://unafold.rna.albany.edu/?q=mfold/RNA-Folding-Form; Zuker, 2003) at 37°C resulted in 8 predicted rather similar secondary structures (see Appendix Fig. 7.2). For further visualization the MFE-based prediction secondary structure provided by RNAfold was chosen.

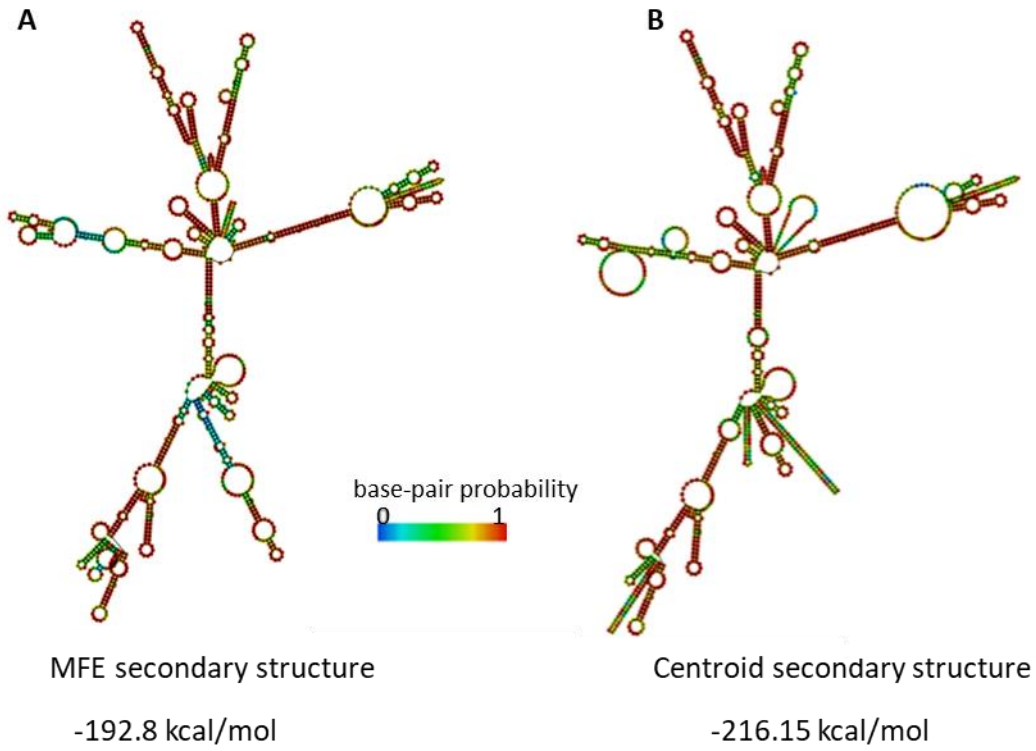

Figure 4.7: Secondary structure prediction of SSR42. Secondary structure of SSR42 was predicted using the web server RNAfold. Two different prediction approaches **A)** MFE-based and **B)** centroid-based were used. Colour code depicts base-pairing propabilities.

The MFE-based predicted secondary structure exhibited 10 stem loop structures (Fig. 4.8). Each stem loop structure consisted of several loop areas, which could serve as potential interaction sites with target mRNAs, proteins or other ncRNAs due to their single-stranded areas. On account of the extraordinary length of SSR42 the secondary structure prediction has to be viewed with a critical eye. Recently it was found that some ncRNAs further fold into a tertiary structure (Abraham et al., 2008) that determines their regulatory role. Thus, the potential secondary structure of the ncRNA molecule might not be found *in vivo* and a potential tertiary structure has to be taken into consideration. However, tertiary structure prediction tools are rather new and do not allow a prediction for a 1232 nt long molecule yet. Experimental analysis of secondary structures for example via digestion with single-strand and double-strand cleaving nucleases followed by sequencing and generating of a PARS-score and subsequent calculation of the secondary structure are limited in the length of the analysed RNA (Righetti et al., 2016; Kertesz et al., 2010). Secondary structure predictions for long RNAs were shown to be inaccurate and only 40% of predicted base pairs are thought to be predicted correctly (Doshi et al., 2004). Therefore, the predicted secondary structure was only used as an illustrative tool for a better visualization of addressed sequence areas.

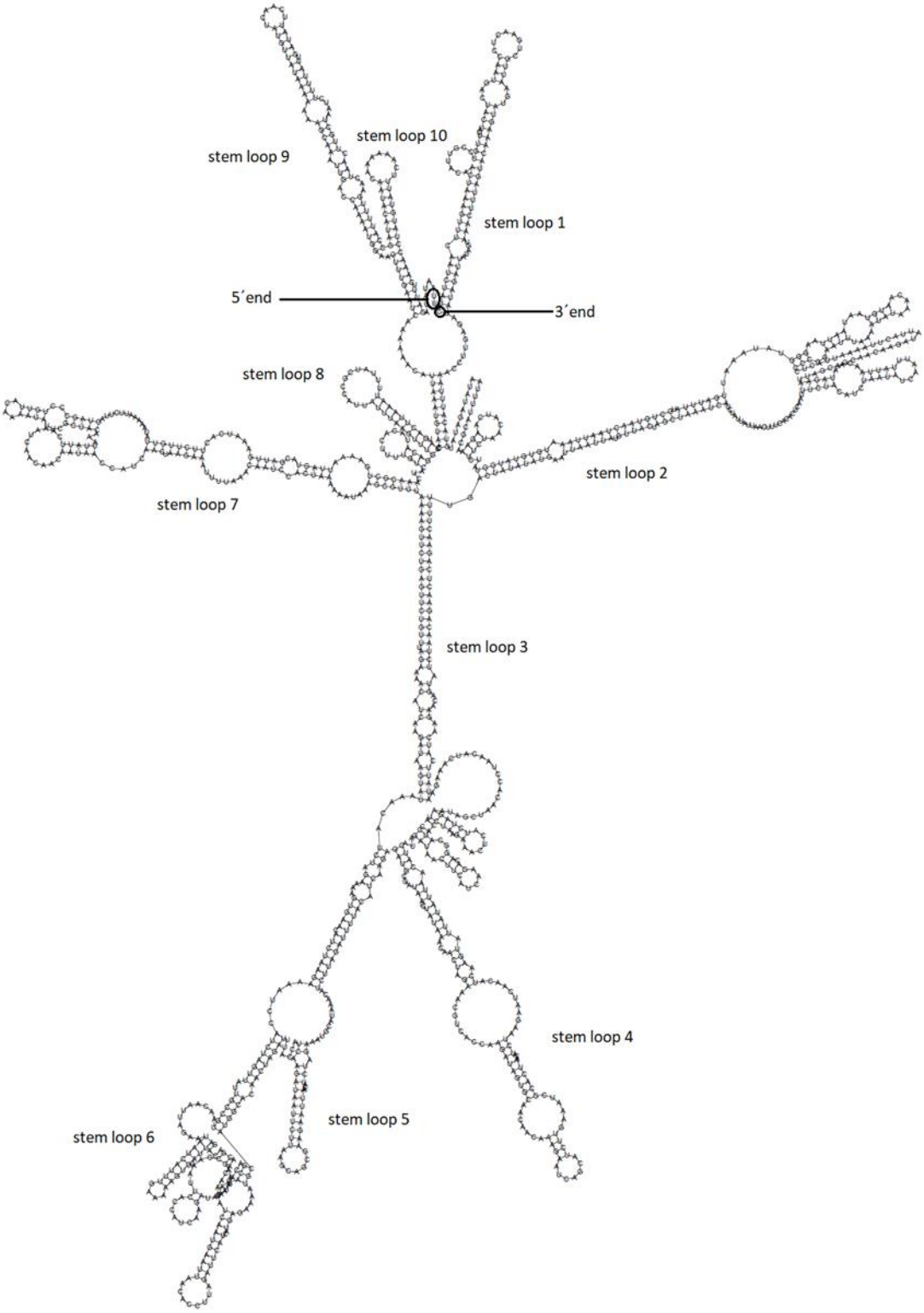

Figure 4.8: Analysis of stem loop structures within the predicted secondary structure of SSR42. MFE-based secondary structure prediction of SSR42. Stem loop regions are numbered consecutively clockwise.

4.2 Regulation of haemolysis by Rsp and SSR42

The 891 nt long transcript of SSR42 was described to be implicated in regulating haemolysis in two *S. aureus* strains, UAMS-1 and USA300. Further transcripton of Panton-Valentine leukocidin, protein A and capsular genes were found to be dependent on presence of SSR42 (Morrison et al., 2012a). Since in this study only 891 nt of SSR42 were deleted from the genome of *S. aureus* but complementation was performed with the full senquence of the gene encoding SSR42 the haemolysis deficits of the mutant could be successfully restored. Regulation of haemolysis by 1232 nt SSR42 was therefore recapitulated in this chapter. Further, Rsp, an AraC-type transcriptional regulator was identified recently to regulate the transcription of SSR42. Lack of *rsp* resulted in reduction of haemolysis and reduced transcription of haemolysins such as α-toxin (Das et al., 2016; Li et al., 2016). Whether haemolysis is indirectly regulated by Rsp via transcriptional regulation of SSR42 was investigated in this chapter.

4.2.1 SSR42 is required for wild-type haemolysis in *S. aureus* 6850

S. aureus expresses several haemolysins which cause lysis of erythrocytes (Vandenesch et al., 2012). The activity of those haemolysins can be tested by growing *S. aureus* on sheep blood agar plates. While α-toxin-mediated erythrocyte lysis is represented by a characteristic bright and clear zone around the staphylococcal colonies on agar supplemented with sheep blood, β-haemolysin causes a fainter clearance zone, which is characterized by an incomplete rupture of erythrocytes (Fig. 4.9A). This is referred to as α-haemolysis while the complete rupture of erythrocytes is called β-haemolysis. Lysis of erythrocytes leads to liberation of haemoglobin. Due to the red colouring of haemoglobin the haemolytic activity of *S. aureus* can be quantified by measuring the liberated haemoglobin spectrophotometrically at 405 nm. Investigating the role of SSR42 for the haemolytic activity of *S. aureus* culture supernatants of *S. aureus* 6850 wild-type bacteria, ΔSSR42 mutant and complemented mutant were spotted on agar plates supplemented with 5% sheep blood. The ΔSSR42 mutant exhibited a strongly reduced haemolysis zone on sheep blood agar compared to that of wild-type bacteria (Fig. 4.9B). While the α-haemolysis zone caused by β-toxin was not affected in the mutant, the β-haemolysis zone was drastically reduced. Likewise, a SSR42 transposon insertion mutant from USA300 JE2 background (JE2 2500639R, see Appendix Figure 7.3) exhibited a reduced haemolysis zone on sheep blood containing agar. Haemolytic activities were successfully restored in both genetic backgrounds via ectopically expression of SSR42 in trans.

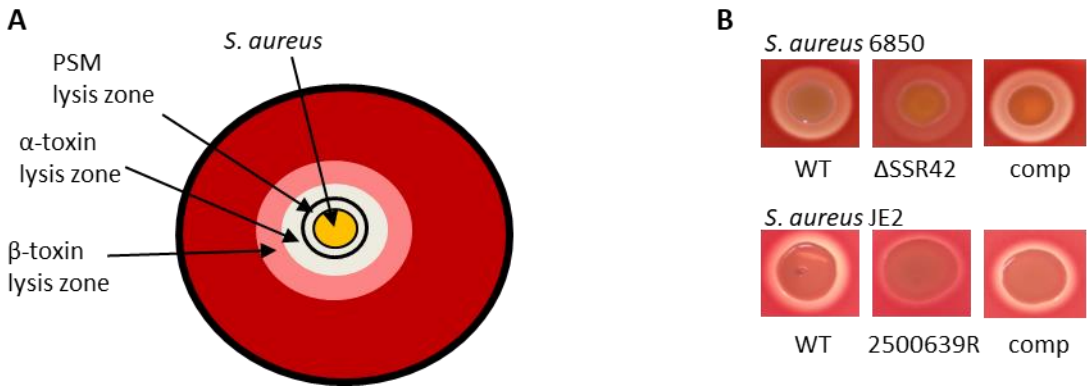

Figure 4.9: SSR42 is required for efficient haemolysis. A) Schematic representation of typical haemolysis zones of *S. aureus* grown on sheep blood agar. **B)** Lack of functional SSR42 affected haemolysis on sheep blood agar. Overnight cultures of *S. aureus* 6850 wild-type, ΔSSR42 mutant and complemented mutant (upper panel) as well as JE2 wild-type bacteria, insertional SSR42 mutant 2500639R and complemented mutant (lower panel) were spotted on sheep blood agar. Haemolysis zones were drastically reduced in case of SSR42 mutants.

Using a quantitative erythrocyte lysis assay the haemolytic activity of *S. aureus* 6850 ΔSSR42 was shown to be significantly and drastically reduced to 30.7% ($p=4.2*10^{-8}$) compared to the haemolytic activity of wild-type bacteria from the same strain background. Haemolysis was successfully restored to wild-type levels when SSR42 was complemented in trans. In order to exclude polar effects caused by a potential damage of upstream (RSAU_002216) or downstream genes (*rsp*, RSAU_002218) the ΔSSR42 mutant was complemented in trans using several plasmids: pSSR42, pSSR42-rsp and p2216-2218 (Fig. 4.10A). Complementation of haemolysis was successfully obtained by using plasmid pSSR42, harbouring the complete sequence of SSR42 and upstream gene RSAU_002216 which overlap in 5 nt in both their 3´-ends. Haemolysis was further successfully restored using plasmid pSSR42-rsp containing the complete sequence of SSR42, RSAU_002216, and *rsp* as well as when plasmid p2216-2218 harbouring all of the four ORFs was used (Fig. 4.10B). Plasmid pSSR42 was used in the following experiments to complement for ncRNA SSR42 in trans. Influence of both upstream and downstream genes in haemolysis regulation was further ruled out by spotting overnight cultures of mutants in RSAU_002216 (NE1614; RSAU_002216 corresponds to SAUSA300_2325 in strain JE2) and RSAU_002218 (NE954; RSAU_002218 corresponds to SAUSA300_2327 in strain JE2) obtained from the Nebraska mutant library (Fey et al., 2013). Insertional disruption of both ORFs did not influence the haemolytic activity of *S. aureus* JE2 (Fig. 4.10C). Involvement of *rsp* in haemolysis regulation was further addressed in section 4.2.3. *S. aureus* possesses several haemolysins capable of lysing erythrocytes. Among such is the well-studied α-toxin. The expression of α-toxin was therefore analysed via Western blotting of overnight culture supernatants. The amount of secreted α-toxin was significantly reduced in the ΔSSR42 mutant (FC=0.7; p=0.00097; Fig. 4.10D) compared to that of wild-type bacteria and was successfully complemented by expressing SSR42 in trans hence providing an

explanation for the reduced haemolytic activity of mutants lacking ncRNA SSR42. In line with this, *hla* mRNA levels were found to be significantly decreased ($FClog_{10}$: -0.34; p=0.011, Fig. 4.10E) in the SSR42 knockout mutant. *hla* transcript levels were successfully restored to wild-type levels in the mutant by complementing for SSR42 in trans.

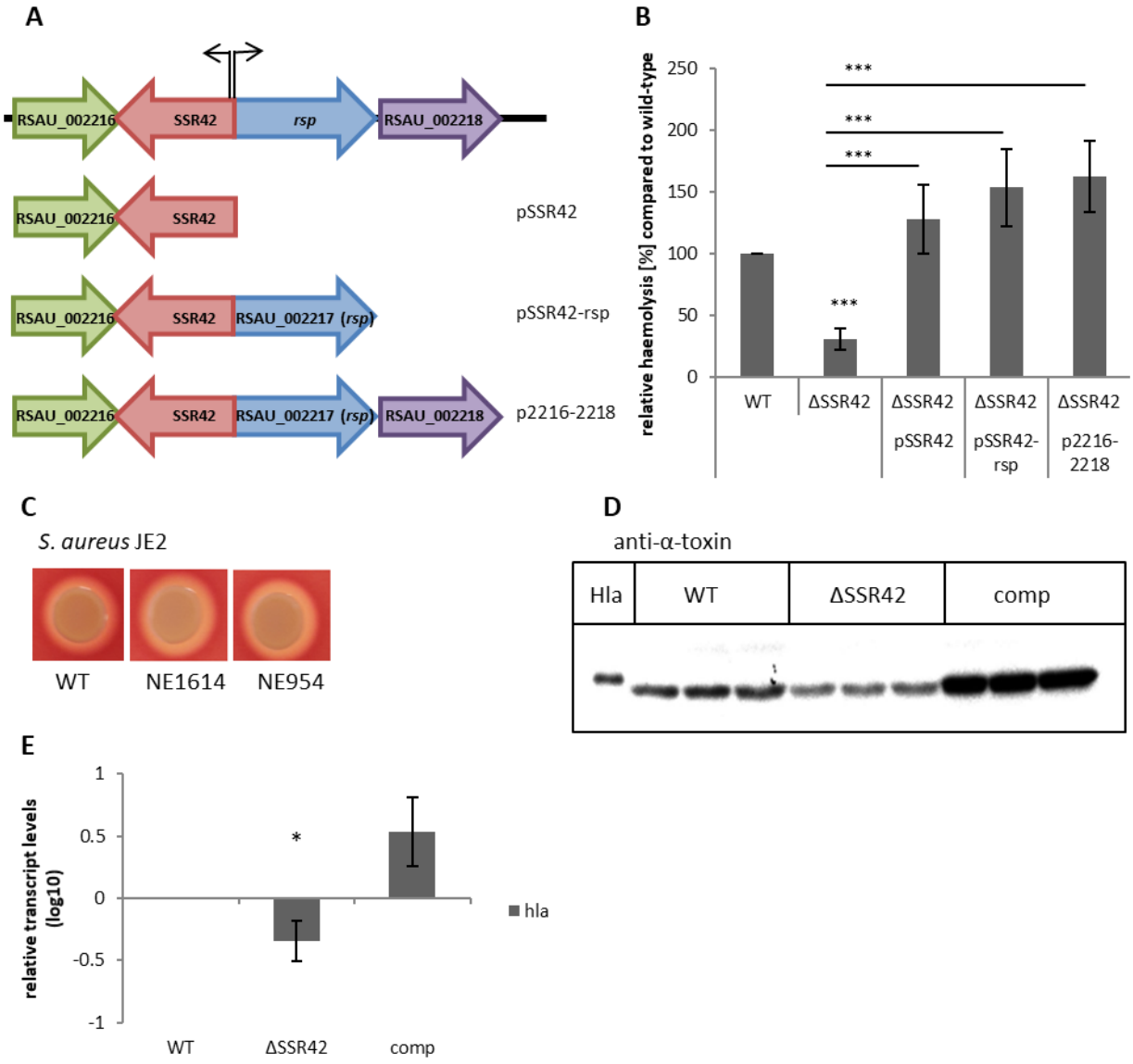

Figure 4.10: Deletion of SSR42 affects lysis of sheep erythrocytes by reduction of α-toxin expression. A) Schematic representation of various complementation plasmids containing SSR42 and neighbouring genes. **B)** Lack of SSR42 reduced the haemolytic activity of *S. aureus* 6850 significantly. Quantitative haemolysis assay using stationary growth phase supernatants of *S. aureus* 6850 wild-type, ΔSSR42 and various complementation mutants demonstrated the requirement of SSR42 for efficient lysis of sheep erythrocytes. The haemolytic activity of wild-type supernatants was set to 100%. **C)** Insertional disruption of neighbouring genes RSAU_002216 (SAUSA_2325; NE1614) and RSAU_002218 (SAUSA_2327; NE954) did not affect haemolyis as observed on sheep blood agar. **D)** Deletion of SSR42 affected expression of α-toxin (Hla) as observed by immunoblotting using stationary phase culture supernatants of each biological triplicates of 6850 wild-type, ΔSSR42 and complemented mutant. **E)** SSR42 is required for *hla* transcription. qRT-PCR analysis of stationary phase RNA revealed significantly less *hla* transcript levels in a ΔSSR42 mutant. Statistical analysis was performed using Student´s t-test.

4.2.2 Induced transcription of SSR42 is sufficient for *hla* transcription but not for haemolysis

Using an anhydrous tetracycline inducible promotor system (pAHT-SSR42) SSR42 was expressed in trans in the ΔSSR42 mutant. While inducible transcription of SSR42 in stationary growth phase resulted in a restored haemolytic activity, haemolysis could not be restored when SSR42 was ectopically transcribed in logarithmic growth phase (OD_{600}=0.4) and remained comparable in both non-induced and induced samples (Fig. 4.11A). Analysing transcript levels of logarithmic growth phase bacteria confirmed the successful complementation of SSR42 and *hla* upon AHT-induced transcription of SSR42 (p=0.08). Transcript levels of *hla* were not only complemented by induction of ectopically SSR42 transcription but found to be strongly enhanced compared to that in wild-type bacteria treated with AHT (p=0.03, Fig. 4.11B). Thus, although high *hla* mRNA levels were present upon transcriptional induction of SSR42 in logarithmic growth phase, haemolysis could not be restored indicating the involvement of other factors for translational regulation of α-toxin such as the quorum-sensing effector RNAIII. However, RNAIII can only be detected in high amounts during stationary growth phase (Boisset et al., 2007; Yarwood et al., 2002; Chabelskaya et al., 2014; Xiong et al., 2002) while being essential for translation initiation of *hla* mRNA (Morfeldt et al., 1995). When the promotor activity of RNAIII (P_{agrP3}) was analysed using a GFP reporter construct granting transcriptional fusion of *agr* and GFP, P_{agrP3} activity was found to slowly start increasing at transition from logarithmic to stationary growth phase (Fig. 4.11C). At an OD_{600} of 0.4 where ectopically transcription of SSR42 was induced only a low activity of P_{agrP3} was observed providing an explanation for the failure to restore haemolysis.

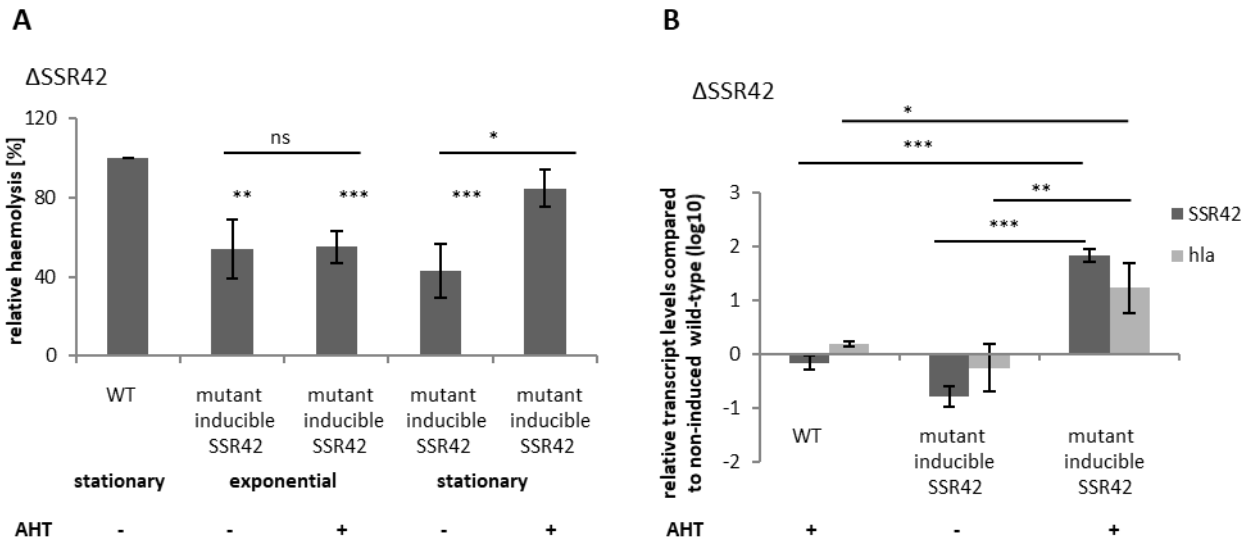

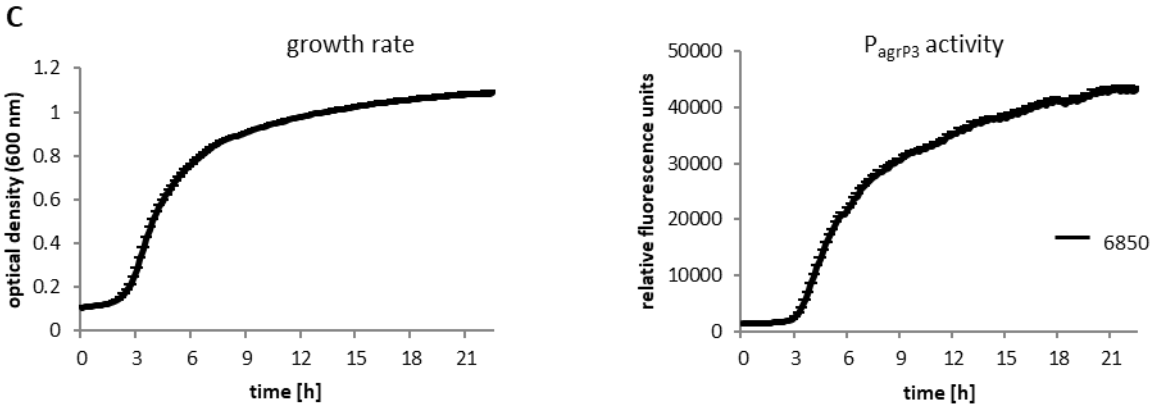

Figure 4.11: Growth phase dependent effects of inducible SSR42 transcription. A) Induction of SSR42 during stationary growth phase restored haemolysis defects of a ΔSSR42 mutant. Haemolytic activities of *S. aureus* ΔSSR42 culture supernatants were only restored to wild-type levels by anhydrous tetracycline-induced complementation of SSR42 (pAHT-SSR42) in stationary but not in exponential growth phase. + AHT indicates addition of anhydrous tetracycline. For quantification of haemolytic activities sheep erythrocytes were treated with bacterial culture supernatants. The haemolytic activity of wild-type supernatants was set to 100%. Statistical analysis was performed using Student´s t-test: *: p< 0.05; ***: p< 0.001. **B)** Analysing *hla* transcript levels of exponential growth phase ΔSSR42 mutant after AHT-induced transcription of SSR42 (pAHT-SSR42) via qRT-PCR demonstrated successful complementation of *hla* transcription upon induction of SSR42 expression. Statistical analysis was performed using Student´s t-test: *: p< 0.05; ***: p< 0.001. **C)** Growth curve and *agr* P3 promotor (P_{agrP3}) activity profile in wild-type *S. aureus* 6850. *agr* P3 promotor activity started to increase upon entry of stationary growth phase in *S. aureus* 6850.

4.2.3 SSR42 is required for restoring haemolysis in a ΔSSR42-*rsp* mutant

Distinguishing whether Rsp is regulating haemolysis in *S. aureus* directly or indirectly via transcriptional regulation of ncRNA SSR42 the haemolytic properties were investigated in a ΔSSR42 and a mutant lacking both SSR42 and *rsp* (ΔSSR42-*rsp*; Fig. 4.12A). Double knockout mutant *S. aureus* 6850 ΔSSR42-*rsp* exhibited a significantly reduced haemolytic activity towards sheep erythrocytes (Fig. 4.12B-C; 23.5%; $p=5.4*10^{-4}$) compared to that of wild-type bacteria. The haemolytic activity of the double knockout mutant was of similar extent as seen in a single ΔSSR42 mutant (30.7%). In order to identify which of both regulatory factors is responsible for the observed reduced haemolysis phenotype, the double knockout mutant ΔSSR42-*rsp* was complemented in trans for either SSR42 (pSSR42), *rsp* (pS2217) or both factors (pSSR42-rsp; Fig. 4.12C). Haemolysis could only be successfully restored when both ncRNA SSR42 and *rsp* were introduced in trans via plasmid pSSR42-rsp.

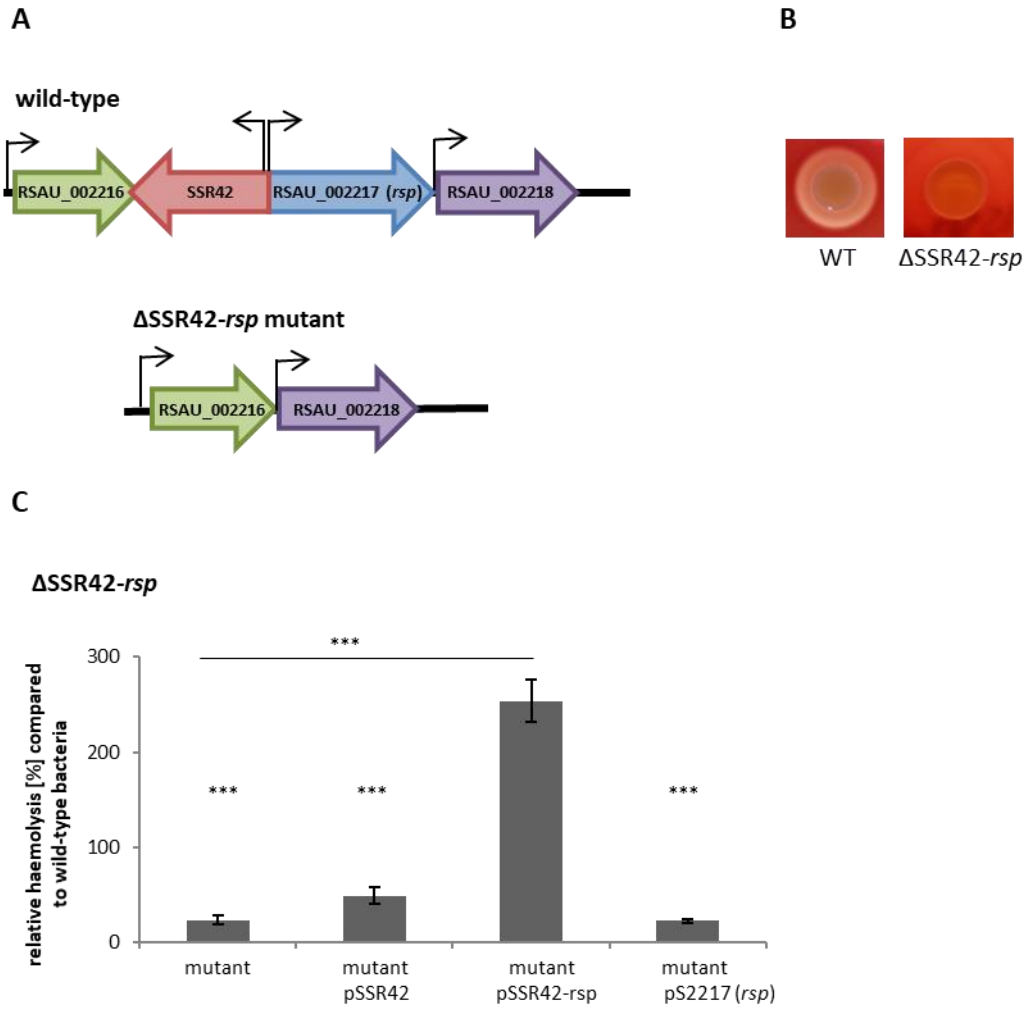

Figure 4.12: A double knockout mutant in SSR42 and *rsp* displays similar defects regarding the haemolytic activity as a ΔSSR42 mutant. A) Genomic localization of SSR42 and *rsp* in *S. aureus* 6850 and genomic situation in a ΔSSR42-*rsp* mutant. Arrows indicate transcription start sides. **B)** Lack of SSR42 and *rsp* results in reduced haemolytic activity as observed on sheep blood agar. Overnight cultures of *S. aureus* 6850 wild-type and ΔSSR42-*rsp* mutant were spotted on sheep blood agar. Haemolysis zones were drastically reduced in case of the ΔSSR42-*rsp* mutant. **C)** Quantitative analysis of haemolytic activities of *S. aureus* 6850 ΔSSR42-*rsp* mutant and various complemented mutants demonstrated a successful complementation only when both SSR42 and *rsp* were expressed in trans (pSSR42-rsp). Episomal complementation with only SSR42 (pSSR42) or *rsp* (pS2217) did not suffice in restoring haemolytic activities in the double knockout mutant ΔSSR42-*rsp*. For quantification of haemolytic activities sheep erythrocytes were treated with bacterial culture supernatants. Wild-type haemolytic activities were set to 100%. Statistical analysis was performed using Student´s t-test: *: p< 0.05; ***: p< 0.001.

To elaborate this further transcriptional analysis using qRT-PCR was performed. Whereas transcription of SSR42 could only be complemented using plasmid pSSR42-rsp*,* transcription of *rsp* was restored using either pSSR42-rsp or pS2217 for complementation (Fig. 4.13A). Instead, transcription was only restored to wild-type levels when both SSR42 and *rsp* were expressed (pSSR42-rsp) in trans. Thus, neither complementation of only *rsp* nor SSR42 was sufficient to restore transcription of *hla*. Furthermore, previous findings demonstrating a regulatory role for Rsp on transcription of SSR42 (Das et al., 2016) were confirmed since transcription was not obtainable in the double knockout mutant when SSR42 was under control of its native promotor (pSSR42).

To exclude secondary side-effects caused by potential mutations in global regulators such as the agr quorum-sensing system or the SaeRS two-component system, which depict hot spots for secondary site mutations, the transcription of the agr effector RNAIII as well as *saeS* was investigated. While RNAIII transcript levels did not differ significantly between wild-type bacteria, mutant and all of the complemented mutants, *saeS* mRNA levels were found to be significantly elevated compared to the transcript levels in wild-type bacteria when both SSR42 and *rsp* were expressed ectopically using plasmid pSSR42-rsp ($p=0.025$).

Considering that *hla* transcription could only be successfully restored to wild-type levels when both SSR42 and *rsp* were expressed but not when *rsp* alone was expressed, it was hypothesized that SSR42, not Rsp, is executing the transcriptional regulation of α-toxin. Confirming this assumption double knockout mutant ΔSSR42-*rsp* was complemented in trans for either SSR42 (pAHT-SSR42) or *rsp* (pAHT-rsp) under control of an anhydrous tetracycline inducible promotor allowing timely targeted expression neglecting the regulatory relationship of both factors and assuring SSR42 transcription in absence of Rsp (Fig. 4.13B). Transcript levels of SSR42, *rsp* and *hla* were analysed upon transcriptional induction via an AHT pulse in logarithmic growth phase ($OD_{600}=0.4$). Only upon induction of SSR42 transcription a significant increase in *hla* mRNA levels was observed ($p=0.0007$) compared to the transcript levels in non-induced bacteria. Induction of *rsp* transcription instead led to a slight increase in *hla* mRNA levels comparable to the increase observed in wild-type bacteria, which were stimulated with AHT indicating only a side-effect of AHT-treatment.

Thus, induction of SSR42 transcription was sufficient to restore *hla* transcription in the double knockout mutant ΔSSR42-*rsp.*

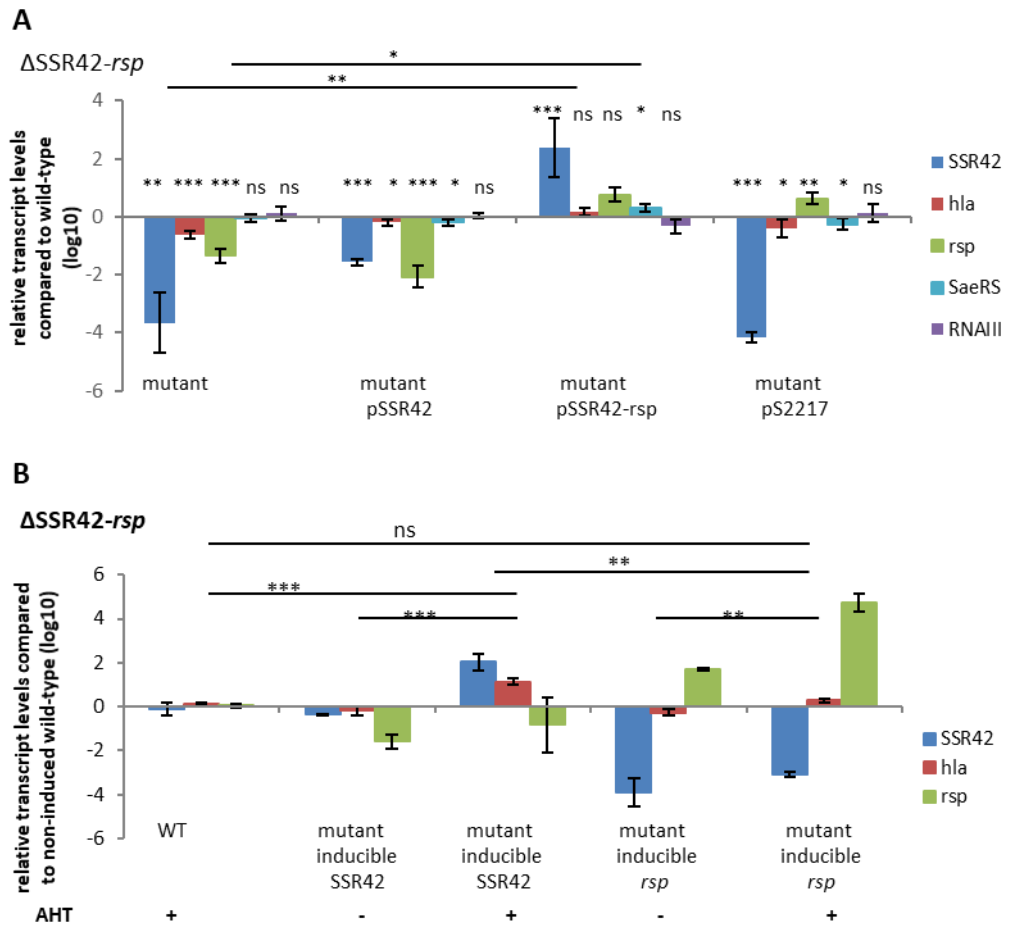

Figure 4.13: SSR42 is required for haemolysis in *S. aureus* while Rsp mediates transcription of SSR42. A) *hla* transcription was only successfully restored by episomal complementation of both SSR42 and *rsp* (pSSR42-rsp) but not by either only SSR42 (pSSR42) or *rsp* (pS2217). qRT-PCR analysis of SSR42, *hla*, *rsp*, *sae*S and RNAIII levels in *S. aureus* 6850 wild-type, ΔSSR42-*rsp* mutant and various complemented mutants. Transcription of *sae*S and RNAIII was not affected by deletion of both SSR42 and *rsp*. **B)** Expression of SSR42 is required for efficient *hla* transcription. qRT-PCR analysis of *hla* levels in *S. aureus* wild-type, ΔSSR42-*rsp* mutant and mutant complemented with either AHT-inducible expression of SSR42 (pAHT-SSR42) or *rsp* (pAHT-rsp). Only AHT-induced transcription of SSR42 resulted in a significantly increase in *hla* transcript levels and successful complementation of *hla* transcription. Statistical analysis was performed using Student´s t-test: *: p< 0.05; ***: p< 0.001

4.3 ncRNA SSR42 is the main effector of Rsp-mediated virulence in *S. aureus*

With the aid of the double knockout mutant ΔSSR42-*rsp* the regulation of *hla* transcription was deciphered and found to be executed via ncRNA SSR42 whilst Rsp was found to be essential for ensuring transcription of SSR42. Thus, the previously detected reduced haemolytic properties of a Δ*rsp* mutant resulted from loss of SSR42 transcription. Since many virulence factors were found to be differentially regulated in a Δ*rsp* mutant (Das et al., 2016) the impact of SSR42 on regulation of those factors was pursued.

4.3.1 ncRNA SSR42 influences transcription of a plethora of virulence factors

For gene expression profiling by RNA-seq total RNA of stationary growth phase (16 h) and exponential growth phase (OD_{600}=0.6) bacteria was isolated. By using high throughput Illumina sequencing differences in RNA abundances when either SSR42 or both SSR42 and *rsp* were not expressed were uncovered (RNA-seq was performed in collaboration with Bruno Huettel and Richard Reinhardt, Genome Centre Cologne and analysed by Maximilian Klepsch, University Würzburg). Several mRNAs encoding virulence factors were found at different transcript levels in the ΔSSR42 mutant when compared to wild-type bacteria (table 4.2, 4.3, see Appendix tables 7.5, 7.6). These included, for example, in exponential growth phase *psm*α4 (phenol soluble modulin; log_2FC: -2.56; padj= $3.5*10^{-10}$, *ure*B (urease subunit beta; log_2FC: 1.87; padj= 0.00162), *ldh*D (D-lactate dehydrogenase; log_2FC: 2.59; padj= 5.67E-09), and *cap*D (capsular polysaccharide synthesis enzyme; log_2FC: 1.50; padj= 0.00034) and in stationary growth phase *chs* (chemotaxis inhibitory protein; log_2FC :-1.81; padj= 0.000877), *scp*A (staphopain A; log_2FC: -1.80; padj= 7.24E-14), *clf*A (clumping factor A; log_2FC: 2.56, padj= 1.75E-20), *isd*B (haem uptake; log_2FC: -2.35; padj= 7.81E-12) and *ffh* (signal recognition particle; log_2FC: 0.85; padj= 0.00028). Differential expression for several virulence factors was verified using qRT-PCR: in exponential growth phase for *psm*α ($FClog_{10}$:-0.64; p=0.03), *ure*B ($FClog_{10}$:0.47; p=0.002), *ldh*D ($FClog_{10}$: 1.03; p=0.03), *cap*D ($FClog_{10}$:0.36; p=0.02), RSAU_002216 ($FClog_{10}$: -0.81; p=0.01; Fig. 4.14A). However, for *lrg*A, *nir*B and *sar*R no significant differences in transcript levels could be detected in the SSR42 knockout mutant despite a significant differential regulation in the RNA-seq derived data (Fig. 4.14B).

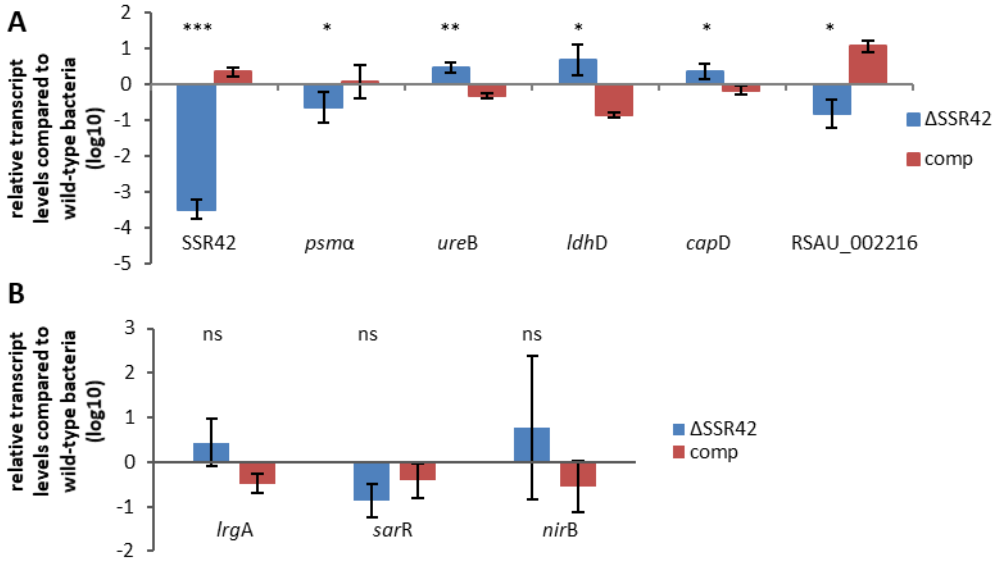

Figure 4.14: SSR42 regulates the expression of various virulence factors during exponential growth phase of *S. aureus* 6850. A) Quantitative real time PCR analysis of *psm*α, *ure*B, *ldh*D, *cap*D and RSAU_002216 transcript levels in *S. aureus* 6850 wild-type, ΔSSR42 mutant and complemented mutant revealed regulation of those genes by ncRNA SSR42**. B)** Quantitative real time PCR analysis of *lrg*A, *sar*R and *nir*B mRNA in *S. aureus* 6850 wild-type, ΔSSR42 mutant and complemented mutant revealed no regulatory impact of SSR42. Statistical analysis was performed using Student´s t-test: *: p< 0.05; ***: p< 0.001.

In stationary growth phase *chs* ($FClog_{10}$:-0.73; p=0.0003), *scp*A ($FClog_{10}$:-0.78; p>0.0001), RSAU_002216 ($FClog_{10}$: -0.83; p=0.0003), *clf*A ($FClog_{10}$:0.78; p=0.003), *isd*B ($FClog_{10}$:-0.84; p>0.0001), *ffh* ($FClog_{10}$: 0.21; p=0.001) and *esx*A ($FClog_{10}$: 0.82; p=0.03) were found to be significant differentially expressed in the ΔSSR42 mutant (Fig. 4.15A). However, no significant differences between expression levels in wild-type bacteria and ΔSSR42 mutant were found for *ess*A, *sar*X, *gpx*A and *ess*B (Fig. 4.15B).

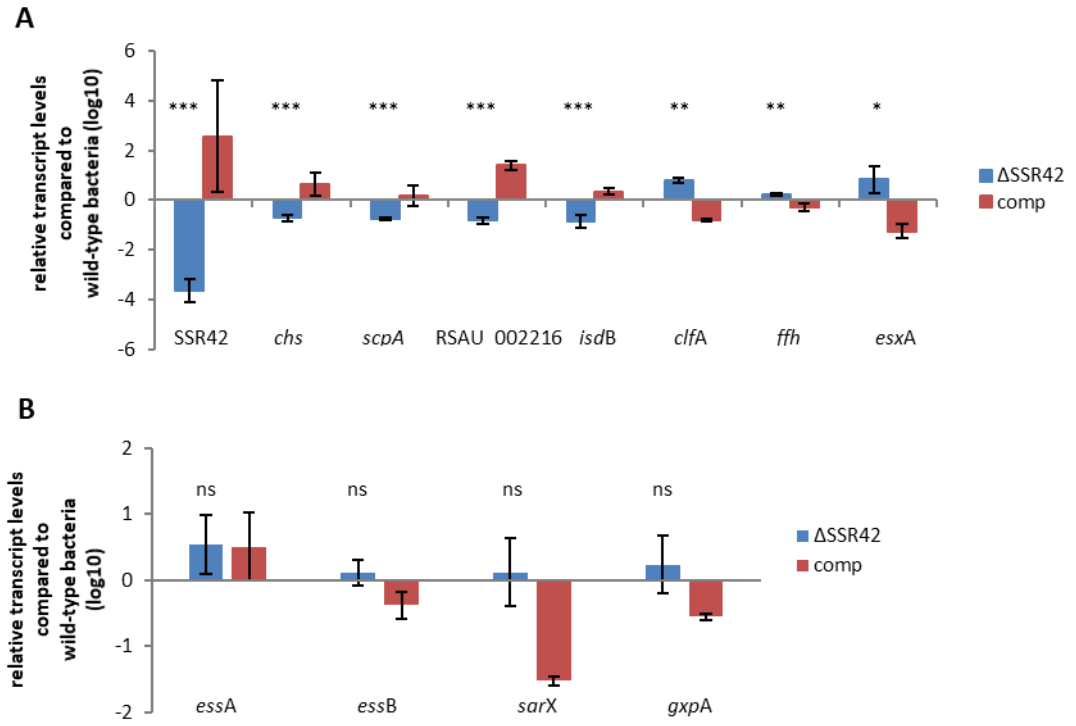

Figure 4.15: SSR42 regulates the expression of various virulence factors during stationary growth phase of *S. aureus* 6850. A) Quantitative real time PCR analysis of *chs*, *scp*A, RSAU_002216, *isd*B, *ffh* and *esx*A transcript levels in *S. aureus* 6850 wild-type, ΔSSR42 mutant and complemented mutant revealed regulation of those genes by ncRNA SSR42. **B)** Quantitative real time PCR analysis of *ess*A, *ess*B, *sar*X and *gxp*A mRNA in *S. aureus* 6850 wild-type, ΔSSR42 mutant and complemented mutant revealed no regulatory impact of SSR42. Statistical analysis was performed using Student´s t-test: *: p< 0.05; ***: p< 0.001.

Ruling out potential side-effects on expression of up-stream ORF RSAU_002216 caused by deletion of SSR42 the ΔSSR42 mutant was complemented in trans with an AHT-inducible complementation plasmid (pAHT-SSR42; Fig. 4.16) that only harbours the SSR42 encoding sequence and no up- or downstream sequences. AHT-inducible complementation restored the expression of RSAU_002216 successfully verifying regulation by SSR42 and ruling out secondary side-effects of the targeted deletion of SSR42.

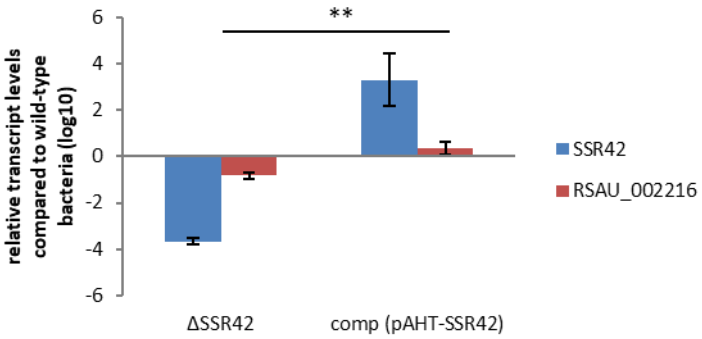

Figure 4.16: Expression of RSAU_002216 is regulated by SSR42. Quantitative real time PCR analysis of RSAU_02216 transcript levels in *S. aureus* 6850, ΔSSR42 and complemented mutant (pAHT-SSR42). Expression of RSAU_002216 was not reduced due to secondary site mutations but is regulated by SSR42 as observed in qRT-PCR. Transcription of RSAU_002216 was successfully complemented by AHT-inducible expression of SSR42. Statistical analysis was performed using Student´s t-test: *: p< 0.05; ***: p< 0.001

In order to decipher the regulatory impact of SSR42 and Rsp special consideration was given to the comparison of the transcriptome of a single ΔSSR42 and the double knockout mutant ΔSSR42-*rsp* (table 4.4, 4.5; see Appendix tables 7.7-7.10). Only a few mRNAs were found to differ between mutants lacking either only SSR42 or both SSR42 and *rsp*. Among these *his*D (histidinol dehydrogenase, log_2FC 1.74; padj=0.02), *isa*B (immune dominant antigen B; log_2FC 1.29; padj=0.031), *luk*G (leucocidin subunit G; log_2FC 1.23; padj= 0.006) and *ssa*A3 (secretory antigen precursor SsaA; log_2FC -1.54; padj=0.032) were detected. Astonishingly, no additional gene other than *rsp* was found to be differentially expressed during stationary growth phase in the double knockout mutant compared to the expression patterns in the ΔSSR42 mutant. Differences in transcript levels of those genes were analysed using qRT-PCR, thereby comparing the transcript levels of *S. aureus* 6850 wild-type bacteria, ΔSSR42-*rsp* mutant and the double knockout mutant complemented only for *rsp* (pS2217; Fig. 4.17). A differential regulation in ΔSSR42-*rsp* could only be confirmed for *his*D ($FClog_{10}$: 1.12; p>0.0001), *ssa*A3 ($FClog_{10}$: -0.79; p= 0.007) and *luk*G ($FClog_{10}$: 0.53; p=0.027). For transcript levels of *isa*B no significant difference was detected.

Thus, the transcription of a majority of previous identified Rsp-regulated target genes is only indirectly modulated by Rsp via transcriptional regulation of ncRNA SSR42.

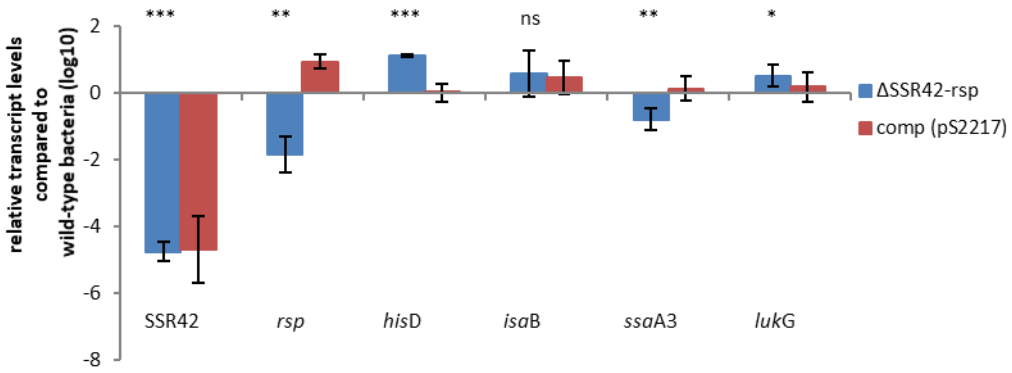

Figure 4.17: Rsp regulates the expression of *his*D, *ssa*A3 and *luk*G in *S. aureus* 6850. Quantitative real time PCR analysis of *his*D, *isa*B, *ssa*A3 and *luk*G transcript levels in *S. aureus* 6850 wild-type, ΔSSR42-*rsp* double knockout mutant and mutant complemented for *rsp* expression revealed regulation of *his*D, *ssa*A3 and *luk*G but not *isa*B. Statistical analysis was performed using Student´s t-test: *: p< 0.05; ***: p< 0.001

Table 4.2: Top 10 genes up-regulated in S. aureus 6850 ΔSSR42 in exponential and stationary growth phase respectively.

gene	log_2Fold change[1]	adjusted p-value	product
exponential growth phase			
nirB	2.72	0.026	assimilatory nitrite reductase [NAD(P)H] large subunit putative
RSAU_002525	2.67	0.001	ATP phosphorribosyl-transferase regulatory regulatory subunit
ldhD	2.58	$1.01*10^{-8}$	D-lactate dehydrogenase
RSAU_000366	2.39	$1.35*10^{-11}$	hypothetical protein
hisA	2.39	0.005	1-(5-phosphoribosyl)-5-[(5-phosphoribosyl-amino) methyl-ideneamino] imidazole-4-carboxamide isomerase HisA
RSAU_001467	2.14	0.0004	LamB/YcsF family protein
ureB	1.89	$2.07*10^{-5}$	urease β- subunit
RSAU_000185	1.81	0.01	flavohemoprotein putative
hisF	1.80	0.047	imidazole glycerol phosphate synthase cyclase subunit HisF
RSAU_001651	1.78	0.046	calcium-binding lipoprotein putative
stationary growth phase			
RSAU_002545	2.56	$7.0*10^{-6}$	hypothetical protein
clfA	2.54	$1.4*10^{-19}$	clumping factor A
fadE	2.51	$5.0*10^{-07}$	acyl-CoA synthetase putative
RSAU_000180	2.42	$8.0*10^{-07}$	coenzyme A transferase
RSAU_000249	2.34	$7.4*10^{-05}$	putative lipoprotein
RSAU_000228	2.18	$4.2*10^{-10}$	WxG Protein EsxA (Typ VII secretion system)
RSAU_000608	2.17	$9.0*10^{-18}$	bacteriophage tail tape measure protein TP901 family
fadD	2.15	0.0002	acyl-CoA dehydrogenase putative
RSAU_000760	2.06	0.002	hypothetical protein
RSAU_000762	2.04	0.002	lipoprotein putative

[1]Compared to transcript levels in *S. aureus* 6850 wild-type bacteria

Table 4.3: Top 10 genes down-regulated in *S. aureus* 6850 ΔSSR42 in exponential and stationary growth phase respectively.

gene	log_2Fold change[1]	adjusted p-value	product
exponential growth phase			
RSAU_002216	-4.13	$1.28*10^{-33}$	hypothetical protein
psmA4	-2.56	$3.47*10^{-10}$	phenol-soluble modulin alpha 4
RSAU_000768	-2.40	$9.7*10^{-5}$	hypothetical protein
sarR	-2.34	$3.8*10^{-09}$	staphylococcal accessory regulator R
psmA2	-2.05	0.001	phenol-soluble modulin alpha 2
psmA1	-1.90	0.04	phenol-soluble modulin alpha 1
psmA3	-1.82	0.0005	phenol-soluble modulin alpha 3
pyrF	-1.79	$1.6*10^{-6}$	orotidine 5-phosphate decarboxylase
pyrP	-1.62	0.03	uracil permease PyrP putative
pyrAB	-1.57	$1.0*10^{-8}$	carbamoyl-phosphate synthase large subunit PyrAB
stationary growth phase			
RSAU_002545	2.56	$7.0*10^{-6}$	hypothetical protein
clfA	2.54	$1.4*10^{-19}$	clumping factor A
fadE	2.51	$5.0*10^{-07}$	acyl-CoA synthetase putative
RSAU_000180	2.42	$8.0*10^{-07}$	coenzyme A transferase
RSAU_000249	2.34	$7.4*10^{-05}$	putative lipoprotein
RSAU_000228	2.18	$4.2*10^{-10}$	WxG Protein EsxA (Typ VII secretion system)
RSAU_000608	2.17	$9.0*10^{-18}$	bacteriophage tail tape measure protein TP901 family
fadD	2.15	0.0002	acyl-CoA dehydrogenase putative
RSAU_000760	2.06	0.002	hypothetical protein
RSAU_000762	2.04	0.002	lipoprotein putative

[1]Compared to transcript levels in *S. aureus* 6850 wild-type bacteria

Table 4.4: Top 5 genes up-regulated in *S. aureus* 6850 ΔSSR42-*rsp* in exponential and stationary growth phase respectively compared to transcript levels in *S. aureus* 6850 ΔSSR42.

Gene	log_2Fold change[1]	adjusted p-value	product
exponential growth phase			
psmA1	1.87	$1.6*10^{-3}$	phenol-soluble modulin alpha 1
RSAU_000315	1.65	$2.7*10^{-5}$	staphylococcal enterotoxin putative
hisD	1.59	$1.4*10^{-3}$	histidinol dehydrogenase HisD
RSAU_000317	1.43	$1.4*10^{-4}$	putative lipoprotein putative
RSAU_002223	1.33	$1.9*10^{-4}$	hypothetical protein
RSAU_000030	1.32	$1.3*10^{-3}$	hypothetical protein
isaB	1.29	$5.4*10^{-4}$	immunodominant antigen B IsaB
RSAU_000782	1.31	$5.9*10^{-4}$	arsenate reductase putative
psmA4	1.26	$6.9*10^{-4}$	phenol-soluble modulin alpha 4
lukG	1.21	$9.9*10^{-5}$	F subunit LuKF-G putative
stationary growth phase			
-	-	-	-

[1]Compared to transcript levels in *S. aureus* 6850 ΔSSR42 mutant

Table 4.5: Top 5 genes down-regulated in *S. aureus* 6850 ΔSSR42-*rsp* in exponential and stationary growth phase respectively compared to transcript levels in *S. aureus* 6850 ΔSSR42.

Gene	log_2Fold change[1]	adjusted p-value	product
exponential growth phase			
rsaF	-1.56	$3.8*10^{-4}$	Non-coding RNA
RSAU_002132	-1.56	$7.2*10^{-4}$	secretory antigen precursor SsaA putative
RSAU_001730	-1.57	$1.3*10^{-4}$	tRNA-Ser
RSAU_001729	-1.59	$1.9*10^{-5}$	tRNA-Met
RSAU_001687	-1.59	$2.7*10^{-4}$	tRNA-Phe
stationary growth phase			
rsp	-7.53	$2.1*10^{-22}$	Repressor of surface proteins

[1]Compared to transcript levels in *S. aureus* 6850 ΔSSR42 mutant

4.3.2 ncRNA SSR42 influences the protein levels of a multitude of virulence factors

Analysis of the transcriptome of a ΔSSR42 mutant revealed several virulence factors, which are regulated by SSR42. Further analysing the regulatory impact of SSR42 on the cytosolic and extracellular proteome of stationary growth phase (16 h) and exponential growth phase (OD_{600}=0.6), bacteria were analysed using mass spectrometry (table 4.6; 4,7, Appendix table 7.11, mass spectrometry was performed by Andreas Otto and Dörte Becher, University of Greifswald and analysed by Maximilian Klepsch, University Würzburg). Relative protein abundances in *S. aureus* 6850 wild-type bacteria and isogenic ΔSSR42 and ΔSSR42-*rsp* mutant were analysed (Appendix table 7.12) and compared focusing again on the overlap of differentially regulated proteins in both mutants (table 4.8; 4.9, see Appendix table 7.13). In the ΔSSR42 mutant several virulence associated proteins such as EsaA (RSAU_000229, FC: 2.56; p=0.0068) and SarA (RSAU_000573 , FC: 1.76; p=0.019) were enriched in the cytosolic fraction, while in the extracellular fraction virulence factors such as EsxA (RSAU_000228, FC: 7.6; $2.6*10^{-6}$), Sbi (RSAU_002257, FC: 1.8; p=0.00091), β-haemolysin HlgB (RSAU_002260, FC: 4.3; p= 0.022) and γ-haemolysin HlgC (RSAU_002259, FC: 3.6 p=0.004) were found in higher amount in the SSR42 mutant (see Appendix table 7.11). When analysing the proteome of double knockout mutant ΔSSR42-*rsp* similarities to a high degree to that of a ΔSSR42 mutant were detected again confirming the high regulatory impact of SSR42. Differences between the ΔSSR42 and double knockout mutant ΔSSR42-*rsp* were detected in exponential growth phase for example for Luk-H (RSAU_001838; FC: 1.82; p=0.048) and in stationary growth phase for catalase (RSAU_001216; FC: 1.56; p=0.002). In summary, while most of the virulence factors, which were differential expressed in a mutant lacking *rsp* (Das et al., 2016),

were shown to be regulated by ncRNA SSR42, only a small subset of virulence factors was identified to be regulated by AraC-type transcriptional regulator Rsp independently of SSR42.

Table 4.6: Top 5 hits of proteins with higher abundance in *S. aureus* 6850 ΔSSR42 in exponential and stationary growth phase respectively.

gene	fold change[1]	adjusted p-value	fraction	product
exponential growth phase				
RSAU_000228	7.6	$2.6*10^{-6}$	extracellular	WxG Protein EsxA (Typ VII secretion system)
RSAU_002260	4.3	0.022	extracellular	gamma-hemolysin component B precursor, HlgB
RSAU_001040	2.5	0.0003	extracellular	Efb, extracellular fibrinogen binding protein
RSAU_001833	2.5	0.005	extracellular	map-like protein
RSAU_000940	2.2	$4.4*10^{-6}$	extracellular	Atl, Autolysin
stationary growth phase				
RSAU_002514	7.05	0.001	extracellular	lipase precursor
RSAU_002340	7.0	0.0001	extracellular	FnbB
RSAU_002259	3.6	0.004	extracellular	gamma haemolysin HlgC
RSAU_001553	3.6	0.007	cytosolic	methylcitrat synthase
RSAU_1083	3.2	$8.6*10^{-5}$	cytosolic	aspartat carbamoyltransferase (PyrB)

[1]Compared to transcript levels in *S. aureus* 6850 wild-type bacteria (ΔSSR42/WT)

Table 4.7: Top 5 hits of proteins with lower abundance in *S. aureus* 6850 ΔSSR42 in exponential and stationary growth phase respectively.

gene	fold change[1]	adjusted p-value	fraction	product
exponential growth phase				
RSAU_000449	0.4	0.0002	cytosolic	hypoxanthine phosphoribosysl-transferase
RSAU_001860	0.4	0.02	extracellular	60 kDa chaperonin GroEL
RSAU_001445	0.4	0.0009	extracellular	chaperone protein DnaK
RSAU_000452	0.4	$2.0*10^{-6}$	extracellular	cysteine synthase A
RSAU_000754	0.6	0.002	extracellular	enolase
stationary growth phase				
RSAU_001372	0.37	0.02	cytosolic	glucose-6-P-1-dehydrogenase (Zwf)
RSAU_002532	0.4	0.003	cytosolic	YceI domain protein
RSAU_001094	0.4	0.049	cytosolic	primosomal assembly protein PriA
RSAU_000449	0.4	0.006	extracellular	hypoxanthine phosphoribosysmtransferase
RSAU_000323	0.45	0.009	cytosolic	alkyl hydroperoxid reductase subunit F (AhpF)

[1]Compared to transcript levels in *S. aureus* 6850 wild-type bacteria (ΔSSR42/WT)

Table 4.8: Influence of Rsp on virulence factor protein levels. Top 5 hits of proteins with higher abundance in *S. aureus* ΔSSR42-*rsp* compared to ΔSSR42.

Gene	fold change[1]	p-value	fraction	Product
exponential growth phase				
RSAU_000524	2.4	0.02	cytosolic	hexulose-6-phosphate synthase
RSAU_001966	1.91	0.0004	cytosolic	DNA-directed RNA polymerase
RSAU_001213	1.9	0.0019	cytosolic	hydrolase haloacid dehalogenase-like family
RSAU_001942	1.86	0.03	cytosolic	F_OF_1-ATP synthase subunit gamma
RSAU_001838	1.82	0.048	extracellular	Leukocidin S subunit LukS-H
stationary growth phase				
RSAU_000494	1.9	0.025	extracellular	DNA-dependent RNA polymerase C beta subunit
RSAU_000936	1.72	0.0015	extracellular	glutamyl endopeptidase precursor putative
RSAU_001192	1.57		extracellular	glutamine synthetase type I
RSAU_001216	1.56	0.002	extracellular	catalase
RSAU_000009	1.56	0.005	extracellular	seryl-tRNA synthetase

[1]Compared to transcript levels in *S. aureus* 6850 ΔSSR42 (ΔSSR42-*rsp*/ΔSSR42)

Table 4.9: Influence of Rsp on virulence factor protein levels. Top 5 hits of proteins with lower abundance in *S. aureus* ΔSSR42-*rsp* compared to ΔSSR42.

Gene	fold change[1]	p-value	fraction	Product
exponential growth phase				
RSAU_000940	0.34	0.014	cytosolic	autolysin Atl
RSAU_002146	0.42	0.013	cytosolic	formate dehydrogenase alpha subunit putative
RSAU_001094	0.43	0.03	cytosolic	primosomal assembly protein PriA
RSAU_000495	0.46	0.02	cytosolic	DNA directed RNA polymerase beta-prime chain putative
RSAU_000494	0.48	0.03	cytosolic	DNA-dependent RNA polymerase beta subunit
stationary growth phase				
RSAU_000857	0.41	0.045	extracellular	hypothetical protein
RSAU_001029	0.55	0.02	cytosolic	thioredoxin TrxA
RSAU_001488	0.57	0.005	cytosolic	transcriptional regulator
RSAU_001588	0.59	0.03	cytosolic	formate-tetrahydrofolate ligase
RSAU_001615	0.68	0.003	cytosolic	leucyl-tRNA synthetase

[1]Compared to transcript levels in *S. aureus* 6850 ΔSSR42 (ΔSSR42-*rsp*/ΔSSR42)

4.3.3 Role of ncRNA in *S. aureus*-induced cell death

Analogue to the transcriptional analysis most differentially regulated proteins in the ΔSSR42-*rsp* mutant were also found to be differentially regulated in the single SSR42 mutant indicating an important role for SSR42 regulating virulence factor expression. Thus, the previous reported regulatory role for Rsp was considered to be executed indirectly via ncRNA SSR42. Considering the strong impact of SSR42 on the regulation of a plethora of virulence factors it was hypothesized that the previously found phenotypic properties of a *rsp* mutant could result from lack of SSR42 transcription rather than from Rsp itself. Regarding haemolysis regulation this hypothesis was already validated (see section 4.2.3).

Rsp was reported to be essential for intracellular cytotoxicity of infected host cells with mutants displaying strongly reduced cytolytic properties (Das et al., 2016). The role of SSR42 in triggering host cell death was therefore analysed. For this, HeLa 2000 cells were infected with a MOI of 10 with wild-type bacteria, ΔSSR42 and complemented mutant from 6850 strain background and cell death was measured 4 h post infection. LDH release was used as an indicator for dying host cells and found to be at significantly lower levels when HeLa 2000 cells were infected with the ΔSSR42 mutant (Fig. 4.18A; 58.15% normalized to wild-type levels of LDH release; p=0.003) compared to cells infected with wild-type bacteria of the same strain background. The reduced cytotoxic activity of the ΔSSR42 mutant was successfully restored when SSR42 was ectopically expressed (comp; 101.1%). Further LDH release from HeLa 200 cells infected with either a Δ*rsp* (54.4%; p=0.004) or a Δ*hla* (52.5%; p=0.0002) mutant was found to be significantly less compared to cells infected with wild-type bacteria from the same strain background (Fig. 4.18B). Interestingly, the LDH release of the cells infected with those mutants was at comparable levels to cells infected with the ΔSSR42 mutant. Thus, knockout of either *rsp*, SSR42 or *hla* resulted in a similar phenotype regarding intracellular killing of host cells. Enumerating the colony forming units (CFU) from the infected cells 90 min after infection revealed no differences between the four groups indicating that similar bacterial abundances were present in the host cells at the initial stages of infection ruling out potential invasion defects (Fig. 4.18C). Since mutants in *rsp* and SSR42 displayed similar reduced cytolytic activities towards host cells it was concluded that SSR42 is responsible for the previous reported reduced cell-death phenotype of Δ*rsp* mutants. α-toxin, which was previously shown to be regulated by ncRNA SSR42, was identified as the potential factor eliciting host cell death from within the infected cells.

By expression of a plethora of cytolytic virulence factors *S. aureus* is not only able to kill cells from within, but further the culture supernatant displays toxicity towards host cells. The toxicity of *S. aureus* culture supernatants was analysed by intoxicating HeLa 2000 cells with 10% of supernatants collected from wild-type bacteria, ΔSSR42 and complemented mutant. The culture supernatants obtained from

the mutant lacking SSR42 exhibited significantly less toxicity towards HeL2000 cells measured by LDH release (Fig. 4.18D; 41.47%; p>0.001). The effect was successfully recovered by complementation of SSR42 (120.85%). Thus, SSR42 was shown to regulate virulence factors implicated in eliciting host cell death.

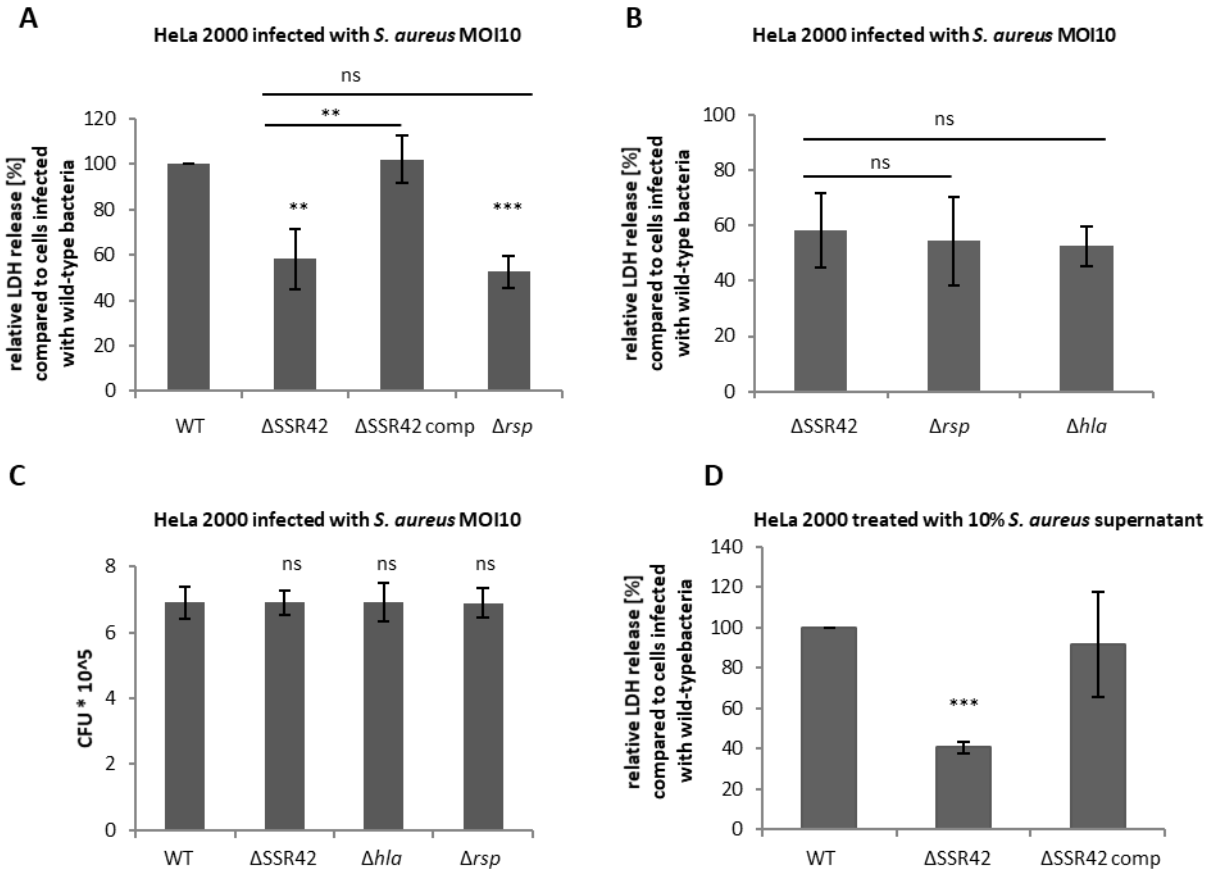

Figure 4.18: ncRNA SSR42 affects host cell death but not invasion. A) Deletion of SSR42 significantly reduces toxicity of *S. aureus* 6850 towards HeLa 2000 cells as observed by LDH release from host cells. Death of HeLa 2000 cells infected with *S. aureus* 6850 wild-type, ΔSSR42 mutant, complemented mutants and Δ*rsp* mutant was quantified via measuring LDH release. **B)** Deletion of either *hla*, SSR42 or *rsp* affects host cell death in a similar way as detected by LDH release from infected HeLa 2000 cells. **C)** Invasion of *S. aureus* 6850 into HeLa 2000 cells is not affected by knockout of either SSR42, *hla* or *rsp*. Enumeration of CFU obtained from infected HeLa 2000 cells after 1.5 h of infection. **D)** Stationary growth phase supernatant of *S. aureus* 6850 ΔSSR42 exhibited significantly less cytotoxic activity towards HeLa 2000 cells. HeLa 2000 cells were treated with 10% stationary growth phase supernatant of *S. aureus* 6850 wild-type, ΔSSR42 mutant and complemented mutant. Cell death was measured via quantification of LDH release. Statistical analysis was performed using Student´s t-test: *: p< 0.05; ***: p< 0.001.

4.3.4 Role of SSR42 in biofilm formation of *S. aureus*

Biofilm formation of *S. aureus* depicts a serious problem in health-care associated infections especially regarding medical device-associated infections due to the higher antibiotic tolerance of bacterial cells residing inside biofilms. Biofilm formation in *Staphylococcus* spp. is described to be a four-step process of adherence, aggregation, maturation, and dispersal (Büttner et al., 2015). During the critical adherence phase of biofilm formation fibronectin binding proteins were reported to be of great importance (O´Neill et al., 2008; McCourt et al., 2014). Higher abundances of *fnbA* mRNA and FnbB protein levels (see sections 4.3.1, 4.3.2) were found in a mutant deficient of SSR42 both indicating a possible enhancement of biofilm formation in *S. aureus*. Hence, the ability to form biofilms was analysed in mutants lacking SSR42 by measuring optical densities of crystal violet stained biofilms. Significantly stronger biofilm formation was detected in case of the ΔSSR42 mutant (Fig. 4.19; FC: 121%; p>0.0001) compared to the ability of wild-type bacteria to form biofilms, whereas the effect was recovered in case of SSR42 complementation (FC: 98.98%).

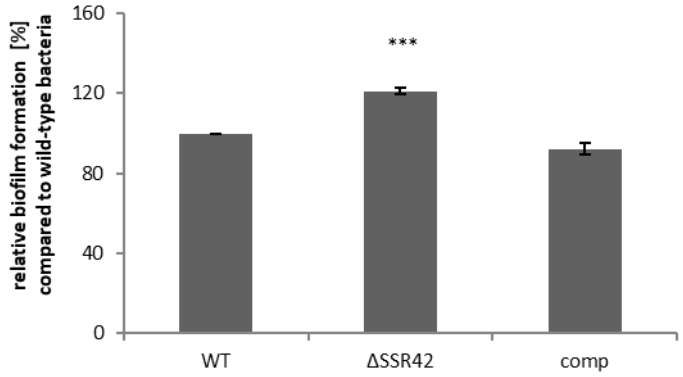

Figure 4.19: SSR42 affects biofilm formation *in S. aureus* 6850. Deletion of SSR42 results in significantly enhanced biofilm formation as observed by quantification of crystal violet stained biofilms in *S. aureus* 6850 wild-type, ΔSSR42 and complemented mutant. Biofilm formation was normalized to growth of bacteria and biofilm formation of wild-type bacteria was set to 100%. Statistical analysis was performed using Student´s t-test: *: p< 0.05; ***: p< 0.001.

4.3.5 SSR42 influences persistence of *S. aureus* in EA.Hy926 cells

Rsp was shown to be an important virulence regulator especially considering virulence, eliciting death of host cells and intracellular residence (Das et al., 2016; Li et al., 2016). While residing in host cells for extended periods the full cytotoxic potential of *rsp* mutants was reported to be only observable in later stages of infection (Das et al., 2016). A strategy for persisting inside host cells is the formation of small colony variants (SCV). Using a long-term infection model EA.Hy926 cells were infected with wild-type bacteria, a ΔSSR42 and Δ*rsp* mutant from *S. aureus* 6850 strain background (experiment was perfomed by Lorena Tuchscherr, University hospital Jena). Enumerating the CFU of infected cells at day 0, 2 and 7 post infection revealed no significant differences between the three groups (Fig. 4.20A).

However, while at day 7 of infection CFU counts did not differ between the used strains, significantly more SCVs could be isolated from cells infected with either the Δ*rsp* (p=0.045) or ΔSSR42 (p= 0.023) mutant (Fig. 4.20B-C). Therefore, it was demonstrated that mutants lacking SSR42 or *rsp* tend to form SCVs during long term infection.

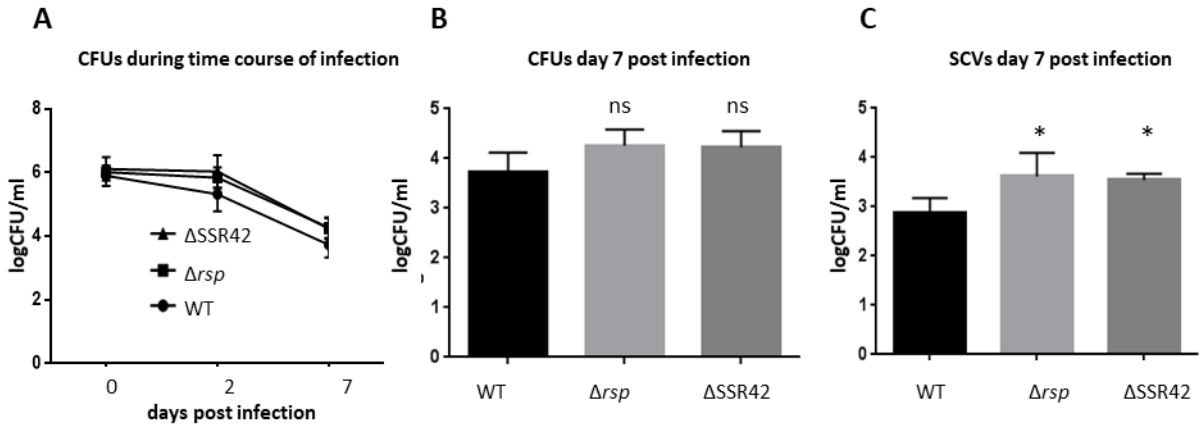

Figure 4.20: ncRNA SSR42 has an impact on formation of small colony variants. A) CFU enumeration of *S. aureus* 6850 wild-type, ΔSSR42 and Δ*rsp* mutant obtained from infected EA.Hy926 cells after 2 and **B)** 7 days of infection reveals no significantly differences between the three groups. **C)** Mutants in either SSR42 or *rsp* tend to form more small colony variants during long term colonization of EA.Hy926 cells as observed by CFU enumeration. Significantly more SCVs were observed for mutants in SSR42 and *rsp* after 7 days of infection of EA.Hy926 cells. Statistical analysis was performed using Student´s t-test: *: p< 0.05; ***: p< 0.001.

4.3.6 SSR42 plays a crucial role for pathogenesis of *S. aureus*

For investigating the influence of SSR42 on virulence in murine infection models, mice were infected with 10^6 CFU of both wild-type, Δ*rsp* and ΔSSR42 mutant from 6850 background (experiment was perfomed by Eva Medina, Helmholtz Centre Braunschweig). After 7 days mice were sacrificed and CFU enumeration from infected tibia, kidneys and livers was performed (Fig. 4.21). For all three infection models both mutants were found at significantly lower CFU numbers (Fig. 4.21A-C; tibia: Δ*rsp*: p= 0.0005, ΔSSR42: p=0.0001; kindey: Δ*rsp*: p= 0.0005, ΔSSR42: p=0.0013; liver: Δ*rsp*: p= <0.0001, ΔSSR42 p= <0.0001). Due to the detected lower number of mutants lacking SSR42 in the infected organs and tibia of mice competition experiments were performed in order to assess potential fitness defects of the ΔSSR42 mutant. A spectinomycin resistant mutant was used to distinguish between wild-type and ΔSSR42 mutant. This mutant was constructed analogue to the previously used ΔSSR42 mutant by placing a spectinomycin cassette between the sequence of RSAU_002216 and the ORF encoding *rsp*. Growth defects were excluded via monitoring the planktonic growth in TSB over a time-course of 23 h (see Appendix Fig. 7.4). Competition experiments were performed by infecting mice with 10^6 CFU of a 1:1 mixture of both wild-type and ΔSSR42-spec^r mutant. After two days of infection half of the mice

were sacrificed and CFU was enumerated from tibia and kidney homogenates plated on plain TSA and TSA containing spectinomycin (Fig. 4.21D). Significantly lower CFUs were detected for the mutant lacking SSR42 from both tibia (p=0.0104) and kidney homogenates (p=0.041) indicating fitness defects during the colonization phase of infection. Analysing the fitness of both wild-type and mutant in a chronic infection, mice were sacrificed 14 days post infection and CFU from tibia and kidney was enumerated (Fig. 4.21D). Interestingly, while CFU numbers of the ΔSSR42 mutant dropped drastically during the initial stages of infection (2 days), bacteria were not completely eradicated by the host´s immune system from tibia (p=0.002) nor kidneys (p=0.0002) and still detectable after 14 days of infection.

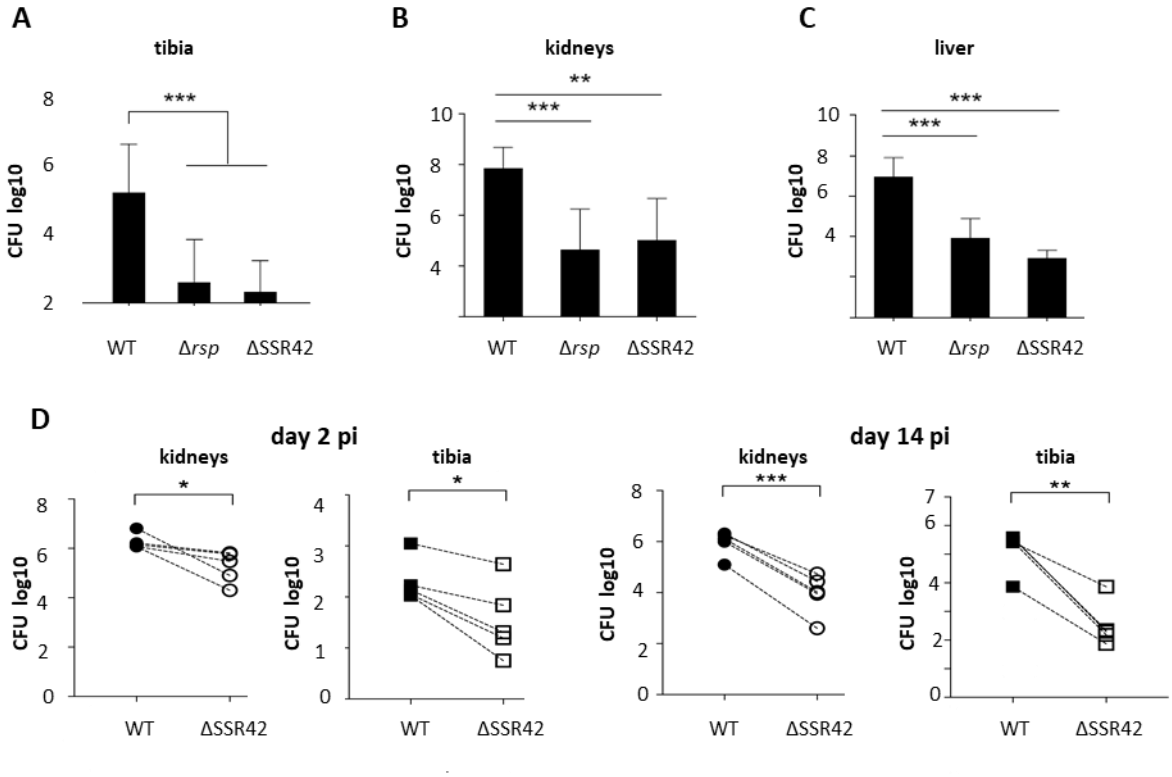

Figure 4.21: SSR42 is required for efficient virulence of *S. aureus* 6850 in murine tibia, kidney and liver infection models. CFU enumeration of *S. aureus* 6850 wild-type, ΔSSR42 and Δ*rsp* mutant harvested from infected murine tibia (**A**), kidneys (**B**) and liver (**C**). Significantly less CFUs were obtained for mutants in *rsp* and SSR42 from all three infection models after 7 days of infection. **D)** Comparison of CFUs obtained from infected murine kidneys and tibia after two days (left panel) and 14 days (right panel) of infection. For the competition experiment mice were infected with a 1:1 mixture of *S. aureus* wild-type and spectinomycin resistant ΔSSR42 mutant. CFUs were enumerated after 2 and 14 days of infection. While CFUs number of the ΔSSR42 mutant were significantly decreased at both time points compared to the CFU numbers of wild-type bacteria, the ΔSSR42 mutant was not completely eradicated by the host after 14 days of infection. Statistical analysis was performed using Student´s t-test: *: p< 0.05; ***: p< 0.001.

4.4 ncRNA SSR42 mediates haemolysis via regulation of the SaeRS two-component system in *S. aureus*

Haemolysis regulation in *S. aureus* is governed by a plethora of different virulence factors. Most important in this process are the agr quorum-sensing system with RNAIII regulating translation of *hla* mRNA (Morfeldt et al., 1995) and the two-component system SaeRS, which is essential for transcription of *hla* (Mainiero et al., 2010).

4.4.1 Influence of ncRNA SSR42 on transcription of various major regulators in *S. aureus*

While SSR42 was shown to regulate the expression of a plethora of virulence factors, thus granting a global regulatory role, the mechanism of regulation remains elusive. The high number of SSR42-regulated factors obviated a direct interaction of SSR42 with all of the target mRNAs. Instead a mechanism involving the interaction with a global regulator was proposed. Most of the differentially regulated genes in a mutant lacking SSR42 were reported to be under control of other major regulators such as the agr quorum-sensing system (AgrA and RNAIII), two-component system SaeRS, alternative σ-factor σB (encoded by *rpoF*) or global repressor CodY (reviewed in Junecko et al., 2012, see table 4.10). Identifying the regulatory mechanism of SSR42 the transcription of the above-mentioned factors was analysed in absence of SSR42 (Fig. 4.22). While knockout of SSR42 did not affect transcript levels of RNAII (*agr*B), RNAIII, *rpo*F and *cod*Y the transcript levels of *sae*S were detected at significant decreased levels ($FClog_{10}$: 0.42; p=0.002) indicating a potential regulatory relationship.

Table 4.10: Exemplary genes whose transcript abundances differed in *S. aureus* 6850 ΔSSR42 and their regulation by global regulators.

gene	log_2Fold change[1]	Adjusted p-value	regulation
nirB	2.72	0.026	YhcSR (Yan et al., 2011)
hisA	2.39	0.005	CodY (Pohl et al., 2009)
ureB	1.89	$2.07*10^{-5}$	Rot (Saïd-Salim et al., 2003) SaeRS (Voyich et al., 2009) agr system (Queck et al., 2008)
hisF	1.80	0.047	CodY (Pohl et al., 2009)
gntK	1.76	0.006	agr system (Queck et al., 2008)
hisD	1.75	0.03	CodY (Majerczyk et al., 2010)
lrgA	1.74	0.013	LytRS (Brunskill and Bayles, 1996) SaeRS (Voyich et al., 2009)
capD	1.71	$6.84*10^{-5}$	MgrA (Gupta et al., 2015) CodY (Pohl et al., 2009)
asd	1.66	0.03	CodY (Pohl et al., 2009)
fnbA	1.58	$1.48*10^{-7}$	CodY (Pohl et al., 2009)
ureA	1.58	0.0007	agr system (Queck et al., 2008)
opuCA	1.53	0.0003	CodY (Pohl et al., 2009)

psmA4	-2.56	$3.47*10^{-10}$	AgrA (Queck et al., 2008)
psmA2	-2.05	0.001	AgrA (Queck et al., 2008)
psmA1	-1.90	0.04	AgrA (Queck et al., 2008)
psmA3	-1.82	0.0005	AgrA (Queck et al., 2008)
pyrF	-1.79	$1.6*10^{-6}$	ThyA (Kriegeskorte et al., 2014) agr system (Queck et al., 2008)
pyrP	-1.62	0,0303307	CodY (Pohl et al., 2009)
pyrAB	-1.57	$1.0*10^{-8}$	ClpP (Michel et al., 2006)
pyrAA	-1.57	0.0005	agr system (Queck et al., 2008)
pyrE	-1.56	$1.45*10^{-8}$	agr system (Queck et al., 2008)
RSAU_001681	-1.51	0.01	agr system (Queck et al., 2008)
capH1	1.87	0.002	CodY (Pohl et al., 2009)
fadB	1.79	$4.5*10^{-9}$	CodY (Pohl et al., 2009)
sarX	1.42	$6.3*10^{-6}$	MgrA (Manna and Cheung 2006b)
splB	-1.87	0.0012	SaeRS (Voyich et al., 2009)
scpA	-1.83	$1.1*10^{-14}$	VfrB (Bose et al., 2014) SarA (Jones et al., 2008) agr system (Queck et al., 2008),
mtlF	-1.78	$3.0*10^{-15}$	MgrA (Luong et al., 2006)
splA	-1.61	$1.4*10^{-7}$	agr system (Queck et al., 2008) MgrA (Luong et al., 2006) σB (Ziebandt et al., 2001) SaeRS (Rogasch et al., 2006)

[1]Compared to transcript levels in *S. aureus* 6850 wild-type bacteria (ΔSSR42/WT)

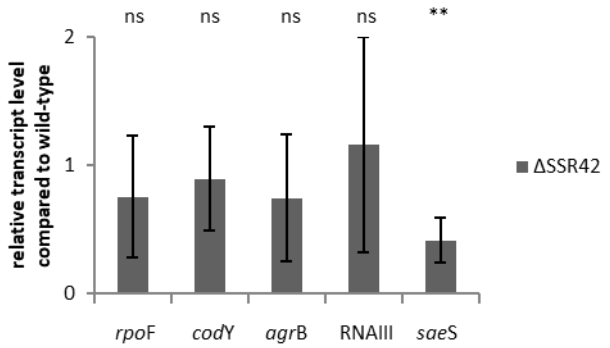

Figure 4.22: Influence of SSR42 on the expression of various global regulators. Quantitative real time PCR analysis of *S. aureus* wild-type and ΔSSR42 mutant indicates regulation of *sae*S expression by SSR42. While transcript levels of *rpo*F, *cod*Y, *agr*B and RNAIII remained unaltered only transcript levels of *sae*S differed significantly a mutant lacking SSR42. Statistical analysis was performed using Student´s t-test: *: p< 0.05; ***: p< 0.001.

4.4.2 SSR42 induces transcription of the *sae* operon and major targtes of the two-component system SaeRS

Transcript levels of *sae*S were found to be significantly decreased in a mutant lacking SSR42. Deciphering the impact of SSR42 on SaeRS further transcription of both *sae*S and *sae*P was analysed in a ΔSSR42 mutant complemented in trans for SSR42 under the control of an AHT-inducible promotor.

While under non-inducing conditions transcript levels of *sae*S ($FClog_{10}$: -0.4, p=0.008) and *sae*P ($FClog_{10}$: -0.22, p=0.012) were significantly reduced, upon induction of SSR42 expression transcript levels of *sae*S and *sae*P were found significantly elevated (*sae*S: $FClog_{10}$: 0.92, p=0.004; *sae*P: $FClog_{10}$: 0.81, p>0.001; Fig. 4.23A). As described earlier, induced transcription of SSR42 resulted in significantly increased transcript levels of *hla* (Fig. 4.11B), a direct class II target of the SaeRS system. Further, the expression of SaeRS class I targets *coa* ($FClog_{10}$: 0.72, p=0.001), *eap* ($FClog_{10}$: 0.999, p>0.001) and *emp* ($FClog_{10}$: 1.12, p>0.001) was significantly enhanced upon AHT-induced transcription of SSR42 (Fig. 4.23B). Instead, *eap*, *emp* and *coa* mRNA were detected at significantly reduced levels in the non-induced control when compared to that of wild-type bacteria (*coa*: $FClog_{10}$: -0.19; p=0.022, *eap:* $FClog_{10}$: -0.43, p>0.001 and *emp:* $FClog_{10}$: -0.29, p=0.031). Thus, a role for SSR42 in regulating virulence factors via regulation of *sae*RS transcript levels was identified.

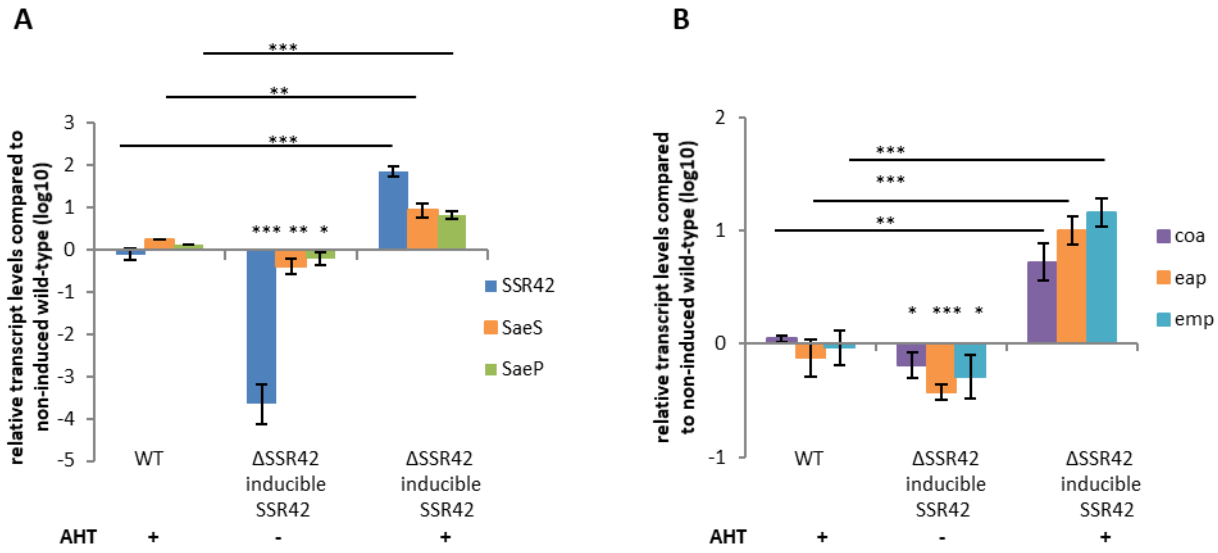

Figure 4.23: SSR42 modulated the expression of the *sae* operon and SaeRS class I target genes. **A)** Inducible transcription of SSR42 results in significantly increased *sae*S and *sae*P transcript levels as observed by qRT-PCR analysis of *S. aureus* 6850 wild-type and ΔSSR42 mutant complemented in trans with AHT-inducible transcription of SSR42. Significantly elevated *sae*S and *sae*P transcript levels were observed when SSR42 transcription was induced by an AHT pulse. + AHT indicates addition of anhydrous tetracycline. **B)** Elevated *coa*, *eap* and *emp* levels were observed using qRT-PCR upon AHT-induced transcription of SSR42. Transcript analysis of *S. aureus* 6850 wild-type and ΔSSR42 mutant complemented in trans with AHT-inducible transcription of SSR42. + AHT indicates addition of anhydrous tetracycline. Statistical analysis was performed using Student´s t-test: *: p< 0.05; ***: p< 0.001.

4.4.3 Regulation of *hla* transcription by SSR42 is dependent on functional SaeRS two-component system

In order to elaborate the regulatory relationship between ncRNA SSR42 and the two-component system SaeRS the transcription of SaeRS target genes was analysed in a SaeR deficient genetic background. For that, the plasmid pAHT-SSR42 granting AHT-inducible SSR42 transcription was

introduced into a transposon insertion mutant in *sae*R (*sae*R::Bursa; NE1622) obtained from the Nebraska library (Fey et al., 2013) and wild-type bacteria from the same strain background (JE2). AHT-inducible transcription of SSR42 resulted in a strong overexpression of SSR42 in bacteria from both wild-type ($FClog_{10}$: 2.77; p=0.008) and *sae*R::Bursa background ($FClog_{10}$: 1.23 ; p=0.03). However, only in wild-type bacteria *hla* mRNA levels were found significantly increased upon induction of SSR42 transcription (Fig. 4.24A; $FClog_{10}$: 0.84; p=0.0011), while they remained unaltered in the *sae*R mutant (p=0.44). Hence, the SSR42-dependent regulation of *hla* transcription was demonstrated to be dependent on functional SaeRS. Affirming the conclusion that SSR42 operates upstream of the SaeRS system the expression of the class II target genes *coa*, *eap* and *emp* was analysed in this context. Similar to *hla* the transcription of *coa* and *eap* could not be restored to wild-type levels in a non-functional SaeR mutant despite induced overexpression of SSR42 (Fig. 4.24B). Although significantly increased *emp* mRNA levels ($FClog_{10}$: 0.16; p=0.02) were detected in the *saeR* mutant upon AHT-induced SSR42 transcription this was most likely caused by side-effects of AHT since treatment with AHT lead to a similar higher *emp* expression in bacteria from wild-type background ($FClog_{10}$: 0.16). It was thus concluded that the reduced haemolysis observed in a ΔSSR42 mutant is caused by reduced expression of the SaeRS two-component system and that ncRNA SSR42 regulates virulence partially via regulation of the SaeRS system.

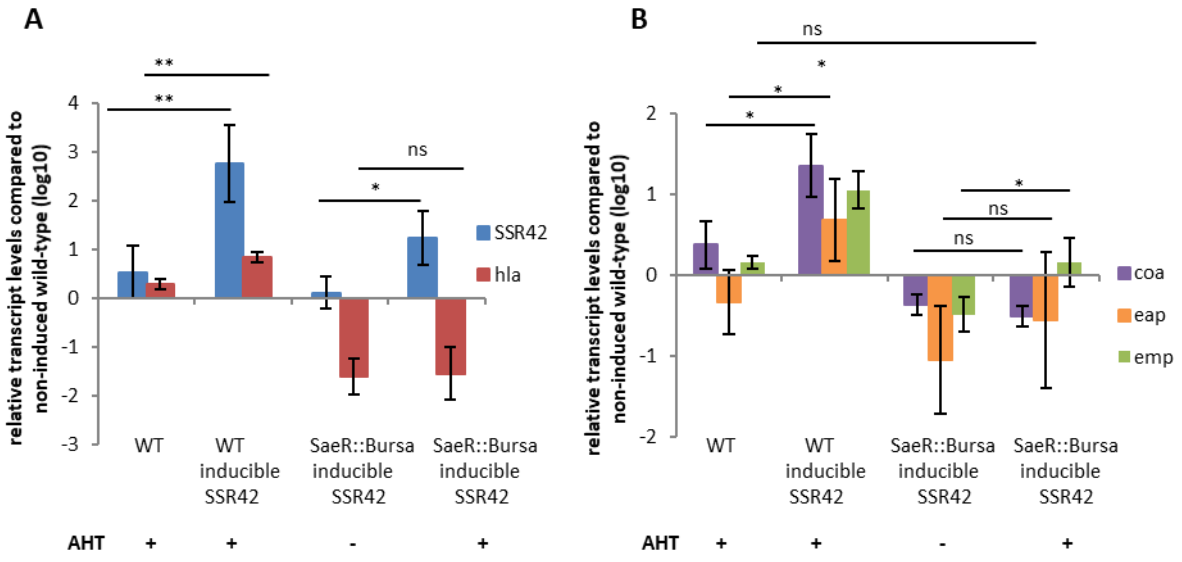

Figure 4.24: SSR42 induced up-regulation of *hla*, *coa*, *emp* and *eap* expression is dependent on functional SaeRS. Quantitative real time PCR analysis of *hla* (**A**) and *coa*, *eap* and *emp* (**B**) transcript levels in *S. aureus* JE2 wild-type bacteria and insertional *sae*R mutant (NE1622; *sae*R::Bursa). Expression of SSR42 was ectopically induced by an AHT pulse (pAHT-SSR42) in wild-type and *sae*R mutant indicated by +AHT. Induced transcription of SSR42 resulted in significantly enhanced *hla*, *coa*, *eap* and *emp* transcript levels in wild-type bacteria as observed by qRT-PCR. In *sae*R mutants however, induction of SSR42 transcription did not alter the transcript levels of the analysed genes. Statistical analysis was performed using Student´s t-test: *: p< 0.05; ***: p< 0.001.

4.4.4 SSR42 regulates the stability of T1 and T2 transcripts of the *sae*PQRS operon

The two-component system SaeRS is transcribed from a four gene operon further encoding the auxiliary genes *sae*P and *sae*Q (see section 2.4.1.2). Transcription is governed from two distinct promotors (P1 and P3). Transcription initiated at *sae* P1 results in unstable transcript T1 encoding the whole operon while transcription from *sae* P3 results in a transcript (T3) encoding only *sae*R and *sae*S (Steinhuber et al., 2003, Jeong et al., 2011). While *sae* P3 is described to be constitutively active (Jeong et al., 2011), P1 is considered to be modulatory (Geiger et al., 2008; Kuroda et al., 2007).

Although ncRNA SSR42 was demonstrated to execute part of its regulatory properties via regulating the transcription of two-component system SaeRS, the mechanism of this regulation remains elusive. One possibility by which ncRNA SSR42 could regulate SaeRS is on the level of transcription. Since both *saeS* and *saeP* transcript levels were affected by SSR42 overexpression, it was hypothesized that the activity of promotor *sae* P1 could be regulated by SSR42. However, while monitoring the *sae* P1 activity using a GFP-reporter (pP_{saeP1}-GFP) construct granting transcriptional fusion of *sae* P1 and GFP in both *S. aureus* 6850 wild-type bacteria and ΔSSR42 mutant no significant differences were detected (Fig. 4.25A). Activity of *sae* P3 promotor was not investigated due to its constitutive activity (Jeong et al., 2011).

Another mechanism by which ncRNA SSR42 could regulate the transcript level of *sae*RS is by affecting the turnover of *sae* transcripts. Therefore, the stability of *sae* transcripts was analysed using a rifampicin assay to arrest de novo transcription (Fig. 4.25B-C). Despite a lower detected level of T1 and T2 transcripts the stability of both transcripts was found significantly reduced 20 min after addition of rifampicin in mutants lacking SSR42 (T1: FC: 0.73, $p>0.001$; T2: FC: 0.71, $p>0.001$). The reduced stability of both transcripts in the ΔSSR42 mutant would explain the reduced transcript levels of *sae*S and *sae*P in mutants lacking SSR42 (Fig. 4.23) and how overexpression of SSR42 could result in higher *sae*S and *sae*P transcript levels.

Thus, a potential mechanism for regulation of sae transcript levels by ncRNA SSR42 was identified. However, analysing the protein amount of SaeR and SaeS in stationary growth phase of *S. aureus* 6850 did not reveal any significant differences in a ΔSSR42 mutant (Fig. 4.26).

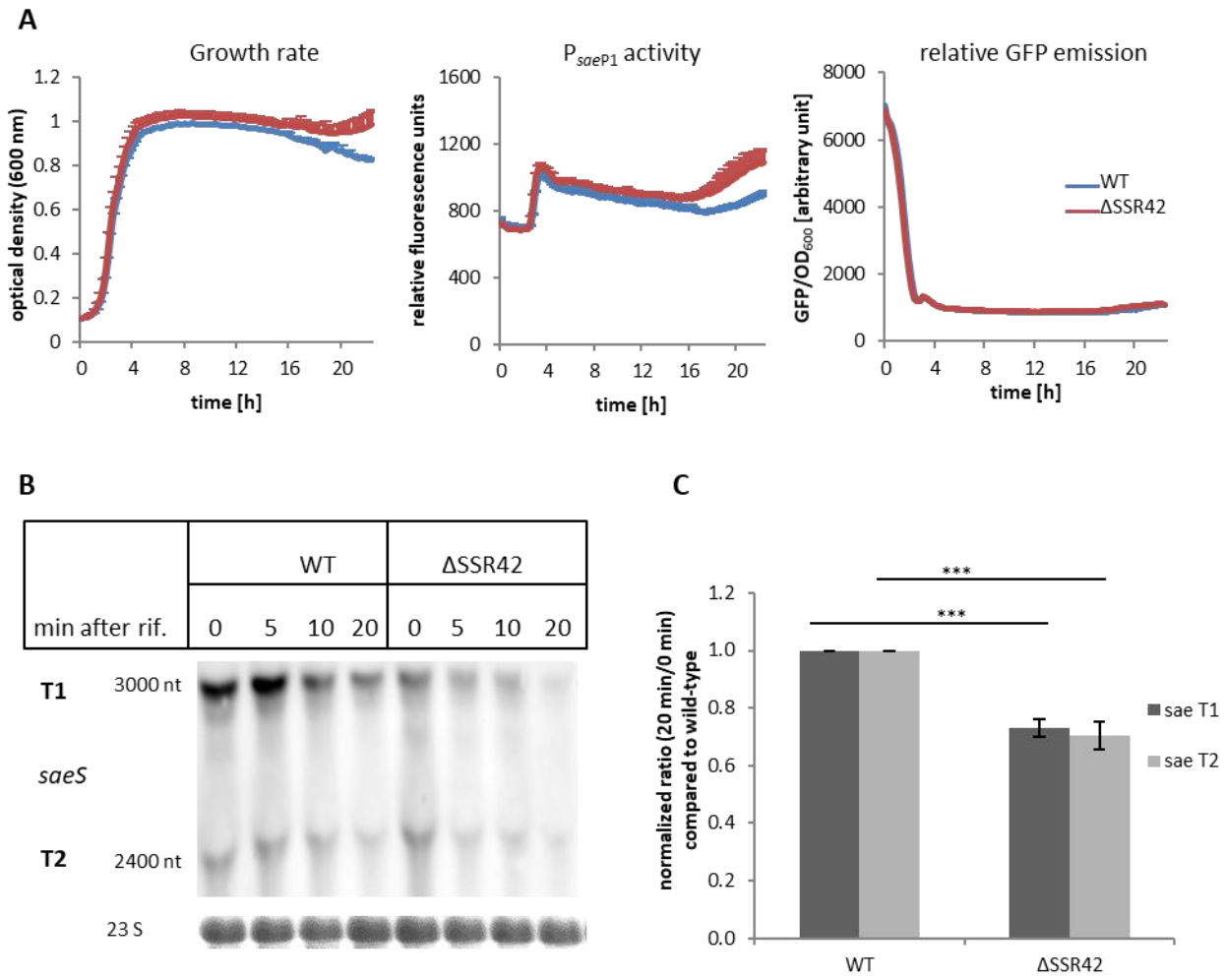

Figure 4.25: SSR42 enhances the stability of *sae* transcripts. A) Growth curve, P_{saeP1} activity profile and normalization of GFP emission to bacterial growth (GFP/OD_{600}) in wild-type *S. aureus* 6850 and isogenic ΔSSR42 mutant. Promotor activity of *sae* P1 was unaltered in mutants lacking SSR42 as observed by using transcriptional fusion of P_{saeP1} and a promotorless GFP. OD_{600} and GFP emission were measured over a time course of 23 h in a TECAN Infinite M200 plate reader. **B)** SSR42 affects stability of *sae* transcripts T1 and T2 as detected by rifampicin assay followed by Northern blot analysis. Rifampicin assay was performed for *S. aureus* 6850 wild-type and ΔSSR42 mutants (left panel) and revealed significantly less stability *for* sae transcript T1 and T2 in case of ΔSSR42 mutant. Chemiluminescence signals of Northern blots were quantified via ImageJ (right panel). Stability ratio of wild-type bacteria was set to 1. Statistical analysis was performed using Student´s t-test: *: p< 0.05; ***: p< 0.001.

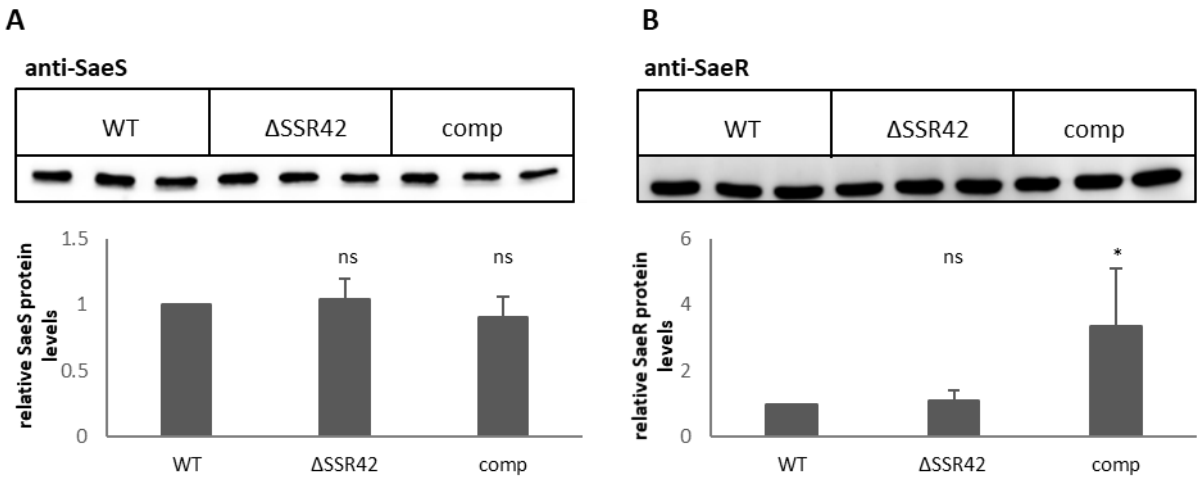

Figure 4.26: SaeR and SaeS protein levels remain unaltered in absence of SSR42. Immunoblotting of proteins obtained from stationary phase *S. aureus* 6850, ΔSSR42 mutant and complemented mutant using polyclonal antibodies against SaeS (**A**) or SaeR (**B**). Depicted are each biological triplicates. Chemiluminescent signals (upper panels) were quantified using ImageJ (lower panels) which revealed no significant differences for SaeS or SaeR levels in mutants lacking SSR42. Statistical analysis was performed using Student´s t-test: *: p< 0.05; ***: p< 0.001.

4.4.5 ncRNA SSR42 regulates the promotor activities of *hla*, *coa* and *psm*α

It was demonstrated that ncRNA SSR42 influences the transcript levels of multiple virulence factors including *hla, coa, ldh*D and *psm*α (see section 4.3). For regulation of *hla* and *coa*, which are both known targets of the SaeRS system a mechanism via modulation of this two-component system was assumed (see section 4.4.4). Since SaeR is known to regulate the expression of *hla* and *coa* by binding to distinct sequences in their promotor regions (Mainiero et al., 2010; Sun et al., 2010; Nygaard et al., 2010), the promotor activites of both genes were analysed in *S. aureus* 6850 of wild-type and SSR42 deficient background using GFP reporter constructs granting transcriptional fusion of P_{hla} and P_{coa}, respectively (Fig. 4.27A-B). The promotor activities were assessed via monitoring the GFP fluorescence over a time period of 23 h. In wild-type bacteria activity of P_{hla} was found maximal in late stationary growth phase. Expression of *hla* was previously reported to be induced and stabilized during stationary growth phase by factors such as the response regulator SaeR and transcriptional regulator SarA (Nygaard et al., 2010; Morrison et al., 2012b). In contrast, P_{hla} activity was drastically reduced in mutants lacking SSR42 (9 h post inoculation: $p=7.34 * 10^{-5}$ normalized to optical density) confirming the previous finding that ncRNA SSR42 regulates α-toxin expression and confirming previous data obtained for 891 nt long SSR42 (Morrison et al., 2012a). Analysing the activity of P_{coa} in both wild-type bacteria and ΔSSR42 mutant revealed a maximal activity upon reaching stationary growth phase. While the overall activity of P_{coa} in mutants lacking ncRNA SSR42 was reduced, maximal P_{coa} activity was reached approximately 2 h in advance. However, this was most likely caused by a better growth rate of the ΔSSR42 mutant. Thus, SSR42 was shown to regulate the expression of *coa* and *hla* by modulating the

promotor activities of both genes which strengthens the hypothesis that SSR42 regulates virulence in part via the SaeRS system.

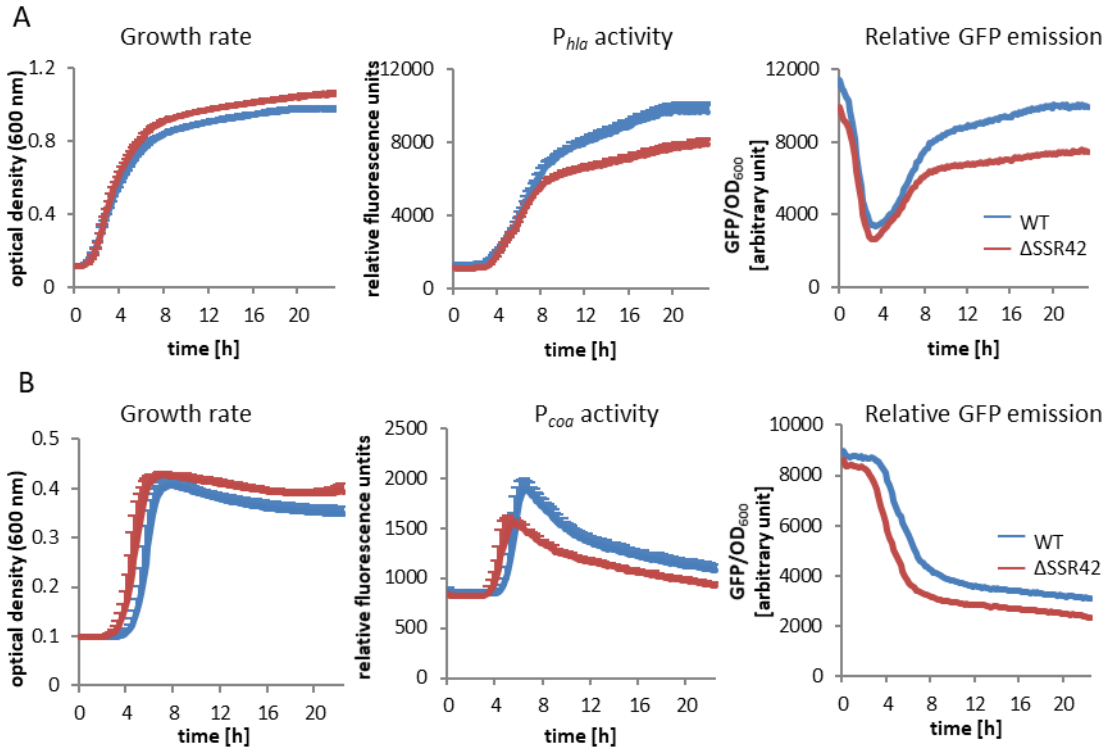

Figure 4.27: SSR42 regulates expression of *hla* and *coa* via modulating the promotor activity. A) Analysis of growth curve, *hla* promtor (P_{hla}) activity profile and normalization of GFP emission to bacterial growth rates (GFP/OD_{600}) in wild-type *S. aureus* 6850 and isogenic ΔSSR42 mutant revealed a significantly lower P_{hla} activity in mutants lacking SSR42 as observed by using a transcriptional fusion of P_{hla} and promotorless GFP. **B)** Promotor activity of coa (P_{coa}) was significantly reduced in a ΔSSR42 mutant during stationary growth phase of *S. aureus* 6850 as measured using a transcriptional fusion construct of P_{coa} and promotorless GFP. Growth rate (OD_{600}) and GFP emission were measured over a time course of 23 h in a TECAN Infinite M200 plate reader. GFP emission was normalized to growth rate of bacteria.

To investigate whether the regulation of other identified targets of ncRNA SSR42 is likewise accomplished via altering the promotor activities the *psm*α operon and *ldh*D were chosen. The activity of $P_{psm\alpha}$ and P_{ldhD} was analysed in both wild-type and ΔSSR42 mutant using GFP reporter constructs (Fig. 4.28). While the activity of $P_{psm\alpha}$ was significantly reduced over time in the ΔSSR42 mutant (Fig. 4.28A) the activity of P_{ldhD} was only affected slightly by deletion of SSR42 (Fig. 4.28B). The observed enhancement of fluorescence corresponding to the P_{ldhD} activity was most likely caused by a slightly better growth of mutants lacking SSR42 and was not observed in the normalized data set.

SSR42 was thus demonstrated to regulate the expression of various target genes via modulating promotor activities. For *hla* and *coa* this is presumably accomplished indirectly via the SaeRS system. However, the activity of P_{ldhD} was found to be unaltered by deletion of SSR42 indicating that regulation by SSR42 occurs via another mechanism illustrating the complex regulatory role of ncRNA SSR42.

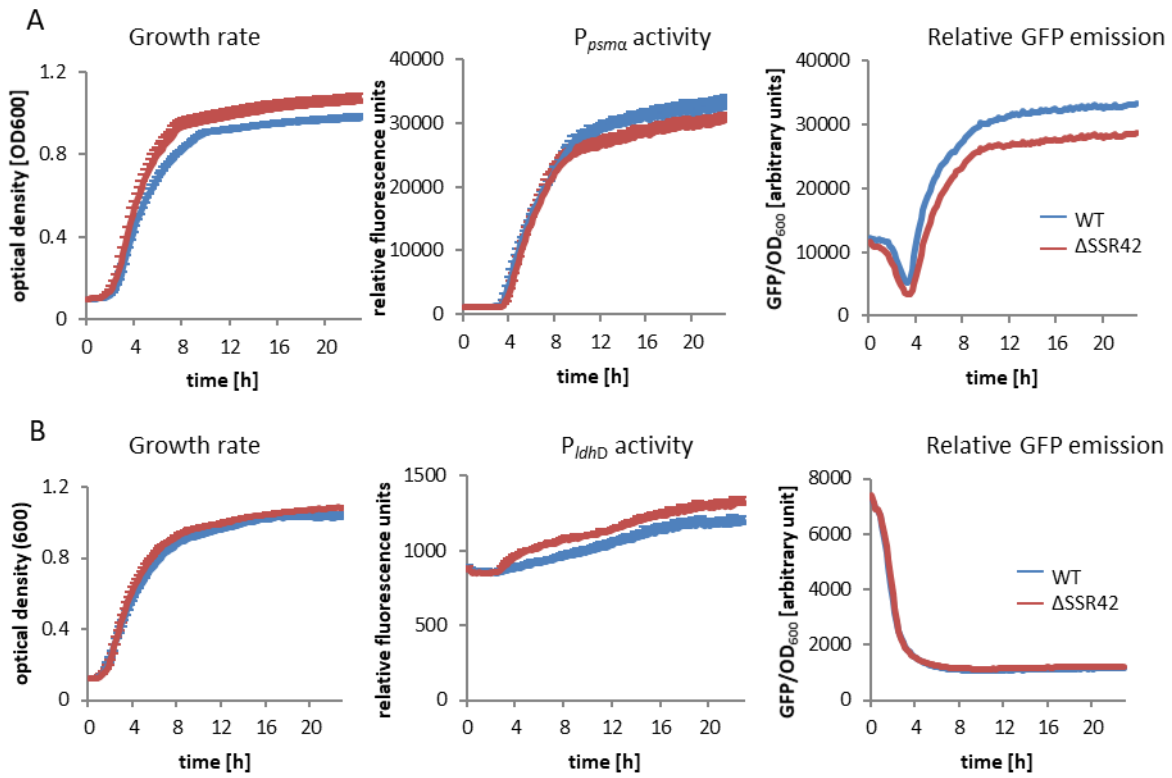

Figure 4.28: SSR42 regulates the promotor activity of *psmα* but not of *ldh*D. A) Monitoring of growth curve, *psmα* and *ldhD* promtor ($P_{psmα}$, P_{ldhD}) activity profile and normalization of GFP emission to bacterial growth rate (GFP/OD_{600}) in wild-type *S. aureus* 6850 and isogenic ΔSSR42 mutant revealed significantly differences for the activity of $P_{psmα}$ (**A**) but not for P_{ldhD} (**B**). Activity of $P_{psmα}$ was significantly reduced in mutants lacking SSR42 as demonstrated using a transcriptional fusion of the respective promotor and a promotorless GFP. Growth rate (OD_{600}) and GFP emission were measured in parallel over a time course of 23 h in a TECAN Infinite M200 plate reader. GFP emission was normalized to growth rate of bacteria.

4.5 Transcription of ncRNA SSR42 in *S. aureus* is induced by various stresses

Previous studies have shown that SSR42 transcript levels are maximal in stationary growth phase where SSR42 is highly stable (Morrison et al., 2012a). However, it remained elusive under which conditions transcription of SSR42 is induced and hence it was addressed in this chapter.

4.5.1 Transcription of SSR42 in *S. aureus* 6850 is maximal in stationary growth phase

Previous studies addressing ncRNA SSR42 (Morrison et al., 2012a) did not completely elucidate the expression profile during the growth of *S. aureus*. Hence, SSR42 transcript levels were measured in *S. aureus* 6850 during early exponential, exponential, stationary and late stationary growth phase using qRT-PCR and were found to increase continuously from early exponential to late stationary growth phase (Fig. 4.29A). Confirming previous studies (Morrison et al., 2012a) transcript levels were found to be maximal in late stationary growth phase.

For further analysis of transcription, a construct allowing transcriptional fusion of the SSR42 promotor (P_{SSR42}) and GFP was exploited. Fluorescence corresponding to the promotor activity of SSR42 was recorded over a time course of 23 h in *S. aureus* 6850 (Fig. 4.29B). In line with the transcript level analysis the activity of P_{SSR42} increased over time climaxing upon entry of stationary growth phase. After reaching the maximum, the activity of P_{SSR42} slowly declined. Comparison of the promotor activity profile and the transcript level profile lead to the assumption that the high transcript levels in late stationary growth phase resulted from stabilization of ncRNA SSR42 since the promotor activity during that growth phase was already decreasing. Using rifampicin to arrest de novo transcription the stability of SSR42 was analysed in late stationary growth phase using Northern blotting (Fig. 4.29C). The half-life of SSR42 was determined to be approximately 60 min confirming previous findings, which described a high stability of SSR42 in stationary growth phase (Morrison et al., 2012a). ncRNA SSR42 thus is detectable during all growth phases of *S. aureus* 6850. During transition to stationary growth phase the promotor activity of SSR42 is strongest while stabilization of the molecule further increases the amount of SSR42 transcripts.

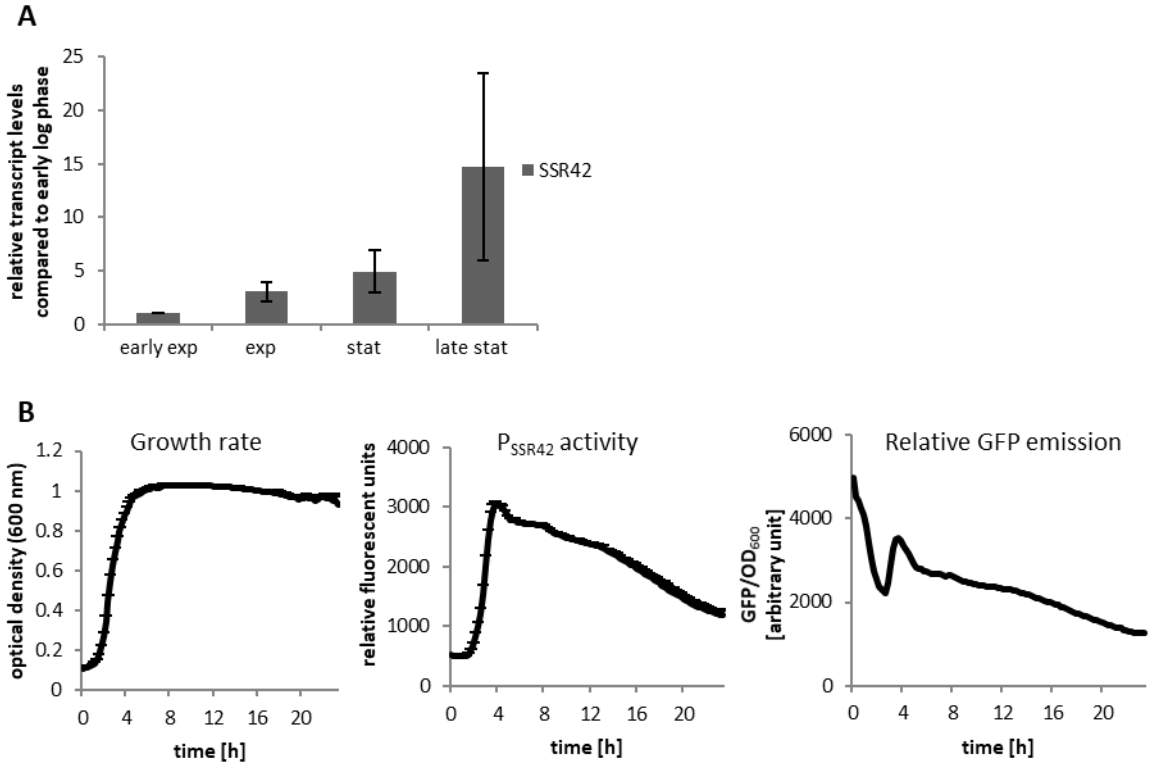

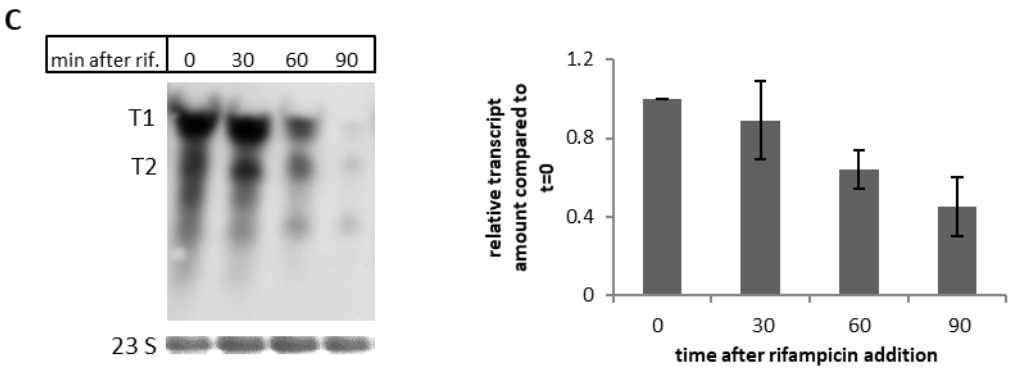

Figure 4.29: Expression and stability of SSR42 is maximal during stationary growth phase. A) qRT-PCR analysis of SSR42 transcript levels in *S. aureus* 6850 during early exponential, exponential, stationary and late stationary growth phase demonstrated a growth phase dependent increase in SSR42 transcript levels. SSR42 transcript levels were detected at highest amount during late stationary growth of S. aureus 6850. **B)** Promotor activity of P_{SSR42} peaked at transition to stationary growth phase in *S. aureus* 6850 as demonstrated by monitoring the growth curve and SSR42 promotor activity (P_{SSR42}) in wild-type *S. aureus* 6850 in parallel over a time course of 23 h using a TECAN Infinite M200 plate reader. GFP emission was normalized to growth rate of bacteria. **C)** SSR42 transcript is highly stable during stationary growth phase of *S. aureus* 6850 as observed with rifampicin assay followed by Northern blot analysis (left panel). Chemiluminescence signals were quantified using ImageJ (right panel).

4.5.2 Promotor activity profiles of ncRNA SSR42 vary in different *S. aureus* strains

SSR42 is encoded with high conservation in the genome of all known *S. aureus* strains and isolates (see section 4.1.1). To analyse the expression pattern of SSR42 in various *S. aureus* strains the previous employed promotor activity assay was used to monitor the activity of P_{SSR42} in the MRSA strains JE2, MW2, COL, the laboratory strain RN4220, the non-cytotoxic strain Cowan I, the osteomyelitis isolate UAMS-1 and strains Newman and HG003 (Fig. 4.30). Excluding secondary effects, the highly conserved promotor region of SSR42 was taken from strain 6850 and used for constructing the GFP reporter contruct. By analysing the promotor profile in the mentioned strains two major profile types were identified: While promotor activity peaked upon entry of stationary growth phase in the strains 6850, RN4220, COL, HG003 and Cowan I, a sigmoid activation profile was observed in *S. aureus* USA300 JE2, MW2 and Newman. The promotor activity of SSR42 in UAMS-1, however, was detected at very low levels.

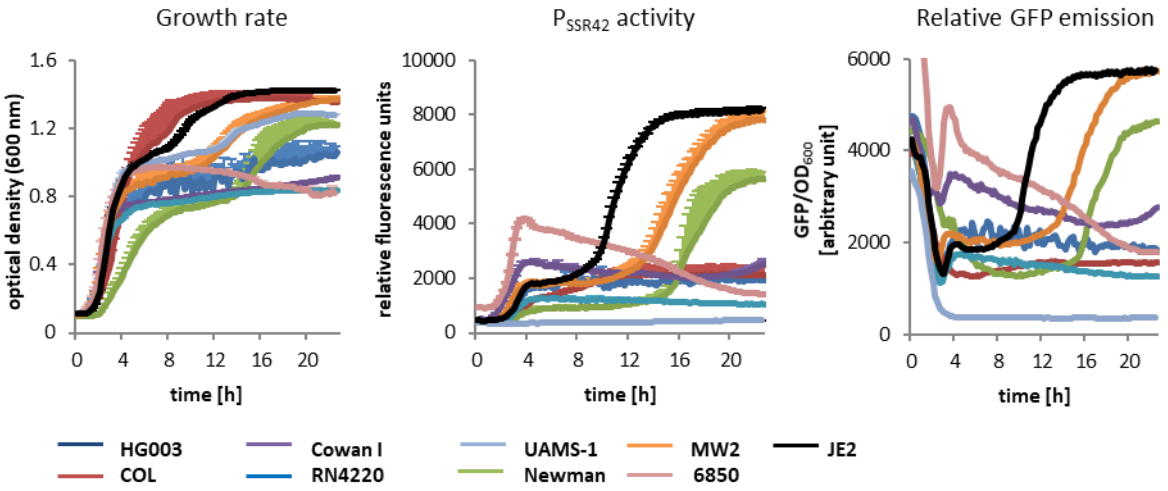

Figure 4.30: P_{SSR42} activity profile displays significantly different progressions dependent on the genetic background. Monitoring of growth curve (OD_{600}) and P_{SSR42} activity over a time course of 23 h in a TECAN Infinite M200 plate reader using a transcriptional fusion of P_{SSR42} and promotorless GFP revealed significant differences in the course of P_{SSR42} activity in diverse *S. aureus* strains. *S. aureus* 6850, HG003, COL, RN4220 and Cowan I displayed a one-peak activity profile while strains JE2, Newman and MW2 displayed a sigmoid shaped profile whereas P_{SSR42} activity was nearly undetectable in strain USAM-1. P_{SSR42} activity was normalized to growth of the respective strain (GFP/OD_{600}).

Rsp was previously described to be essential for transcription of SSR42 with mutants in *rsp* lacking expression of SSR42 (Das et al., 2016). It was therefore hypothesized that strain-specific differences in *rsp* expression could be responsible for the different P_{SSR42} activity profiles. Searching for a cause for the observed differences in the SSR42 promotor activity profiles, strain 6850 and JE2 were chosen as representatives for both profile types. Therefore, the activity of the promotor driving *rsp* transcription was monitored in *S. aureus* 6850 and JE2 and compared to the activity profile of P_{SSR42} (Fig. 4.31A-B). While for MRSA strain JE2 the activity of P_{rsp} showed a likewise sigmoid profile, the activity of P_{rsp} in 6850 peaked upon entry of stationary growth phase as observed for P_{SSR42}. The similarities of both promotor activity profiles in the respective strain supported the hypothesis that the distinct P_{SSR42} activity profiles result from a strain-specific expression pattern of *rsp*. Confirming this hypothesis, the expression of Rsp was analysed. Due to the absence of a Rsp-specific antibody the expression of a triple FLAG-tagged Rsp under control of the native promotor was analysed in mutants lacking wild-type Rsp (6850 Δ*rsp* and JE2 NE1304; Fig. 4.31C). While Rsp-3xFLAG protein levels in strain JE2 increased continuously from exponential to stationary growth phase they remained rather unaltered in MSSA strain 6850 reflecting the observed strain-specific differences in the promotor activity profile. Thus, the higher SSR42 expression in strain JE2 seems to be a direct outcome of elevated Rsp levels.

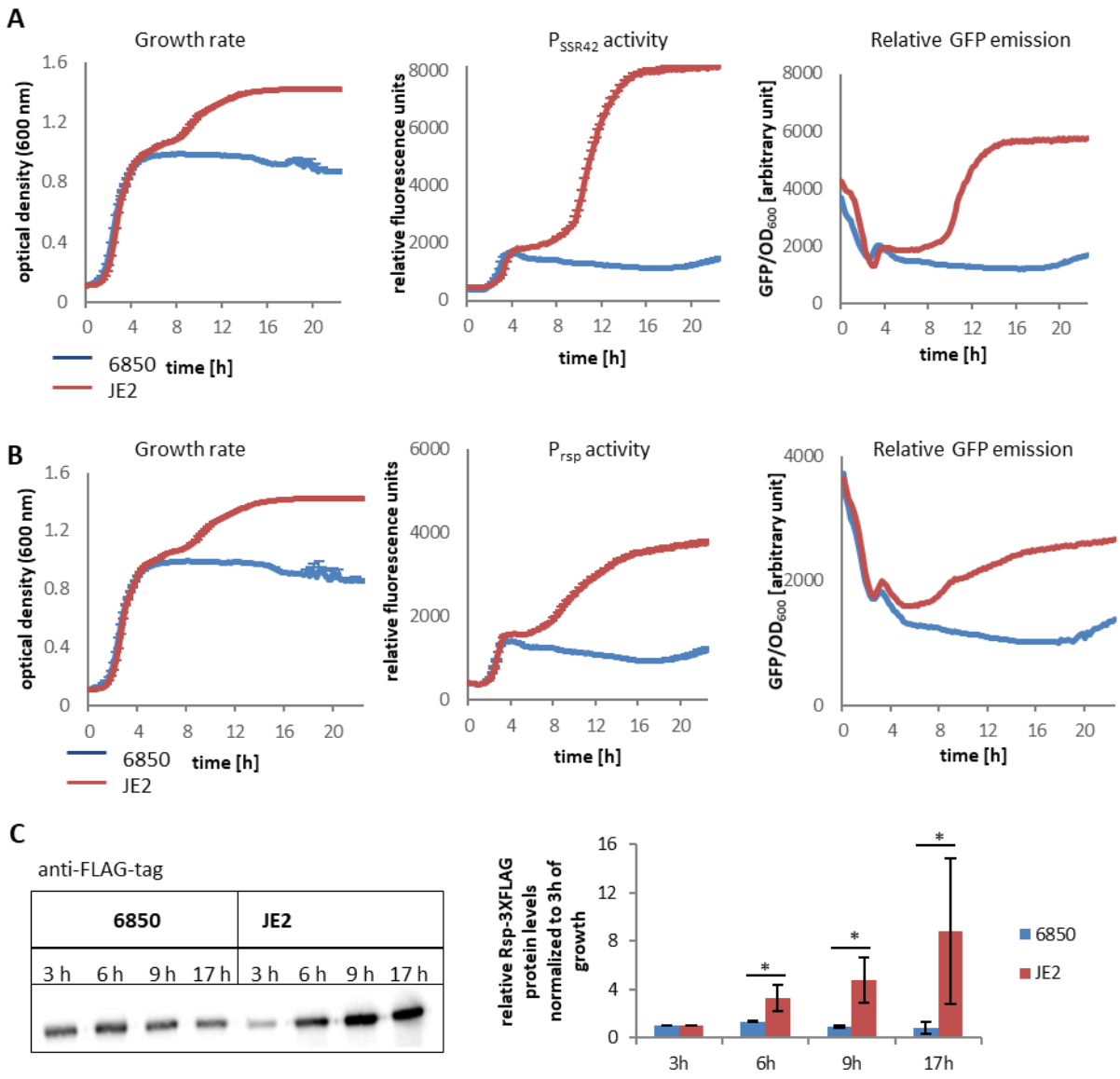

Figure 4.31: P_{SSR42} is strictly dependent on P_{rsp} activity and subsequent Rsp protein levels in *S. aureus* strain 6850 and JE2. Monitoring of growth curve (OD_{600}) and P_{SSR42} (**A**), respectively P_{rsp} (**B**) activity over a time course of 23 h in a TECAN Infinite M200 plate reader. A transcriptional fusion of P_{SSR42} and P_{rsp} with GFP revealed similarities in both profiles in the respective genetic background of 6850 and JE2. Promotor activity was normalized to growth rate of bacteria. **C)** JE2 expresses significantly more Rsp than strain 6850 as observed by immunoblotting of triple FLAG-tagged Rsp in *S. aureus* 6850 and JE2 (left panel). Chemiluminescent signals were quantified using ImageJ (right panel). Statistical analysis was performed using Student´s t-test: *: p< 0.05; ***: p< 0.001.

This regulatory relationship between SSR42 and Rsp was further observed for osteomyelitis isolate UAMS-1. Here, the drastically reduced SSR42 levels (FC: 0.0014 compared to mRNA levels in strain 6850; p>0.001) were accompanied by significantly reduced *rsp* mRNA levels (FC: 0.34; p=0.02). However, for the other tested strains this dependence of Rsp was not observed (Fig. 4.32). While expression of SSR42 in strain Newman was significantly elevated (FC: 10.95; p=0.006) compared to transcript levels in strain 6850, *rsp* transcript levels were detected at comparable levels. In the non-

cytotoxic strain Cowan I instead, *rsp* mRNA was detected at drastically reduced levels (FC: 0.097; p>0.001) whereas SSR42 transcript levels did not differ significantly to that found in strain 6850. Moreover, SSR42 transcript levels in laboratory strain RN4220 were found significantly reduced compared to the levels in strain 6850 (FC: 0.203; p>0.001) while *rsp* mRNA did not differ significantly. The discrepancy between SSR42 and *rsp* levels in the tested strains disproveed the hypothesis that the Rsp level determines the SSR42 promotor activity and that strain-specific differences in Rsp expression could be responsible for the observed differences in SSR42 transcription. While for strain JE2 this hypothesis could be confirmed (Fig. 4.31C) and the elevated SSR42 transcript levels seemed to be a direct outcome of the Rsp protein levels, the regulation of SSR42 transcription seems to differ in the other tested strains. The regulation of SSR42 transcription was further addressed in chapter 4.6.

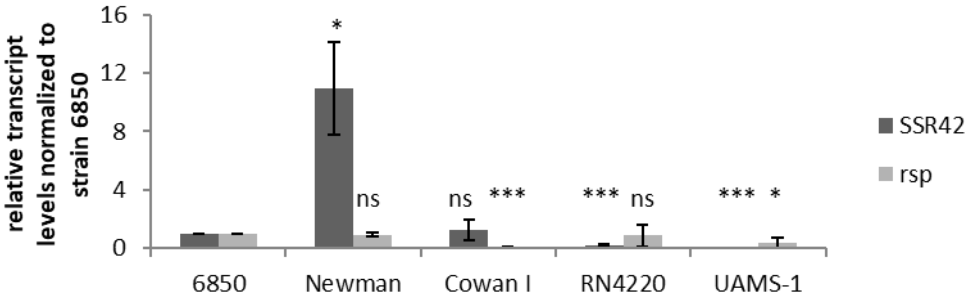

Figure 4.32: Expression of SSR42 and *rsp* is dependent on the genetic background in *S. aureus*. Quantitative real time PCR analysis of RNA obtained from stationary phase *S. aureus* 6850, Newman, Cowan I, RN4220 and UAMS-1 revealed significant differences regarding transcript levels of SSR42 and *rsp*. Statistical analysis was performed using Student´s t-test: *: p< 0.05; ***: p< 0.001.

4.5.3 Antibiotics treatment and various stresses influence the activity of P_{SSR42}

The analysis of P_{SSR42} activity and transcript levels revealed a growth phase dependent expression and stabilization of SSR42. Despite the growth phase the stimuli activating P_{SSR42} remain rather ambiguous. Until now only neutrophil-derived stimuli were reported to induce SSR42 transcription via up-regulation of *rsp* expression (Das et al., 2016). In this section the activity of P_{SSR42} upon treatment with various antibiotics, chemicals and fatty acids was analysed using β-galactosidase and GFP reporter constructs in order to gain further insight into stimuli modulating SSR42 transcription. For analysing the impact of antibiotics on the activity of P_{SSR42} a reporter construct harbouring a transcriptional fusion of P_{SSR42} to the open reading frame *bga*B encoding a β-galactosidase was generated. Detection of blue indigo dye on agar plates containing X-Gal served as a marker for induction of P_{SSR42} activity. Various antibiotics were tested using a disc diffusion assay and induction of P_{SSR42} promotor activity was observed upon treatment with imipenem, meropenem, cefpodoxime and oxacillin, ofloxacin, cefoxitin and trimethoprim-sulphamethoxazole (Fig. 4.33; table 4.2). Activation of P_{SSR42} activity was found to be dependent on functional Rsp since in a Δ*rsp* mutant blue indigo dye production was only observed

when the ORF encoding *rsp* was re-introduced via the reporter plasmid (Fig. 4.33B). Using an oxacillin MIC strip the production of the blue indigo dye was only detected in distinct zones in which sub-inhibitory concentrations were present (Fig. 4.33C). Induction of P_{SSR42} activity using oxacillin and imipenem was further tested in the MRSA strain USA300 JE2 (Fig. 4.33D). In JE2 stimulation with those antibiotics led to a likewise formation of the indigo dye. Stimulation with 1 µg of oxacillin resulted in a distinct large indigo blue zone, which was accompanied by reduced growth of *S. aureus* without the presence of a complete growth inhibition zone due to the resistance of strain JE2 against oxacillin.

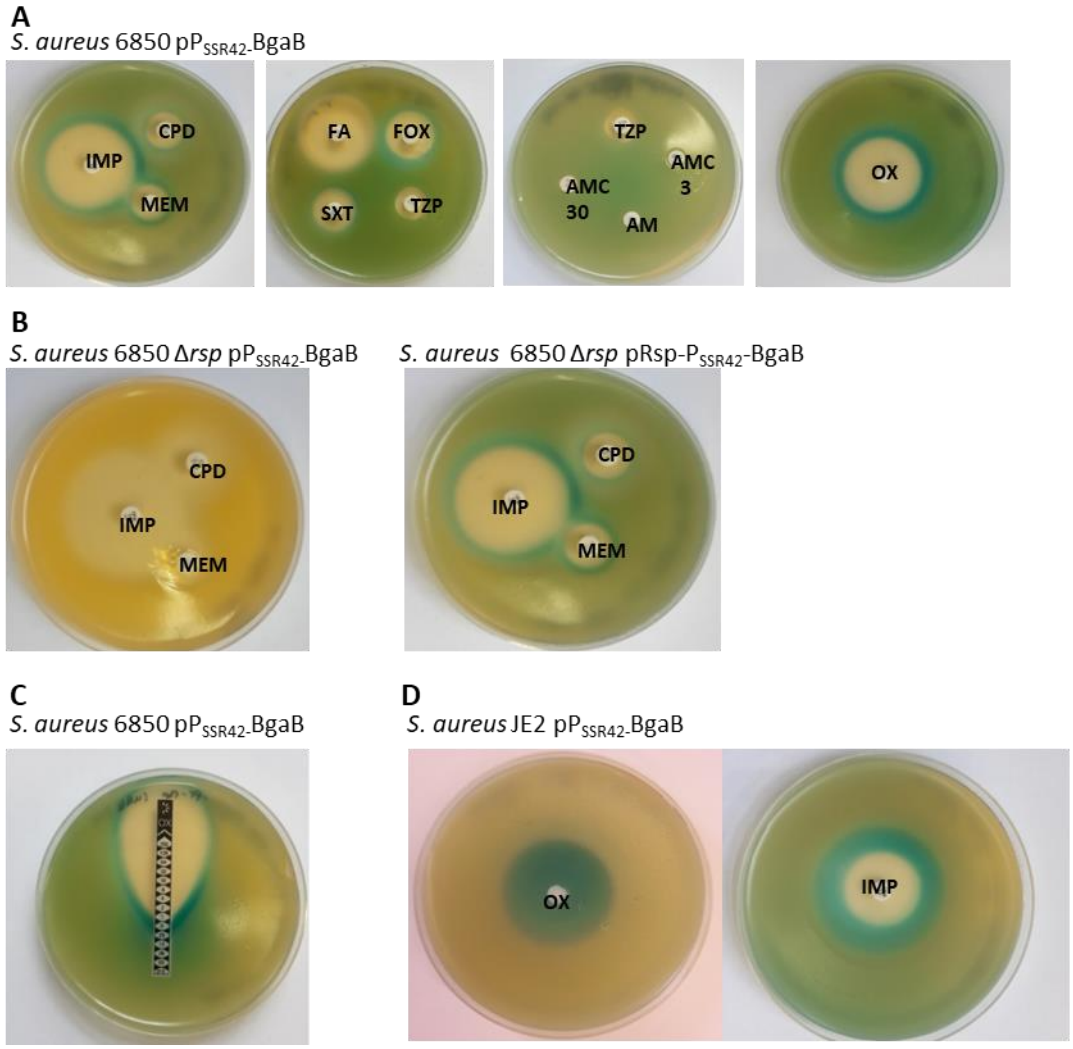

Figure 4.33: SSR42 promotor P_{SSR42} is activated upon exposure to sub-inhibitory concentrations of various antibiotics in a Rsp-dependent way. Disc diffusion assay of *S. aureus* 6850 monitoring the activity of P_{SSR42} upon stimulation with various antibiotics. A transcriptional fusion construct of P_{SSR42} with β-galactosidase BgaB was used to observe the activity of P_{SSR42} by production of indigo dye on X-Gal agar plates. **A)** Testing the influence of imipenem (IMP), cefpodoxim (CPD), meropenem (MEM), fusidic acid (FA), cefoxitin (FOX), trimethoprim-sulphamethoxazole (SXT), piperacillin-tazobactam (TZP), ampicillin (AC), amoxicillin-clavulanate (AMC) and oxacillin (OX) on X-Gal agar plates. **B)** Induction of P_{SSR42} activity is strictly dependent on presence of Rsp as demonstrated by disc diffusion assay with wild-type *S. aureus* 6850 and Δ*rsp* mutant harbouring transcriptional fusion construct of P_{SSR42} with BgaB. **C)** P_{SSR42} activity is induced by sub-inhibitory concentrations of oxacillin in *S. aureus* 6850 as demonstrated by using an oxacillin MIC strip. **D)** Induction of P_{SSR42} activity in *S. aureus* JE2 with oxacillin and imipenem on X-Gal agar plates.

Interestingly, while most of the positively tested antibiotics affect cell wall turnover, induction of promotor activity was further observed challenging *S. aureus* with the DNA damaging agent mitomycin C (Fig. 4.34). The SOS response in *S. aureus* was reported to be induced by various antibiotics as well as DNA-damaging substances such as mitomycin C (Maiques et al., 2006; Cirz et al., 2007; Anderson et al., 2006). Thus, it was tested whether induction of P_{SSR42} activity was part of the SOS response in *S. aureus*. For this, the mutant *lex*A-G94E, which is unable to autoproteolytic cleave LexA (Schröder et al., 2013) and thus can not induce SOS-response was used. Treatment of both mutant *lex*A-G94E and isogenic wild-type HG001 with mitomycin C resulted in comparable formation of the blue indigo dye indicating that induction of P_{SSR42} is not mediated via the SOS response in *S. aureus.*

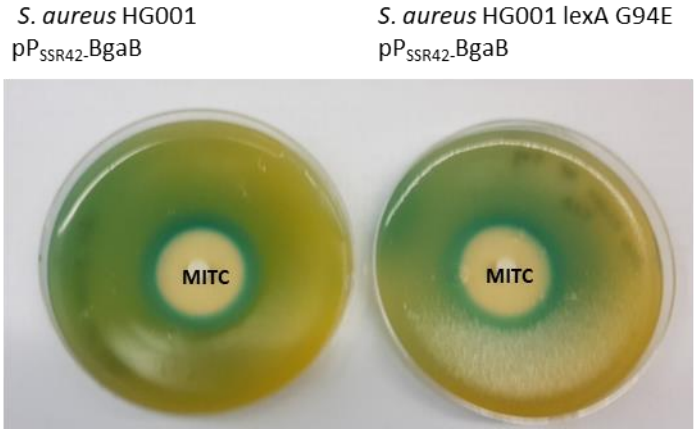

Figure 4.34: SSR42 promotor activity is stimulated by sub-inhibitory concentrations of DNA-damaging substance mitomycin C in a LexA independent fashion. Disc diffusion assay of *S. aureus* HG001 wild-type and *lex*A-G94E mutant harbouring a transcriptional fusion construct of P_{SSR42} with β-galactosidase BgaB was used to monitor the activity of P_{SSR42} upon stimulation with mitomycin C. Production of indigo dye on X-Gal agar plates was observed for wild-type bacteria and *lex*A mutant upon stimulation with mitomycin C (MITC).

Treatment with colistin which leads to disruption of cell membranes instead lead to a slightly reduced indigo blue dye formation (Fig. 4.35A) that was further analysed using the previously described GFP reporter construct during 23 h of planktonic growth of *S. aureus* JE2 and 6850 (Fig. 4.35B-C). While in strain JE2 treatment with colistin resulted in reduction of P_{SSR42} activity in a concentration-dependent manner, this effect was not observed for strain 6850.

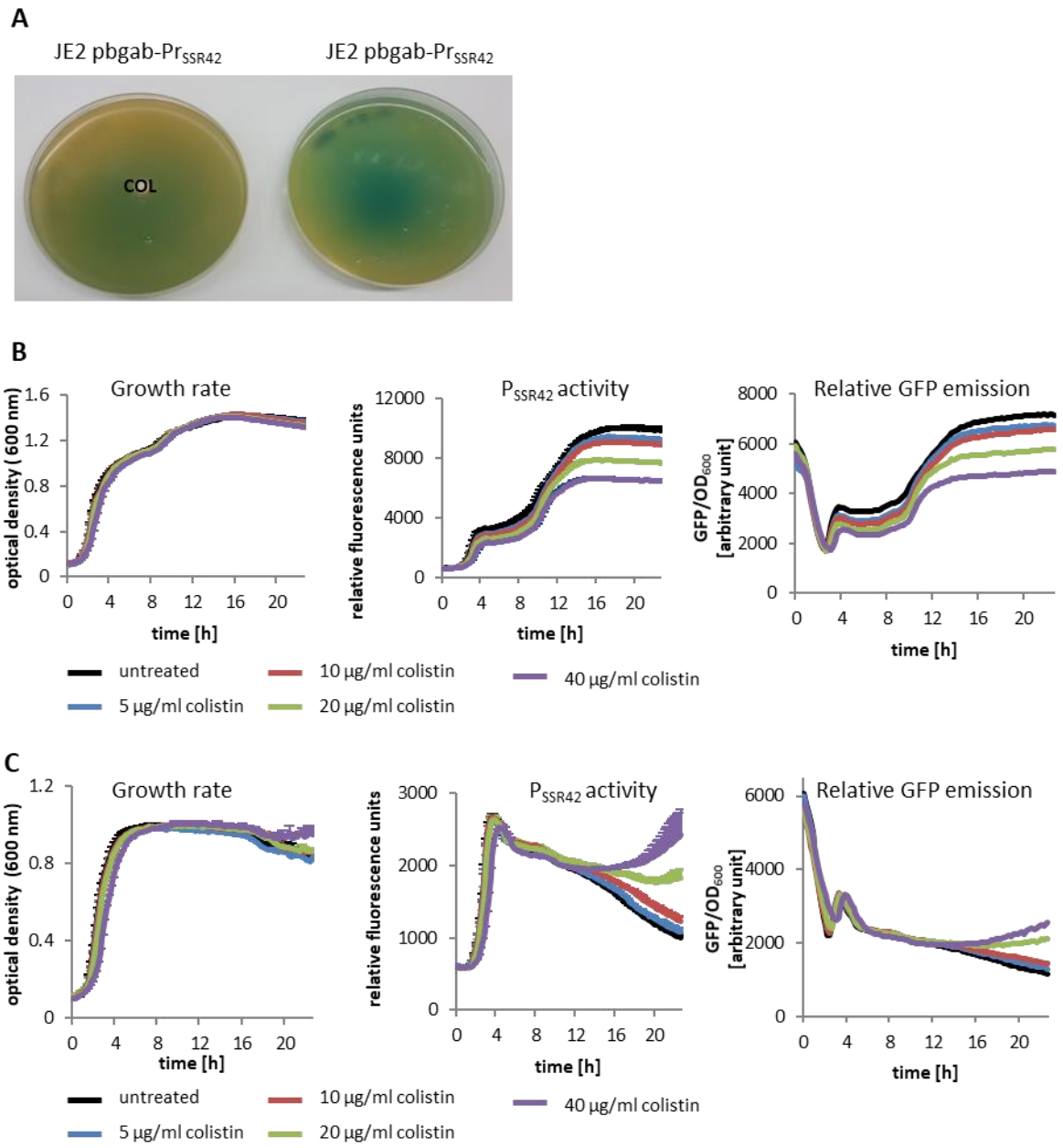

Figure 4.35: P_{SSR42} activity is inhibited by sub-inhibitory concentrations of colistin in *S. aureus* JE2. A) Disc diffusion assay of *S. aureus* JE2 harbouring a transcriptional fusion construct of P_{SSR42} with β-galactosidase BgaB. Stimulation of *S. aureus* JE2 with 40 µg of colistin reduced the formation of blue indigo dye on X-Gal agar plates. **B)** Growth curve and P_{SSR42} activity were tracked in *S. aureus* JE2 harbouring a transcriptional fusion of P_{SSR42} with GFP. Bacteria were treated with increasing sub-inhibitory concentrations of colistin which resulted in a significantly decrease in P_{SSR42} activity. **C)** Instead stimulation of *S. aureus* 6850 with colistin did not affect P_{SSR42} activity significantly as observed by monitoring P_{SSR42} activities of bacteria harbouring a transcriptional fusion of P_{SSR42} with GFP. Promotor activity was normalized to growth rate of bacteria.

Similarly, to the effects observed on agar plates, oxacillin treatment during planktonic growth of *S. aureus* JE2 revealed a distinct effect on P_{SSR42} activity (Fig. 4.36). While high concentrations of oxacillin (64, 10 µg/ml) inhibited growth of JE2 and thus no activity of P_{SSR42} was detectable, exposure to a slightly inhibitory concentration of oxacillin (0.05 µg/ml) affected the promotor activity of SSR42 (Fig. 4.36A). Upon exposure to 0.05 µg/ml oxacillin P_{SSR42} activity was initially reduced and ascended afterwards reaching even higher activity levels than in untreated bacteria. In contrast, treatment of *S. aureus* strain 6850 with sub-inhibitory concentrations of oxacillin (0.025 µg/ml) enhanced the overall activity of P_{SSR42} significantly (Fig. 4.36B).

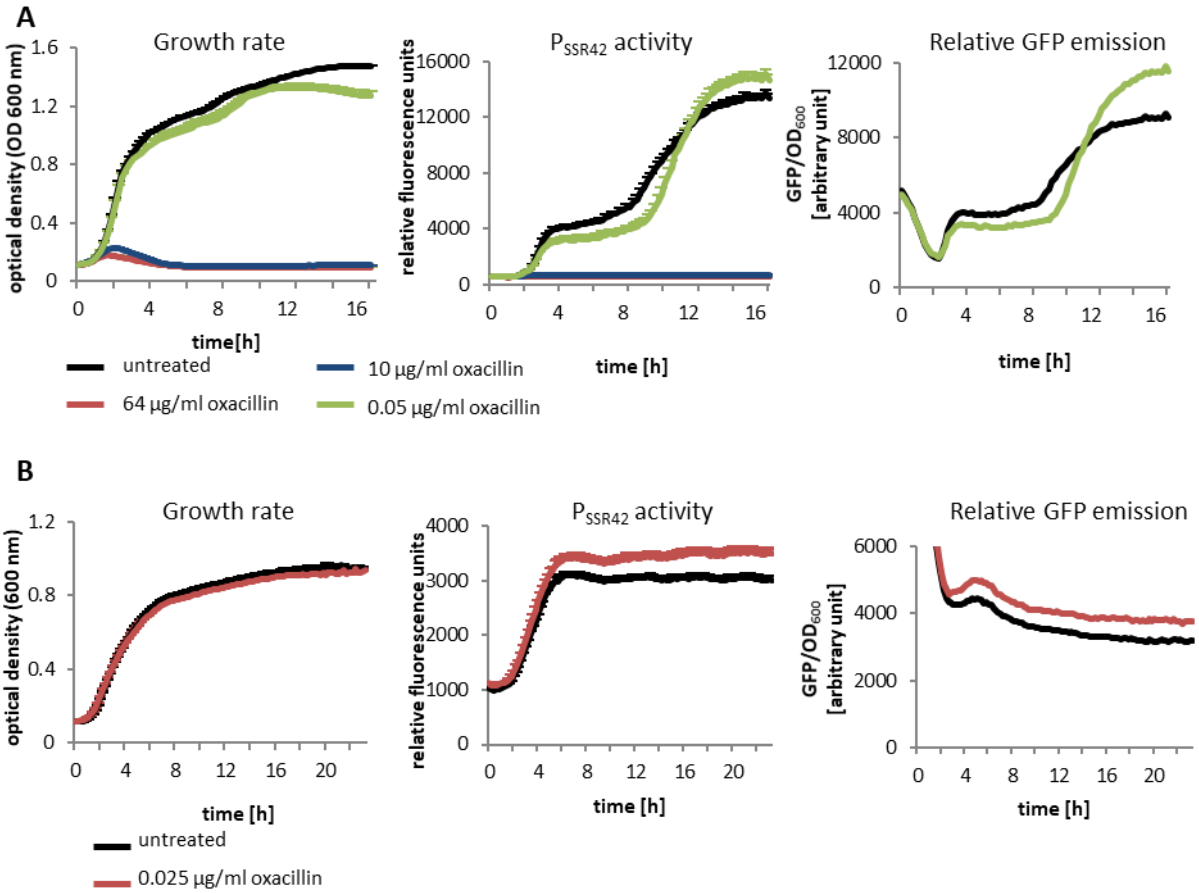

Figure 4.36: Sub-inhibitory concentrations of oxacillin increase the activity of P_{SSR42}. Monitoring of P_{SSR42} activity and growth of *S. aureus* JE2 (**A**) and 6850 **(B**) harbouring a transcriptional fusion of P_{SSR42} with GFP upon treatment with oxacillin. While high oxacillin concentrations inhibited bacterial growth and subsequent P_{SSR42} activity, challenging *S. aureus* JE2 with sub-inhibitory concentrations of oxacillin (0.05 µg/ml) resulted in a growth phase dependent alteration of P_{SSR42} activity. **B)** In contrast sub-inhibitory concentrations of oxacillin resulted in an increase in P_{SSR42} activity in *S aureus* 6850. Promotor activity was normalized to growth rate of bacteria.

Further, the effect of fatty acids on the activity of P_{SSR42} was analysed using the GFP reporter construct. Treatment of *S. aureus* with 0.001% oleic acid reduced the activity of P_{SSR42} in comparable amount in both MRSA JE2 (Fig. 4.37A) and MSSA 6850 (Fig. 4.37B). A similar effect was observed for treatment of strains JE2 and 6850 with either 12.5 µg/ml or 6.25 µg/ml myristic acid (Fig. 4.38). Thus, the activity of P_{SSR42} can be modulated by treatment with various substances ranging from β-lactam antibiotics, DNA damaging substance to fatty acids (table 4.11).

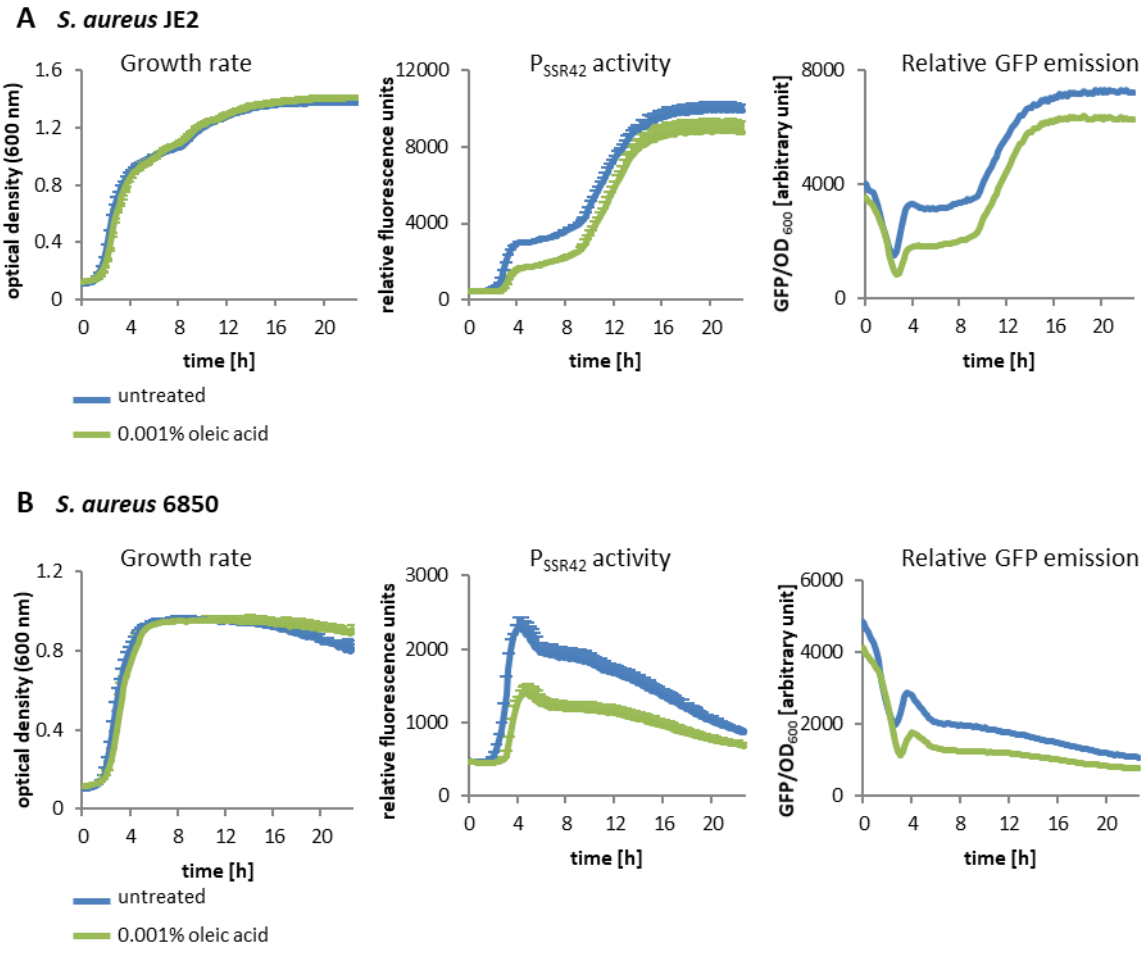

Figure 4.37: P_{SSR42} activity is inhibited by oleic acid in *S. aureus* JE2 and 6850. Treatment of sub-inhibitory concentrations with oleic acid (0.001%) resulted in a significantly decrease in P_{SSR42} activity as observed by monitoring the P_{SSR42} activity and growth of *S. aureus* JE2 (**A**) and 6850 (**B**) harbouring a transcriptional fusion of P_{SSR42} with GFP. Promotor activity was normalized to growth rate of bacteria.

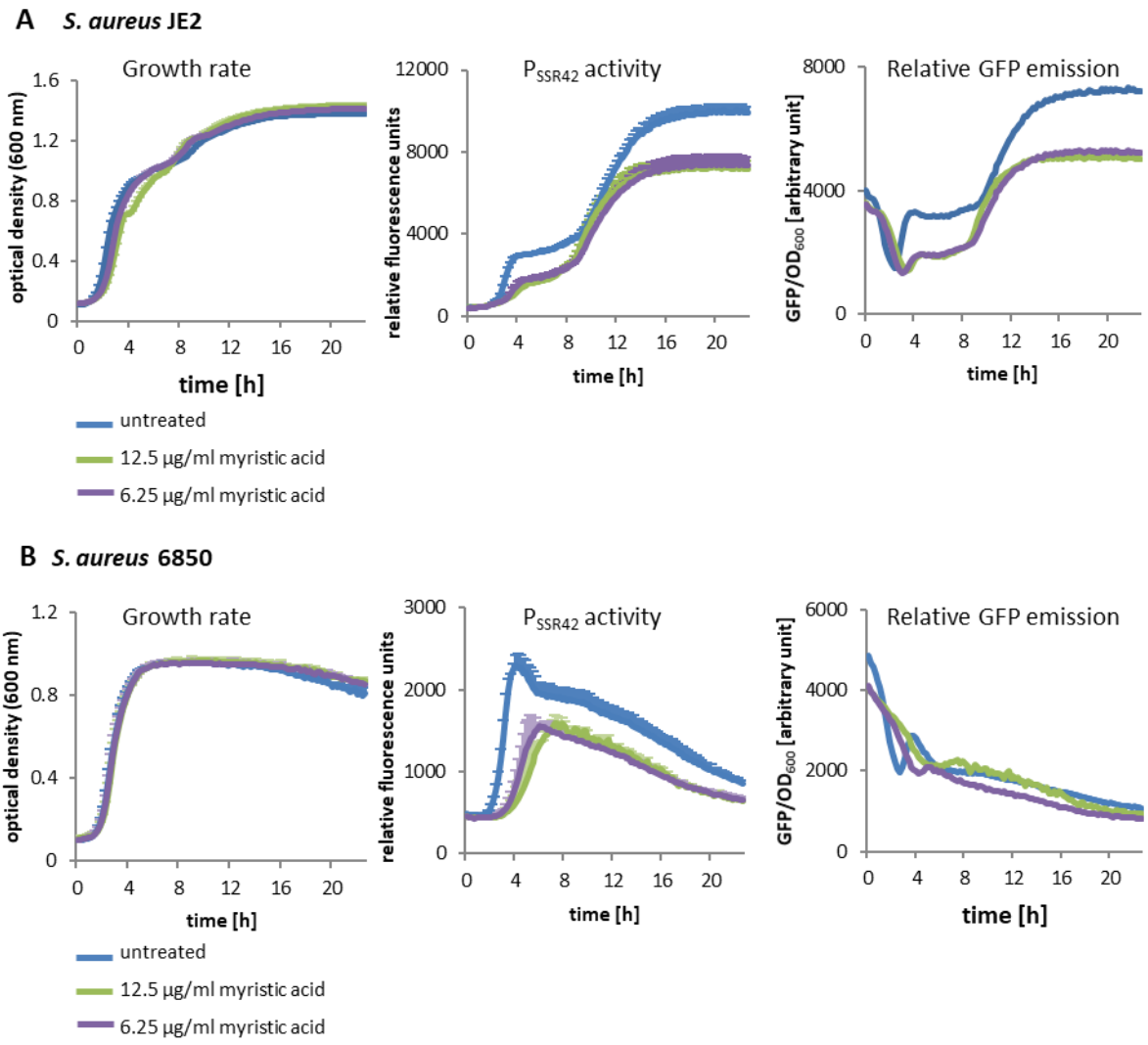

Figure 4.38: P_{SSR42} activity is inhibited by myristic acid in both *S. aureus* JE2 and 6850. Monitoring the P_{SSR42} activity and growth of *S. aureus* JE2 (**A**) and 6850 (**B**) harbouring a transcriptional fusion of P_{SSR42} with GFP. Treatment with sub-inhibitory concentrations of myristic acid (12.5 µg/ml, 6.25 µg/ml) resulted in a significantly decrease in P_{SSR42} activity in both *S. aureus* JE2 and 6850. Promotor activity was normalized to growth rate of bacteria.

Table 4.11: Influence of chemical on the activity of P_{SSR42}.

Substance	Used amount	Influence on SSR42 promotor activity
fluorchinolones		
ofloxacin	9 µg	activating
cephalosporines		
cefpodoxim	10 µg	activating
cefoxitin	30 µg	activating
β-lactam antibiotics		
amoxicillin-clavulanate	20 µg / 10µg	no influence
ampicillin	10 µg	no influence
imipenem	10 µg	activating
meropenem	10 µg	activating

oxacillin	10 µg	activating
piperacillin-tazobactam	30 µg/ 60 µg	no influence
miscellaneous		
colistin	0.6 mg	inhibitory in JE2
fusidic acid	10 µg	no influence
trimethoprim-sulphamethoxazole	16 µg/ 80 µg	activating
mitomycin C	10 µg	activating
fatty acids		
myristic acid	6.5 µg/ml	inhibitory
oleic acid	0.001%	inhibitory

4.5.4 Glucose-dependent regulation of SSR42

Most pathogenic bacteria are capable of surviving within different microenvironments inside the host. For adaption to these changing environments virulence has to be closely linked to the metabolic state of the bacteria in order to adjust the virulence potential to the availability of nutrients to overcome nutrient defieciency inside the different host niches.

Whether the availability of glucose had an impact on expression of regulatory RNA SSR42 was analysed by challenging *S. aureus* during planktonic growth with different concentrations of glucose (6.3-25.2mM). Bacteria used in this experiment harboured the previous mentioned construct allowing transcriptional coupling of P_{SSR42} and GFP. Bacteria were grown in TSB supplemented with either no glucose, 6.3 mM, 12.6 mM or 25.2 mM glucose. Activity of P_{SSR42} was monitored over 23 h of growth (Fig. 4.39). When *S. aureus* strain JE2 was grown in TSB containing standard glucose concentration (12.6 mM) the previously recorded sigmoid shaped activity curve of P_{SSR42} was observed. In contrast, the activity of P_{SSR42} was reduced approximately by half when bacteria were grown in TSB containing 6.3 mM or no glucose (Fig. 4.39A). Further, reducing the glucose availability circumvented the second rise in the promotor activity profile, which can be observed when strain JE2 is grown using standard glucose concentrations. Instead, growth of *S. aureus* JE2 in TSB containing the double amount of glucose (25.2 mM) led to an even more drastic reduction in P_{SSR42} activity reaching levels similar to the activity observed in strain 6850 when grown in standard glucose concentration (12.6 mM). However, these effects were not observable in MSSA strain 6850. Here, an increased glucose concentration (25.2 mM) resulted in a slightly reduced activity of P_{SSR42} while a reduction of glucose availability led to a higher activity (Fig. 4.39B). Interestingly, while both, a complete lack or reduction of glucose enhanced the activity of P_{SSR42} drastically starting approximately at 5 h of growth, a reduction of glucose to 6.3 mM resulted in a sigmoid shaped P_{SSR42} activity profile resembling the activity profile of strain JE2. Besides modulating the activity of P_{SSR42} the availability of glucose further affected the growth of *S. aureus*. Reducing the glucose availability or growing *S. aureus* under glucose deprived conditions resulted in an enhanced growth. While growth of *S. aureus* JE2 was reduced in TSB containing 25.2

mM glucose compared to growth under standard conditions this was not found for growth of strain 6850. Hence, it was concluded that the metabolic state of *S. aureus* can influence the activity of P_{SSR42} in a strain dependent manner.

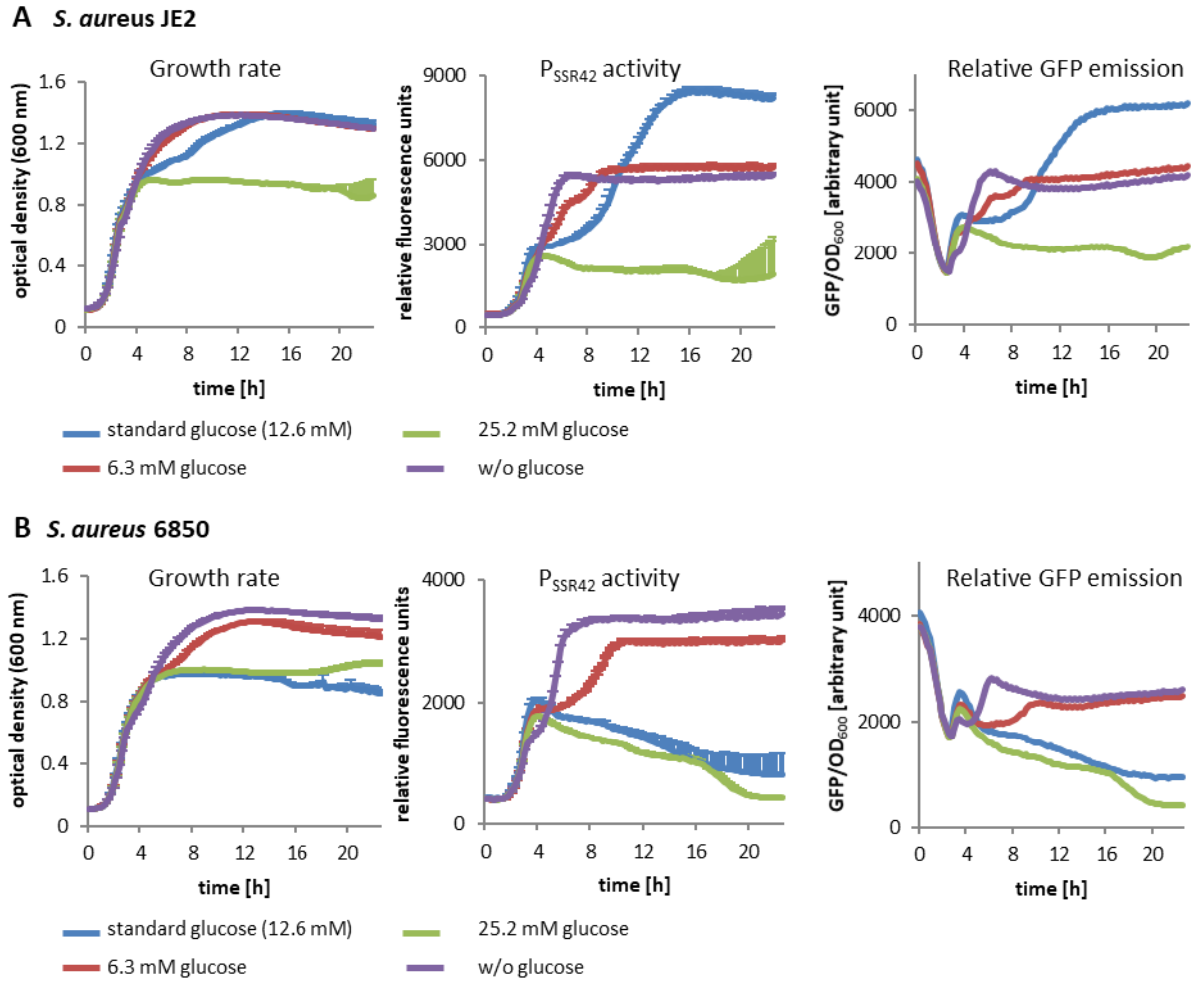

Figure 4.39: P_{SSR42} activity is modulated by glucose. Growing *S. aureus* in other than standard glucose concentrations resulted in significantly alterations in the P_{SSR42} activity in both *S. aureus* JE2 (**A**) and 6850 (**B**) as observed by monitoring the P_{SSR42} activity and growth of *S. aureus* harbouring a transcriptional fusion of P_{SSR42} with GFP. Promotor activity was normalized to growth rate of bacteria.

P_{SSR42} activity was similar in *S. aureus* 6850 or JE2 grown in BHI and in TSB, which both did not contain glucose (Fig. 4.40A). Interestingly, growing strain 6850 in another TSB broth which already contains 2.5 g/L glucose in the prepared media powder (corresponds to 12.6 mM; Sigma Aldrich, T8907) resulted in an enhanced P_{SSR42} activity compared to bacteria grown in TSB supplemented with 12.6 mM glucose (Fig. 4.40B). When strain JE2 was grown in that media the activity of P_{SSR42} instead was reduced and the second activitation peak of P_{SSR42} activity was lost indicating that not only availability of glucose but a further hitherto unknown metabolic factor modulates the activity of P_{SSR42}.

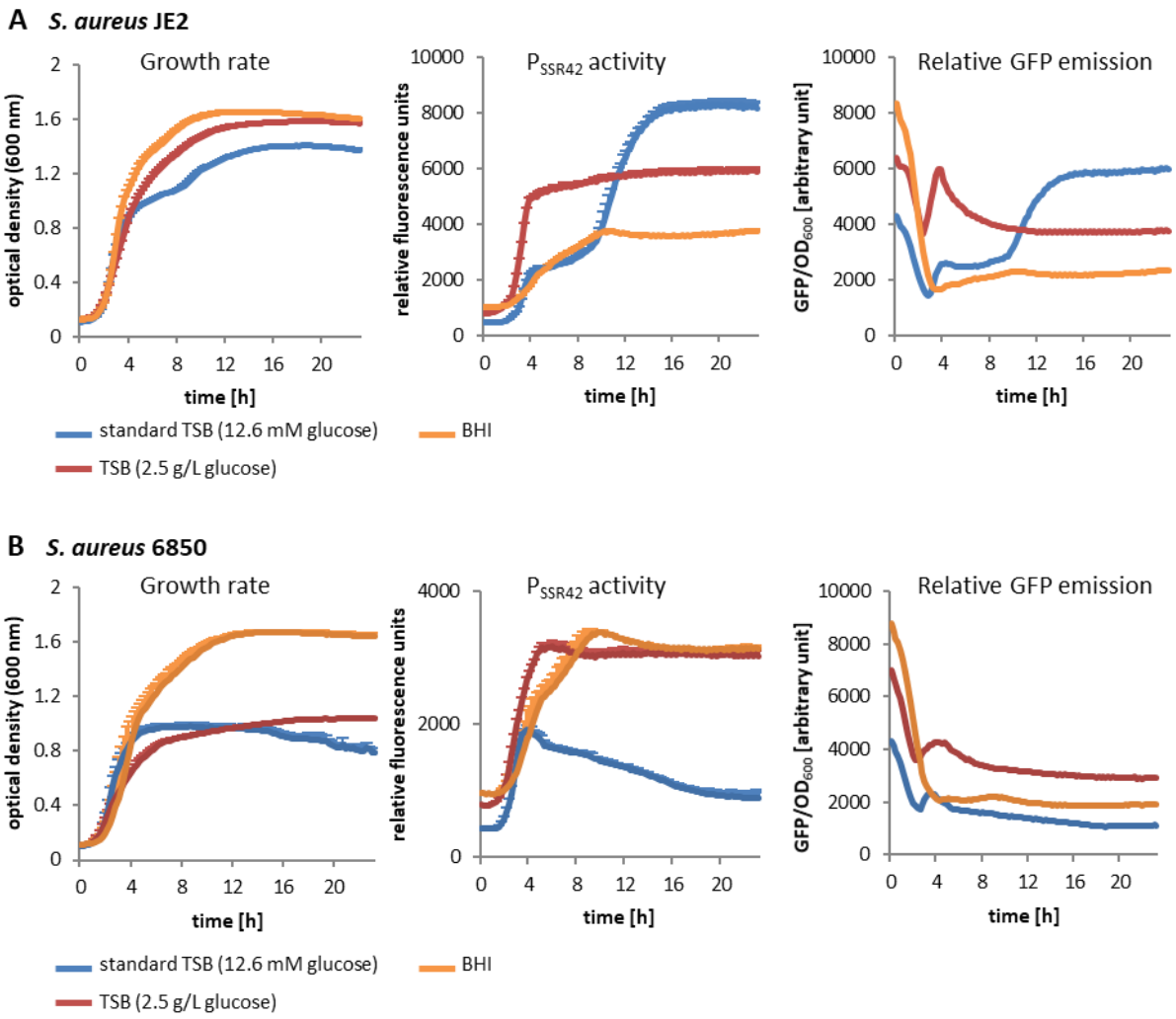

Figure 4.40: Variation of P_{SSR42} activity under growth of *S. aureus* in different media. P_{SSR42} shows significantly alterations in the activity when *S. aureus* JE2 (**A**) and 6850 (**B**) are cultivated in different media. P_{SSR42} activity and growth of *S. aureus* harbouring a transcriptional fusion of P_{SSR42} with GFP were monitored over a time course of 23 h. Promotor activity was normalized to growth rate of bacteria.

4.5.5 Role of SSR42 in oxacillin-induced haemolysis up-regulation

Expression of virulence factors such as α-toxin, PVL and TSST-1 have been reported to be modulated in presence of sub-inhibitory concentrations of antibiotics (Rudkin et al., 2014; Ohlsen et al., 1998; Dumitrescu et al., 2007; Dickgiesser and Wallach, 1987). Further, lincosamines, erythromycin, and chloramphenicol were shown to alter the fibronectin binding abilities of *S. aureus* (Proctor et al., 1983), while clindamycin and doxycycline enhanced the uptake of bacteria by polymorphnuclear neutrophils (Milatovic, 1982). Sub-inhibitory concentrations of antibiotics were further demonstrated to influence virulence traits such as biofilm formation (Mirani and Jamil, 2011; Haddadin et al., 2010; Subrt et al., 2011) and haemolytic activity (Ohlsen et al., 1998; Kuroda et al., 2007). Especially β-lactam antibiotics

were investigated in this regard and found to induce transcriptional up-regulation of *saeRS* (Kuroda et al., 2007) resulting in enhanced haemolytic properties of *S. aureus* (Kuroda et al., 2007; Ohlsen et al., 1998).

Since ncRNA SSR42 was shown to regulate haemolysis and the activity of P_{SSR42} was demonstrated to be inducible by sub-inhibitory concentrations of oxacillin, it was hypothesized that SSR42 could be responsible for the reported oxacillin-inducible up-regulation of *hla* expression (Kuroda et al., 2007; Ohlsen et al., 1998). To test this hypothesis liquid cultures of wild-type *S. aureus* 6850 and isogenic ΔSSR42 mutant were spotted on sheep blood agar. An oxacillin containing disc (1 µg) was placed with equal distance to both strains. While wild-type bacteria grown in small distance to the antibiotic disc displayed stronger haemolysis than bacteria further away from the disc, haemolysis was unaltered in presence of oxacillin in the ΔSSR42 mutant (Fig. 4.41A). In line with this, challenging wild-type bacteria with sub-inhibitory concentrations of oxacillin (0.025 µg/ml) resulted in elevated α-toxin levels in wild-type *S. aureus* 6850 (Fig. 4.41B; FC: 1.8; p>0.001). In contrast, oxacillin had no significant effect on α-toxin levels in a mutant lacking SSR42 while ectopic expression of SSR42 restored the oxacillin-induced phenotype in the ΔSSR42 mutant (FC: 1.3; p=0.012).

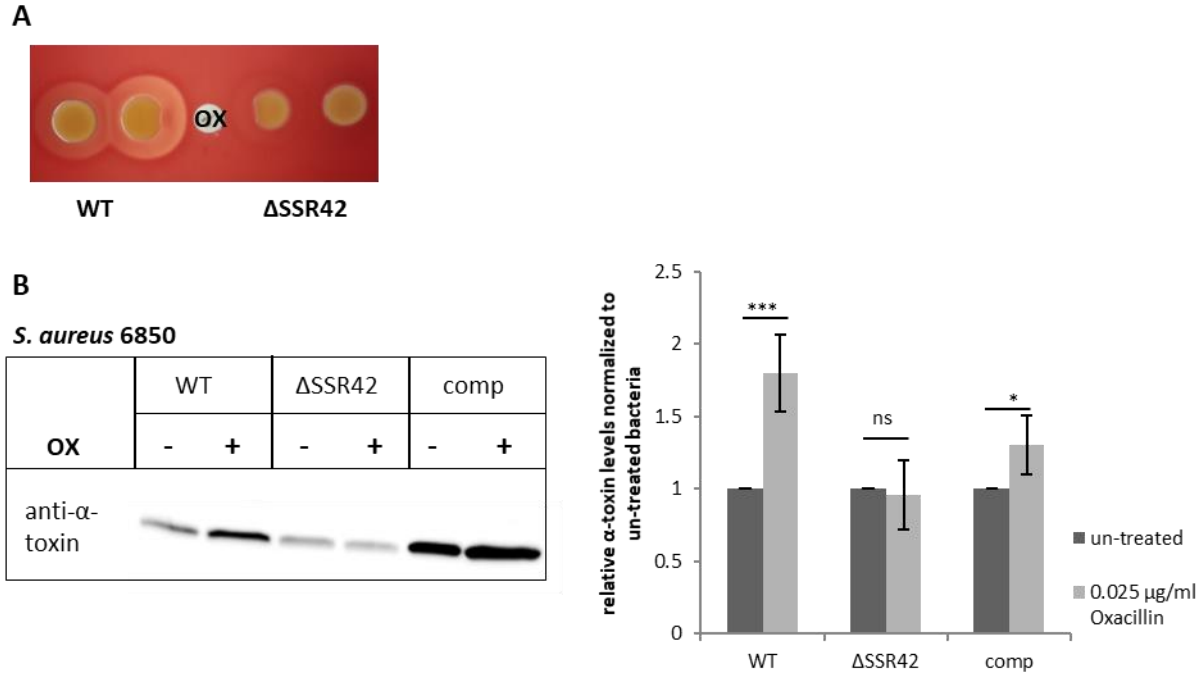

Figure 4.41: SSR42 is required for oxacillin-induced up-regulation of α-toxin expression. A) Haemolysis on sheep blood agar is significantly increased in *S. aureus* 6850 wild-type bacteria but not in a ΔSSR42 when sub-inhibitory concentrations of oxacillin are present as observed by spotting stationary phase cultures on sheep blood agar. An oxacillin disc was placed in equal distance to both wild-type and SSR42 mutant. **B)** Treatment of *S. aureus* with sub-inhibitory concentrations of oxacillin (0.025 µg/ml) resulted in increased α-toxin protein levels in wild-type and complemented mutant but not in absence of SSR42 as observed by immunoblotting of stationary phase culture supernatants (left panel) and subsequent quantification of chemiluminescence signals using ImageJ (right panel). Statistical analysis was performed using Student´s t-test: *: p< 0.05; ***: p< 0.001.

Sub-inhibitory concentrations of oxacillin were previously reported to induce activity of P_{hla} (Ohlsen et al., 1998). Therefore, the activity of P_{hla} upon exposure to sub-inhibitory concentrations of oxacillin was analysed in *S. aureus* wild-type bacteria and a ΔSSR42 mutant using a GFP reporter system (Fig. 4.42). Upon treatment of bacteria with sub-inhibitory concentrations of oxacillin (0.025 µg/ml) the promotor activity of *hla* was found to be strongly enhanced in *S. aureus* 6850 wild-type bacteria, while in mutants lacking SSR42 no influence of oxacillin on the activity of P_{hla} was observed (Fig. 4.42A). This activation of P_{hla} upon treatment with sub-inhibitory concentrations of oxacillin was further observed in the MRSA strain JE2 but not in the transposon insertion mutant 2500639R lacking functional SSR42 (Fig. 4.42B). Due to the resistance of strain JE2 towards oxacillin higher concentrations had to be used (0.01 µg/ml). Thus, a role for SSR42 in the oxacillin-induced up-regulation of haemolysis was confirmed in both MRSA and MSSA strains.

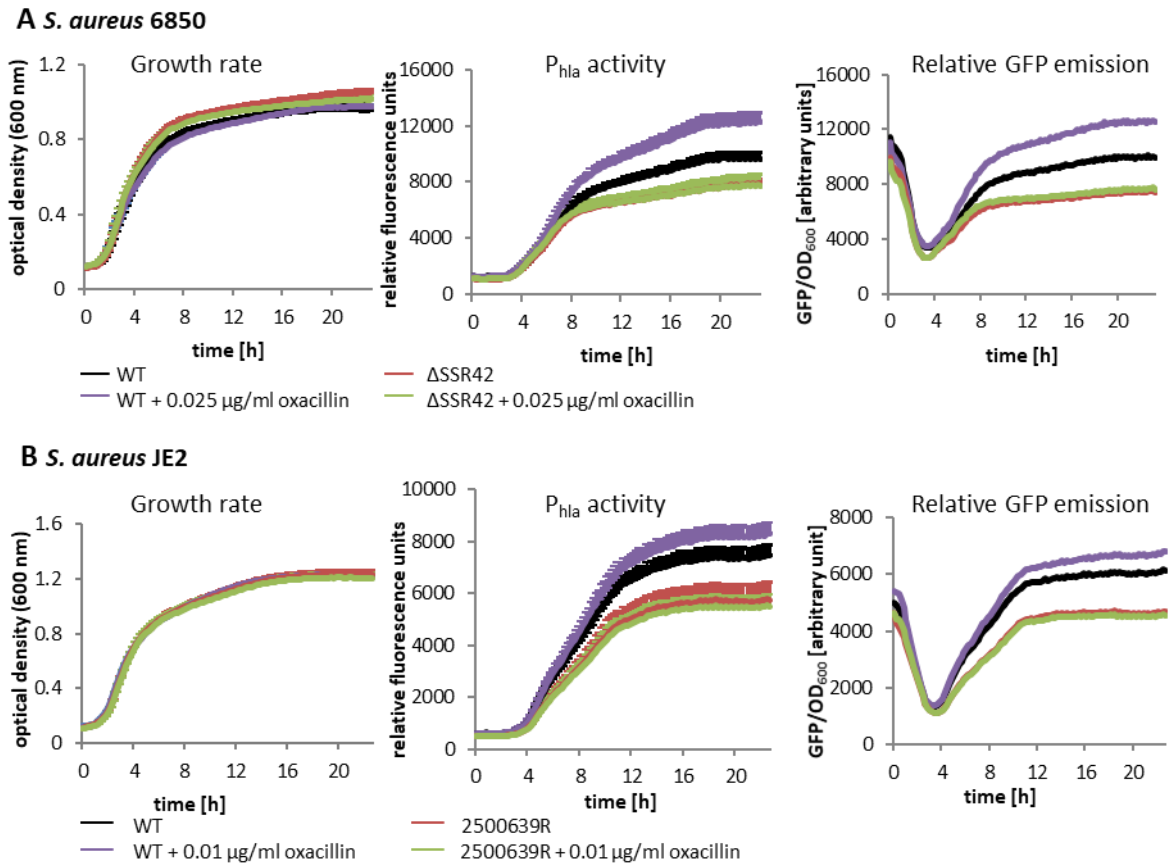

Figure 4.42: Transcription of *hla* is enhanced in the presence sub-inhibitory concentrations of oxacillin in a SSR42 dependent fashion. A) P_{hla} activity is significantly increased in the prescence of sub-inhibitory concentrations of oxacillin in *S. aureus* 6850 wild-type bacteria but not in 6850 ΔSSR42. **B)** Similar, sub-inhibitory concentrations of oxacillin resulted in enhanced P_{hla} activity in *S. aureus* JE2 wild-type bacteria but an insertional SSR42 mutant (JE2 2500639R). P_{hla} activity and growth of *S. aureus* harbouring a transcriptional fusion of P_{hla} with GFP were monitored over a time course of 23 h using a TECAN Infinite M200 plate reader. Promotor activity was normalized to growth rate of bacteria.

4.5.6 Sub-inhibitory concentrations of oxacillin enhance virulence of *S. aureus* 6850 in a SSR42-dependent manner

ncRNA SSR42 was found to play a decisive role in inducing cell death of infected host cells (see chapter 4.3.3). Mutants in SSR42 displayed a reduced cytotoxic phenotype towards HeLa 2000 cells similar to mutants lacking α-toxin. Considering the impact of α-toxin on cytotoxicity and the observed oxacillin-dependent induction of α-toxin expression the influence of oxacillin on cell death was analysed in mutants lacking SSR42. For analysing whether treatment with oxacillin alters the cytotoxic properties of *S. aureus*, HeLa 2000 cells were infected with wild-type *S. aureus* 6850 for 4 h. Infected cells were treated with various concentrations of oxacillin (2.5 - 0.025 µg/ml) during the last 2.5 h of infection where bacteria are considered to escape from the phagosomes, in which they reside after invasion of host cells (Fig. 4.43). CFU enumeration 4 h post infection demonstrated that the oxacillin concentrations used had no impact on the viability of intracellular bacteria, thus classifying the concentrations used as sub-inhibitory for bacterial growth (Fig. 4.43A). Cell death was measured exploiting LDH release from infected cells (Fig. 4.43B). Relative LDH release was found significantly enhanced when infected host cells were treated with 0.5 µg/ml oxacillin (FC: 1.41; p=0.001) compared to non-treated infected host cells, while no differences were found for the further tested oxacillin concentrations. Uninfected host cells were treated with the highest tested oxacillin concentration (2.5 µg/ml) to exclude potential cytotoxic properties of oxacillin on host cells. No significant difference in LDH release was detected between non-treated and oxacillin-treated cells (FC: 0.26; p=0.22).

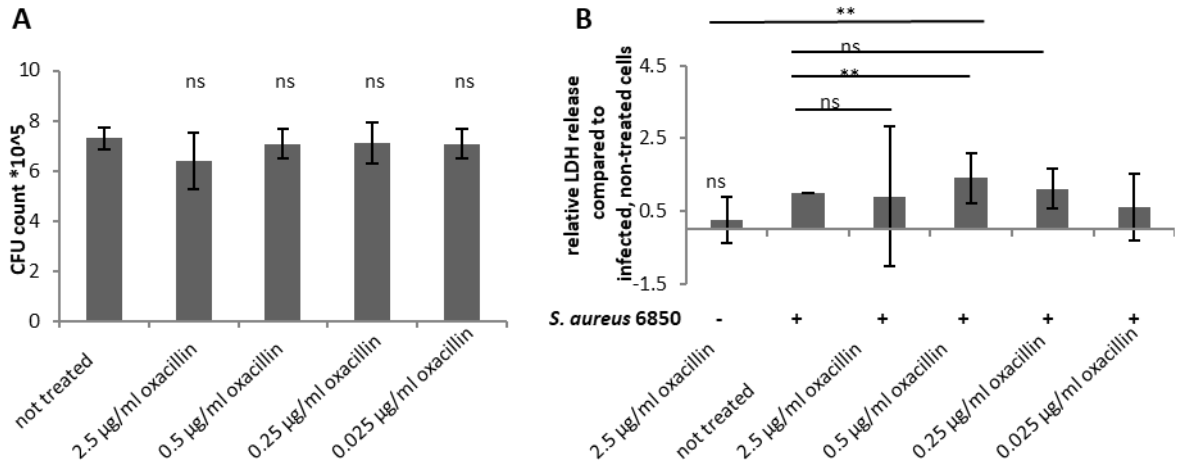

Figure 4.43: Cytotoxicity of *S. aureus* 6850 is enhanced in the presence of sub-inhibitory concentrations of oxacillin. A) Establishment of intracellular sub-inhibitory concentrations of oxacillin. HeLa 2000 cells were infected with *S. aureus* 6850 with a MOI of 10 for 4 h. Cells were treated with various oxacillin concentrations for the last 2.5 h of infection. The used oxacillin concentrations were classified as sub-inhibitory for *S. aureus* 6850 as observed by CFU enumeration. **B)** Treatment of infected HeLa 2000 cells with 0.5 µg/ml oxacillin resulted in significantly enhanced cytotoxicity of *S. aureus* 6850 as observed by measuring released LDH levels. HeLa 2000 cells were infected with *S. aureus* 6850 with a MOI of 10 for 4 h. LDH release was measured. LDH release from uninfected cells was set to 1. Statistical analysis was performed using sSudent´s t-test: *: p< 0.05; ***: p< 0.001.

Analysing the role of SSR42 in the oxacillin-induced enhanced cytotoxicity, HeLa 2000 cells were infected with wild-type bacteria, isogenic ΔSSR42 mutant, complemented mutant and a Δ*hla* mutant for 4 h (Fig. 4.44). Effects caused by different sensitivities against oxacillin were excluded by performing a MIC test for wild-type bacteria, ΔSSR42 and Δ*hla* mutant (Fig. 4.44A). The MIC was determined to be approximately 0.25 µg on Müller-Hinton agar. Infected HeLa 2000 cells were treated with 0.5 µg/ml oxacillin during the last 2.5 h of infection. LDH release was measured as an indicator for cell death (Fig. 4.44B). While relative LDH release was found to be approximately two-fold elevated in oxacillin-treated cells infected with wild-type bacteria (FC: 2.06; p> 0.0001), no significant differences in LDH release were found for cells infected with either a ΔSSR42 or Δ*hla* mutant. The oxacillin-induced enhancement of cytotoxic activity towards HeLa 2000 cells was recovered after complementation of SSR42 in trans (FC: 2.1; p> 0.0001). An oxacillin-induced enhancement of cytotoxicity was likewise not observable for cells infected with the Δ*hla* mutant.

Thus, it was concluded that the enhancement of cytotoxicity resulted from oxacillin-induced expression of α-toxin. This oxacillin provoked induction of cell death was strictly dependent on ncRNA SSR42.

In summary, analysing the LDH release of infected HeLa 2000 revealed an important role for ncRNA SSR42 in the observed oxacillin-induced enhancement of cytotoxicity of wild-type *S. aureus* via regulation of α-toxin.

A

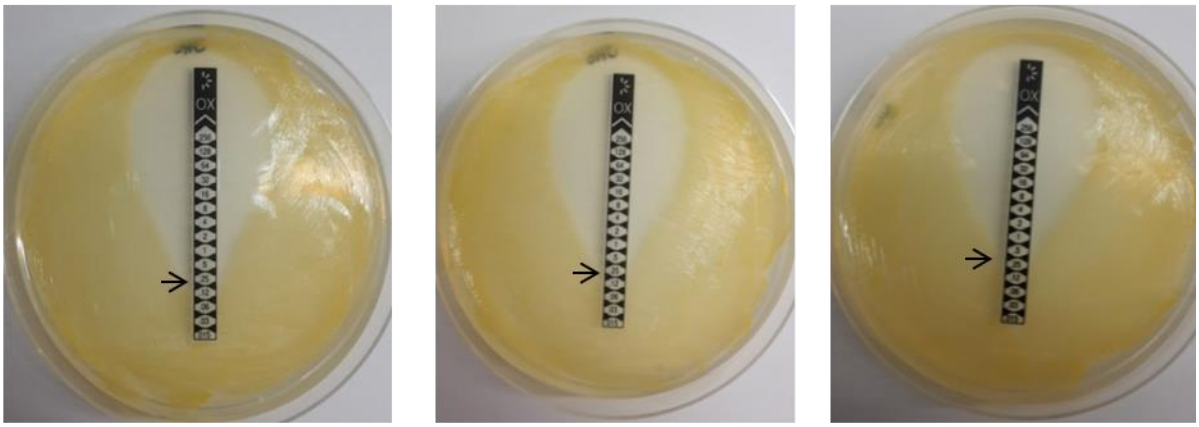

S. aureus 6850 WT ΔSSR42 Δ*hla*

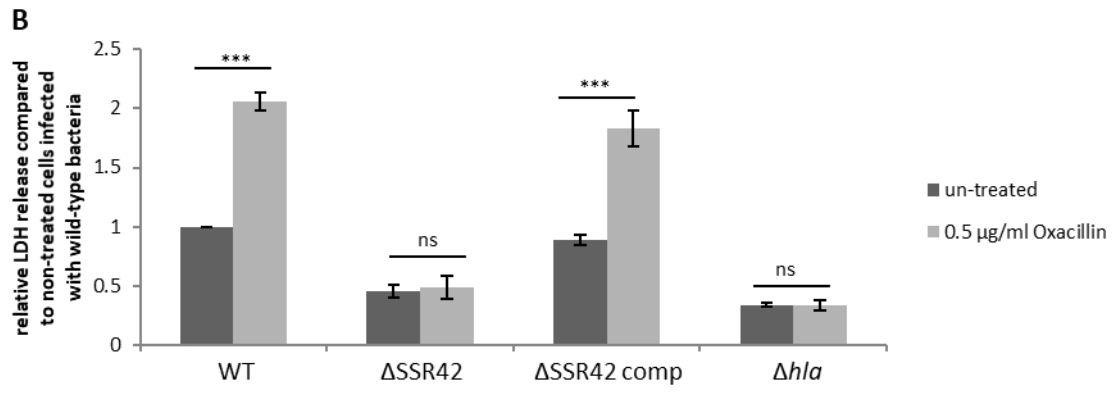

Figure: 4.44 Oxacillin-induced enhancement of cytotoxicity is dependent on presence of SSR42 in *S. aureus* 6850. A) Oxacillin MIC test of *S. aureus* 6850 wild-type bacteria, ΔSSR42 and Δ*hla* mutant revealed no differences in the MIC for the three groups on Müller-Hinton agar plates. **B)** SSR42 mediates oxacillin-induced enhancement of cytotoxicity on HeLa 2000 cells via regulation of *hla* expression as observed by measuring LDH release of infected cells. HeLa 2000 cells were infected with a MOI of 10 with *S. aureus* 6850 wild-type, ΔSSR42 and Δ*hla* mutant for 4 h. Cells were treated with sub-inhibitory conenetrations of oxacillin (0.5 µg/ml) 1.5 h post infection. LDH release was measured after 4 h of infection. LDH release from untreated cells infected with wild-type bacteria was set to 1. Treatment with oxacillin resulted in a significant increase in LDH release form HeLa 2000 cells infected with either wild-type bacteria or complemented SSR42 mutant. In contrast oxacillin treatment of cells infected with either ΔSSR42 or Δ*hla* mutant did not affect LDH release. Statistical analysis was performed using Student´s t-test: *: p< 0.05; ***: p< 0.001.

4.6 Transcription of ncRNA SSR42 is regulated by various major regulators in *S. aureus*

Despite regulation by AraC-type transcriptional regulator Rsp (Das et al., 2016) the regulation of SSR42 transcription remains elusive. However, analysing the impact of *rsp* mRNA levels on transcription of SSR42 in various *S. aureus* strains (see section 4.5.2) suggested the implication of further factors. Applying SSR42 promotor activity assays in various mutants obtained from the Nebraska library as well as knockout mutants, the regulation of SSR42 transcription was deciphered. The impact of various regulatory factors on transcriptional regulation of SSR42 was analysed recording the activity of P_{SSR42} over a time course of 23 h (Fig. 4.45-4.50). All tested mutants obtained from the Nebraska library where freshly transduced into JE2 wild-type background to exclude effects caused by secondary site mutations. All described effects of the various regulators on activity of P_{SSR42} are summarized in a heatmap illustrating the differences in P_{SSR42} activity between each mutant and wild-type bacteria (Fig. 4.51, heatmap created by Maximilian Klepsch, University Würzburg).

4.6.1 Regulation of SSR42 by Rsp

A strong regulatory impact of **Rsp** on transcriptional regulation of ncRNA SSR42 has been reported previously with mutants in *rsp* lacking SSR42 transcription completely (Das et al., 2016). Therefore, the activity of P_{SSR42} was analysed in an insertional mutant in *rsp* (NE1304) using the GFP reporter construct

pP$_{SSR42}$-GFP (Fig. 4.45). Confirming previous findings, no activity of P$_{SSR42}$ was detected in mutant NE1304 illustrating the essential role of Rsp on regulation of SSR42 transcription.

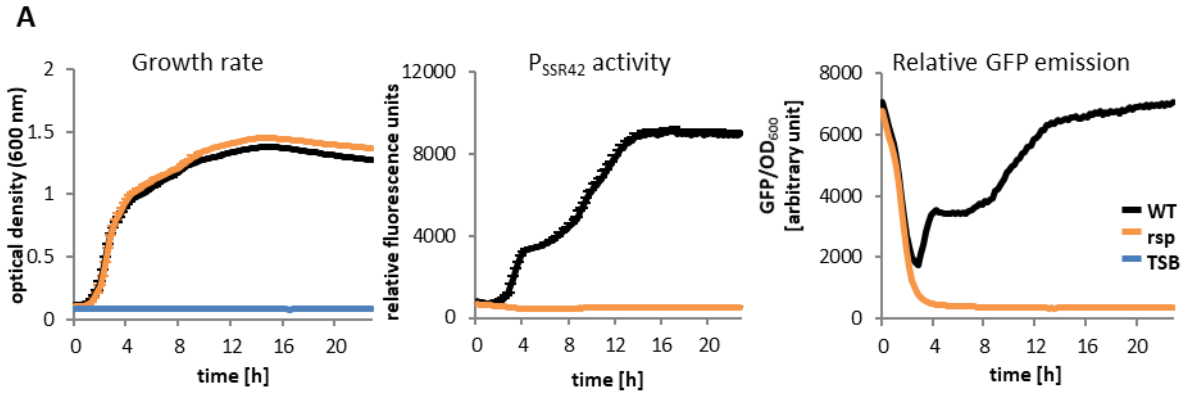

Figure 4.45: Rsp is required for transcription of SSR42. Insertional mutant of *S. aureus* JE2 in *rsp* was obtained from the NTML mutant library (Fey et al., 2013) and was used for monitoring the promotor activity of SSR42 (P$_{SSR42}$) in a time course of 23 h using a transcriptional fusion of SSR42 and promotorless GFP. Growth curve was measured in parallel and GFP intensity was normalized to growth of the bacteria (GFP/OD$_{600}$). Lack of functional Rsp (NE1304) resulted in a complete abolishement of P$_{SSR42}$ activity illustrating the requirement of Rsp for SSR42 transcription. Modified after Horn et al., 2018b.

4.6.2 Regulation of SSR42 by two-component systems

Two-component systems play a major role in transcriptional regulation. The two-component systems ArlRS, SrrAB and VraRS have been implicated in influencing the sensitivity towards oxacillin in *S. aureus* (Matsuo et al., 2010) and were thus analysed regarding regulation of SSR42 (Fig. 4.46). Further, the activity of P$_{SSR42}$ was studied in mutants of the major virulence regulatory systems *sae*RS and *agr* as well as in *vfr*B encoding a regulator of the SaeRS two-component system.

As a first candidate to regulate SSR42 transcription, the **agr quorum-sensing system** was chosen due to the importance of this system in matters of viruelence regulation, especially haemolysis. Promotor activity of SSR42 was found to be drastically altered in mutants lacking a functional agr quorum-sensing system (*agr*A: NE1532). Insertional disruption of *agr*A drastically altered the profile of P$_{SSR42}$ activity delaying the second peak in up-regulation (approximately after 17 h of growth) and subsequently resulting in higher activity during late time points in growth of *S. aureus* JE2 (Fig. 4.46A).

Due to the observed role for SSR42 in stabilizing *sae* transcripts a potential regulatory impact of the **SaeRS** two-component system on the activity of P$_{SSR42}$ was analysed. The activity of P$_{SSR42}$ in an insertional mutant in *sae*S (NE1296) was strongly enhanced during later time points during growth (~12 h; Fig. 4.46B)). However, disruption of *sae*R (NE1622) had no effect on the activity of P$_{SSR42}$ (Fig. 4.46C).

Insertional inactivation of the two-component system **ArlRS** (*arlR*::Bursa NE1684, *arlS*::Bursa NE1183) resulted in an overall higher activity of P_{SSR42} compared to that of wild-type bacteria (Fig. 4.46D). Enhanced promotor activity was especially prominent during later time points of growth of *S. aureus* (~12 h).

Lack of two-component system **VraRS** (*vra*R::BursaNE554, *vraS*::Bursa NE823) resulted in an overall slight decrease in P_{SSR42} activity (Fig. 4.46E) indicating a minor role for two-component system VraRS in regulation of SSR42 transcription.

Due to a reported role of two-component system **SrrAB** in regulation of oxacillin sensitivity (Matsuo et al., 2010) P_{SSR42} activity in the insertional mutants in *srr*A and *srr*B (*srr*A::Bursa NE1309, *srr*B::Bursa NE588) was analysed (Fig. 4.46F). While mutants in *srr*A displayed a reduced P_{SSR42} activity mostly during the early growth phases of *S. aureus* JE2 (~3-11 h), insertional disruption of *srr*B resulted in a decrease of P_{SSR42} activity only during later time points of growth (~11-23 h).

In contrast, the P_{SSR42} activity in a mutant lacking the SaeRS-regulatory protein **VfrB** (NE229) was reduced over the whole 23 h of growth (Fig. 4.46G).

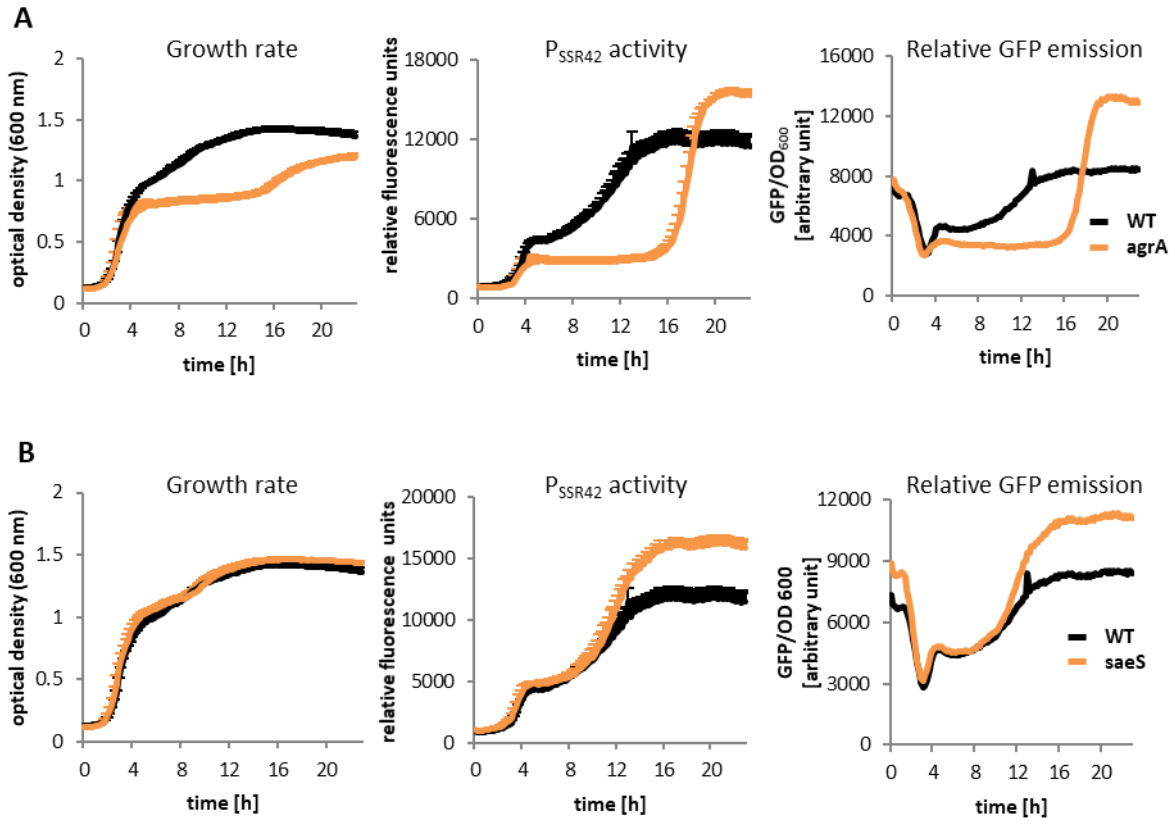

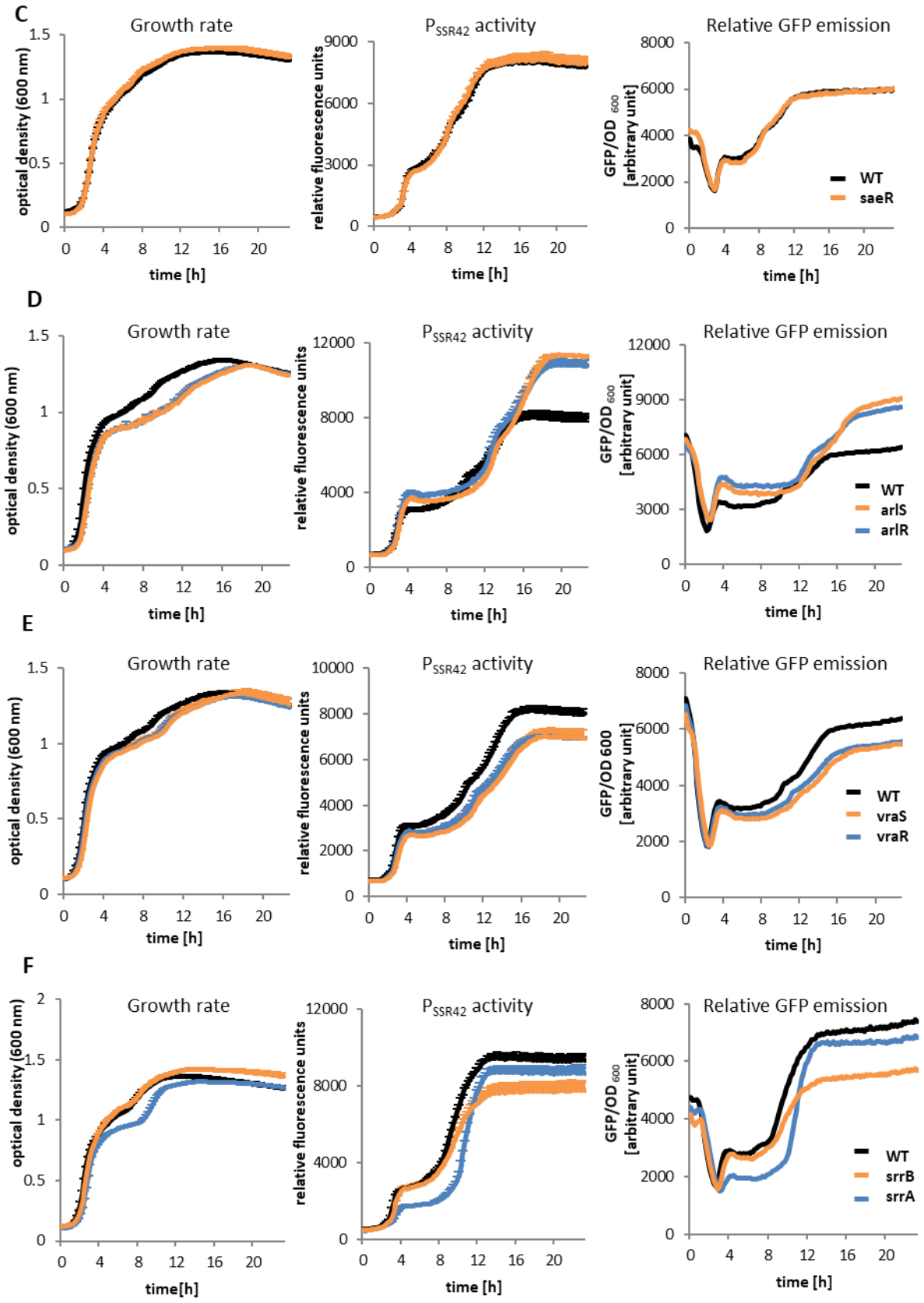
C
Growth rate
optical density (600 nm)
time [h]
P SSR42 activity
relative fluorescence units
time [h]
Relative GFP emission
GFP/OD 600 [arbitrary unit]
time [h]
WT
saeR
D
Growth rate
optical density (600 nm)
time [h]
P SSR42 activity
relative fluorescence units
time [h]
Relative GFP emission
GFP/OD 600 [arbitrary unit]
time [h]
WT
arlS
arlR
E
Growth rate
optical density (600 nm)
time [h]
P SSR42 activity
relative fluorescence units
time [h]
Relative GFP emission
GFP/OD 600 [arbitrary unit]
time [h]
WT
vraS
vraR
F
Growth rate
optical density (600 nm)
time[h]
P SSR42 activity
relative fluorescence units
time [h]
Relative GFP emission
GFP/OD 600 [arbitrary unit]
time [h]
WT
srrB
srrA

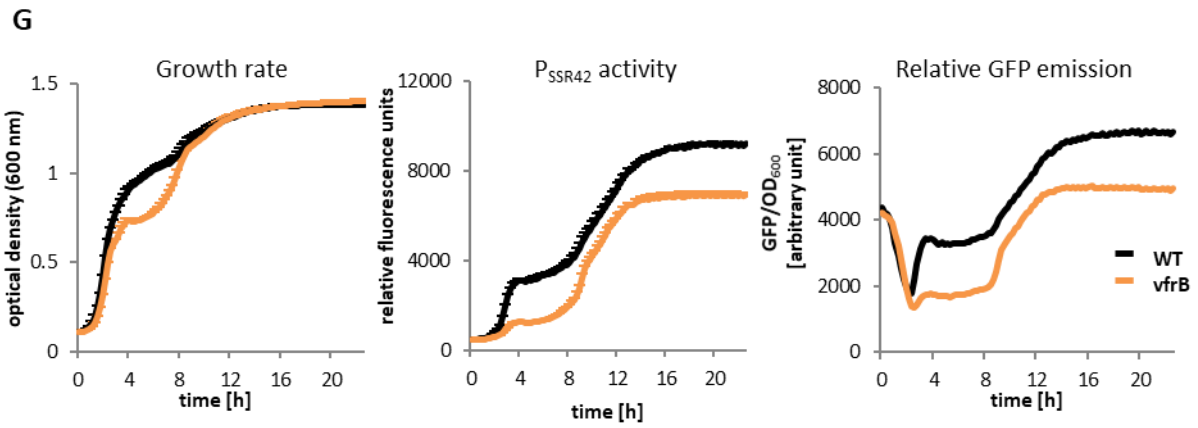

Figure 4.46: Several two-component systems are involved in regulation of SSR42 transcription. Insertional mutants of *S. aureus* JE2 in various two-component systems were obtained from the NTML mutant library (Fey et al., 2013) and were used for monitoring the promotor activity of SSR42 (P_{SSR42}) in a time course of 23 h using a transcriptional fusion of SSR42 and promotorless GFP. Growth curve was measured in parallel and GFP fluoresence was normalized to growth of the bacteria (GFP/OD_{600}). **A)** Insertional inactivation of *agr*A (NE1532) resulted in a strong alteration in the P_{SSR42} activity profile. While P_{SSR42} was nearly inactive during the first 16 h of growth P_{SSR42} activity strongly increased afterwards. **B)** Inactivation of *sae*S (NE1296) enhanced the activity of P_{SSR42} during late phases of growth. **C)** In contrast, disruption of *sae*R (NE1622) did not affect the activity of P_{SSR42}. **D)** Lack of functional two-component system ArlRS (NE1684, NE1183) resulted in an enhancement of P_{SSR42} activity starting at 16 of growth in *S. aureus* JE2. **E)** Insertional disruption of *vra*S (NE823) and *vra*R (NE554) slightly decreased the activity of P_{SSR42} **F)** as well as insertional disruption of *srr*A (NE1309) and *srr*B (NE588). **G)** Insertional disruption of fatty acid kinase encoding gene *vfr*B (NE229) resulted in an overall decrease in the activity of P_{SSR42}. Modified after Horn et al., 2018b.

4.6.3 Regulation of SSR42 by SarA-family transcriptional regulators

Besides two-component system virulence regulation in *S. aureus* is governed by members of the SarA-family of transcriptional regulators (Cheung et al., 2008). Hence, the impact of SarA, SarT, SarU and rot on regulation of SSR42 transcription was analysed (Fig. 4.47).

Insertional disruption of the genes encoding either ***sar*A** (NE1193) or ***sar*T** (NE514) did not influence the activity of P_{SSR42} in *S. aureus* strain JE2 (Fig. 4.47A). Lack of functional **SarU** (NE96) instead strongly altered the profile of P_{SSR42} activity leading to a delay in the second activity peak and resulting in a subsequently higher activity of P_{SSR42} during later time points (Fig. 4.47B), hence resembling the effects observed in mutants lacking a functional agr system (Fig. 4.46A). In contrast, insertional mutation in *rot* (NE386) revealed a minor role for **Repressor of toxins** (**Rot**) with regard to SSR42 transcription control (Fig. 4.47C). Mutants lacking functional Rot displayed a slight enhanced P_{SSR42} activity during early time points in growth (3-10 h) compared to wild-type bacteria and a subsequently reduced activity during later time points.

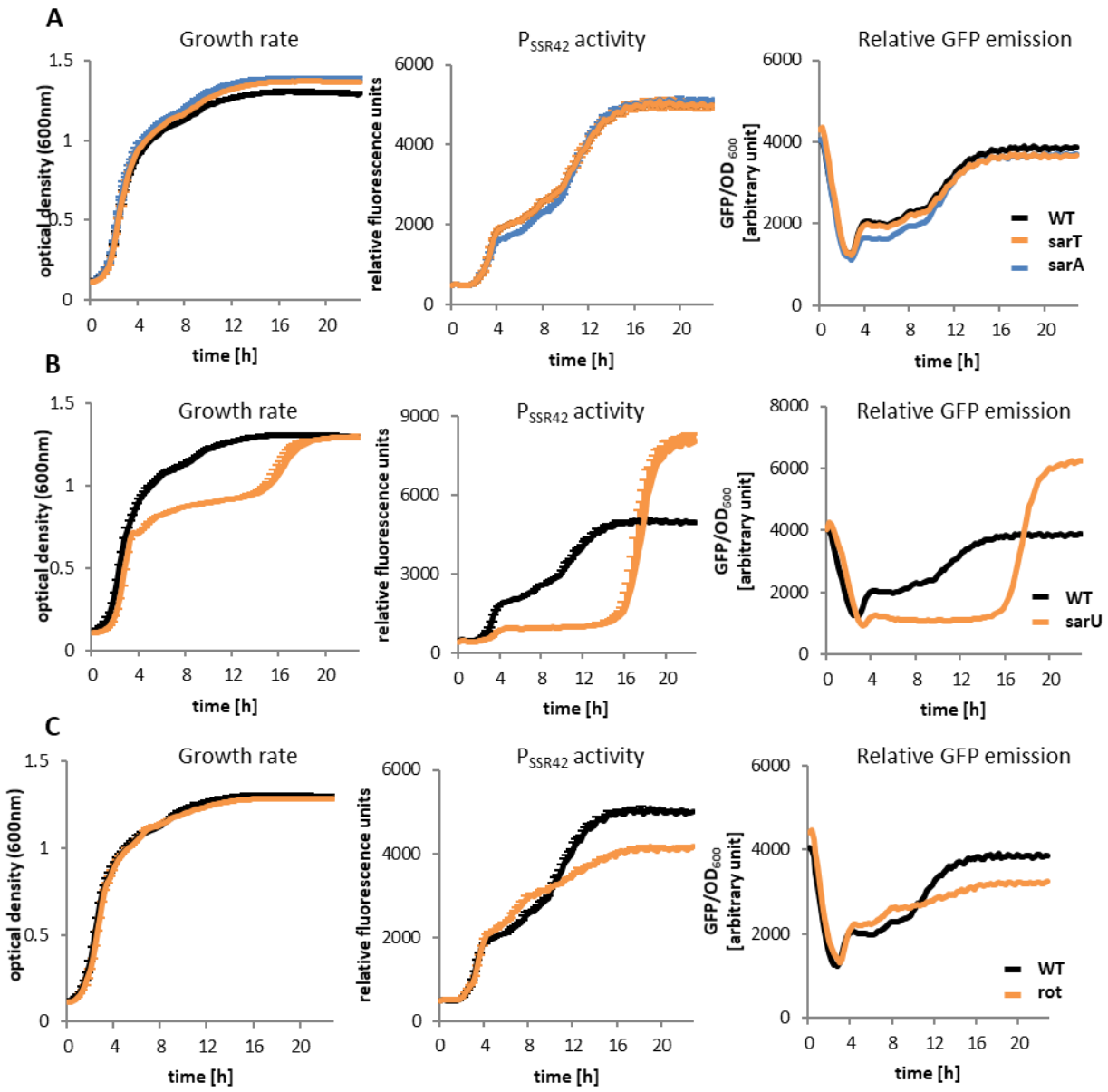

Figure 4.47: Several important SarA-family transcriptional regulators are involved in regulation of SSR42 transcription. Mutants of *S. aureus* JE2 harbouring insertions in SarA-family transcriptional regulators obtained from the NTML mutant library (Fey et al., 2013) and were used for monitoring the promotor activity of SSR42 (P_{SSR42}) in a time course of 23 h using a transcriptional fusion of SSR42 and promotorless GFP. **A)** No regulatory impact for SarA (NE1193) and SarT (NE514) on the activity of P_{SSR42} was observed. **B)** In contrats, insertional disruption of *sar*U (NE96) resulted in a similar P_{SSR42} activity profile as observed for mutants in *agr*A. **C)** Mutation in *rot* (NE386) significantly reduced the activity of P_{SSR42} during late stationary growth in *S. aureus* JE2. Modified after Horn et al., 2018b.

4.6.4 Regulation of SSR42 by alternative sigma-factors

Alternative sigma-factors are known to regulate transcription of certain genes in response to stresses (Kazmierczak et al., 2005). Thus, their impact on regulation of SSR42 transcription was chosen to be studied.

Transcription of extraplasmatic function sigma-factor (ECF) **σS** was previously reported to be inducible in response to external stresses, delivered by DNA and cell-wall damaging substances (Miller et al., 2012), thus constituting a good candidate for investigation of SSR42 regulation. Indeed, activity of P_{SSR42} was slightly reduced in a Δ*sig*S mutant (Fig. 4.48A) indicating a regulatory role for this alternative sigma-factor.

σB was reported to regulate the switch to the persisting SCV phenotype promoting survival during chronic infections (Tuchscherr et al., 2015). Since mutants lacking SSR42 were prone to form SCVs during long-term infection of EA.Hy296 cells (see chapter 4.3.5), the effect of insertional disruption of σB (encoded by *rpo*F, NE1109) on activity of P_{SSR42} was investigated. Interestingly, lack of functional σB in strain JE2 did not only reduce the activity of P_{SSR42} drastically but prevented the second rise in promotor activity completely (Fig. 4.48B). The resulting promotor activity curve in a σB mutant was comparable to that of strains such as 6850, COL and RN4220 that naturally do not display a sigmoid shaped P_{SSR42} activity. Further insertional disruption of σB-regulatory protein *rsb*U (NE1607) led to a similar P_{SSR42} activity (Fig. 4.48B) confirming the role of σB for regulation of SSR42.

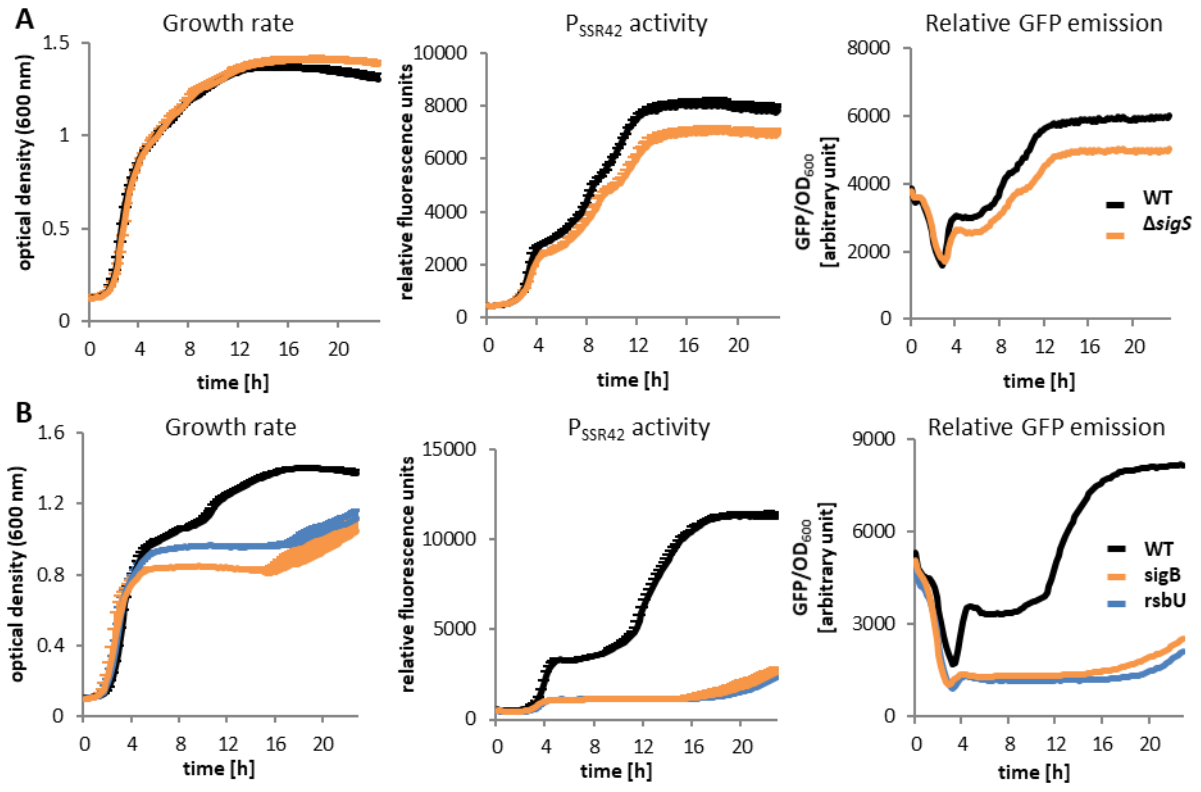

Figure 4.48: Alternative sigma-factors are involved in regulation of SSR42 transcription. A deletion mutant in Δ*sig*S and mutants of *S. aureus* JE2 harbouring insertions in *rsb*U and σB (*rpo*F), which were obtained from the NTML mutant library (Fey et al., 2013) were used for monitoring the promotor activity of SSR42 (P_{SSR42}) in a time course of 23 h using a transcriptional fusion of SSR42 and promotorless GFP. **A)** Deletion of *sig*S (Δ*sig*S) resulted in a slight decrease in P_{SSR42} activity. **B)** In contrast insertional disruption of *rpo*F (NE1109) and *rsb*U (NE1607) had a strong regulatory impact on the activity profile of P_{SSR42} resulting in a strong overall decrease. Modified after Horn et al., 2018b.

4.6.5 Regulation of SSR42 by miscellaneous regulators

Transcription of SSR42 was shown to be susceptible to the availability of glucose (see chapter 4.5.4) revealing a potential regulatory connection between the metabolism and virulence regulation. This connecting virulence is governed by factors such as RpiRc, CodY and CcpE. Hence, the impact of those regulators on the activity of P_{SSR42} was analysed (Fig. 4.49).

Knockout of transcriptional regulator **RpiRc** (Δ*rpi*Rc) strongly reduced the activity of P_{SSR42} to approximately 50% of wild-type activity (Fig. 4.49A). Further, the second activity peak of P_{SSR42} was hardly detectable in mutants lacking *rpi*Rc.

CodY represents another major regulatory protein linking metabolism of *S. aureus* to virulence regulation and serves mainly as a repressor of virulence genes (Majerczyk et al., 2010; Pohl et al., 2009). Insertional disruption of *cod*Y (NE1555) resulted in a drastically reduced activity of P_{SSR42} characterized by an absence of a second activity peak (Fig. 4.49B) comparable to mutants lacking functional σB (Fig. 4.48B). Due to the observed regulatory role for CodY on SSR42 transcription, the connection of CodY and the stringent response (Geiger et al., 2012), the activity of P_{SSR42} was analysed in a triple knockout mutant lacking *rsh*, *relp* and *relq* (Δ*rsh*Δ*relp*Δ*relq*; Fig. 4.49C). Knockout of those alarmone producing genes did not lead to significant changes in the activity of P_{SSR42} ruling out a potential effect of stringent response on the transcription of SSR42.

A third linkage between virulence gene regulation and metabolism represents catabolite control protein **CcpE.** It has been demonstrated that in presence of glucose CcpE represses virulence associated genes such as RNAIII, *cap*A, *hla* and TCA cycle genes (Hartmann et al., 2014; Ding et al., 2014). Activity of P_{SSR42} was analysed in a mutant lacking functional CcpE (NE1560; Fig. 4.49D) and found to be highly similar to that of mutants lacking functional CodY or σB which also lack the second activity peak in P_{SSR42} activity.

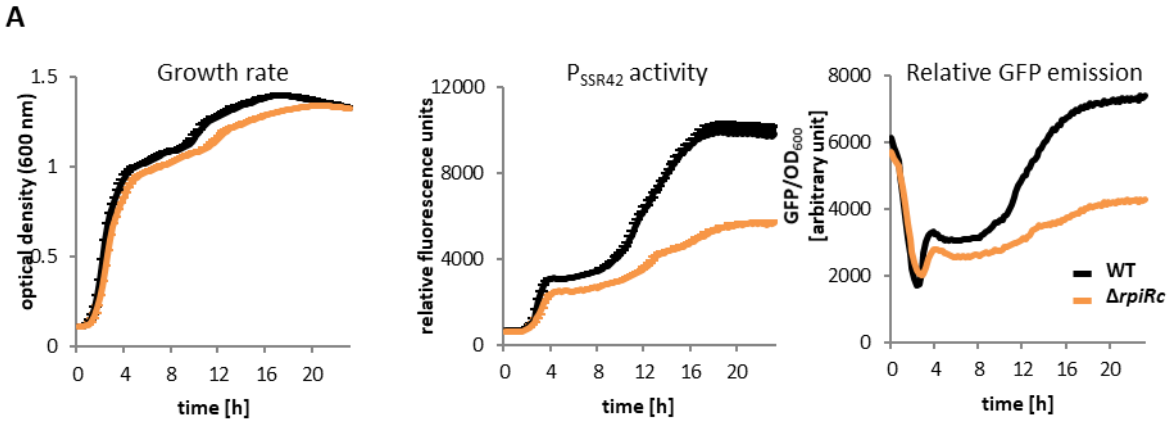

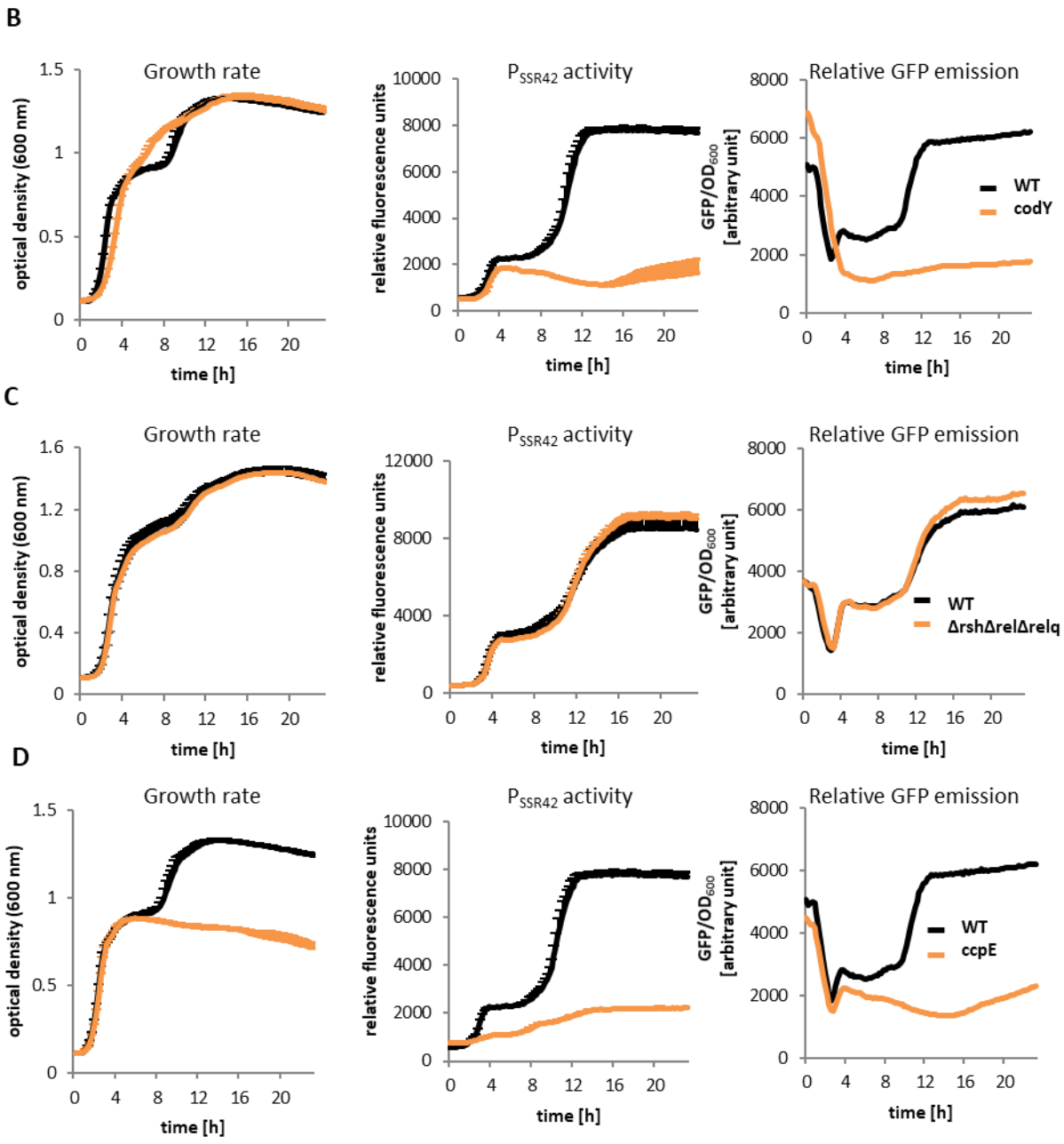

Figure 4.49: Various metabolite-responsive regulators affect the activity of P_{SSR42}. Deletion mutants Δ*rpiRc* and Δ*rsh*Δ*relp*Δ*relq* and insertional mutants in *cod*Y and *ccp*E of *S. aureus* JE2 which were obtained from the NTML mutant library (Fey et al., 2013) were used for monitoring the promotor activity of SSR42 (P_{SSR42}) in a time course of 23 h using a transcriptional fusion of SSR42 and promotorless GFP. **A)** Lack of *rpi*Rc resulted in a strong decrease in P_{SSR42} activity. **B)** Insertional disruption *cod*Y (NE1555) in contrast reduced the activity of P_{SSR42} even more drastic. **C)** P_{SSR42} activity in triple knockout mutant Δ*rsh*Δ*relp*Δ*relq* was not alterted. **D)** Insertional mutation in *ccp*E (NE1560) affected the activity of P_{SSR42} in a similar way than mutation in *cod*Y. Modified after Horn et al., 2018b.

The eukaryotic-like serine/ threonine kinase **PknB** is involved in resistance towards β-lactam antibiotics with mutants exhibiting a higher sensitivity (Tamber et al., 2010). Hence, the activity of P_{SSR42} was

investigated in an insertional mutant in *pkn*B (NE217). Insertional disruption of *pkn*B resulted in a reduced P_{SSR42} activity approximately 11 h after inoculation of bacteria (Fig. 4.50A). Subsequently, P_{SSR42} activity reached wild-type levels at later time points (approximately 17 h) indicating role for PknB in regulation of SSR42 during early time points of growth.

Virulence regulation in *S. aureus* is further executed by endoribonucleases. **RNase Y** displays a major role in initiating the degradation of hundred mRNA species and a few small non-coding RNAs (Khemici et al., 2015; Marincola et al., 2012). ncRNA SSR42 has been identified in a global EMOTE screen to be potentially processed by RNase Y, which was further analysed in this study using Northern blots (Fig. 4.5). Thus, activity of P_{SSR42} was analysed in a knockout mutant lacking *rny* (Fig. 4.50B). Comparing the SSR42 promotor activity profiles of Δ*rny* and wild-type bacteria revealed no significant differences indicating no regulatory role for RNase Y on transcription of ncRNA SSR42.

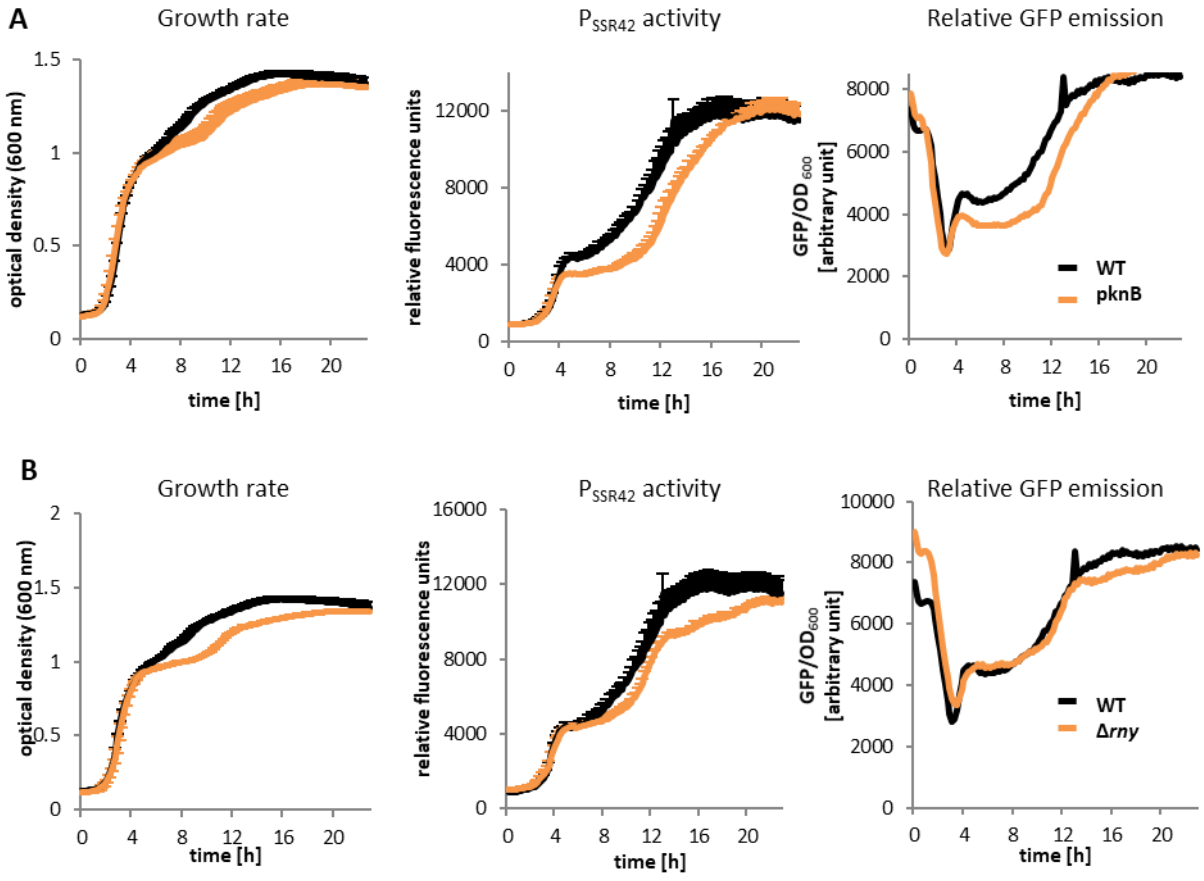

Figure 4.50: Mutation in *pkn*B but not deletion of *rny* affects the activity of P_{SSR42}. Deletion mutant Δ*rny* and an insertional mutant in *pkn*B of *S. aureus* JE2, which was obtained from the NTML mutant library (Fey et al., 2013) were used for monitoring the promotor activity of SSR42 (P_{SSR42}) in a time course of 23 h using a transcriptional fusion of SSR42 and promotorless GFP. **A)** Insertional disruption of *pkn*B (NE217) decreased the activity of P_{SSR42} between 4 and 16 h of growth of *S. aureus* JE2. **B)** Lack of RNase Y instead affected the activity of P_{SSR42} only slightly. Modified after Horn et al., 2018b.

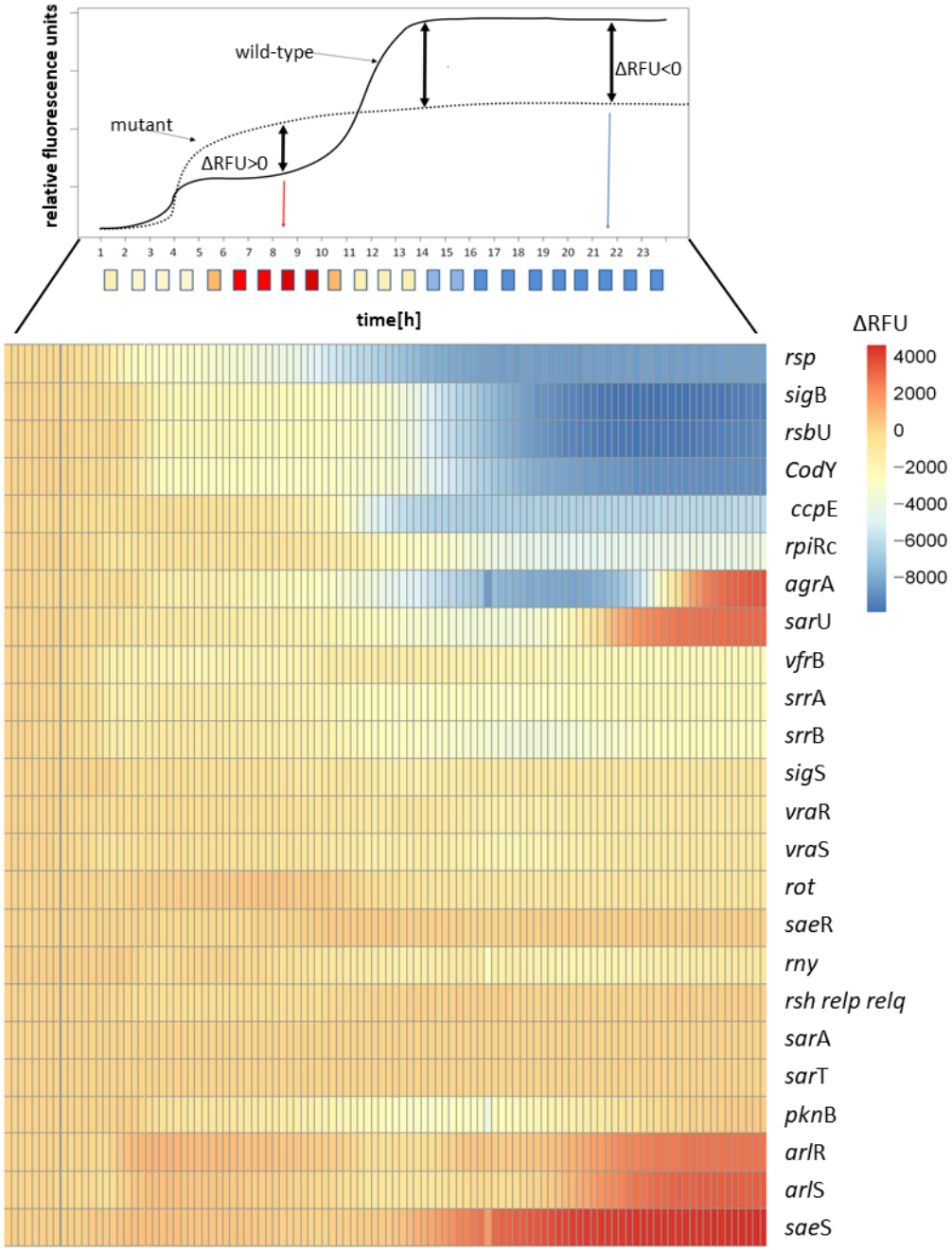

Figure 4.51: Summary of the impact of various global regulators on transcription of SSR42. Heatmap summarizing the factors affecting P*SSR42* activity compared to the activity of *S. aureus* JE2 wild-type. Differences in the P_{SSR42} activity (ΔRFU) are illustrated by a colour code (modified after Horn et al., 2018b, constructed by Maximilian Klepsch, University Würzburg).

Verifying the previous findings transcript levels of ncRNA SSR42 were analysed in some of the tested mutants (Fig. 4.52). While for mutants in *agr*A, *vra*R, *srr*B, *sar*U, *sig*S, *rpo*F, *ccp*E and *pkn*B SSR42 transcript levels were significantly decreased compared to wild-type bacteria at 15 h of growth, for mutants in *cod*Y and *rpi*Rc no significant differences in SSR42 transcript levels were detected (Fig. 4.52A), despite a previous observed lower activity of P_{SSR42} during that time point of growth. Since the promotor activity curve indicated an up-regulation of P_{SSR42} activity in the *agr*A mutant during late time points in growth, bacteria were harvested after 23 h of growth and SSR42 transcript levels were compared to that of an earlier time point (15 h). After 23 h of growth SSR42 transcript levels in an insertional mutant in *agr*A were significantly increased when compared to the transcript levels of the earlier time point (15 h; Fig. 4.52B). However, they did not differ significantly when compared to SSR42 transcript levels in wild-type bacteria.

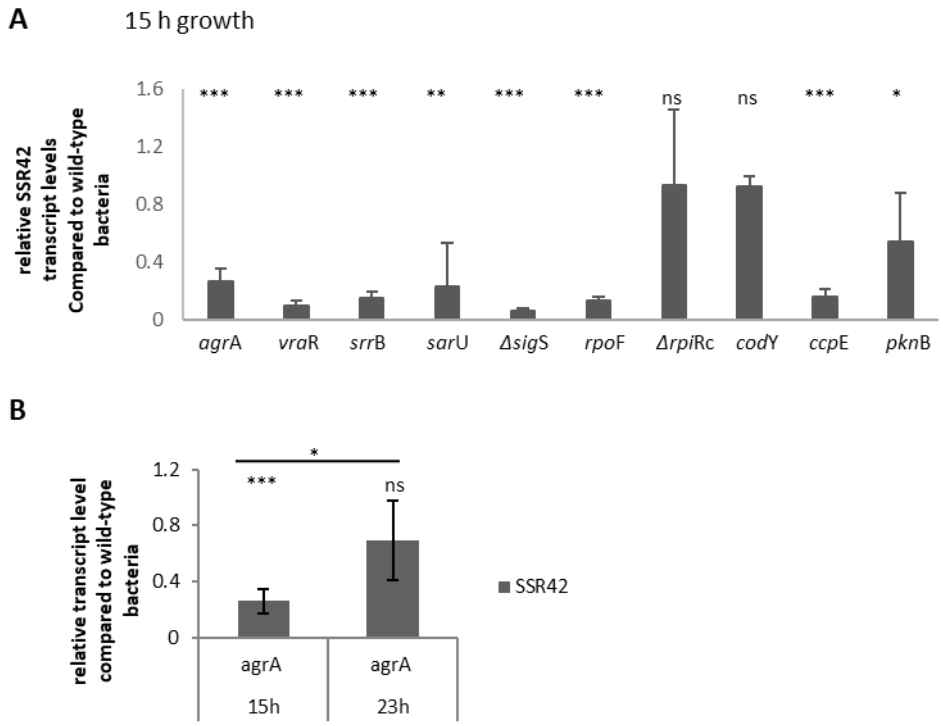

Figure 4.52: Analysis of SSR42 transcript levels in various mutants in global regulators. A) Quantitative real time PCR analysis of SSR42 transcript levels of stationary phase *S. aureus* JE2 (15 h of growth) and various insertional mutants and *sig*S and *rpi*Rc deletion mutants. Insertional mutants were obtained from the NTML library (Fey et al., 2013). Modified after Horn et al., 2018b. **B)** SSR42 transcript levels were significantly increased during late stationary growth phase (23 h) compared to during 15 h of growth in *S. aureus* JE2 harbouring an insertional mutation in *agr*A (NE1532). Statistical analysis was performed using Student´s t-test: *: p< 0.05; ***: p< 0.001.

4.6.6 Regulation of *rsp* transcription

The essential role of Rsp for transcription of SSR42 lead to the hypothesis that the previously observed factors regulating the promotor activity of SSR42 could already act via regulation of Rsp. Thus, the activity of the promotor operating *rsp* transcription (P_{rsp}) was analysed in some of the previous tested mutants using transcriptional fusion of P_{rsp} and GFP. The obtained data is summarized in a heatmap resulting from comparison of P_{rsp} activity in wild-type bacteria and mutants (Fig. 4.53, heatmap was constrcted by Maximilian Klepsch, University Würzburg).

While mutation in some of the tested regulators (*rpi*Rc, *ccp*E, *agr*A, *cod*Y, *arl*R) had a similar effect on *rsp* promotor activity, mutants in *vfr*B, *srr*AB, *rsb*U and *sae*S showed no, respectively opposite effects on P_{rsp} than on P_{SSR42} activity (Fig. 4.54) indicating that those factors possibly regulate SSR42 promotor activity by other means than by regulating *rsp* transcription.

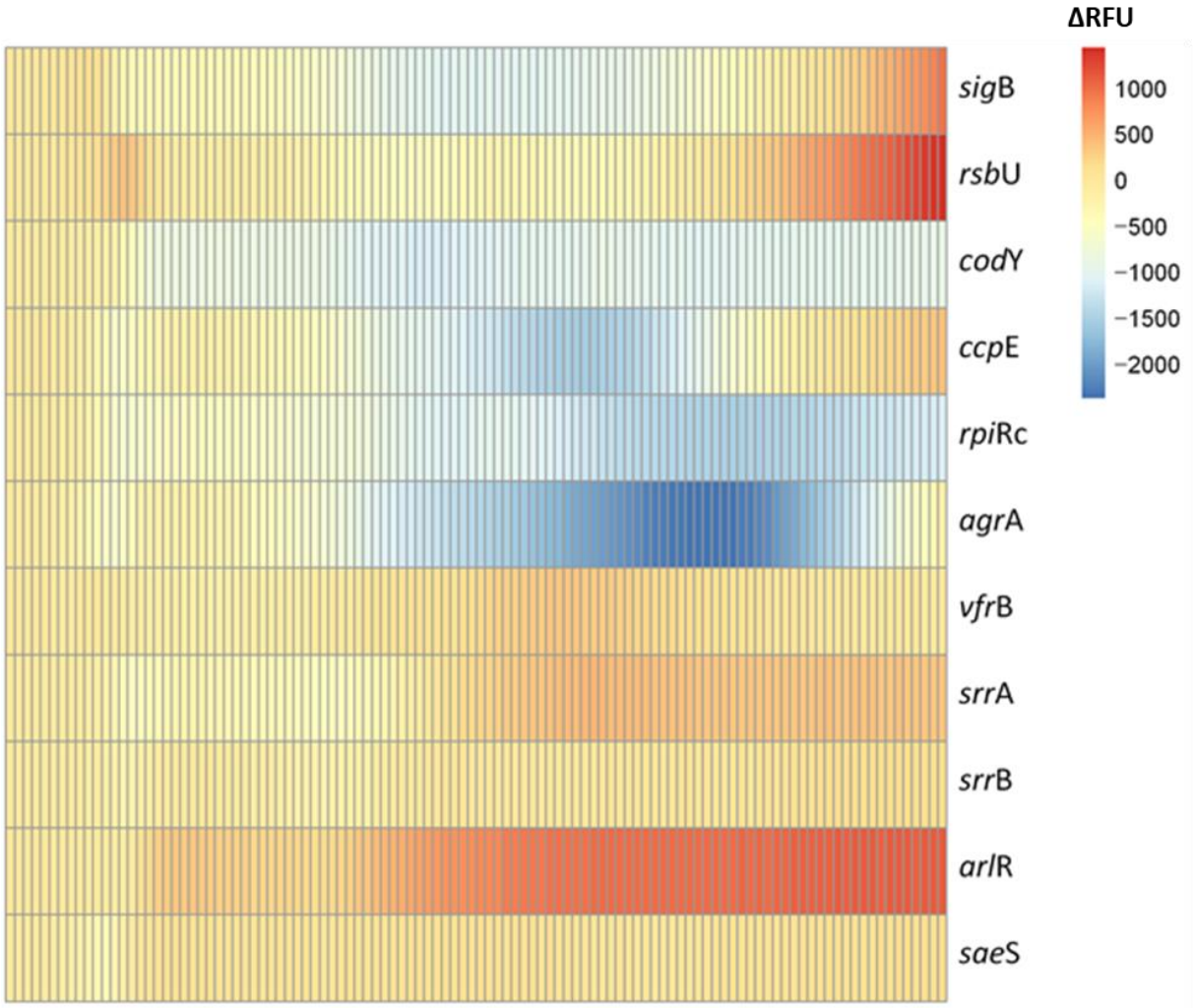

Figure 4.53: Summary of the impact of various global regulators on transcription of *rsp*. Summary of factors affecting P_{rsp} activity compared to the activity of wild-type *S. aureus* JE2 illustrated in a heatmap. Differences in the P_{rsp} activity (ΔRFU) are illustrated by a colour code (modified from Horn et al., 2018b, constructed by Maximilian Klepsch, University Würzburg).

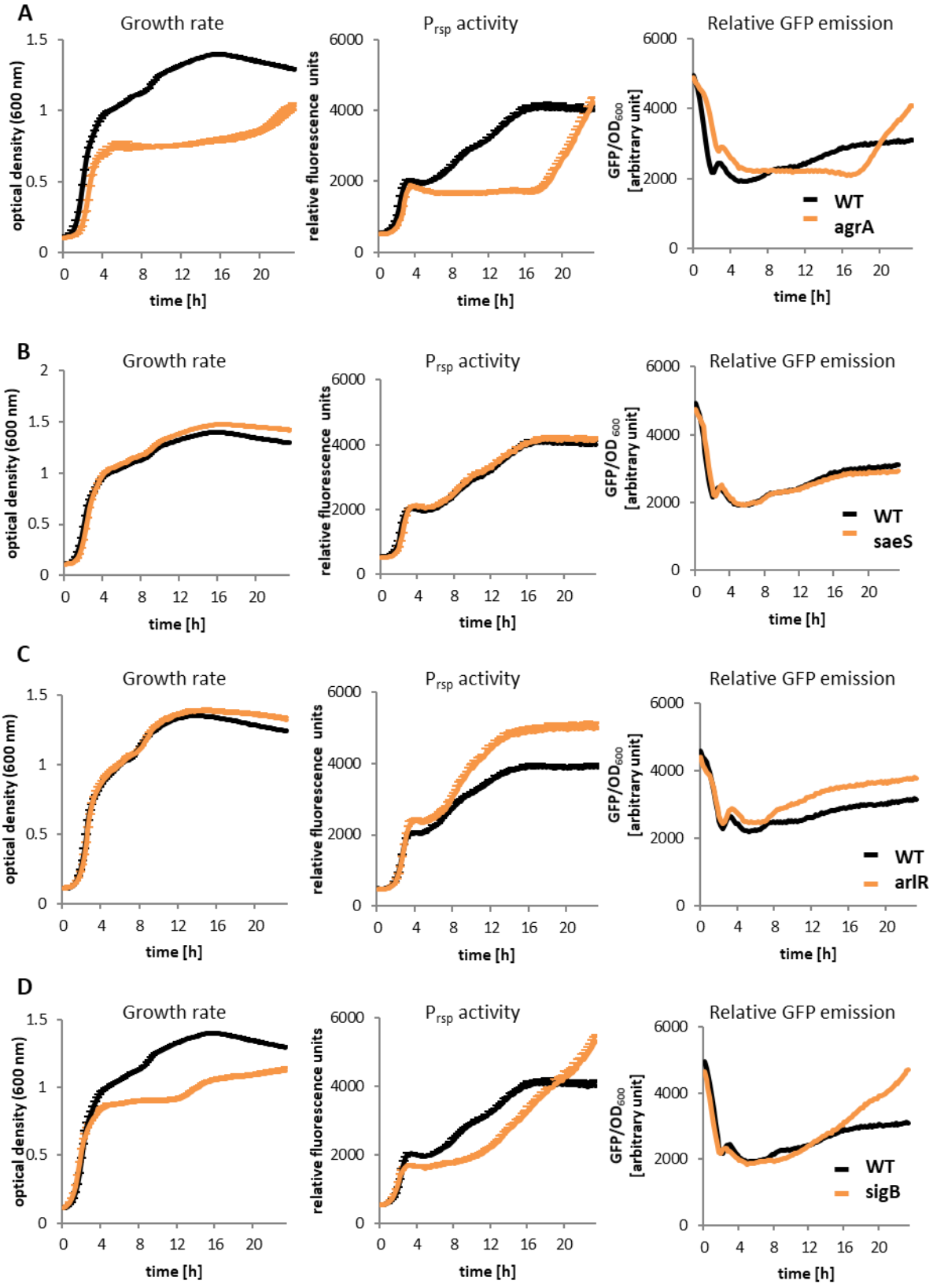
A
Growth rate
optical density (600 nm)
time [h]
P rsp activity
relative fluorescence units
time [h]
Relative GFP emission
GFP/OD600 [arbitrary unit]
time [h]
WT
agrA
B
Growth rate
optical density (600 nm)
time [h]
P rsp activity
relative fluorescence units
time [h]
Relative GFP emission
GFP/OD 600 [arbitrary unit]
time [h]
WT
saeS
C
Growth rate
optical density (600 nm)
time [h]
P rsp activity
relative fluorescence units
time [h]
Relative GFP emission
GFP/OD600 [arbitrary unit]
time [h]
WT
arlR
D
Growth rate
optical density (600 nm)
time [h]
P rsp activity
relative fluorescence units
time [h]
Relative GFP emission
GFP/OD600 [arbitrary unit]
time [h]
WT
sigB

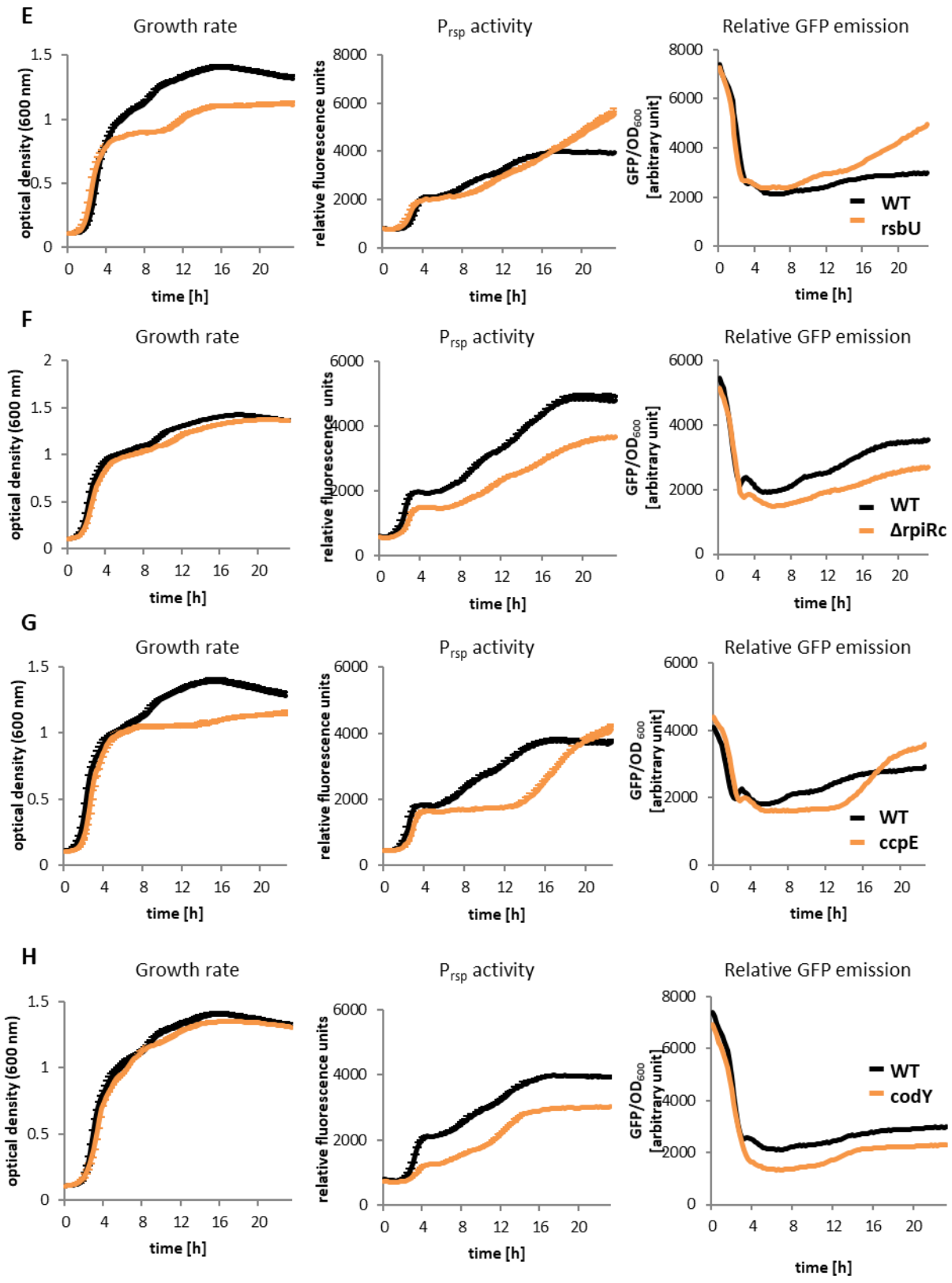
E
Growth rate
optical density (600 nm)
time [h]
P rsp activity
relative fluorescence units
time [h]
Relative GFP emission
GFP/OD600 [arbitrary unit]
time [h]
WT
rsbU
F
Growth rate
optical density (600 nm)
time [h]
P rsp activity
relative fluorescence units
time [h]
Relative GFP emission
GFP/OD600 [arbitrary unit]
time [h]
WT
ΔrpiRc
G
Growth rate
optical density (600 nm)
time [h]
P rsp activity
relative fluorescence units
time [h]
Relative GFP emission
GFP/OD 600 [arbitrary unit]
time [h]
WT
ccpE
H
Growth rate
optical density (600 nm)
time [h]
P rsp activity
relative fluorescence units
time [h]
Relative GFP emission
GFP/OD600 [arbitrary unit]
time [h]
WT
codY

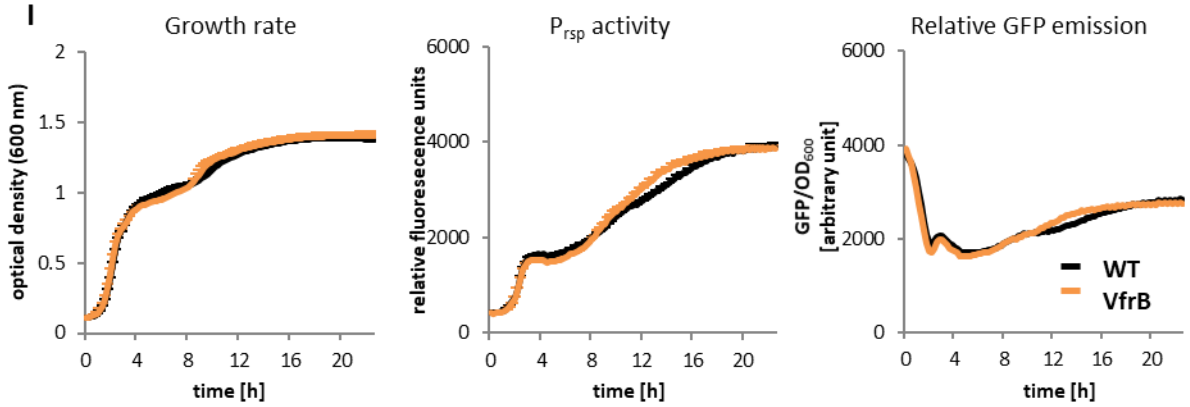

Figure 4.54: Various regulators affect the activity of P_{rsp}. Insertional mutants of *S. aureus* JE2 in regulators were obtained from the NTML mutant library (Fey et al., 2013) and were used for monitoring the promotor activity of rsp (P_{rsp}) in a time course of 23 h using a transcriptional fusion of *rsp* and promotorless GFP. Growth curve was measured in parallel and GFP fluoresence was normalized to growth of the bacteria (GFP/OD_{600}). **A)** Insertional disruption of *agr*A (NE1532) affected the activity of P_{rsp} during late stationary growth phase of *S. aureus* JE2. **B)** In contrats disruption of *sae*S (NE1296) did not affect the activity of P_{rsp}. **C)** Disruption of *arl*R (1684) resulted in an increase in the activity of P_{rsp}. **D)** Lack of functional σB (*rpo*F; NE1109) resulted in a slight increase in P_{rsp} activity during late stationary growth phase. **E)** Similarly, insertional disruption of *rsb*U (NE1607) resulted in a similar P_{rsp} profile. **F)** Knockout of *rpi*Rc decreased the activity of P_{rsp} mainly during stationary growth phase of *S. aureus* JE2. **G)** Insertional mutation in *ccp*E (NE1560) decreased the activity of P_{rsp} and resulted in an enhanced activity during late stationary growth phase. **H)** A regulatory impact of CodY on the activity of P_{rsp} was observed with mutants in *cod*Y (NE1555) displaying reduced P_{rsp} activity. **I)** In contrast, no regulatory role for VfrB on transcription of *rsp* was observed in insertional mutants in *vfr*B (NE229). Modified after Horn et al., 2018b.

4.7 Molecular characterization of ncRNA SSR42

ncRNA SSR42 was demonstrated to display a versatile role for *S. aureus´* virulence regulating haemolysis, host cell death, biofilm and SCV formation. However, the regulatory mechanism remains elusive. Analysing functional domains of SSR42 identified a region essential for haemolysis regulation and two stabilizing domains. Potential interaction partners of ncRNA SSR42 were identified via gradient sequencing and interaction predictions.

4.7.1 Identification of stabilizing and functional regions in ncRNA SSR42

For characterization of stabilizing or functional domains within SSR42 small, approximately 70 nt long sequences were deleted from the sequence of SSR42 and introduced into *S. aureus* 6850 ΔSSR42 via modified versions of complementation plasmid pSSR42 (Fig. 4.55A-B, see Appendix Fig. 7.10). The resulting complemented mutants were screened for haemolysis defects using an erythrocyte lysis assay and compared to the complemented mutant expressing wild-type SSR42 in trans (Fig. 4.55C).

Three out of the eight mutants displayed signififcantly reduced haemolytic activities when compared to the haemolytic activity of the complemented mutant expressing wild-type SSR42. Deletion of a 76 nt region (Δ1; 2,352,023-2,352,099 bp) resulted in significantly reduced haemolysis to 75.52% (p>0.001). Deletion of a 63 nt region (Δ6; 2,352,688-2,352,742 bp) and a 65 nt deletion (Δ7; 2,352,858-2,352,794 bp) spanning the previously identified potential 5'-end of 891 nt SSR42 (Morrison et al., 2012a) was further found to influence the haemolytic activity of *S. aureus* (Δ6: 42.6%, p>0.001; Δ7: 43.72%, p=0.003). Interestingly, deletion of a 62 nt region upstream of the predicted RNase Y cleavage site (Δ8; 2,352,917-2,352,978 bp) did not affect haemolysis. Analysis of transcript levels of SSR42 via Northern blotting revealed a strong reduction of SSR42 transcripts in mutant Δ6 and an accumulation of SSR42 degradation products in mutant Δ7 (Fig. 4.55C). Instead, transcript levels of full-length SSR42 and smaller transcripts were detected at a similar level in mutant Δ1 compared to the levels in the control strain (Fig. 4.55C). The reduced SSR42 transcript levels and the accumulation of degradation products in mutants Δ6 and Δ7 indicated that those regions are most likely involved in stabilization and processing of SSR42, whereas region Δ1 is involved in regulation of haemolysis.

To investigate whether region Δ1 (2,352,023-2,352,099 bp) would be sufficient to restore haemolysis in a ΔSSR42 mutant the stem loop structure encompassing this region was introduced in trans (pStemLoop2; Fig. 4.55D). Using Northern blotting SSR42 transcripts could not be detected in the mutant expressing the stem loop structure in trans (data not shown). Transcript levels of both SSR42 (RT-PCR oligonucleotides: pSL2 RT F and pSL2 RT R; FC: 0.061; p>0.001) and *hla* (FC: 0.22; p>0.001) were significantly reduced when only this certain stem loop structure of SSR42 was reintroduced in trans. Yet, compared to the expression levels in a ΔSSR42 mutant SSR42 and *hla* transcript levels were significantly enriched (SSR42: p=0.0061; hla: p=0.047). Hence, it was concluded that this specific stem loop structure has to be rather unstable, explaining the extremely reduced SSR42 transcript levels. *hla* transcript levels were subsequently reduced due the unsuccessful complementation. Thus, expression of only this certain stem loop structure (Stem loop2: 2,352,023-2,352,099 bp) of SSR42 was not sufficient to restore haemolysis in a ΔSSR42 mutant.

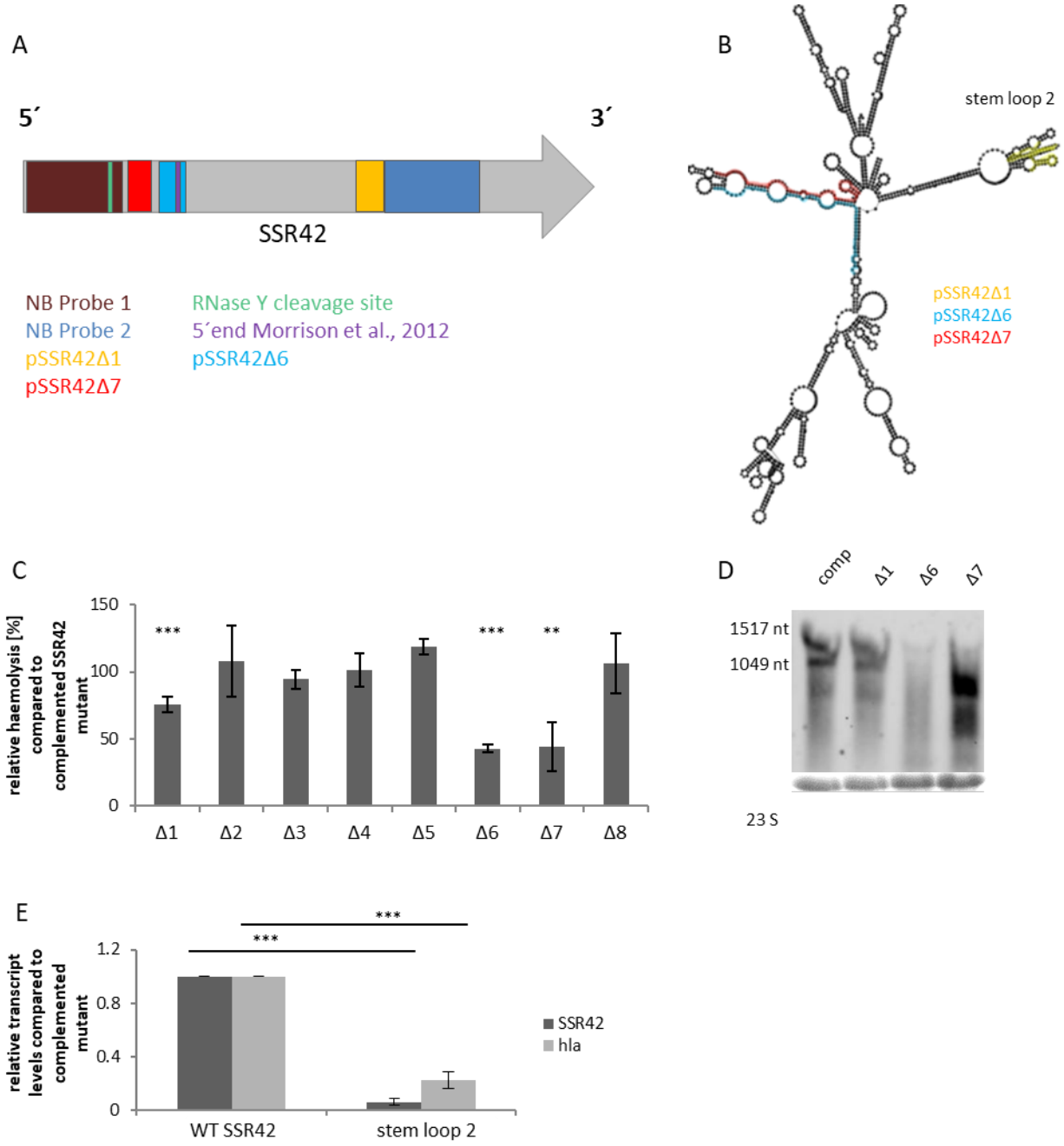

Figure 4.55: Mutational analysis of SSR42 identified three domains implicated in stabilization of ncRNA SSR42 and haemolysis regulation. A) Schematic representation of the SSR42 sequence. Highlighted are regions addressed in mutational analysis. **B)** Schematic illustration of the predicted secondary structure of SSR42 with highlighted regions affecting stability and haemolysis regulation. **C)** Three regions in SSR42 were identified affecting the haemolytic activity of *S. aureus* 6850. Sheep erythrocytes were challenged with stationary culture supernatants from *S. aureus* 6850 expressing wild-type SSR42 and various mutated versions of SSR42. Deletion of region 1, 6 and 7 affected the haemolytic activity significantly. **D)** Deletion of region 6 and 7 altered the SSR42 transcript level in *S. aureus* 6850 as observed by Northern blot analysis. **E)** Expression of only a stem loop structure of SSR42 encompassing region Δ1 was not sufficient to restore SSR42 and *hla* transcription in *S. aureus* 6850 ΔSSR42 as observed by qRT-PCR analysis. Statistical analysis was performed using Student´s t-test: *: p< 0.05; ***: p< 0.001.

4.7.2 Construction of minimal versions of ncRNA SSR42

Introducing small mutations in SSR42 revealed a broad sequence range within SSR42, which was not implicated in haemolysis regulation. This region was further addressed by creation of minimal versions of SSR42. These minimal ncRNAs were constructed since complementation of only a stem loop structure of SSR42 (2,352,023-2,352,099 bp) was not sufficient for restoring haemolysis and indicated the necessity of additional sequence parts for stabilization of SSR42.

Two minimal versions of SSR42 (mini-1, mini-2) were therefore constructed spanning the previously identified regions implicated in stabilization and haemolysis regulation (Δ1: 2,52,023-2,352,099 bp; Δ6: 2,352,688-2,352,742 bp and Δ7: 2,352,858-2,352,794 bp; Fig. 4.56, see Appendix Fig. 7.11). For creation of minimal SSR42 version 1 (mini-1) a 795 nt sequence of SSR42 was introduced into *S. aureus* 6850 ΔSSR42 via complementation plasmid pSSR42_mini-1, which resulted from deleting a 437 nt sequence (bp 2,351,972-2,352,410) from the original complementation plasmid pSSR42. A second SSR42 deletion version (mini-2) was constructed by deleting an additional 128 nt region at the 5'-region of SSR42(bp 2,353,043-2,352,915 bp) that included the predicted RNase Y cleavage site (Khemici et al., 2015) creating a 668 nt long RNA molecule. Both resulting sequences were analysed with RNAfold (Fig. 4.56A). Prediction confirmed the conversation of the previous observed potential secondary structure characteristics of full-length SSR42. The resulting plasmids were introduced in *S. aureus* 6850 ΔSSR42 and the haemolytic activity of the supernatants obtained from those mutants was analysed (Fig. 4.56C). The haemolytic activities were compared to ΔSSR42 complemented in trans with wild-type SSR42. Complementation with either of both minimal SSR42 versions failed to recover the haemolytic activity of culture supernatants to wild-type levels. Complementation with minimal version 1 partially restored haemolysis in a ΔSSR42 mutant (75.64%, $p>0.001$). In contrast, haemolysis could not be restored when minimal SSR42 version 2 was used for complementation (33.71%, $p>0.001$). Expression of both minimal SSR42 molecules was analysed via Norther blotting (Fig. 4.56D). While transcript levels of wild-type SSR42 and minimal version 1 were detected at comparable amounts minimal SSR42 version 2 could not be detected, indicating a high instability of this RNA molecule. The failure to restore haemolysis using minimal SSR42 version 2 thus resulted from the drastically reduced SSR42 transcript levels most likely caused by a reduced stability of the RNA molecule. Instead, expression of mini-1 partially restored the haemolytic activities and SSR42 transcript levels were found at similar amounts compared to full-length SSR42, thus indicating that additional sequence parts are necessary for a complete recovery of a wild-type haemolytic potential.

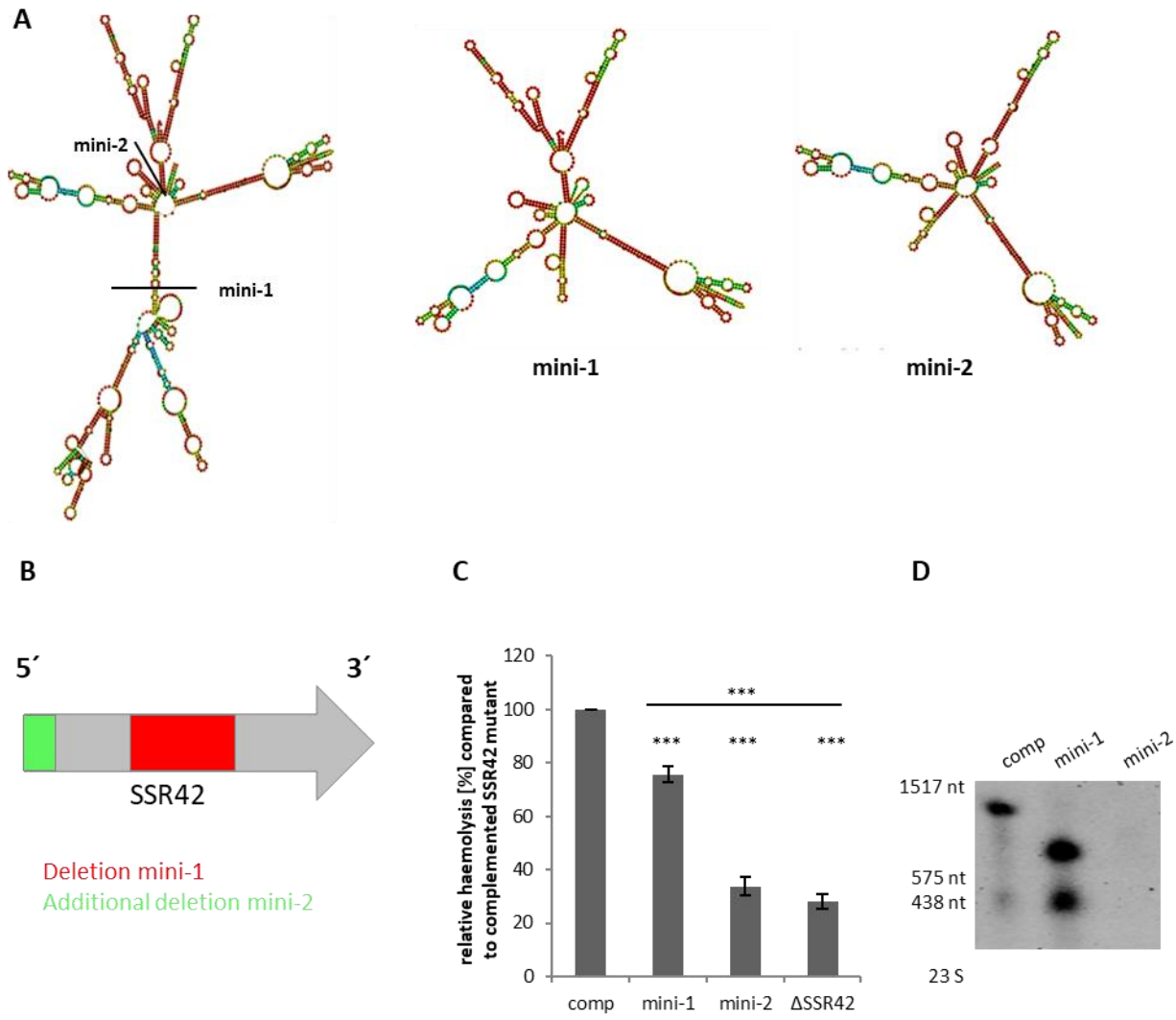

Figure 4.56: Construction and functional analysis of minimal versions of SSR42. A) Schematic representation of the secondary structure of SSR42 (left panel) and of minimal SSR42 versions 1 (middle panel) and version 2 (right panel). **B)** Illustration of deleted regions for creation of minimal version 1 and 2 within the sequence of SSR42. **C)** Haemolytic activity of *S. aureus* 6850 ΔSSR42 is partially restored by introducing minimal SSR42 version 1. Introduction of minimal version 2 did not restore haemolysis in *S. aureus* ΔSSR42 as observed by treating sheep erythrocytes with stationary culture supernatants of *S. aureus* 6850 expressing either wild-type SSR42, minimal SSR42 versions 1 or 2 and a ΔSSR42 mutant. Statistical analysis was performed using Student´s t-test: *: p< 0.05; ***: p< 0.001. **D)** SSR42 transcript levels of minimal SSR42 version 2 were not detectable in *S. aureus* 6850 using Northern blot analysis.

4.7.3 Analysis of implication of putative ORF 3 in haemolysis regulation

A previous study addressing SSR42 already analysed a potential role of the predicted putative ORFs within SSR42. In this study no role for those described putative ORFs regarding haemolysis regulation was found (Morrison et al., 2012a). However, due to the underestimation of the length of SSR42 some ORFs were missed in that study. Prediction of ORFs revealed a rather long putative ORF of 123 nt length (ORF 3, see section 4.1.4). Due to the length of this putative ORF a potential implication in haemolysis

regulation can not be excluded. Therefore, the start codon of this putative ORF was mutated (TTG → TCG), thereby preventing transcription (Fig. 4.57, see Appendix Fig. 7.12). This mutated SSR42 sequence was introduced in trans in a ΔSSR42 mutant via a modified version of complementation plasmid pSSR42-rsp. Analysing the haemolytic activity of supernatants obtained from *S. aureus* 6850 ΔSSR42 complemented either with wild-type SSR42 or with SSR42 harbouring the mutation in the putative start codon revealed no significant differences between the two tested groups (Fig. 4.57B). Thus, a potential peptide encoded by ORF 3 would not affect haemolysis regulation.

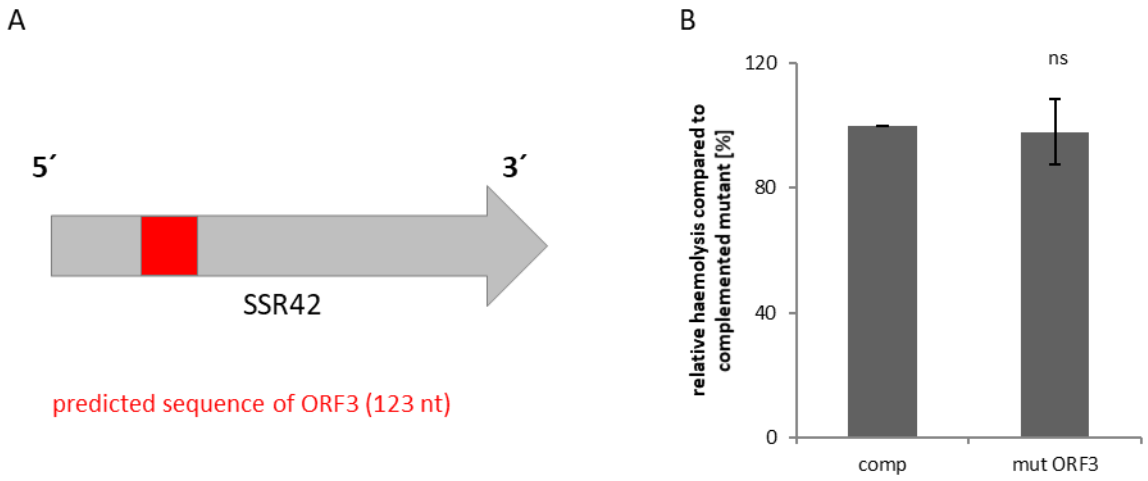

Figure 4.57: Predicted open reading frame 3 within SSR42 is not required for regulation of haemolysis in *S. aureus* 6850. A) Schematic representation of SSR42 with highlighted predicted ORF 3. **B)** Mutation of ORF 3 within SSR42 did not affect haemolysis in *S. aureus* 6850 as demonstrated by an erythrocyte lysis assay. Sheep erythrocytes were treated with stationary phase culture supernatants of *S. aureus* 6850 expressing wild-type SSR42 and SSR42 harbouring a mutation within the start codon of ORF 3 preventing potential translation. Haemolytic activity of *S. aureus* ΔSSR42 complemented with wild-type SSR42 was set to 100%. Statistical analysis was performed using Student´s t-test: *: p< 0.05; ***: p< 0.001.

4.8 Attempt to decipher the regulatory mechanism of ncRNA SSR42

4.8.1 Identifying potential interaction partners of SSR42 via Grad-seq

Identifying potential interaction partners of SSR42 could pioneer the decryption of a regulatory mechanism and serve as a further validation for the previously observed regulatory impact of SSR42. Gradient profiling by sequencing (Grad-seq) was recently established to draft RNA landscapes in a global approach. Exploiting physical properties of shared RNA-protein interactions this method enables the partitioning of RNAs into diverse groups. Grad-seq facilitates the grouping of RNAs with likely similar function into collectives. Thereby, common protein partners can be identified (Smirnov et al., 2016). Grad-seq is based on a sedimentation of RNAs and proteins in a glycerol gradient. In the glycerol

gradient complexes are sorted by size and shape. The resulting different sedimentation behaviours are used to assess potential interaction of RNAs and proteins. However, the appearance of two RNAs or an RNA and protein in the same glycerol fraction does not necessarily result from a direct interaction but from interaction with a common RNA-binding protein or a similar size and shape of complexes. Using gradient profiling by sequencing an RNA interactome for *S. aureus* was created according to the sedimentation coefficient of RNA complexes. For this, t-SNE two-component analysis was applied. Grad-Seq was performed in collaboration with Alexandr Smirnov and Konrad Förstner in *S. aureus* HG003 (Fig. 4.58). According to the sedimentation coefficient of RNA complexes an interactome of all RNAs of *S. aureus* was generated using t-SNE two-component analysis (Fig. 4.58A). t-SNE two-component analysis revealed a distinct cluster for non-coding RNAs including RNAIII, SprD, RsaF, RsaH, RsaE, RsaA, RNase P, SSR42, 6S rRNA, srrA, RsaOG, RsaI and ffh indicating the interaction with potential common RNA-binding proteins. Further, tRNAs were detected in this cluster.

Sequence reads of SSR42 were detected over a wide fraction range and found to be most abundant in fraction 2 and 9 (Fig. 4.58B). While appearance in fraction 2 could indicate free and not interacting SSR42 molecules or RNA-RNA interactions, the appearance in fraction 9 indicates an interaction with proteins. SSR42 reads were only detected in a low amount in the pellet fraction. Appearance of a factor in the last or pellet fraction is associated with interaction with high molecular weight complexes such as ribosomes. A low abundance of sequence reads from the pellet fraction is thus distinctive for ncRNAs. Using correlation calculations (pearson correlation) potential RNA interaction partners of SSR42 were predicted. For this, the pattern of detected sequence reads of SSR42 in the gradient fractions was compared to the pattern of all other detected RNAs. Thus, a high correlation coefficient results from a high resemblance to the sequence read profile of SSR42. The results of RNAs with very high correlation are listed in table 4.12. Among the RNAs with high correlation to the Grad-seq profile of SSR42 also several previously detected targets of SSR42 were found. mRNAs of *esxa* (pearson correlation coefficient: 0.91), *chs* (pearson correlation coefficient: sense: 0.62; antisense: 0.69), *clfA* (pearson correlation coefficient: 0.96) and *atl* (pearson correlation coefficient: 0.89) displayed a high correlation with the Grad-seq profile of SSR42 (table 4.13). Grad-seq profiling of cellular proteins could not be performed due to degradation of the samples. Since Grad-Seq displays the physical properties of RNA-RNA and RNA-protein complexes but not necessarily reveals direct interaction of two RNA molecules, direct interaction partners were sought to be identified using a RNA-pulldown. However, neither MS2-pulldown nor an Oligo-capture approach provided an insight into interaction partners of SSR42 since the establishment of both methods failed in *S. aureus* (see Appendix Fig. 7.5, 7.6).

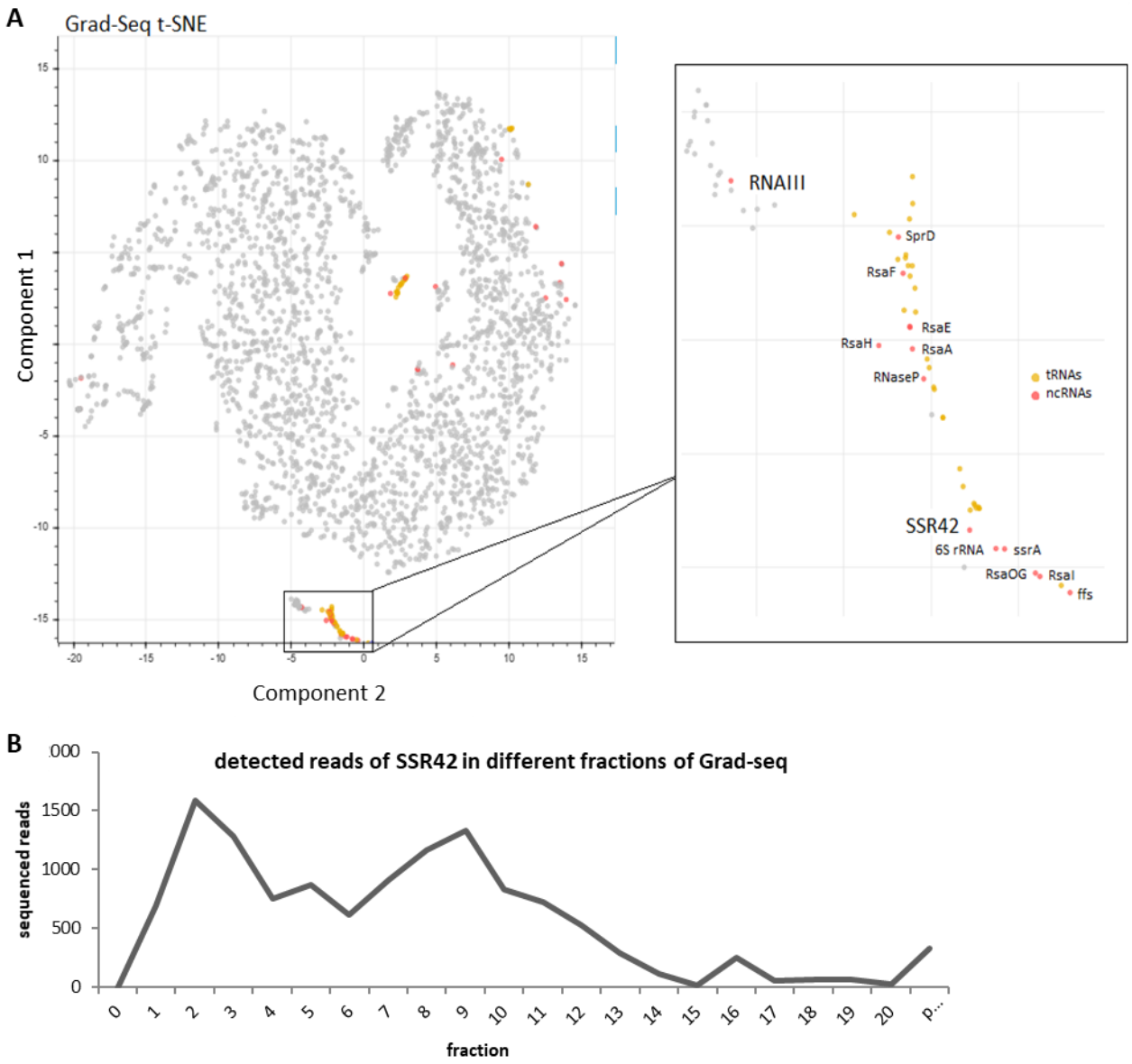

Figure 4.58: Grad-seq analysis revealed an interactome of RNAs in *S. aureus* HG003. A) Two-component analysis of Grad-Seq reads of total RNA from 21 glycerol gradient fractions reveals a cluster of non-coding RNAs and tRNAs. SSR42 was detected in exact that cluster indicating potential interaction with other ncRNAs or commen RNA-binding proteins. Two-component analysis was performed by Konrad Förstner. **B)** Sequence read profile of ncRNA SSR42 from 21 glycerol gradient fractions. Sequence reads were detected at highest levels in fraction 2 and 9. Grad-seq was performed by Alexandr Smirnov and analysed by Konrad Förstner, IMIB Würzburg.

Table 4.12: Top hits of RNAs displaying high correlation with the Grad-seq profile of ncRNA SSR42.

Gene	Product	pearson correlation coefficent
RSAU_002216		0.999
***rpl*0**	50S ribosomal protein L15	0.989
sRNA_00320	sRNA	0.978
***ldh*1**	L-lactate dehydrogenase 1	0.969
***ahp*F**	alkyl hydroperoxid reductase subunit F	0.965
Ssb	Single stranded DNA binding protein	0.961

***usp*A_1**	universal stress protein	0.958
***hut*U**	urocanate hydratase	0.959
***pdh*C**	dihydrolipoamide S-acetyltransferase component PdhC	0.957
***rpl*Q**	50S ribosomal protein L17	0.957
***clf*A**	Clumping factor A	0.956
***rpl*N**	50S ribosomal protein L14	09.54
***brn*Q**	branched-chain amino acid transport system II carrier protein putative	09.44
***rib*A**	Protein from nitrogen regulatory protein P-II family YAAQ	0.943
***qox*C**	cytochrome aa3 quinol oxidasesubunit III	0.942
***rpl*V**	50S ribosomal protein L22	0.941
tuf	Translogation elongator factor	0.940
***rpl*B**	50S ribosomal protein L2	0.937
iolE	sugar phosphate isomeras/epimerase protein	0.936
***yko*E**	substrate specific component YkoE of thiamin-regulated ECF transporter HydroxyMethylPyrimidine	0.936
***dna*A**	chromosomal replicator initiator protein	0.936
***fmh*B**	Peptidogylcan pentaglycine interpeptide biosynthesis protein	0.936
***suc*A**	2-oxoglutarate dehydrogenase E1 component	0.935
***gnt*P**	Telomeric repeat binding factor 2 family protein	0.934
***yko*D**	ABC-Transporter	0.934
***pdh*A**	pyruvate dehydrogenase complex E1 component alpha subunit PdhA	0.933
adk	Adenlyate kinase	0.933
***rpl*K**	50S ribosomal protein L11	0.933
***asn*S**	asparaginyl-tRNA synthetase	0.933
***wal*K**	Sensor histidine kinase WalK	0.929
***put*P**	High affinity proline permease	0.927
***rps*E**	ribosomal protein S5	0.926
***aus*A**	Non-ribosomal peptide synthetase	0.923
sRNA_00095	sRNA	0.922
***rps*J**	30S ribosomal protein S10	0.921
***cop*A**	copper-translocating P-type ATPase CopA	0.920
***yjd*L**	Proton-dependent oligopeptide transporter	0.919
***moe*A**	molybdopterin biosynthesis protein A MoeA putative	0.919
***crt*O**	putative glycosyl-4-4´diaponeurosporenoate acetyltransferase	0.914
***rpl*Q**	50S ribosomal protein L17	0.912
hup	DNA-binding protein HU	0.911
***agr*B**	accessory gene regulator protein B	0.908
***gvp*P**	Gas vesicle protein	0.908
***agc*S**	Sodium alanine symporter family protein	0.908
***cta*B**	protoheme IX farnesyltransferase	0.904
***mqo*2**	malate:quinone oxidoreductase 2	0.903
***ywl*G**	UPF0340 protein ECTR2_1970	0.903
***dgk*A**	Surface protein of unknown function	0.902
***nar*H**	Nitrogen reductase beta chain	0.902
***man*P**	PTS-system, fructose specific	0.902
***rps*I**	30S ribosomal protein S9	0.901

Table 4.13: Comparison of SSR42 targets displaying high correlation with the Grad-seq profile of SSR42 with data obtained by proteomics and transcriptomics.

gene	product	pearson correlation coefficent (Grad-seq)	log_2Fold Change (RNA-Seq)	logFold change (proteomics)
***clf*A**	clumping factor A	0.958	2.56	1.7
***esx*A**	Type VII secreted factor	0.908	2.19	7.6
atl	autolysin	0.893	ns	2.2
***ldh*D**	D-lactate dehydrogenase	0.832	2.59	ns
frp	NAD(P)H-flavin oxidoreductase	0.830	1.54	ns
sbi	immunoglobulin G-binding protein SBI	0.822	ns	1.8
***clp*C**	Clp Protease C	0.764	ns	1.8
***nir*B**	assimilatory nitrite reductase [NAD(P)H] large subunit putative	0.762	2.75	ns
***fnb*B**	fibronectin binding protein B	0.748	ns	7.0
***sar*R**	staphylococcal accessory regulator R	0.750	-2.22	ns
***lrg*A**	holin-like murein hydrolase regulator LrgA	0.745	1.70	ns
***pyr*F**	orotidine 5-phosphate decarboxylase	0.729	-1.68	ns
***sar*X**	staphylococcal accessory regulator X	0.707	1.41	ns
***ldh*D (5´UTR)**	D-lactate dehydrogenase	0.696	2.59	ns
***ess*A**	Type VII secretion system	0.695	1.64	2.56
***chs* (anti-sense)**	chemotaxis inhibitory protein	0.688	-1.81	ns
***his*F**	imidazole glycerol phosphate synthase cyclase subunit HisF	0.662	2.04	ns
***hlg*B**	gamma-hemolysin component B precursor, hlgB	0.660	ns	4.3
chs	chemotaxis inhibitory protein	0.621	-1.81	ns
***hlg*C**	gamma-hemolysin component C	0.604	ns	3.6
***scp*A**	staphopain A	0.568	-1.80	ns
***Sar*A (anti-sense)**	staphylococcal accessory regulator A	0.503	ns	1.76

4.8.2 Identifying potential interaction partners of SSR42 via target prediction

Since the identification of direct interaction partners of SSR42 failed via performing RNA-pulldowns, potential target mRNAs were predicted using the IntaRNA web server (http://rna.informatik.uni-freiburg.de/IntaRNA; Mann et al., 2017; Wright et al., 2014; Busch et al., 2008). Target prediction using this web server only allows the analysis of ncRNAs up to a length of 750 nt. Therefore, the sequence of ncRNA SSR42 was split in halves and both parts were analysed separately. The results of the prediction for both halves of the molecule was combined and is shown in table 4.14 (see also Appendix

table 7.14). Among the predicted target mRNAs of SSR42 with a p-value below 0.05 previously identified factors such as *esx*A, *ureA* and *spl*B were found. Those virulence factors were already identified in the RNA-seq to be differentially expressed in a ΔSSR42 mutant (see section 4.3.1). Regulation of these factors could hence be governed by a direct interaction of ncRNA SSR42 with the respective mRNAs. Interestingly, the list of predicted potential target mRNAs included δ-haemlysin mRNA which is encoded on RNAIII as well as Hfq encoding mRNA.

Although not found in the previous prediction analysis, the sequence of SSR42 and the *sae* operon were analysed using IntaRNA for a potential base-pairing. This was done since the previous experiments indicated the stabilization of *sae* mRNA by SSR42. A potential base-pairing between nt 791-832 of SSR42 and nt 434-474 of *sae*Q mRNA was predicted (Fig. 4.59, see appendix Fig. 7.13). The exact nucleotides are highlighted in the sequences below. The energy of the base-pairing was calculated to be -14.18 kcal/mol. Thus, it is likely that SSR42 could stabilize *sae* transcripts via binding to *sae*Q mRNA encoded in *sae* transcript T1 or T2 which would be in line with the previous experimental findings.

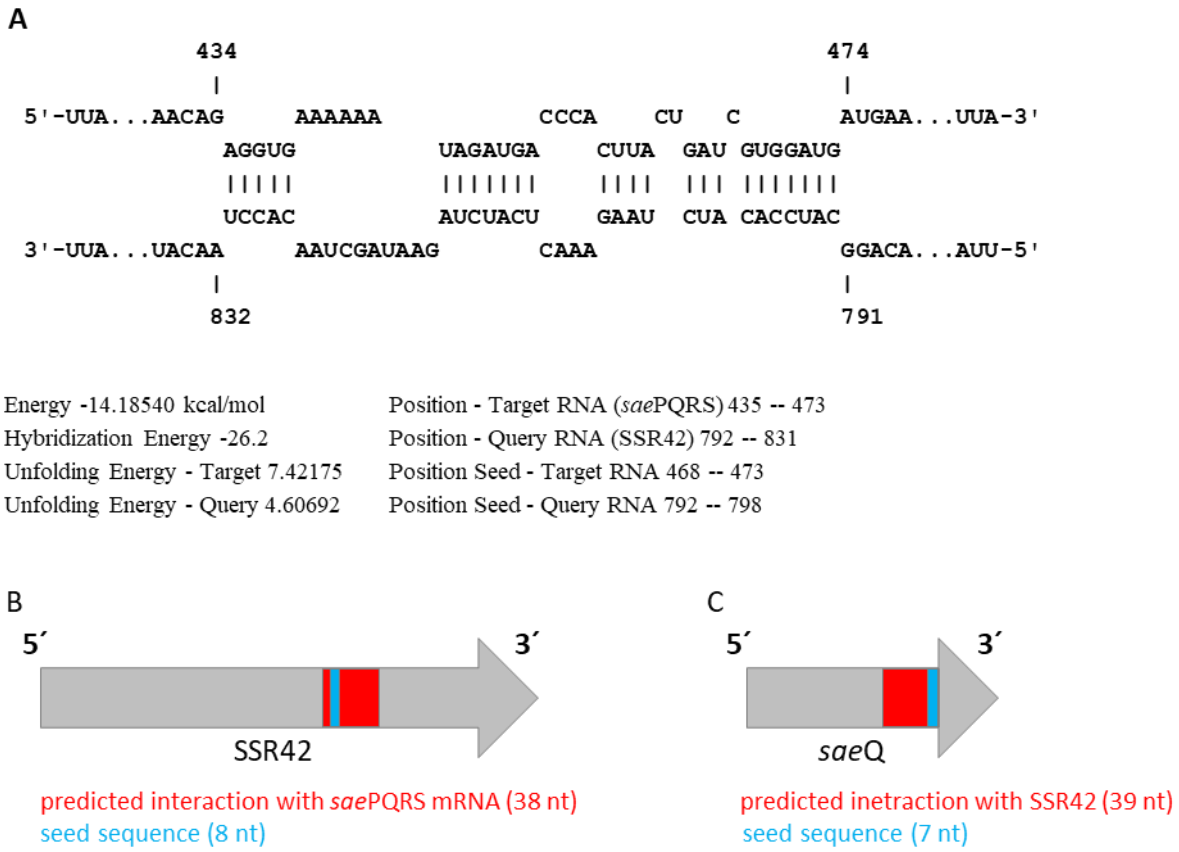

Figure 4.59: Interaction prediction indicates direct interaction of SSR42 and *sae* mRNA. A) Interaction prediction of SSR42 with *sae* mRNA performed by webserved IntaRNA. **B)** Schematic representation of SSR42 sequence with highlighted sequence predicted to interact with *sae* mRNA. **C)** Schematic representation of *sae*Q sequence with highlighted region predicted by IntaRNA to interact with SSR42.

Table 4.14: Top hits obtained from prediction of potential direct interaction partners of SSR42.

Gene	product	position in target	position in SSR42	hybridization energy kJ/mol
RSAU_002489	putative surface anchored protein SasF	19 — 149	658—804	-21.40
RSAU_002374	Phosphotransferase system IIC-related protein	81 — 124	823—866	-21.12
RSAU_001452	DNA internalization-related competence protein ComEC/Rec2	69 — 129	449 — 508	-20.91
RSAU_000953	phosphoribosylaminoimidazole-succinocarboxamidesynthase PurC	76 — 95	1000—1018	-20.40
RSAU_002131	transcriptional regulator putative	8 — 108	195 — 291	-20.00
RSAU_000557	aldo-keto reductase putative	53 — 138	744—837	-19.98
RSAU_002517	histidine biosynthesis bifunctional protein HisIE	1 — 91	188 — 278	-19.51
RSAU_000580	monovalent cation/H antiporter subunit C putative	72 — 141	732—799	-19.30
RSAU_001242	methionine sulfoxide reductase A	47 — 100	194 — 239	-19.15
RSAU_002191	teicoplanin resistance-associated transcriptional regulator TcaR	14 — 64	778—833	-18.92
RSAU_001081	uracil phosphoribosyltransferase PyrR	72 — 108	470 — 506	-18.84
RSAU_002153	amino acid permease	8 — 88	392 — 472	-18.66
RSAU_000397	hypothetical protein	81 — 137	196 — 242	-18.61
RSAU_000167	putative two-component response regulator AraC family	82 — 107	1118—1144	-18.49
RSAU_001463	5-methylthioadenosine/S-adenosylhomocysteine nucleosidase	36 — 92	231 — 284	-18.46
RSAU_001328	bifunctional biotin operon-related protein / biotin-acetyl-CoA-carboxylase putative	1 — 53	261 — 316	-18.38
RSAU_001019	NPQTN-specific sortase B	85 — 132	212 — 254	-18.33
RSAU_001407	competence protein ComGC	4 — 150	713—843	-18.19
RSAU_001961	transcriptional regulator	57 — 145	749—831	-18.15
RSAU_002230	two component sensor histidine kinase	73 — 149	843—924	-18.09
RSAU_001398	hypothetical protein	60 — 145	899—965	-18.05
RSAU_000580	monovalent cation/H antiporter subunit C	1 — 41	826—860	-17.79
RSAU_001980	mannose-6-phosphate isomerase	1 — 19	914—931	-17.55
RSAU_000376	hypothetical protein	93 — 135	907—950	-17.47
RSAU_000401	acetyltransferase GNAT family	81 — 137	888—960	-17.38
RSAU_000228	putative WxG domain protein EsxA	83 — 118	422 — 461	-17.35
RSAU_001398	hypothetical protein	74 — 145	723—795	-17.32
RSAU_001056	HAD superfamily hydrolase	12 — 105	988—1063	-17.28
RSAU_001113	3-oxoacyl-[acyl-carrier protein] reductase	97 — 150	880—936	-17.21
RSAU_001285	5-bromo-4-chloroindolyl phosphate hydrolysis protein XpaC	95 — 142	725—771	-17.14
RSAU_002084	50S ribosomal protein L23	10 — 25	1127—1142	-17.06

RSAU_001527	delta-aminolevulinic acid dehydratase	88 — 150	195 — 268	-17.06
RSAU_002450	antibiotic biosynthesis monooxygenase	14 — 150	811—957	-16.99
RSAU_001153	ribosome-binding factor A	81 — 137	195 — 254	-16.97
RSAU_000439	ribose-phosphate pyrophosphokinase	10 — 58	753—795	-16.96
RSAU_001117	signal recognition particle-docking protein FtsY	52 — 80	912—938	-16.91
RSAU_002392	ferrous iron transport protein A (FeoA)	12 — 123	166 — 295	-16.8
RSAU_000755	hypothetical protein	1 — 27	259 — 299	-16.84
RSAU_001265	phosphate transport system regulatory protein	101 — 115	424 — 438	-16.82
RSAU_002253	EmrB-QacA subfamily drug resistance transporter	62 — 148	419 — 523	-16.78
RSAU_000664	aldo/keto reductase	51 — 149	385 — 467	-16.76
RSAU_001669	serine protease SplB	100 — 134	1179—1211	-16.74
RSAU_000726	ComF operon protein 3-like amidophosphoribosyltransferase	82 — 125	828—880	-16.74
RSAU_001242	methionine sulfoxide reductase A	83 — 144	744—803	-16.65
RSAU_002123	urease alpha subunit	16 — 67	727--793	-16.63

5 DISCUSSION

S. aureus regulates virulence via the global transcriptional regulator Rsp. Among the Rsp-regulated factors a 1232 nt long ncRNA, SSR42, was identified (Das et al., 2016), which was previously shown to regulate virulence factor expression (Morrison et al., 2012a). However, since previous studies underestimated the length of this ncRNA the full regulatory impact and the relationship with Rsp remain elusive. The aim of the present study was to characterize SSR42 on a molecular and functional basis and to estimate the position of SSR42 in the hierarchy of staphylococcal virulence regulation.

5.1 Strain-specific expression of 1232 nt long ncRNA SSR42

Rsp, which is encoded in antiparallel orientation to SSR42, was recently identified as a global regulator affecting various virulence traits ranging from haemolysis to cytotoxicity. Further, the study determined the length of the primary SSR42 transcript by TEX-treatment RNA-seq as 1232 nt (Das et al., 2016), which exceeded the previously established length determination of 891 nt (Morrison et al., 2012a).

In order to address this discrepancy, the SSR42 transcript was analysed in the present study. Northern blotting confirmed the presence of an approximately 1200 nt long transcript in various *S. aureus* strains (Fig. 4.4) including the strains used in the previous study by Morrison et al., 2012a, thereby corroborating the data from Das, et al. 2016. In addition, other studies identified a RNA that exceeded 1100 nt: Teg27: 1176 nt (Beaume et al., 2010), srn_4470: 1174 nt (Sassi et al., 2015), or RsaX28: 1177 nt (Khemici et al., 2015). Also, a genome-wide identification of RNase Y processing sites identified a single cleavage site within SSR42, there termed RsaX28 (Khemici et al., 2015). In the present study at least one smaller SSR42 transcript was identified, which was found to result from RNase Y cleavage. While deletion or mutation of the predicted RNase Y cleavage site did not omit cleavage of SSR42 (Fig. 4.5), it was concluded that not the sequence is initiating cleavage but rather a structural element in SSR42 is required for processing by RNase Y. Already for processing of *sae* transcript T1 a downstream structural element in the mRNA was shown to determine the cleavage by RNase Y (Marincola and Wolz, 2017). However, although RNase Y cleavage is thought to initiate the further degradation of RNA species (Khemici et al., 2015), RNase Y cleavage was not found to affect the stability of SSR42 transcript T1 (Fig. 4.6). Moreover, regarding *sae* transcripts even a stabilizing role for RNase Y was observed in processing of unstable transcript T1 resulting in stable transcript T2 (Marincola and Wolz, 2017). Therefore, the role of RNase Y cleavage on SSR42 needs further investigation.

Comparing P_{SSR42} activity profiles in various *S. aureus* strains revealed significant differences in the course and intensity of the promotor activity. In general, two distinct P_{SSR42} activity profiles were observed: a one-peak profile as observed in strain 6850 and a sigmoid profile as in strain JE2 (Figs. 4.30,

4.31) indicating strain-specific differences in the regulation of SSR42 transcription. While the strong regulatory dependency of Rsp on SSR42 transcription was verified using promotor activity assays (Fig. 4.45), comparison of the promotor activities of P_{SSR42} and P_{rsp} in both *S. aureus* 6850 and strain JE2 revealed similarities to a high degree regarding the course of activity (Fig. 4.31). The highly similar course of P_{rsp} activity indicated an important role for Rsp expression for determination of the SSR42 promotor activity in both strains 6850 and JE2. Indeed, analysing Rsp protein levels in both strains during different growth phases reflected the strain-specific differences in P_{rsp} activity (Fig. 4.31C). In addition to the observed strong regulatory relationship of SSR42 and Rsp in strain JE2 a similar modulation of P_{rsp} and P_{SSR42} activity in mutants in *agr*A, *rpi*Rc, *cod*Y and *arl*R was observed (Fig. 4.54). This suggests that for those regulators SSR42 transcription is indirectly mediated via transcriptional regulation of *rsp*.

However, the strict connection between Rsp levels and SSR42 transcription was not observed in the other strains tested and significant differences between SSR42 and *rsp* transcript levels were found for strain Newman, Cowan I and RN4220 (Fig. 4.52). Whereas strain Newman exhibited a strong and significant increase in SSR42 transcript levels compared to strain 6850, *rsp* transcript levels were unaltered. In contrast, strain Cowan I displayed significantly reduced *rsp* transcript levels while SSR42 transcript levels were unaltered compared to strain 6850, whereas the laboratory strain RN4220 exhibited strongly decreased SSR42 transcript levels and unaltered *rsp* transcript levels. Overall transcript levels of SSR42 in strain UAMS-1 were detected only at a very low amount. This may correlate with the inability of strain UAMS-1 to produce a functional α-toxin due to a non-sense mutation within *hla* (Cassat et al., 2013).

Analysing the *rsp* transcript levels in diverse *S. aureus* strains hence suggested a strain-specific impact of Rsp on SSR42 transcript levels. Thus, Rsp may exhibit less impact on transcriptional regulation of SSR42 in strain Newman, Cowan I and RN4220 and regulation of SSR42 transcription could be governed by other, transcriptional regulators. The present study identified agr and SaeS as further transcriptional regulators of SSR42 (Fig. 4.51). While strain Cowan I and RN4220 are characterized by inactive agr systems (Nair et al., 2011, Grundmeier et al., 2010) and strain Newman exhibits a constitutively active kinase SaeS (Schäfer et al., 2009) the discrepancies regarding the regulation of SSR42 could be the result of the mutations in those regulators. However, strain-specific differences in post-transcriptional regulation of *rsp* cannot be excluded and hence differences in *rsp* transcript levels may not be reflected in the Rsp protein levels of the respective strains. As a potential reason for the strain-specific differences in the relationship between Rsp and transcriptional regulation of SSR42 differences in the sequence of Rsp were excluded due to the high conservation among *S. aureus* strains.

Comparing the transcriptome of the ΔSSR42 mutant in strain 6850 (table 4.2, 4.3) with the transcriptome conducted in a previous study encompassing a 891 nt deletion of SSR42 within strain UAMS-1 and LAC (Morrsion et al., 2012a), revealed only a slight overlap of regulated genes including *isa*B, *hla* and capsular genes. However, comparing the regulated genes within strain UAMS-1 and LAC already revealed substantial differences within the set of regulated genes. Among the overlapping genes within both strains only three genes including *rsp* were detected (Morrison et al., 2012a). Expression of *rsp* was found repressed by SSR42 during stationary growth phase in those strains. In *S. aureus* 6850, however, no differential regulation of *rsp* in stationary (padj= 0.27) nor in exponential growth phase (padj= 0.59, see Appendix Fig. 7.8) was detected in mutants lacking SSR42. This further suggests that SSR42 may display different regulatory properties in different *S. aureus* strains despite the high sequence conservation among all *S. aureus* strains. The substantial differences within the transcriptome indicate that ncRNA SSR42 executes different roles regarding virulence gene regulation dependent on the genetic background. Strain-specific differences in regulatory capacities have already been observed for other regulatory factors in *S. aureus* such as RNAIII (Queck et al., 2008; Geisinger at al., 2012). The differences in the set of target genes regulated by SSR42 presumably results from the strain-specific expression patterns and expression levels of SSR42 observed in this study, which may result from differences in the regulation of SSR42 transcription. The SSR42 promotor activity profile was found to differ significantly dependent on the genetic background. While promotor activity of SSR42 was detected at extremely low levels in strain UAMS-1, P_{SSR42} activity displayed a peak during transition to stationary growth phase in strain 6850 (Fig. 4.30). In strain JE2, however, a sigmoid promotor activity profile was observed. Since expression of SSR42 was further shown to be modulated by the availability of glucose (Fig. 4.39) and the presence of antibiotics (Fig. 4.33), it was suggested that strain-specific differences in the glucose metabolism or the ability to cope with stresses could influence SSR42 transcript levels and hence the impact of SSR42 on regulation of virulence factors.

5.2 Rsp and SSR42: a new virulence regulator system with the ncRNA SSR42 as effector of Rsp

Expression of α-toxin in *S. aureus* is governed by various global regulators such as the agr system and SaeRS (Queck et al., 2008; Mainiero et al., 2010). Another factor, the ncRNA SSR42, was implicated in haemolysis regulation via modulating the promotor activity of *hla* (Morrison et al., 2012a). Rsp was recently identified to strongly affect the haemolytic activity of *S. aureus* and expression of SSR42 (Das et al., 2016). The complete absence of SSR42 transcripts in *rsp* mutants suggested a role for SSR42 in executing parts of Rsp-mediated virulence (Das et al., 2016).

In the present study, mutants harbouring a deletion in the locus encompassing 1232 nt SSR42 displayed a strongly reduced haemolytic activity towards sheep erythrocytes, which was demonstrated to be due

to reduced α-toxin expression. Lack of SSR42 transcription was successfully complemented by inducible expression either in stationary or exponential growth phase (Fig. 4.11). While inducible expression of SSR42 resulted in enhanced *hla* transcript levels independent of the respective growth phase of bacteria, haemolysis could only be restored by inducible transcription of SSR42 in stationary growth phase. Hence, these data suggested the involvement of a further factor involved in *hla* translation regulation. Translation regulation of *hla* is governed by RNAIII via rendering the Shine-Dalgarno sequence accessible for the ribosome (Morfeldt et al., 1995). Since RNAIII is essential for translation of *hla* mRNA (Morfeldt et al., 1995) but only detectable in high amounts during stationary growth phase (Boisset et al., 2007; Yarwood et al., 2002; Chabelskaya et al., 2014; Xiong et al., 2002, Fig. 4.11) it would explain the discrepancy between SSR42 expression and haemolysis re-establishment during exponential growth phase. These data thus indicate the requirement of two long regulatory RNAs in haemolysis regulation: SSR42 for transcriptional regulation of *hla* and 514 nt long RNAIII for liberating the Shine-Dalgarno sequence within *hla* mRNA and granting translation.

Complementation studies of a double knockout mutant in SSR42 and *rsp* were used to distinguish the role of both regulators for haemolysis regulation (Fig. 4.12, 4.13). While an essential role for Rsp in transcriptional regulation of SSR42 was confirmed (Das et al., 2016, Fig. 4.45), only a minor role for Rsp in haemolysis regulation was found (Fig. 4.13). Via inducible expression of SSR42 in a ΔSSR4-*rsp* mutant an important role for SSR42 in haemolysis regulation was confirmed and SSR42 was identified as the effector of Rsp regarding haemolysis regulation (Fig. 4.13). Thus, the reduced haemolytic activity in *rsp* mutants results from lack of SSR42 expression.

In a previous study the deletion of SSR42 affected haemolysis as well. However, the construct used for complementation of this 891 nt long deletion by chance encompassed the whole 1232 nt long SSR42 locus thereby explaining the efficient re-establishment of haemolysis in the mutant (Morrison et al., 2012a). In the present study the importance of 1232 nt long SSR42 for haemolysis regulation was demonstrated by mutational approaches where deletion of the region spanning the previous identified 5´-end resulted in a strongly reduced stability of the ncRNA and a subsequent reduced haemolytic activity of *S. aureus* (Fig. 4.55).

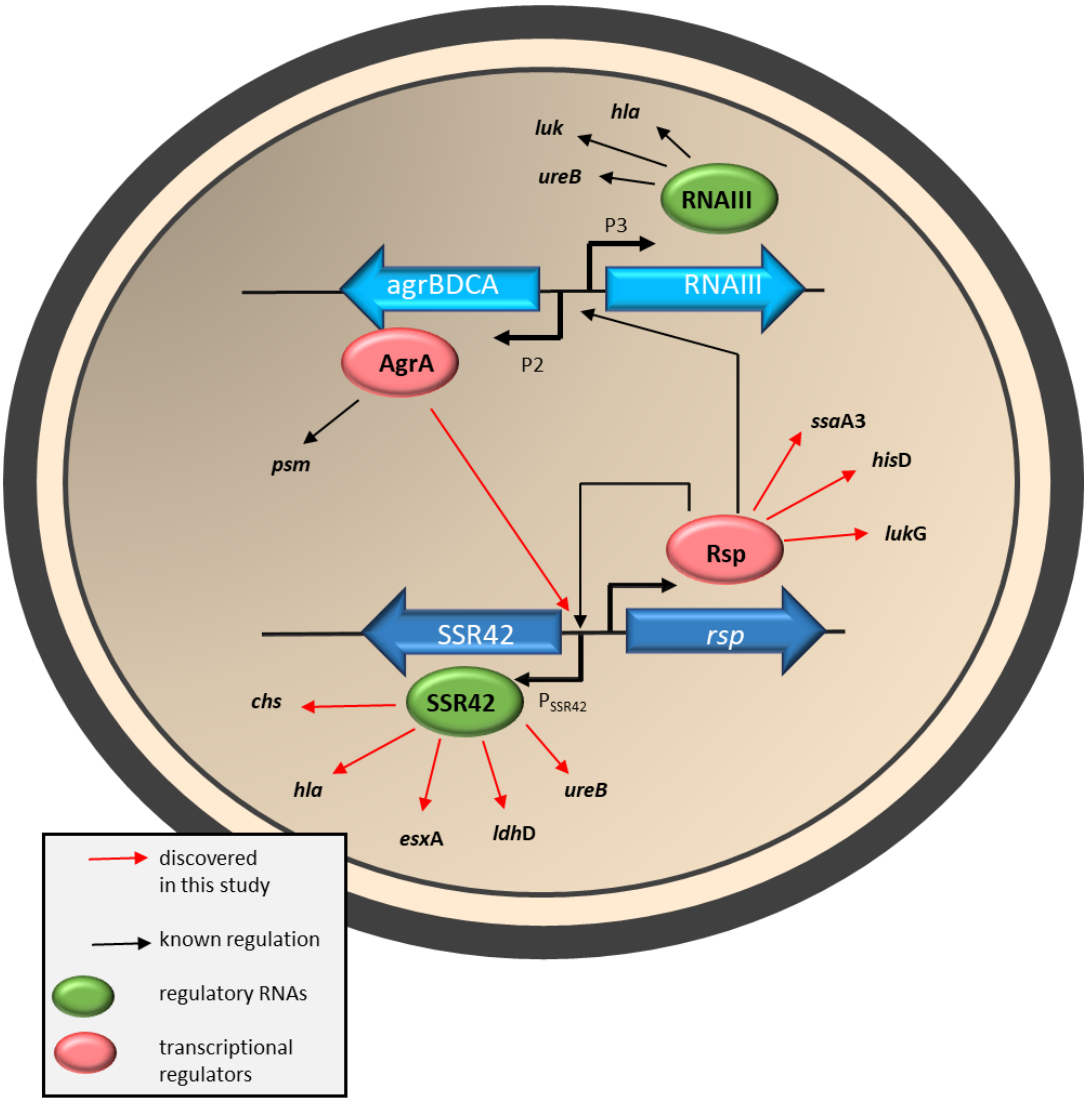

Figure 5.1: Schematic illustration of transcriptional units agr/RNAIII and Rsp/SSR42. The scheme summarizes the similarities between agr/RNAIII and Rsp/SSR42 and the findings from this study (red arrows). *agr*BDCA and RNAIII as well as *rsp* and SSR42 are situated in antiparallel orientation and are transcribed from each two divergent promotors. Both ncRNAs SSR42 and RNAIII regulate the expression of a variety of virulence genes, which overlap partially. While Rsp regulates transcription of *agr* a regulatory role for AgrA on transcriptional regulation of SSR42 was identified in this study.

Analysing the transcriptome of mutants in SSR42 revealed the impact of SSR42 on a variety of different virulence factors including *esx*A, *clf*A, *ldh*D, *ure*B and *psm*α (table 4.2, 4.3). Since most of the differentially regulated genes were already detected in mutants lacking functional Rsp the transcriptome and proteome of a ΔSSR42-*rsp* mutant was compared to that of a mutant lacking only SSR42. By applying transcriptome analysis, the regulon of both regulators was determined and SSR42 was identified as the main effector of Rsp-regulated genes. Interestingly, only the expression of *luk*G, *his*D and *ssa*A3 was found to differ between the ΔSSR42 mutant and the double knockout mutant (Fig. 4.17), thus indicating SSR42-independent regulation by Rsp. SSR42 and *rsp* are encoded in antiparallel

orientation in close genetic proximity and are transcribed from two divergent promotors (Fig. 5.1). This is similar to another major regulatory element in *S. aureus*: the agr quorum-sensing system (reviewed in Novick, 2003). For the agr system the regulatory RNA (RNAIII) mainly executes regulation of virulence gene expression while the transcriptional regulator, AgrA, only regulates a small subset of target genes independently of RNAIII (Queck et al., 2008). Similar for Rsp and SSR42 the regulatory RNA, SSR42, was identified to mainly regulate target gene expression. For Rsp instead only a small subset of virulence genes, including *luk*G, *his*D and *ssa*A3 was identified.

The connection of a regulatory protein and a non-coding RNA to mediate target gene expression could therefore not be unique and restricted to AgrA/RNAIII but evolved in parallel in *S. aureus.* Targets, which have to be regulated quickly upon sensing a specific stimulus would most likely be regulated by the non-coding RNA due to the possibility of a much quicker response whereas other target genes would be regulated directly by the transcription factor protein. This facilitates the regulation of a wide range of target genes via different mechanisms during different time points in growth. The Rsp/SSR42 system not only shows resemblances to the agr system (Fig. 5.1) but is also connected to this system via regulation of *agr* transcription by Rsp (Li et al., 2016). A functional agr-system in turn regulates SSR42 transcription in late stationary growth phase of *S. aureus* (Fig. 4.46). Hence, Rsp/SSR42 could act in concert with the agr quorum-sensing system to modulate virulence factor expression.

5.3 SSR42: a new master regulator affecting various virulence phenotypes

Rsp, transcriptional regulator of SSR42, was first identified and therefore named Repressor of surface proteins since deletion resulted in overexpression of surface proteins and enhancement of biofilm formation (Lei et al., 2011). In a further study, a transposon mutant screen identified Rsp as an important regulator of haemolysis and intracellular virulence. Interestingly, mutants lacking functional Rsp not only displayed reduced cytotoxicity but further prolonged intracellular residence in host cells (Das et al., 2016). Since the present study identified SSR42 as the executing factor of Rsp-mediated haemolysis and virulence gene expression regulation, the further phenotypes of *rsp* mutants were analysed in a ΔSSR42 mutant.

While characterizing a ΔSSR42 mutant ncRNA SSR42 was demonstrated to have an impact on haemolysis, cytotoxicity, virulence in a murine infection model and biofilm formation (Figs. 5.2, 4.10, 4.18, 4.21, 4.19). In line with the increased *fnb*A and *fnb*B transcript and protein levels (see Appendix table 7.6, 7.11) biofilm formation in mutants lacking SSR42 was found to be increased (Fig. 4.19). Fibronectin binding proteins were reported to be required for the initial step of biofilm formation mediating the adherence to a substrate (O´Neill et al., 2008; McCourt et al., 2014). Moreover, expression of *fnb*A was shown to be repressed by Rsp via binding to the *fnb*A promotor region (Lei et

al., 2011). However, by comparing the transcript levels of *fnb*A in a ΔSSR42 (*fnb*A: $FClog_{10}$: 1.58; p>0.001) and ΔSSR42-*rsp* mutant (*fnb*A: $FClog_{10}$: 1.71; p>0.001) no significant differences were found (see Appendix Fig. 7.7). Thus, these data suggest that rather SSR42 regulates transcription of *fnb*A in *S. aureus* 6850. The discrepancies between these data and the previous study suggesting regulation by Rsp (Lei et al., 2011) could be explained by the usage of different strains or by the fact that for the binding studies of Rsp and the *fnb*A promotor sequence only the helix-turn-helix-motif instead of the whole protein was used (Lei et al., 2011). Furthermore, it is supposable that SSR42 and Rsp together modulate expression of *fnb*A. Due to the minimal differences in the transcript levels of *fnb*A in the double knockout mutant compared to the transcript levels in the single SSR42 mutant (*fnb*A: ΔSSR42-*rsp* vs ΔSSR42: $FClog_{10}$: 0.12; p>0.852), such a conjoint regulation by SSR42 and Rsp could have been missed in the transcriptome analysis. Thus, analysis of *fnb*A regulation needs further investigations.

Infecting HeLa 2000 cells with a ΔSSR42 mutant revealed the importance of SSR42 for mediating host cell death. LDH release from infected cells was significantly reduced to similar levels when cells were infected with either mutants lacking SSR42 or *rsp* (Fig. 4.18) confirming the previously found role for SSR42 as effector of Rsp-mediated virulence regulation. As an effector of cell death α-toxin was identified, which was demonstrated to be under the control of SSR42 (Figs. 4.10, 4.27A; Morrison et al., 2012a) and which has previously been reported to provoke host cell death in various studies (Bantel et al., 2001; Essmann et al., 2003, Suttorp and Habben, 1988). Further, supernatants of a ΔSSR42 mutant displayed significantly less cytotoxicity towards HeLa 2000 cells (Fig. 4.18) indicating that a SSR42-regulated secreted factor mediates cell death from outside host cells. As observed in the transcriptome and proteome, SSR42 regulates the expression of various cytolytic pore-forming toxins such as PSMα, HlgB and α-toxin (tables 4.2, 4.3, 4.6, 4.7). Due to the highly cytolytic activity towards a variety of host cells (Bhakdi et al., 1989; Bhakdi and Tranum-Jensen, 1991; Walev et al., 1994) and the high protein levels found in *S. aureus* stationary phase culture supernatants α-toxin was suggested as the effector of the observed effects of bacterial supernatants on epithelial cells. Moreover, α-toxin has been identified as a potent apoptosis inducing factor of *S. aureus* culture supernatants (Bantel et al., 2001). The positive regulation of α-toxin transcription by SSR42 would thus explain the reduced cytotoxic activities of culture supernatants obtained from mutants lacking ncRNA SSR42. Hence, SSR42 was demonstrated to effect host cell death, presumably via regulation of α-toxin expression from both outside and within cells.

Lack of SSR42 or Rsp was further shown to favour the formation of small colony variants in similar amounts during long time infection of EA.Hy926 cells (Fig. 4.20). A previous study demonstrated that mutation of *rsp* leads not only to an attenuated cytotoxic phenotype but also to a prolonged intracellular residence of bacteria (Das et al. 2016). A prolonged intracellular residence of *S. aureus* has

been reported in various studies (Hamill et al., 1986; Kubica et al., 2008; Lowy et al., 1988; Tuchscherr et al., 2011) and is considered to promote chronic staphylococcal infections. Bacteria isolated from long-term infections are often less haemolytic and cytotoxic, display reduced growth-rates and were thus named small colony variants (SCV) (Bulger and Bulger, 1967; Proctor et al., 1994). SCVs are further characterized by higher tolerance against antibiotics and reactive oxygen species (Agarwal et al., 2007; Kahl et al., 1998; Proctor et al., 1995). In line with that SSR42 was demonstrated to positively affect both haemolysis and cytotoxicity (Figs. 4.10; 4.18). Hence, mutants lacking SSR42 display typical characteristics of SCVs and were demonstrated to form SCVs during long-term infections. Lack of SSR42 may thus provoke the shift from a highly virulent to a quiescent, non-haemolytic and non-cytotoxic SCV phenotype. Moreover, mutants lacking SSR42 displayed a strongly reduced virulence in murine tibia, kidney and liver infection models from where they were recovered at significantly lower amounts than wild-type bacteria (Fig. 4.21). During the acute and chronic phases of infection ΔSSR42 mutants displayed a significant fitness defect (Fig. 4.21D). Interestingly, while CFUs of ΔSSR42 mutants already strongly dropped during the acute infection phase, the CFU number remained rather unaltered afterwards during the chronic infection stages and bacteria lacking SSR42 were not completely cleared by the host immune system. This is in line with the previous findings indicating that SSR42 is mediating SCV formation, a form of persistence. Thus, SSR42 may represent a new factor involved in intracellular residence and SCV formation and serve as a virulence switch for *S. aureus*. Recently, a study analysing differences in the transcriptome of *S. aureus* during *in vitro* and *in vivo* growth identified several virulence encoding genes whose transcription was up-regulated during *in vivo* conditions in mice (Szafranska et al., 2014). Among the differential regulated genes a high number of previously identified SSR42 target genes were identified strengthening the importance of SSR42 during *in vivo* growth: *spl*F, *spl*A, *spl*B, *scp*A, *aur*, *clp*C, *clp*B, *ahp*F, *ahp*C, *hla*, *clf*A and *fnb*A (Szafranska et al., 2014; tables 7.5, 7.6). However, SSR42 could not be analysed in that study since it was not annotated in the used reference genome. Thus, SSR42 represents a major virulence regulator especially required for intracellular virulence. While mutants in SSR42 display reduced cytotoxicity, they seem to be better adapted to the harsh conditions faced inside host cells and could subsequently promote persistent or reoccurring infections. However, the mechanism of SCV formation or the reason why SSR42 mutants are not completely cleared by the host immune system remains elusive and needs further investigation.

In summary, the attenuated cytotoxicity of *rsp* mutants (Das et al., 2016) was also a characteristic of a ΔSSR42 mutant, therefore it was concluded that Rsp mediates cytotoxicity only indirect via regulation of SSR42 transcription. Moreover, SSR42 was suggested to be responsible for the prolonged intracellular residence inside host cells as reported for *rsp* mutants (Das et al., 2016). Considering the similar phenotypes regarding host cell death and SCV formation and the high overlap of the transcriptomes and proteomes of a Δ*rsp* and ΔSSR42 mutant it is likely that more phenotypes

described for the *rsp* mutant are secondary effects caused by lack of SSR42 transcription. Thus, SSR42 was considered to be the main-effector of Rsp-mediated virulence in *S. aureus*.

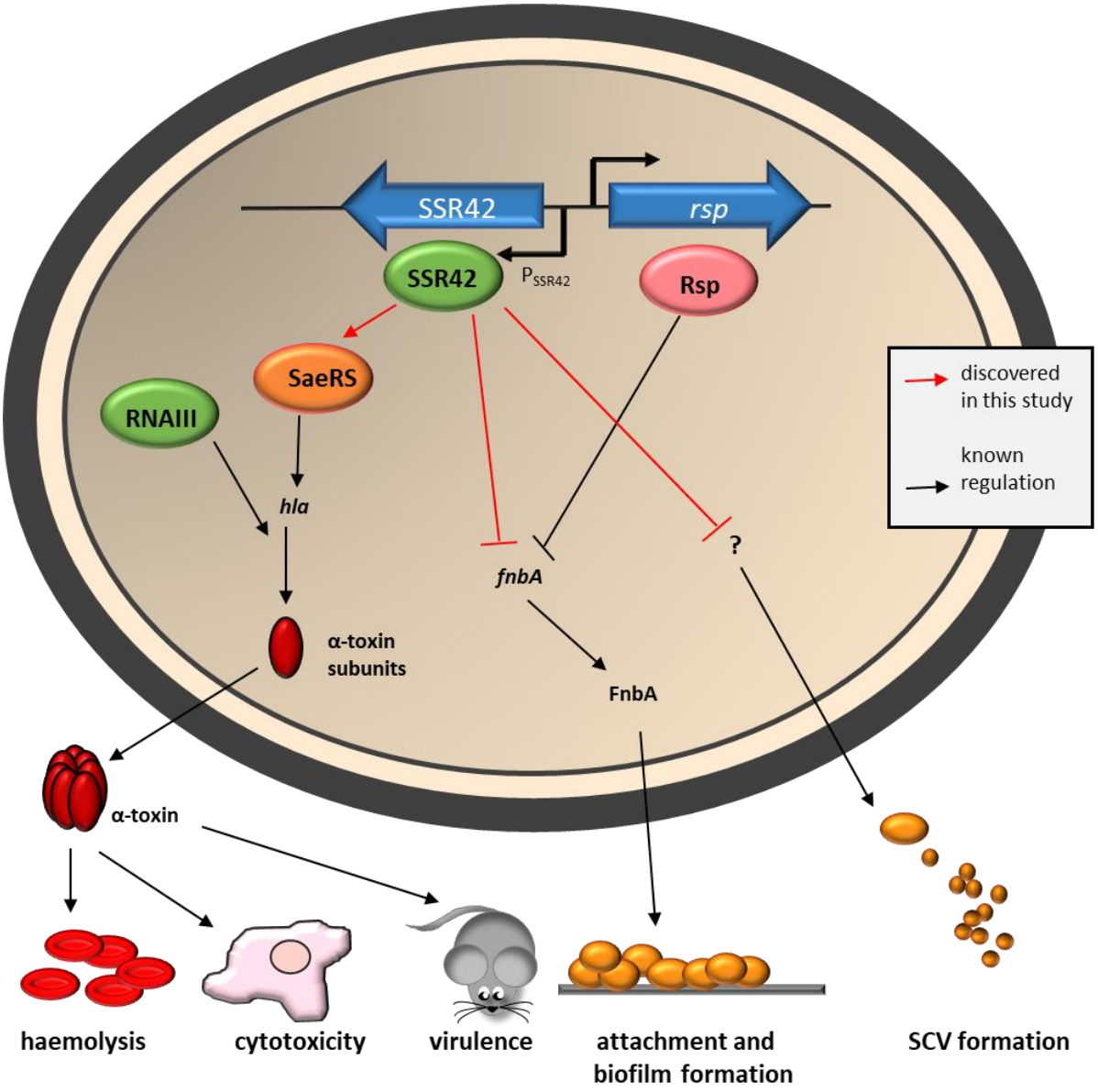

Figure 5.2: A graphical overview of phenotypes affected by SSR42. Summary of observed phenotypes of a SSR42 mutant and the regulation of the factors involved in those phenotypes. Newly identified regulations are marked with red arrows. Mutants in SSR42 are characterized by reduced haemolysis. In this study regulation of *hla* was identified to be executed via modulation of *sae* transcript stability. Regulation of α-toxin expression affected haemolysis, cytotoxicity and virulence. ΔSSR42 mutants further displayed enhanced biofilm formation which was suggested to be the result of repression of *fnb*A expression. Further mutants lacking SSR42 tend to form SCVs during long term infection of host cells. This is modulated via a yet unknown factor illustrated by a question mark.

5.4 Potential interaction of SSR42 with other regulators

SSR42 was demonstrated to mediate the expression of various virulence factors thereby executing a global regulatory role. Among the down-regulated genes the operon upstream of SSR42, RSAU_002216 was detected. In mutants lacking SSR42 the expression of RSAU_002216 was drastically decreased in stationary as well as exponential growth phase indicating a strong dependency on SSR42 for transcriptional regulation (Fig. 4.16, table 4.2, 4.3). Since the gene encoding SSR42 and ORF RSAU_002216 overlap at both 3'-ends, transcription of RSAU_002216 was analysed when SSR42 was complemented using an AHT-inducible plasmid which did not harbour the ORF RSAU_002216 (pAHT-SSR42; Fig. 4.16). Expression of SSR42 was sufficient to restore transcription of RSAU_002216, thus it was concluded that SSR42 regulates the expression of this ORF. Further, disruption of this ORF in strain USA300 JE2 (NE1614; RSAU_002216 in 6850 correlates to SAUSA300_2325 in JE2) did not affect haemolysis (Fig. 4.10). Moreover, literature search revealed no evidence for RSAU_002216 in haemolysis or virulence regulation thus a potential regulatory role for RSAU_002216 regarding haemolysis regulation was excluded.

The high number of SSR42 regulated genes indicated an indirect regulatory mechanism involving other virulence regulators (table 4.10). SSR42 was demonstrated by the present study not only to induce expression of *sae*S and *sae*P but also various SaeRS class I target genes as well as the class II target gene *hla* (Fig. 4.23). Inducible SSR42 transcription in mutants lacking a functional SaeRS system further demonstrated the essentiality of SaeRS for *hla* regulation (Fig. 4.24) and expression of the class I target genes. SSR42 regulates the expression of virulence factors such as *coa* and *hla* via modulating their promotor activities (Fig. 4.25), which is in line with the proposed mechanism that SSR42 mediates the expression of a subset of target genes indirectly via SaeRS since transcription of both *coa* and *hla* is induced via binding of SaeR-P to the respective promotor regions (Giraudo et al., 1997; Mainiero et al., 2010). Thus, SSR42 acts upstream of SaeRS.

Recording the activity of P_{hla} over time revealed that the SSR42-dependent regulation begins at transition to stationary growth phase of bacteria further confirming the hypothesis that SSR42 operates upstream of SaeRS since SaeR has been shown to induce transcription of *hla* predominantly in post-exponential growth phase (Giraudo et al., 1997; Novick and Jiang, 2003). The reduced transcript levels of *sae*S and *sae*P in a ΔSSR42 mutant indicated either modulation of the promotor activity of *sae* P1 which drives transcription of *sae* T1 or modulation of the transcript stability. The reduction of P_{hla} activity in a ΔSSR42 mutant (Fig. 4.27) indicated a subtle modulation of SaeRS rather than a strict expression regulation which in line with the observation that ncRNA SSR42 modulates the stability of the *sae* transcripts T1 and T2 (Fig. 4.25). In contrast, a complete lack of SaeR activity would result in an absolute loss of P_{hla} activity (Xiong et al., 2006).

In an attempt to identify functional regions within SSR42 an approximately 70 nt long sequence was identified to be required for haemolysis regulation (Fig. 4.55). This sequence could either be implicated in binding and stabilizing *sae* mRNA or in another, yet unknown mechanism. Using an ncRNA-mRNA interaction prediction tool a potential interaction of SSR42 and *sae*Q mRNA (Fig. 4.59), which is encoded on *sae* transcript T1 and T2, was suggested. This would reflect experimental findings of SSR42 modulating *sae* T1 and T2 stabilities. However, the predicted sequence was only partially (Δ2, 10 nt) addressed by the performed deletion studies where it had no impact on haemolysis regulation (Fig. 4.55). Since the complete predicted sequence was not mutated and especially the seed sequence was still present in deletion mutant Δ2, no exact conclusion can be drawn whether this sequence is important for SaeRS-mediated haemolysis regulation. In addition, RNA interaction predictions for such long RNAs are rather imprecise and the predicted interaction of SSR42 and *sae*Q mRNA may have only occured by chance. Moreover, experimental approaches rather indicated involvement of region Δ1 in haemolysis regulation (Fig. 4.55). It is supposable that SSR42 may interact via this sequence with *sae* mRNA. However, expression of only a stem loop structure encompassing region Δ1 was not sufficient to restore haemolysis in *S. aureus* ΔSSR42 (Fig. 4.55). The failure to restore *hla* transcription was caused by unsuccessful complementation of SSR42 most likely resulting from a strongly decreased stability of the molecule. Further, complementation with minimal versions of SSR42 was not successful for restoring wild-type haemolytic activities in a SSR42 mutant (Fig. 4.56). However, using minimal version 1 for complementation of SSR42 significantly increased haemolytic activities (approximately 75% of wild-type levels) were achieved indicating a reqirement of further sequences within SSR42 for granting the full regulatory properties of SSR42 regarding haemolysis regulation. Though, mutational studies did further only reveal two sequences implicated in stabilization of SSR42 (Fig. 4.55), which were preserved in SSR42 mini-1 it was concluded that the sum of deleted regions affected the stability of SSR42, thereby impeding full complementation of haemolytic activities. A high amount of a smaller approximatley 400 nt transcript was observed for mutants complemented with mini-1 which could serve as a hint for differences in the stability of SSR42 (Fig. 4.56).

Another indirect mechanism of mediating the *sae* transcript stability could be by means of endoribonuclease RNase Y. Both SSR42 and *sae* T1 transcript are processed by RNase Y, whereas only for *sae* mRNA the stability is affected by RNase Y cleavage (Marincola et al., 2012, Fig. 4.6). SSR42 could interact with RNase Y and thereby modulate *sae* mRNA stabilities. However, further experimental proof is required to decipher the regulatory mechanism of how SSR42 mediates *sae* stability.

Further, the activity of P_{SSR42} was found enhanced in mutants lacking functional SaeS but not in mutants lacking SaeR (Fig. 4.46). This interdependency between SSR42 and SaeS could constitute a negative feedback loop independent of SaeR limiting the transcript levels of SSR42 during late stationary growth phase of *S. aureus*. However, since protein levels of SaeS and SaeR were unaltered in a ΔSSR42 mutant

(Fig. 4.26) and expression of *sae* targets has been shown to be independent of the *sae*RS mRNA dosage (Mainiero et al., 2010) it is questionable if the observed reduced stability of *sae* transcripts in a ΔSSR42 mutant would be sufficient for the drastic decrease in haemolytic activity. Additionally, lack of Rsp has been shown to increase transcription of *sae* in strain LAC (Das et al., 2016). However, this was not observed in the double knockout mutant ΔSSR42-*rsp* in strain 6850 (Fig. 4.13). The exact role of SSR42 on regulation of SaeRS is complicated by potential feed back mechanisms and therefore needs further investigations.

For modulating the promotor activity of *psm*α a further mechanism has to be employed by SSR42 since expression of *psm*α is not under control of the SaeRS system. Most of the differential regulated genes found in a ΔSSR42 mutant are under control of further global regulators such as CodY, σB, agr, Rot, CcpA, SarA-family proteins and ArlRS (table 4.10). Via transcript level analysis a regulatory mechanism involving the modulating of either *cod*Y, *rpo*F (σB) or *agr* expression was excluded (Fig. 4.22). While most of the target genes were found to be under control of the agr quorum-sensing system a direct interaction of SSR42 and agr was excluded (Figs. 4.13, 4.22). The agr system itself is regulated by various members of the SarA-family of transcriptional regulators (reviewed in Cheung et al., 2008). Via RNA-Seq and mass spectrometry analysis elevated *sarX* transcript levels and elevated SarA protein levels were detected in the ΔSSR42 mutant (see Appendix tables 7.5, 7.11). SarX is a negative regulator of the agr quorum-sensing system inhibiting agr-regulated genes by inhibiting the *agr* P2 promotor activity (Manna and Cheung, 2006b), while SarA induces up-regulation of several exotoxins including α-toxin, β-toxin, and δ-toxin during the post-exponential growth phase (Cheung et al., 2004; Cheung and Zhang, 2002) by binding to the promotor region of *agr* (Sterba et al., 2003). Hence, SarA-familiy proteins would be ideal candidates by which SSR42 could execute regulation of virulence factors.

Further, SSR42 may regulate some of the target genes directly. Potential mechanisms could include base-pairing of SSR42 and target mRNAs, thereby granting or blocking ribosomal access and mediating translation efficiencies. Stabilization of target mRNAs or recruitment of RNases, such as RNase Y, could be further mechanisms exploited by SSR42. These mechanisms have been reported for RNAIII (Morfeldt et al., 1995; Geisinger et al., 2006; Boisset et al., 2007; Chevalier et al., 2010) and thus it is likely that they are also used by SSR42. Performing a whole genome wide interaction prediction using IntaRNA a potential direct interaction with *esx*A, *ure*A and *spl*B mRNA was identified (table 4.14, Appendix table 7.14). The expression of those genes was found to differ significantly between wild-type bacteria and a ΔSSR42 mutant. The expression of those genes could thus be governed by a direct interaction with SSR42 using one of the above-mentioned mechanisms. However, further analysis is required to identify the additional regulatory mechanisms employed by ncRNA SSR42. RNA-Pulldown approaches and gradient sequencing (Grad-seq) were applied as approaches to identify direct targets and interaction partners of SSR42. However, the establishment of RNA-pulldown approaches was not

successful and Grad-seq could only be used for establishment of a RNA interactome due to degradation of the protein fractions. Correlation analysis of Grad-seq obtained sequence reads revealed several mRNAs that displayed high resemblance to the sequence read profile of SSR42 (table 4.13). However, Grad-seq exploits physical properties for separation of single RNA, RNA-RNA or RNA-protein complexes (Smirnov et al., 2016). Thus, Grad-seq does not necessarily reveal direct interaction of RNAs but rather indicates similarities in physical properties or potential similar binding partners such as RNA-binding proteins. Interaction of RNAs with a similar RNA-binding protein may therefore result in complexes of similar size and physical properties, which would be represented by similar Grad-seq profiles. Appearance of a ncRNA together with target mRNAs in a specific gradient does not confirm a direct interaction but could further strengthen the previous findings and give a hint for the involvement of further factors such as RNA-binding proteins implicated in the regulatory process (Smirnov et al., 2016). Unfortunately, the protein fractions could not be analysed and thus the interaction of SSR42 with RNA-binding proteins remains elusive. Among the mRNAs, which displayed the highest similarity towards the Grad-seq profile of SSR42 RSAU_002216 mRNA, diverse ribosomal protein encoding mRNAs, *wal*K, two sRNAs of unknown function (sRNA_00095; sRNA_00320) and *agrB* were detected (table 4.12). The high similarities of those RNA species towards the SSR42 profile indicates potential interaction with common RNA-binding proteins or the involvement of those RNAs in common RNA-protein complexes. *S. aureus* expresses various RNA-binding proteins such as the RNA-chaperon Hfq, DEAD-box RNA helicase CshA and several ribonucleases like RNase Y, RNase III, RNase J1 and J2, PNPase and MazF. Further, regulatory proteins such as SarA were demonstrated to exhibit RNA-binding abilities (Roberts et al., 2006). While interaction of SSR42 with RNase Y was predicted by a global EMOTE screen (Khemici et al., 2015) and demonstrated via Northern blot analysis in the present study (Fig. 4.5) not much is known about other proteins interacting with SSR42.

Despite being part of the degradosome complex of *S. aureus* and affecting the bulk mRNA turnover (Giraud et al., 2015) DEAD-box RNA-helicase CshA was reported to confer a protecting role for most house-keeping mRNAs, *sar*A mRNA and several sRNAs against degradation by toxin MazF (Kim et al., 2016). The protective function of CshA is thought to result from stabilization of selected RNAs thereby enhancing the survival of *S. aureus* during stress-related MazF induction (Kim et al., 2016). Besides sRNAs such as teg049, SSR42 was detected amongst the RNAs, which displayed reduced stability in absence of *csh*A upon induction of toxin MazF (Kim et al., 2016). The protective role of CshA is most likely carried out by a direct interaction of SSR42 and RNA-binding protein CshA thereby enhancing the stability of this ncRNA. Moreover, *clf*A transcripts were found less abundant in *csh*A mutants after induction of ribonuclease MazF (Kim et al., 2016). In the present study *clf*A was identified as a target of SSR42. Further the *clf*A mRNA exhibited a strong correlation with SSR42 in the Grad-seq profile (pearson correlation coefficient: 0.96). Thus, DEAD box helicase CshA is a potential interaction partner

of SSR42 and *clf*A mRNA potentially forming a complex involving both molecules. Regulation of *clf*A by SSR42 could therefore involve the action of RNA-binding protein CshA.

SarA itself has been shown to mediate the stability and degradation properties of a variety of RNA species in *S. aureus* UAMS-1 (Roberts et al., 2006) including that of several mRNAs which displayed a strong correlation with the SSR42 Grad-seq profile conducted in the present study (table 4.11; *rpl*O, *rpl*Q, *rpl*N, *rpl*K, *rsp*E, *ahp*F, *pdh*A, *pdh*C, *ssb*, *hup* and *tuf*). Thus, next to CshA, these data suggested SarA as one of the RNA-binding proteins interacting with SSR42 to form complexes with other mRNAs. As another potential interaction partner of SSR42 and the mRNAs exhibiting a high correlation towards the SSR42 Grad-seq profile Hfq, a RNA-chaperon facilitating ncRNA-mRNA interactions, was suggested. In strain 8325-4 deletion of *hfq* has been shown to result in down-regulation of various genes (Liu et al., 2010) whose expression was also affected by deletion of SSR42: *spl*A, *spl*B, *spl*C, *spl*F, *coa*, *fnb*B and *lrg*A (table 4.2, 4.3, see Appendix table 7.5, 7.6). Pulldown of Hfq in the same study revealed interaction next to *spl*A, *spl*B, *spl*C, *spl*F with *rpl*Q, *rpl*O and *rpl*K (Liu et al., 2010), which were top hits in the Grad-seq correlation study (table 4.12, 4.13). The high overlap between factors down-regulated in Δ*hfq* or ΔSSR42 mutants indicates a potential interaction of both factors. Hfq could thus be involved in facilitating the interaction between SSR42 and target mRNAs such as *spl*A, *spl*B thus, explaining the overlap of the SSR42 and Hfq regulon.

Further, a high number of mRNA species, previously identified as targets of SSR42 during the transcriptome and proteome studies, displayed high correlation with the SSR42 Grad-seq profile of SSR42 confirming regulation by SSR42 once more (table 4.13). Using interaction prediction *esx*A was suggested to directly interact with SSR42. The high similarity of the Grad-seq profile of both SSR42 and *esx*A strengthend this hypothesis further.

Grad-seq further obviated potential translation of the predicted ORFs within the sequence of *S. aureus* due to the absence of SSR42 in the highest fractions in which ribosomal protein complexes typically appear (Smirnov et al., 2016). Morover, mutation of the start codon of the largest predicted ORF within SSR42 (ORF 3, Fig. 4.57) did not affect haemolysis regulation confirming the non-coding nature of SSR42.

In summary, SSR42 was identified as an important global regulator affecting virulence, pathogenesis in murine infection models and intracellularity via formation of SCVs. While for regulation of haemolysis an interaction with SaeRS via stabilization of *sae* transcript T1 and T2 was idenfied the further regulatory mechanisms remain elusive. Grad-seq and interaction predictions provided hints for direct interaction of ncRNA SSR42 with target mRNAs such as *esx*A as well as regulation via interaction with RNA-binding proteins such as Hfq, CshA and SarA.

5.5 SSR42 - an important point of intersection for virulence regulation

Virulence regulation in *S. aureus* displays a complex hierarchical process integrating a plethora of different regulators. In order to estimate the position and function of SSR42 in this regulatory network, the activity of P_{SSR42} was analysed in a variety of mutants. While in mutants lacking functional Rsp no P_{SSR42} activity was detected, hence confirming previous data (Das et al., 2016, Fig. 4.45), P_{SSR42} activity was drastically and significantly altered in mutants in *agr*A, *sar*U, *cod*Y, σB, *sae*S, *arl*RS, *ccp*E and *rpi*Rc (Figs. 5.3, 4.46-51). In contrast, mutation in σS, *vra*RS, *srr*AB, *pkn*B, *vfr*B and *rot* did affect P_{SSR42} activity less drastic while mutation of *sae*R, *sar*A, *sar*T and *rny* did not affect the promotor activity of SSR42. Disruption of *agr* expression resulted in a P_{SSR42} activity profile characterized by a long phase of reduced activity followed by a strong activity starting approximately at 16 h of growth. Finally, P_{SSR42} activity exceeded that of wild-type bacteria afterwards (Fig. 4.46A). With *sar*U as an activator of *agr* (Manna and Cheung, 2003) the P_{SSR42} activity reflected that of *agr*A mutants (Fig. 4.47B). In contrast, insertional disruption of *arl*RS resulted in a higher P_{SSR42} activity (Fig. 4.46D). Two-component system ArlRS was shown to positively regulate the expression of *agr* (Liang et al., 2005). However, its influence on haemolysis is controversial (Fournier et al., 2001; Walker et al., 2013; Radin et al., 2016). In an early study lack of *arlR* resulted in an increase of α-toxin production and transcriptional fusion revealed a role for ArlR in repression of *hla* transcription (Fournier et al., 2001), which would be in line with the observed higher activity of P_{SSR42} in mutants in *arlR* or *arlS*. However, newer studies could not confirm regulation of *hla* by ArlRS (Walker et al., 2013; Radin et al., 2016; Liang et al., 2005). Thus, the impact of ArlRS on SSR42 transcription and hence haemolysis regulation needs further investigation. Disruption of two other two-component systems, SrrAB and VraRS, which are implicated in altered β-lactam susceptibility (Kuroda et al., 2003; Matsuo et al., 2010), only slightly reduced the activity of P_{SSR42} (Fig. 4.46 E-F), while lack of functional σB, *rsb*U, *cod*Y and *ccp*E resulted in a strong overall reduction of P_{SSR42} activity (Figs. 4.48, 4.49). In addition to the reduced activity the second peak of activation, which occurs in wild-type JE2 typically after 9 h of growth was lost. Appearance of such a sigmoid P_{SSR42} activity profile was further found to be dependent on the genetic background and observed in *S. aureus* JE2, MW2 and Newman. In strains 6850, COL, Cowan I, HG003 and RN4220 instead, the P_{SSR42} activity peaked at transition to stationary growth phase (Fig. 4.30). Since this one-peak activity profile was observed in both highly cytotoxic (6850) as well as laboratory non-cytotoxic strains (RN4220, Cowan I), it was concluded that the expression profile does not correlate with virulence, haemolysis nor methicillin resistance.

σB has been demonstrated to positively affect the regulation of 120 genes in response to various conditions (Pané-Farré et al., 2006; Bischoff et al., 2004). Among the target genes other transcriptional regulators such as SarA and SarS, SA2147 (BglG family/DNA-binding protein) and SA2555 (LysR-type transcriptional regulator) (Pané-Farré, et al., 2006; Bischoff et al., 2004) were found. Despite the strong

impact of σB on P_{SSR42} activity no typical binding sites were found in the promotor region of SSR42. Thus, regulation of SSR42 by σB has to be executed indirectly. In line with this lack of functional RsbU, an activator of σB (Pané-Farré et al., 2009), resulted in a similar P_{SSR42} activity. σB mutants are characterized by increased haemolysis (Mitchell et al., 2013), enhanced *sae* P1 activity (Geiger et al., 2008) and hence increased *sae* transcript levels (Cheung et al., 1999). Whereas stabilization of *sae* T1 and T2 transcripts was found to be modulated by SSR42 (Fig. 4.25B-C) and P_{SSR42} activity is strongly affected by σB (Fig. 4.48), deletion of σB should thus result in reduced SSR42 and *sae* mRNA levels and subsequent reduced haemolysis. However, since σB is regulating a plethora of other regulators such as SarS (Bischoff et al., 2004), an inhibitor of *hla* expression (Tegmark et al., 2000; Oscarsson et al., 2006), the lack of σB could result in increased haemolysis by means of reduced *sar*S transcription. Moreover, σB could act in concert with additional other activators or repressors, which would result in the observed effect on haemolysis regulation.

Insertional disruption of *cod*Y resulted in a strong decrease in P_{SSR42} activity (Fig. 4.49B). The profile of P_{SSR42} activity strongly resembled that of mutants in σB and *rsb*U (Fig. 4.48B). Since the promotor sequence of SSR42 lacks typical *cod*Y binding motives and SSR42 was not identified among the direct binding partners of CodY (Majerczyk et al., 2010), data suggested that CodY may regulate SSR42 transcription indirectly by means of other regulatory factors. Potential factors by which SSR42 transcription regulation could be governed include RsbU, the activator of σB and RpiRc, which were both found under control of CodY (Majerczyk et al., 2010). The strongly reduced P_{SSR42} activity in insertional mutants in *cod*Y should result in reduced *sae* levels since SSR42 was demonstrated to stabilize *sae* T1 and T2 transcripts (Fig. 4.25). However, two CodY binding sites were recently identified in the *sae* P1 promotor suggesting direct regulation of *sae* expression by CodY (Mlynek et al., 2018). Hence, expression of *sae* was found enhanced in mutants lacking functional CodY. In addition, mutants in *codY* were reported to display enhanced *hla* mRNA and α-toxin levels and subsequent enhanced haemolytic activity (Majerczyk et al., 2008) which would be contradictory to the decreased P_{SSR42} activity since SSR42 was demonstrated to be required for efficient *hla* transcription. CodY regulates the expression of a total 203 genes among which 179 are repressed by CodY (Majerczyk et al., 2010). Direct targets of CodY include the quorum-sensing response regulator encoding gene *agr*A and its effector RNAIII as well as *sae*S (Majerczyk et al., 2010). Knockout of *cod*Y was further shown to negatively affect transcription of SarA family transcriptional regulator SarS, σB activator RsbU and other transcriptional regulators (Majerczyk et al., 2010). Haemolysis regulation is a complex multifactorial process involving a plethora of different regulators. Hence, enhanced haemolysis in mutants lacking CodY could be governed by overexpression of *agr* and *sae* despite reduced SSR42 transcript levels. In addition, the reduced SarS levels would diminish its repressing effect on *hla* transcription.

Insertional disruption of *ccp*E drastically diminished the activity of P_{SSR42} preventing the second peak in promotor activation (Fig. 4.49D), usually observed in wild-type bacteria during late stationary growth phase. Despite reduced SSR42 transcript levels *hla* transcript levels were reported to be enhanced in *ccp*E mutants. Besides enhanced *hla* transcription mutants in *ccp*E exhibit increased RNAIII levels (Hartmann et al., 2014). Hence, enhanced *hla* transcription may be governed indirectly by RNAIII via inhibition of translation of *rot* mRNA, encoding an inhibitor of *hla* transcription (Geisinger et al., 2006). Deletion of *rpi*Rc reduced the activity of P_{SSR42} significantly (Fig. 4.49A). RpiRc was shown to function as a metabolite-responsive modulator affecting both metabolism via regulation of pentose phosphate pathway genes as well as virulence via regulation of RNAIII (Gaupp et al., 2016). Mutants in *rpi*Rc were characterized by increased RNAIII and *hla* levels resulting in increased haemolysis (Gaupp et al., 2016) despite reduced SSR42 transcription. The impact of RpiRc on RNAIII and haemolysis regulation was suggested to be executed by the help of other regulators such as SarA and σB (Gaupp et al., 2016). However, while σB was shown to modulate P_{SSR42} activity, no role for SarA was detected in this process. Moreover, insertional disruption of factty acid kinase encoding gene *vfr*B reduced the SSR42 promotor activity (Fig. 4.46G). Fatty acid kinase VfrB was firstly identified in a transposon mutant screen searching for mutants with altered haemolytic activities. Mutants in *vfr*AB are characterized by reduced haemolysis on sheep blood agar (Bose et al., 2014) and VfrB was later implicated in regulation of *hla* and *coa* promotor activities via modulation of the SaeRS system (Krute et al., 2017). The relationship found between VfrB and SSR42 hence is in accordance with the demonstrated regulatory impact of SSR42 on regulation of *coa* and *hla* promotor activities (Fig. 4.27). Lack of VfrB hence results in decreased SSR42 levels and subsequent reduced transcription of *coa*, and *hla*. The data obtained in the present study suggest that SSR42 is mediating the observed effects of *vfr*B mutants, hence constituting the executing factor for regulation of the SaeRS two-component system while only an indirect role for VfrB was suggested.

SSR42 was thus shown to be regulated by various global regulators including two-component systems, alternative sigma-factors and metabolite-responsive modulators. The complex regulation by various factors suggests that SSR42 may constitute an important point of intersection for handling the input from various regulators in order to modulate virulence accordingly. Estimating the position of SSR42 in the regulatory complex of haemolysis regulation, thus illustrated the involvement of multiple global regulators in haemolysis regulation and highlighted the complexity of this process in *S. aureus*. However, due to the complexity the complete regulatory network is not yet understood in its entirety and further investigations will be required.

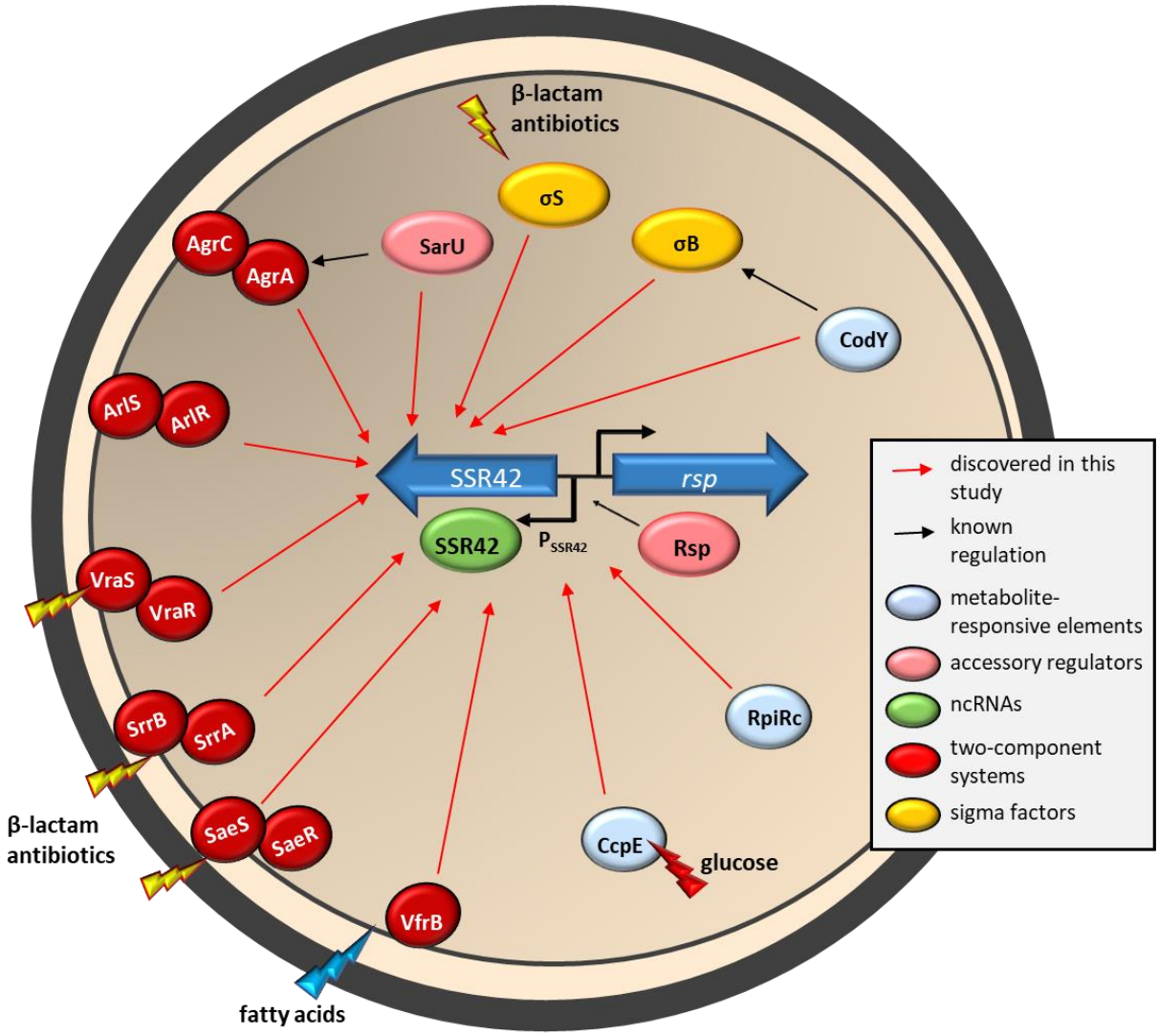

Figure 5.3: Schematic summary of transcriptional regulation of SSR42 by various global regulators. Summary of the regulators modulating transcription of SSR42 identified in this study. Newly identified regulatory relationships are illustrated by red arrows while known regulations are shown in black. Various substances were identified to modulate transcription of SSR42. Influence of those substances on regulators implicated in transcriptional regulation of SSR42 are pictured by lightning bolts. Adapted from Horn et al., 2018b.

5.6 ncRNA SSR42 - a new link between metabolism and virulence

S. aureus is a successful pathogen colonizing and infecting various environments. Part of its success as a pathogen is the ability to easily adapt to the different environments inside the host. A prerequisite for the adaption is the sensing of differences in nutrient, oxygen and iron availability and the capability to modulate the expression of virulence determinants accordingly. For this, *S. aureus* expresses several so-called metabolite-responsive modulators including CodY, RpiRc and CcpE.

In this study SSR42 was demonstrated to be under control of various global regulators. However, whereas SSR42 promotor activities in *cod*Y and *rpi*Rc mutants were drastically reduced (Fig. 4.49), SSR42 transcript levels were found unaltered in the mutants compared to wild-type bacteria (Fig. 4.52).

While the transcript level analysis was performed with bacteria aerobically cultured in Erlenmeyer flasks the promotor activity studies were performed in a TECAN Infinite M200 microplate reader in which rather imperfect, microaerophilic growth conditions predominate due to the reduced flask-to-medium ratio (Somerville and Proctor, 2013). *S. aureus* is a facultative anaerobe and hence well adapted to low-oxygen environments. During growth in oxygen-limited environments the metabolome of *S. aureus* was reported to change, which is illustrated by a reduced TCA cycle activity (Ledala et al., 2014). The changes in the metabolome result in accumulation of incompletely oxidized carbon compounds such as lactic and acetic acid (Somerville et al., 2003), which alter the pH of the culture medium. Such changes in the metabolism could be perceived by metabolite-responsive regulators such as CodY or RpiRc. Thus, the discrepancies between the regulatory impact of CodY and RpiRc on SSR42 transcription regulation could have resulted from the different growth conditions and subsequent differences in metabolic activities.

Growing *S. aureus* in the presence of various glucose concentrations resulted in differences in the P_{SSR42} activity. Interestingly, while P_{SSR42} activity was dependent on the genetic background when bacteria were grown under standard glucose concentrations, varying the glucose concentrations had similar end results on the P_{SSR42} activity profile (Fig. 4.39). Increasing the glucose concentration resulted in a decrease of the activity of P_{SSR42} in both *S. aureus* 6850 and JE2. While a decrease in the glucose concentrations enhanced the activity of P_{SSR42} in strain 6850, the activity was reduced in strain JE2 to a similar level observed in strain 6850. Further, omission of glucose enhanced the growth of both JE2 and 6850 and resulted in similar P_{SSR42} activities in both strains characterized by a peak at transition to stationary growth phase. In addition, expression of α-toxin was reported to be modulated in response to different glucose concentrations (Duncan and Cho, 1972). Since SSR42 was demonstrated to be required for *hla* transcription and SSR42 transcription was found to vary in presence of different glucose concentrations, SSR42 was proposed to be responsible for the glucose-dependent differences in α-toxin expression observed by Duncan and Cho (Duncan and Cho, 1972). These differences observed in SSR42 transcription may modulate the impact of SSR42 on virulence regulation, thereby resulting in glucose-dependent changes in virulence regulation. The initial differences in the P_{SSR42} activity observed in different strains (see section 5.1) could thus not only be governed by differences in the regulation of SSR42 transcription but further result from metabolic differences.

The response of P_{SSR42} activity to the glucose concentration of the surrounding environment may represent a mechanism of *S. aureus* to adapt virulence to the respective host environment. Different host environments are characterized by distinct glucose concentrations. While the low glucose concentration (6.3 mM) used in this study reflects the concentration typically found in human blood (Guemes et al., 2016), the higher glucose concentrations may instead reflect the situation found in distinct tissue and organs such as the liver (Wals and Katz, 1993). Thus, the glucose-dependent

transcriptional regulation of SSR42 may illustrate an adaption mechanism towards different host niches to establish different manifestations of infection.

In the present study SSR42 transcription was demonstrated to be under control of various metabolite-responsive factors such as CcpE, which was reported to repress transcription of TCA cycle genes as well as various virulence factor encoding genes as well as RNAIII in the presence of glucose (Hartmann et al., 2014). CcpE would thus constitute an ideal factor governing glucose-dependent transcription of SSR42. Further factors governing glucose-dependent SSR42 regulation could constitute CodY, RpiRc or CcpA. While for CcpA a role in glucose-dependent regulation of virulence genes was reported (Seidl et al., 2009), CodY and RpiRc are not known to regulate gene expression dependent on the glucose availability. Next to glycolysis, glucose can be metabolized via the pentose-phosphate pathway, which is regulated by RpiRc (Gaupp et al., 2016). Thus, the glucose concentration could be indirectly linked to RpiRc via regulation of the pentose-phosphate pathway. In absence of glucose *S. aureus* can utilize amino acids as carbon source which would reduce the pool of branched-chain amino acids and the regulatory impact of CodY (Majerczyk et al., 2010). This could indirectly link SSR42 transcription, that was shown to be strongly dependent on CodY, to the glucose availability and the metabolic state of *S. aureus*.

The stationary growth phase of bacteria is characterized by a slow growth rate resulting from a decrease in an essential nutrient such as glucose or by accumulation of growth-inhibitory by-products of metabolism such as lactic and acetic acid. Accumulation of those substances results in a decrease in the pH of the surrounding medium (Somerville et al., 2003). As previously discussed, the activity of P_{SSR42} was found to differ significantly between *S. aureus* JE2 and 6850 during stationary growth phase and was assumed to partially result from differences in metabolic activities. In addition, measuring the pH of consumed culture supernatant revealed another difference between strain 6850 and JE2. While culture supernatants were acidified for strain 6850 (pH: 5.2), supernatants of strain JE2 remained rather neutral (pH: 8.0). *S. aureus* JE2 harbours the arginine catabolic mobile element (ACME), which is prevalent among methicillin-resistant isolates of sequence type 8. ACME harbours the *arc* genes encoding components of an arginine deaminase pathway, which metabolizes L-arginine to CO_2, ATP and ammonia (Shore et al., 2011). ACME contributes to the success of isolates from sequence type 8 facilitating the persistence on human skin and within cutaneous abscesses due to a higher resistance against organic acids and polyamines in the skin (Thurlow et al., 2013). ACME further promotes the survival of *S. aureus* in acidic conditions via accumulation of ammonia which buffers the pH of the surrounding environment (Thurlow et al., 2013). The elevated pH of consumed culture supernatant of strain JE2, therefore results from disarming the growth-inhibiting effect of accumulating acids via production of ammonia. This can further be observed in the higher growth rate of strain JE2 compared to strain 6850. Expression of the arginine deaminase and the resulting metabolism and growth

advantages may contribute to the higher transcription of SSR42. However, ACME is not present in strains Newman and MW2, which exhibited the sigmoid shaped P_{SSR42} activity profile as well.
In summary, SSR42 transcription is modulated by the availability of glucose presumably via metabolite-responsive elements such as CcpE, CcpA, CodY or RpiRc. Thus, SSR42 constitutes a further factor linking metabolism and virulence gene expression in *S. aureus* and may contribute to the success of the pathogen.

5.7 Defence mechanism: SSR42-dependent induction of virulence under sub-lethal concentrations of antibiotics

The enhancement of haemolysis and toxin production upon exposure to sub-inhibitory concentrations of antibiotics, especially β-lactam antibiotics, is a long-known phenomenon. Lincosamines, erythromycin and chloramphenicol were reported to alter the fibronectin binding abilities of *S. aureus* (Proctor et al., 1983), whereas clindamycin and doxycycline were shown to enhance uptake of bacteria by polymorphonuclear neutrophils (Milatovic, 1982). Sub-inhibitory concentrations of antibiotics were further demonstrated to influence the production of toxic shock syndrome toxin-1 (TSST-1) (Dickgiesser and Wallach, 1987), to affect the expression of Panton-Valentine leukocidin (Dumitrescu et al., 2007) and biofilm formation (Mirani and Jamil, 2011; Haddadin et al., 2010; Subrt et al., 2011). In this regard especially β-lactam antibiotics such as oxacillin were found to alter the toxin expression profile (Rudkin et al., 2014) and enhance *hla* transcription in *S. aureus* (Ohlsen et al., 1998). Since sub-inhibitory concentrations of oxacillin have been previously reported to enhance haemolysis (Kuroda et al., 2007; Ohlsen et al., 1998) and induce the activity of the *hla* promotor (Ohlsen et al., 1998), the role of SSR42 in this process was investigated. Using β-galactosidase and GFP reporter constructs the promotor activity of SSR42 was found enhanced upon challenge with various antibiotics (Figs. 4.33, 4.36). Especially sub-inhibitory concentrations of β-lactam antibiotics were found to enhance the activity of P_{SSR42} (Figs. 4.33, 4.36). Interestingly the DNA-damaging agent mitomycin C induced P_{SSR42} activity similar to β-lactam antibiotics (Fig. 4.34). β-lactam antibiotics and Mitomycin C are long known to induce the bacterial SOS response, which was also demonstrated for *S. aureus* (Anderson et al., 2006). However, the mitomycin C dependent activation of P_{SSR42} activity was still observed in a *lex*A-G94E mutant (Fig. 4.34) incapable of triggering SOS response (Schröder et al., 2013). Since the *lex*A mutant was still capable of mitomycin C-dependent induction of P_{SSR42} activity, it was concluded that SSR42 transcription is independent of LexA derepression. However, it can not be excluded that a mechanism other than SOS response is involved in the activation of P_{SSR42}. The exact mechanisms of transcriptional activation of SSR42 upon stimulation with antibiotics and mitomycin C thus needs further investigations.

In addition, SSR42 was demonstrated to induce haemolysis by means of *hla* transcription upon stimulation with sub-inhibitory concentrations of oxacillin (Figs. 4.41, 4.42). Although exhibiting resistance against oxacillin, the SSR42 dependent increase in P_{hla} activity was further observed for strain JE2. However, higher oxacillin concentrations had to be used (Fig. 4.42B). With α-toxin as a previously identified major factor triggering host cell death in strain 6850 (Fig. 4.18), toxicity towards HeLa 2000 cells was found enhanced when sub-inhibitory concentrations of oxacillin were present in the cell culture medium. This oxacillin dependent enhancement in cytotoxicity of *S. aureus* was strictly dependent on presence of SSR42 (Fig. 4.43). However, due to the low half-live of oxacillin and the reduced intracellular activity (Jo et al., 2011; Egert et al., 1977) a high concentration of oxacillin had to be used. CFU enumeration, though, obviated a potential bactericidal or cytotoxic effect. During the course of infection bacteria can be exposed to sub-inhibitory concentrations of antibiotics at the beginning and end of treatment with antibiotics or during low-dosage therapy and could thus encounter a so-called post-antibiotic sub-MIC effect (Odenholt, 2001). Bacterial cells inside a biofilm were further shown to receive only lower dosages of antibiotics than single cells (Singh et al., 2010). Treatment with too low dosages of antibiotics or with antibiotics for which resistances exist could thus induce up-regulation of SSR42 transcription, which would hence enhance haemolytic and cytotoxic activity. α-toxin was demonstrated to play a crucial role in pathogenesis of a multiplicity of infections such as pneumonia (Bubeck Wardenburg and Schneewind, 2008), corneal infection (O`Callaghan et al., 1997) and sepsis (Powers et al., 2015), thus stressing the importance of ncRNA SSR42 in virulence regulation and especially stress-related virulence regulation of *S. aureus*. The enhancement of SSR42 transcription and subsequent *hla* transcription observed suggests that treatment with the wrong antibiotics or low application rates may enhance bacterial pathogenesis and disease outcome via transcriptional up-regulation of ncRNA SSR42 and hence could rather worsen than improve the outcome of staphylococcal infections. Thus, antibiotic treatment of *S. aureus* infections could in some cases not only be ineffective but even worsen the course of infection. The mechanisms underlying the perception of antibiotics are highly unknown in *S. aureus*. The expression of *sae*RS and alternative sigma-factor *sig*S were demonstrated to be inducible by sub-inhibitory concentrations of oxacillin (Miller et al., 2012, Geiger et al., 2008; Ohlsen et al., 1998; Kuroda et al., 2007) and may thus be involved in this process. Further, two-component system VraRS was shown to play a crucial role in resistance against β-lactam antibiotics (Yin et al., 2006; Gardete et al., 2006). However, no role for VraRS in haemolysis regulation is known. Thus, the exact mechanism of antibiotic perception and up-regulation of SSR42 transcription remains elusive and needs further investigations.

Treatment of *S. aureus* JE2 but not strain 6850 with sub-inhibitory concentrations of colistin reduced the activity of P_{SSR42} drastically (Fig. 4.35). A recent study investigated the transcriptome of *S. aureus* HG001 under diverse growth conditions and found transcription of SSR42 to be reduced in the

presence of colistin (Mäder et al., 2016; SSR42 = gene/segment S1036) confirming the data conducted for strain JE2. Since in strain 6850 colistin did not reduce P_{SSR42} activity, it was concluded that colistin would decrease SSR42 transcription dependent on the genetic background. Moreover, analysis of the transcriptome of *S. aureus* HG001 did not reveal any significant differences in SSR42 transcription during different growth conditions (Mäder et al., 2016). A recent study demonstrated that treatment of *S. aureus* with myristic as well as oleic acid decreased the promotor activity of *coa*. Interestingly, for the reduction of P_{hla} activity by fatty acids a strong dependence on fatty acid kinase VfrB was reported (Krute et al., 2017). While reduction of promotor activities of the SaeRS class I target gene *coa* was less dependent on presence of VfrB, transcription of class II gene *hla* in response to myristic acid was strictly dependent on VfrB (Krute et al., 2017). In the present study, a decrease in P_{SSR42} activity upon treatment of *S. aureus* 6850 or JE2 with either oleic acid or myristic acid was demonstrated (Fig. 4.37, 4.38) as well as a SSR42-dependent regulation of P_{coa} and P_{hla} activity (Fig. 4.27). In addition to that, insertional disruption of *vfr*B resulted in an overall decrease in SSR42 promotor activity (Fig. 4.46). Since regulation of P_{hla} activity was demonstrated to be mediated by SSR42 (Fig. 4.27) this ncRNA was suggested to also be involved in the down-regulation of *hla* in the presence of myristic acid. The same mechanism would be possible for regulation of P_{coa} in the presence of fatty acids. While VfrB was identified as the factor involved in perception of myristic acid (Krute et al., 2017), the mechanism of oleic acid perception remains elusive and needs further investigation. The conducted data therefore suggest the involvement of SSR42 in executing fatty acid-dependent regulation of SaeRS class I and II target genes. The human skin produces diverse fatty acids, which exhibit bactericidal function (Cartron et al., 2014; Drake et al., 2008). Perception of fatty acids could therefore be a mechanism exploited by *S. aureus* to adapt virulence gene expression while colonizing human skin via down-regulation of SSR42. With this mechanism *S. aureus* could shift from a highly cytotoxic phenotype to a colonizing and non-cytotoxic phenotype.

In summary, transcription of SSR42 was demonstrated to be influenced by presence of subinhibitory concentrations of diverse antibiotics, mitomycin C, colistin and fatty acids. Moreover, an important role for SSR42 in the oxacillin-induced enhancement of haemolysis and cytotoxicity was identified illustrating potential challenges during antibiotic treatment of staphylococcal infections.

5.8 Future perspectives

This study aimed to characterize the 1232 nt long non-coding RNA SSR42 of *S. aureus*. By applying transcriptome and proteome analysis the regulon of SSR42 was identified and the regulatory relationship of SSR42 and AraC-transcriptional regulator Rsp was determined.

SSR42 was identified as the main regulator of Rsp-mediated virulence regarding virulence phenotypes such as haemolysis and cytotoxicity. In a recent study Rsp was identified as an important factor

mediating cytotoxicity towards neutrophils and survival upon phagocytosis by neutrophils (Das et al., 2016), thus it would be of great importance to investigate the impact of SSR42 for this phenotype.

SSR42 was identified to regulate haemolysis by means of stabilizing *sae* transcripts. However, the exact mechanism has to be investigated in further experiments. Interaction prediction as well as mutational studies suggested two sequences within SSR42, which could be implicated in direct binding to *sae* mRNA. Thus, a direct interaction of SSR42 and *sae* mRNA could be analysed using electromobility shift assays.

The identification of direct binding partners should be the focus of further studies. However, oligo-capture pulldown experiments of SSR42 failed so far due to the required long incubation which resulted in degradation of RNAs. An alternative for the pulldown approaches could exploit *in vitro* transcribed SSR42, which would be added to a precleared cell lysate of *S. aureus*. By using this approach unspecific binding of proteins and RNAs to a biotin-labelled oligo would be reduced, which would facilitate the binding of SSR42. Moreover, using this approach would the incubation time could be drastically reduced which would hence limit potential processing events and degradation by RNases.

Further Grad-seq should be repeated for strain 6850 and JE2 to identify potential interaction partners and to gain further insight into potential protein-RNA complexes involving SSR42. Comparison of Grad-seq profiles from different strains could further reveal differences in the regulatory impact of SSR42.

By using promotor activity studies the position of SSR42 within the regulator network of virulence regulation in *S. aureus* was estimated. Since for several regulators such as σB and CodY a direct interaction with SSR42 is unlikely due to the absence of typical bindig sites, the mechanism of transcriptional regulation should be the focus of further studies. For this, the promotor activity of SSR42 should be investigated in several double or triple mutants of regulators. Further, successful pulldown approaches or analysis of the protein fractions of Grad-seq could reveal potential interactions with regulators.

Since in this thesis a strong role of the genetic background on SSR42 transcription and the impact on virulence regulation was observed, comparative analysis of different strains should be performed in order to gain insight into strain-specific regulatory differences. For this, transcriptomes and proteomes of SSR42 mutants from different genetic backgrounds could be compared. Further, it would be of great interest to identify differences in the regulation of SSR42 in different *S. aureus* strains. This could be achieved by transferring the insertional mutations from JE2 obtained from the Nebraska mutant library into the genetic background of other strains. The SSR42 promotor activity could subsequently be analysed in those mutants and differences in the regulation of SSR42 would be identified.

In this thesis a SSR42 dependent up-regulation of haemolysis and cytotoxicity upon stimulation with sub-inhibitory concentrations of antibiotics was demonstrated. However, cell culture-based studies often do not reflect *in vivo* situations. Thus, infection experiments should be performed *in vivo*

investigating the role of SSR42 in oxacillin-induced up-regulation of α-toxin expression. Since α-toxin plays a crucial role for establishment of pneumonia, murine lung infection models should be used for these experiments. Mice could therefore be infected with wild-type bacteria and mutants lacking SSR42 and simultaneously be challenged with sub-inhibitory concentrations of oxacillin. However, due to the reduced intracellular activity of oxacillin the pharmacokinetics and availability of oxacillin have to be investigated beforehand, in order to establish sub-inhibitory concentrations in the lungs. For simplification the oxacillin resistant strain JE2 could be used and higher oxacillin concentrations could be applied. This would overcome the necessity of using exact sub-inhibitory concentration. Thus, oxacillin could be applied in a concentration, which would normally be used for treatment of infections. Further, the identification of the factors mediating perception of sub-inhibitory concentrations of antibiotics and subsequent transcriptional activation of SSR42 would be of great interest. Candidates, which should be the focus of further studies, are the SaeRS two-component system, VraRS and σS. The oxacillin-induced enhancement of P_{SSR42} activity and the SSR42-dependent up-regulation of haemolysis should hence be analysed in mutants of above mentioned regulators. Moreover, the glucose dependent regulation of SSR42 should be addressed and studied in metabolite-responsive mutants such as CodY, RpiRc and CcpE. In addition, the perception of fatty acids and modulation of SSR42 transcription should be analysed in further studies. Since data suggested that fatty acid dependent down-regulation of P_{coa} and P_{hla} is mediated via SSR42, the promotor profiles of both *coa* and *hla* should be analysed upon stimulation with fatty acids in mutants lacking SSR42. Further, the impact of SSR42 on the stability of *sae* mRNA should be investigated after stimulation with β-lactam antibiotics or fatty acids, since regulation of *hla* and *coa* expression presumably is carried out via regulation of *sae*.

Investigating the regulatory mechanism of SSR42 a precise secondary structure would help to identify potential functional structures within SSR42. However, experimental analysis of secondary structures is limited for long RNAs. Thus, further studies constructing stable minimal versions of SSR42 that are still functional regarding haemolysis regulation would help to artificially create a shorter functional RNA molecule that could be used in experimental approaches to investigate the secondary structure of SSR42.

In this study a potential role for SSR42 in mediating SCV formation and persistence was found. During chronic infection a ΔSSR42 mutant was not completely eradicated by the host immune system. Therefore, it would be of great importance to compare the transcriptome of wild-type bacteria and ΔSSR42 mutant during the acute and chronic phase of infection. By doing so, further factors involved in this pre-stage of persistence could be identified and serve as potential targets for new antibacterial strategies to eradicate persistent and reoccurring infections. This would be of great value since treatment of staphylococcal infection is impeded by the rise of antibiotic resistances.

6 REFERENCES

Abraham M, Dror O, Nussinov R, Wolfson HJ. 2008. Analysis and classification of RNA tertiary structures. RNA 14:2274-2289.

Abu-Qatouseh LF, Chinni SV, Seggewiss J, Proctor RA, Brosius J, Rozhdestvensky TS, Peters G, von Eiff C, Becker K. 2010. Identification of differentially expressed small non-protein-coding RNAs in *Staphylococcus aureus* displaying both the normal and the small-colony variant phenotype. J Mol Med (Berl) 88:565-75.

Adhikari RP, Novick RP. 2008. Regulatory organization of the staphylococcal *sae* locus. Microbiology 154:949-59.

Agarwal H, Verrall R, Singh SP, Tang YW, Wilson G. 2007. Small colony variant *Staphylococcus aureus* multiorgan infection. Pediatr Infect Dis J 26:269-71.

Agerer F, Michel A, Ohlsen K, Hauck CR. 2003. Integrin-mediated invasion of *Staphylococcus aureus* into human cells requires Src family protein-tyrosine kinases. J Biol Chem 278:42524-31.

Alonzo F, Torres VJ. 2014. The Bicomponent Pore-Forming Leucocidins of *Staphylococcus aureus*. Microbiology and Molecular Biology Reviews : MMBR 78:199-230.

Alonzo F, 3rd, Kozhaya L, Rawlings SA, Reyes-Robles T, DuMont AL, Myszka DG, Landau NR, Unutmaz D, Torres VJ. 2013. CCR5 is a receptor for *Staphylococcus aureus* leukotoxin ED. Nature 493:51-5.

Alonzo F, 3rd, Benson MA, Chen J, Novick RP, Shopsin B, Torres VJ. 2012. *Staphylococcus aureus* leucocidin ED contributes to systemic infection by targeting neutrophils and promoting bacterial growth in vivo. Mol Microbiol 83:423-35.

Anderson KL, Roux CM, Olson MW, Luong TT, Lee CY, Olson R, Dunman PM. 2010. Characterizing the effects of inorganic acid and alkaline shock on the *Staphylococcus aureus* transcriptome and messenger RNA turnover. FEMS Immunol Med Microbiol 60:208-50.

Anderson KL, Roberts C, Disz T, Vonstein V, Hwang K, Overbeek R, Olson PD, Projan SJ, Dunman PM. 2006. Characterization of the *Staphylococcus aureus* heat shock, cold shock, stringent, and SOS responses and their effects on log-phase mRNA turnover. J Bacteriol 188:6739-56.

Archer NK, Mazaitis MJ, Costerton JW, Leid JG, Powers ME, Shirtliff ME. 2011. *Staphylococcus aureus* biofilms: Properties, regulation and roles in human disease. Virulence 2:445-459.

Athanasopoulos AN, Economopoulou M, Orlova VV, Sobke A, Schneider D, Weber H, Augustin HG, Eming SA, Schubert U, Linn T, Nawroth PP, Hussain M, Hammes H-P, Herrmann M, Preissner KT, Chavakis T. 2006. The extracellular adherence protein (Eap) of *Staphylococcus aureus* inhibits wound healing by interfering with host defense and repair mechanisms. Blood 107:2720-2727.

Appelbaum PC. 2007. Reduced glycopeptide susceptibility in methicillin-resistant *Staphylococcus aureus* (MRSA). Int J Antimicrob Agents 30:398-408.

Baba T, Takeuchi F, Kuroda M, Yuzawa H, Aoki K, Oguchi A, Nagai Y, Iwama N, Asano K, Naimi T, Kuroda H, Cui L, Yamamoto K, Hiramatsu K. 2002. Genome and virulence determinants of high virulence community-acquired MRSA. Lancet 359:1819-27.

Balasubramanian D, Ohneck EA, Chapman J, Weiss A, Kim MK, Reyes-Robles T, Zhong J, Shaw LN, Lun DS, Ueberheide B, Shopsin B, Torres VJ. 2016. *Staphylococcus aureus* Coordinates Leukocidin Expression and Pathogenesis by Sensing Metabolic Fluxes via RpiRc. MBio 7.

Bandyra KJ, Said N, Pfeiffer V, Gorna MW, Vogel J, Luisi BF. 2012. The seed region of a small RNA drives the controlled destruction of the target mRNA by the endoribonuclease RNase E. Mol Cell 47:943-53.

Bantel H, Sinha B, Domschke W, Peters G, Schulze-Osthoff K, Janicke RU. 2001. alpha-Toxin is a mediator of *Staphylococcus aureus*-induced cell death and activates caspases via the intrinsic death pathway independently of death receptor signaling. J Cell Biol 155:637-48.

Barrio MB, Rainard P, Prevost G. 2006. LukM/LukF'-PV is the most active *Staphylococcus aureus* leukotoxin on bovine neutrophils. Microbes Infect 8:2068-74.

Bateman BT, Donegan NP, Jarry TM, Palma M, Cheung AL. 2001. Evaluation of a tetracycline-inducible promoter in *Staphylococcus aureus* in vitro and in vivo and its application in demonstrating the role of sigB in microcolony formation. Infect Immun 69:7851-7.

Bayles KW, Wesson CA, Liou LE, Fox LK, Bohach GA, Trumble WR. 1998. *Intracellular Staphylococcus aureus* escapes the endosome and induces apoptosis in epithelial cells. Infect Immun 66:336-42.

Beasley FC, Vines ED, Grigg JC, Zheng Q, Liu S, Lajoie GA, Murphy ME, Heinrichs DE. 2009. Characterization of staphyloferrin A biosynthetic and transport mutants in *Staphylococcus aureus*. Mol Microbiol 72:947-63.

Beaume M, Hernandez D, Farinelli L, Deluen C, Linder P, Gaspin C, Romby P, Schrenzel J, Francois P. 2010. Cartography of methicillin-resistant *S. aureus* transcripts: detection, orientation and temporal expression during growth phase and stress conditions. PLoS One 5:e10725.

Beenken KE, Mrak LN, Griffin LM, Zielinska AK, Shaw LN, Rice KC, Horswill AR, Bayles KW, Smeltzer MS. 2010. Epistatic relationships between sarA and agr in *Staphylococcus aureus* biofilm formation. PLoS One 5:e10790.

Benito Y, Kolb FA, Romby P, Lina G, Etienne J, Vandenesch F. 2000. Probing the structure of RNAIII, the *Staphylococcus aureus* agr regulatory RNA, and identification of the RNA domain involved in repression of protein A expression. RNA 6:668-679.

Benton BM, Zhang JP, Bond S, Pope C, Christian T, Lee L, Winterberg KM, Schmid MB, Buysse JM. 2004. Large-Scale Identification of Genes Required for Full Virulence of *Staphylococcus aureus*. Journal of Bacteriology 186:8478-8489.

Berman DS, Schaefler S, Simberkoff MS, Rahal JJ. 1987. *Staphylococcus aureus* colonization in intravenous drug abusers, dialysis patients, and diabetics. J Infect Dis 155:829-31.

Bhakdi S, Tranum-Jensen J. 1991. Alpha-toxin of *Staphylococcus aureus*. Microbiol Rev 55:733-51.

Bhakdi S, Muhly M, Korom S, Hugo F. 1989. Release of interleukin-1 beta associated with potent cytocidal action of staphylococcal alpha-toxin on human monocytes. Infect Immun 57:3512-9.

Bingham RJ, Rudino-Pinera E, Meenan NA, Schwarz-Linek U, Turkenburg JP, Hook M, Garman EF, Potts JR. 2008. Crystal structures of fibronectin-binding sites from *Staphylococcus aureus* FnBPA in complex with fibronectin domains. Proc Natl Acad Sci U S A 105:12254-8.

Bischoff M, Dunman P, Kormanec J, Macapagal D, Murphy E, Mounts W, Berger-Bächi B, Projan S. 2004. Microarray-Based Analysis of the *Staphylococcus aureus* σ(B) Regulon. Journal of Bacteriology 186:4085-4099.

Blättner S, Das S, Paprotka K, Eilers U, Krischke M, Kretschmer D, Remmele CW, Dittrich M, Muller T, Schuelein-Voelk C, Hertlein T, Mueller MJ, Huettel B, Reinhardt R, Ohlsen K, Rudel T, Fraunholz MJ.

2016. *Staphylococcus aureus* Exploits a Non-ribosomal Cyclic Dipeptide to Modulate Survival within Epithelial Cells and Phagocytes. PLoS Pathog 12:e1005857.

Boden MK, Flock JI. 1992. Evidence for three different fibrinogen-binding proteins with unique properties from *Staphylococcus aureus* strain Newman. Microb Pathog 12:289-98.

Bohn C, Rigoulay C, Bouloc P. 2007. No detectable effect of RNA-binding protein Hfq absence in *Staphylococcus aureus*. BMC Microbiol 7:10.

Bohn C, Rigoulay C, Chabelskaya S, Sharma CM, Marchais A, Skorski P, Borezee-Durant E, Barbet R, Jacquet E, Jacq A, Gautheret D, Felden B, Vogel J, Bouloc P. 2010. Experimental discovery of small RNAs in *Staphylococcus aureus* reveals a riboregulator of central metabolism. Nucleic Acids Res 38:6620-36.

Boles BR, Horswill AR. 2008. agr-Mediated Dispersal of *Staphylococcus aureus* Biofilms. PLoS Pathogens 4:e1000052.

Boisset S, Geissmann T, Huntzinger E, Fechter P, Bendridi N, Possedko M, Chevalier C, Helfer AC, Benito Y, Jacquier A, Gaspin C, Vandenesch F, Romby P. 2007. *Staphylococcus aureus* RNAIII coordinately represses the synthesis of virulence factors and the transcription regulator Rot by an antisense mechanism. Genes & Development 21:1353-1366.

Bose JL, Daly SM, Hall PR, Bayles KW. 2014. Identification of the *Staphylococcus aureus vfr*AB Operon, a Novel Virulence Factor Regulatory Locus. Infection and Immunity 82:1813-1822.

Bronesky D, Wu Z, Marzi S, Walter P, Geissmann T, Moreau K, Vandenesch F, Caldelari I, Romby P. 2016. *Staphylococcus aureus* RNAIII and Its Regulon Link Quorum Sensing, Stress Responses, Metabolic Adaptation, and Regulation of Virulence Gene Expression. Annu Rev Microbiol 70:299-316.

Brunskill EW, Bayles KW. 1996. Identification of LytSR-regulated genes from *Staphylococcus aureus*. Journal of Bacteriology 178:5810-5812.

Bubeck Wardenburg J, Bae T, Otto M, Deleo FR, Schneewind O. 2007. Poring over pores: alpha-hemolysin and Panton-Valentine leukocidin in *Staphylococcus aureus* pneumonia. Nat Med 13:1405-6.

Bubeck Wardenburg J, Schneewind O. 2008. Vaccine protection against *Staphylococcus aureus* pneumonia. J Exp Med 205:287-94.

Bulger RJ, Bulger RE. 1967. Ultrastructure of small colony variants of a methicillin-resistant *Staphylococcus aureus*. Journal of Bacteriology 94:1244-1246.

Bunikowski R, Mielke ME, Skarabis H, Worm M, Anagnostopoulos I, Kolde G, Wahn U, Renz H. 2000. Evidence for a disease-promoting effect of *Staphylococcus aureus*-derived exotoxins in atopic dermatitis. J Allergy Clin Immunol 105:814-9.

Burgui S, Gil C, Solano C, Lasa I, Valle J. 2018. A Systematic Evaluation of the Two-Component Systems Network Reveals That ArlRS Is a Key Regulator of Catheter Colonization by *Staphylococcus aureus*. Front Microbiol 9:342.

Burke FM, Di Poto A, Speziale P, Foster TJ. 2011. The A domain of fibronectin-binding protein B of *Staphylococcus aureus* contains a novel fibronectin binding site. Febs j 278:2359-71.

Burian M, Wolz C, Goerke C. 2010. Regulatory Adaptation of *Staphylococcus aureus* during Nasal Colonization of Humans. PLoS ONE 5:e10040.

Burton DC, Edwards JR, Horan TC, Jernigan JA, Fridkin SK. 2009. Methicillin-resistant *Staphylococcus aureus* central line-associated bloodstream infections in US intensive care units, 1997-2007. Jama 301:727-36.

Busch A, Richter AS, Backofen R. 2008. IntaRNA: efficient prediction of bacterial sRNA targets incorporating target site accessibility and seed regions. Bioinformatics 24:2849-56.

Büttner H, Mack D, Rohde H. 2015. Structural basis of *Staphylococcus epidermidis* biofilm formation: mechanisms and molecular interactions. Frontiers in Cellular and Infection Microbiology 5:14.

Carpousis AJ. 2007. The RNA degradosome of *Escherichia coli*: an mRNA-degrading machine assembled on RNase E. Annu Rev Microbiol 61:71-87.

Cartron ML, England SR, Chiriac AI, Josten M, Turner R, Rauter Y, Hurd A, Sahl HG, Jones S, Foster SJ. 2014. Bactericidal activity of the human skin fatty acid cis-6-hexadecanoic acid on *Staphylococcus aureus*. Antimicrob Agents Chemother 58:3599-609.

Cassat JE, Hammer ND, Campbell JP, Benson MA, Perrien DS, Mrak LN, Smeltzer MS, Torres VJ, Skaar EP. 2013. A secreted bacterial protease tailors the *Staphylococcus aureus* virulence repertoire to modulate bone remodeling during osteomyelitis. Cell host & microbe 13:759-772.

Cassidy P, Harshman S. 1976. Studies on the binding of staphylococcal 125I-labeled alpha-toxin to rabbit erythrocytes. Biochemistry 15:2348-55.

Castro SL, Nelman-Gonzalez M, Nickerson CA, Ott CM. 2011. Induction of attachment-independent biofilm formation and repression of Hfq expression by low-fluid-shear culture of *Staphylococcus aureus*. Appl Environ Microbiol 77:6368-78.

Cedergren L, Andersson R, Jansson B, Uhlen M, Nilsson B. 1993. Mutational analysis of the interaction between staphylococcal protein A and human IgG1. Protein Eng 6:441-8.

Chabelskaya S, Bordeau V, Felden B. 2014. Dual RNA regulatory control of a *Staphylococcus aureus* virulence factor. Nucleic Acids Res 42:4847-58.

Chambers JR, Sauer K. 2013. Small RNAs and their role in biofilm formation. Trends Microbiol 21:39-49.

Chatterjee SS, Joo H-S, Duong AC, Dieringer TD, Tan VY, Song Y, Fischer ER, Cheung GYC, Li M, Otto M. 2013. Essential *Staphylococcus aureus* toxin export system. Nature medicine 19:364-367.

Chavakis T, Hussain M, Kanse SM, Peters G, Bretzel RG, Flock JI, Herrmann M, Preissner KT. 2002. *Staphylococcus aureus* extracellular adherence protein serves as anti-inflammatory factor by inhibiting the recruitment of host leukocytes. Nat Med 8:687-93.

Chavakis T, Wiechmann K, Preissner KT, Herrmann M. 2005. *Staphylococcus aureus* interactions with the endothelium: the role of bacterial "secretable expanded repertoire adhesive molecules" (SERAM) in disturbing host defense systems. Thromb Haemost 94:278-85.

Chen PR, Bae T, Williams WA, Duguid EM, Rice PA, Schneewind O, He C. 2006. An oxidation-sensing mechanism is used by the global regulator MgrA in *Staphylococcus aureus*. Nat Chem Biol 2:591-5.

Cheng AG, Kim HK, Burts ML, Krausz T, Schneewind O, Missiakas DM. 2009. Genetic requirements for *Staphylococcus aureus* abscess formation and persistence in host tissues. Faseb j 23:3393-404.

Cheng AG, McAdow M, Kim HK, Bae T, Missiakas DM, Schneewind O. 2010. Contribution of coagulases towards *Staphylococcus aureus* disease and protective immunity. PLoS Pathog 6:e1001036.

Cheung GYC, Duong AC, Otto M. 2012. Direct and synergistic hemolysis caused by *Staphylococcus* phenol-soluble modulins: implications for diagnosis and pathogenesis. Microbes and Infection / Institut Pasteur 14:380-386.

Cheung GYC, Joo H-S, Chatterjee SS, Otto M. 2014. Phenol-soluble modulins – critical determinants of staphylococcal virulence. FEMS microbiology reviews 38:698-719.

Cheung AL, Bayer AS, Zhang G, Gresham H, Xiong YQ. 2004. Regulation of virulence determinants in vitro and in vivo in *Staphylococcus aureus*. FEMS Immunol Med Microbiol 40:1-9.

Cheung AL, Nishina KA, Pous MPT, Tamber S. 2008. The SarA protein family of *Staphylococcus aureus*. The international journal of biochemistry & cell biology 40:355-361.

Cheung AL, Yeaman MR, Sullam PM, Witt MD, Bayer AS. 1994. Role of the sar locus of *Staphylococcus aureus* in induction of endocarditis in rabbits. Infect Immun 62:1719-25.

Cheung AL, Zhang G. 2002. Global regulation of virulence determinants in *Staphylococcus aureus* by the SarA protein family. Front Biosci 7:d1825-42.

Cheung AL, Chien Y-t, Bayer AS. 1999. Hyperproduction of Alpha-Hemolysin in a sigB Mutant Is Associated with Elevated SarA Expression in *Staphylococcus aureus*. Infection and Immunity 67:1331-1337.

Chevalier C, Boisset S, Romilly C, Masquida B, Fechter P, Geissmann T, Vandenesch F, Romby P. 2010. *Staphylococcus aureus* RNAIII binds to two distant regions of *coa* mRNA to arrest translation and promote mRNA degradation. PLoS Pathog 6:e1000809.

Cho KH. 2017. The Structure and Function of the Gram-Positive Bacterial RNA Degradosome. Frontiers in Microbiology 8:154.

Cho H, Jeong DW, Liu Q, Yeo WS, Vogl T, Skaar EP, Chazin WJ, Bae T. 2015. Calprotectin Increases the Activity of the SaeRS Two Component System and Murine Mortality during *Staphylococcus aureus* Infections. PLoS Pathog 11:e1005026.

Choi CS, Yin CS, Bakar AA, Sakewi Z, Naing NN, Jamal F, Othman N. 2006. Nasal carriage of *Staphylococcus aureus* among healthy adults. J Microbiol Immunol Infect 39:458-64.

Choi JH, Seo HS, Lim SY, Park K. 2014. Cutaneous Immune Defenses Against *Staphylococcus aureus* Infections. Journal of Lifestyle Medicine 4:39-46.

Cirz RT, Jones MB, Gingles NA, Minogue TD, Jarrahi B, Peterson SN, Romesberg FE. 2007. Complete and SOS-mediated response of *Staphylococcus aureus* to the antibiotic ciprofloxacin. J Bacteriol 189:531-9.

Clarke SR, Mohamed R, Bian L, Routh AF, Kokai-Kun JF, Mond JJ, Tarkowski A, Foster SJ. 2007. The *Staphylococcus aureus* surface protein IsdA mediates resistance to innate defenses of human skin. Cell Host Microbe 1:199-212.

Clemens DL, Lee BY, Horwitz MA. 2004. Virulent and avirulent strains of *Francisella tularensis* prevent acidification and maturation of their phagosomes and escape into the cytoplasm in human macrophages. Infect Immun 72:3204-17.

Coleman D, Knights J, Russell R, Shanley D, Birkbeck TH, Dougan G, Charles I. 1991. Insertional inactivation of the *Staphylococcus aureus* beta-toxin by bacteriophage phi 13 occurs by site- and orientation-specific integration of the phi 13 genome. Mol Microbiol 5:933-9.

Cook HA, Furuya EY, Larson E, Vasquez G, Lowy FD. 2007. Heterosexual transmission of community-associated methicillin-resistant *Staphylococcus aureus*. Clin Infect Dis 44:410-3.

Cooper LZ, Madoff MA, Weinstein L. 1964. Hemolysis of rabbit erythrocytes by purified Staphylococcal alpha-toxin II. : Effects of Inhibitors on the Hemolytic Sequence. Journal of Bacteriology 87:136-144.

Corey GR. 2009. *Staphylococcus aureus* bloodstream infections: definitions and treatment. Clin Infect Dis 48 Suppl 4:S254-9.

Costerton JW, Stewart PS, Greenberg EP. 1999. Bacterial biofilms: a common cause of persistent infections. Science 284:1318-22.

Costerton JW, Lewandowski Z, Caldwell DE, Korber DR, Lappin-Scott HM. 1995. Microbial biofilms. Annu Rev Microbiol 49:711-45.

Crass BA, Bergdoll MS. 1986. Toxin involvement in toxic shock syndrome. J Infect Dis 153:918-26.

Crosby HA, Schlievert PM, Merriman JA, King JM, Salgado-Pabón W, Horswill AR. 2016. The *Staphylococcus aureus* Global Regulator MgrA Modulates Clumping and Virulence by Controlling Surface Protein Expression. PLOS Pathogens 12:e1005604.

Cue D, Lei MG, Luong TT, Kuechenmeister L, Dunman PM, O'Donnell S, Rowe S, O'Gara JP, Lee CY. 2009. Rbf Promotes Biofilm Formation by *Staphylococcus aureus* via Repression of *icaR*, a Negative Regulator of *ica*ADBC. Journal of Bacteriology 191:6363-6373.

Dale SE, Sebulsky MT, Heinrichs DE. 2004. Involvement of SirABC in iron-siderophore import in *Staphylococcus aureus*. J Bacteriol 186:8356-62.

Dantes R, Mu Y, Belflower R, Aragon D, Dumyati G, Harrison LH, Lessa FC, Lynfield R, Nadle J, Petit S, Ray SM, Schaffner W, Townes J, Fridkin S. 2013. National burden of invasive methicillin-resistant *Staphylococcus aureus* infections, United States, 2011. JAMA Intern Med 173:1970-8.

Darouiche RO, Landon GC, Patti JM, Nguyen LL, Fernau RC, McDevitt D, Greene C, Foster T, Klima M. 1997. Role of *Staphylococcus aureus* surface adhesins in orthopaedic device infections: are results model-dependent? J Med Microbiol 46:75-9.

Das S, Lindemann C, Young BC, Muller J, Österreich B, Ternette N, Winkler A-C, Paprotka K, Reinhardt R, Förstner KU, Allen E, Flaxman A, Yamaguchi Y, Rollier CS, van Diemen P, Blättner S, Remmele CW, Selle M, Dittrich M, Müller T, Vogel J, Ohlsen K, Crook DW, Massey R, Wilson DJ, Rudel T, Wyllie DH, Fraunholz MJ. 2016. Natural mutations in a *Staphylococcus aureus* virulence regulator attenuate cytotoxicity but permit bacteremia and abscess formation. Proceedings of the National Academy of Sciences of the United States of America 113:E3101-E3110.

David MZ, Daum RS. 2010. Community-associated methicillin-resistant *Staphylococcus aureus*: epidemiology and clinical consequences of an emerging epidemic. Clin Microbiol Rev 23:616-87.

Deivanayagam CCS, Wann ER, Chen W, Carson M, Rajashankar KR, Höök M, Narayana SVL. 2002. A novel variant of the immunoglobulin fold in surface adhesins of *Staphylococcus aureus*: crystal structure of the fibrinogen-binding MSCRAMM, clumping factor A. The EMBO Journal 21:6660-6672.

DeLeo FR, Otto M, Kreiswirth BN, Chambers HF. 2010. Community-associated meticillin-resistant *Staphylococcus aureus*. Lancet 375:1557-68.

Descloux E, Perpoint T, Ferry T, Lina G, Bes M, Vandenesch F, Mohammedi I, Etienne J. 2008. One in five mortality in non-menstrual toxic shock syndrome versus no mortality in menstrual cases in a balanced French series of 55 cases. Eur J Clin Microbiol Infect Dis 27:37-43.

de Haas CJC, Veldkamp KE, Peschel A, Weerkamp F, Van Wamel WJB, Heezius ECJM, Poppelier MJJG, Van Kessel KPM, van Strijp JAG. 2004. Chemotaxis Inhibitory Protein of *Staphylococcus aureus*, a Bacterial Antiinflammatory Agent. The Journal of Experimental Medicine 199:687-695.

Desjardins M, Huber LA, Parton RG, Griffiths G. 1994. Biogenesis of phagolysosomes proceeds through a sequential series of interactions with the endocytic apparatus. J Cell Biol 124:677-88.

DeVries AS, Lesher L, Schlievert PM, Rogers T, Villaume LG, Danila R, Lynfield R. 2011. Staphylococcal toxic shock syndrome 2000-2006: epidemiology, clinical features, and molecular characteristics. PLoS One 6:e22997.

Dickgiesser N, Wallach U. 1987. Toxic shock syndrome toxin-1 (TSST-1): influence of its production by subinhibitory antibiotic concentrations. Infection 15:351-3.

Ding Y, Liu X, Chen F, Di H, Xu B, Zhou L, Deng X, Wu M, Yang CG, Lan L. 2014. Metabolic sensor governing bacterial virulence in *Staphylococcus aureus*. Proc Natl Acad Sci U S A 111:E4981-90.

Doshi KJ, Cannone JJ, Cobaugh CW, Gutell RR. 2004. Evaluation of the suitability of free-energy minimization using nearest-neighbor energy parameters for RNA secondary structure prediction. BMC Bioinformatics 5:105.

Drake DR, Brogden KA, Dawson DV, Wertz PW. 2008. Thematic review series: skin lipids. Antimicrobial lipids at the skin surface. J Lipid Res 49:4-11.

Dumitrescu O, Boisset S, Badiou C, Bes M, Benito Y, Reverdy M-E, Vandenesch F, Etienne J, Lina G. 2007. Effect of Antibiotics on *Staphylococcus aureus* Producing Panton-Valentine Leukocidin. Antimicrobial Agents and Chemotherapy 51:1515-1519.

DuMont AL, Nygaard TK, Watkins RL, Smith A, Kozhaya L, Kreiswirth BN, Shopsin B, Unutmaz D, Voyich JM, Torres VJ. 2011. Characterization of a new cytotoxin that contributes to *Staphylococcus aureus* pathogenesis. Molecular Microbiology 79:814-825.

Duncan JL, Cho GJ. 1972. Production of Staphylococcal Alpha Toxin II. Glucose Repression of Toxin Formation. Infection and Immunity 6:689-694.

Dunne DW, Resnick D, Greenberg J, Krieger M, Joiner KA. 1994. The type I macrophage scavenger receptor binds to gram-positive bacteria and recognizes lipoteichoic acid. Proceedings of the National Academy of Sciences of the United States of America 91:1863-1867.

Durand S, Gilet L, Bessières P, Nicolas P, Condon C. 2012. Three Essential Ribonucleases—RNase Y, J1, and III—Control the Abundance of a Majority of *Bacillus subtilis* mRNAs. PLoS Genetics 8:e1002520.

Duthie ES, Lorenz LL. 1952. Staphylococcal coagulase; mode of action and antigenicity. J Gen Microbiol 6:95-107.

Dziewanowska K, Patti JM, Deobald CF, Bayles KW, Trumble WR, Bohach GA. 1999. Fibronectin binding protein and host cell tyrosine kinase are required for internalization of *Staphylococcus aureus* by epithelial cells. Infect Immun 67:4673-8.

Edgell CJ, McDonald CC, Graham JB. 1983. Permanent cell line expressing human factor VIII-related antigen established by hybridization. Proc Natl Acad Sci U S A 80:3734-7.

Edwards AM, Potts JR, Josefsson E, Massey RC. 2010. *Staphylococcus aureus* Host Cell Invasion and Virulence in Sepsis Is Facilitated by the Multiple Repeats within FnBPA. PLoS Pathogens 6:e1000964.

Edwards AM, Bowden MG, Brown EL, Laabei M, Massey RC. 2012. *Staphylococcus aureus* Extracellular Adherence Protein Triggers TNFα Release, Promoting Attachment to Endothelial Cells via Protein A. PLoS ONE 7:e43046.

Egert J, Carrizosa J, Kaye D, Kobasa WD. 1977. Comparison of methicillin, nafcillin, and oxacillin in therapy of *Staphylococcus aureus* endocarditis in rabbits. J Lab Clin Med 89:1262-8.

Engemann JJ, Carmeli Y, Cosgrove SE, Fowler VG, Bronstein MZ, Trivette SL, Briggs JP, Sexton DJ, Kaye KS. 2003. Adverse clinical and economic outcomes attributable to methicillin resistance among patients with *Staphylococcus aureus* surgical site infection. Clin Infect Dis 36:592-8.

Entenza J-M, Moreillon P, Senn MM, Kormanec J, Dunman PM, Berger-Bächi B, Projan S, Bischoff M. 2005. Role of σ(B) in the Expression of *Staphylococcus aureus* Cell Wall Adhesins ClfA and FnbA and Contribution to Infectivity in a Rat Model of Experimental Endocarditis. Infection and Immunity 73:990-998.

Entenza JM, Foster TJ, Ni Eidhin D, Vaudaux P, Francioli P, Moreillon P. 2000. Contribution of Clumping Factor B to Pathogenesis of Experimental Endocarditis due to *Staphylococcus aureus*. Infection and Immunity 68:5443-5446.

Eriksen NH, Espersen F, Rosdahl VT, Jensen K. 1995. Carriage of *Staphylococcus aureus* among 104 healthy persons during a 19-month period. Epidemiol Infect 115:51-60.

Essmann F, Bantel H, Totzke G, Engels IH, Sinha B, Schulze-Osthoff K, Janicke RU. 2003. *Staphylococcus aureus* alpha-toxin-induced cell death: predominant necrosis despite apoptotic caspase activation. Cell Death Differ 10:1260-72.

Fagerlund A, Granum PE, Havarstein LS. 2014. *Staphylococcus aureus* competence genes: mapping of the SigH, ComK1 and ComK2 regulons by transcriptome sequencing. Mol Microbiol 94:557-79.

Fairn GD, Grinstein S. 2012. How nascent phagosomes mature to become phagolysosomes. Trends Immunol 33:397-405.

Fedtke I, Mader D, Kohler T, Moll H, Nicholson G, Biswas R, Henseler K, Götz F, Zähringer U, Peschel A. 2007. A *Staphylococcus aureus ypf*P mutant with strongly reduced lipoteichoic acid (LTA) content: LTA governs bacterial surface properties and autolysin activity. Molecular Microbiology 65:1078-1091.

Felden B, Vandenesch F, Bouloc P, Romby P. 2011. The *Staphylococcus aureus* RNome and Its Commitment to Virulence. PLoS Pathogens 7:e1002006.

Feng Y, Chen CJ, Su LH, Hu S, Yu J, Chiu CH. 2008. Evolution and pathogenesis of *Staphylococcus aureus*: lessons learned from genotyping and comparative genomics. FEMS Microbiol Rev 32:23-37.

Ferran AA, Liu J, Toutain P-L, Bousquet-Mélou A. 2016. Comparison of the In vitro Activity of Five Antimicrobial Drugs against *Staphylococcus pseudintermedius* and *Staphylococcus aureus* Biofilms. Frontiers in Microbiology 7:1187.

Fey PD, Endres JL, Yajjala VK, Widhelm TJ, Boissy RJ, Bose JL, Bayles KW. 2013. A Genetic Resource for Rapid and Comprehensive Phenotype Screening of Nonessential *Staphylococcus aureus* Genes. mBio 4:e00537-12.

Finck-Barbancon V, Prevost G, Piemont Y. 1991. Improved purification of leukocidin from *Staphylococcus aureus* and toxin distribution among hospital strains. Res Microbiol 142:75-85.

Fischer B, Vaudaux P, Magnin M, el Mestikawy Y, Proctor RA, Lew DP, Vasey H. 1996. Novel animal model for studying the molecular mechanisms of bacterial adhesion to bone-implanted metallic devices: role of fibronectin in *Staphylococcus aureus* adhesion. J Orthop Res 14:914-20.

Flock M, Flock J-I. 2001. Rebinding of Extracellular Adherence Protein Eap to *Staphylococcus aureus* Can Occur through a Surface-Bound Neutral Phosphatase. Journal of Bacteriology 183:3999-4003.

Flügge, C. 1886. Die Mikroorganismen.

Forsgren A, Nordstrom K. 1974. Protein A from *Staphylococcus aureus*: the biological significance of its reaction with IgG. Ann N Y Acad Sci 236:252-66.

Foster TJ, McDevitt D. 1994. Surface-associated proteins of *Staphylococcus aureus*: their possible roles in virulence. FEMS Microbiol Lett 118:199-205.

Foster TJ, Hook M. 1998. Surface protein adhesins of *Staphylococcus aureus*. Trends Microbiol 6:484-8.

Foster TJ, Geoghegan JA, Ganesh VK, Hook M. 2014. Adhesion, invasion and evasion: the many functions of the surface proteins of *Staphylococcus aureus*. Nat Rev Microbiol 12:49-62.

Fournier B, Klier A, Rapoport G. 2001. The two-component system ArlS-ArlR is a regulator of virulence gene expression in *Staphylococcus aureus*. Mol Microbiol 41:247-61.

Fowler VG, Jr., Miro JM, Hoen B, Cabell CH, Abrutyn E, Rubinstein E, Corey GR, Spelman D, Bradley SF, Barsic B, Pappas PA, Anstrom KJ, Wray D, Fortes CQ, Anguera I, Athan E, Jones P, van der Meer JT, Elliott TS, Levine DP, Bayer AS. 2005. *Staphylococcus aureus* endocarditis: a consequence of medical progress. Jama 293:3012-21.

Fraser J, Arcus V, Kong P, Baker E, Proft T. 2000. Superantigens - powerful modifiers of the immune system. Mol Med Today 6:125-32.

Fraunholz M, Sinha B. 2012. Intracellular *Staphylococcus aureus*: live-in and let die. Front Cell Infect Microbiol 2:43.

Freer JH, Arbuthnott JP, Billcliffe B. 1973. Effects of staphylococcal -toxin on the structure of erythrocyte membranes: a biochemical and freeze-etching study. J Gen Microbiol 75:321-32.

Friedrich R, Panizzi P, Fuentes-Prior P, Richter K, Verhamme I, Anderson PJ, Kawabata S, Huber R, Bode W, Bock PE. 2003. Staphylocoagulase is a prototype for the mechanism of cofactor-induced zymogen activation. Nature 425:535-9.

Gaballa A, Antelmann H, Aguilar C, Khakh SK, Song KB, Smaldone GT, Helmann JD. 2008. The *Bacillus subtilis* iron-sparing response is mediated by a Fur-regulated small RNA and three small, basic proteins. Proc Natl Acad Sci U S A 105:11927-32.

Gaillard JL, Berche P, Mounier J, Richard S, Sansonetti P. 1987. In vitro model of penetration and intracellular growth of *Listeria monocytogenes* in the human enterocyte-like cell line Caco-2. Infection and Immunity 55:2822-2829.

Galbusera E, Renzoni A, Andrey DO, Monod A, Barras C, Tortora P, Polissi A, Kelley WL. 2011. Site-Specific Mutation of *Staphylococcus aureus* VraS Reveals a Crucial Role for the VraR-VraS Sensor in the Emergence of Glycopeptide Resistance. Antimicrobial Agents and Chemotherapy 55:1008-1020.

Gallegos MT, Schleif R, Bairoch A, Hofmann K, Ramos JL. 1997. Arac/XylS family of transcriptional regulators. Microbiology and Molecular Biology Reviews 61:393-410.

Ganesh VK, Barbu EM, Deivanayagam CCS, Le B, Anderson AS, Matsuka YV, Lin SL, Foster TJ, Narayana SVL, Höök M. 2011. Structural and Biochemical Characterization of *Staphylococcus aureus* Clumping Factor B/Ligand Interactions. The Journal of Biological Chemistry 286:25963-25972.

Gardete S, Wu SW, Gill S, Tomasz A. 2006. Role of VraSR in antibiotic resistance and antibiotic-induced stress response in *Staphylococcus aureus*. Antimicrob Agents Chemother 50:3424-34.

Garzoni C, Francois P, Huyghe A, Couzinet S, Tapparel C, Charbonnier Y, Renzoni A, Lucchini S, Lew DP, Vaudaux P, Kelley WL, Schrenzel J. 2007. A global view of *Staphylococcus aureus* whole genome expression upon internalization in human epithelial cells. BMC Genomics 8:171.

Gaupp R, Wirf J, Wonnenberg B, Biegel T, Eisenbeis J, Graham J, Herrmann M, Lee CY, Beisswenger C, Wolz C, Tschernig T, Bischoff M, Somerville GA. 2016. RpiRc Is a Pleiotropic Effector of Virulence Determinant Synthesis and Attenuates Pathogenicity in *Staphylococcus aureus*. Infect Immun 84:2031-41.

Geiger T, Francois P, Liebeke M, Fraunholz M, Goerke C, Krismer B, Schrenzel J, Lalk M, Wolz C. 2012. The Stringent Response of *Staphylococcus aureus* and Its Impact on Survival after Phagocytosis through the Induction of Intracellular PSMs Expression. PLoS Pathogens 8:e1003016.

Geiger T, Goerke C, Mainiero M, Kraus D, Wolz C. 2008. The Virulence Regulator Sae of S*taphylococcus aureus*: Promoter Activities and Response to Phagocytosis-Related Signals. Journal of Bacteriology 190:3419-3428.

Geiger T, Kästle B, Gratani FL, Goerke C, Wolz C. 2014. Two Small (p)ppGpp Synthases in *Staphylococcus aureus* Mediate Tolerance against Cell Envelope Stress Conditions. Journal of Bacteriology 196:894-902.

Geisinger E, Adhikari RP, Jin R, Ross HF, Novick RP. 2006. Inhibition of *rot* translation by RNAIII, a key feature of agr function. Mol Microbiol 61:1038-48.

Geisinger E, Chen J, Novick RP. 2012. Allele-Dependent Differences in Quorum-Sensing Dynamics Result in Variant Expression of Virulence Genes in *Staphylococcus aureus*. Journal of Bacteriology 194:2854-2864.

Geissmann T, Chevalier C, Cros M-J, Boisset S, Fechter P, Noirot C, Schrenzel J, François P, Vandenesch F, Gaspin C, Romby P. 2009. A search for small noncoding RNAs in *Staphylococcus aureus* reveals a conserved sequence motif for regulation. Nucleic Acids Research 37:7239-7257.

Genestier AL, Michallet MC, Prevost G, Bellot G, Chalabreysse L, Peyrol S, Thivolet F, Etienne J, Lina G, Vallette FM, Vandenesch F, Genestier L. 2005. *Staphylococcus aureus* Panton-Valentine leukocidin directly targets mitochondria and induces Bax-independent apoptosis of human neutrophils. J Clin Invest 115:3117-27.

George NP, Wei Q, Shin PK, Konstantopoulos K, Ross JM. 2006. *Staphylococcus aureus* adhesion via Spa, ClfA, and SdrCDE to immobilized platelets demonstrates shear-dependent behavior. Arterioscler Thromb Vasc Biol 26:2394-400.

Geraci J, Neubauer S, Pollath C, Hansen U, Rizzo F, Krafft C, Westermann M, Hussain M, Peters G, Pletz MW, Loffler B, Makarewicz O, Tuchscherr L. 2017. The *Staphylococcus aureus* extracellular matrix protein (Emp) has a fibrous structure and binds to different extracellular matrices. Sci Rep 7:13665.

Ghuysen JM, Strominger JL. 1963. Structure of the cell wall of *Staphylococcus aureus*, strain Copenhagen. I. Preparation of fragments by enzymatic hydrolysis. Biochemistry 2:1110-9.

Giachino P, Engelmann S, Bischoff M. 2001. Sigma(B) activity depends on RsbU in *Staphylococcus aureus*. J Bacteriol 183:1843-52.

Giese B, Dittmann S, Paprotka K, Levin K, Weltrowski A, Biehler D, Lâm T-T, Sinha B, Fraunholz MJ. 2009. Staphylococcal Alpha-Toxin Is Not Sufficient To Mediate Escape from Phagolysosomes in Upper-Airway Epithelial Cells. Infection and Immunity 77:3611-3625.

Giese B, Glowinski F, Paprotka K, Dittmann S, Steiner T, Sinha B, Fraunholz MJ. 2011. Expression of delta-toxin by *Staphylococcus aureus* mediates escape from phago-endosomes of human epithelial and endothelial cells in the presence of beta-toxin. Cell Microbiol 13:316-29.

Gill SR, Fouts DE, Archer GL, Mongodin EF, DeBoy RT, Ravel J, Paulsen IT, Kolonay JF, Brinkac L, Beanan M, Dodson RJ, Daugherty SC, Madupu R, Angiuoli SV, Durkin AS, Haft DH, Vamathevan J, Khouri H, Utterback T, Lee C, Dimitrov G, Jiang L, Qin H, Weidman J, Tran K, Kang K, Hance IR, Nelson KE, Fraser CM. 2005. Insights on Evolution of Virulence and Resistance from the Complete Genome Analysis of an Early Methicillin-Resistant *Staphylococcus aureus* Strain and a Biofilm-Producing Methicillin-Resistant *Staphylococcus epidermidis* Strain. Journal of Bacteriology 187:2426-2438.

Gillaspy AF, Hickmon SG, Skinner RA, Thomas JR, Nelson CL, Smeltzer MS. 1995. Role of the accessory gene regulator (agr) in pathogenesis of staphylococcal osteomyelitis. Infection and Immunity 63:3373-3380.

Gillet Y, Issartel B, Vanhems P, Fournet JC, Lina G, Bes M, Vandenesch F, Piemont Y, Brousse N, Floret D, Etienne J. 2002. Association between *Staphylococcus aureus* strains carrying gene for Panton-Valentine leukocidin and highly lethal necrotising pneumonia in young immunocompetent patients. Lancet 359:753-9.

Giraud C, Hausmann S, Lemeille S, Prados J, Redder P, Linder P. 2015. The C-terminal region of the RNA helicase CshA is required for the interaction with the degradosome and turnover of bulk RNA in the opportunistic pathogen *Staphylococcus aureus*. RNA Biol 12:658-74.

Giraudo AT, Cheung AL, Nagel R. 1997. The sae locus of *Staphylococcus aureus* controls exoprotein synthesis at the transcriptional level. Arch Microbiol 168:53-8.

Gomez MI, Lee A, Reddy B, Muir A, Soong G, Pitt A, Cheung A, Prince A. 2004. *Staphylococcus aureus* protein A induces airway epithelial inflammatory responses by activating TNFR1. Nat Med 10:842-8.

Götz F, Bannerman, T, Schleifer, K-H. 2006. The Genera Staphylococcus and Macrococcus. In The Prokaryotes (Eds, Dworkin M, Falkow S, Rosenberg E, Schleifer K-H, Stackebrandt E) Springer US, pp.5-75.

Gravet A, Colin DA, Keller D, Girardot R, Monteil H, Prevost G. 1998. Characterization of a novel structural member, LukE-LukD, of the bi-component staphylococcal leucotoxins family. FEBS Lett 436:202-8.

Grigg JC, Vermeiren CL, Heinrichs DE, Murphy ME. 2007. Haem recognition by a *Staphylococcus aureus* NEAT domain. Mol Microbiol 63:139-49.

Greenberg JW, Fischer W, Joiner KA. 1996. Influence of lipoteichoic acid structure on recognition by the macrophage scavenger receptor. Infect Immun 64:3318-25.

Grosz M, Kolter J, Paprotka K, Winkler AC, Schafer D, Chatterjee SS, Geiger T, Wolz C, Ohlsen K, Otto M, Rudel T, Sinha B, Fraunholz M. 2014. Cytoplasmic replication of *Staphylococcus aureus* upon phagosomal escape triggered by phenol-soluble modulin alpha. Cell Microbiol 16:451-65.

Gruber AR, Lorenz R, Bernhart SH, Neuböck R, Hofacker IL. 2008. The Vienna RNA Websuite. Nucleic Acids Research 36:W70-W74.

Gründling A, Schneewind O. 2007. Synthesis of glycerol phosphate lipoteichoic acid in *Staphylococcus aureus*. Proceedings of the National Academy of Sciences of the United States of America 104:8478-8483.

Grundmeier M, Tuchscherr L, Bruck M, Viemann D, Roth J, Willscher E, Becker K, Peters G, Loffler B. 2010. Staphylococcal strains vary greatly in their ability to induce an inflammatory response in endothelial cells. J Infect Dis 201:871-80.

Guemes M, Rahman SA, Hussain K. 2016. What is a normal blood glucose? Arch Dis Child 101:569-74.

Guillet J, Hallier M, Felden B. 2013. Emerging Functions for the *Staphylococcus aureus* RNome. PLoS Pathogens 9:e1003767.

Gupta RK, Luong TT, Lee CY. 2015. RNAIII of the *Staphylococcus aureus* agr system activates global regulator MgrA by stabilizing mRNA. Proceedings of the National Academy of Sciences of the United States of America 112:14036-14041.

Haag AF, Bagnoli F. 2017. The Role of Two-Component Signal Transduction Systems in *Staphylococcus aureus* Virulence Regulation. Curr Top Microbiol Immunol 409:145-198.

Haddadin RN, Saleh S, Al-Adham IS, Buultjens TE, Collier PJ. 2010. The effect of subminimal inhibitory concentrations of antibiotics on virulence factors expressed by *Staphylococcus aureus* biofilms. J Appl Microbiol 108:1281-91.

Haggar A, Hussain M, Lönnies H, Herrmann M, Norrby-Teglund A, Flock J-I. 2003. Extracellular Adherence Protein from *Staphylococcus aureus* Enhances Internalization into Eukaryotic Cells. Infection and Immunity 71:2310-2317.

Hamill RJ, Vann JM, Proctor RA. 1986. Phagocytosis of *Staphylococcus aureus* by cultured bovine aortic endothelial cells: model for postadherence events in endovascular infections. Infect Immun 54:833-6.

Hammer ND, Skaar EP. 2011. Molecular mechanisms of *Staphylococcus aureus* iron acquisition. Annu Rev Microbiol 65:129-47.

Hanahan D. 1983. Studies on transformation of *Escherichia coli* with plasmids. J Mol Biol 166:557-80.

Hanselman BA, Kruth SA, Rousseau J, Low DE, Willey BM, McGeer A, Weese JS. 2006. Methicillin-resistant *Staphylococcus aureus* colonization in veterinary personnel. Emerg Infect Dis 12:1933-8.

Hartleib J, Kohler N, Dickinson RB, Chhatwal GS, Sixma JJ, Hartford OM, Foster TJ, Peters G, Kehrel BE, Herrmann M. 2000. Protein A is the von Willebrand factor binding protein on *Staphylococcus aureus*. Blood 96:2149-56.

Hartman BC, Leedom J, Lewis WP, Weintraub P. 1984. Postsurgical toxic shock syndrome: report of a case in which full syndrome manifestations were aborted by early recognition and therapy. J Am Osteopath Assoc 84:356-9.

Hartmann T, Baronian G, Nippe N, Voss M, Schulthess B, Wolz C, Eisenbeis J, Schmidt-Hohagen K, Gaupp R, Sunderkotter C, Beisswenger C, Bals R, Somerville GA, Herrmann M, Molle V, Bischoff M. 2014. The catabolite control protein E (CcpE) affects virulence determinant production and pathogenesis of *Staphylococcus aureus*. J Biol Chem 289:29701-11.

Haslinger-Löffler B, Kahl BC, Grundmeier M, Strangfeld K, Wagner B, Fischer U, Cheung AL, Peters G, Schulze-Osthoff K, Sinha B. 2005. Multiple virulence factors are required for *Staphylococcus aureus*-induced apoptosis in endothelial cells. Cell Microbiol 7:1087-97.

Haslinger B, Strangfeld K, Peters G, Schulze-Osthoff K, Sinha B. 2003. *Staphylococcus aureus* alpha-toxin induces apoptosis in peripheral blood mononuclear cells: role of endogenous tumour necrosis factor-alpha and the mitochondrial death pathway. Cell Microbiol 5:729-41.

Hasman H, Moodley A, Guardabassi L, Stegger M, Skov RL, Aarestrup FM. 2010. Spa type distribution in Staphylococcus aureus originating from pigs, cattle and poultry. Vet Microbiol 141:326-31.

Harper L, Balasubramanian D, Ohneck EA, Sause WE, Chapman J, Mejia-Sosa B, Lhakhang T, Heguy A, Tsirigos A, Ueberheide B, Boyd JM, Lun DS, Torres VJ. 2018. *Staphylococcus aureus* Responds to the Central Metabolite Pyruvate To Regulate Virulence. MBio 9.

Hendrix H, Lindhout T, Mertens K, Engels W, Hemker HC. 1983. Activation of human prothrombin by stoichiometric levels of staphylocoagulase. J Biol Chem 258:3637-44.

Heilmann C. 2011. Adhesion mechanisms of staphylococci. Adv Exp Med Biol 715:105-23.

Heilmann C, Niemann S, Sinha B, Herrmann M, Kehrel BE, Peters G. 2004. *Staphylococcus aureus* fibronectin-binding protein (FnBP)-mediated adherence to platelets, and aggregation of platelets induced by FnBPA but not by FnBPB. J Infect Dis 190:321-9.

Herbert S, Ziebandt AK, Ohlsen K, Schafer T, Hecker M, Albrecht D, Novick R, Gotz F. 2010. Repair of global regulators in *Staphylococcus aureus* 8325 and comparative analysis with other clinical isolates. Infect Immun 78:2877-89.

Herzer CM. 2001. Toxic shock syndrome: broadening the differential diagnosis. J Am Board Fam Pract 14:131-6.

Hoover DG, Gray RJ. 1977. Function of cell wall teichoic acid in thermally injured *Staphylococcus aureu*s. J Bacteriol 131:477-85.

Hopkins PA, Fraser JD, Pridmore AC, Russell HH, Read RC, Sriskandan S. 2005. Superantigen recognition by HLA class II on monocytes up-regulates toll-like receptor 4 and enhances proinflammatory responses to endotoxin. Blood 105:3655-62.

Horn J, Stelzner K, Rudel T, Fraunholz M. 2018a. Inside job: *Staphylococcus aureus* host-pathogen interactions. Int J Med Microbiol 308:607-624.

Horn J, Klepsch M, Manger M, Wolz C, Rudel T, Fraunholz M. 2018b. The long non-coding RNA SSR42 controls *Staphylococcus aureus* α-toxin transcription in response to environmental stimuli. Journal of Bacteriology doi:10.1128/jb.00252-18.

Hudson MC, Ramp WK, Frankenburg KP. 1999. *Staphylococcus aureus* adhesion to bone matrix and bone-associated biomaterials. FEMS Microbiol Lett 173:279-84.

Huntzinger E, Boisset S, Saveanu C, Benito Y, Geissmann T, Namane A, Lina G, Etienne J, Ehresmann B, Ehresmann C, Jacquier A, Vandenesch F, Romby P. 2005. *Staphylococcus aureus* RNAIII and the endoribonuclease III coordinately regulate *spa* gene expression. Embo j 24:824-35.

Hussain M, Haggar A, Heilmann C, Peters G, Flock J-I, Herrmann M. 2002. Insertional Inactivation of eap in *Staphylococcus aureus* Strain Newman Confers Reduced Staphylococcal Binding to Fibroblasts. Infection and Immunity 70:2933-2940.

Hussain M, Becker K, von Eiff C, Schrenzel J, Peters G, Herrmann M. 2001. Identification and Characterization of a Novel 38.5-Kilodalton Cell Surface Protein of *Staphylococcus aureus* with Extended-Spectrum Binding Activity for Extracellular Matrix and Plasma Proteins. Journal of Bacteriology 183:6778-6786.

Huveneers S, Truong H, Fassler R, Sonnenberg A, Danen EH. 2008. Binding of soluble fibronectin to integrin alpha5 beta1 - link to focal adhesion redistribution and contractile shape. J Cell Sci 121:2452-62.

Ibarra JA, Pérez-Rueda E, Carroll RK, Shaw LN. 2013. Global analysis of transcriptional regulators in Staphylococcus aureus. BMC Genomics 14:126-126.

Ingavale S, van Wamel W, Luong TT, Lee CY, Cheung AL. 2005. Rat/MgrA, a Regulator of Autolysis, Is a Regulator of Virulence Genes in *Staphylococcus aureus*. Infection and Immunity 73:1423-1431.

Inoshima I, Inoshima N, Wilke GA, Powers ME, Frank KM, Wang Y, Bubeck Wardenburg J. 2011. A *Staphylococcus aureus* pore-forming toxin subverts the activity of ADAM10 to cause lethal infection in mice. Nat Med 17:1310-4.

Inoue S, Moriyama T, Horinouchi Y, Tachibana T, Okada F, Maruo K, Yoshiya S. 2013. Comparison of clinical features and outcomes of *staphylococcus aureus* vertebral osteomyelitis caused by methicillin-resistant and methicillin-sensitive strains. Springerplus 2:283.

Inouye S, Nakazawa A, Nakazawa T. 1986. Nucleotide sequence of the regulatory gene *xyl*S on the *Pseudomonas putida* TOL plasmid and identification of the protein product. Gene 44:235-42.

Issa NC, Thompson RL. 2001. Staphylococcal toxic shock syndrome. Suspicion and prevention are keys to control. Postgrad Med 110:55-6, 59-62.

Iwamoto M, Mu Y, Lynfield R, Bulens SN, Nadle J, Aragon D, Petit S, Ray SM, Harrison LH, Dumyati G, Townes JM, Schaffner W, Gorwitz RJ, Lessa FC. 2013. Trends in invasive methicillin-resistant *Staphylococcus aureus* infections. Pediatrics 132:e817-24.

Janzon L, Arvidson S. 1990. The role of the delta-lysin gene (*hld*) in the regulation of virulence genes by the accessory gene regulator (agr) in *Staphylococcus aureus*. The EMBO Journal 9:1391-1399.

Janzon L, Lofdahl S, Arvidson S. 1989. Identification and nucleotide sequence of the delta-lysin gene, hld, adjacent to the accessory gene regulator (agr) of *Staphylococcus aureus*. Mol Gen Genet 219:480-5.

Jeong D-W, Cho H, Jones MB, Shatzkes K, Sun F, Ji Q, Liu Q, Peterson SN, He C, Bae T. 2012. The auxiliary protein complex SaePQ activates the phosphatase activity of sensor kinase SaeS in the SaeRS two-component system of *Staphylococcus aureus*. Molecular microbiology 86:331-348.

Jeong D-W, Cho H, Lee H, Li C, Garza J, Fried M, Bae T. 2011. Identification of the P3 Promoter and Distinct Roles of the Two Promoters of the SaeRS Two-Component System in *Staphylococcus aureus*. Journal of Bacteriology 193:4672-4684.

Jevon M, Guo C, Ma B, Mordan N, Nair SP, Harris M, Henderson B, Bentley G, Meghji S. 1999. Mechanisms of internalization of *Staphylococcus aureus* by cultured human osteoblasts. Infect Immun 67:2677-81.

Jevons MP. 1961. “Celbenin” - resistant Staphylococci. British Medical Journal 1:124-125.

Ji G, Beavis RC, Novick RP. 1995. Cell density control of staphylococcal virulence mediated by an octapeptide pheromone. Proceedings of the National Academy of Sciences of the United States of America 92:12055-12059.

Jin T, Bokarewa M, Foster T, Mitchell J, Higgins J, Tarkowski A. 2004. *Staphylococcus aureus* resists human defensins by production of staphylokinase, a novel bacterial evasion mechanism. J Immunol 172:1169-76.

Jo DS, Montgomery CP, Yin S, Boyle-Vavra S, Daum RS. 2011. Improved Oxacillin Treatment Outcomes in Experimental Skin and Lung Infection by a Methicillin-Resistant *Staphylococcus aureus* Isolate with a *vra*SR Operon Deletion. Antimicrobial Agents and Chemotherapy 55:2818-2823.

Johnson M, Cockayne A, Morrissey JA. 2008. Iron-regulated biofilm formation in *Staphylococcus aureus* Newman requires *ica* and the secreted protein Emp. Infect Immun 76:1756-65.

Jones RC, Deck J, Edmondson RD, Hart ME. 2008. Relative quantitative comparisons of the extracellular protein profiles of *Staphylococcus aureus* UAMS-1 and its *sar*A, *agr*, and *sar*A *agr* regulatory mutants using one-dimensional polyacrylamide gel electrophoresis and nanocapillary liquid chromatography coupled with tandem mass spectrometry. J Bacteriol 190:5265-78.

Josse J, Laurent F, Diot A. 2017. Staphylococcal Adhesion and Host Cell Invasion: Fibronectin-Binding and Other Mechanisms. Frontiers in Microbiology 8:2433.

Junecko JM, Zielinska AK, Mrak LN, Ryan DC, Graham JW, Smeltzer MS, Lee CY. 2012. Transcribing virulence in *Staphylococcus aureus.* World J Clin Infect Dis 2:63-76.

Kahl B, Herrmann M, Everding AS, Koch HG, Becker K, Harms E, Proctor RA, Peters G. 1998. Persistent infection with small colony variant strains of *Staphylococcus aureus* in patients with cystic fibrosis. J Infect Dis 177:1023-9.

Kaito C, Morishita D, Matsumoto Y, Kurokawa K, Sekimizu K. 2006. Novel DNA binding protein SarZ contributes to virulence in *Staphylococcus aureus*. Mol Microbiol 62:1601-17.

Kaito C, Saito Y, Ikuo M, Omae Y, Mao H, Nagano G, Fujiyuki T, Numata S, Han X, Obata K, Hasegawa S, Yamaguchi H, Inokuchi K, Ito T, Hiramatsu K, Sekimizu K. 2013. Mobile genetic element SCCmec-encoded psm-mec RNA suppresses translation of *agr*A and attenuates MRSA virulence. PLoS Pathog 9:e1003269.

Kalinka J, Hachmeister M, Geraci J, Sordelli D, Hansen U, Niemann S, Oetermann S, Peters G, Löffler B, Tuchscherr L. 2014. *Staphylococcus aureus* isolates from chronic osteomyelitis are characterized by high host cell invasion and intracellular adaptation, but still induce inflammation. International Journal of Medical Microbiology 304:1038-1049.

Kazmierczak MJ, Wiedmann M, Boor KJ. 2005. Alternative Sigma Factors and Their Roles in Bacterial Virulence. Microbiology and Molecular Biology Reviews 69:527-543.

Keane FM, Loughman A, Valtulina V, Brennan M, Speziale P, Foster TJ. 2007. Fibrinogen and elastin bind to the same region within the A domain of fibronectin binding protein A, an MSCRAMM of *Staphylococcus aureus*. Mol Microbiol 63:711-23.

Kerrigan SW, Clarke N, Loughman A, Meade G, Foster TJ, Cox D. 2008. Molecular basis for *Staphylococcus aureus*-mediated platelet aggregate formation under arterial shear in vitro. Arterioscler Thromb Vasc Biol 28:335-40.

Kertesz M, Wan Y, Mazor E, Rinn JL, Nutter RC, Chang HY, Segal E. 2010. Genome-wide Measurement of RNA Secondary Structure in Yeast. Nature 467:10.1038/nature09322.

Khanna T, Friendship R, Dewey C, Weese JS. 2008. Methicillin resistant *Staphylococcus aureus* colonization in pigs and pig farmers. Vet Microbiol 128:298-303.

Khemici V, Prados J, Linder P, Redder P. 2015. Decay-Initiating Endoribonucleolytic Cleavage by RNase Y Is Kept under Tight Control via Sequence Preference and Sub-cellular Localisation. PLoS Genet 11:e1005577.

Killikelly A, Benson MA, Ohneck EA, Sampson JM, Jakoncic J, Spurrier B, Torres VJ, Kong XP. 2015. Structure-based functional characterization of repressor of toxin (Rot), a central regulator of *Staphylococcus aureus* virulence. J Bacteriol 197:188-200.

Kim S, Corvaglia A-R, Léo S, Cheung A, Francois P. 2016. Characterization of RNA Helicase CshA and Its Role in Protecting mRNAs and Small RNAs of *Staphylococcus aureus* Strain Newman. Infection and Immunity 84:833-844.

Kinkel TL, Roux CM, Dunman PM, Fang FC. 2013. The *Staphylococcus aureus* SrrAB Two-Component System Promotes Resistance to Nitrosative Stress and Hypoxia. mBio 4:e00696-13.

Kintarak S, Whawell SA, Speight PM, Packer S, Nair SP. 2004. Internalization of *Staphylococcus aureus* by Human Keratinocytes. Infection and Immunity 72:5668-5675.

Kipp F, Ziebuhr W, Becker K, Krimmer V, Hoss N, Peters G, von Eiff C. 2003. Detection of *Staphylococcus aureus* by 16S rRNA directed in situ hybridisation in a patient with a brain abscess caused by small colony variants. Journal of Neurology, Neurosurgery, and Psychiatry 74:1000-1002.

Kluytmans J, van Belkum A, Verbrugh H. 1997. Nasal carriage of *Staphylococcus aureus*: epidemiology, underlying mechanisms, and associated risks. Clin Microbiol Rev 10:505-20.

Ko YP, Kuipers A, Freitag CM, Jongerius I, Medina E, van Rooijen WJ, Spaan AN, van Kessel KP, Hook M, Rooijakkers SH. 2013. Phagocytosis escape by a *Staphylococcus aureus* protein that connects complement and coagulation proteins at the bacterial surface. PLoS Pathog 9:e1003816.

Koenig RL, Ray JL, Maleki SJ, Smeltzer MS, Hurlburt BK. 2004. *Staphylococcus aureus* AgrA Binding to the RNAIII-agr Regulatory Region. Journal of Bacteriology 186:7549-7555.

Kollef MH, Shorr A, Tabak YP, Gupta V, Liu LZ, Johannes RS. 2005. Epidemiology and outcomes of health-care-associated pneumonia: results from a large US database of culture-positive pneumonia. Chest 128:3854-62.

Koop G, Vrieling M, Storisteanu DML, Lok LSC, Monie T, van Wigcheren G, Raisen C, Ba X, Gleadall N, Hadjirin N, Timmerman AJ, Wagenaar JA, Klunder HM, Fitzgerald JR, Zadoks R, Paterson GK, Torres C, Waller AS, Loeffler A, Loncaric I, Hoet AE, Bergström K, De Martino L, Pomba C, de Lencastre H, Ben Slama K, Gharsa H, Richardson EJ, Chilvers ER, de Haas C, van Kessel K, van Strijp JAG, Harrison EM, Holmes MA. 2017. Identification of LukPQ, a novel, equid-adapted leukocidin of *Staphylococcus aureus.* Scientific Reports 7:40660.

Kreiswirth BN, Lofdahl S, Betley MJ, O'Reilly M, Schlievert PM, Bergdoll MS, Novick RP. 1983. The toxic shock syndrome exotoxin structural gene is not detectably transmitted by a prophage. Nature 305:709-12.

Kretschmer D, Gleske AK, Rautenberg M, Wang R, Koberle M, Bohn E, Schoneberg T, Rabiet MJ, Boulay F, Klebanoff SJ, van Kessel KA, van Strijp JA, Otto M, Peschel A. 2010. Human formyl peptide receptor 2 senses highly pathogenic *Staphylococcus aureus*. Cell Host Microbe 7:463-73.

Kriegeskorte A, Konig S, Sander G, Pirkl A, Mahabir E, Proctor RA, von Eiff C, Peters G, Becker K. 2011. Small colony variants of *Staphylococcus aureus* reveal distinct protein profiles. Proteomics 11:2476-90.

Kriegeskorte A, Block D, Drescher M, Windmüller N, Mellmann A, Baum C, Neumann C, Lorè NI, Bragonzi A, Liebau E, Hertel P, Seggewiss J, Becker K, Proctor RA, Peters G, Kahl BC. 2014. Inactivation of *thy*A in *Staphylococcus aureus* Attenuates Virulence and Has a Strong Impact on Metabolism and Virulence Gene Expression. mBio 5:e01447-14.

Kroh HK, Panizzi P, Bock PE. 2009. Von Willebrand factor-binding protein is a hysteretic conformational activator of prothrombin. Proceedings of the National Academy of Sciences of the United States of America 106:7786-7791.

Krute CN, Rice KC, Bose JL. 2017. VfrB Is a Key Activator of the *Staphylococcus aureus* SaeRS Two-Component System. Journal of Bacteriology 199:e00828-16.

Kubica M, Guzik K, Koziel J, Zarebski M, Richter W, Gajkowska B, Golda A, Maciag-Gudowska A, Brix K, Shaw L, Foster T, Potempa J. 2008. A potential new pathway for *Staphylococcus aureus* dissemination: the silent survival of *S. aureus* phagocytosed by human monocyte-derived macrophages. PLoS One 3:e1409.

Kuroda M, Ohta T, Uchiyama I, Baba T, Yuzawa H, Kobayashi I, Cui L, Oguchi A, Aoki K, Nagai Y, Lian J, Ito T, Kanamori M, Matsumaru H, Maruyama A, Murakami H, Hosoyama A, Mizutani-Ui Y, Takahashi NK, Sawano T, Inoue R, Kaito C, Sekimizu K, Hirakawa H, Kuhara S, Goto S, Yabuzaki J, Kanehisa M, Yamashita A, Oshima K, Furuya K, Yoshino C, Shiba T, Hattori M, Ogasawara N, Hayashi H, Hiramatsu K. 2001. Whole genome sequencing of meticillin-resistant *Staphylococcus aureus*. Lancet 357:1225-40.

Kuroda H, Kuroda M, Cui L, Hiramatsu K. 2007. Subinhibitory concentrations of beta-lactam induce haemolytic activity in *Staphylococcus aureus* through the SaeRS two-component system. FEMS Microbiol Lett 268:98-105.

Kuroda M, Kuroda H, Oshima T, Takeuchi F, Mori H, Hiramatsu K. 2003. Two-component system VraSR positively modulates the regulation of cell-wall biosynthesis pathway in *Staphylococcus aureus*. Mol Microbiol 49:807-21.

Laarman AJ, Mijnheer G, Mootz JM, van Rooijen WJ, Ruyken M, Malone CL, Heezius EC, Ward R, Milligan G, van Strijp JA, de Haas CJ, Horswill AR, van Kessel KP, Rooijakkers SH. 2012. *Staphylococcus aureus* Staphopain A inhibits CXCR2-dependent neutrophil activation and chemotaxis. Embo j 31:3607-19.

Lammers A, Nuijten PJ, Smith HE. 1999. The fibronectin binding proteins of *Staphylococcus aureus* are required for adhesion to and invasion of bovine mammary gland cells. FEMS Microbiol Lett 180:103-9.

Lasa I, Toledo-Arana A, Dobin A, Villanueva M, de los Mozos IR, Vergara-Irigaray M, Segura V, Fagegaltier D, Penades JR, Valle J, Solano C, Gingeras TR. 2011. Genome-wide antisense transcription drives mRNA processing in bacteria. Proc Natl Acad Sci U S A 108:20172-7.

Laudien M, Gadola SD, Podschun R, Hedderich J, Paulsen J, Reinhold-Keller E, Csernok E, Ambrosch P, Hellmich B, Moosig F, Gross WL, Sahly H, Lamprecht P. 2010. Nasal carriage of *Staphylococcus aureus* and endonasal activity in Wegener s granulomatosis as compared to rheumatoid arthritis and chronic Rhinosinusitis with nasal polyps. Clin Exp Rheumatol 28:51-5.

Laupland KB, Lyytikainen O, Sogaard M, Kennedy KJ, Knudsen JD, Ostergaard C, Galbraith JC, Valiquette L, Jacobsson G, Collignon P, Schonheyder HC. 2013. The changing epidemiology of *Staphylococcus aureus* bloodstream infection: a multinational population-based surveillance study. Clin Microbiol Infect 19:465-71.

Ledala N, Zhang B, Seravalli J, Powers R, Somerville GA. 2014. Influence of Iron and Aeration on *Staphylococcus aureus* Growth, Metabolism, and Transcription. Journal of Bacteriology 196:2178-2189.

Lee LY, Miyamoto YJ, McIntyre BW, Hook M, McCrea KW, McDevitt D, Brown EL. 2002. The *Staphylococcus aureus* Map protein is an immunomodulator that interferes with T cell-mediated responses. J Clin Invest 110:1461-71.

Lehnik-Habrink M, Lewis RJ, Mader U, Stulke J. 2012. RNA degradation in *Bacillus subtilis*: an interplay of essential endo- and exoribonucleases. Mol Microbiol 84:1005-17.

Lei MG, Cue D, Roux CM, Dunman PM, Lee CY. 2011. Rsp inhibits attachment and biofilm formation by repressing *fnb*A in *Staphylococcus aureus* MW2. J Bacteriol 193:5231-41.

Lei L, Altstaedt J, von der Ohe M, Proft T, Gross U, Rink L. 2001. Induction of interleukin-8 in human neutrophils after MHC class II cross-linking with superantigens. J Leukoc Biol 70:80-6.

Li T, He L, Song Y, Villaruz AE, Joo H-S, Liu Q, Zhu Y, Wang Y, Qin J, Otto M, Li M. 2016. AraC-Type Regulator Rsp Adapts *Staphylococcus aureus* Gene Expression to Acute Infection. Infection and Immunity 84:723-734.

Liang X, Yu C, Sun J, Liu H, Landwehr C, Holmes D, Ji Y. 2006. Inactivation of a two-component signal transduction system, SaeRS, eliminates adherence and attenuates virulence of *Staphylococcus aureus*. Infect Immun 74:4655-65.

Liang X, Zheng L, Landwehr C, Lunsford D, Holmes D, Ji Y. 2005. Global Regulation of Gene Expression by ArlRS, a Two-Component Signal Transduction Regulatory System of *Staphylococcus aureus*. Journal of Bacteriology 187:5486-54

Liese J, Rooijakkers SH, van Strijp JA, Novick RP, Dustin ML. 2013. Intravital two-photon microscopy of host-pathogen interactions in a mouse model of *Staphylococcus aureus* skin abscess formation. Cell Microbiol 15:891-909.

Lina G, Jarraud S, Ji G, Greenland T, Pedraza A, Etienne J, Novick RP, Vandenesch F. 1998. Transmembrane topology and histidine protein kinase activity of AgrC, the agr signal receptor in *Staphylococcus aureus*. Mol Microbiol 28:655-62.

Lindsay JA, Moore CE, Day NP, Peacock SJ, Witney AA, Stabler RA, Husain SE, Butcher PD, Hinds J. 2006. Microarrays reveal that each of the ten dominant lineages of *Staphylococcus aureus* has a unique combination of surface-associated and regulatory genes. J Bacteriol 188:669-76.

Link TM, Valentin-Hansen P, Brennan RG. 2009. Structure of *Escherichia coli* Hfq bound to polyriboadenylate RNA. Proc Natl Acad Sci U S A 106:19292-7.

Liu Y, Wu N, Dong J, Gao Y, Zhang X, Mu C, Shao N, Yang G. 2010. Hfq is a global regulator that controls the pathogenicity of *Staphylococcus aureus*. PLoS One 5.

Liu Y, Manna AC, Pan C-H, Kriksunov IA, Thiel DJ, Cheung AL, Zhang G. 2006. Structural and function analyses of the global regulatory protein SarA from *Staphylococcus aureus*. Proceedings of the National Academy of Sciences of the United States of America 103:2392.

Liu Q, Cho H, Yeo W-S, Bae T. 2015. The Extracytoplasmic Linker Peptide of the Sensor Protein SaeS Tunes the Kinase Activity Required for Staphylococcal Virulence in Response to Host Signals. PLoS Pathogens 11:e1004799.

Liu M, Tanaka WN, Zhu H, Xie G, Dooley DM, Lei B. 2008. Direct hemin transfer from IsdA to IsdC in the iron-regulated surface determinant (Isd) heme acquisition system of *Staphylococcus aureus*. J Biol Chem 283:6668-76.

Liu Y, Manna A, Li R, Martin WE, Murphy RC, Cheung AL, Zhang G. 2001. Crystal structure of the SarR protein from *Staphylococcus aureus*. Proceedings of the National Academy of Sciences of the United States of America 98:6877-6882.

Livak KJ, Schmittgen TD. 2001. Analysis of relative gene expression data using real-time quantitative PCR and the 2(-Delta Delta C(T)) Method. Methods 25:402-8.

Lowy FD, Fant J, Higgins LL, Ogawa SK, Hatcher VB. 1988. *Staphylococcus aureus*--human endothelial cell interactions. J Ultrastruct Mol Struct Res 98:137-46.

Lowy FD. 1998. *Staphylococcus aureus* infections. N Engl J Med 339:520-32.

Luong TT, Dunman PM, Murphy E, Projan SJ, Lee CY. 2006. Transcription Profiling of the *mgr*A Regulon in *Staphylococcus aureus*. Journal of Bacteriology 188:1899-1910.

Mäder U, Nicolas P, Depke M, Pane-Farre J, Debarbouille M, van der Kooi-Pol MM, Guerin C, Derozier S, Hiron A, Jarmer H, Leduc A, Michalik S, Reilman E, Schaffer M, Schmidt F, Bessieres P, Noirot P, Hecker M, Msadek T, Volker U, van Dijl JM. 2016. *Staphylococcus aureus* Transcriptome Architecture: From Laboratory to Infection-Mimicking Conditions. PLoS Genet 12:e1005962.

McCourt J, O'Halloran DP, McCarthy H, O'Gara JP, Geoghegan JA. 2014. Fibronectin-binding proteins are required for biofilm formation by community-associated methicillin-resistant *Staphylococcus aureus* strain LAC. FEMS Microbiol Lett 353:157-64.

McLaughlin JR, Murray CL, Rabinowitz JC. 1981. Unique features in the ribosome binding site sequence of the gram-positive *Staphylococcus aureus* beta-lactamase gene. J Biol Chem 256:11283-91.

Mainiero M, Goerke C, Geiger T, Gonser C, Herbert S, Wolz C. 2010. Differential target gene activation by the *Staphylococcus aureus* two-component system *sae*RS. J Bacteriol 192:613-23.

Maiques E, Ubeda C, Campoy S, Salvador N, Lasa I, Novick RP, Barbe J, Penades JR. 2006. beta-lactam antibiotics induce the SOS response and horizontal transfer of virulence factors in *Staphylococcus aureus*. J Bacteriol 188:2726-9.

Majerczyk CD, Dunman PM, Luong TT, Lee CY, Sadykov MR, Somerville GA, Bodi K, Sonenshein AL. 2010. Direct targets of CodY in Staphylococcus aureus. J Bacteriol 192:2861-77.

Majerczyk CD, Sadykov MR, Luong TT, Lee C, Somerville GA, Sonenshein AL. 2008. *Staphylococcus aureus* CodY negatively regulates virulence gene expression. J Bacteriol 190:2257-65.

Manav MC, Beljantseva J, Bojer MS, Tenson T, Ingmer H, Hauryliuk V, Brodersen DE. 2018. Structural basis for (p)ppGpp synthesis by the *Staphylococcus aureus* small alarmone synthetase RelP. J Biol Chem 293:3254-3264.

Mandin P, Repoila F, Vergassola M, Geissmann T, Cossart P. 2007. Identification of new noncoding RNAs in *Listeria monocytogenes* and prediction of mRNA targets. Nucleic Acids Research 35:962-974.

Mann M, Wright PR, Backofen R. 2017. IntaRNA 2.0: enhanced and customizable prediction of RNA-RNA interactions. Nucleic Acids Res 45:W435-w439.

Manna AC, Cheung AL. 2003. *sar*U, a *sar*A homolog, is repressed by SarT and regulates virulence genes in *Staphylococcus aureus*. Infect Immun 71:343-53.

Manna A, Cheung AL. 2001. Characterization of *sar*R, a modulator of sar expression in *Staphylococcus aureus*. Infect Immun 69:885-96.

Manna AC, Cheung AL. 2006a. Transcriptional regulation of the agr locus and the identification of DNA binding residues of the global regulatory protein SarR in *Staphylococcus aureus*. Molecular Microbiology 60:1289-1301.

Manna AC, Cheung AL. 2006b. Expression of SarX, a negative regulator of agr and exoprotein synthesis, is activated by MgrA in *Staphylococcus aureus*. J Bacteriol 188:4288-99.

Manna AC, Ingavale SS, Maloney M, van Wamel W, Cheung AL. 2004. Identification of *sar*V (SA2062), a new transcriptional regulator, is repressed by SarA and MgrA (SA0641) and involved in the regulation of autolysis in *Staphylococcus aureus*. J Bacteriol 186:5267-80.

Marincola G, Schafer T, Behler J, Bernhardt J, Ohlsen K, Goerke C, Wolz C. 2012. RNase Y of *Staphylococcus aureus* and its role in the activation of virulence genes. Mol Microbiol 85:817-32.

Marincola G, Wolz C. 2017. Downstream element determines RNase Y cleavage of the *sae*PQRS operon in *Staphylococcus aureus*. Nucleic Acids Res 45:5980-5994.

Marraffini LA, DeDent AC, Schneewind O. 2006. Sortases and the Art of Anchoring Proteins to the Envelopes of Gram-Positive Bacteria. Microbiology and Molecular Biology Reviews 70:192-221.

Mascher T. 2014. Bacterial (intramembrane-sensing) histidine kinases: signal transfer rather than stimulus perception. Trends Microbiol 22:559-65.

Matsuo M, Kato F, Oogai Y, Kawai T, Sugai M, Komatsuzawa H. 2010. Distinct two-component systems in methicillin-resistant *Staphylococcus aureus* can change the susceptibility to antimicrobial agents. Journal of Antimicrobial Chemotherapy 65:1536-1537.

Mazmanian SK, Skaar EP, Gaspar AH, Humayun M, Gornicki P, Jelenska J, Joachmiak A, Missiakas DM, Schneewind O. 2003. Passage of heme-iron across the envelope of *Staphylococcus aureus*. Science 299:906-9.

McAdow M, Kim HK, Dedent AC, Hendrickx AP, Schneewind O, Missiakas DM. 2011. Preventing *Staphylococcus aureus* sepsis through the inhibition of its agglutination in blood. PLoS Pathog 7:e1002307.

McCormick JK, Yarwood JM, Schlievert PM. 2001. Toxic shock syndrome and bacterial superantigens: an update. Annu Rev Microbiol 55:77-104.

McDevitt D, Francois P, Vaudaux P, Foster TJ. 1995. Identification of the ligand-binding domain of the surface-located fibrinogen receptor (clumping factor) of *Staphylococcus aureus*. Mol Microbiol 16:895-907.

McDougal LK, Steward CD, Killgore GE, Chaitram JM, McAllister SK, Tenover FC. 2003. Pulsed-field gel electrophoresis typing of oxacillin-resistant *Staphylococcus aureus* isolates from the United States: establishing a national database. J Clin Microbiol 41:5113-20.

McGavin MH, Krajewska-Pietrasik D, Rydén C, Höök M. 1993. Identification of a *Staphylococcus aureus* extracellular matrix-binding protein with broad specificity. Infection and Immunity 61:2479-2485.

Mehlin C, Headley CM, Klebanoff SJ. 1999. An inflammatory polypeptide complex from *Staphylococcus epidermidis*: isolation and characterization. J Exp Med 189:907-18.

Mempel M, Schmidt T, Weidinger S, Schnopp C, Foster T, Ring J, Abeck D. 1998. Role of *Staphylococcus aureus* surface-associated proteins in the attachment to cultured HaCaT keratinocytes in a new adhesion assay. J Invest Dermatol 111:452-6.

Menestrina G, Dalla Serra M, Comai M, Coraiola M, Viero G, Werner S, Colin DA, Monteil H, Prevost G. 2003. Ion channels and bacterial infection: the case of beta-barrel pore-forming protein toxins of *Staphylococcus aureus*. FEBS Lett 552:54-60.

Menestrina G, Serra MD, Prevost G. 2001. Mode of action of beta-barrel pore-forming toxins of the staphylococcal alpha-hemolysin family. Toxicon 39:1661-72.

Menestrina G. 1986. Ionic channels formed by *Staphylococcus aureus* alpha-toxin: voltage-dependent inhibition by divalent and trivalent cations. J Membr Biol 90:177-90.

Menzies BE, Kourteva I. 2000. *Staphylococcus aureus* alpha-toxin induces apoptosis in endothelial cells. FEMS Immunol Med Microbiol 29:39-45.

Mera RM, Suaya JA, Amrine-Madsen H, Hogea CS, Miller LA, Lu EP, Sahm DF, O'Hara P, Acosta CJ. 2011. Increasing role of *Staphylococcus aureus* and community-acquired methicillin-resistant *Staphylococcus aureus* infections in the United States: a 10-year trend of replacement and expansion. Microb Drug Resist 17:321-8.

Michel A, Agerer F, Hauck CR, Herrmann M, Ullrich J, Hacker J, Ohlsen K. 2006. Global Regulatory Impact of ClpP Protease of *Staphylococcus aureus* on Regulons Involved in Virulence, Oxidative Stress Response, Autolysis, and DNA Repair. Journal of Bacteriology 188:5783-5796.

Miller M, Cespedes C, Vavagiakis P, Klein RS, Lowy FD. 2003. *Staphylococcus aureus* colonization in a community sample of HIV-infected and HIV-uninfected drug users. Eur J Clin Microbiol Infect Dis 22:463-9.

Miller HK, Carroll RK, Burda WN, Krute CN, Davenport JE, Shaw LN. 2012. The extracytoplasmic function sigma factor sigmaS protects against both intracellular and extracytoplasmic stresses in *Staphylococcus aureus*. J Bacteriol 194:4342-54.

Milatovic D. 1982. Effect of subinhibitory antibiotic concentrations on the phagocytosis of *Staphylococcus aureus*. Eur J Clin Microbiol 1:97-101.

Mirani ZA, Jamil N. 2011. Effect of sub-lethal doses of vancomycin and oxacillin on biofilm formation by vancomycin intermediate resistant *Staphylococcus aureus*. J Basic Microbiol 51:191-5.

Mitchell G, Fugère A, Pépin Gaudreau K, Brouillette E, Frost EH, Cantin AM, Malouin F. 2013. SigB Is a Dominant Regulator of Virulence in *Staphylococcus aureus* Small-Colony Variants. PLoS ONE 8:e65018.

Miyazaki E, Chen J-M, Ko C, Bishai WR. 1999. The *Staphylococcus aureus* rsbW (orf159) Gene Encodes an Anti-Sigma Factor of SigB. Journal of Bacteriology 181:2846-2851.

Mlynek KD, Sause WE, Moormeier DE, Sadykov MR, Hill KR, Torres VJ, Bayles KW, Brinsmade SR. 2018. Nutritional regulation of the Sae two-component system by CodY in *Staphylococcus aureus*. J Bacteriol doi:10.1128/jb.00012-18.

Montgomery CP, Boyle-Vavra S, Daum RS. 2010. Importance of the Global Regulators Agr and SaeRS in the Pathogenesis of CA-MRSA USA300 Infection. PLOS ONE 5:e15177.

Montoya M, Gouaux E. 2003. Beta-barrel membrane protein folding and structure viewed through the lens of alpha-hemolysin. Biochim Biophys Acta 1609:19-27.

Morfeldt E, Taylor D, von Gabain A, Arvidson S. 1995. Activation of alpha-toxin translation in *Staphylococcus aureus* by the trans-encoded antisense RNA, RNAIII. The EMBO Journal 14:4569-4577.

Morgan M. 2008. Methicillin-resistant *Staphylococcus aureus* and animals: zoonosis or humanosis? J Antimicrob Chemother 62:1181-7.

Morikawa K, Takemura AJ, Inose Y, Tsai M, Nguyen Thi le T, Ohta T, Msadek T. 2012. Expression of a cryptic secondary sigma factor gene unveils natural competence for DNA transformation in *Staphylococcus aureus*. PLoS Pathog 8:e1003003.

Morrison JM, Miller EW, Benson MA, Alonzo F, 3rd, Yoong P, Torres VJ, Hinrichs SH, Dunman PM. 2012a. Characterization of SSR42, a novel virulence factor regulatory RNA that contributes to the pathogenesis of a *Staphylococcus aureus* USA300 representative. J Bacteriol 194:2924-38.

Morrison JM, Anderson KL, Beenken KE, Smeltzer MS, Dunman PM. 2012b. The Staphylococcal Accessory Regulator, SarA, is an RNA-Binding Protein that Modulates the mRNA Turnover Properties of Late-Exponential and Stationary Phase *Staphylococcus aureus* Cells. Frontiers in Cellular and Infection Microbiology 2:26.

Münzenmayer L, Geiger T, Daiber E, Schulte B, Autenrieth SE, Fraunholz M, Wolz C. 2016. Influence of Sae-regulated and Agr-regulated factors on the escape of *Staphylococcus aureus* from human macrophages. Cell Microbiol 18:1172-83.

Musser JM, Schlievert PM, Chow AW, Ewan P, Kreiswirth BN, Rosdahl VT, Naidu AS, Witte W, Selander RK. 1990. A single clone of *Staphylococcus aureus* causes the majority of cases of toxic shock syndrome. Proc Natl Acad Sci U S A 87:225-9.

Muryoi N, Tiedemann MT, Pluym M, Cheung J, Heinrichs DE, Stillman MJ. 2008. Demonstration of the iron-regulated surface determinant (Isd) heme transfer pathway in *Staphylococcus aureus*. J Biol Chem 283:28125-36.

Nair D, Memmi G, Hernandez D, Bard J, Beaume M, Gill S, Francois P, Cheung AL. 2011. Whole-genome sequencing of *Staphylococcus aureus* strain RN4220, a key laboratory strain used in virulence research, identifies mutations that affect not only virulence factors but also the fitness of the strain. J Bacteriol 193:2332-5.

Nakamura Y, Oscherwitz J, Cease KB, Chan SM, Munoz-Planillo R, Hasegawa M, Villaruz AE, Cheung GY, McGavin MJ, Travers JB, Otto M, Inohara N, Nunez G. 2013. *Staphylococcus* delta-toxin induces allergic skin disease by activating mast cells. Nature 503:397-401.

Nicholas RO, Li T, McDevitt D, Marra A, Sucoloski S, Demarsh PL, Gentry DR. 1999. Isolation and characterization of a sigB deletion mutant of *Staphylococcus aureus*. Infect Immun 67:3667-9.

Nielsen JS, Olsen AS, Bonde M, Valentin-Hansen P, Kallipolitis BH. 2008. Identification of a sigma B-dependent small noncoding RNA in *Listeria monocytogenes*. J Bacteriol 190:6264-70.

Nilsson IM, Bremell T, Rydén C, Cheung AL, Tarkowski A. 1996. Role of the staphylococcal accessory gene regulator (sar) in septic arthritis. Infection and Immunity 64:4438-4443.

Novick RP, Iordanescu S, Projan SJ, Kornblum J, Edelman I. 1989. pT181 plasmid replication is regulated by a countertranscript-driven transcriptional attenuator. Cell 59:395-404.

Novick RP, Ross HF, Projan SJ, Kornblum J, Kreiswirth B, Moghazeh S. 1993. Synthesis of staphylococcal virulence factors is controlled by a regulatory RNA molecule. The EMBO Journal 12:3967-3975.

Novick RP. 2003. Autoinduction and signal transduction in the regulation of staphylococcal virulence. Mol Microbiol 48:1429-49.

Novick RP, Projan SJ, Kornblum J, Ross HF, Ji G, Kreiswirth B, Vandenesch F, Moghazeh S. 1995. The agr P2 operon: an autocatalytic sensory transduction system in *Staphylococcus aureus*. Mol Gen Genet 248:446-58.

Novick RP, Jiang D. 2003. The staphylococcal *sae*RS system coordinates environmental signals with agr quorum sensing. Microbiology 149:2709-17.

Nygaard TK, Pallister KB, Ruzevich P, Griffith S, Vuong C, Voyich JM. 2010. SaeR binds a consensus sequence within virulence gene promoters to advance USA300 pathogenesis. J Infect Dis 201:241-54.

O'Brien LM, Walsh EJ, Massey RC, Peacock SJ, Foster TJ. 2002. *Staphylococcus aureus* clumping factor B (ClfB) promotes adherence to human type I cytokeratin 10: implications for nasal colonization. Cell Microbiol 4:759-70.

O'Callaghan RJ, Callegan MC, Moreau JM, Green LC, Foster TJ, Hartford OM, Engel LS, Hill JM. 1997. Specific roles of alpha-toxin and beta-toxin during *Staphylococcus aureus* corneal infection. Infect Immun 65:1571-8.

Odenholt I. 2001. Pharmacodynamic effects of subinhibitory antibiotic concentrations. Int J Antimicrob Agents 17:1-8.

Ogston A. 1882. Micrococcus Poisoning. Journal of Anatomy and Physiology 17:24-58.

Ohlsen K, Ziebuhr W, Koller K-P, Hell W, Wichelhaus TA, Hacker J. 1998. Effects of Subinhibitory Concentrations of Antibiotics on Alpha-Toxin (*hla*) Gene Expression of Methicillin-Sensitive and Methicillin-Resistant *Staphylococcus aureus* Isolates. Antimicrobial Agents and Chemotherapy 42:2817-2823.

Olsen K, Falch BM, Danielsen K, Johannessen M, Ericson Sollid JU, Thune I, Grimnes G, Jorde R, Simonsen GS, Furberg AS. 2012. *Staphylococcus aureus* nasal carriage is associated with serum 25-hydroxyvitamin D levels, gender and smoking status. The Tromso Staph and Skin Study. Eur J Clin Microbiol Infect Dis 31:465-73.

Olson PD, Kuechenmeister LJ, Anderson KL, Daily S, Beenken KE, Roux CM, Reniere ML, Lewis TL, Weiss WJ, Pulse M, Nguyen P, Simecka JW, Morrison JM, Sayood K, Asojo OA, Smeltzer MS, Skaar EP, Dunman PM. 2011. Small Molecule Inhibitors of *Staphylococcus aureus* RnpA Alter Cellular mRNA Turnover, Exhibit Antimicrobial Activity, and Attenuate Pathogenesis. PLoS Pathogens 7:e1001287.

Olson R, Nariya H, Yokota K, Kamio Y, Gouaux E. 1999. Crystal structure of staphylococcal LukF delineates conformational changes accompanying formation of a transmembrane channel. Nat Struct Biol 6:134-40.

O'Neill E, Pozzi C, Houston P, Humphreys H, Robinson DA, Loughman A, Foster TJ, O'Gara JP. 2008. A Novel *Staphylococcus aureus* Biofilm Phenotype Mediated by the Fibronectin-Binding Proteins, FnBPA and FnBPB. Journal of Bacteriology 190:3835-3850.

Oscarsson J, Kanth A, Tegmark-Wisell K, Arvidson S. 2006. SarA Is a Repressor of hla (α-Hemolysin) Transcription in *Staphylococcus aureus*: Its Apparent Role as an Activator of *hla* in the Prototype Strain NCTC 8325 Depends on Reduced Expression of *sar*S. Journal of Bacteriology 188:8526-8533.

Oun S, Redder P, Didier JP, Francois P, Corvaglia AR, Buttazzoni E, Giraud C, Girard M, Schrenzel J, Linder P. 2013. The CshA DEAD-box RNA helicase is important for quorum sensing control in *Staphylococcus aureus*. RNA Biol 10:157-65.

Palazzolo-Ballance AM, Reniere ML, Braughton KR, Sturdevant DE, Otto M, Kreiswirth BN, Skaar EP, DeLeo FR. 2008. Neutrophil microbicides induce a pathogen survival response in community-associated methicillin-resistant *Staphylococcus aureus*. J Immunol 180:500-9.

Panton PN, Valentine FCO. 1932. Staphylococcal toxin. The Lancet 219:506-508.

Painter KL, Strange E, Parkhill J, Bamford KB, Armstrong-James D, Edwards AM. 2015. *Staphylococcus aureus* adapts to oxidative stress by producing H_2O_2-resistant small-colony variants via the SOS response. Infect Immun 83:1830-44.

Painter KL, Krishna A, Wigneshweraraj S, Edwards AM. 2014. What role does the quorum-sensing accessory gene regulator system play during *Staphylococcus aureus* bacteremia? Trends Microbiol 22:676-85.

Palma M, Cheung AL. 2001. sigma(B) activity in *Staphylococcus aureus* is controlled by RsbU and an additional factor(s) during bacterial growth. Infect Immun 69:7858-65.

Palma M, Haggar A, Flock J-I. 1999. Adherence of *Staphylococcus aureus* Is Enhanced by an Endogenous Secreted Protein with Broad Binding Activity. Journal of Bacteriology 181:2840-2845.

Palmqvist N, Foster T, Fitzgerald JR, Josefsson E, Tarkowski A. 2005. Fibronectin-binding proteins and fibrinogen-binding clumping factors play distinct roles in staphylococcal arthritis and systemic inflammation. J Infect Dis 191:791-8.

Pané-Farré J, Jonas B, Forstner K, Engelmann S, Hecker M. 2006. The sigmaB regulon in *Staphylococcus aureus* and its regulation. Int J Med Microbiol 296:237-58.

Pané-Farré J, Jonas B, Hardwick SW, Gronau K, Lewis RJ, Hecker M, Engelmann S. 2009. Role of RsbU in Controlling SigB Activity in *Staphylococcus aureus* following Alkaline Stress. Journal of Bacteriology 191:2561-2573.

Panizzi P, Nahrendorf M, Figueiredo JL, Panizzi J, Marinelli B, Iwamoto Y, Keliher E, Maddur AA, Waterman P, Kroh HK, Leuschner F, Aikawa E, Swirski FK, Pittet MJ, Hackeng TM, Fuentes-Prior P, Schneewind O, Bock PE, Weissleder R. 2011. In vivo detection of *Staphylococcus aureus* endocarditis by targeting pathogen-specific prothrombin activation. Nat Med 17:1142-6.

Patel AH, Nowlan P, Weavers ED, Foster T. 1987. Virulence of protein A-deficient and alpha-toxin-deficient mutants of *Staphylococcus aureus* isolated by allele replacement. Infect Immun 55:3103-10.

Peacock SJ, Foster TJ, Cameron BJ, Berendt AR. 1999. Bacterial fibronectin-binding proteins and endothelial cell surface fibronectin mediate adherence of *Staphylococcus aureus* to resting human endothelial cells. Microbiology 145 (Pt 12):3477-86.

Peschel A, Vuong C, Otto M, Gotz F. 2000. The D-alanine residues of *Staphylococcus aureus* teichoic acids alter the susceptibility to vancomycin and the activity of autolytic enzymes. Antimicrob Agents Chemother 44:2845-7.

Peschel A, Otto M. 2013. Phenol-soluble modulins and staphylococcal infection. Nat Rev Microbiol 11:667-73.

Peschel A, Otto M, Jack RW, Kalbacher H, Jung G, Gotz F. 1999. Inactivation of the dlt operon in *Staphylococcus aureus* confers sensitivity to defensins, protegrins, and other antimicrobial peptides. J Biol Chem 274:8405-10.

Papenfort K, Vogel J. 2010. Regulatory RNA in bacterial pathogens. Cell Host Microbe 8:116-27.

Pichon C, Felden B. 2005. Small RNA genes expressed from *Staphylococcus aureus* genomic and pathogenicity islands with specific expression among pathogenic strains. Proc Natl Acad Sci U S A 102:14249-54.

Pishchany G, Haley KP, Skaar EP. 2013. *Staphylococcus aureus* growth using human hemoglobin as an iron source. Journal of visualized experiments : JoVE doi:10.3791/50072:10.3791/50072 50072.

Plouin-Gaudon I, Clement S, Huggler E, Chaponnier C, Francois P, Lew D, Schrenzel J, Vaudaux P, Lacroix JS. 2006. Intracellular residency is frequently associated with recurrent *Staphylococcus aureus* rhinosinusitis. Rhinology 44:249-54.

Pohl K, Francois P, Stenz L, Schlink F, Geiger T, Herbert S, Goerke C, Schrenzel J, Wolz C. 2009. CodY in *Staphylococcus aureus*: a regulatory link between metabolism and virulence gene expression. J Bacteriol 191:2953-63.

Postma B, Poppelier MJ, van Galen JC, Prossnitz ER, van Strijp JA, de Haas CJ, van Kessel KP. 2004. Chemotaxis inhibitory protein of *Staphylococcus aureus* binds specifically to the C5a and formylated peptide receptor. J Immunol 172:6994-7001.

Powers ME, Becker REN, Sailer A, Turner JR, Wardenburg JB. 2015. Synergistic Action of *Staphylococcus aureus* α-Toxin on Platelets and Myeloid Lineage Cells Contributes to Lethal Sepsis. Cell host & microbe 17:775-787.

Pragman AA, Yarwood JM, Tripp TJ, Schlievert PM. 2004. Characterization of virulence factor regulation by SrrAB, a two-component system in *Staphylococcus aureus*. J Bacteriol 186:2430-8.

Prasse D, Ehlers C, Backofen R, Schmitz RA. 2013. Regulatory RNAs in archaea: first target identification in Methanoarchaea. Biochem Soc Trans 41:344-9.

Prévost G, Cribier B, Couppié P, Petiau P, Supersac G, Finck-Barbançon V, Monteil H, Piemont Y. 1995. Panton-Valentine leucocidin and gamma-hemolysin from *Staphylococcus aureus* ATCC 49775 are encoded by distinct genetic loci and have different biological activities. Infection and Immunity 63:4121-4129.

Proctor RA, Balwit JM, Vesga O. 1994. Variant subpopulations of *Staphylococcus aureus* as cause of persistent and recurrent infections. Infect Agents Dis 3:302-12.

Proctor RA, van Langevelde P, Kristjansson M, Maslow JN, Arbeit RD. 1995. Persistent and relapsing infections associated with small-colony variants of *Staphylococcus aureus*. Clin Infect Dis 20:95-102.

Proctor RA, von Eiff C, Kahl BC, Becker K, McNamara P, Herrmann M, Peters G. 2006. Small colony variants: a pathogenic form of bacteria that facilitates persistent and recurrent infections. Nat Rev Microbiol 4:295-305.

Proctor RA, Olbrantz PJ, Mosher DF. 1983. Subinhibitory concentrations of antibiotics alter fibronectin binding to *Staphylococcus aureus*. Antimicrobial Agents and Chemotherapy 24:823-826

Radin JN, Kelliher JL, Párraga Solórzano PK, Kehl-Fie TE. 2016. The Two-Component System ArlRS and Alterations in Metabolism Enable *Staphylococcus aureus* to Resist Calprotectin-Induced Manganese Starvation. PLoS Pathogens 12:e1006040.

Reffuveille F, Josse J, Vallé Q, Mongaret C, Gangloff S. 2017. *Staphylococcus aureus* Biofilms and their Impact on the Medical Field. 10.5772/66380.

Reniere ML, Ukpabi GN, Harry SR, Stec DF, Krull R, Wright DW, Bachmann BO, Murphy ME, Skaar EP. 2010. The IsdG-family of haem oxygenases degrades haem to a novel chromophore. Mol Microbiol 75:1529-38.

Reyes D, Andrey DO, Monod A, Kelley WL, Zhang G, Cheung AL. 2011. Coordinated Regulation by AgrA, SarA, and SarR To Control agr Expression in *Staphylococcus aureus*. Journal of Bacteriology 193:6020-6031.

Righetti F, Nuss AM, Twittenhoff C, Beele S, Urban K, Will S, Bernhart SH, Stadler PF, Dersch P, Narberhaus F. 2016. Temperature-responsive in vitro RNA structurome of *Yersinia pseudotuberculosis*. Proceedings of the National Academy of Sciences of the United States of America 113:7237-7242.

Roberts C, Anderson KL, Murphy E, Projan SJ, Mounts W, Hurlburt B, Smeltzer M, Overbeek R, Disz T, Dunman PM. 2006. Characterizing the Effect of the *Staphylococcus aureus* Virulence Factor Regulator, SarA, on Log-Phase mRNA Half-Lives. Journal of Bacteriology 188:2593-2603.

Rogasch K, Rühmling V, Pané-Farré J, Höper D, Weinberg C, Fuchs S, Schmudde M, Bröker BM, Wolz C, Hecker M, Engelmann S. 2006. Influence of the Two-Component System SaeRS on Global Gene Expression in Two Different *Staphylococcus aureus* Strains. Journal of Bacteriology 188:7742-7758.

Rolo J, Miragaia M, Turlej-Rogacka A, Empel J, Bouchami O, Faria NA, Tavares A, Hryniewicz W, Fluit AC, de Lencastre H. 2012. High genetic diversity among community-associated *Staphylococcus aureus* in Europe: results from a multicenter study. PLoS One 7:e34768.

Rubinstein E, Kollef MH, Nathwani D. 2008. Pneumonia caused by methicillin-resistant *Staphylococcus aureus*. Clin Infect Dis 46 Suppl 5:S378-85.

Rudkin JK, Laabei M, Edwards AM, Joo HS, Otto M, Lennon KL, O'Gara JP, Waterfield NR, Massey RC. 2014. Oxacillin alters the toxin expression profile of community-associated methicillin-resistant *Staphylococcus aureus*. Antimicrob Agents Chemother 58:1100-7.

Que Y-A, Haefliger J-A, Piroth L, François P, Widmer E, Entenza JM, Sinha B, Herrmann M, Francioli P, Vaudaux P, Moreillon P. 2005. Fibrinogen and fibronectin binding cooperate for valve infection and invasion in *Staphylococcus aureus* experimental endocarditis. The Journal of Experimental Medicine 201:1627-1635.

Queck SY, Jameson-Lee M, Villaruz AE, Bach T-HL, Khan BA, Sturdevant DE, Ricklefs SM, Li M, Otto M. 2008. RNAIII-independent target gene control by the agr quorum-sensing system: insight into the evolution of virulence regulation in *Staphylococcus aureus*. Molecular cell 32:150-158.

Queck SY, Khan BA, Wang R, Bach TH, Kretschmer D, Chen L, Kreiswirth BN, Peschel A, Deleo FR, Otto M. 2009. Mobile genetic element-encoded cytolysin connects virulence to methicillin resistance in MRSA. PLoS Pathog 5:e1000533.

Saha R, Saha N, Donofrio RS, Bestervelt LL. 2013. Microbial siderophores: a mini review. J Basic Microbiol 53:303-17.

Saïd-Salim B, Dunman PM, McAleese FM, Macapagal D, Murphy E, McNamara PJ, Arvidson S, Foster TJ, Projan SJ, Kreiswirth BN. 2003. Global Regulation of *Staphylococcus aureus* Genes by Rot. Journal of Bacteriology 185:610-619.

Sansonetti PJ, Ryter A, Clerc P, Maurelli AT, Mounier J. 1986. Multiplication of *Shigella flexneri* within HeLa cells: lysis of the phagocytic vacuole and plasmid-mediated contact hemolysis. Infection and Immunity 51:461-469.

Sassi M, Augagneur Y, Mauro T, Ivain L, Chabelskaya S, Hallier M, Sallou O, Felden B. 2015. SRD: a *Staphylococcus* regulatory RNA database. Rna 21:1005-17.

Schäfer D, Lâm T-T, Geiger T, Mainiero M, Engelmann S, Hussain M, Bosserhoff A, Frosch M, Bischoff M, Wolz C, Reidl J, Sinha B. 2009. A Point Mutation in the Sensor Histidine Kinase SaeS of *Staphylococcus aureus* Strain Newman Alters the Response to Biocide Exposure. Journal of Bacteriology 191:7306-7314.

Scherr TD, Heim CE, Morrison JM, Kielian T. 2014. Hiding in Plain Sight: Interplay between Staphylococcal Biofilms and Host Immunity. Frontiers in Immunology 5:37.

Schleif R. 2010. AraC protein, regulation of the l-arabinose operon in *Escherichia coli*, and the light switch mechanism of AraC action. FEMS Microbiol Rev 34:779-96.

Schmidt KA, Manna AC, Gill S, Cheung AL. 2001. SarT, a repressor of alpha-hemolysin in *Staphylococcus aureus*. Infect Immun 69:4749-58.

Schmidt KA, Manna AC, Cheung AL. 2003. SarT influences *sar*S expression in *Staphylococcus aureus*. Infect Immun 71:5139-48.

Schneider CA, Rasband WS, Eliceiri KW. 2012. NIH Image to ImageJ: 25 years of Image Analysis. Nature methods 9:671-675.

Schröder A, Kland R, Peschel A, von Eiff C, Aepfelbacher M. 2006. Live cell imaging of phagosome maturation in *Staphylococcus aureus* infected human endothelial cells: small colony variants are able to survive in lysosomes. Med Microbiol Immunol 195:185-94.

Schröder W, Goerke C, Wolz C. 2013. Opposing effects of aminocoumarins and fluoroquinolones on the SOS response and adaptability in *Staphylococcus aureus*. J Antimicrob Chemother 68:529-38.

Schumacher MA, Pearson RF, Moller T, Valentin-Hansen P, Brennan RG. 2002. Structures of the pleiotropic translational regulator Hfq and an Hfq-RNA complex: a bacterial Sm-like protein. Embo j 21:3546-56.

Schwan WR, Langhorne MH, Ritchie HD, Stover CK. 2003. Loss of hemolysin expression in *Staphylococcus aureus* agr mutants correlates with selective survival during mixed infections in murine abscesses and wounds. FEMS Immunol Med Microbiol 38:23-8.

Schwarz-Linek U, Hook M, Potts JR. 2004. The molecular basis of fibronectin-mediated bacterial adherence to host cells. Mol Microbiol 52:631-41.

Schwarz-Linek U, Werner JM, Pickford AR, Gurusiddappa S, Kim JH, Pilka ES, Briggs JA, Gough TS, Hook M, Campbell ID, Potts JR. 2003. Pathogenic bacteria attach to human fibronectin through a tandem beta-zipper. Nature 423:177-81.

Seidl K, Leemann M, Zinkernagel AS. 2018. The ArlRS two-component system is a regulator of *Staphylococcus aureus*-induced endothelial cell damage. Eur J Clin Microbiol Infect Dis 37:289-292.

Seidl K, Muller S, Francois P, Kriebitzsch C, Schrenzel J, Engelmann S, Bischoff M, Berger-Bachi B. 2009. Effect of a glucose impulse on the CcpA regulon in *Staphylococcus aureus*. BMC Microbiol 9:95.

Sendi P, Proctor RA. 2009. *Staphylococcus aureus* as an intracellular pathogen: the role of small colony variants. Trends Microbiol 17:54-8.

Senn L, Basset P, Nahimana I, Zanetti G, Blanc DS. 2012. Which anatomical sites should be sampled for screening of methicillin-resistant *Staphylococcus aureus* carriage by culture or by rapid PCR test? Clin Microbiol Infect 18:E31-3.

Senn MM, Giachino P, Homerova D, Steinhuber A, Strassner J, Kormanec J, Flückiger U, Berger-Bächi B, Bischoff M. 2005. Molecular Analysis and Organization of the σ(B) Operon in *Staphylococcus aureus.* Journal of Bacteriology 187:8006-8019.

Shannon O, Uekotter A, Flock JI. 2005. Extracellular fibrinogen binding protein, Efb, from *Staphylococcus aureus* as an antiplatelet agent in vivo. Thromb Haemost 93:927-31.

Shannon O, Flock JI. 2004. Extracellular fibrinogen binding protein, Efb, from *Staphylococcus aureus* binds to platelets and inhibits platelet aggregation. Thromb Haemost 91:779-89.

Sheen TR, Ebrahimi CM, Hiemstra IH, Barlow SB, Peschel A, Doran KS. 2010. Penetration of the blood-brain barrier by *Staphylococcus aureus*: contribution of membrane-anchored lipoteichoic acid. J Mol Med (Berl) 88:633-9.

Shinji H, Yosizawa Y, Tajima A, Iwase T, Sugimoto S, Seki K, Mizunoe Y. 2011. Role of Fibronectin-Binding Proteins A and B in In Vitro Cellular Infections and In Vivo Septic Infections by *Staphylococcus aureus.* Infection and Immunity 79:2215-2223.

Shore AC, Rossney AS, Brennan OM, Kinnevey PM, Humphreys H, Sullivan DJ, Goering RV, Ehricht R, Monecke S, Coleman DC. 2011. Characterization of a novel arginine catabolic mobile element (ACME) and staphylococcal chromosomal cassette mec composite island with significant homology to *Staphylococcus epidermidis* ACME type II in methicillin-resistant *Staphylococcus aureus* genotype ST22-MRSA-IV. Antimicrob Agents Chemother 55:1896-905.

Shaw LN, Lindholm C, Prajsnar TK, Miller HK, Brown MC, Golonka E, Stewart GC, Tarkowski A, Potempa J. 2008. Identification and characterization of sigma, a novel component of the *Staphylococcus aureus* stress and virulence responses. PLoS One 3:e3844.

Sheehy SH, Atkins BA, Bejon P, Byren I, Wyllie D, Athanasou NA, Berendt AR, McNally MA. 2010. The microbiology of chronic osteomyelitis: prevalence of resistance to common empirical anti-microbial regimens. J Infect 60:338-43.

Shi S, Zhang X. 2012. Interaction of *Staphylococcus aureus* with osteoblasts (Review). Exp Ther Med 3:367-370.

Shompole S, Henon KT, Liou LE, Dziewanowska K, Bohach GA, Bayles KW. 2003. Biphasic intracellular expression of *Staphylococcus aureus* virulence factors and evidence for Agr-mediated diffusion sensing. Mol Microbiol 49:919-27.

Shorr AF, Tabak YP, Gupta V, Johannes RS, Liu LZ, Kollef MH. 2006. Morbidity and cost burden of methicillin-resistant *Staphylococcus aureus* in early onset ventilator-associated pneumonia. Crit Care 10:R97.

Shorr AF, Haque N, Taneja C, Zervos M, Lamerato L, Kothari S, Zilber S, Donabedian S, Perri MB, Spalding J, Oster G. 2010. Clinical and economic outcomes for patients with health care-associated *Staphylococcus aureus* pneumonia. J Clin Microbiol 48:3258-62.

Siboo IR, Cheung AL, Bayer AS, Sullam PM. 2001. Clumping Factor A Mediates Binding of *Staphylococcus aureus* to Human Platelets. Infection and Immunity 69:3120-3127.

Skaar EP, Humayun M, Bae T, DeBord KL, Schneewind O. 2004a. Iron-source preference of *Staphylococcus aureus* infections. Science 305:1626-8.

Skaar EP, Gaspar AH, Schneewind O. 2004b. IsdG and IsdI, heme-degrading enzymes in the cytoplasm of *Staphylococcus aureus*. J Biol Chem 279:436-43.

Sinha B, Francois PP, Nusse O, Foti M, Hartford OM, Vaudaux P, Foster TJ, Lew DP, Herrmann M, Krause KH. 1999. Fibronectin-binding protein acts as *Staphylococcus aureus* invasin via fibronectin bridging to integrin alpha5beta1. Cell Microbiol 1:101-17.

Sinha B, Francois P, Que YA, Hussain M, Heilmann C, Moreillon P, Lew D, Krause KH, Peters G, Herrmann M. 2000. Heterologously expressed *Staphylococcus aureus* fibronectin-binding proteins are sufficient for invasion of host cells. Infect Immun 68:6871-8.

Singh R, Ray P, Das A, Sharma M. 2010. Penetration of antibiotics through *Staphylococcus aureus* and *Staphylococcus epidermidis* biofilms. J Antimicrob Chemother 65:1955-8.

Smirnov A, Förstner KU, Holmqvist E, Otto A, Günster R, Becher D, Reinhardt R, Vogel J. 2016. Grad-seq guides the discovery of ProQ as a major small RNA-binding protein. Proceedings of the National Academy of Sciences 113:11591-11596.

Smyth CJ, Möllby R, Wadström T. 1975. Phenomenon of hot-cold hemolysis: chelator-induced lysis of sphingomyelinase-treated erythrocytes. Infection and Immunity 12:1104-1111.

Sollid JU, Furberg AS, Hanssen AM, Johannessen M. 2014. *Staphylococcus aureus*: determinants of human carriage. Infect Genet Evol 21:531-41.

Somerville GA, Proctor RA. 2013. Cultivation conditions and the diffusion of oxygen into culture media: The rationale for the flask-to-medium ratio in microbiology. BMC Microbiology 13:9-9.

Somerville GA, Said-Salim B, Wickman JM, Raffel SJ, Kreiswirth BN, Musser JM. 2003. Correlation of acetate catabolism and growth yield in *Staphylococcus aureus*: implications for host-pathogen interactions. Infect Immun 71:4724-32.

Song L, Hobaugh MR, Shustak C, Cheley S, Bayley H, Gouaux JE. 1996. Structure of staphylococcal alpha-hemolysin, a heptameric transmembrane pore. Science 274:1859-66.

Soong G, Martin FJ, Chun J, Cohen TS, Ahn DS, Prince A. 2011. *Staphylococcus aureus* protein A mediates invasion across airway epithelial cells through activation of RhoA GTPase signaling and proteolytic activity. J Biol Chem 286:35891-8.

Speziale P, Pietrocola G, Rindi S, Provenzano M, Provenza G, Di Poto A, Visai L, Arciola CR. 2009. Structural and functional role of *Staphylococcus aureus* surface components recognizing adhesive matrix molecules of the host. Future Microbiol 4:1337-52.

Springer B, Orendi U, Much P, Hoger G, Ruppitsch W, Krziwanek K, Metz-Gercek S, Mittermayer H. 2009. Methicillin-resistant *Staphylococcus aureus*: a new zoonotic agent? Wien Klin Wochenschr 121:86-90.

Steidl R, Pearson S, Stephenson RE, Ledala N, Sitthisak S, Wilkinson BJ, Jayaswal RK. 2008. *Staphylococcus aureus* cell wall stress stimulon gene-lacZ fusion strains: potential for use in screening for cell wall-active antimicrobials. Antimicrob Agents Chemother 52:2923-5.

Steinhuber A, Goerke C, Bayer MG, Döring G, Wolz C. 2003. Molecular Architecture of the Regulatory Locus sae of *Staphylococcus aureus* and Its Impact on Expression of Virulence Factors. Journal of Bacteriology 185:6278-6286.

Sterba KM, Mackintosh SG, Blevins JS, Hurlburt BK, Smeltzer MS. 2003. Characterization of *Staphylococcus aureus* SarA Binding Sites. Journal of Bacteriology 185:4410-4417.

Stewart PS, Costerton JW. 2001. Antibiotic resistance of bacteria in biofilms. Lancet 358:135-8.

Strobel M, Pfortner H, Tuchscherr L, Volker U, Schmidt F, Kramko N, Schnittler HJ, Fraunholz MJ, Loffler B, Peters G, Niemann S. 2016. Post-invasion events after infection with *Staphylococcus aureus* are strongly dependent on both the host cell type and the infecting S. aureus strain. Clin Microbiol Infect 22:799-809.

Stryjewski ME, Chambers HF. 2008. Skin and soft-tissue infections caused by community-acquired methicillin-resistant *Staphylococcus aureus*. Clin Infect Dis 46 Suppl 5:S368-77.

Subrt N, Mesak LR, Davies J. 2011. Modulation of virulence gene expression by cell wall active antibiotics in *Staphylococcus aureus*. J Antimicrob Chemother 66:979-84.

Sun F, Li C, Jeong D, Sohn C, He C, Bae T. 2010. In the *Staphylococcus aureus* two-component system sae, the response regulator SaeR binds to a direct repeat sequence and DNA binding requires phosphorylation by the sensor kinase SaeS. J Bacteriol 192:2111-27.

Sutherland R, Rolinson GN. 1964. Characteristics of methicillin-resistant Staphylococci. J Bacteriol 87:887-99.

Suttorp N, Habben E. 1988. Effect of staphylococcal alpha-toxin on intracellular Ca2+ in polymorphonuclear leukocytes. Infect Immun 56:2228-34.

Svensson SL, Sharma CM. 2016. Small RNAs in Bacterial Virulence and Communication. Microbiol Spectr 4.

Szafranska AK, Oxley APA, Chaves-Moreno D, Horst SA, Roßlenbroich S, Peters G, Goldmann O, Rohde M, Sinha B, Pieper DH, Löffler B, Jauregui R, Wos-Oxley ML, Medina E. 2014. High-Resolution Transcriptomic Analysis of the Adaptive Response of *Staphylococcus aureus* during Acute and Chronic Phases of Osteomyelitis. mBio 5:e01775-14.

Talan DA, Krishnadasan A, Gorwitz RJ, Fosheim GE, Limbago B, Albrecht V, Moran GJ. 2011. Comparison of *Staphylococcus aureus* from skin and soft-tissue infections in US emergency department patients, 2004 and 2008. Clin Infect Dis 53:144-9.

Tamber S, Schwartzman J, Cheung AL. 2010. Role of PknB kinase in antibiotic resistance and virulence in community-acquired methicillin-resistant *Staphylococcus aureus* strain USA300. Infect Immun 78:3637-46.

Tegmark K, Karlsson A, Arvidson S. 2000. Identification and characterization of SarH1, a new global regulator of virulence gene expression in *Staphylococcus aureus*. Mol Microbiol 37:398-409.

Thoendel M, Horswill AR. 2009. Identification of *Staphylococcus aureus* AgrD residues required for autoinducing peptide biosynthesis. J Biol Chem 284:21828-38.

Thomason MK, Storz G. 2010. Bacterial antisense RNAs: How many are there and what are they doing? Annual review of genetics 44:167-188.

Thomer L, Schneewind O, Missiakas D. 2013. Multiple ligands of von Willebrand factor-binding protein (vWbp) promote *Staphylococcus aureus* clot formation in human plasma. J Biol Chem 288:28283-92.

Throup JP, Zappacosta F, Lunsford RD, Annan RS, Carr SA, Lonsdale JT, Bryant AP, McDevitt D, Rosenberg M, Burnham MK. 2001. The *srh*SR gene pair from *Staphylococcus aureus*: genomic and

proteomic approaches to the identification and characterization of gene function. Biochemistry 40:10392-401.

Thurlow LR, Joshi GS, Clark JR, Spontak JS, Neely CJ, Maile R, Richardson AR. 2013. Functional modularity of the arginine catabolic mobile element contributes to the success of USA300 methicillin-resistant *Staphylococcus aureus*. Cell Host Microbe 13:100-7.

Toledo-Arana A, Dussurget O, Nikitas G, Sesto N, Guet-Revillet H, Balestrino D, Loh E, Gripenland J, Tiensuu T, Vaitkevicius K, Barthelemy M, Vergassola M, Nahori MA, Soubigou G, Regnault B, Coppee JY, Lecuit M, Johansson J, Cossart P. 2009. The *Listeria* transcriptional landscape from saprophytism to virulence. Nature 459:950-6.

Tong SY, Davis JS, Eichenberger E, Holland TL, Fowler VG, Jr. 2015. *Staphylococcus aureus* infections: epidemiology, pathophysiology, clinical manifestations, and management. Clin Microbiol Rev 28:603-61.

Treiber T, Treiber N, Plessmann U, Harlander S, Daiss JL, Eichner N, Lehmann G, Schall K, Urlaub H, Meister G. 2017. A Compendium of RNA-Binding Proteins that Regulate MicroRNA Biogenesis. Mol Cell 66:270-284.e13.

Troidle L, Eisen T, Pacelli L, Finkelstein F. 2007. Complications associated with the development of bacteremia with *Staphylococcus aureus*. Hemodial Int 11:72-5.

Tsubakishita S, Kuwahara-Arai K, Sasaki T, Hiramatsu K. 2010. Origin and molecular evolution of the determinant of methicillin resistance in staphylococci. Antimicrob Agents Chemother 54:4352-9.

Tuazon CU, Perez A, Kishaba T, Sheagren JN. 1975. *Staphylococcus aureus* among insulin-injecting diabetic patients. An increased carrier rate. Jama 231:1272.

Tuchscherr L, Medina E, Hussain M, Volker W, Heitmann V, Niemann S, Holzinger D, Roth J, Proctor RA, Becker K, Peters G, Loffler B. 2011. *Staphylococcus aureus* phenotype switching: an effective bacterial strategy to escape host immune response and establish a chronic infection. EMBO Mol Med 3:129-41.

Tuchscherr L, Heitmann V, Hussain M, Viemann D, Roth J, von Eiff C, Peters G, Becker K, Loffler B. 2010. *Staphylococcus aureus* small-colony variants are adapted phenotypes for intracellular persistence. J Infect Dis 202:1031-40.

Tuchscherr L, Bischoff M, Lattar SM, Noto Llana M, Pfortner H, Niemann S, Geraci J, Van de Vyver H, Fraunholz MJ, Cheung AL, Herrmann M, Volker U, Sordelli DO, Peters G, Loffler B. 2015. Sigma Factor SigB Is Crucial to Mediate *Staphylococcus aureus* Adaptation during Chronic Infections. PLoS Pathog 11:e1004870.

Rosenbach, FJ 1884. Mikroorganismen bei den Wundinfektionskrankheiten des Menschen.

Ubukata K, Nonoguchi R, Song MD, Matsuhashi M, Konno M. 1990. Homology of *mec*A gene in methicillin-resistant *Staphylococcus haemolyticus* and *Staphylococcus simulans* to that of *Staphylococcus aureus*. Antimicrob Agents Chemother 34:170-2.

Urban JH, Vogel J. 2007. Translational control and target recognition by *Escherichia coli* small RNAs in vivo. Nucleic Acids Research 35:1018-1037.

Valentin-Hansen P, Eriksen M, Udesen C. 2004. The bacterial Sm-like protein Hfq: a key player in RNA transactions. Mol Microbiol 51:1525-33.

Valeva A, Palmer M, Hilgert K, Kehoe M, Bhakdi S. 1995. Correct oligomerization is a prerequisite for insertion of the central molecular domain of staphylococcal alpha-toxin into the lipid bilayer. Biochim Biophys Acta 1236:213-8.

Valeva A, Schnabel R, Walev I, Boukhallouk F, Bhakdi S, Palmer M. 2001. Membrane insertion of the heptameric staphylococcal alpha-toxin pore. A domino-like structural transition that is allosterically modulated by the target cell membrane. J Biol Chem 276:14835-41.

Vandenesch F, Lina G, Henry T. 2012. *Staphylococcus aureus* Hemolysins, bi-component Leukocidins, and Cytolytic Peptides: A Redundant Arsenal of Membrane-Damaging Virulence Factors? Frontiers in Cellular and Infection Microbiology 2:12.

van Wamel WJ, Rooijakkers SH, Ruyken M, van Kessel KP, van Strijp JA. 2006. The innate immune modulators staphylococcal complement inhibitor and chemotaxis inhibitory protein of *Staphylococcus aureus* are located on beta-hemolysin-converting bacteriophages. J Bacteriol 188:1310-5.

Vann JM, Proctor RA. 1987. Ingestion of *Staphylococcus aureus* by bovine endothelial cells results in time- and inoculum-dependent damage to endothelial cell monolayers. Infect Immun 55:2155-63.

Veloso TR, Chaouch A, Roger T, Giddey M, Vouillamoz J, Majcherczyk P, Que Y-A, Rousson V, Moreillon P, Entenza JM. 2013. Use of a Human-Like Low-Grade Bacteremia Model of Experimental Endocarditis To Study the Role of *Staphylococcus aureus* Adhesins and Platelet Aggregation in Early Endocarditis. Infection and Immunity 81:697-703.

Ventura CL, Malachowa N, Hammer CH, Nardone GA, Robinson MA, Kobayashi SD, DeLeo FR. 2010. Identification of a novel *Staphylococcus aureus* two-component leukotoxin using cell surface proteomics. PLoS One 5:e11634.

Vesga O, Groeschel MC, Otten MF, Brar DW, Vann JM, Proctor RA. 1996. *Staphylococcus aureus* small colony variants are induced by the endothelial cell intracellular milieu. J Infect Dis 173:739-42.

Vogel J, Luisi BF. 2011. Hfq and its constellation of RNA. Nat Rev Microbiol 9:578-89.

von Eiff C, Becker K, Machka K, Stammer H, Peters G. 2001. Nasal carriage as a source of *Staphylococcus aureus* bacteremia. Study Group. N Engl J Med 344:11-6.

Voss A, Loeffen F, Bakker J, Klaassen C, Wulf M. 2005. Methicillin-resistant *Staphylococcus aureus* in Pig Farming. Emerging Infectious Diseases 11:1965-1966.

Voyich JM, Vuong C, DeWald M, Nygaard TK, Kocianova S, Griffith S, Jones J, Iverson C, Sturdevant DE, Braughton KR, Whitney AR, Otto M, DeLeo FR. 2009. The SaeR/S Gene Regulatory System is Essential for Innate Immune Evasion by *Staphylococcus aureus*. The Journal of infectious diseases 199:1698-1706.

Walev I, Palmer M, Martin E, Jonas D, Weller U, Hohn-Bentz H, Husmann M, Bhakdi S. 1994. Recovery of human fibroblasts from attack by the pore-forming alpha-toxin of *Staphylococcus aureus*. Microb Pathog 17:187-201.

Walker B, Krishnasastry M, Zorn L, Bayley H. 1992. Assembly of the oligomeric membrane pore formed by Staphylococcal alpha-hemolysin examined by truncation mutagenesis. J Biol Chem 267:21782-6.

Walker JN, Crosby HA, Spaulding AR, Salgado-Pabon W, Malone CL, Rosenthal CB, Schlievert PM, Boyd JM, Horswill AR. 2013. The *Staphylococcus aureus* ArlRS two-component system is a novel regulator of agglutination and pathogenesis. PLoS Pathog 9:e1003819.

Wallace RG, Lee N, Fowler AV. 1980. The *ara*C gene of *Escherichia coli*: transcriptional and translational start-points and complete nucleotide sequence. Gene 12:179-90.

Wals PA, Katz J. 1993. A concentration gradient of glucose from liver to plasma. Metabolism 42:1492-6.

Walsh EJ, O'Brien LM, Liang X, Hook M, Foster TJ. 2004. Clumping factor B, a fibrinogen-binding MSCRAMM (microbial surface components recognizing adhesive matrix molecules) adhesin of *Staphylococcus aureus*, also binds to the tail region of type I cytokeratin 10. J Biol Chem 279:50691-9.

Wang R, Braughton KR, Kretschmer D, Bach TH, Queck SY, Li M, Kennedy AD, Dorward DW, Klebanoff SJ, Peschel A, DeLeo FR, Otto M. 2007. Identification of novel cytolytic peptides as key virulence determinants for community-associated MRSA. Nat Med 13:1510-4.

Weidenmaier C, Goerke C, Wolz C. 2012. *Staphylococcus aureus* determinants for nasal colonization. Trends Microbiol 20:243-50.

Weinberg ED. 1978. Iron and infection. Microbiological Reviews 42:45-66.

Weinrick B, Dunman PM, McAleese F, Murphy E, Projan SJ, Fang Y, Novick RP. 2004. Effect of mild acid on gene expression in *Staphylococcus aureus*. J Bacteriol 186:8407-23.

Wertheim HF, Melles DC, Vos MC, van Leeuwen W, van Belkum A, Verbrugh HA, Nouwen JL. 2005. The role of nasal carriage in *Staphylococcus aureu*s infections. Lancet Infect Dis 5:751-62.

Wesson CA, Liou LE, Todd KM, Bohach GA, Trumble WR, Bayles KW. 1998. *Staphylococcus aureus* Agr and Sar global regulators influence internalization and induction of apoptosis. Infect Immun 66:5238-43.

Wilke GA, Bubeck Wardenburg J. 2010. Role of a disintegrin and metalloprotease 10 in S*taphylococcus aureus* alpha-hemolysin-mediated cellular injury. Proc Natl Acad Sci U S A 107:13473-8.

Williams REO. 1963. Healthy carriage of *Staphylococcus aureus*: Its prevalence and importance. Bacteriological Reviews 27:56-71.

Witte W, Strommenger B, Stanek C, Cuny C. 2007. Methicillin-resistant *Staphylococcus aureus* ST398 in humans and animals, Central Europe. Emerg Infect Dis 13:255-8.

Wright PR, Georg J, Mann M, Sorescu DA, Richter AS, Lott S, Kleinkauf R, Hess WR, Backofen R. 2014. CopraRNA and IntaRNA: predicting small RNA targets, networks and interaction domains. Nucleic Acids Research 42:W119-W123.

Wulf MW, Sorum M, van Nes A, Skov R, Melchers WJ, Klaassen CH, Voss A. 2008. Prevalence of methicillin-resistant *Staphylococcus aureus* among veterinarians: an international study. Clin Microbiol Infect 14:29-34.

Xia G, Kohler T, Peschel A. 2010. The wall teichoic acid and lipoteichoic acid polymers of *Staphylococcus aureus*. Int J Med Microbiol 300:148-54.

Xie C, Alcaide P, Geisbrecht BV, Schneider D, Herrmann M, Preissner KT, Luscinskas FW, Chavakis T. 2006. Suppression of experimental autoimmune encephalomyelitis by extracellular adherence protein of *Staphylococcus aureus*. J Exp Med 203:985-94.

Xiong YQ, Van Wamel W, Nast CC, Yeaman MR, Cheung AL, Bayer AS. 2002. Activation and transcriptional interaction between agr RNAII and RNAIII in *Staphylococcus aureus* in vitro and in an experimental endocarditis model. J Infect Dis 186:668-77.

Xiong YQ, Willard J, Yeaman MR, Cheung AL, Bayer AS. 2006. Regulation of *Staphylococcus aureus* alpha-toxin gene (*hla*) expression by *agr*, *sar*A, and *sae* in vitro and in experimental infective endocarditis. J Infect Dis 194:1267-75.

Xue T, Zhang X, Sun H, Sun B. 2014. ArtR, a novel sRNA of *Staphylococcus aureus*, regulates alpha-toxin expression by targeting the 5' UTR of *sar*T mRNA. Med Microbiol Immunol 203:1-12.

Xu SX, Gilmore KJ, Szabo PA, Zeppa JJ, Baroja ML, Haeryfar SM, McCormick JK. 2014. Superantigens subvert the neutrophil response to promote abscess formation and enhance *Staphylococcus aureus* survival in vivo. Infect Immun 82:3588-98.

Yan M, Yu C, Yang J, Ji Y. 2011. The Essential Two-Component System YhcSR Is Involved in Regulation of the Nitrate Respiratory Pathway of *Staphylococcus aureus*. Journal of Bacteriology 193:1799-1805.

Yarwood JM, McCormick JK, Schlievert PM. 2001. Identification of a Novel Two-Component Regulatory System That Acts in Global Regulation of Virulence Factors of *Staphylococcus aureus*. Journal of Bacteriology 183:1113-1123.

Yarwood JM, McCormick JK, Paustian ML, Kapur V, Schlievert PM. 2002. Repression of the *Staphylococcus aureus* accessory gene regulator in serum and in vivo. J Bacteriol 184:1095-101.

Yin S, Daum RS, Boyle-Vavra S. 2006. VraSR two-component regulatory system and its role in induction of *pbp*2 and *vra*SR expression by cell wall antimicrobials in *Staphylococcus aureus*. Antimicrob Agents Chemother 50:336-43.

Yoon JH, Srikantan S, Gorospe M. 2012. MS2-TRAP (MS2-tagged RNA affinity purification): tagging RNA to identify associated miRNAs. Methods 58:81-7.

Yoong P, Torres VJ. 2013. The effects of *Staphylococcus aureus* leukotoxins on the host: cell lysis and beyond. Current opinion in microbiology 16:63-69.

Zapotoczna M, McCarthy H, Rudkin JK, O'Gara JP, O'Neill E. 2015. An Essential Role for Coagulase in *Staphylococcus aureus* Biofilm Development Reveals New Therapeutic Possibilities for Device-Related Infections. J Infect Dis 212:1883-93.

Zhang L, Ji G. 2004. Identification of a Staphylococcal AgrB Segment(s) Responsible for Group-Specific Processing of AgrD by Gene Swapping. Journal of Bacteriology 186:6706-6713.

Zhu Y, Nandakumar R, Sadykov MR, Madayiputhiya N, Luong TT, Gaupp R, Lee CY, Somerville GA. 2011. RpiR homologues may link *Staphylococcus aureus* RNAIII synthesis and pentose phosphate pathway regulation. J Bacteriol 193:6187-96.

Ziebandt AK, Weber H, Rudolph J, Schmid R, Hoper D, Engelmann S, Hecker M. 2001. Extracellular proteins of *Staphylococcus aureus* and the role of SarA and sigma B. Proteomics 1:480-93.

Ziebandt AK, Becher D, Ohlsen K, Hacker J, Hecker M, Engelmann S. 2004. The influence of agr and sigmaB in growth phase dependent regulation of virulence factors in *Staphylococcus aureus*. Proteomics 4:3034-47.

Zou D, Kaneko J, Narita S, Kamio Y. 2000. Prophage, phiPV83-pro, carrying panton-valentine leukocidin genes, on the *Staphylococcus aureus* P83 chromosome: comparative analysis of the genome structures of phiPV83-pro, phiPVL, phi11, and other phages. Biosci Biotechnol Biochem 64:2631-43.

Zuker M. 2003. Mfold web server for nucleic acid folding and hybridization prediction. Nucleic Acids Res 31:3406-15.

Theses

Das S. 2016. Genome-wide identification of virulence-associated genes in *Staphylococcus aureus* using Transposon insertion-site deep sequencing. PhD thesis.

Feuerbaum S. 2015. Untersuchung der Promoteraktivität des Virulenzregulators Rsp in *Staphylococcus aureus*. Master thesis.

Figures:

Figure 2.1: www.helmholtz-hzi.de

Figure 2.2: https://upload.wikimedia.org/wikipedia/commons/2/29/Human_body_schemes.png

https://www.freepik.com/free-vector/human-organs_595348.htm#term=kidney&page=1&position=2

7 APPENDIX

7.1 Abbreviations

Abbreviation	Meaning
agr	accessory gene regulator
AHT	Anhydrous tetracycline
AM	Ampicillin
AMC	Amoxicillin-clavulanate
BSA	Bovine Serum Albumin
bp	Base pairs
Cam	Chloramphenicol
cDNA	Complementary DNA
CFUs	Colony-forming units
COL	Colistin
Comp	Complemented mutant
CPD	Cefpodoxim
dNTP	deoxyribonucleosid trisphosphate
DMSO	dimethyl sulfoxid
DNA	Desoxyribonucleic acid
EtOH	Ethanol
exp	Exponential growth phase
FA	Fusidic acid
FCS/FBS	Fetal calf serum/ fetal bovine serum
FOX	Cefoxitin
fwd	forward
GFP	Green fluorescent protein
h	hours
IMP	Imipenem
kb	Kilo base
kDA	Kilo Dalton
Ko	Kock-out
LB	Luria-Bertani
log	Logarithmic growth phase
M	molar
MEM	Meropenem
MITC	Mitomycin C
MIC	Minimal inhibitory concentration
MOI	Multiplicity of infection
MOPS	N-Morpholino propanesulfonic acid
MRSA	Methicillin-resistant *S. aureus*
MSSA	Methicillin-sensitive *S. aureus*
mRNA	Messenger RNA
ncRNA	Non-coding RNA
ni	Not induced/ not infected
nt	nucleotides
OD	Optical density
OX	Oxacillin
p	p-value
PBS	Phosphate buffered saline
PCR	Polymerase chain reaction
p.i.	Post infection
qRT-PCR	Quantitative real time PCR
rev	reverse

Rif	Rifampicin
RNA	Ribonucleic acid
rpm	Revolutions per minute
RT	Room temperature
SCV	Small colony variants
SNT	supernatant
stat	Stationary growth phase
SXT	Trimethoprim-sulphamethoxazole
t	Time
TSA	Tryptic soy agar
TSB	Tryptic soy broth
TZP	Piperacillin-tazobactam
WT	wild-type
w/v	Weight per volume
V	volt
v/v	Volume per volume

7.2 List of figures

7.3 List of tables

7.4 Supplementary information

Figure 7.1

Staphylococcus argenteus MSHR1132 complete genome sequence
Sequence ID: **FR821777.2** Length: 2762785 Number of Matches: 1
Range 1: 2385363 to 2386602

Score	Expect	Identities	Gaps	Strand	Frame
1860 bits(2062)	0.0()	1171/1245(94%)	18/1245(1%)	Plus/Minus	

Features:

```
Query  1        TTAATATAGATTTCAAACCTATGTATTTCAAAAAACAATACATAGCCATTTTGAACTAAC  60
Sbjct  2386602  TTAATATAGATTTCAAACCTATGTATTTCATAAAACAATACATGGCCATTTTGAACTAAT  2386543
Query  61       TTGCTAATCTTTTATTGATATTCAACTATGTTATaaaaaaaGCAAATTGACCAAAATGGA  120
Sbjct  2386542  ATGCTAATATTTTTTTGATATTCAACTATGTTATAAAAAAAGCATGTTGACCAAAATGGA  2386483
Query  121      AGTTTGAATCAAAAAACATTAAATGTACCCATGACTTAAATTTTATCGCCATTATTTAAG  180
Sbjct  2386482  AGTTTGAATCAAAAAACATTAAATGTACCCATTACTTAAATTTTATCGCCATTATTTAAG  2386423
Query  181      TTTGGACATACACTTTTGTCATCAAACGCTGAAAATTAGTACGATTGAAATCACTTCTTG  240
Sbjct  2386422  TTTTGACATACACTTAAGTCATCGAACGCTAGAATTTAGTACGATTGAACTCACTTCTTG  2386363
Query  241      TT-ATAAAAATTCTTAGTAGCCCTGTTACAAAATATTCGCTACAAA-TTATTCAAATCAA  298
Sbjct  2386362  TTTATAAAAATTCTTAGTAGCCCTGTTACAAAGTATTCGCTACAAAATTATTCAATCCAA  2386303
Query  299      -CAACAATAACCATCAACTAAGAAATTTTAAACAATCCACTAAAAAATAAAGCGTTTAAA  357
Sbjct  2386302  ACAACAATAACCATCAACTAAGAAATTTTAAACAATCTACAAAATAA--AAGCGTTTAAA  2386245
Query  358      A-GTTCTGTTTAGAAAA-CATCAAGATAAGTATAAACATCTAGAAAAGTGAACATCTAAG  415
Sbjct  2386244  AAGTTCTGTTTAGAAAAACATCAAGATAAGTATAAACATCTAGAAAAGTGAACATCTAAG  2386185
Query  416      AAAATCCATCTAGTTATTGCCGTAACAATTAGAATAATCATTTGAAAAAGTGCATTAGAC  475
Sbjct  2386184  AACATCCATCTTGTTATTGCCGTAACAATTAGAATAATCATTAGAAAA-GTGCATTAGAC  2386126
Query  476      AGCGA-AATTCACCATCAAGATAATGAAGCAACAAGAAACAGCACACATCAATGAATTAA  534
Sbjct  2386125  AACGAGAATTCACCATCGAGATAATGAAACAACAAGAATCAGCACGCAACAATGAATTAA  2386066
Query  535      CACCTTAGATTCATCATGAGAAAATGCATGGCACAACTAGATTTACCATCAAGATAATTC  594
Sbjct  2386065  CACCTTAGATTCATCATGAGAAAATGCATGACACAACTAGATTTACCATCAAGATAATTC  2386006
Query  595      TTAAGCAGCGAAGAATTAACATCTAGAAATGCATAAACATCTTAGATTTTACATCAAGAG  654
Sbjct  2386005  TTAAGCAGCGAAGAATTAACATCTAGAAATGCATAAACACCTTAGATTTACCATCAAGAG  2385946
Query  655      ATGCGATAACT-ATAAACAACTAGAAACGTCACCAAGATAGTGCAACAACAAAGAATCAG  713
```

Figure 7.1: Conservation of SSR42 in *Staphylococcus argenteus*. Schematic representation of sequence identity of SSR42 from *S. aureus* 6850 in *Staphylococcus argenteus*.

Figure 7.2

1

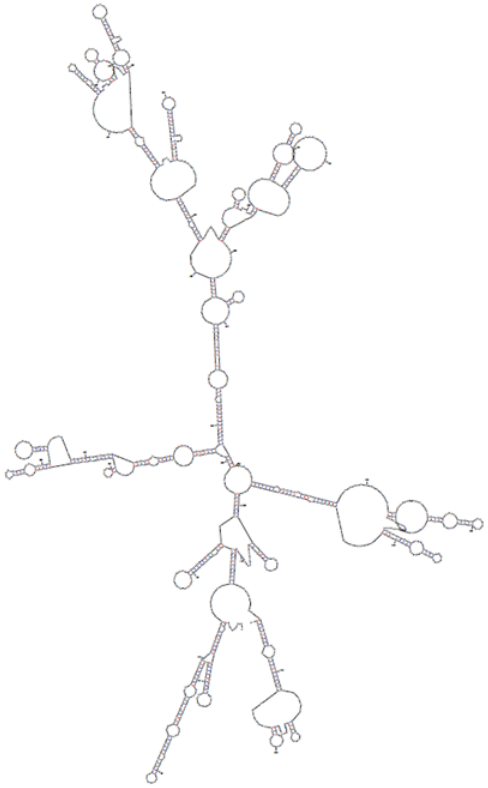

dG= -170.04

2

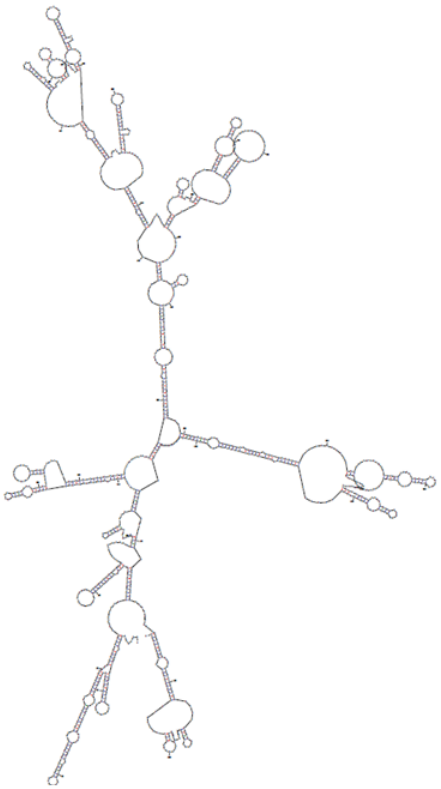

dG= -166.20

3

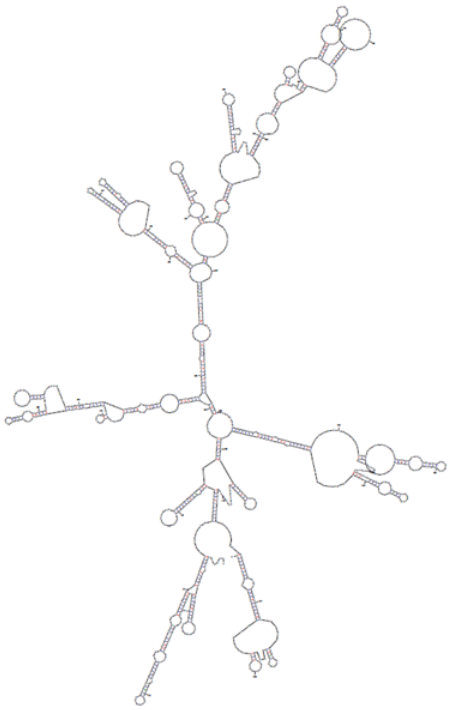

dG= -165.28

4

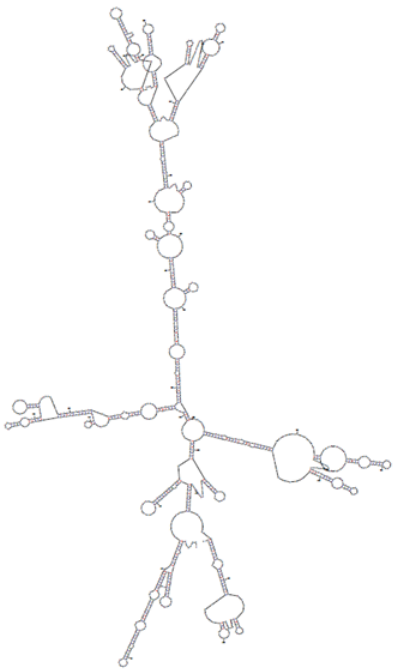

dG= -1621

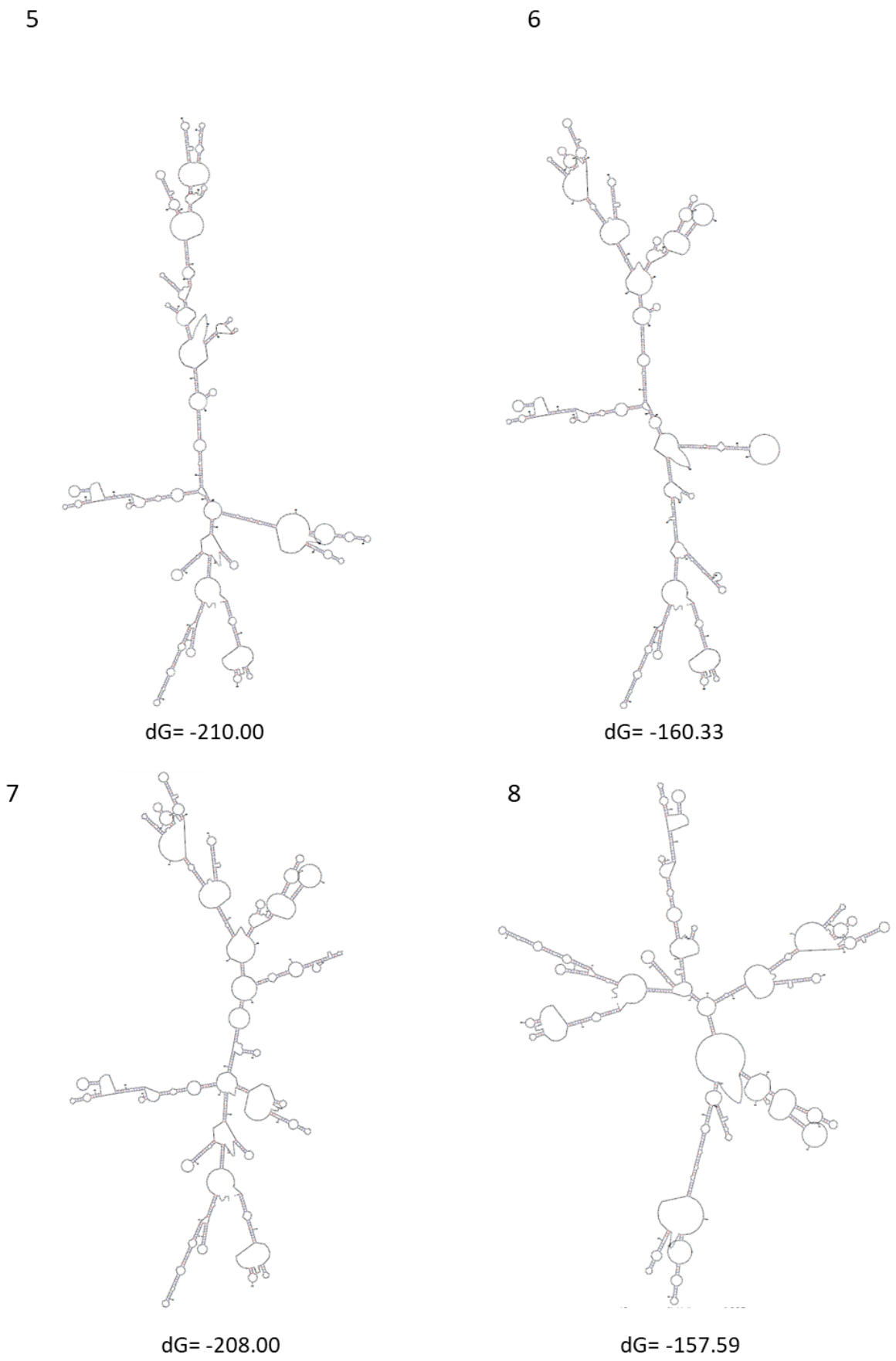

Figure 7.2: Schematic depiction of secondary structure prediction of SSR42 using mFold. 8 different secondary structures were predicted.

Figure 7.3

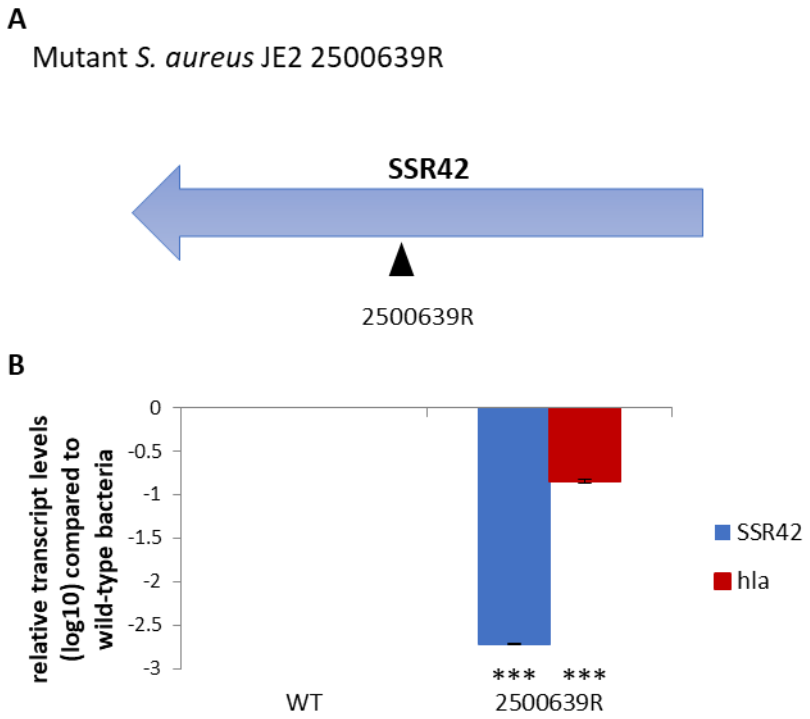

Figure 7.3: Insertional mutant in SSR42. A) Schematic representation of insertional mutation in SSR42 in *S. aureus* JE2 (2500639R). **B)** qRT-PCR analysis of SSR42 and hla transcript levels in mutant JE2 2500639R compared to transcript levels in *S. aureus* JE2 wild-type bacteria.

Figure 7.4

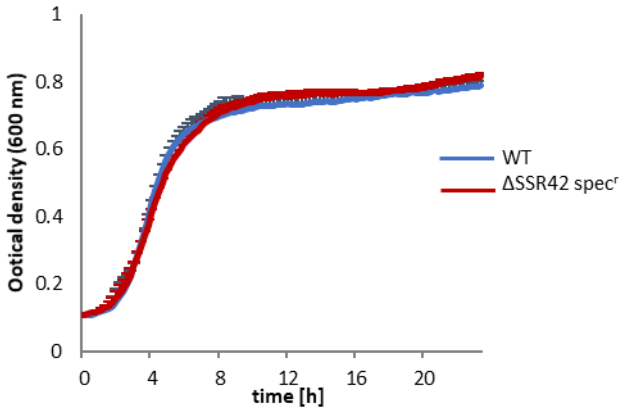

Figure 7.4: Mutant ΔSSR42-spec^r does not exhibit any growth defects. Replacement of SSR42 with a spectinomycin resistance cassette does not affect growth of *S. aureus* 6850 as observed by monitoring the growth of S. aureus in a TECAN Infinite M200 plate reader over a time course of 23 h.

Figure 7.5

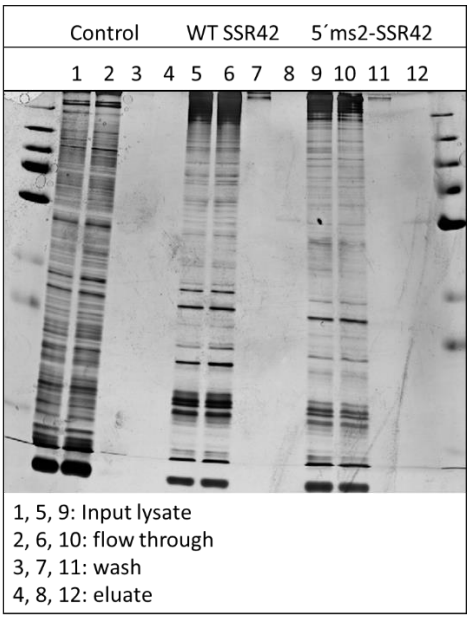

Figure 7.5: MS2-pulldown. MS2-pulldown approach failed as observed by silver stained SDS-PAGE of samples obtained from MS2-pulldown of wild-type *S. aureus* 6850, 5´-ms-tagged SSR42 expressing *S. aureus*. *S. aureus* expressing the ms2-tag was used as a control.

Figure 7.6

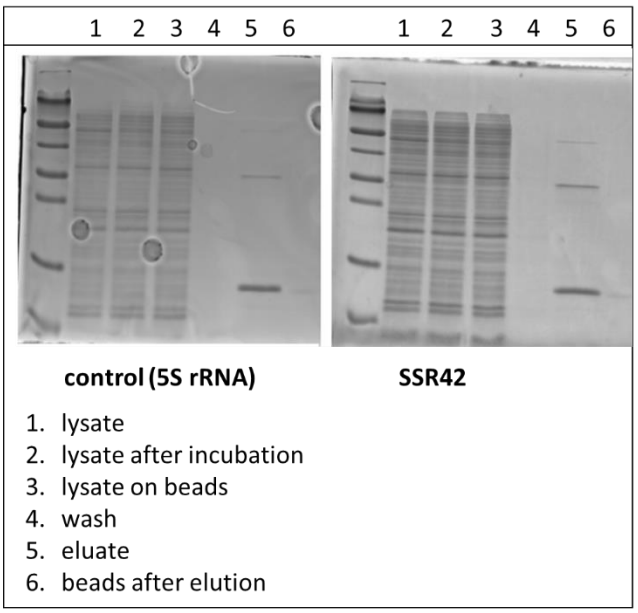

Figure 7.6: Oligo capture pulldown. Failiure of establishement of oligo capture-pulldown approach as observed by silver stained SDS-PAGE of samples obtained from oligo capture-pulldown experiment. 5S rRNA was used as a control. 5S rRNA and SSR42 were expressed harbouring a 5´- 14 nt long oligo tag in *S. aureus* 6850.

Figure 7.7

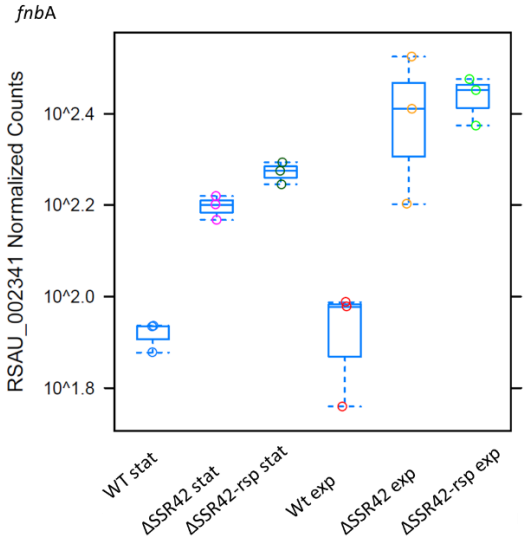

Figure 7.7: *fnb*A transcript levels do not differ significantly between *S. aureus* ΔSSR42 and ΔSSR42-*rsp* mutant. Comparison of *fnb*A expression levels in *S. aureus* 6850 wild-type bacteria, ΔSSR42 and ΔSSR42-*rsp* mutant. Transcriptome analysis obtained data pictured in a boxplot.

Figure 7.8

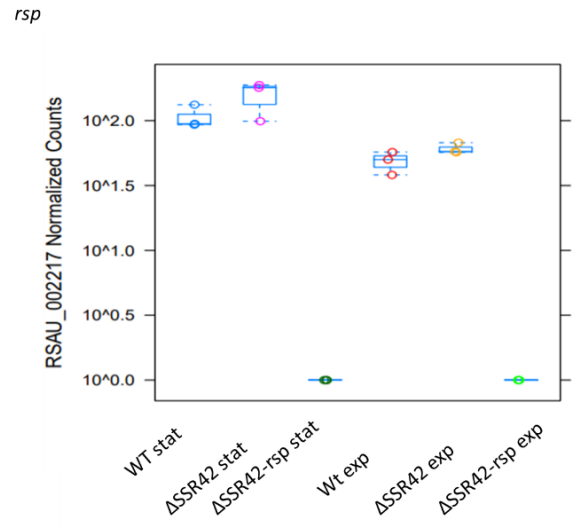

Figure 7.8: *rsp* transcript levels do not differ significantly between *S. aureus* ΔSSR42 and wild-type bacteria. Comparison of *rsp* expression levels in *S. aureus* 6850 wild-type bacteria, ΔSSR42 and ΔSSR42-*rsp* mutant. Transcriptome analysis obtained data pictured in a boxplot.

Figure 7.9

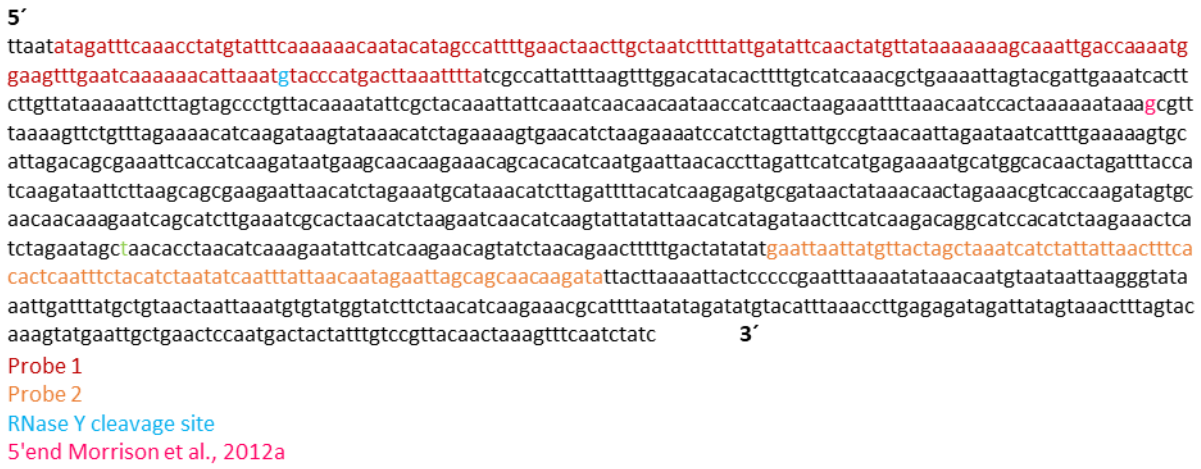

Figure 7.9: Schematic overview of Northern blot probes within the sequence of SSR42. Depicted in colour are the used probes for analysis of SSR42 transcript levels.

Figure 7.10

Figure 7.10: Schematic illustration of mutated sequences within SSR42. Depicted in colour are the deleted sequences for functional analysis of SSR42.

Figure 7.11

5´
ttaatatagatttcaaacctatgtatttcaaaaaacaatacatagccattttgaactaacttgctaatcttttattgatattcaactatgttataaaaaaagcaaattgaccaaaatg
gaagtttgaatcaaaaaacattaaatgtacccatgacttaaattttatcgccattatttaagtttggacatacacttttgtcatcaaacgctgaaaattagtacgattgaaatcactt
cttgttataaaaattcttagtagccctgttacaaaatattcgctacaaattattcaaatcaacaacaataaccatcaactaagaaattttaaacaatccactaaaaaataaagcgt
ttaaaagttctgtttagaaaacatcaagataagtataaacatctagaaaagtgaacatctaagaaaatccatctagttattgccgtaacaattagaataatcatttgaaaaagtg
cattagacagcgaaattcaccatcaagataatgaagcaacaagaaacagcacacatcaatgaattaacaccttagattcatcatgagaaaatgcatggcacaactagatttac
catcaagataattcttaagcagcgaagaattaacatctagaaatgcataaacatcttagattttacatcaagagatgcgataactataaacaactagaaacgtcaccaagatag
tgcaacaacaaagaatcagcatcttgaaatcgcactaacatctaagaatcaacatcaagtattatattaacatcatagataacttcatcaagacaggcatccacatctaagaaa
ctcatctagaatagctaacacctaacatcaaagaatattcatcaagaacagtatctaacagaacttttgactatatatgaattaattatgttactagctaaatcatctattattaa
ctttcacactcaatttctacatctaatatcaatttattaacaatagaattagcagcaacaagatattacttaaaattactcccccgaatttaaaatataaacaatgtaataattaag
ggtataaattgatttatgctgtaactaattaaatgtgtatggtatcttctaacatcaagaaacgcattttaatatagatatgtacatttaaaccttgagagatagattatagtaaact
ttagtacaaagtatgaattgctgaactccaatgactactatttgtccgttacaactaaagtttcaatctatc 3´

Deletion mini-1
Additional deletion mini-2

Figure 7.11: Schematic representation of mutated sequences within SSR42 to create minimal versions. Depicted in colour are the deleted sequences for functional analysis of minimal SSR42 versions.

Figure 7.12

5´
ttaatatagatttcaaacctatgtatttcaaaaaacaatacatagccattttgaactaacttgctaatcttttattgatattcaactatgttataaaaaaagcaaattgaccaaaatgg
aagtttgaatcaaaaaacattaaatgtacccatgacttaaattttatcgccattatttaagtttggacatacacttttgtcatcaaacgctgaaaattagtacgattgaaatcacttctt
gttataaaaattcttagtagccctgttacaaaatattcgctacaaattattcaaatcaacaacaataaccatcaactaagaaattttaaacaatccactaaaaaataagcgtttaa
aagttctgtttagaaaacatcaagataagtataaacatctagaaaagtgaacatctaagaaaatccatctagttattgccgtaacaattagaataatcatttgaaaaagtgcattag
acagcgaaattcaccatcaagataatgaagcaacaagaaacagcacacatcaatgaattaacaccttagattcatcatgagaaaatgcatggcacaactagatttaccatcaag
ataattcttaagcagcgaagaattaacatctagaaatgcataaacatcttagattttacatcaagagatgcgataactataaacaactagaaacgtcaccaagatagtgcaacaa
caaagaatcagcatcttgaaatcgcactaacatctaagaatcaacatcaagtattatattaacatcatagataacttcatcaagacaggcatccacatctaagaaactcatctaga
atagctaacacctaacatcaaagaatattcatcaagaacagtatctaacagaacttttgactatatatgaattaattatgttactagctaaatcatctattattaactttcacactca
atttctacatctaatatcaatttattaacaatagaattagcagcaacaagatattacttaaaattactcccccgaatttaaaatataaacaatgtaataattaagggtataaattgatt
tatgctgtaactaattaaatgtgtatggtatcttctaacatcaagaaacgcattttaatatagatatgtacatttaaaccttgagagatagattatagtaaactttagtacaaagtatg
aattgctgaactccaatgactactatttgtccgttacaactaaagtttcaatctatc 3´

predicted sequence of ORF3
performed mutation in start codon of ORF3 (T→C)

Figure 7.12: Schematic representation of mutated start codon within putative ORF 3. Depicted in colour is the sequence of putative ORF 3 and the performed mutation within the start codon.

Figure 7.13

A

5´

ttaatatagatttcaaacctatgtatttcaaaaaacaatacatagccattttgaactaacttgctaatcttttattgatattcaactatgttataaaaaaagcaaattgaccaaaatggaa
gtttgaatcaaaaaacattaaatgtacccatgacttaaatttttatcgccattatttaagtttggacatacacttttgtcatcaaacgctgaaaattagtacgattgaaatcacttcttgtta
taaaaattcttagtagccctgttacaaaatattcgctacaaattattcaaatcaacaacaataaccatcaactaagaaattttaaacaatccactaaaaaataaagcgtttaaaagttc
tgtttagaaaacatcaagataagtataaacatctagaaaagtgaacatctaagaaaatccatctagttattgccgtaacaattagaataatcatttgaaaaagtgcattagacagcg
aaattcaccatcaagataatgaagcaacaagaaacagcacacatcaatgaattaacaccttagattcatcatgagaaaatgcatggcacaactagatttaccatcaagataattctt
aagcagcgaagaattaacatctagaaatgcataaacatcttagattttacatcaagagatgcgataactataaacaactagaaacgtcaccaagatagtgcaacaacaaagaatca
gcatcttgaaatcgcactaacatctaagaatcaacatcaagtattatattaacatcatagataacttcatcaagacaggcatccacatctaagaaactcatctagaatagctaacacct
aacatcaaagaatattcatcaagaacagtatctaacagaacttttgactatatatgaattaattatgttactagctaaatcatctattattaactttcacactcaatttctacatctaata
tcaatttattaacaatagaattagcagcaacaagatattacttaaaattactcccccgaatttaaaatataaacaatgtaataattaagggtataaattgatttatgctgtaactaatta
aatgtgtatggtatcttctaacatcaagaaacgcattttaatatagatatgtacatttaaaccttgagagatagattatagtaaactttagtacaaagtatgaattgctgaactccaatg
actactatttgtccgttacaactaaagtttcaatctatc **3´**

SSR42
predicted interaction with *sae*PQRS mRNA (43 nt)
seed sequence (8 nt)

B

5´

atgaataaattattgctactcgttacatttatcattcgtgtgggttcaggtattgttatgttaatgcaaggctacgaaaaattaacgggcggatttacgctgaaaggtttagtaccagtca
tcgctaacaatactgattcaccagagtggtataagtggtttttcgcaaatatagttgcacatacgacgtcattatttgatattgttgtcccactcggagagattgcaattggattaggttt
aatttttggagtttttgcatatgctgctagtttctttggagcctttgttatgataaattatatcttagcagatatgatatttacgtatcctcttcaattaactttctttatccttttactaatgag
tcactcattgttaaaacagatttcacttaaagaaatcattaattactttagaggtcgtaagaacagaggtgaaaaaatagatgacccacttactgatcgtggatga **3´**

*sae*Q
predicted interaction with SSR42
seed sequence

Figure 7.13: Schematic illustration of predicted interacting sequences within SSR42 and *sae*Q. Depicted in colour are the sequences within SSR42 and *sae*Q mRNA which were predicted to interact using IntaRNA.

Table 7.1: Conservation of SSR42 in *S. aureus.*

Description	Max score	Total score	Query cover	E value	Ident	Accession
Staphylococcus aureus subsp. aureus 6850, complete genome	2276	2276	100%	0.0	100%	CP006706.1
Staphylococcus aureus subsp. aureus Tager 104, complete genome	2270	2270	100%	0.0	99%	CP012409.1
Staphylococcus aureus subsp. aureus SA268, complete genome	2265	2265	100%	0.0	99%	CP006630.1
Staphylococcus aureus subsp. aureus SA40, complete genome	2265	2265	100%	0.0	99%	CP003604.1
Staphylococcus aureus subsp. aureus SA957, complete genome	2265	2265	100%	0.0	99%	CP003603.1
Staphylococcus aureus subsp. aureus M013, complete genome	2265	2265	100%	0.0	99%	CP003166.1
Staphylococcus aureus subsp. aureus strain FDAARGOS_5 chromosome, complete genome	2259	2259	100%	0.0	99%	CP007539.3
Staphylococcus aureus subsp. aureus strain 2148.N chromosome, complete genome	2259	2259	100%	0.0	99%	CP016856.2
Staphylococcus aureus subsp. aureus strain EDCC5458 chromosome, complete genome	2259	2259	100%	0.0	99%	CP022290.1
Staphylococcus aureus subsp. aureus isolate Clinical isolate genome assembly, chromosome: I	2259	2259	100%	0.0	99%	LT671859.1
Staphylococcus aureus subsp. aureus strain HG001, complete genome	2259	2259	100%	0.0	99%	CP018205.1
Staphylococcus aureus subsp. aureus strain Gv88, complete genome	2259	2259	100%	0.0	99%	CP012018.1
Staphylococcus aureus subsp. aureus strain Gv51, complete genome	2259	2259	100%	0.0	99%	CP012015.1
Staphylococcus aureus subsp. aureus strain Be62, complete genome	2259	2259	100%	0.0	99%	CP012013.1
Staphylococcus aureus subsp. aureus strain HC1335, complete genome	2259	2259	100%	0.0	99%	CP012012.1
Staphylococcus aureus subsp. aureus strain HC1340, complete genome	2259	2259	100%	0.0	99%	CP012011.1
Staphylococcus aureus subsp. aureus DSM 20231, complete genome	2259	2259	100%	0.0	99%	CP011526.1
Staphylococcus aureus subsp. aureus DNA, complete genome, strain: TMUS2134	2259	2259	100%	0.0	99%	AP014653.1
Staphylococcus aureus subsp. aureus DNA, complete genome, strain: TMUS2126	2259	2259	100%	0.0	99%	AP014652.1
Staphylococcus aureus subsp. aureus strain Gv69, complete genome	2259	2259	100%	0.0	99%	CP009681.1
Staphylococcus aureus subsp. aureus CN1, complete genome	2259	2259	100%	0.0	99%	CP003979.1
Staphylococcus aureus subsp. aureus T0131, complete genome	2259	2259	100%	0.0	99%	CP002643.1

Staphylococcus aureus subsp. aureus ED133, complete genome	2259	2259	100%	0.0	99%	CP001996.1
Staphylococcus aureus subsp. aureus TW20, complete genome	2259	2259	100%	0.0	99%	FN433596.1
Staphylococcus aureus subsp. aureus COL, complete genome	2259	2259	100%	0.0	99%	CP000046.1
Staphylococcus aureus subsp. aureus NCTC 8325, complete genome	2259	2259	100%	0.0	99%	CP000253.1
Staphylococcus aureus subsp. aureus NCTC 8325 clone sabac-126, complete sequence	2259	2259	100%	0.0	99%	AC090968.14
Staphylococcus aureus strain MSSA476, complete genome	2259	2259	100%	0.0	99%	BX571857.1
Staphylococcus aureus subsp. aureus MW2 DNA, complete genome	2259	2259	100%	0.0	99%	BA000033.2
Staphylococcus aureus subsp. aureus strain USA300_2014.C01 chromosome, complete genome	2254	2254	100%	0.0	99%	CP012119.2
Staphylococcus aureus subsp. aureus strain 1971.C01 chromosome, complete genome	2254	2254	100%	0.0	99%	CP016858.2
Staphylococcus aureus subsp. aureus strain 5118.N chromosome, complete genome	2254	2254	100%	0.0	99%	CP016855.2
Staphylococcus aureus subsp. aureus strain USA300_2014.C02 chromosome, complete genome	2254	2254	100%	0.0	99%	CP012120.2
Staphylococcus aureus subsp. aureus strain 2148.C01 chromosome, complete genome	2254	2254	100%	0.0	99%	CP017094.2
Staphylococcus aureus subsp. aureus strain 1969.N chromosome, complete genome	2254	2254	100%	0.0	99%	CP016861.2
Staphylococcus aureus subsp. aureus strain 3020.C01 chromosome, complete genome	2254	2254	100%	0.0	99%	CP025495.1
Staphylococcus aureus subsp. aureus strain 1625.C01 chromosome, complete genome	2254	2254	100%	0.0	99%	CP016863.2
Staphylococcus aureus subsp. aureus strain ISU926, complete genome	2254	2254	100%	0.0	99%	CP017091.1
Staphylococcus aureus subsp. aureus strain ATCC 6538, complete genome	2254	2254	100%	0.0	99%	CP020020.1
Staphylococcus aureus subsp. aureus strain UCI 28, complete genome	2254	2254	100%	0.0	99%	CP018768.1
Staphylococcus aureus subsp. aureus strain UCI62, complete genome	2254	2254	100%	0.0	99%	CP018766.1
Staphylococcus aureus subsp. aureus strain USA300_SUR1, complete genome	2254	2254	100%	0.0	99%	CP009423.1
Staphylococcus aureus subsp. aureus strain LA-MRSA ST398 isolate E154,	2254	2254	100%	0.0	99%	CP013218.1

Staphylococcus aureus subsp. aureus ST228 complete genome, isolate 18583	2254	2254	100%	0.0	99%	HE579073.1
Staphylococcus aureus subsp. aureus ST228 complete genome, isolate 18412	2254	2254	100%	0.0	99%	HE579071.1
Staphylococcus aureus subsp. aureus ST228 complete genome, isolate 18341	2254	2254	100%	0.0	99%	HE579069.1
Staphylococcus aureus subsp. aureus ST228 complete genome, isolate 16125	2254	2254	100%	0.0	99%	HE579067.1
Staphylococcus aureus subsp. aureus ST228 complete genome, isolate 16035	2254	2254	100%	0.0	99%	HE579065.1
Staphylococcus aureus subsp. aureus ST228 complete genome, isolate 15532	2254	2254	100%	0.0	99%	HE579063.1
Staphylococcus aureus subsp. aureus ST228 complete genome, isolate 10497	2254	2254	100%	0.0	99%	HE579061.1
Staphylococcus aureus subsp. aureus ST228 complete genome, isolate 10388	2254	2254	100%	0.0	99%	HE579059.1
Staphylococcus aureus subsp. aureus 71193 genome	2254	2254	100%	0.0	99%	CP003045.1
Staphylococcus aureus subsp. aureus VC40, complete genome	2254	2254	100%	0.0	99%	CP003033.1
Staphylococcus aureus subsp. aureus 11819-97, complete genome	2254	2254	100%	0.0	99%	CP003194.1
Staphylococcus aureus subsp. aureus ECT-R 2 complete genome	2254	2254	100%	0.0	99%	FR714927.1
Staphylococcus aureus subsp. aureus TCH60, complete genome	2254	2254	100%	0.0	99%	CP002110.1
Staphylococcus aureus subsp. aureus ST398 complete genome	2254	2254	100%	0.0	99%	AM990992.1
Staphylococcus aureus subsp. aureus ED98, complete genome	2254	2254	100%	0.0	99%	CP001781.1
Staphylococcus aureus subsp. aureus USA300_TCH1516, complete genome	2254	2254	100%	0.0	99%	CP000730.1
Staphylococcus aureus subsp. aureus USA300_TCH1516, complete genome	2254	2254	100%	0.0	99%	CP000730.1
Staphylococcus aureus subsp. aureus Mu3 DNA, complete genome	2254	2254	100%	0.0	99%	AP009324.1
Staphylococcus aureus subsp. aureus JH1, complete genome	2254	2254	100%	0.0	99%	CP000736.1
Staphylococcus aureus subsp. aureus JH9, complete genome	2254	2254	100%	0.0	99%	CP000703.1
Staphylococcus aureus subsp. aureus Mu50 DNA, complete genome	2254	2254	100%	0.0	99%	BA000017.4
Staphylococcus aureus subsp. aureus USA300_FPR3757, complete genome	2254	2254	100%	0.0	99%	CP000255.1
Staphylococcus aureus subsp. aureus N315 DNA, complete genome	2254	2254	100%	0.0	99%	BA000018.3
Staphylococcus aureus subsp. aureus strain MRSA252, complete genome	2254	2254	100%	0.0	99%	BX571856.1
Staphylococcus aureus subsp. aureus Z172, complete genome	2252	2252	100%	0.0	99%	CP006838.1
Staphylococcus aureus subsp. aureus USA300 strain NRS384	2250	2250	100%	0.0	99%	CP027476.1

Staphylococcus aureus subsp. aureus strain EDCC5464 chromosome, complete genome	2248	2248	100%	0.0	99%	CP022291.1
Staphylococcus aureus subsp. aureus strain ATCC 25923, complete genome	2248	2248	100%	0.0	99%	CP009361.1
Staphylococcus aureus subsp. aureus strain H-EMRSA-15, complete genome	2248	2248	100%	0.0	99%	CP007659.1
Staphylococcus aureus subsp. aureus 55/2053, complete genome	2248	2248	100%	0.0	99%	CP002388.1
Staphylococcus aureus subsp. aureus HO 5096 0412 complete genome	2248	2248	100%	0.0	99%	HE681097.1
Staphylococcus aureus subsp. aureus LGA251 complete genome sequence	2248	2248	100%	0.0	99%	FR821779.1
Staphylococcus aureus subsp. aureus JKD6159, complete genome	2248	2248	100%	0.0	99%	CP002114.2
Staphylococcus aureus subsp. aureus strain Newman_D2C chromosome, complete genome	2222	2222	100%	0.0	99%	CP023391.1
Staphylococcus aureus subsp. aureus str. Newman strain NYU_Newman chromosome, complete genome	2222	2222	100%	0.0	99%	CP023390.1
Staphylococcus aureus subsp. aureus str. Newman DNA, complete genome	2222	2222	100%	0.0	99%	AP009351.1

Table 7.2: Blast hits of SSR42 in other species than *S. aureus.*

Description	Max score	Total score	Query cover	E value	Ident	Accession
Staphylococcus argenteus MSHR1132 complete genome sequence	1860	1860	100%	0.0	94%	FR821777.2
Staphylococcus argenteus strain BN75 genome	1856	1856	100%	0.0	94%	CP015758.1
Staphylococcus argenteus strain XNO106 chromosome, complete genome	1851	1851	100%	0.0	94%	CP025023.1
Staphylococcus argenteus strain XNO62 chromosome, complete genome	1851	1851	100%	0.0	94%	CP023076.1
PREDICTED: Ceratosolen solmsi marchali WASH complex subunit 7 (LOC105366870), mRNA	46.4	46.4	5%	2.3	77%	XM_011505461.1
Dracunculus medinensis genome assembly D_medinensis_Ghana, scaffold DME_scaffold0000003	46.4	46.4	3%	2.3	82%	LK978191.1
Schistosoma curassoni genome assembly S_curassoni_Dakar, scaffold SCUD_contig0006651	44.6	44.6	3%	8.1	85%	LM088298.1

Table 7.3: Conservation of genetic locus surrounding SSR42 in *S. aureus.*

Description	Max score	Total score	Query cover	E value	Ident	Accession
Staphylococcus aureus subsp. aureus 6850, complete genome	8361	8361	100%	0.0	99%	CP006706.1
Staphylococcus aureus subsp. aureus Tager 104, complete genome	8309	8309	100%	0.0	99%	CP012409.1
Staphylococcus aureus subsp. aureus ED133, complete genome	8224	8224	100%	0.0	99%	CP001996.1
Staphylococcus aureus subsp. aureus JKD6159, complete genome	8197	8197	100%	0.0	99%	CP002114.2
Staphylococcus aureus subsp. aureus LGA251 complete genome sequence	8188	8188	100%	0.0	99%	FR821779.1
Staphylococcus aureus subsp. aureus SA268, complete genome	8163	8163	100%	0.0	99%	CP006630.1
Staphylococcus aureus subsp. aureus SA40, complete genome	8163	8163	100%	0.0	99%	CP003604.1
Staphylococcus aureus subsp. aureus SA957, complete genome	8154	8154	100%	0.0	99%	CP003603.1
Staphylococcus aureus subsp. aureus M013, complete genome	8154	8154	100%	0.0	99%	CP003166.1
Staphylococcus aureus subsp. aureus strain ISU926, complete genome	8147	8147	100%	0.0	99%	CP017091.1
Staphylococcus aureus subsp. aureus strain LA-MRSA ST398 isolate E154, complete genome	8147	8147	100%	0.0	99%	CP013218.1
Staphylococcus aureus subsp. aureus 71193 genome	8147	8147	100%	0.0	99%	CP003045.1
Staphylococcus aureus subsp. aureus ST398 complete genome	8141	8141	100%	0.0	99%	AM990992.1
Staphylococcus aureus subsp. aureus strain EDCC5464 chromosome, complete genome	8138	8138	100%	0.0	99%	CP022291.1
Staphylococcus aureus subsp. aureus strain H-EMRSA-15, complete genome	8138	8138	100%	0.0	99%	CP007659.1
Staphylococcus aureus subsp. aureus HO 5096 0412 complete genome	8138	8138	100%	0.0	99%	HE681097.1
Staphylococcus aureus subsp. aureus strain FORC_001, complete genome	8132	8132	100%	0.0	99%	CP009554.1
Staphylococcus aureus subsp. aureus strain MRSA252, complete genome	8132	8132	100%	0.0	99%	BX571856.1
Staphylococcus aureus subsp. aureus 55/2053, complete genome	8123	8123	100%	0.0	99%	CP002388.1
Staphylococcus aureus subsp. aureus strain ATCC 25923, complete genome	8120	8120	100%	0.0	99%	CP009361.1
Staphylococcus aureus subsp. aureus TCH60, complete genome	8098	8098	100%	0.0	99%	CP002110.1
Staphylococcus aureus subsp. aureus strain JS395, complete genome	8083	8083	100%	0.0	99%	CP012756.1
Staphylococcus aureus subsp. aureus strain EDCC5458 chromosome, complete genome	8055	8055	98%	0.0	99%	CP022290.1
Staphylococcus aureus subsp. aureus isolate Clinical isolate genome assembly, chromosome: I	8055	8055	98%	0.0	99%	LT671859.1

Staphylococcus aureus subsp. aureus strain FDAARGOS_5 chromosome, complete genome	8051	8051	98%	0.0	99%	CP007539.3
Staphylococcus aureus subsp. aureus strain HG001, complete genome	8051	8051	98%	0.0	99%	CP018205.1
Staphylococcus aureus subsp. aureus strain Gv88, complete genome	8051	8051	98%	0.0	99%	CP012018.1
Staphylococcus aureus subsp. aureus strain Be62, complete genome	8051	8051	98%	0.0	99%	CP012013.1
Staphylococcus aureus subsp. aureus strain HC1335, complete genome	8051	8051	98%	0.0	99%	CP012012.1
Staphylococcus aureus subsp. aureus strain HC1340, complete genome	8051	8051	98%	0.0	99%	CP012011.1
Staphylococcus aureus subsp. aureus DSM 20231, complete genome	8051	8051	98%	0.0	99%	CP011526.1
Staphylococcus aureus subsp. aureus strain Gv69, complete genome	8051	8051	98%	0.0	99%	CP009681.1
Staphylococcus aureus subsp. aureus TW20, complete genome	8051	8051	98%	0.0	99%	FN433596.1
Staphylococcus aureus subsp. aureus COL, complete genome	8051	8051	98%	0.0	99%	CP000046.1
Staphylococcus aureus subsp. aureus T0131, complete genome	8046	8046	98%	0.0	99%	CP002643.1
Staphylococcus aureus subsp. aureus NCTC 8325 clone sabac-126, complete sequence	8046	8046	98%	0.0	99%	AC090968.14
Staphylococcus aureus subsp. aureus strain OXLIM chromosome, complete genome	8042	8042	98%	0.0	99%	CP029032.1
Staphylococcus aureus subsp. aureus strain CAR chromosome, complete genome	8042	8042	98%	0.0	99%	CP029030.1
Staphylococcus aureus subsp. aureus strain CIT chromosome, complete genome	8042	8042	98%	0.0	99%	CP029031.1
Staphylococcus aureus subsp. aureus strain USA300_2014.C01 chromosome, complete genome	8042	8042	98%	0.0	99%	CP012119.2
Staphylococcus aureus subsp. aureus strain 1971.C01 chromosome, complete genome	8042	8042	98%	0.0	99%	CP016858.2
Staphylococcus aureus subsp. aureus strain 5118.N chromosome, complete genome	8042	8042	98%	0.0	99%	CP016855.2
Staphylococcus aureus subsp. aureus strain USA300_2014.C02 chromosome, complete genome	8042	8042	98%	0.0	99%	CP012120.2
Staphylococcus aureus subsp. aureus strain 2148.C01 chromosome, complete genome	8042	8042	98%	0.0	99%	CP017094.2
Staphylococcus aureus subsp. aureus strain 1969.N chromosome, complete genome	8042	8042	98%	0.0	99%	CP016861.2

Staphylococcus aureus subsp. aureus strain USA300_SUR1, complete genome	8042	8042	98%	0.0	99%	CP009423.1
Staphylococcus aureus subsp. aureus strain Gv51, complete genome	8042	8042	98%	0.0	99%	CP012015.1
Staphylococcus aureus subsp. aureus Z172, complete genome	8042	8042	98%	0.0	99%	CP006838.1
Staphylococcus aureus subsp. aureus USA300_TCH1516, complete genome	8042	8042	98%	0.0	99%	CP000730.1
Staphylococcus aureus subsp. aureus NCTC 8325, complete genome	8042	8042	98%	0.0	99%	CP000253.1
Staphylococcus aureus subsp. aureus USA300_FPR3757, complete genome	8042	8042	98%	0.0	99%	CP000255.1
Staphylococcus aureus subsp. aureus USA300 strain NRS384	8038	8038	98%	0.0	99%	CP027476.1
Staphylococcus aureus subsp. aureus VC40, complete genome	8038	8038	98%	0.0	99%	CP003033.1
Staphylococcus aureus subsp. aureus strain Newman_D2C chromosome, complete genome	8013	8013	98%	0.0	99%	CP023391.1
Staphylococcus aureus subsp. aureus str. Newman strain NYU_Newman chromosome, complete genome	8013	8013	98%	0.0	99%	CP023390.1
Staphylococcus aureus subsp. aureus str. Newman DNA, complete genome	8013	8013	98%	0.0	99%	AP009351.1
Staphylococcus aureus subsp. aureus strain 2148.N chromosome, complete genome	7934	7934	98%	0.0	98%	CP016856.2
Staphylococcus aureus subsp. aureus DNA, complete genome, strain: TMUS2134	7934	7934	98%	0.0	98%	AP014653.1
Staphylococcus aureus subsp. aureus DNA, complete genome, strain: TMUS2126	7934	7934	98%	0.0	98%	AP014652.1
Staphylococcus aureus subsp. aureus CN1, complete genome	7934	7934	98%	0.0	98%	CP003979.1
Staphylococcus aureus subsp. aureus strain UCI 28, complete genome	7928	7928	98%	0.0	98%	CP018768.1
Staphylococcus aureus subsp. aureus strain UCI62, complete genome	7928	7928	98%	0.0	98%	CP018766.1
Staphylococcus aureus subsp. aureus ECT-R 2 complete genome	7928	7928	98%	0.0	98%	FR714927.1
Staphylococcus aureus subsp. aureus JH1, complete genome	7928	7928	98%	0.0	98%	CP000736.1
Staphylococcus aureus subsp. aureus JH9, complete genome	7928	7928	98%	0.0	98%	CP000703.1
Staphylococcus aureus subsp. aureus N315 DNA, complete genome	7928	7928	98%	0.0	98%	BA000018.3

Staphylococcus aureus subsp. aureus strain USA300_SUR1, complete genome	8042	8042	98%	0.0	99%	CP009423.1
Staphylococcus aureus subsp. aureus strain Gv51, complete genome	8042	8042	98%	0.0	99%	CP012015.1
Staphylococcus aureus subsp. aureus Z172, complete genome	8042	8042	98%	0.0	99%	CP006838.1
Staphylococcus aureus subsp. aureus USA300_TCH1516, complete genome	8042	8042	98%	0.0	99%	CP000730.1
Staphylococcus aureus subsp. aureus NCTC 8325, complete genome	8042	8042	98%	0.0	99%	CP000253.1
Staphylococcus aureus subsp. aureus USA300_FPR3757, complete genome	8042	8042	98%	0.0	99%	CP000255.1
Staphylococcus aureus subsp. aureus USA300 strain NRS384	8038	8038	98%	0.0	99%	CP027476.1
Staphylococcus aureus subsp. aureus VC40, complete genome	8038	8038	98%	0.0	99%	CP003033.1
Staphylococcus aureus subsp. aureus strain Newman_D2C chromosome, complete genome	8013	8013	98%	0.0	99%	CP023391.1
Staphylococcus aureus subsp. aureus str. Newman strain NYU_Newman chromosome, complete genome	8013	8013	98%	0.0	99%	CP023390.1
Staphylococcus aureus subsp. aureus str. Newman DNA, complete genome	8013	8013	98%	0.0	99%	AP009351.1
Staphylococcus aureus subsp. aureus strain 2148.N chromosome, complete genome	7934	7934	98%	0.0	98%	CP016856.2
Staphylococcus aureus subsp. aureus DNA, complete genome, strain: TMUS2134	7934	7934	98%	0.0	98%	AP014653.1
Staphylococcus aureus subsp. aureus DNA, complete genome, strain: TMUS2126	7934	7934	98%	0.0	98%	AP014652.1
Staphylococcus aureus subsp. aureus CN1, complete genome	7934	7934	98%	0.0	98%	CP003979.1
Staphylococcus aureus subsp. aureus strain UCI 28, complete genome	7928	7928	98%	0.0	98%	CP018768.1
Staphylococcus aureus subsp. aureus strain UCI62, complete genome	7928	7928	98%	0.0	98%	CP018766.1
Staphylococcus aureus subsp. aureus ECT-R 2 complete genome	7928	7928	98%	0.0	98%	FR714927.1
Staphylococcus aureus subsp. aureus JH1, complete genome	7928	7928	98%	0.0	98%	CP000736.1
Staphylococcus aureus subsp. aureus JH9, complete genome	7928	7928	98%	0.0	98%	CP000703.1
Staphylococcus aureus subsp. aureus N315 DNA, complete genome	7928	7928	98%	0.0	98%	BA000018.3

Table 7.4: Blast hits of putative ORFs within SSR42.

ORF1:

hypothetical protein (*Chryseobacterium* sp. OV279)

Sequence IF: WP_072924482.1. Length: 493. Number of Matches: 1

Score	Expect	Identities	Positives	Gaps
32.9 bits (70)	2.9	10/15 (67%)	10/15 (66%)	4/15 (26%)

ORF 1	1	MY- - - - FKKQYIAIL	11
		MY FKKQYI IL	
hypothetical protein	1	MYMKPIFKKQYIVIL	15

ORF 2:

hypothetical protein CBD98_02640 (*Flavobacteriaceae* bacterium TMED238)

Sequence IF: OUX01526.1. Length: 229. Number of Matches: 1

Score	Expect	Identities	Positives	Gaps
35 bits (75)	3.6	12/20 (60%)	13/20 (65%)	6/20 (30%)

ORF 2	3	IHFCHQTLKISTIEITSCYK	22
		IHFC KIS +I SCYK	
hypothetical protein	146	IHFC- - - - KIS- - DIASCYK	159

ORF 4:

hypothetical protein DICPUDRAFT_73920 (*Dictyostelium purpureum*)

Sequence IF: XP_003282892.1. Length: 453. Number of Matches: 1

Score	Expect	Identities	Positives	Gaps
33.3 bits (71)	5.9	11/16 (69%)	12/16 (75%)	1/16 (6%)

ORF 4	1	LLQNIRYKLFKSTTIT	16
		LLQNI YKL TT T	
Hypothetical protein	342	LLQNIKYKLI-PTTVT	356

ORF 5:

AAA family ATPase (*Burkholderia cepacia*)

Sequence IF: WP_059232660.1. Length: 542. Number of Matches: 1

Score	Expect	Identities	Positives	Gaps
33.3 bits (71)	3.0	9/12 (75%)	10/12 (82%)	0/12 (0%)

ORF 5	1 LFRKHQDKYKHL 12	
	LFR HQD YK L	
AAA family ATPase	141 LFRTHQDRYKQL 152	

ORF 6:

conserved hypothetical protein (*Leishmania mexicana* MHOM/GT/2001/U1103)

Sequence IF: OUX01526.1. Length: 229. Number of Matches: 1

Score	Expect	Identities	Positives	Gaps
31.6 bits (67)	9.8	9/10 (90%)	9/10 (90%)	0/10 (0%)

ORF 6	4 CIRQRNSPSR 13	
	CI QRNSPSR 13	
Hypothetical protein	61 CISQRNSPSR 70	

ORF 7:

structural maintenance of chromosomes protein 2 (*Schistosoma haematobium*)

Sequence IF: XP_012795727.1. Length: 1204. Number of Matches: 1

Score	Expect	Identities	Positives	Gaps
35 bits (75)	0.74	11/14 (79%)	12/14 (85%)	1/14 (7%)

ORF 7	1 MKQQE-TAGINELT 13	
Structural maintenance of	MKQ E-TA I ELT 13	
chromosomes protein 2	434 MKQKELTAHIDELT 447	

ORF 8:

DUF4038 domain-containing protein (*Lachnoclostridium* sp. AN169)

Sequence IF: WP_087160745.1. Length: 521. Number of Matches: 1

Score	Expect	Identities	Positives	Gaps
33.3 bits (71)	2.5	9/11 (82%)	10/11 (90%)	0/11 (0%)

ORF 8	1	MRKCMAQLDLP	11
		MRKCMAQLDLP	
DUF4038	465	MRKCMAHLDLP	475

ORF 9:

putative uncharacterized protein (*Bacteroides uniformis* CAG:3)

Sequence IF: CDE00215.1. Length: 356. Number of Matches: 1

Score	Expect	Identities	Positives	Gaps
34.1 bits (73)	4.0	10/13 (77%)	11/13 (84%)	0/13 (0%)

ORF 9	7	FTIKIILKQRRIN	19
		F IK ILKQRRI	
hypothetical protein	120	FQIKTILKQRRID	132

ORF 10:

glutaminyl-peptide cyclotransferase, putative (*Plamodium* sp. gorilla clade G3)

Sequence IF: SOV83336.1. Length: 383. Number of Matches: 1

Score	Expect	Identities	Positives	Gaps
33.7 bits (72)	8.7	11/16 (69%)	11/16 (68%)	4/16 (25%)

ORF 10	9	IKRCDNYKQ----LET	20
		I RCDNYKQ LET	
glutamyl-peptide cyclotransferase	310	IERCDNYKQIKNKLET	325

ORF 11:

hypothetical protein (*Psychroserpens damuponensis*)

Sequence IF: WP_040281346.1. Length: 177. Number of Matches: 1

Score	Expect	Identities	Positives	Gaps
38.8 bits (84)	0.24	13/21 (62%)	15/21 (71%)	0/21 (0%)

ORF 11	2	TIYELIMLLAKSSIINFHTQF	22
		TIYELI LL SSI T F	
hypothetical protein	9	TIYELIKLLSQSSIADYNTIF	29

ORF 12:

Pentatricopeptide repeat-containing protein (*Apostasia shenzhenica*)

Sequence IF: PKA59515.1. Length: 513. Number of Matches: 1

Score	Expect	Identities	Positives	Gaps
32.5 bits (69)	40	10/11 (91%)	10/11 (90%)	1/11 (9%)

ORF 12	3	IY-ELIMLLAK	12
pentatricopeptide repeat		IY ELIMLLAK	
containing protein	406	IYKELIMLLAK	416

Table 7.5: Differential regulated genes during stationary growth phase in *S. aureus* ΔSSR42.

gene	log_2Fold change[1]	Adjusted p-value
gapA	1.99	$2.9*10^{-11}$
RSAU_000572	1.98	$7.9*10^{-6}$
RSAU_000124	1.94	0.0001
RSAU_002433	1.94	$6.8*10^{-6}$
RSAU_001358	1.91	0.002
RSAU_000255	1.88	$5.8*10^{-7}$
capH1	1.87	0.002
RSAU000487	1.86	$1.8*10^{-8}$
RSAU_000250	1.80	$6.0*10^{-10}$
fadB	1.79	$4.5*10^{-9}$
RSAU_002017	1.70	0.002
mnhG1	1.68	$8.6*10^{-5}$
RSAU_000799	1.66	$6.2*10^{-19}$
RSAU_002368	1.58	0.0003
essB	1.55	0.001
frp	1.51	$2.6*10^{-9}$

RSAU_000122	1.50	0.002
RSAU_000226	1.50	0.0003
essA	1.48	0.007
gpxA	1.46	6.3 *10^{-6}
sarX	1.42	4.7 *10^{-6}
RSAU_002293	1.41	0.0095
RSAU_000254	1.41	0.0002
***sdr*E**	1.38	3.4 *10^{-7}
RSAU_000375	1.37	0.003
***nix*A**	1.37	6.3 *10^{-6}
efb	1.36	0.0002
***crt*N**	1.35	0.009
RSAU_000350	1.35	1.7 *10^{-5}
RSAU_002463	1.34	0.049
RSAU_002429	1.33	0.02
RSAU_000745	1.33	1.47 *10^{-5}
***yab*J**	1.32	0.0002
***ald*A1**	1.31	1.2*10^{-5}
RSAU_002363	1.31	0.0001
***ldh*D**	1.30	0.013
***spo*VG**	1.29	9.7 *10^{-5}
RSAU_000325	1.29	7.1 *10^{-5}
RSAU_000548	1.28	8.8 *10^{-8}
RSAU_002176	1.27	0.001
***cys*M**	1.27	3.6 *10^{-5}
RSAU_001644	1.25	4.2 *10^{-5}
RSAU_000798	1.25	1.6*10^{-12}
RSAU_002164	1.24	0.01
***esa*A**	1.21	0.0001
RSAU_000376	1.21	0.0005
RSAU_000393	1.21	1.7 *10^{-5}
***mn*F1**	1.20	0.0001
RSAU_001553	1.20	0.0001
***uhp*T**	1.19	0.0002
RSAU_000773	1.19	2.4*10^{-5}
RSAU_000351	1.18	6.1*10^{-7}
RSAU000488	1.18	0.0002
RSAU_002043	1.17	5.5 *10^{-8}
RSAU_002350	1.17	0.002
***fdh*D**	1.16	2.8 *10^{-7}
RSAU_000154	1.16	0.0007
***pro*P**	1.13	0.0002
RSAU_000378	1.12	0.001
***yyc*J**	1.12	1.8*10^{-5}
RSAU_000778	1.11	0.001
RSAU_001332	1.11	0.0007
RSAU_002323	1.10	1.9*10^{-5}
***nor*A**	1.10	0.0002
RSAU_000928	1.10	4.2*10^{-5}
***bud*B**	1.09	5.0*10^{-7}
RSAU000485	1.083	0.004
***asp*2**	1.07	0.0003
***roc*A**	1.07	0.003
***csp*B**	1.07	0.003
RSAU_002312	1.06	0.003
RSAU_001357	1.05	0.0007
***acs*A**	1.04	0.003
***mop*B**	1.04	1.5 *10^{-7}
RSAU_002318	1.03	0.0002
RSAU_001485	1.03	1.3 *10^{-5}
veg	1.00	0.0007

***sar*R**	-1.02	0.002
RSAU_001845	-1.03	4.0 *10^{-5}
***pyr*AA**	-1.05	0.002
***spl*F**	-1.13	0.0007
RSAU_002394	-1.14	0.003
***cid*A**	-1.14	4.1 *10^{-6}
***phn*E2**	-1.14	0.0004
plc	-1.15	7.5 *10^{-5}
***ilv*A**	-1.18	9.7 *10^{-6}
RSAU_001746	-1.21	0.004
***phn*E**	-1.24	7.1 *10^{-5}
***luk*D**	-1.24	0.002
***pyr*B**	-1.25	0.004
***isd*A**	-1.27	1.4 *10^{-6}
RSAU_001985	-1.32	0.001
RSAU_000073	-1.36	1.1 *10^{-5}
***spl*C**	-1.38	3.9 *10^{-6}
RSAU_002306	-1.50	0.002
***sbn*C**	-1.51	3.6 *10^{-6}
***isd*F**	-1.55	0.0004
RSAU_001935	-1.56	1.0 *10^{-6}
***spl*A**	-1.61	9.5 *10^{-10}
RSAU_001659	-1.65	0.004
RSAU_001986	-1.73	1.6 *10^{-7}
mtlf	-1.78	6.2 *10^{-18}
RSAU_000070	-1.78	3.6 *10^{-5}
chs	-1.79	4.6 *10^{-5}
RSAU_000071	-1.83	0.002
***scp*A**	-1.83	1.1 *10^{-14}
***spl*B**	-1.87	0.001
***isd*B**	-2.34	4.5 *10^{-9}
RSAU_002216	-7.73	2.7 *10^{-82}

[1]Compared to transcript levels in *S. aureus* 6850 wild-type bacteria

Table 7.6: Differential regulated genes during exponential growth phase in *S. aureus* ΔSSR42

gene	log_2Fold change[1]	Adjusted p-value
***nir*B**	2.72	0.03
RSAU_002525	2.67	0.001
***ldh*D**	2.58	1.0*10^{-8}
RSAU_000366	2.39	1.3 *10^{-11}
***his*A**	2.39	0.005
RSAU_001467	2.15	0.0004
***ure*B**	1.89	2.1 *10^{-5}
RSAU_000185	1.81	0.01
***his*F**	1.80	0.047
RSAU_001651	1.78	0.006
***gnt*K**	1.76	0.006
***his*D**	1.75	0.03
***lrg*A**	1.74	0.01
***cap*D**	1.71	6.8 *10^{-5}
***dha*L**	1.71	0.01
RSAU_000184	1.67	0.04
asd	1.66	0.03
RSAU_000123	1.60	0.004

***fnb*A**	1.58	$1.5*10^{-7}$
***ure*A**	1.58	0.0007
***opu*CA**	1.53	0.0003
RSAU_001971	1.52	0.0005
***opp*B1**	1.50	0.03
***fnb*B**	1.49	0.0005
***pro*P**	1.47	$8.2 *10^{-5}$
RSAU_001652	1.45	0.002
RSAU_002444	1.44	0.03
RSAU_002120	1.40	$1.8 *10^{-5}$
RSAU_002350	1.38	0.006
RSAU_000060	1.38	$2.3 *10^{-6}$
***acs*A**	1.37	0.006
***gnt*P**	1.37	0.02
***lys*C**	1.36	0.04
***glp*F**	1.35	0.04
***opp*A1**	1.34	0.04
RSAU_002164	1.34	0.01
RSAU_000161	1.33	0.02
RSAU_000236	1.33	0.04
RSAU_000062	1.33	0.006
RSAU_002400	1.31	0.02
RSAU_002290	1.26	$3.1 *10^{-5}$
RSAU_002401	1.23	0.02
RSAU_001466	1.21	0.002
RSAU_000820	1.21	0.04
RSAU_000375	1.19	0.01
***glc*B**	1.19	0.046
RSAU_000254	1.19	0.004
***ilv*D**	1.13	0.02
***ess*C**	1.13	0.002
RSAU_001170	1.13	0.03
***glp*D**	1.11	0.01
***roc*A**	1.14	0.045
***nix*A**	1.08	0.0005
RSAU_000351	1.05	0.001
RSAU_000350	1.05	0.02
RSAU_000228	1.05	0.02
RSAU_002312	1.04	0.046
RSAU_000788	1.02	0.048
***mop*B**	1.01	$5.7 *10^{-5}$
RSAU_001970	1.00	0.02
RSAU_001525	-1.00	0.0005
***pyr*R**	-1.04	0.01
***cys*K**	-1.07	$1.3 *10^{-7}$
***clp*B**	-1.08	0.03
***pmt*C**	-1.13	0.04
***czr*B**	-1.16	0.0003
hla	-1.18	0.02
RSAU_000977	-1.19	0.04
RSAU_000061	-1.20	0.02

nuc	-1.21	0.02
ftn	-1.22	0.007
***scp*A**	-1.27	$5.0 *10^{-5}$
***pyr*B**	-1.35	0.04
***sar*S**	-1.35	0.04
***pyr*C**	-1.41	0.001
chs	-1.42	0.03
RSAU_001681	-1.51	0.009
***pyr*E**	-1.56	$1.5 *10^{-8}$
***pyr*AA**	-1.57	0.0005
***pyr*AB**	-1.57	$1.0 *10^{-8}$
***pyr*P**	-1.62	0.03
***pyr*F**	-1.79	$1.6 *10^{-6}$
***psm*A3**	-1.82	0.0005
***psm*A1**	-1.90	0.04
***psm*A2**	-2.05	0.001
***sar*R**	-2.24	$3.8 *10^{-9}$
RSAU_000768	-2.40	$9.7 *10^{-5}$
***psm*A4**	-2.56	$3.5 *10^{-10}$
RSAU_002216	-4.13	$1.3 *10^{-33}$

[1]Compared to transcript levels in *S. aureus* 6850 wild-type bacteria

Table 7.7: Differential regulated genes during stationary growth phase in *S. aureus* ΔSSR42-*rsp*.

gene	log_2Fold change[1]	adjusted p-value
RSAU_000377	3.05	$8.3 *10^{-6}$
***fad*E**	2.95	$4.4 *10^{-10}$
RSAU_000180	2.83	$1.5 *10^{-9}$
RSAU_000762	2.47	$3.1 *10^{-5}$
***fad*D**	2.39	$1.8 *10^{-5}$
RSAU_000249	2.36	$3.4 *10^{-5}$
RSAU_001358	2.15	0.0002
***clf*A**	2.14	$8.7 *10^{-14}$
***gap*A**	2.12	$5.5 *10^{-13}$
RSAU_002017	1.97	0.0001
***fad*B**	1.94	$8.0 *10^{-11}$
RSAU000487	1.93	$2.0 *10^{-9}$
RSAU_000608	1.89	$2.1 *10^{-13}$
RSAU_000549	1.88	0.007
***cap*H1**	1.87	$9.0 *10^{-7}$
***sdr*E**	1.87	0.001
RSAU_000517	1.85	$2.9 *10^{-13}$
efb	1.83	$7.4 *10^{-6}$
RSAU_000760	1.82	0.007
RSAU_000572	1.80	$4.3 *10^{-5}$
RSAU000485	1.80	$4.4 *10^{-5}$
RSAU000488	1.76	$1.9 *10^{-6}$
RSAU_000376	1.69	$3.7 *10^{-5}$
***ess*B**	1.66	0.0003
RSAU_000226	1.65	$1.9 *10^{-5}$

RSAU_001040	1.63	1.0 *10^{-6}
RSAU_000255	1.61	2.6 *10^{-5}
RSAU_000228	1.57	2.1 *10^{-5}
RSAU_000124	1.50	0.005
RSAU_001553	1.48	7.6 *10^{-5}
***accB*2**	1.48	0.008
RSAU_000250	1.48	6.1 *10^{-7}
RSAU_000236	1.47	0.03
RSAU_000799	1.43	7.2 *10^{-14}
RSAU_002043	1.43	6.0*10^{-7}
***asp*2**	1.41	4.2 *10^{-5}
***asp*1**	1.41	0.01
RSAU_002463	1.39	0.03
RSAU_002322	1.39	0.047
RSAU_002044	1.39	0.005
RSAU_000362	1.37	0.002
***esa*A**	1.35	7.3 *10^{-6}
RSAU_000378	1.28	0.002
***bud*B**	1.27	4.2 *10^{-7}
RSAU_000798	1.27	7.2 *10^{-11}
***sas*F**	1.27	4.2 *10^{-5}
RSAU_000548	1.26	4.3 *10^{-7}
***ess*A**	1.24	0.03
***gpx*A**	1.22	0.0002
RSAU_002433	1.22	0.01
RSAU_001357	1.22	0.001
***asp*3**	1.21	0.04
***cap*C1**	1.21	0.002
***fad*A**	1.20	2.9 *10^{-6}
RSAU_002168	1.20	0.01
RSAU_000254	1.20	0.002
***mop*B**	1.19	1.7 *10^{-7}
RSAU_001041	1.18	0.001
***acc*C2**	1.18	0.003
RSAU_000351	1.18	2.9 *10^{-5}
***fnb*A**	1.17	0.0003
***fnb*B**	1.14	0.01
***gcv*T**	1.13	0.0005
veg	1.13	0.003
***rec*Q1**	1.13	1.3 *10^{-5}
***roc*D2**	1.13	0.01
***suc*C**	1.12	0.02
***fdh*D**	1.11	3.4 *10^{-5}
***pck*A**	1.11	0.005
RSAU_001467	1.11	0.03
RSAU_000142	1.10	0.04
RSAU_000154	1.10	0.01
frp	1.10	3.7 *10^{-5}
***cys*M**	1.09	0.0005
RSAU_001471	1.09	0.04
***ald*A1**	1.09	0.0004

RSAU_000350	1.08	0.0009
***ess*C**	1.07	0.002
***ebp*S**	1.06	0.003
RSAU_001245	1.05	0.004
***fts*Y**	1.04	0.002
RSAU_000668	1.04	0.0008
RSAU_002323	1.04	0.0009
RSAU_001118	1.03	0.03
RSAU_001485	1.03	0.0003
RSAU_002176	1.03	0.01
***csp*B**	1.03	0.04
ffh	1.01	$2.4 * 10^{-6}$
***odh*A**	1.01	0.02
***cit*C**	1.00	0.0004
RSAU_000182	1.00	0.001
***fem*B**	0.99	$3.7 * 10^{-5}$
RSAU_000393	0.99	0.007
***odh*B**	0.96	0.03
RSAU_000669	0.96	0.01
***hsl*U**	0.96	0.01
RSAU_001428	0.96	0.006
RSAU_000474	0.95	0.008
RSAU_000475	0.95	0.03
RSAU_001652	0.93	0.04
***roc*F**	0.93	0.02
RSAU_001402	0.93	0.007
RSAU_000283	0.93	0.003
***cts*R**	0.91	0.0007
***sar*X**	0.91	0.008
***cap*G**	0.91	0.047
***yyc*J**	0.90	0.008
***ure*A**	0.89	0.01
RSAU_000745	0.89	0.009
***mut*M**	0.89	0.004
***asp*23**	0.88	0.049
RSAU_001028	0.87	0.04
***din*B**	0.87	$3.8 * 10^{-6}$
***cap*F**	0.87	0.04
***men*F**	0.86	0.02
***yab*J**	0.84	0.03
RSAU_002145	0.83	0.0001
***msr*B**	0.83	0.004
***ure*G**	0.83	0.0009
RSAU_001027	0.82	0.03
RSAU_002324	0.81	0.02
RSAU_000880	0.81	0.02
***spo*VG**	0.79	0.04
RSAU_002363	0.79	0.04
***nix*A**	0.79	0.02
***men*H**	0.79	0.02
***sec*A2**	0.78	0.0008

RSAU_000325	0.78	0.03
***ure*F**	0.78	0.04
RSAU_000929	0.77	0.03
***ure*E**	0.77	0.049
***cap*D**	0.76	0.003
***yaa*T**	0.75	0.005
***fem*A**	0.75	0.001
***men*D**	0.72	0.01
***yyc*H**	0.72	0.03
RSAU_001247	0.71	0.01
***uvr*B**	0.67	0.01
RSAU_002175	0.67	0.02
RSAU_000748	0.66	0.02
RSAU_001401	0.65	0.0003
RSAU_002206	0.65	0.004
***lat*S**	0.64	0.02
RSAU_000284	0.63	0.04
RSAU_001613	0.62	0.01
***cit*B**	0.59	0.04
lip	0.59	0.01
RSAU_002279	0.57	0.01
RSAU_001960	0.56	0.01
RSAU_000694	0.55	0.04
***vic*K**	0.54	0.04
rho	0.53	0.003
***yyc*I**	0.52	0.009
***men*E**	0.52	0.03
***pri*A**	0.51	0.04
RSAU_001058	0.47	0.03
***trm*U**	0.46	0.01
RSAU_001090	0.45	0.03
***acc*C1**	-0.46	0.0007
***atp*D**	-0.49	0.02
***nrd*R**	-0.49	0.03
upp	-0.50	0.049
***acc*B1**	-0.50	0.04
***atp*C**	-0.51	0.005
***thr*S**	-0.51	0.02
***mnh*D2**	-0.51	0.03
RSAU_000787	-0.53	0.02
***prf*B**	-0.55	0.02
***rbf*A**	-0.55	0.049
***fab*Z**	-0.56	0.02
RSAU_000443	-0.57	0.01
***cys*K**	-0.59	0.01
***glt*A**	-0.61	0.049
RSAU_000148	-0.61	0.03
***glt*B**	-0.61	0.01
***atp*E**	-0.62	0.008
***ahp*C**	-0.63	0.00
***met*N**	-0.63	0.03

***atp*I**	-0.63	0.02
RSAU_000149	-0.65	0.03
RSAU_000847	-0.65	$3.8 * 10^{-5}$
RSAU_002212	-0.65	0.049
***dna*B**	-0.67	0.02
RSAU_000129	-0.67	0.02
RSAU_001952	-0.67	0.009
***met*K**	-0.68	0.049
***mna*A**	-0.68	0.0004
rplO	-0.69	0.03
***atp*A**	-0.70	0.003
RSAU_000936	-0.71	0.04
RSAU_001525	-0.71	0.02
***agr*A**	-0.72	$6.5 * 10^{-5}$
***sec*Y1**	-0.72	0.04
***thr*B**	-0.72	0.02
RSAU_000297	-0.72	0.049
RSAU_002413	-0.74	0.049
RSAU_000074	-0.75	0.049
RSAU_001163	-0.75	0.04
***sas*H**	-0.76	0.0008
***atp*B**	-0.76	0.0004
***pyr*AB**	-0.77	0.01
RSAU_002129	-0.77	0.02
RSAU_001866	-0.78	0.047
RSAU_000131	-0.79	0.02
***rpm*D**	-0.79	0.01
RSAU_000365	-0.81	0.02
***pmt*D**	-0.83	0.02
RSAU_002243	-0.83	0.02
***pyr*F**	-0.85	0.02
***mnh*G2**	-0.86	0.007
putative ncRNA: 2,533,432-2,533,704 bp	-0.88	0.046
RSAU_002529	-0.88	0.04
RSAU_001840	-0.88	0.0009
RSAU_000326	-0.88	0.04
***lyt*R**	-0.90	0.001
aur	-0.90	0.006
RSAU_001830	-0.90	0.049
RSAU_000078	-0.90	0.03
***mnh*F2**	-0.90	0.003
***ahp*F**	-0.92	$3.3 * 10^{-9}$
hup	-0.92	0.03
RSAU_001512	-0.94	0.006
***spx*A**	-0.95	0.002
RSAU_001410	-0.96	$1.1 * 10^{-5}$
***deo*D1**	-0.96	0.03
RSAU_001738	-0.97	0.03
RSAU_001740	-0.97	0.02
***phn*E2**	-0.98	0.01
RSAU_000174	-0.99	0.02

RSAU_000061	-1.01	0.047
RSAU_000299	-1.01	7.4 *10^{-6}
***sbn*C**	-1.02	0.01
putative ncRNA: 581,468-581,758 bp	-1.02	0.008
***pyr*AA**	-1.02	0.03
RSAU_000526	-1.04	0.0001
RSAU_002437	-1.05	0.0013
RSAU_001739	-1.05	0.04
sak	-1.06	0.002
***spl*C**	-1.10	0.003
***isd*A**	-1.10	0.0005
***spl*F**	-1.101	0.013
***yqe*Z**	-1.11	3.2 *10^{-5}
***cid*A**	-1.13	0.0001
***hts*C**	-1.14	4.2 *10^{-5}
RSAU_001438	-1.14	7.5 +10^{-7}
***luk*D**	-1.15	0.02
***per*R**	-1.16	0.0001
scn	-1.17	0.001
RSAU_002306	-1.19	0.046
RSAU_001723	-1.21	0.03
RSAU_000364	-1.30	0.009
RSAU_000070	-1.36	0.008
***isd*F**	-1.36	0.01
RSAU_000073	-1.39	8.0 *10^{-5}
***sar*R**	-1.41	0.0005
RSAU_000071	-1.45	0.01
RSAU_001986	-1.47	0.0003
***phn*E**	-1.54	3.1 *10^{-5}
***spl*B**	-1.56	0.006
***spr*D**	-1.56	0.03
***luk*E**	-1.58	0.002
RSAU_002308	-1.59	0.006
***opp*1D**	-1.61	0.003
RSAU_002242	-1.62	0.04
***mtl*F**	-1.63	2.7 *10^{-13}
***spl*A**	-1.65	9.09*10^{-9}
chs	-1.67	0.003
RSAU_001746	-1.67	0.001
***scp*A**	-1.69	5.1 *10^{-13}
plc	-1.81	5.1 *10^{-8}
***isd*C**	-1.94	0.0003
***isd*B**	-2.35	3.8 *10^{-10}
RSAU_001935	-2.41	1.2 *10^{-11}
RSAU_002216	-6.42	7.4 *10^{-5}
RSAU_002217	-6.99	1.8 *10^{-16}

[1]Compared to transcript levels in *S. aureus* 6850 wild-type bacteria

Table 7.8: Differential regulated genes during exponential growth phase in *S. aureus* ΔSSR42-*rsp.*

gene	log_2Fold change[1]	Adjusted p-value
***nir*B**	3.70	0.0001
***his*B**	3.68	0.0002
RSAU_002525	3.58	$2.9 *10^{-7}$
***nir*D**	3.51	0.001
***his*A**	3.49	$5.4 *10^{-7}$
***his*C1**	3.39	$1.1 *10^{-6}$
***his*D**	3.34	$4.1 *10^{-8}$
RSAU_002236	3.23	0.0007
RSAU_001717	3.091	$9.6 *10^{-5}$
***nar*H**	2.92	0.005
RSAU_001716	2.87	0.0001
***arg*G**	2.86	0.0002
***nar*T**	2.78	0.008
***arg*H**	2.73	0.0002
***his*G**	2.71	0.0002
RSAU_000185	2.71	$1.7*10^{-6}$
***nar*J**	2.70	0.007
***ldh*D**	2.66	$2.2 *10^{-9}$
***nar*G**	2.65	0.006
***his*H**	2.51	$2.8 *10^{-5}$
asd	2.47	$2.8 *10^{-5}$
RSAU_001467	2.46	$3.9 *10^{-6}$
RSAU_000184	2.42	$9.1 *10^{-5}$
***his*F**	2.41	0.0005
RSAU_000366	2.38	$9.6 *10^{-12}$
RSAU_002530	2.30	0.01
RSAU_001651	2.24	$2.9 *10^{-5}$
RSAU_000375	2.20	$5.8 *10^{-9}$
RSAU_000377	2.13	0.0001
RSAU_002239	2.12	0.02
RSAU_000673	2.11	0.0002
***mal*A**	2.11	0.004
***ure*B**	2.10	$2.7 *10^{-7}$
***opp*A1**	2.10	$2.1 *10^{-5}$
RSAU_001652	2.06	$1.9 *10^{-7}$
RSAU_000062	2.06	$1.9 *10^{-7}$
***luk*G**	2.04	$2.4 *10^{-8}$
***opu*CA**	2.04	$3.2 *10^{-8}$
RSAU_000788	2.02	$3.2 *10^{-8}$
***adh*A**	1.97	0.009
RSAU_000161	1.97	$7.0 *10^{-6}$
***gnt*K**	1.95	0.0003
***pfl*B**	1.93	0.01
***lrg*A**	1.91	0.0008
RSAU_000762	1.89	0.0007
RSAU_001971	1.87	$1.4 *10^{-7}$
***lrg*B**	1.87	0.0001
***lys*C**	1.81	0.003

***dha*M**	1.81	0.0004
***nar*I**	1.81	0.0005
RSAU_002232	1.81	0.0006
RSAU_000820	1.81	$4.2 * 10^{-5}$
RSAU_002464	1.81	0.01
RSAU_002427	1.80	0.005
***ilv*C**	1.77	0.04
***acc*C2**	1.76	0.0002
RSAU_001659	1.75	0.03
RSAU_002400	1.74	0.0001
***luk*H**	1.72	$1.9 * 10^{-5}$
***isa*B**	1.72	0.0001
***fnb*A**	1.71	$6.4 * 10^{-9}$
RSAU_000060	1.70	$8.5 * 10^{-10}$
RSAU_002401	1.70	$5.1 * 10^{-5}$
***cap*D**	1.69	$1.9 * 10^{-5}$
***opp*C1**	1.69	0.003
***sda*AB**	1.66	0.0008
***ure*A**	1.66	$5.1 * 10^{-5}$
***opp*B1**	1.64	0.002
***gnt*P**	1.64	0.0004
***dha*L**	1.63	0.003
alr	1.62	0.0003
***nrd*D**	1.62	0.003
RSAU_001581	1.62	$3.9 * 10^{-6}$
RSAU_001470	1.61	0.004
RSAU_000030	1.60	0.001
RSAU_000821	1.60	$9.6 * 10^{-5}$
RSAU_002044	1.60	0.049
***hisI*E**	1.60	0.005
RSAU_000254	1.59	$3.2 * 10^{-6}$
RSAU_002231	1.58	0.0005
***cap*H1**	1.57	0.01
***lct*P**	1.57	0.007
***pur*Q**	1.57	0.002
***fd*A**	1.56	$4.4 * 10^{-6}$
RSAU_002463	1.55	0.003
RSAU_000059	1.55	$6.8 * 10^{-8}$
***opu*CB**	1.55	0.0005
RSAU_002531	1.54	0.01
***dap*A**	1.54	0.002
RSAU_000143	1.54	0.02
RSAU_001970	1.53	$9.0 * 10^{-6}$
RSAU_001466	1.53	$3.8 * 10^{-6}$
RSAU_001981	1.52	0.0006
***nrd*G**	1.51	0.01
RSAU_000386	1.51	0.01
RSAU_000162	1.50	$1.7 * 10^{-5}$
***clp*L**	1.49	0.0007
***adh*E**	1.49	0.002
***tre*C**	1.48	0.0008

***roc*A**	1.47	0.0005
RSAU_000160	1.44	0.006
***ndh*F**	1.43	0.01
RSAU_002310	1.42	0.0002
***rps*A**	1.42	$5.0 *10^{-5}$
RSAU_000572	1.41	0.0006
RSAU_002164	1.41	0.001
***pur*C**	1.41	0.01
***cap*G**	1.40	0.005
RSAU_002444	1.40	0.008
RSAU_002323	1.38	$1.7 *10^{-6}$
***acs*A**	1.38	0.001
RSAU_001358	1.37	0.02
RSAU_002229	1.34	0.001
RSAU_000031	1.33	0.04
***glp*D**	1.33	0.0002
RSAU_000123	1.32	0.006
RSAU_000683	1.32	0.003
***fnb*B**	1.32	0.0007
RSAU_000551	1.31	0.002
***pur*K**	1.31	0.0001
RSAU_000760	1.30	0.01
RSAU_000132	1.30	0.01
RSAU_001207	1.30	$5.1 *10^{-5}$
RSAU_000771	1.30	0.005
RSAU_001978	1.30	0.004
***glc*B**	1.29	0.005
RSAU_000317	1.29	0.004
***ess*B**	1.28	0.004
RSAU_000745	1.28	$1.5 *10^{-5}$
***hch*A**	1.27	$8.2*10^{-6}$
RSAU_000727	1.27	0.04
RSAU_000395	1.27	0.03
***opp*F1**	1.26	0.001
RSAU_002120	1.26	$3.1 *10^{-5}$
RSAU_001577	1.26	0.002
RSAU_002350	1.25	0.004
RSAU_000251	1.25	0.03
RSAU_000236	1.23	0.02
RSAU_000789	1.23	0.0007
RSAU_000226	1.22	$5.1 *10^{-5}$
RSAU_000376	1.22	0.00203
efb	1.22	0.0008
RSAU_002223	1.22	0.004
***arc*D**	1.22	0.0009
RSAU_000255	1.21	0.0003
RSAU_000351	1.21	$2.2 *10^{-5}$
RSAU_001567	1.20	0.04
RSAU_001471	1.18	0.047
RSAU_002482	1.18	0.02
RSAU_002526	1.17	0.004

RSAU_000315	1.17	0.01
***dap*B**	1.17	0.0002
***opu*CC**	1.16	$2.0*10^{-6}$
RSAU_002404	1.16	0.005
***ilv*D**	1.16	0.004
RSAU_000159	1.14	0.004
RSAU_000502	1.14	0.002
***scd*A**	1.14	0.01
***his*C2**	1.13	$7.8*10^{-6}$
RSAU_000330	1.11	0.02
***ess*C**	1.11	0.0005
RSAU_000260	1.07	0.002
***dha*K**	1.07	0.01
RSAU_002309	1.07	0.006
***ilv*A**	1.07	0.02
RSAU_001960	1.06	$1.4*10^{-8}$
RSAU_002312	1.06	0.001
***crt*M**	1.06	0.02
***dho*M**	1.05	0.03
***pyn*P**	1.02	0.005
***dap*D**	1.02	0.005
***pck*A**	1.02	0.007
RSAU_000965	1.02	0.02
***esa*A**	1.01	0.0003
RSAU_002374	1.01	0.02
RSAU_002500	-1.00	0.047
RSAU_001476	-1.00	0.02
RSAU_001513	-1.00	0.009
***ssa*A2**	-1.00	0.001
***rps*K**	-1.01	0.01
RSAU_000205	-1.01	0.01
aur	-1.02	0.01
***dlt*D**	-1.02	0.007
RSAU_002089	-1.02	0.005
***sec*Y1**	-1.04	0.0004
RSAU_000716	-1.04	0.003
***ssa*A4**	-1.04	0.005
fur	-1.04	$5.4*10^{-6}$
***rlp*F**	-1.0	0.006
***hem*N**	-1.04	0.005
***men*A**	-1.0	0.002
***coa*W**	-1.05	$9.9*10^{-5}$
***rps*B**	-1.05	0.001
RSAU_001316	-1.05	$1.7*10^{-5}$
RSAU_000879	-1.05	0.005
***ula*A**	-1.05	0.0002
***pot*A**	-1.05	0.03
RSAU_001222	-1.06	0.03
***inf*B**	-1.06	0.0006
***rpl*Q**	-1.06	0.0005
***rps*H**	-1.06	0.004

guaA	-1.06	0.0003
***isa*A**	-1.06	$2.9 *10^{-5}$
***rpl*N**	-1.06	0.007
hla	-1.06	0.01
RSAU_002187	-1.06	0.02
RSAU_000714	-1.06	0.0004
***rps*N2**	-1.07	0.006
RSAU_001190	-1.07	$1.5 *10^{-6}$
RSAU_001681	-1.07	0.03
***kdp*C**	-1.08	$1.8 *10^{-5}$
***typ*A**	-1.08	0.0006
***rim*P**	-1.10	0.0006
RSAU_001315	-1.10	0.0004
RSAU_002212	-1.11	$8.3 *10^{-5}$
RSAU_002534	-1.11	0.001
RSAU_001181	-1.11	$7.4 *10^{-5}$
gcp	-1.12	$7.1 *10^{-5}$
RSAU_001425	-1.13	0.001
***rpl*E**	-1.13	0.004
***pyr*R**	-1.13	0.001
RSAU_002194	-1.14	0.02
RSAU_002186	-1.14	0.004
RSAU_001920	-1.15	$2.0 *10^{-5}$
***trm*Fo**	-1.15	0.0009
***acc*A**	-1.16	$7.3 *10^{-9}$
***rps*Q**	-1.16	0.008
RSAU_001525	-1.16	$6.3 *10^{-6}$
***que*E**	-1.17	0.0005
***rpo*C**	-1.17	0.001
***rpl*X**	-1.18	0.002
cdh	-1.18	0.0003
***csp*B**	-1.18	0.006
RSAU_000007	-1.18	$2.8 *10^{-6}$
***rnh*B**	-1.19	0.04
***scp*A**	-1.20	$2.9 *10^{-5}$
***clp*B**	-1.21	0.002
RSAU_002142	-1.22	0.0004
RSAU_000545	-1.22	0.0002
***pyr*G**	-1.23	$2.7 *10^{-5}$
RSAU_001737	-1.24	0.002
***opu*D**	-1.24	$1.7 *10^{-8}$
***pot*C**	-1.24	0.02
RSAU_000906	-1.24	0.0005
***rpo*B**	-1.25	0.0002
RSAU_000294	-1.25	0.02
***rpm*C**	-1.26	0.006
RSAU_002328	-1.26	0.001
***als*T**	-1.26341769	$6.2 *10^{-5}$
RSAU_001133	-1.27	$6.8 *10^{-8}$
***fad*E**	-1.27	0.03
RSAU_001616	-1.28	$6.3 *10^{-6}$

RSAU_000407	-1.28	0.001
***glt*S**	-1.28	0.0002
RSAU_001507	-1.28	$6.7 *10^{-5}$
RSAU_001039	-1.29	0.0004
***sir*B**	-1.29	0.0003
***sir*A**	-1.29	0.006
RSAU_001740	-1.30	$3.4 *10^{-5}$
***psm*A4**	-1.30	0.0004
RSAU_002220	-1.31	0.0009
RSAU_000655	-1.32	0.0007
***rpm*A**	-1.33	$2.0 *10^{-5}$
***pyr*B**	-1.33	0.01
***ars*R**	-1.34	0.002
RSAU_000465	-1.35	0.005
RSAU_001353	-1.36	0.0004
***rpm*F**	-1.36	$1.9 *10^{-5}$
***rpm*G2**	-1.36	$7.5 *10^{-6}$
RSAU_001731	-1.36	0.0004
***rpl*B**	-1.37	$8.1 *10^{-5}$
RSAU_000630	-1.38	$7.5 *10^{-6}$
***rpl*P**	-1.39	0.001
RSAU_002308	-1.41	0.0005
***pot*D**	-1.41	0.003
***rpm*I**	-1.42	$9.9 *10^{-5}$
RSAU_000391	-1.42	0.0009
RSAU_002370	-1.42	0.0001
RSAU_001688	-1.43	0.007
RSAU_001847	-1.43	0.0008
RSAU_000993	-1.43	0.0005
RSAU_000791	-1.45	0.0003
RSAU_001746	-1.46	0.002
chs	-1.46	0.005
RSAU_001679	-1.46	0.03
ssb	-1.47	$2.4*10^{-6}$
***rpl*V**	-1.48	0.0005
RSAU_002292	-1.48	$4.3 *10^{-6}$
***rps*C**	-1.48	0.0004
RSAU_002100	-1.48	0.0002
RSAU_001726	-1.50	0.0004
RSAU_002361	-1.51	0.0001
RSAU_001738	-1.51	$2.6 *10^{-7}$
***rps*T**	-1.51	$9.8 *10^{-6}$
***rpl*M**	-1.51	$4.0 *10^{-7}$
***pyr*E**	-1.52	$2.4 *10^{-8}$
RSAU_000766	-1.52	0.001
RSAU_001732	-1.52	$8.7 *10^{-6}$
RSAU_002003	-1.52	$1.5 *10^{-5}$
RSAU_001684	-1.53	0.0002
***rpl*K**	-1.53	$3.9 *10^{-5}$
***rps*R**	-1.54	$6.0 *10^{-8}$
***czr*B**	-1.54	8.2316E-08

***rps*F**	-1.54	5.8 *10^{-6}
***bra*B**	-1.56	7.1*10^{-6}
***rps*I**	-1.56	1.3 *10^{-6}
RSAU_001729	-1.56	1.4 *10^{-6}
RSAU_001680	-1.56	0.04
***rsm*G**	-1.56	0.001
RSAU_001734	-1.57	3.5 *10^{-6}
RSAU_001727	-1.57	3.2 *10^{-6}
RSAU_001721	-1.58	0.001
***spr*D**	-1.59	0.0002
***rp*L**	-1.59	2.8 *10^{-5}
RSAU_001225	-1.60	2.2 *10^{-6}
RSAU_000326	-1.60	7.1 *10^{-6}
***rpl*A**	-1.61	1.2 *10^{-6}
***rpm*E**	-1.61	2.7 *10^{-5}
***bio*W**	-1.62	0.01
***rps*S**	-1.63	0.0003
RSAU_000459	-1.63	0.0007
RSAU_001728	-1.64	2.8 *10^{-5}
RSAU_000354	-1.65	8.1 *10^{-5}
RSAU_001741	-1.65	5.4 *10^{-7}
***rpl*W**	-1.66	0.0001
RSAU_000458	-1.67	0.04
RSAU_001011	-1.67	7.0 *10^{-5}
***inf*C**	-1.67	0.0005
RSAU_001310	-1.67	0.0006
***spl*A**	-1.68	0.02
***rpl*Y**	-1.69	3.4 *10^{-6}
RSAU_000846	-1.70	9.2 *10^{-5}
RSAU_001739	-1.70	4.3 *10^{-6}
***pyr*C**	-1.70	6.3 *10^{-6}
***rim*M**	-1.71	0.007
***rpl*D**	-1.72	0.0002
***rsa*F**	-1.72	0.0008
RSAU_002371	-1.73	6.3 *10^{-5}
fer	-1.74	1.6 *10^{-5}
RSAU_000464	-1.74	0.0004
RSAU_000064	-1.74	5.1 *10^{-5}
RSAU_000220	-1.75	2.9 *10^{-7}
***rpl*S**	-1.76	1.2 *10^{-5}
***rpl*T**	-1.77	1.3 *10^{-6}
RSAU_000983	-1.77	0.001
RSAU_001706	-1.77	2.4 *10^{-7}
RSAU_001687	-1.77	2.0*10^{-6}
RSAU_000921	-1.78	0.0008
***rpm*G3**	-1.78	1.5 *10^{-5}
***trm*D**	-1.78	0.0003
RSAU_001683	-1.80	0.008
RSAU_001733	-1.80	4.4 *10^{-6}
***rpl*J**	-1.80	1.5 *10^{-5}
***pyr*AA**	-1.81	6.7 *10^{-6}

***pot*B**	-1.82	0.007
RSAU_000463	-1.85	0.0004
***pyr*AB**	-1.86	$4.3 *10^{-12}$
RSAU_000461	-1.86	$2.8*10^{-5}$
***rps*O**	-1.88	$1.9 *10^{-7}$
RSAU_001686	-1.89	$2.0 *10^{-5}$
rplC	-1.90	0.0003
RSAU_001685	-1.90	$4.0 *10^{-6}$
RSAU_000768	-1.90	0.0006
***isd*B**	-1.91	$2.0 *10^{-6}$
RSAU_001730	-1.91	$2.4 *10^{-8}$
RSAU_001689	-1.92	0.001
RSAU_001200	-1.92	0.04
RSAU_000926	-1.92	0.0005
***sar*R**	-1.93	$2.3 *10^{-7}$
RSAU_001720	-1.93	$2.0*10^{-6}$
RSAU_001682	-1.94	0.01
***rpm*H**	-1.96	$4.3 *10^{-8}$
rpsP	-1.96	$1.8 *10^{-5}$
RSAU_000616	-1.98	0.02
***rps*J**	-2.01	$2.0*10^{-5}$
RSAU_001896	-2.01	$4.6 *10^{-6}$
RSAU_000061	-2.03	$6.8 *10^{-7}$
***pyr*F**	-2.03	$2.4 *10^{-8}$
***rps*D**	-2.08	$4.1*10^{-8}$
RSAU_001053	-2.10	$1.6 *10^{-5}$
RSAU_001722	-2.11	$4.4 *10^{-8}$
RSAU_000460	-2.18	$5.4 *10^{-7}$
RSAU_001725	-2.21	$7.3 *10^{-9}$
RSAU_000462	-2.22	$6.8 *10^{-7}$
RSAU_002002	-2.24	$3.7 *10^{-7}$
RSAU_001719	-2.30	$1.3 *10^{-8}$
***ssa*A3**	-2.32	$1.2 *10^{-5}$
RSAU_002001	-2.32	$1.0*10^{-6}$
RSAU_001723	-2.43	$3.7 *10^{-9}$
RSAU_000164	-2.46	$2.9 *10^{-5}$
RSAU_001724	-2.50	$2.9 *10^{-7}$
RSAU_001900	-2.67	$1.7*10^{-5}$
RSAU_001901	-2.87	$1.1 *10^{-6}$
RSAU_002216	-4.03	$8.9*10^{-32}$
RSAU_002217	-6.08	$2.5 *10^{-12}$

[1]Compared to transcript levels in *S. aureus* 6850 wild-type bacteria

Table 7.9: Effects of Rsp on transcription of genes. Up-regulated genes in *S. aureus* 6850 double knockout mutant ΔSSR42-rsp compared to ΔSSR42 mutant.

gene	log_2Fold change[1]	Adjusted p-value	product
exponential growth phase			
psmA1	1.87	$1.6*10^{-3}$	phenol-soluble modulin alpha 1
RSAU_000315	1.65	$2.7*10^{-5}$	staphylococcal enterotoxin putative
hisD	1.59	$1.4*10^{-3}$	histidinol dehydrogenase HisD
RSAU_000317	1.43	$1.4*10^{-4}$	putative lipoprotein putative
RSAU_002223	1.33	$1.9*10^{-4}$	hypothetical protein
RSAU_000030	1.32	$1.3*10^{-3}$	hypothetical protein
isaB	1.29	$5.4*10^{-4}$	immunodominant antigen B IsaB
RSAU_000782	1.31	$5.9*10^{-4}$	arsenate reductase putative
psmA4	1.26	$6.9*10^{-4}$	phenol-soluble modulin alpha 4
lukG	1.21	$9.9*10^{-5}$	F subunit LuKF-G putative
rsaF	-1.56	$3.8*10^{-4}$	non-coding RNA
stationary growth phase			
-	-	-	

[1]Compared to transcript levels in *S. aureus* 6850 ΔSSR42

Table 7.10: Effects of Rsp on transcription of genes. Down-regulated genes in *S. aureus* 6850 double knockout mutant ΔSSR42-rsp compared to ΔSSR42 mutant.

gene	log_2Fold change[1]	Adjusted p-value	product
exponential growth phase			
RSAU_001730	-1.57	$1.3*10^{-4}$	tRNA-Ser
RSAU_001729	-1.59	$1.9*10^{-5}$	tRNA-Met
RSAU_001687	-1.59	$2.7*10^{-4}$	tRNA-Phe
RSAU_000460	-1.65	$1.5*10^{-5}$	tRNA-Lys
RSAU_001724	-1.65	$1.0*10^{-4}$	tRNA-Trp
RSAU_001686	-1.68	$1.7*10^{-3}$	tRNA-His
RSAU_001685	-1.69	$4.5*10^{-4}$	tRNA-Gly
RSAU_001722	-1.7	$1.7*10^{-4}$	tRNA-Gln
RSAU_001728	-1.7	$1.7*10^{-4}$	tRNA-Asp
RSAU_001689	-1.78	$3.4*10^{-4}$	tRNA-Trp
RSAU_001723	-1.8	$1.7*10^{-4}$	tRNA-His
RSAU_000125	-1.83	$1.1*10^{-3}$	putative nitrate/nitrite system ATP-binding ABC transporter
RSAU_001901	-2.47	$3.4*10^{-4}$	tRNA-Leu
rsp	-6.4	$1.2*10^{-13}$	Repressor of surface proteins
stationary growth phase down-regulated genes			
rsp	-7.53	$2.1*10^{-22}$	Repressor of surface proteins

[1]Compared to transcript levels in *S. aureus* 6850 ΔSSR42

Table 7.11: Proteins with significantly differential abundances in *S. aureus* 6850 ΔSSR42 in exponential and stationary growth phase respectively.

gene	fold change[1] (ΔSSR42/ WT)	adjusted p-value	fraction	product
exponential growth phase			**extracellular**	
RSAU_000228	7.6	$2.6*10^{-6}$	extracellular	WxG Protein EsxA (Typ VII secretion system)
RSAU_002260	4.3	0.022	extracellular	gamma-hemolysin component B precursor, HlgB
RSAU_001040	2.5	0.0003	extracellular	Efb, extracellular fibrinogen binding protein
RSAU_001833	2.5	0.005	extracellular	map-like protein
RSAU_000940	2.2	$4.4*10^{-6}$	extracellular	Atl, Autolysin
RSAU_002132	2.1	$2.0*10^{-6}$	extracellular	Secretory antigen SSaA3
RSAU_002257	1.8	0.003	extracellular	immunoglobulin G-binding protein SBI
RSAU_000500	0.7	0.005	extracellular	translation elongator factor TU
RSAU_000754	0.6	0.002	extracellular	enolase
RSAU_000452	0.4	$2.0*10^{-6}$	extracellular	cysteine synthase A
RSAU_001445	0.4	0.0009	extracellular	chaperone protein DnaK
RSAU_001860	0.4	0.02	extracellular	60 kDa chaperonin GroEL
exponential growth phase			**cytosolic**	
RSAU_001184	2.1	0.001	cytosolic	aerobic glycerol3P dehydrogenase
RSAU_001127	1.5	0.008	cytosolic	succinyl coA synthetase
RSAU_001938	0.7	0.02	cytosolic	UDP-N-acetylglucosamine 1-carboxyvinyltransferase 1
RSAU_001113	0.6	0.011	cytosolic	3 oxoacyl-reductase
RSAU_001576	0.6	0.011	cytosolic	30 S ribosolmal protein S4
RSAU_002074	0.6	0.03	cytosolic	50 S ribosolmal protein L5
RSAU_000449	0.4	0.0002	cytosolic	hypoxanthine phosphoribosysl-transferase
stationary growth phase			**extracellular**	
RSAU_002514	7.05	0.001	extracellular	lipase precursor
RSAU_002340	7.0	0.0001	extracellular	Fibronectin-binding protein B
RSAU_000517	5.0	0.02	extracellular	Serine aspartate repeat containing protein E (sdrE)
RSAU_002259	3.6	0.011	extracellular	gamma hemolysin hlgC
RSAU_000752	2.7	0.011	extracellular	thiosephosphate isomerase
RSAU_000488	2.5	0.03	extracellular	transcriptional antiterminator NusG
RSAU_002252	2.3	0.0002	extracellular	amino acid ABC transporter binding protein
RSAU_001184	2.1	$6.6*10^{-5}$	extracellular	aerobic glycerol3P dehydrogenase
RSAU_001127	1.5	0.0006	extracellular	succinyl coA synthetase
RSAU_000981	0.82	0.020	extracellular	pyruvat dehydrogenase pdhD
RSAU_001637	0.75	0.004	extracellular	transaldolase
RSAU_001938	0.7	0.02	extracellular	UDP-N-acetylglucosamine 1-carboxyvinyltransferase 1
RSAU_001700	0.64	0.02	extracellular	peptidyl-prolyl isomerase
RSAU_001113	0.6	0.0002	extracellular	3 oxoacyl-reductase
RSAU_001576	0.6	0.01	extracellular	30 S ribosolmal protein S4
RSAU_002074	0.6	0.01	extracellular	50 S ribosolmal protein L5
RSAU_000324	0.6	0.004	extracellular	alkyl hydroperoxid reductase ahpC
RSAU_000976	0.6	0.0001	extracellular	peptid deformylase
RSAU_001780	0.6	0.007	extracellular	ferritin
RSAU_000449	0.4	0.006	extracellular	hypoxanthine phosphoribosysmtransferase
stationary growth phase			**cytosolic**	
RSAU_001553	3.6	0.007	cytosolic	methylcitrat synthase

RSAU_1083	3.2	$8.6*10^{-5}$	cytosolic	aspartat carbamoyltransferase (pyrB)
RSUA_000229	2.56	0.0003	cytosolic	EsaA
RSAU_000500	2.31	0.02	cytosolic	translation elongation factor tu
RSAU_000727	2.3	0.001	cytosolic	ribosome associated inhibitor
RSAU_00974	2.1	0.049	cytosolic	Ribonuclease J1
RSAU_001488	2.1	0.0005	cytosolic	putative transcriptional regulator
RSAU_000707	2.08	0.0004	cytosolic	ribonucleotid diphosphat reductase (nrdF)
RSAU_001879	2	0.003	cytosolic	redox sensing transcriptional repressor
RSAU_000433	1.95	0.04	cytosolic	pur operon repressorr PurR
RSAU_001140	1.9	0.013	cytosolic	uridylate kinase (pyrH)
RSAU_001255	1.9	0.019	cytosolic	Aminoacyltransferase FemA
RSAU_000332	1.84	0.02	cytosolic	Xanthine phophoribosyl transferase
RSAU_000476	1.8	0.006	cytosolic	clp proteasse ClpC
RSAU_001827	1.8	0.005	cytosolic	aldehyde dehydrogenase
RSAU_000573	1.76	0.033	cytosolic	staphylococcal accessory regulator A
RSAU_000765	1.7	0.001	cytosolic	clumping factor A
RSAU_002087	1.7	0.01	cytosolic	30 S ribosolmal protein S10
RSAU_001975	1.6	0.04	cytosolic	deoxyribose phosphat aldolase
RSAU_001386	1.52	0.03	cytosolic	DNA repair protein RecN
RSAU_002252	1.4	0.0001	cytosolic	Amino acid ABD transporter binding protein
RSAU_001568	1.4	0.006	cytosolic	acetate kinase
RSAU_001960	1.3	0.01	cytosolic	aldehyd dehydrogenase
RSAU_000728	1.2	0.02	cytosolic	preprotein translocase SecA subunit (secA1)
RSAU_000980	0.9	0.01	cytosolic	pyruvat dehydrogenase complex (phdC)
RSAU_001806	0.8	0.0008	cytosolic	dipeptidase PepV
RSAU_000999	0.7	0.0002	cytosolic	pyruvat carboxylase
RSAU_001396	0.7	0.04	cytosolic	Xaa-Pro aminopeptidase
RSAU_001523	0.7	0.001	cytosolic	valyl-tRNA synthase
RSAU_001780	0.7	0.04	cytosolic	ferritin
RSAU_001860	0.7	0.0006	cytosolic	60 kDa chaperonin GroEL
RSAU_000524	0.69	0.004	cytosolic	hexulose-6-P-synthase
RSAU_000564	0.64	0.01	cytosolic	arginyl-tRNA synthetase
RSAU_001963	0.6	0.004	cytosolic	fructose bisphosphate aldolase
RSAU_002240	0.6	0.014	cytosolic	3-methyl-2-oxobutanoate hydroxymethyltransferase PanB
RSAU_002443	0.6	0.011	cytosolic	L-lactate dehydrogenase Ldh2
RSAU_002448	0.6	0.04	cytosolic	malate quinone oxidoreductase 2
RSAU_000470	0.54	0.04	cytosolic	pyridoxal biosynthesis lyase (pdxs)
RSAU_000324	0.53	0.02	cytosolic	alkyl hydroperoxid reductase subunit C (ahpC)
RSAU_000335	0.5	0.001	cytosolic	bifunctional GMP transferase synthase /glythamine amidotransferase (guaA)
RSAU_001233	0.5	0.04	cytosolic	4-hydroxybenzol CoA thioesterase
RSAU_001874	0.5	0.009	cytosolic	Sucrose-6-P-hydrolase
RSAU_001951	0.5	0.03	cytosolic	serine hydroxymethyltransferase putative
RSAU_000847	0.46	0.03	cytosolic	coenzyme A disulfide reductase
RSAU_000323	0.45	0.009	cytosolic	alkyl hydroperoxid reductase subunit F (ahpF)
RSAU_001094	0.4	0.049	cytosolic	primosomal assembly protein PriA
RSAU_002532	0.4	0.003	cytosolic	YceI domain protein
RSAU_001372	0.37	0.02	cytosolic	glucose-6-P-1-dehydrogenase (zwf)

[11]Compared to protein levels in *S. aureus* 6850 wild-type bacteria (ΔSSR42/WT)

Table 7.12: Proteins with significantly differential abundances in *S. aureus* 6850 ΔSSR42-*rsp* in exponential and stationary growth phase respectively.

gene	fold change[1] (ΔSSR42-*rsp*/WT)	adjusted p-value	fraction	product
exponential growth phase			**extracellular**	
RSAU_002260	5.68	0.001	extracellular	gamma-hemolysin component B precursor
RSAU_000228	5.01	0.0004	extracellular	putative WxG domain protein EsxA
RSAU_001838	3.83	0.001	extracellular	map-like protein
RSAU_000570	3.39	0.0004	extracellular	hypothetical protein
RSAU_000517	3.08	0.03	extracellular	Serine-aspartate repeat-containing protein E
RSAU_001040	2.84	$5.4*10^{-5}$	extracellular	extracellular fibrinogen/complement-binding protein
RSAU_001833	2.48	0.001	extracellular	superoxide dismutase (SodA2)
RSAU_000940	2.39	$7.4*10^{-7}$	extracellular	autolysin Atl
RSAU_002487	1.94	0.03	extracellular	N-acetylmuramoyl-L-alanine amidase
RSAU_002473	1.9	0.03	extracellular	clumping factor B (ClfB)
RSAU_002132	1.71	0.0002	extracellular	secretory antigen precursor SsaA
RSAU_002257	1.71	0.002	extracellular	immunoglobulin G-binding protein SBI
RSAU_000398	1.70	0.0007	extracellular	hypothetical protein
RSAU_000750	1.56	0.01	extracellular	glyceraldehyde 3-phosphate dehydrogenase 1
RSAU_000500	1.27	0.03	extracellular	translation elongation factor Tu
RSAU_001860	0.53	0.02	extracellular	60 kDa chaperonin GroEL
RSAU_001418	0.39	0.03	extracellular	Extracellular fibrinogen /complement binding protein
exponential growth phase			**cytosolic**	
RSAU_002365	3.35	0.007	cytosolic	D-lactate dehydrogenase
RSAU_001318	2.52	0.02	cytosolic	Cell cycle protein GpsB
RSAU_000503	2.22	0.04	cytosolic	chaperone protein HchA
RSAU_001380	1.91	0.003	cytosolic	disulfide isomerase putative
RSAU_001213	1.9	0.0009	cytosolic	hydrolase haloacid dehalogenase-like family
RSAU_002447	1.83	0.045	cytosolic	fructose-bisphosphate aldolase class 1
RSAU_001942	1.8	0.04	cytosolic	FOF1-ATP synthase subunit gamma
RSAU_001775	1.79	0.02	cytosolic	methionine aminopeptidase 1
RSAU_001963	1.79	0.002	cytosolic	fructose-bisphosphate aldolase
RSAU_001966	1.74	0.01	cytosolic	DNA-directed RNA polymerase delta subunit
RSAU_001704	1.73	0.03	cytosolic	hypothetical protein with DUF964
RSAU_001607	1.72	0.04	cytosolic	D-alanine aminotransferase putative
RSAU_001488	1.7	0.02	cytosolic	transcriptional regulator putative
RSAU_001537	1.65	0.0005	cytosolic	50S ribosomal protein L20
RSAU_001112	1.6	0.02	cytosolic	malonyl CoA-acyl carrier protein transacylase
RSAU_001975	1.55	0.04	cytosolic	deoxyribose-phosphate aldolase
RSAU_001127	1.4	0.049	cytosolic	succinyl-CoA synthetase beta subunit
RSAU_001184	1.23	0.0006	cytosolic	aerobic glycerol-3-phosphate dehydrogenase GlpD
RSAU_001938	0.69	0.02	cytosolic	UDP-N-acetylglucosamine 1-carboxyvinyltransferase 1
RSAU_002069	0.68	0.02	cytosolic	ribosomal protein S5
RSAU_000449	0.65	0.04	cytosolic	hypoxanthine phosphoribosyltransferase
RSAU_001345	0.62	0.04	cytosolic	GTP-binding protein EngA
RSAU_001965	0.54	0.005	cytosolic	CTP synthase

RSAU_000494	0.48	0.02	cytosolic	DNA-dependent RNA polymerase beta subunit
RSAU_002087	0.48	0.0002	cytosolic	30S ribosomal protein S10
RSAU_000495	0.44	0.001	cytosolic	DNA directed RNA polymerase beta-prime chain putative
RSAU_001172	0.28	0.03	cytosolic	2-oxoacid:acceptor oxidoreductase alpha subunit putative
stationary growth phase			**extracellular**	
RSAU_002340	6.88	0.0001	extracellular	Fibronectin-binding protein B
RSAU_000517	6.15	$6.1*10^{-5}$	extracellular	Serine-aspartate repeat-containing protein E
RSAU_002259	3.59	0.004	extracellular	gamma-hemolysin component C precursor
RSAU_000587	3.24	0.02	extracellular	Mn2 ABC transporter substrate-binding lipoprotein putative
RSAU_002514	2.78	0.006	extracellular	Lipase precursor
RSAU_002081	2.75	0.048	extracellular	50S ribosomal protein L22
RSAU_000494	2.7	0.003	extracellular	DNA-dependent RNA polymeras beta subunit
RSAU_000750	2.66	0.002	extracellular	glyceraldehyde 3-phosphate dehydrogenase 1
RSAU_001372	2.48	0.005	extracellular	glucose-6-phosphate 1-dehydrogenase
RSAU000488	2.48	0.007	extracellular	Serine-aspartate repeat-containing protein D truncated
RSAU_002252	2.25	0.02	extracellular	amino acid ABC transporter amino acid-binding protein putative
RSAU_0000093	2.1	0.02	extracellular	Phosphopentomutase putative
RSAU_000495	2.05	0.02	extracellular	DNA directed RNA polymerase beta-prime chain putative
RSAU_000754	1.85	0.048	extracellular	enolase
RSAU_000009	1.78	0.001	extracellular	seryl-tRNA synthetase
RSAU_000503	1.74	0.008	extracellular	Chaperone protein HchA
RSAU_001192	1.51	0.049	extracellular	Glutamine synthetase type I
RSAU_002065	0.64	0.003	extracellular	Adenylate kinase
RSAU_000976	0.58	0.003	extracellular	Peptide deformylase
RSAU_00170	0.55	$2.8*10^{-5}$	extracellular	Peptidyl-prolyl cis/trans isomerase
RSAU_000324	0.45	$7.1*10^{-6}$	extracellular	alkyl hydroperoxide reductase subunit C
RSAU_001833	0.41	0.009	extracellular	Map-like protein
stationary growth phase			**cytosolic**	
RSAU_001553	25.37	0.001	cytosolic	methylcitrate synthase
RSAU_000433	21.56	0.03	cytosolic	Pur operon repressor PurR
RSAU_000229	13.72	0.003	cytosolic	EsaA
RSAU_001974	11.4	0.02	cytosolic	Pyrimidine-nucleoside phosphorylase
RSAU_001255	9.6	0.0002	cytosolic	Aminoacyltransferase FemA
RSAU_001568	8.26	0.002	cytosolic	Acetate kinase
RSAU_001386	7.3	0.033	cytosolic	DNA repair protein RecN
RSAU_001615	7	0.006	cytosolic	leucyl-tRNA synthetase
RSAU_001326	4.49	0.003	cytosolic	asparaginyl-tRNA synthetase putative
RSAU_000974	4.32	0.012	cytosolic	Ribonuclease J 1 putative
RSAU_001094	3.3	0.02	cytosolic	primosomal assembly protein PriA
RSAU_000323	2.9	0.0002	cytosolic	alkyl hydroperoxide reductase subunit F
RSAU_000976	2.29	0.02	cytosolic	Peptide deformylase
RSAU_000765	2.1	0.0004	cytosolic	Clumping factor A
RSAU_000507	1.88	0.008	cytosolic	haloacid dehalogenase-like hydrolase
RSAU_002443	1.86	0.03	cytosolic	L-lactate dehydrogenase Ldh2
RSAU_001083	1.79	$8.4*10^{-5}$	cytosolic	aspartate carbamoyltransferase catalytic chain A PyrB
RSAU_001807	1.51	0.005	cytosolic	aldehyde dehydrogenase putative

RSAU_000470	1.46	0.007	cytosolic	pyridoxal biosynthesis lyase PdxS putative
RSAU_001216	1.3	0.007	cytosolic	catalase
RSAU_001402	1.22	0.0008	cytosolic	glycine cleavage system P protein subunit 1
RSAU_000792	1.2	0.0008	cytosolic	FeS assembly ATPase SufC putative
RSAU_001697	1.1	0.013	cytosolic	Histidine triad protein putative
RSAU_002252	1.1	0.043	cytosolic	amino acid ABC transporte amino acid-binding protein putative
RSAU_000728	0.92	0.02	cytosolic	preprotein translocase SecA subunit putative
RSAU_000980	0.92	0.043	cytosolic	pyruvate dehydrogenase complex E2 dihydrolipoamide S-acetyltransferase component PdhC
RSAU_001372	0.9	$5.9*10^{-5}$	cytosolic	glucose-6-phosphate 1-dehydrogenase
RSAU_000301	0.82	0.02	cytosolic	glucose-6-phosphate 1-dehydrogenase
RSAU_001168	0.64	0.04	cytosolic	recombinase A
RSAU_001293	0.56	0.02	cytosolic	2-oxoglutarate dehydrogenase E1 putative
RSAU_001074	0.56	0.02	cytosolic	isoleucyl-tRNA synthetase
RSAU_001608	0.55	0.02	cytosolic	dipeptidase PepV putative
RSAU_001588	0.5	0.0004	cytosolic	formate-tetrahydrofolate ligase
RSAU_000476	0.42	0.002	cytosolic	ATP-dependent Clp protease ATP-binding subunit ClpC
RSAU_001951	0.42	0.03	cytosolic	serine hydroxymethyltransferase putative
RSAU_000334	0.4	0.01	cytosolic	Inosine-5'-monophosphate dehydrogenase
RSAU_000727	0.4	0.0003	cytosolic	ribosome-associated inhibitor protein putative
RSAU_001396	0.39	0.044	cytosolic	Xaa-Pro aminopeptidase putative
RSAU_000479	0.37	0.04	cytosolic	glutamyl-tRNA synthetase GluRS
RSAU_001224	0.35	0.02	cytosolic	transketolase
RSAU_001347	0.26	0.009	cytosolic	30S ribosomal protein S1
RSAU_001523	0.26	0.002	cytosolic	valyl-tRNA synthetase
RSAU_000564	0.21	0.002	cytosolic	arginyl-tRNA synthetase
RSAU_002448	0.2	0.002	cytosolic	malate:quinone oxidoreductase 2
RSAU_001950	0.19	0.002	cytosolic	uracil phosphoribosyl transferase
RSAU_001960	0.183	0.0009	cytosolic	aldehyde dehydrogenase putative
RSAU_000845	0.14	0.01	cytosolic	fumarylacetoacetate hydrolase family protein
RSAU_000847	0.12	0.008	cytosolic	coenzyme A disulfide reductase putative
RSAU_001963	0.12	0.009	cytosolic	fructose-bisphosphate aldolase
RSAU_001601	0.11	0.004	cytosolic	thioredoxin putative
RSAU_001780	0.11	0.03	cytosolic	ferritin putative
RSAU_000500	0.1	0.02	cytosolic	translation elongation factor Tu
RSAU_001860	0.1	0.006	cytosolic	60 kDa chaperonin GroEL
RSAU_000999	0.09	0.009	cytosolic	pyruvate carboxylase
RSAU_000335	0.05	0.0001	cytosolic	bifunctional GMP synthase/glutamine amidotransferase protein
RSAU_000324	0.03	0.0002	cytosolic	alkyl hydroperoxide reductase subunit C
RSAU_001704	0.02	0.02	cytosolic	hypothetical protein with DUF964
RSAU_001029	0.014	0.02	cytosolic	thioredoxin TrxA

[11]Compared to protein levels in *S. aureus* 6850 wild-type bacteria (ΔSSR42-*rsp*/WT)

Table 7.13: Proteins with significantly differential abundances in *S. aureus* 6850 ΔSSR42-*rsp* in exponential and stationary growth phase respectively compared to protein levels in *S. aureus* ΔSSR42.

gene	fold change[1] ΔSSR42-*rsp*/ΔSSR42	adjusted p-value	fraction	product
exponential growth phase			**extracellular**	
RSAU_001838	1.82	0.048	extracellular	leukocidin S subunit LukS-H
RSAU_000500	1.81	$6.2 *10^{-5}$	extracellular	translation elongation factor Tu
RSAU_002132	0.82	0.026	extracellular	secretory antigen precursor SsaA
RSAU_000228	0.66	0.014	extracellular	putative WxG domain protein EsxA
exponential growth phase			**cytosolic**	
RSAU_000524	2.4	0.02	cytosolic	hexulose-6-phosphate synthase
RSAU_001966	1.91	0.0004	cytosolic	DNA-directed RNA polymerase
RSAU_001213	1.9	0.0019	cytosolic	hydrolase haloacid dehalogenase-like family
RSAU_001942	1.86	0.03	cytosolic	FOF1-ATP synthase subunit gamma
RSAU_001113	1.68	0.01	cytosolic	3-oxoacyl-[acyl-carrier protein] reductase
RSAU_001975	1.66	0.019	cytosolic	deoxyribose-phosphate aldolase
RSAU_001537	1.65	0.0006	cytosolic	50S ribosomal protein L20
RSAU_000488	1.64	0.048	cytosolic	transcription antitermination protein NusG
RSAU_001384	1.64	0.047	cytosolic	2-oxoisovalerate dehydrogenase E1 component alpha subunit
RSAU_001963	1.56	0.012	cytosolic	fructose-bisphosphate aldolase
RSAU_001576	1.53	0.014	cytosolic	30S ribosomal protein S4
RSAU_001526	1.48	0.03	cytosolic	glutamate-1-semialdehyde aminotransferase
RSAU_002074	1.46	0.011	cytosolic	50S ribosomal protein L5
RSAU_002080	0.96	0.015	cytosolic	30S ribosomal protein S3
RSAU_000976	0.79	0.04	cytosolic	peptide deformylase
RSAU_000796	0.73	0.02	cytosolic	FeS assembly protein SufB
RSAU_001386	0.68	0.049	cytosolic	DNA repair protein RecN
RSAU_001074	0.56	0.04	cytosolic	isoleucyl-tRNA synthetase
RSAU_002087	0.54	0.002	cytosolic	30S ribosomal protein S10
RSAU_000494	0.48	0.03	cytosolic	DNA-dependent RNA polymerase beta subunit
RSAU_000495	0.46	0.02	cytosolic	DNA directed RNA polymerase beta-prime chain putative
RSAU_001094	0.43	0.03	cytosolic	primosomal assembly protein PriA
RSAU_002146	0.42	0.013	cytosolic	formate dehydrogenase alpha subunit putative
RSAU_000940	0.34	0.014	cytosolic	autolysin Atl
stationary growth phase			**extracellular**	
RSAU_000494	1.9	0.03	extracellular	DNA-dependent RNA polymerase beta subunit
RSAU_000936	1.72	0.002	extracellular	glutamyl endopeptidase precursor putative
RSAU_001192	1.57	0.03	extracellular	glutamine synthetase type I
RSAU_000009	1.56	0.005	extracellular	seryl-tRNA synthetase
RSAU_001216	1.56	0.002	extracellular	catalase
RSAU_001224	1.5	0.01	extracellular	Transketolase
RSAU_000876	1.37	0.002	extracellular	oligoendopeptidase F
RSAU_000857	0.41	0.045	extracellular	hypothetical protein
stationary growth phase			**cytosolic**	
RSAU_000435	1.4	0.04	cytosolic	stage V sporulation protein G
RSAU_001950	1.4	0.03	cytosolic	uracil phosphoribosyl transferase

RSAU_001402	1.34	0.0003	cytosolic	glycine cleavage system P protein
RSAU_001615	0.68	0.003	cytosolic	leucyl-tRNA synthetase
RSAU_001588	0.59	0.03	cytosolic	formate-tetrahydrofolate ligase
RSAU_001488	0.57	0.005	cytosolic	transcriptional regulator
RSAU_001029	0.55	0.02	cytosolic	thioredoxin TrxA

[11]Compared to protein levels in *S. aureus* 6850 ΔSSR42 mutant (ΔSSR42-*rsp*/ ΔSSR42)

Table 7.14: Prediction of potential direct interaction partners of SSR42.

gene	product	position in target	position in SSR42	hybridization energy kJ/mol
RSAU_002489	putative surface anchored protein SasF	19 -- 149	658--804	-21.40
RSAU_002374	Phosphotransferase system IIC-related protein	81 -- 124	823--866	-21.12
RSAU_001452	DNA internalization-related competence protein ComEC/Rec2	69 -- 129	449 -- 508	-20.91
RSAU_000953	phosphoribosylaminoimidazole-succinocarboxamidesynthase PurC	76 -- 95	1000--1018	-20.398
RSAU_002131	transcriptional regulator putative	8 -- 108	195 -- 291	-20.00
RSAU_000557	aldo-keto reductase putative	53 -- 138	744--837	-19.98
RSAU_002517	histidine biosynthesis bifunctional protein HisIE	1 -- 91	188 -- 278	-19.51
RSAU_000580	monovalent cation/H antiporter subunit C putative	72 -- 141	732--799	-19.30
RSAU_001242	methionine sulfoxide reductase A	47 -- 100	194 -- 239	-19.15
RSAU_002191	teicoplanin resistance-associated transcriptional regulator TcaR	14 -- 64	778--833	-18.92
RSAU_001081	uracil phosphoribosyltransferase PyrR	72 -- 108	470 -- 506	-18.84
RSAU_002153	amino acid permease	8 -- 88	392 -- 472	-18.66
RSAU_000397	hypothetical protein	81 -- 137	196 -- 242	-18.61
RSAU_000167	putative two-component response regulator AraC family	82 -- 107	1118--1144	-18.49
RSAU_001463	5-methylthioadenosine/S-adenosylhomocysteine nucleosidase	36 -- 92	231 -- 284	-18.46
RSAU_001328	bifunctional biotin operon-related protein / biotin-acetyl-CoA-carboxylase putative	1 -- 53	261 -- 316	-18.38
RSAU_001019	NPQTN-specific sortase B	85 -- 132	212 -- 254	-18.33
RSAU_001407	competence protein ComGC	4 -- 150	713--843	-18.19
RSAU_001961	transcriptional regulator	57 -- 145	749--831	-18.15
RSAU_002230	two component sensor histidine kinase	73 -- 149	843--924	-18.09
RSAU_001398	hypothetical protein	60 -- 145	899--965	-18.05
RSAU_000580	monovalent cation/H antiporter subunit C	1 -- 41	826--860	-17.7864
RSAU_001980	mannose-6-phosphate isomerase	1 -- 19	914--931	-17.55
RSAU_000376	hypothetical protein	93 -- 135	907--950	-17.47
RSAU_000401	acetyltransferase GNAT family	81 -- 137	888--960	-17.38
RSAU_000228	putative WxG domain protein EsxA	83 -- 118	422 -- 461	-17.35
RSAU_001398	hypothetical protein	74 -- 145	723--795	-17.32
RSAU_001056	HAD superfamily hydrolase	12 -- 105	988--1063	-17.28
RSAU_001113	3-oxoacyl-[acyl-carrier protein] reductase	97 -- 150	880--936	-17.21
RSAU_001285	5-bromo-4-chloroindolyl phosphate hydrolysis protein XpaC	95 -- 142	725--771	-17.14

RSAU_002084	50S ribosomal protein L23	10 -- 25	1127--1142	-17.06
RSAU_001527	delta-aminolevulinic acid dehydratase	88 -- 150	195 -- 268	-17.06
RSAU_002450	antibiotic biosynthesis monooxygenase	14 -- 150	811--957	-16.99
RSAU_001153	ribosome-binding factor A	81 -- 137	195 -- 254	-16.97
RSAU_000439	ribose-phosphate pyrophosphokinase	10 -- 58	753--795	-16.96
RSAU_001117	signal recognition particle-docking protein FtsY	52 -- 80	912--938	-16.91
RSAU_002392	ferrous iron transport protein A (FeoA)	12 -- 123	166 -- 295	-16.8
RSAU_000755	hypothetical protein	1 -- 27	259 -- 299	-16.84
RSAU_001265	phosphate transport system regulatory protein	101 -- 115	424 -- 438	-16.82
RSAU_002253	EmrB-QacA subfamily drug resistance transporter	62 -- 148	419 -- 523	-16.78
RSAU_000664	aldo/keto reductase	51 -- 149	385 -- 467	-16.76
RSAU_001669	serine protease splB	100 -- 134	1179--1211	-16.74
RSAU_000726	ComF operon protein 3-like amidophosphoribosyltransferase	82 -- 125	828--880	-16.74
RSAU_001242	methionine sulfoxide reductase A	83 -- 144	744--803	-16.65
RSAU_002123	urease alpha subunit	16 -- 67	727--793	-16.63
RSAU_000445	RNA-binding S4 domain proteinputative	72 -- 149	380 -- 470	-16.60
RSAU_000303	cystathionine gamma-synthase superfamily protein	91 -- 150	190 -- 254	-16.59
RSAU_001892	3-isopropylmalate dehydratase large subunit	18 -- 91	189 -- 267	-16.45
RSAU_000392	cysteine synthase	5 -- 99	1126--1210	-16.41
RSAU_001032	succinate dehydrogenase flavoprotein subunit sdhA	54 -- 146	730--816	-16.37
RSAU_002423	cobalamin synthesis-related protein CobW	32 -- 150	788--890	-16.31
RSAU_001110	fatty acid biosynthesis transcriptional regulator	22 -- 96	231 -- 315	-16.28
RSAU_000617	staphylokinase precursor	41 -- 53	820--832	-16.28
RSAU000488	Serine-aspartate repeat-containing protein D truncated	63 -- 141	421 -- 505	-16.26
RSAU_000275	ascorbate-specific PTS system enzyme IIC	67 -- 147	727--799	16.17
RSAU_002148	inositol monophosphatase family protein	47 -- 105	727--781	-16.17
RSAU_001635	CAAX amino terminal protease family protein	121 -- 146	1056--1083	-16.13
RSAU_001938	UDP-N-acetylglucosamine 1-carboxyvinyltransferase 1	57 -- 125	191 -- 281	-16.09
RSAU_000481	cysteinyl-tRNA synthetase	6 -- 53	192 -- 242	-16.03
RSAU_002123	urease alpha subunit	9 -- 69	514 -- 576	-16.02
RSAU_000889	enoyl-(acyl-carrier-protein) reductase FabI	87 -- 142	542 -- 596	-15.99
RSAU_001393	acetyl-CoA biotin carboxylase	36 -- 69	1196--1228	-15.98
RSAU_001242	methionine sulfoxide reductase A	86 -- 150	525 -- 585	-15.90
RSAU_001868	delta-hemolysin	117 -- 150	230 -- 255	-15.88
RSAU_000823	NA+/H+ antiporter subunit G	126 -- 150	965--990	-15.87
RSAU_001521	leader peptidase	89 -- 141	737--797	-15.83
RSAU_001882	O-sialoglycoprotein endopeptidase	66 -- 132	744--816	-15.78
RSAU_001908	toxin mazF	73 -- 146	868--937	-15.78
RSAU_001399	lipoate-protein ligase A	47 -- 136	233 -- 293	-15.77
RSAU_001572	thiamine biosynthesis protein ThiI	15 -- 47	236 -- 263	-15.76
RSAU_000012	homoserine O-acetyltransferase	108 -- 138	1006--1036	-15.64
RSAU_002264	biotin synthase	32 -- 61	210 -- 239	-15.59
RSAU_002459	citrate transporter	67 -- 123	911--963	-15.50
RSAU_001452	DNA internalization-related competence protein ComEC/Rec2	105 -- 148	740--794	-15.45

RSAU_000506	branched-chain amino acid aminotransferase	36 -- 141	768--853	-15.43
RSAU_000609	bacteriophage tail protein	51 -- 63	230 -- 242	-15.43
RSAU_001064	UDP-N-acetylmuramoyl-L-alanyl-D-glutamate synthetase MurD	1 -- 105	713--841	-15.42
RSAU_002514	lipase precursor	89 -- 150	727--797	-15.38
RSAU_000208	two-component response regulator LytR	102 -- 149	892--932	-15.37
RSAU_000421	DNA-directed DNA polymerase III delta prime subunit	5 -- 147	782--897	-15.37
RSAU_001081	uracil phosphoribosyltransferase PyrR	72 -- 127	912--969	-15.36
RSAU_001558	acetyl-CoA carboxylase carboxyl transferase beta subunit	102 -- 141	474 -- 505	-15.36
RSAU_002283	2-dehydropantoate 2-reductase	110 -- 149	392 -- 435	-15.34
RSAU_002146	formate dehydrogenase alpha subunit	44 -- 100	1001--1061	-15.33
RSAU_001581	haloacid dehalogenase-like protein	88 -- 127	743--798	-15.30

7.5 Publications and presentations

7.5.1 Publications

Horn J, Stelzner K, Rudel T, Fraunholz M. 2018. Inside job: *Staphylococcus aureus* host-pathogen interactions. Int J Med Microbiol 308:607-624.

Horn J, Klepsch M, Manger M, Wolz C, Rudel T, Fraunholz M. 2018. The long non-coding RNA SSR42 controls *Staphylococcus aureus* α-toxin transcription in response to environmental stimuli. Journal of Bacteriology doi:10.1128/jb.00252-18.

7.5.2 Poster presentations

Horn J., Klepsch M., Hüttel B., Reinhardt R., Rudel T., Fraunholz M.J. The 1232 nt long non-coding RNA SSR42 regulates virulence in *Staphylococcus aureus* on a transcriptional level. Joint DGHM & VAAM Conference; 69th Annual DGHM (2016, Würzburg, Germany)

7.5.3 Oral presentations

Horn J., Rudel T., Fraunholz M.J. Characterization of Rsp and the long ncRNA SSR42 from *Staphylococcus aureus*. PhD meeting, DFG Transregional Collaborative Research Centre 34 (2015, Würzburg, Germany)

Horn J., Feuerbaum S., Rudel T., Fraunholz M.J. Molecular characterization of the virulence factors Rsp and SSR42 from *Staphylococcus aureus*. PhD meeting, DFG Transregional Collaborative Research Centre 34 (2016, Münster, Germany)

Horn J., Klepsch M., Wolz C., Hüttel B., Reinhardt R., Rudel T., Fraunholz M.J. Molecular characterization of the ncRNA SSR42 from *Staphylococcus aureus*. PhD meeting, DFG Transregional Collaborative Research Centre 34 (2017, Greifswald, Germany)

Horn J., Klepsch M., Manger M., Wolz C., Hüttel B., Reinhardt R., Rudel T., Fraunholz M.J. The long non-coding RNA SSR42 controls virulence of *Staphylococcus aureus* in response to external signals. 70th annual Conference of the german society of hygiene and microbiology (DGHM). (2018, Bochum, Germany)

7.6 Contribution by others

This work was conducted under the supervision of Prof. Dr. Thomas Rudel, Dr. Martin Fraunholz and Prof. Dr. Cynthia Sharma at the Department of Microbiology at the University of Würzburg. Several Parts of this doctoral thesis have been conducted in collaboration with others and are indicated below:

- RNase Y knockout mutant was kindly provided by Prof. Dr. Christiane Wolz at the department of Medical Microbiology and Hygiene at the University hospital in Tübingen, Germany.
- RNA-seq was performed in collaboration with Dr. Bruno Hüttel and Dr. Richrd Reinhardt at the Genome Centre Cologne, Cologne, Germany.
- Mass spectrometry performed in collaboration with Prof. Dr. Dörte Becher and Dr. Andreas Otto at the Institue for Microbiology, University of Greifswald.
- Processing and statistical analysis of RNA-seq and Mass spectrometry was performed by Maximilian Klepsch, Department of Microbiology, University of Würzburg, Germany.
- Initial Cloning of SSR42 promotor activity reporter plasmids (pGFP-Pr_{SSR42}, pbgab-Pr_{SSR42} and pbgab-Pr_{SSR42}-rsp) were performed by Stefanie Feuerbaum during her Master thesis.
- Analysis of transcriptional regulation of SSR42 in miscellaneous mutants obtained from the Nebraska library using the reporter plasmid pGFP-Pr_{SSR42} was performed in collaboration with Michelle Manger during her Master thesis.
- Cloning of complementation plasmid pSSR42 was performed by Dr. Sudip Das.
- Performance of long term infection of EA.Hy926 cells with *S. aureus* was performed by Dr. Lorena Tuchscherr, Medical Microbiology Department, University hospital Jena, Germany.
- Mouse experiments were performed by Dr. Eva Medina and her team at the Helmholtz Centre for Infection Research, Braunschweig, Germany.
- Grad-Seq experiments were performed by Pooja Tanwer and Dr. Alexandr Smirnov. Statistical analysis was performed by Konrad Förstner, Institute for Molecular Infection Biology, Würzburg, Germany.

7.7 Danksagung

An dieser Stelle möchte ich mich ganz herzlich bei allen bedanken, die zur Entstehung meiner Arbeit beigetragen haben.

Herrn Prof. Dr. Thomas Rudel danke ich für die Chance meine Doktorarbeit am Lehrstuhl für Mikrobiologie anfertigen zu dürfen, für die Betreuung und all die konstruktive Kritik und Denkanstöße, die zur Verbesserung meiner Arbeit beigetragen haben.

Besonders möchte ich mich bei Dr. Martin Fraunholz für die gute Betreuung, die konstruktiven Diskussionen und vor allem für die tolle Unterstützung bedanken. Danke, dass du immer an mein Projekt geglaubt hast und deine Tür jeder Zeit für mich offenstand.

Ich möchte mich auch herzlich bei Prof. Dr. Cynthia Sharma bedanken für die Übernahme des Zweitgutachtens. Bei meinen Kooperationspartnern möchte ich mich an dieser Stelle für die gute Zusammenarbeit und Unterstützung bedanken (Maximilian Klepsch, Dr. Eva Medina, Dr. Christiane Wolz, Dr. Gabriela Marincola, Lisa Bleul, Dr. Richard Reinhardt, Dr. Buno Hüttel, Dr. Andreas Otto, Dr. Dörte Becher, Prof. Dr. Jörg Vogel, Dr. Konrad Förstner, Dr. Lorena Tuchscherr, Dr. Alexandr Smirnov)

Weiterhin bedanke ich mich bei meinem we-lab, der Staphylokokkengruppe. Danke, für die Zusammenarbeit, die Hilfe und für die tolle Arbeitsstimmung. Danke, dass ihr jeden Tag etwas lustiger und angenehmer gemacht habt. Ebenfalls möchte ich mich herzlich bei dem gesamten Lehrstuhl für Mikrobiologie für die tolle Arbeitsatmosphäre und Zusammenarbeit bedanken. Besonders bedanke ich mich bei meinen Leidensgenossen und ehemaligen Kollegen Max, Dani, Kathrin, Franzi, Anastasija und Franzi, aus denen gute Freunde wurden. Danke, dass ihr die letzten vier Jahre für mich besonders gemacht habt. Danke für die Hilfe, Aufmunterung, die ganzen lustigen Kaffeepausen und vor allem für die seelische Unterstützung. Danke für die großartige Zeit und für einfach alles! Ein ganz besonderer Dank möchte ich an dieser Stelle Max aussprechen. Danke für die Auswertung meiner NGS und Proteom Daten und für jegliche Hilfe bei statistischen Fragen. Außerdem möchte ich mich für die konstruktiven Diskussionen bedanken und für die lustige Stimmung im Büro. Einen großen Dank auch an meine Frühstücksmädels Kerstin, Manu, Kerstin, Elke, Regina, Franzi. Danke, dass mit euch jeder Tag lustig gestartet hat.

Ein ganz großer Dank möchte ich auch meiner Familie aussprechen, die so manches Gejammer während der Doktorandenzeit ertragen musste. Danke, dass ihr mir das Studium ermöglicht habt und immer hinter mir gestanden habt. Vielen Dank für eure seelische Unterstützung und euren permanenten Glauben an mich. Ich bin euch wahnsinnig dankbar für eure permanente Unterstützung und Liebe! Als letztes möchte ich mich bei Patrick bedanken. Danke, dass du mich in den letzten zwei Jahren begleitet hast, mir Mut und Kraft gegeben hast und meine schlechten Launen und das Gemecker ertragen hast. Danke für die tägliche Aufmunterung, die Hilfe und Unterstützung und den stetigen Zuspruch.

7.8 Affidavit

Eidesstattliche Erklärungen nach §7 Abs. 2 Satz 3, 4, 5 der Promotionsordnung der Fakultät für Biologie

I hereby declare that my thesis entitled: „**Molecular and functional characterization of the long non-coding RNA SSR42 in *Staphylococcus aureus***" is the result of my own work. I did not receive any help or support from commercial consultants. All sources and / or materials applied are listed and specified in the thesis.

Furthermore, I verify that the thesis has not been submitted as part of another examination process neither in identical nor in similar form.

Besides, I declare that if I do not hold the copyright for figures and paragraphs, I obtained it from the rights holder and that paragraphs and figures have been marked according to law or for figures taken from the internet the hyperlink has been added accordingly.

Würzburg,

Hiermit erkläre ich an Eides statt, die Dissertation: „ **Molecular and functional characterization of the long non-coding RNA SSR42 in *Staphylococcus aureus*** ", eigenständig, d. h. insbesondere selbständig und ohne Hilfe eines kommerziellen Promotionsberaters, angefertigt und keine anderen, als die von mir angegebenen Quellen und Hilfsmittel verwendet zu haben.

Ich erkläre außerdem, dass die Dissertation weder in gleicher noch in ähnlicher Form bereits in einem anderen Prüfungsverfahren vorgelegen hat.

Weiterhin erkläre ich, dass bei allen Abbildungen und Texten bei denen die Verwertungsrechte (Copyright) nicht bei mir liegen, diese von den Rechtsinhabern eingeholt wurden und die Textstellen bzw. Abbildungen entsprechend den rechtlichen Vorgaben gekennzeichnet sind sowie bei Abbbildungen, die dem Internet entnommen wurden, der entsprechende Hypertextlink angegeben wurde.

Würzburg,